

Report Prepared by:  
Francisco J. Presuel-Moreno  
With  
Wendy Arias  
Victor Echevarria  
Scott Shill  
Yu-You Wu

## **Final Report**

Diffusion vs. Concentration of Chloride Ions in Concrete  
BDK79-977-03

Submitted to  
Florida Department of Transportation Research Center  
605 Suwannee Street  
Tallahassee, Florida 32399

Submitted by  
Francisco Presuel-Moreno  
Principal Investigator  
Department of Ocean and Mechanical Engineering  
Center for Marine Materials  
Florida Atlantic University  
SeaTech Research Center  
101 North Beach Road  
Dania Beach, Florida 33004

June 2014

### **Disclaimer**

The opinions, findings, and conclusions expressed in this publication are those of the author and not necessarily those of the State of Florida Department of Transportation.

# SI\* (MODERN METRIC) CONVERSION FACTORS

## APPROXIMATE CONVERSIONS TO SI UNITS

Symbol	When You Know	Multiply By	To Find	Symbol
<b>LENGTH</b>				
in	inches	25.4	millimeters	mm
ft	feet	0.305	meters	m
yd	yards	0.914	meters	m
mi	miles	1.61	kilometers	km
<b>AREA</b>				
in <sup>2</sup>	square inches	645.2	square millimeters	mm <sup>2</sup>
ft <sup>2</sup>	square feet	0.093	square meters	m <sup>2</sup>
yd <sup>2</sup>	square yard	0.836	square meters	m <sup>2</sup>
ac	acres	0.405	hectares	ha
mi <sup>2</sup>	square miles	2.59	square kilometers	km <sup>2</sup>
<b>VOLUME</b>				
fl oz	fluid ounces	29.57	milliliters	mL
gal	gallons	3.785	liters	L
ft <sup>3</sup>	cubic feet	0.028	cubic meters	m <sup>3</sup>
yd <sup>3</sup>	cubic yards	0.765	cubic meters	m <sup>3</sup>
NOTE: volumes greater than 1000 L shall be shown in m <sup>3</sup>				
<b>MASS</b>				
oz	ounces	28.35	grams	g
lb	pounds	0.454	kilograms	kg
T	short tons (2000 lb)	0.907	megagrams (or "metric ton")	Mg (or "t")
<b>TEMPERATURE (exact degrees)</b>				
°F	Fahrenheit	5 (F-32)/9 or (F-32)/1.8	Celsius	°C
<b>ILLUMINATION</b>				
fc	foot-candles	10.76	lux	lx
fl	foot-Lamberts	3.426	candela/m <sup>2</sup>	cd/m <sup>2</sup>
<b>FORCE and PRESSURE or STRESS</b>				
lbf	poundforce	4.45	newtons	N
lbf/in <sup>2</sup>	poundforce per square inch	6.89	kilopascals	kPa

## APPROXIMATE CONVERSIONS FROM SI UNITS

Symbol	When You Know	Multiply By	To Find	Symbol
<b>LENGTH</b>				
mm	millimeters	0.039	inches	in
m	meters	3.28	feet	ft
m	meters	1.09	yards	yd
km	kilometers	0.621	miles	mi
<b>AREA</b>				
mm <sup>2</sup>	square millimeters	0.0016	square inches	in <sup>2</sup>
m <sup>2</sup>	square meters	10.764	square feet	ft <sup>2</sup>
m <sup>2</sup>	square meters	1.195	square yards	yd <sup>2</sup>
ha	hectares	2.47	acres	ac
km <sup>2</sup>	square kilometers	0.386	square miles	mi <sup>2</sup>
<b>VOLUME</b>				
mL	milliliters	0.034	fluid ounces	fl oz
L	liters	0.264	gallons	gal
m <sup>3</sup>	cubic meters	35.314	cubic feet	ft <sup>3</sup>
m <sup>3</sup>	cubic meters	1.307	cubic yards	yd <sup>3</sup>
<b>MASS</b>				
g	grams	0.035	ounces	oz
kg	kilograms	2.202	pounds	lb
Mg (or "t")	megagrams (or "metric ton")	1.103	short tons (2000 lb)	T
<b>TEMPERATURE (exact degrees)</b>				
°C	Celsius	1.8C+32	Fahrenheit	°F
<b>ILLUMINATION</b>				
lx	lux	0.0929	foot-candles	fc
cd/m <sup>2</sup>	candela/m <sup>2</sup>	0.2919	foot-Lamberts	fl
<b>FORCE and PRESSURE or STRESS</b>				
N	newtons	0.225	poundforce	lbf
kPa	kilopascals	0.145	poundforce per square inch	lbf/in <sup>2</sup>

\*SI is the symbol for the International System of Units. Appropriate rounding should be made to comply with Section 4 of ASTM E380. (Revised March 2003)

**Technical Report Documentation Page**

1. Report No.	2. Government Accession No.	3. Recipient's Catalog No.	
4. Title and Subtitle Diffusion vs. Concentration of Chloride Ions in Concrete		5. Report Date June 2014	
		6. Performing Organization Code FAU-OE-CMM-08-3	
7. Author(s) Francisco Presuel-Moreno, Wendy Arias, Victor Echevarria, Scott Shill, Yu-You Wu		8. Performing Organization Report No. BDK79-977-03	
9. Performing Organization Name and Address Center for Marine Materials Florida Atlantic University – SeaTech 101 North Beach Road Dania Beach, Florida 33004		10. Work Unit No. (TRAIS)	
		11. Contract or Grant No. BDK79-977-03	
12. Sponsoring Agency Name and Address Florida Department of Transportation 605 Suwannee Street, MS 30 Tallahassee, FL 32399		13. Type of Report and Period Covered Final Report May 18 2011 – June 4, 2014	
		14. Sponsoring Agency Code	
15. Supplementary Notes			
16. Abstract This investigation was performed to gain insight and assist in determining the long-term durability of reinforced concrete structures where the external chloride concentrations are different than those typically observed at the permanently immersed, tidal, and splash zones of partially immersed bridges. Insight into the diffusion properties of the concrete at these locations may lead to changes in the state's policy on corrosion control of reinforced concrete structures. Structures at locations where the external chloride concentrations may have spatial, let alone time, variation are of interest. Additionally, at elevations above the splash zone, the amount of chlorides deposited would be lower, and the concrete close to the surface not saturated. Similarly, the section of structures that extend inland would be subjected to seawater spray and the concrete close to the surface would usually not be water saturated. The performance in regard to chloride penetration of specimens made with three base compositions (the supplementary cementitious materials were: 20% fly ash; 20% fly ash + 8% silica fume; and 50% slag), and water-to-cementitious ratios of 0.35, 0.41, or 0.47 were investigated here. Experiments investigated the diffusion of chloride ions into concrete samples that were exposed in scenarios that simulated the splash, tidal, and immersed portions of a marine structure, with the solution ranging from brackish water to 10% seawater, to seawater. Bulk diffusion experiments were conducted in solutions that contained 0.6%, 3%, and 16.5% NaCl. Rapid migration tests and resistivity measurements were also performed several times over two years, and the non-saturated migration coefficient vs. resistivity values were correlated. The apparent diffusion values from the bulk diffusion tests were correlated to corresponding equivalent resistivity values. Samples exposed for over 18 years, simulating tidal exposure were also part of this investigation. The field component investigated the chloride concentration as a function of elevation. Other experiments were conducted which involved controlling the degree of saturation and exposing a designated surface to finely ground salt. These apparent diffusion results were compared to the apparent diffusion results from specimens in which the chloride transport was due to natural marine atmosphere.			
17. Key Word Bridge substructures, chloride surface concentration, bulk diffusion, apparent diffusion coefficient, non-saturated concrete, resistivity,		18. Distribution Statement No restrictions. This document is available to the public through NTIS, Springfield, VA 22161	
19. Security Classif. (of this report) Unclassified	20. Security Classif. (of this page) Unclassified	21. No. of Pages: 320	22. Price

## **ACKNOWLEDGMENTS**

The authors are indebted to the FDOT State Materials Office (SMO) for assisting in preparing the different concrete specimens and conducting several tests and initial curing at SMO for this study and, in particular, Mr. Mario Paredes, Mr. Ronald Simmons, and several SMO Technicians (Dennis Baldi, Richard Delorenzo, Pat Carlton, Thomas Frank, Jason Burchfield, Teresa Risher, Cody Owen). The assistance of several students that work as graduate/undergraduate research assistants (Bongeon Seo, Omar Ramos, Lin Li, Yali Sun, Yanbo Liu) is also acknowledged.

## Executive Summary

Material selection and design for reinforced concrete structures is critical to maintaining the reliability of the infrastructure of highway and municipal service systems. To design reinforced concrete structures with a minimum 75 years of service life, the Florida Department of Transportation has implemented the use of concrete with low water-to-cement ratio with pozzolans and/or slag cement replacement material, plastic control chemical admixtures, and thick concrete cover. Much of the State's reinforced concrete infrastructure is exposed to chloride environments which can cause concrete deterioration by corrosion of reinforcing steel.

This investigation was performed to gain insight and assist in determining the long-term durability of reinforced concrete structures where the external chloride concentrations are different than those observed at the permanently immersed, tidal, and splash zone. Insight into the diffusion properties of the concrete at these locations may lead to changes in the state's policy on corrosion control of reinforced concrete structures. Structures at locations where the external chloride concentrations may have spatial, let alone time, variation are of interest. Additionally, at elevations above the splash zone, the amount of chlorides deposited would be lower, and the concrete close to the surface not saturated. Similarly, the portion of a structure that is inland would be subjected to seawater spray, with the concrete close to the surface not saturated.

Experiments investigated the diffusion of chloride ions into concrete samples that were exposed in scenarios that simulated the splash, tidal, atmospheric, and immersed portions of a marine structure with the solution ranging from brackish water to 10% seawater to seawater. Bulk diffusion experiments were conducted in solutions that contained 0.6%, 3%, and 16.5% NaCl by wt%. Rapid migration tests and resistivity measurements were performed several times over two years, and these values were correlated. The apparent diffusion values from the bulk diffusion tests were correlated to the calculated equivalent resistivity values.

Samples exposed for over 18 years simulating tidal exposure were also part of this investigation. The field component also investigated the chloride concentration as a function of elevation. Other experiments were conducted in which the degree of saturation was controlled, and these results were compared to the chloride transport of specimens exposed to the marine atmosphere. Study results showed that the apparent diffusion of specimens exposed to bulk diffusion were significantly larger than the apparent diffusivity obtained from specimens exposed to simulated tidal/splash in seawater or brackish water. The difference in  $D_{app}$  is due in part to the presence of the mortar layer on the latter type of specimens (tidal/splash), but also to chemical compounds that are known to form within the pore structure when the solution is seawater (or brackish water).

The apparent diffusion of specimens exposed to marine atmosphere (natural chloride deposition from seawater spray particles at locations 100 m to 200 m from the sea) was as small as  $0.02 \times 10^{-12} \text{ m}^2/\text{s}$ , and significantly smaller than that measured on specimens under controlled water saturation degree where the smaller apparent diffusion value was  $0.5 \times 10^{-12} \text{ m}^2/\text{s}$ . This difference might be due to the large difference in chloride ions at the surface for both of these exposures.

## TABLE OF CONTENTS

DISCLAIMER .....	ii
CONVERSION FACTOR TABLE .....	iii
TECHNICAL REPORT DOCUMENTATION PAGE .....	iv
ACKNOWLEDGEMENTS .....	v
EXECUTIVE SUMMARY .....	vi
LIST OF FIGURES .....	xii
LIST OF TABLES .....	xviii
1 Introduction .....	1
1.1 Background Statement .....	1
1.2 Objectives .....	1
1.3 Methodology .....	2
1.4 Structure of Report .....	2
2 Literature Review and Background.....	3
2.1 Introduction .....	3
2.2 Mechanisms of Chloride Ion Transport in Marine Environments .....	4
2.3 Chloride Diffusion into Chloride .....	4
2.4 Time-Dependent Diffusivity .....	6
2.5 Effect of Chloride Surface Concentration on Diffusivity .....	8
2.6 Field Chloride Surface Concentration at Low Tide and Below .....	8
2.7 Field Chloride Surface Concentration at Mid-To-High Tide Section, and Splash Zone .....	9
2.8 Chloride Deposition above the Splash Zone .....	9
2.9 Chloride Saturation of Concrete.....	13
2.10 Controlled Degree of Water Saturation on Diffusion .....	13
2.11 Chloride Binding .....	16
2.12 Chloride Profiles.....	17
2.13 Existing Test Methods used in this Project .....	17
2.13.1 Resistivity Measurement.....	18
2.13.2 Density, Absorption, and Voids in Hardened Concrete.....	18
2.13.3 Rapid Chloride Migration Test (RCMT) .....	18
2.13.4 Bulk Diffusion .....	18
2.13.5 Wet Candle Test.....	19

2.13.6 Chloride Content Analysis .....	19
2.14 Conclusions from Literature Review .....	19
3 Experimental Program.....	20
3.1 Introduction .....	20
3.2 New Specimens .....	20
3.2.1 Concrete Mix Prepared .....	20
3.2.2 Concrete Mixes for Specimens at FAU Prepared Previously.....	21
3.2.3 Additional Concrete Mixes for Specimens at SMO .....	21
3.3 Specimen Geometry .....	22
3.3.1 New Specimens.....	22
3.3.2 Geometry of Specimens Previously Prepared and Exposed at FAU .....	24
3.3.3 Specimens Exposed at SMO.....	25
3.4 Water Sealant Application on Specimens Exposed at FAU.....	30
3.5 Indoor and Outdoor Exposure: Partially Immersed Specimens .....	32
3.5.1 Tidal Simulation.....	32
3.5.2 Splash Simulation .....	34
3.5.3 Partial Immersion Exposure: Barge Scenario .....	36
3.6 Atmospheric Exposure .....	37
3.6.1 Exposure Locations.....	37
3.6.2 G2 Slabs .....	40
3.6.3 G4 Slabs .....	41
3.7 Milling.....	42
3.8 Coring and Milling .....	43
3.9 Bulk Diffusion .....	45
3.9.1 Exposure in 3% and 16.5% NaCl .....	45
3.9.2 Bulk Diffusion in Low Chloride Concentration (0.6% NaCl).....	46
3.9.3 Chloride Diffusion on Concrete Under Controlled Partial Saturation.....	48
3.10 Other Tests .....	52
3.10.1 Surface Resistivity of Concrete .....	52
3.10.2 Rapid Chloride Migration Test (RCMT).....	53

3.10.3	Wet Candle Test.....	55
3.10.4	Chloride Analysis of Concrete Powders.....	56
3.10.5	Porosity.....	56
4	Experimental Results.....	57
4.1	Resistivity.....	57
4.2	Rapid Chloride Migration Coefficients (RCMT).....	62
4.3	Porosity.....	68
4.4	Profiles after Bulk Diffusion and Fully Immersed Locations.....	70
4.4.1	Specimens Exposed to Low Concentration of Sodium Chloride Solution (0.1M NaCl) ..	70
4.4.2	Specimens Exposed to High Concentration of Sodium Chloride Solutions (3% and 16.5% NaCl).....	75
4.4.3	Specimen Exposed to Simulated Field Conditions.....	81
4.5	Free Chlorides Concentration Profiles.....	87
4.5.1	Specimens Exposed to Low Concentration of Sodium Chloride Solution (0.1M NaCl) ..	87
4.5.2	Specimens Exposed to High Concentrations of Sodium Chloride Solutions (3% and 16.5% NaCl) ..	90
4.6	Nomenclature for Specimens Partially Immersed at Elevations above Water.....	94
4.6.1	Tidal Exposure Chloride Concentration Profiles.....	95
4.6.2	Tidal Exposure: Chloride Surface Concentration Calculated and First Layer.....	101
4.6.3	Splash Exposure Chloride Concentration Profiles.....	104
4.6.4	Splash Exposure: Chloride Surface Concentration Calculated and First Layer.....	104
4.6.5	Chloride Concentration Profiles of Specimens Exposed at the Barge.....	109
4.7	Barge Exposure: Chloride Surface Concentration Calculated and First Layer.....	116
4.8	Specimens Exposed to 70%, 80%, 90%, and 100% SD.....	117
4.8.1	Absorption of Specimens.....	117
4.8.2	Chloride Concentration Profiles.....	118
4.8.3	Effect of Mortar on the Chloride Diffusion (100% Degree of Saturation).....	120
4.8.4	Chloride Surface Concentration.....	122
4.9	Marine Atmospheric Exposure Chloride Profiles.....	124
4.10	Wet Candle Deposition.....	131
4.11	Specimens Subjected to Tidal Simulation for >18 Years: Chloride Profiles.....	135

4.12	Partial Immersion at SMO .....	140
5	Discussion .....	143
5.1	Aging Factor Using Resistivity.....	143
5.2	Aging Factor (Using Resistivity) vs. Time.....	146
5.2.1	Aging Factor vs. Time for Specimens under RT Curing.....	146
5.2.2	Effect of Cementitious Material Content on Aging Factor vs. Time.....	148
5.3	Resistivity vs. $D_{nssm}$ .....	150
5.4	Apparent Diffusion Coefficient .....	154
5.4.1	Specimens Exposed to Low Concentration of Sodium Chloride Solution (0.1M NaCl)	154
5.4.2	Specimens Exposed to High Concentration of Sodium Chloride Solutions (3% and 16.5% NaCl).....	154
5.4.3	Specimens Exposed to Simulated Field Conditions .....	157
5.5	Comparison of Apparent Diffusivity Coefficient (Free vs. Total) .....	168
5.5.1	Specimens Exposed to Low Concentration of Sodium Chloride Solution (0.1M NaCl)	168
5.5.2	Specimens Exposed to High Concentrations of Sodium Chloride Solutions (3% and 16.5% NaCl) .....	168
5.6	Additional $D_{app}$ Analysis for Cores Obtained at Elevation A or from Bulk Diffusion ...	170
5.6.1	Effect of w/cm Ratio on Specimens Exposed to 0.1 M NaCl.....	170
5.6.2	Effect of Supplementary Cementitious Material Type Based on Specimens Exposed to 3% or 16.5% NaCl .....	172
5.6.3	Effect of Sodium Chloride Concentration Solution and w/cm .....	173
5.6.4	Effect of Exposure Time.....	175
5.6.5	Effect of Exposure Condition .....	176
5.7	Specimens Subjected to Tidal Simulation for >18 Years at SMO.....	180
5.7.1	$D_{app}$ vs. Elevation .....	180
5.8	Chloride Binding Capacity .....	185
5.9	Correlation between Apparent Diffusivity and Equivalent Resistivity .....	189
5.10	$D_{app}$ of Specimens Exposed to 70%, 80%, 90%, and 100% Saturation Degree.....	194
5.10.1	Effect of Mortar Layer on $D_{app}$ for Sections Exposed in 100% SD .....	197
5.11	$D_{app}$ for Specimen Exposure Outdoors to Marine Atmosphere.....	199
6	Compilation of Previous Field Visits and New Field Visits .....	212
6.1	Chloride Profiles .....	215

6.2	$D_{app}$ vs. Elevation .....	219
6.3	$D_{app}$ from cores obtained at elevations higher than 2 m .....	221
6.4	$D_{app}$ vs. Resistivity .....	223
7	Conclusions .....	224
	References .....	227
	Appendices .....	234
	Appendix A: Core Collection for Field Simulations .....	234
	Appendix B: Exposure Date and Coring Ages for G2 Specimens .....	235
	Appendix C: Resistivity vs. Time .....	236
	Appendix D: DCL4, 5, 7, 8, 10a, 10b, and 11: Chloride Concentration for Specimens Exposed to 0.1M NaCl Solution vs. Depth .....	238
	Appendix E: Chloride Profiles for Specimens Exposed to 3% and 16.5% NaCl Solutions .....	240
	Appendix F: Chloride Profiles for Tidal Simulated Exposure .....	253
	Appendix G: Chloride Profiles for Splash Simulated Exposure .....	263
	Appendix H: Chloride Profiles for Specimens Exposed at Barge .....	267
	Appendix I: Inverse Resistivity vs. Time (Log-Log Scale) .....	269
	Appendix J: Apparent Diffusivity Coefficient of Specimens Exposed at SMO .....	271
	Appendix K: DCL3, 6, and 9: Apparent Diffusivity Coefficient of Specimens Exposed to 0.1M NaCl Solution .....	278
	Appendix L: DCL7, 8, and 9: Apparent Diffusivity Coefficient of Specimens Exposed to Tidal and Splash .....	279
	Appendix M: DCL7, 8, 9, and 10b: Free vs. Total Chloride Contents .....	280
	Appendix N: Computed Equivalent Resistivity Values for DCL Mixes (Bulk Diffusion) .....	281
	Appendix O: Historical Weather and Wind Data (Ft. Lauderdale Airport) .....	283
	Appendix P: Compilation of $D_{app}$ from Previous Projects Sorted by Bridge Number .....	286

## LIST OF FIGURES

Figure 2-1: Units of chloride concentration [23] .....	5
Figure 2-2: Effects of wind speed on salt concentration from previous studies [47] .....	10
Figure 2-3: Graph showing the relation of humidity and chloride content [48].....	11
Figure 2-4: Studies of chloride deposition as a function of distance [41] .....	12
Figure 2-5: The relationship between total chloride amount and time [41] .....	13
Figure 2-6: Diffusivity and resistivity vs. saturation [63].....	15
Figure 2-7: Diffusivity vs. saturation degree [63] .....	15
Figure 2-8: Chloride profiles for two different compositions of concrete exposed for the same time [67].....	17
Figure 3-1: Specimen design used for tidal exposure.....	26
Figure 3-2: Diagram of tank used for tidal exposure simulation .....	27
Figure 3-3: Tidal simulated samples at SMO .....	28
Figure 3-4: Cored location on specimens subjected to tidal exposure at SMO .....	28
Figure 3-5: Partial immersion samples at SMO.....	29
Figure 3-6: Cored location on specimens subjected to partial immersion at SMO .....	29
Figure 3-7: Thoroseal-coated G4 specimen.....	31
Figure 3-8: Tidal simulation exposure conditions .....	33
Figure 3-9: Tidal simulation (low tide seawater height = 7").....	33
Figure 3-10: Tidal simulation .....	34
Figure 3-11: Splash simulation block .....	35
Figure 3-12: Splash simulation .....	35
Figure 3-13: Barge scenario.....	36
Figure 3-14: Satellite image of SeaTech showing locations of the concrete samples .....	37
Figure 3-15: East property exposure.....	38
Figure 3-16: West property: away from the fence .....	39
Figure 3-17: West property: adjacent to the fence.....	39
Figure 3-18: G2 – east property -horizontally oriented with exposure side eastward .....	40
Figure 3-19: G2 – west property and fence adjacent – horizontally oriented with exposure side skyward.....	41
Figure 3-20: G4 – west property and fence adjacent – vertically oriented with exposure side eastward .....	41

Figure 3-21: G4 – west property – horizontally oriented with exposure side skyward .....	42
Figure 3-22: G4 – east property – horizontally oriented with exposure side eastward .....	42
Figure 3-23: G4 slab (milling performed once) .....	42
Figure 3-24: Typical milling of G4 slabs .....	43
Figure 3-25: Milling setup for 2" diameter cylinder .....	44
Figure 3-26: Bulk diffusion exposure .....	45
Figure 3-27: Saw cut of concrete cylinder .....	46
Figure 3-28: Specimens placed in the container with Ca(OH) <sub>2</sub> solution .....	47
Figure 3-29: Test specimens coated with Sikadur 32 .....	47
Figure 3-30: Bulk diffusion in 0.1 M NaCl .....	48
Figure 3-31: Specimen for 100% SD with and without mortar layer .....	52
Figure 3-32: RMT setup [74] .....	54
Figure 3-33: Wet candle apparatus .....	55
Figure 4-1: Resistivity for DCL specimens cured at RT vs. time .....	58
Figure 4-2: DCL1 resistivity .....	59
Figure 4-3: DCL4 resistivity .....	59
Figure 4-4: DCL7 resistivity .....	60
Figure 4-5: G3 specimens resistivity after 300 days .....	62
Figure 4-6: $D_{nssm}$ vs. resistivity grouped by age at time of testing .....	66
Figure 4-7: DCL1, DCL2 and DCL3 $D_{nssm}$ vs. resistivity .....	66
Figure 4-8: DCL4, DCL5, and DCL6 $D_{nssm}$ vs. resistivity .....	67
Figure 4-9: DCL7, DCL8, and DCL9 $D_{nssm}$ vs. resistivity .....	67
Figure 4-10: DCL2, DCL10b, and DCL11 $D_{nssm}$ vs. resistivity .....	68
Figure 4-11: DCL1, 2 and 3 specimens exposed to 0.1M NaCl solution at 220 and 400 days cured at 14RT/77ET/RT and RT vs. depth .....	72
Figure 4-12: DCL3, 6, and 9 specimens exposed to 0.1M NaCl solution at 220 and 400 days vs. depth .....	73
Figure 4-13: DCL1, 2, and 3 - Average chloride concentrations vs. depth .....	76
Figure 4-14: DCL3, 6, and 9 - Average chloride concentrations vs. depth .....	77
Figure 4-15: DCL3, 6, and 9 - Tidal simulation chloride concentration vs. depth (left and right) .....	82
Figure 4-16: DCL3, 6, and 9- Splash simulation chloride concentration vs. depth .....	84
Figure 4-17: DCL3, 6, and 9- Barge simulation chloride concentration vs. depth (left and right) .....	86

Figure 4-18: DCL1, 2, and 3 Free and total chloride concentration vs. depth (400 days in 0.1M)	88
Figure 4-19: DCL3, 6, and 9 Free and total chloride concentration vs. depth (400 days in 0.1M)	89
Figure 4-20: DCL1, 2, and 3: free and total chloride concentration vs. depth	91
Figure 4-21: DCL3 and 6: free and total chloride concentration vs. depth	92
Figure 4-22: Locations of coring for specimens subjected to tidal simulation (in cm)	95
Figure 4-23: DCL3- Tidal simulation chloride concentration vs. depth (elevations B and C)	96
Figure 4-24: DCL6 - Tidal simulation chloride concentration vs. depth (elevations B and C)	98
Figure 4-25: DCL9- Tidal simulation chloride concentration vs. depth (elevations B and C)	99
Figure 4-26: DCL3, 6 and 9- Tidal chloride profiles (elevation D)	100
Figure 4-27: Chloride profiles for DCL3 splash exposure (elevations B, C, and D)	105
Figure 4-28: Chloride profiles for DCL6 splash exposure (elevations B, C, and D)	106
Figure 4-29: Chloride profiles for DCL9 splash exposure (elevations B, C, and D)	107
Figure 4-30: Chloride profiles for DCL3 Barge exposure (elevations B, C, and D)	110
Figure 4-31: Chloride profiles for DCL6 Barge exposure (elevations B, C, and D)	111
Figure 4-32: Chloride profiles for DCL9 Barge exposure (elevations B, C, and D)	112
Figure 4-33: Chloride profiles for DCL2 Barge exposure (elevations B, C, and D)	113
Figure 4-34: Chloride profiles for DCL10b Barge exposure (elevations B, C, and D)	114
Figure 4-35: Chloride profiles for DCL11 Barge exposure (elevations B, C, and D)	115
Figure 4-36: Measured chloride profiles for DCL2	119
Figure 4-37: Chloride profiles for DCL1, DC2, DC3, DC10b and DCL11 with SD =80%	120
Figure 4-38: Chloride profiles from DCL1, DC2, DC3, DC10b and DCL11 cured in RT with SD =100% under the conditions of exposed surface with and without mortar layers	121
Figure 4-39: DCL3 Atmospheric simulation - chloride concentration vs. depth	125
Figure 4-40: DCL9 Atmospheric simulation - chloride concentration vs. depth	126
Figure 4-41: Chloride profile for DC1 after 24 months of exposure	127
Figure 4-42: Chloride profile for DC2 after 24 months of exposure	128
Figure 4-43: Chloride profile for DC3 after 24 months of exposure	128
Figure 4-44: Chloride profiles at the east location after 24 months of exposure	129
Figure 4-45: Chloride profiles comparing the different mix compositions after 24 months of exposure at the east location	130
Figure 4-46: Chloride profiles for DC7e shown with time of exposure	131
Figure 4-47: Profiles after 18 months of exposure on G4 specimens	132

Figure 4-48: Average chloride deposition values measured at the three stations.....	132
Figure 4-49: Chloride deposition measured at each site per wet-candle setup.....	133
Figure 4-50: Profiles for specimens with Silica Fume (SF) .....	136
Figure 4-51: Profiles for specimens with superfine fly ash (SFFA).....	137
Figure 4-52: Profiles for specimen only with OPC as cementitious material.....	139
Figure 4-53: Measured and fitted profiles for specimen only with OPC.....	140
Figure 4-54: Profiles for specimens with FA (partial immersion).....	141
Figure 5-1: DCL2 and 10 Measured and Projected Resistivity using two aging factor values ..	144
Figure 5-2: Aging factor for DCL1, 2 and 3 mixtures for specimens RT cured.....	146
Figure 5-3: Aging factor for DCL4, 5 and 6 mixtures for specimens RT cured.....	147
Figure 5-4: Aging factor for DCL7, 8, and 9 mixtures for specimens RT cured.....	148
Figure 5-5: Aging factor for DCL2, DCL10b and DCL11 mixtures for specimens RT cured...	149
Figure 5-6: Evolution of the resistivity inverse in log-log scale.....	150
Figure 5-7: $D_{nssm}$ vs. resistivity grouped per entrained air content (90 days values) .....	151
Figure 5-8: $D_{nssm}$ vs. resistivity grouped per specimen age.....	151
Figure 5-9: Correlations that include all values log-log on the left and linear-linear on the right.....	152
Figure 5-10: Relationship between apparent diffusion coefficient and w/cm ratio.....	171
Figure 5-11: DCL1, 2 and 3 Calculated and measured chloride concentration vs. w/cm ratio..	172
Figure 5-12: Relationship between average apparent chloride coefficient and type of cementitious material.....	173
Figure 5-13: Relationship between apparent diffusivity and NaCl concentration solution.....	174
Figure 5-14: Relationship between calculated and measured chloride concentration and NaCl concentration solutions .....	175
Figure 5-15: Relationship between apparent coefficient and exposure time.....	176
Figure 5-16: Relationship between $D_{app}$ and w/cm for various exposure conditions.....	177
Figure 5-17: Relationship between apparent diffusion coefficient and exposure conditions (0.47 w/cm and different compositions).....	178
Figure 5-18: Relationship between apparent diffusion coefficient and exposure conditions (0.41 w/cm with 20% FA and different cementitious amount) .....	179
Figure 5-19: DCL3, 6, and 9 Calculated and measured chloride concentration at the surface and first layer .....	180
Figure 5-20: $D_{app}$ vs. elevation for specimens with superfine fly ash .....	181
Figure 5-21: $D_{app}$ vs. elevation for specimens with silica fume .....	182

Figure 5-22: Average $D_{app}$ vs. elevation computed for specimens exposed to tidal simulation	182
Figure 5-23: $D_{app}$ vs. elevation calculate for each side on specimens with Fly Ash	183
Figure 5-24: Average $D_{app}$ vs. elevation on specimens with Fly Ash	183
Figure 5-25: Relationship between free and total chloride content of DCL1, 2, and 3	186
Figure 5-26: DCL1, DCL2, DCI3, DCL4, DCL5, DCL6, DCL10b, and DCL11 Relationship between free and total chloride content	187
Figure 5-27: Equivalent resistivity curve [91]	190
Figure 5-28: Correlation of apparent diffusivity and equivalent resistivity	191
Figure 5-29: Correlation between $D_{app}$ and equivalent resistivity for specimens exposed to different curing conditions	193
Figure 5-30: Correlation between $D_{app}$ and equivalent resistivity (specimens grouped by mix)	194
Figure 5-31: Chloride diffusivity of DCL2 specimens vs. SD	195
Figure 5-32: Chloride diffusivity of DCL1, DCL2, DCL3 specimens cured in RT vs. SD	196
Figure 5-33: Chloride diffusivity of DCL2, DCL10b, DCL11 cured in RT vs. SD	197
Figure 5-34: $D_{app}$ for specimens in 100% SD during exposure	199
Figure 5-35: $D_{app}$ vs. time marine atmosphere exposure (DCL1 to DCL6)	200
Figure 5-36: $D_{app}$ vs. time marine atmosphere exposure (DCL7 to DCL11)	201
Figure 5-37: $D_{app}$ vs. time marine atmosphere exposure (1C1, 1C2, and 1C3)	202
Figure 5-38: $C_{tot}$ vs. time for specimens with 20%FA (DCL1, DCL2 and DCL3)	203
Figure 5-39: Storm surge during high tide at fence site (Fall 2012)	204
Figure 5-40: $C_{tot}$ values vs. time for DCL4 to DCL9	205
Figure 5-41: $C_{tot}$ values vs. time for DCL10, 10a, 10b, and DCL11	206
Figure 5-42: $C_{tot}$ values vs. time calculated for 1C1, 1C2, and 1C3 (older specimens)	207
Figure 5-43: $C_{tot}$ vs. $D_{ac}$ for DCL1, DCL2, and DCL3 and C1, C2, C3 [41]	209
Figure 6-1: Chloride profiles obtained at sound locations (Sunshine Skyway bridge)	215
Figure 6-2: Location at which cores were obtained south face of trestle caps on pier 44 and 60	216
Figure 6-3: Chloride profiles obtained from elevation close to the MG	216
Figure 6-4: Profiles obtained from test piles at St. George Bridge (#490100)	217
Figure 6-5: Typical profiles obtained at Turkey Creek #700203 bridge (three elevations)	218
Figure 6-6: Typical profiles obtained at Bounces Pass Bridge (#150243)	218
Figure 6-7: $D_{app}$ vs. elevation Key Royale Bridge	219
Figure 6-8: $D_{app}$ vs. elevation for bridges visited during 2013	220

Figure 6-9: $D_{app}$ vs. elevation for Bridges recent and previous visit (empty symbols).....	221
Figure 6-10: $D_{app}$ vs. resistivity (field results).....	223
Figure A.1: Location at which cores were obtained .....	234
Figure C.1: Resistivity vs. time for DCL2, 3, 5, 6, 8 and 9 .....	236
Figure C.2: Resistivity vs. time for DCL10, 10a, 10b, and 11 .....	237
Figure D.1: Chloride profiles for specimens exposed in 0.1 M NaCl for 220 and 400 days (DCL4, 5, 7, 8, 10a, 10b, and 11) .....	238
Figure E.1 Profiles of specimens exposed to bulk diffusion in 16.5% and 3% NaCl .....	240
Figure F.1: Chloride profiles vs. elevation: Tidal simulation: DCL1, 2, 4, 5, 7, 8, 10a, 10b, 11, and FA .....	253
Figure G.1: Chloride profiles vs. elevation: splash simulation: DCL1, 2, 4, 5, 7, 8, 10b, and 11 .....	263
Figure H.1: Chloride profiles vs. elevation: barge simulation FA and FA+SF specimens .....	267
Figure I.1: Conductivity (1/resistivity) vs. time for all mixtures .....	269
Figure K.1: Effect of cm on $D_{app}$ comparing DCL3, 6 and 9 specimen exposed in 0.1 M NaCl .....	278
Figure L.1: Effect of w/cm on $D_{app}$ for DCL7, 8 and 9 at elevation A .....	279
Figure M.1: DCL7, DCL8, DCL9 and DCL10b: Free vs. total chloride contents .....	280
Figure O.1: Wind Speed (mean, minimum and maximum).....	283
Figure O.2: Monthly mean wind direction .....	283
Figure O.3: Monthly mean temperature.....	284
Figure O.4: Mean monthly relative humidity .....	284
Figure O.5: Monthly rainfall.....	285

## LIST OF TABLES

Table 3-1: DCL concrete mix detail .....	20
Table 3-2: Mix detail .....	21
Table 3-3: Concrete mix detail for tidal simulation specimens exposed at SMO .....	21
Table 3-4: Concrete used on specimens exposed partially immersed at SMO.....	22
Table 3-5: Details of concrete specimens .....	22
Table 3-6: DCL cylinder (G3) curing scenarios .....	23
Table 3-7: Details of concrete mixes G0 and G1.....	24
Table 3-8: Details of concrete mix G4.....	24
Table 3-9 Tidal samples age at time of testing .....	26
Table 3-10: Age at coring of partially immersed samples.....	30
Table 3-11: Specimens sides on which Thoroseal was applied.....	30
Table 3-12: Number of cylinders per mix exposed to simulated field conditions.....	32
Table 3-13: Concrete mixes for tidal simulation .....	32
Table 3-14: Concrete mixes for splash simulation .....	34
Table 3-15: Concrete mixes for barge .....	36
Table 3-16: Concrete mixes for atmospheric exposure .....	40
Table 3-17: Core sampling elevations on blocks.....	44
Table 3-18: Concrete cylinders (G3) for study.....	48
Table 3-19: Details of concrete mixes for present study .....	49
Table 3-20: Degree of water saturation (SD) and concrete sections .....	50
Table 3-21: Concrete cylinders and ages for RCMT .....	53
Table 4-1: Mix properties .....	57
Table 4-2: RMT performed on specimens at 90 to 100 days.....	63
Table 4-3: RMT performed on specimens at 365 days of age.....	64
Table 4-4: RMT performed on specimens after 1.5 years and 2 years of age .....	65
Table 4-5: Porosity measured at various ages on specimens of groups DCL1 to DCL6.....	69
Table 4-6: Porosity measured at various ages on specimens of groups DCL7 to DCL11.....	70
Table 4-7: Chloride concentration at surface and first layer for specimens exposed at 220 days	74
Table 4-8: Chloride concentration at surface and first layer for specimens exposed at 400 days	75

Table 4-9: Chloride concentration at surface and at first layers for DCL mixes exposed to 16.5% NaCl solution .....	79
Table 4-10: Chloride concentration at surface and at first layers for DCL mixes exposed to 3% NaCl solution .....	80
Table 4-11: Chloride concentration at surface and at first layer for DCL mixes exposed to tidal simulation for 6, 10, 18 months .....	83
Table 4-12: Chloride concentration at surface at first layers for DCL mixes exposed to splash simulation for 6, 10, 18 months .....	85
Table 4-13: Chloride concentration at surface and at first layers for DCL mixes exposed to barge simulation for 6, 10, 18 months .....	87
Table 4-14: Free and total chloride concentration at surface and at first layer for DCL mixes exposed to 0.1M NaCl solution for 400 days .....	90
Table 4-15: Free and total chloride concentration at surface and at first layer for DCL mixes exposed to 3% NaCl solution for 1 year .....	93
Table 4-16: Free and total chloride concentration at surface and at first layer for DCL mixes exposed to 16.5% NaCl solution for 1 year .....	94
Table 4-17: Concentration at the surface and first layer (Tidal Exposure Elevation B).....	101
Table 4-18: Concentration at the surface and first layer (Tidal Exposure Elevation C).....	102
Table 4-19: Concentration at the surface and first layer (Tidal Exposure Elevation D) .....	103
Table 4-20: Concentration at the surface and first layer (Splash Exposure - Elevation B) .....	108
Table 4-21: Concentration at the surface and first layer (Splash Exposure - Elevation C) .....	108
Table 4-22: Concentration at the surface and first layer (Splash Exposure - Elevation D).....	109
Table 4-23: Fitted concentration at the surface and first layer (Barge Exposure - Elevation B) .....	116
Table 4-24: Fitted concentration at the surface and first layer (Barge Exposure - Elevation C) .....	117
Table 4-25: Concentration at the surface and first layer (Barge Exposure - Elevation D).....	117
Table 4-26: Absorption of specimens (%) .....	118
Table 4-27: Chloride surface contents of DCL2 cured in 14RT/28ET/RT .....	122
Table 4-28: Chloride surface contents of DCL1, DCL2, DCL3, DCL10b and DCL11 in RT... ..	123
Table 4-29: $C_S$ measured and Fitted for 100% SD .....	124
Table 4-30: Cumulative chloride deposition (in $g/m^2$ ) .....	134
Table 5-1: Aging factors $q_0$ and $q_1$ (14RT/77ET/RT) .....	145
Table 5-2: K values as per Nernst-Einstein (units in $10^{-2} kohm \cdot m^3/s$ ) equation obtained at different ages .....	153
Table 5-3: K values grouped by SCM type (units in $\times 10^{-2} kohm \cdot m^3/s$ ) obtained at different ages. ....	153

Table 5-4: $D_{app}$ values for specimens exposed to 0.1M NaCl .....	154
Table 5-5: Average $D_{app}$ diffusion values of concrete mixes exposed to 3% NaCl for 1 year ..	155
Table 5-6: Average $D_{app}$ values of concrete mixes exposed to 16.5% NaCl for 1 year .....	156
Table 5-7: Apparent diffusion values of concrete mixes at tidal simulation (Elevation A) .....	158
Table 5-8: Apparent diffusion values of concrete mixes at tidal simulation (Elevation B) .....	159
Table 5-9: Apparent diffusion values of concrete mixes at tidal simulation (Elevation C) .....	160
Table 5-10: Apparent diffusion values of concrete mixes at tidal simulation (Elevation D) .....	161
Table 5-11: $D_{app}$ values of concrete mixes exposed at splash simulation (elevation A) .....	163
Table 5-12: $D_{app}$ values of concrete mixes exposed at splash simulation (elevation B) .....	163
Table 5-13: $D_{app}$ values of concrete mixes exposed at splash simulation (elevation C) .....	164
Table 5-14: $D_{app}$ values of concrete mixes exposed at splash simulation (elevation D) .....	164
Table 5-15: $D_{app}$ values of concrete mixes at barge simulation (Elevation A) .....	166
Table 5-16: $D_{app}$ values of concrete mixes at barge simulation (Elevation B) .....	166
Table 5-17: $D_{app}$ values of concrete mixes at barge simulation (Elevation C) .....	167
Table 5-18: $D_{app}$ values of concrete mixes at barge simulation (Elevation D) .....	167
Table 5-19: Apparent diffusivity for free and total chloride analyses for DCL mixes exposed to 0.1M NaCl solution for 400 days .....	168
Table 5-20: Apparent diffusivity for free and total chloride analyses for DCL mixes exposed to 3% NaCl solution for 365 days .....	169
Table 5-21: Apparent diffusivity for free and total chloride analyses for DCL mixes exposed to 16.5% NaCl solution for 365 days .....	170
Table 5-22: $D_{app}$ values with and without re-zeroing .....	184
Table 5-23: DCL1, 2, and 3 Chloride binding capacity when cured at NC, AC, NC=AC and exposed to high concentration of NaCl solution .....	185
Table 5-24: Chloride binding capacity for all DCL mixes .....	188
Table 5-25: Correlation between apparent diffusivity and equivalent resistivity .....	192
Table 5-26: Apparent diffusivity for specimens exposed to 100% SD .....	198
Table 5-27: $k_t$ values calculated for specimens with 1C1, 1C2, 1C3 mixtures DCL specimens	207
Table 5-28: $k_t$ values calculated for DCL specimens .....	208
Table 5-29: $k_t$ values reported by Meira[41] .....	208
Table 5-30: $k_d$ values calculated for DCL and 1C specimens .....	210
Table 5-31: $k_d$ values reported by Meira[41] .....	211
Table 6-1: List of sites visited by SMO not previously published .....	212
Table 6-2: Dates at which the fender piles were deployed and cored .....	214

Table 6-3: List of bridges visited during 2013 including $D_{app}$ values .....	214
Table 6-4: List of cores obtained at elevations > 2 m.....	222
Table B.1: Age at which slabs exposed to marine atmosphere were cored.....	235
Table J.1: $D_{app}$ for specimens exposed to bulk diffusion and RT cured for 28 days.....	271
Table J.2: $D_{app}$ for specimens exposed to bulk diffusion and AC cured (14RT/14ET) .....	273
Table J.3: $D_{app}$ for specimens exposed to bulk diffusion, RT cured until resistivity NC=AC....	275
Table N.1: Equivalent resistivity vs. $D_{app}$ .....	281
Table P.1: $D_{app}$ values from previous projects sorted by bridge number .....	286

# 1 Introduction

## 1.1 Background Statement

Material selection and design for reinforced concrete structures is critical to maintaining the reliability of the infrastructure of highway and municipal service systems. To design reinforced concrete structures with a minimum 75 years of service life, the Florida Department of Transportation has implemented the use of concrete with low water-to-cement (or cementitious) ratio with pozzolanic and slag cement replacement material, plastic control chemical admixtures, and thick concrete cover. Much of the State's reinforced concrete infrastructure is exposed to chloride environments which can cause concrete deterioration by corrosion of reinforcing steel.

The durability performance of reinforced concrete structures in marine chloride environments built with the state's design philosophy above the tidal region has been widely considered. Their performance has been within the expectation of design goals and has been the basis for part of the deterioration prediction and maintenance decision adopted by the state.

However, there is interest in determining the long-term durability of reinforced concrete structures where the external chloride concentrations are different. Insight into the diffusion properties of the concrete at these locations may lead to changes in the state's policy on corrosion control of reinforced concrete structures. Several environments such as the immediate tidal/splash areas and the submerged region of marine concrete structures (including joints that may possibly not be continuously wetted) and buried structures with varying water tables are among the locations where the external chloride concentrations may have spatial, let alone time, variation. Additionally, at elevations above the splash zone, the amount of chlorides deposited would be lower and the concrete close to the surface not saturated. . Similarly, the portion of a structure that is inland would be subjected to seawater spray, with the concrete close to the surface not saturated.

This project provides additional insight on the chloride diffusion properties of concrete typically specified by the State. The reported results add to the base of knowledge of expected chloride diffusivities for regions of such structures with different external chloride concentrations.

## 1.2 Objectives

The project objectives are as follows:

To determine the extent of concrete chloride diffusivity variation by external environmental and surface chloride concentration.

To determine the mechanism by which chloride transport may vary by chloride concentration

To identify the significance of concrete saturation in the extent of surface chloride concentration and extent of diffusivity variation.

To provide analytical/semi-empirical quantification of chloride ion diffusivity with variance in surface chloride concentration.

### **1.3 Methodology**

To investigate the objectives described above it was decided to conduct an experimental program where different type of specimens were prepared and their performance compared. The tests ranged from indoor exposure: bulk diffusion in 3 different chloride concentration, diffusion of chlorides under controlled moisture condition, rapid migration test at different ages, resistivity vs. time, and simulated field exposure on larger specimens: tidal and splash environments. The latter two exposed to seawater. Additionally, test outdoors consisted of atmospheric marine exposure (i.e., non-saturated concrete) at three sites and specimens placed on a barge simulating partially immersed conditions. The wet candle test was also performed to monitor chloride deposition and to be able to correlate the deposited amount to the amount penetrating the concrete specimens. Samples simulating outdoor exposure and those exposed outdoors were cored after various periods of time. The cores were milled and chloride profiles were obtained. The exposure periods ranged from 6 months to 30 months. Additionally, chloride profiles and apparent diffusion was determined from cores obtained on specimens that had been exposed for over 18 year in a laboratory setting to tidal simulated conditions or partially immersed conditions all the time. A third component consisted preparing a compendium of apparent diffusivities from previous projects and also apparent diffusion values not reported before (SMO provided profiles). This was complemented with a small number of field visits to bridges, and when possible, cores were obtained at multiple elevations.

### **1.4 Structure of Report**

The report consist of the following chapters. Literature review and background. Experimental, Results, Field component, Discussion, and Conclusions.

## 2 Literature Review and Background

There are a good number of publications that describe the concepts of chloride transport in concrete including several recent publications. Suggested bibliography is included within the references. In here selected topics relevant to the objectives will be covered but not in a comprehensive manner, for additional details the reader is referred to the reviews papers, journal papers and Ph. D dissertations included as references.

### 2.1 Introduction

The Florida Department of Transportation has a large database of chloride profiles and calculated apparent chloride diffusivity ( $D_{app}$ ) values. The traditional approach is to use Fick's second law in one dimension to achieve the best fit to a chloride profile measured to obtain the apparent chloride diffusivity [1,2,3]. Such values have traditionally been used to extrapolate future chloride profiles from which one can determine if a critical concentration would be reached /exceeded at a certain depth. Based on this analysis, a determination is made of whether a structure would meet the expected service life.

A recently completed project for FDOT [4] included correlations of wet resistivity and  $D_{app}$  values from field cores. The  $D_{app}$  values were obtained by fitting to the chloride profiles measured on sliced cores. Other FDOT projects also have reported chloride profiles for reinforced concrete structures through Florida. However, not all determined chloride profiles follow traditional diffusion shapes with the surface concentration being the largest concentration of the profile.

Since mid to late 1990s, it has been suggested replacing the constant apparent chloride diffusivity by a transient one [5-8]. The time dependent diffusivity is in part due to higher degree of hydration with time (aging factor) and to some extent to binding capacity of the concrete and the chloride concentration at the surface. For field structures exposed in marine exposure, interactions between seawater and the mortar close to the surface (cover-concrete) might also affect how the diffusivity changes with time [9-11]. The decrease of chloride diffusivity with time is typically more significant on structures built with high performance concrete. The calculation of time-dependent chloride diffusivity has been primarily carried out on laboratory studies, or outdoor exposed specimens under immersion in seawater or at low tide zone. There are limited field studies with the time-dependent chloride diffusivity [12-14]. A recent publication also suggested that the apparent diffusivity would stop changing after 10 to 15 years [15]. Some predictive models now assume that the diffusivity can be assumed constant after 25 or 30 years (e.g., Life 365 [16]). The time at which the diffusivity stops (or significantly slows down) changing is likely dependent on the concrete composition [17]. The following sections summarize and briefly discuss relevant literature.

## 2.2 Mechanisms of Chloride Ion Transport in Marine Environments

The transport of water and aggressive ions such as chloride ions through concrete in marine environments is controlled by two primary mechanisms: sorption and diffusion. Chloride penetration by permeation also occurs when water is forced through concrete by hydraulic water under pressure but permeability is not one of the important mechanisms in the present study.

The dominant mechanism during short periods of exposure, especially near partially saturated or unsaturated surface is sorption which is defined as the absorption of water by capillary pores and transported by capillary action [18, 19]. At longer times, moisture movement is controlled by transport through the gel pores and moisture diffusion, which is driven by a concentration gradient. It has been reported [20] that both mechanisms can be represented by non-linear function of moisture content in the material. For the situations in which the concrete is not fully water-saturated, the transport of ions will be reduced in relation with the portion of the pores that are filled.

## 2.3 Chloride Diffusion into Concrete

Assuming concrete is homogenous media, chloride diffusion into concrete can be expressed by Fick's laws [21]. There are two types of diffusions: stationary (or steady state) diffusion and non-stationary diffusion.

Stationary diffusion, i.e., there is no change in concentration with time, is described by Fick's first law:

$$J = -D \frac{dC}{dx} \quad (1)$$

where J is the flux of chloride ions or the rate of chloride transfer through unit area of a section, D is the effective diffusion coefficient, C is the time-independent concentration of chloride ions and x is the location variable or section position. It is the case after steady-state conditions have been reached.

In the case of non-steady state diffusion, i.e., when the chloride profile changes with time, the equation that is assumed to describe this process is known as Fick's second law. Equation (2) takes into account the change of the chloride ion concentration in the material as time changes; it is assumed that the chloride ion transport is one dimensional, that the diffusivity (diffusion coefficient) does not change with time, and that the tested specimen approaches a semi-infinite slab. This equation is usually solved by assuming that at any x and t=0 and the initial concentration  $C_x=0$  (or a low initial measured amount). It is also assumed that the concentration at the surface would remain constant at a concentration known as  $C_s$ ; in reality  $C_s$  increases with time until it reaches a balance with the solution (or continue to increase if subjected to wet-dry cycles). Equation (3) represents the chloride concentration at a location x and time t and erf is the Gaussian error function. The apparent diffusion coefficient is calculated by using a curve fitting to the chloride concentration profiles measured at different depths of penetration from the

surface in an experiment [22]. This assumes that surface concentration and exposure time are known.

$$\frac{dC}{dt} = -D_{app} \frac{d^2C}{d^2x} \quad (2)$$

Where,

$D_{app}$  = apparent chloride coefficient [ $m^2/s$ ]  
 $dC/dX$  = gradient of concentration [ $mol/m^4$ ]  
 $t$  = time [s]

This equation's solution can be obtained depending on the initial and boundary conditions as well as the diffusion coefficient. For constant diffusion coefficient, constant chloride surface concentration ( $C_s = C(0,t)$ ) and the initial condition  $C=0$  for all  $x$  and  $t=0$ , the solution of equation (2) is obtained by:

$$C(x,t) = C_s \left[ 1 - \operatorname{erf} \left( \frac{x}{2\sqrt{D_a t}} \right) \right] \quad (3)$$

Where,

$D_{app}$  = apparent chloride coefficient [ $m^2/s$ ]  
 $x$  = depth in the chloride path [m]  
 $t$  = time [s]  
 $C_s$  = Chloride concentration at the surface [ $kg/m^3$ ]

As presented by Andrade [23], the diffusion coefficient can be affected by the chloride concentration units used. Thus, as seen in Figure 1 the presence of chloride ions can be expressed in the following units: [23]

% concrete or g Cl/kg concrete if referred to the concrete unit weight  
 % cement or in g Cl/kg cement if this is referred to the cement content  
 g or mol Cl/l of solution if this is referred to the pore solution  
 % cementitious or in g Cl/kg cementitious if this is referred to the cementitious content  
 Additionally the concentration in  $kg/m^3$  of concrete is sometimes reported

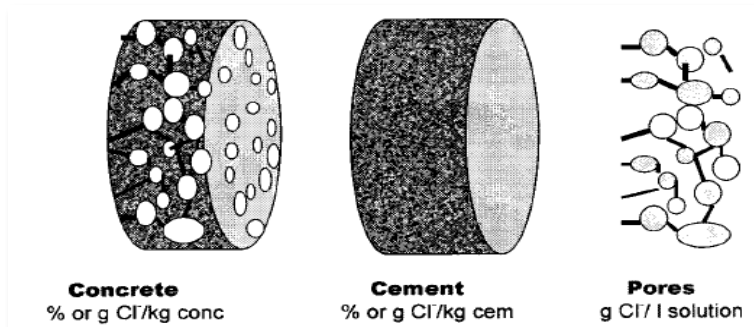


Figure 2-1: Units of chloride concentration [23]

The penetration rate of the chloride ions can be influenced by different factors. For instance, the physical composition of pore solution, the pore structure, tortuosity and connectivity of the cement/mortar paste matrix, which is also affected by the type of material, the water-cement ratio, the amount of hydration, and the age of the concrete; all these parameters would control how fast the chloride is transported in the concrete. In fact, the older the concrete is, the more hydrated the concrete becomes (if additional moisture is applied and reactants are still available) and the more developed and refined the pore structure is (reducing the connectivity and pore diameter). Another important feature is the temperature used during the curing process of the concrete. For example, in the case of material cured at modest elevated temperatures (around 35°C to 40°C) and the concrete immersed, the resistance to chloride penetration of this concrete is better since the concrete is considered to be more mature after a short time than normal room temperature cured concrete of the same age [24]. The cover thickness values ( $x_c$ ) can also determine how fast the chlorides will reach the steel reinforcement in the concrete. When the values of  $x_c$  are low, the corrosion can begin earlier since the chloride will penetrate faster in the concrete reaching the reinforced steel. On the other hand, having a thick cover, properties such as the shrinkage and thermal stress of the concrete might be affected.

In summary, the chloride diffusion coefficient in concrete is a function of multi variables such as time, porosity, degree of concrete hydration (maturity), degree of saturation, aggregate dimension, environmental conditions, etc.

## 2.4 Time-Dependent Diffusivity

As mentioned above, as concrete matures, additional hydration occurs resulting refinement of the pore structure, which then reduces the chloride diffusivity and thus the chloride diffusivity decrease with increase of time. However, the traditional approach does not take account time-dependent changes in either diffusivity or the surface chloride concentration. Depending on exposure conditions, the surface chloride concentration could be constant, for examples, for partially immersed structures, the portion under permanent immersion and the section immediately above known as the low tide zone. Tang found [25] that the diffusivity coefficient of young high strength concrete dramatically decreases with age. Other researchers [26,27] have reported similar findings.

The observed diffusivity reduction for high performance concrete (HPC) changes significantly as it ages. Thomas and Bamforth [8] proposed the following equation to estimate how fast the chloride diffusivity will change: The following equation (4) represents the time-dependent diffusion coefficient ( $D_{app}(t)$ ).

$$D_{app}(t) = D_0 \left( \frac{t_0}{t} \right)^m \quad (4)$$

Where,

$D_{app}(t)$  = apparent diffusion coefficient at time  $t$  [ $m^2/s$ ]

$D_0$  = diffusion coefficient at time  $t_0$  [ $m^2/s$ ]

$m$  = aging factor

It has been suggested that  $m$  can be obtained by taking a minimum of three chloride profiles at different times. Other researchers [5-8, 12, 28] have also described similar equation(s) for cases in which diffusion is the main transport form for the chloride penetration.

It has been found that the values for the aging factor ( $0 \leq m \leq 1$ ) vary depending on the composition of the concrete and the environmental condition ( $m$  varies from 0.32 to 0.91) [17, 29]. It has also been suggested that  $m=0.1$  for a Portland cement concrete. Various methods have been used to calculate the aging factor; for example, bulk diffusion and rapid chloride migration tests have been experimentally performed to derive the value for  $m$  (these tests are described in the next sections). On the other hand, Andrade has determined the aging factor by using the electrical resistivity of concrete based on the Nernst Einstein equation (5).

$$D(cl) = \frac{k}{\rho} \quad (5)$$

Where,

$D(cl)$  = chloride diffusion coefficient [ $m^2/s$ ]

$k$  = constant

$\rho$  = resistivity [ohm/m]

By combining equations 4 and 5, the formula used to calculate the aging factor can be found (eq. 6) [29].

$$m = \frac{\log\left(\frac{\rho_t}{\rho_0}\right)}{\log\left(\frac{t}{t_0}\right)} \quad (6)$$

Where,

$m$  = aging factor

$\rho_t$  = resistivity at time  $t$  [ohm/m]

$\rho_0$  = resistivity at initial time [ohm/m]

$t$  = time [s]

Furthermore, different studies have suggested that the aging factor, found by the bulk diffusion or the resistivity approach is different. In fact, Andrade indicates there should be two aging factor coefficients;  $n$  represents the aging factor calculated by apparent diffusion approach while  $q$  is found via resistivity, and the formula that relates these two parameters is the following: [23, 29]

$$q = 0.798n - 0.0072 \sim 0.8n \quad (7)$$

The main reason to have two different parameters is that the  $n$  value reflects how the diffusion of chlorides changes with time, which can be related to the changes in the microstructure (this is what resistivity accounts), changes in  $C_s$  and the binding properties of the concrete, while  $q$  is related to the microstructure, porosity and tortuosity changes [29]. More recently, it has been reported that the aging factor  $q$  is not constant with time for some concrete compositions [17].

For concrete with only ordinary Portland cement (OPC), the diffusivity will likely experience only a modest change as the concrete ages. Whereas for high performance concrete (HPC)

mixtures, the diffusivity values could experience significant changes and extrapolation from a short-term test could be quite off when predicting long-term performance. Adequate modifications to include the time-dependent chloride diffusivity determination should be documented in the next FDOT modeling generation for high performance concrete. It is likely that the concrete has matured beyond a certain point the microstructure would stop changing (this is dependent on the type and amount of cementitious material used), thus the concrete diffusivity would stop changing.

Recent research supports the idea that the aging factor is not a constant value (depending on the mix composition, time of curing and exposure conditions). Moreover, there have been reports that  $m$  values for some HPC concrete exposed to marine environment might be even steeper.

## **2.5 Effect of Chloride Surface Concentration on Diffusivity**

Using a modified migration test by employing a lower applied potential, for example, smaller electric potential than typical rapid chloride penetration test (RCPT), Zhang and Gjorv [30] found that the diffusivity measured when using dilute solutions was 10 to 20 times greater than that measured when using concentrated solutions (0.01 M vs. 1 M). Similar findings have been reported by Castellote et al. [31] and other groups [32, 33]. The results from these studies suggest that the chloride surface concentration (and the chloride concentration in the solution) would affect the measured diffusivity. Zhang and Gjorv also indicated that chloride diffusivity in concrete is a non-linear function of the chloride surface source concentration and suggested a cubic-root relationship [30]. Fortunately, the diffusivity is more concentration-dependent at lower, rather than at higher, concentration levels. How important is this effect for Florida relevant chloride concentrations requires additional investigation. Rather than using an accelerated transport experiment, bulk diffusion are planned on 3 different sodium chloride concentration solutions as well as from cores obtained from fully immersed concrete portion of partially immersed specimens. Additionally, concrete specimens exposed to marine atmosphere will also be investigated.

## **2.6 Field Chloride Surface Concentration at Low Tide and Below**

The field chloride surface concentration can be obtained by employing the various methods. One approach is by using the fittings on the chloride profiles obtained from sliced concrete cores. Another is by experimental determination – after a concrete core has been obtained, a thin section closest to the surface is sliced or milled and then the chloride surface concentration is determined. FDOT [34] uses a chemical titration to obtain the total chlorides. The value for the first slice (or milled portion) is usually named the field chloride surface concentration (or first layer chloride concentration and depending on the thickness of the layer it might represent the average concentration over a few millimeters).

The assumption that the chloride surface concentration does not change with time is in principle adequate for cases in which the concrete structure is fully immersed or immersed most of time. However, it has recently been reported that even for a low tidal section, the value of chloride surface concentration could increase with time due to some capillary sorption [35] taking place

during the dry periods. Some researchers [36, 37] have suggested that the surface chloride concentration should be considered a time-dependent variable as well when calculating projected profiles that use the time-dependent diffusivity. As a first approximation it might be ok to still assume a constant concentration for the fully immersed portion after some time, and also the portion part of the low tide region might reach a higher stable value after somewhat longer time than for below water.

## **2.7 Field Chloride Surface Concentration at Mid-To-High Tide Section, and Splash Zone**

There is no question that the chloride surface concentration of concrete exposed to tidal/splash zone is time-dependent [36-38]. The field values of surface chloride concentration at mid-to-high tide section and splash zones experience a large scatter and could be larger than the one measured at and below low tide in many cases. The full saturation assumption might no longer be valid in such region, it is possible that with time salt crystals might start forming at the surface. In cases where the maximum chloride concentration from a chloride profile is measured at some depth from the surface, which is from a few millimeters to a couple of centimeters, the chloride concentrations at and to the right of its maximum value could be used to calculate the diffusivity as the water saturation level is high. This assumption could also be implemented in FDOT modeling for chloride transport by resetting distance  $x=0$  to the location where the maximum chloride concentration is found. The location of this maximum might need to be updated as time passes. Some investigators have called this phenomenon the skin effect [23, 39]. The skin effect has been studied for years and is considered to be the result of a combination of environmental conditions and material properties. In the case of Florida marine sites, some environmental parameters such as rain, wet-dry cycles, and preferential wind to name a few affect the chloride at the surface and determine if the skin effect develops or not.

## **2.8 Chloride Deposition above the Splash Zone**

At mid-to-high tide section and splash zones the chloride at the surface of concrete is likely a combination of constant concentration and chloride being deposited via a convection mechanism. At elevations above the splash zone, the chloride concentration at the surface of concrete is due to spray particles that are deposited. The concentration in the spray might be significantly lower than that reaching the region immediately below due to gravity. Recently, a research group led by Meira et al. [40] investigated the chloride transport on marine exposed structures and found the different chloride deposition rate dependence with distance from the ocean. The chloride deposition rate reduced by half from 10 m to 100 m. The approach described [40, 41] could be applied to understand the chloride transport at the regions where the chloride profiles no longer have a maximum concentration at the concrete surface, for example the maximum chloride concentration from the concrete surface. Moreover, at this higher elevation, the concrete close to the outer surface would experience different degrees of water saturation.

One aspect of chloride penetration that is of particular interest to FDOT is the advancement of chlorides in unsaturated concrete above the splash zone. At these higher elevations (or some distance inland), capillary absorption will take place as the structure comes into contact with wind-blown marine aerosols. This will be predominant on the concrete closer to the surface

(skin). In capillary absorption, transport is induced by inter-molecular attractive forces between the concrete and the seawater spray particles. This transport mechanism acting by itself is not typically enough to drive the chlorides deep enough to reach the rebar at the rates observed in the splash or tidal zone. However, there is a need for profiling chloride penetration under scenarios where the water content is controlled and varied.

The marine atmosphere zone is primarily affected by marine aerosols. Marine aerosols are caused by breaking waves in surf zones dispersing particles containing chlorides into the air [42]. The bursting of air bubbles at the sea surface also affect structures near the coast and at areas in the open sea prone to high winds can generate and carry these particles [43, 44].

There are several different mechanisms for which chlorides could penetrate into concrete. For concrete in the marine environment, the mechanism is largely dependent on which region or marine zone the concrete is located. Transportation of chlorides into concrete in the submerged zone occurs via diffusion [45]. In the marine atmosphere, the transport is suggested to occur via the marine aerosols containing the chlorides. The salt is deposited on the concrete of which diffusion and capillary absorption may occur.

The primary mechanism for marine aerosol transport upon being produced is wind [40]. Many research papers point out that salt concentration increases exponentially with wind speed [46]. An increased generation of marine particles and an increase in the percentage of larger particle drops occur as wind increases [44]. Figure 2-2 shows a correlation between sea-salt concentration and wind speed [47]

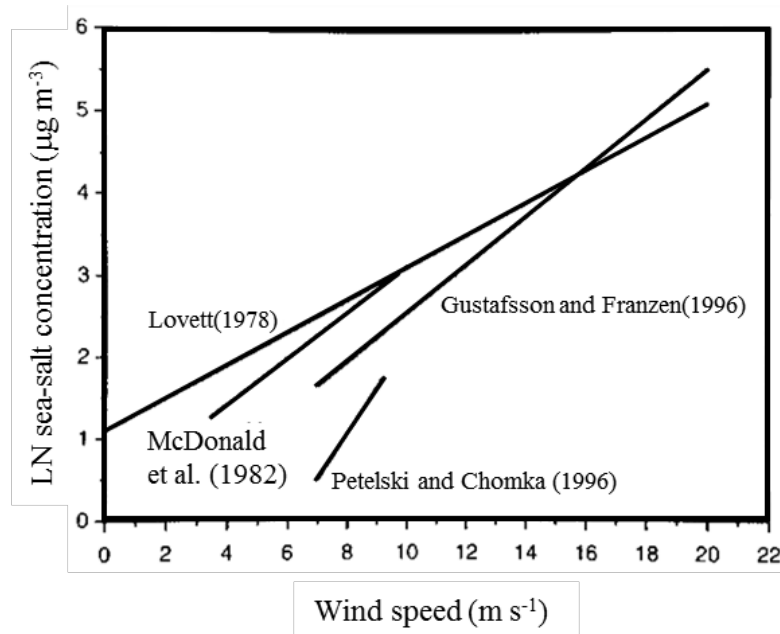


Figure 2-2: Effects of wind speed on salt concentration from previous studies [47]

The marine aerosol particles will travel at a distance inland with the wind direction and speed. Because of the weight and size of the particles, the salts will only be able to travel to a certain

distance, at which the effect of marine aerosol is no longer a contributor. Meira presents results showing that within the first hundred meters from the sea, chlorides from the marine aerosol and the penetration into concrete decreases significantly [40].

While the effects of wind are the predominant source of marine aerosols containing chlorides, it has been observed that several other parameters influence the salt concentrations generated by marine aerosol. Due to the wetting of salt, relative humidity is an important influence on the salt concentration, particularly between the relative humidity range of 50% to 70% [47]. It has also been proposed by Meira that the “washout effect, which, due to rainfall, is more effective at higher relative humidity levels” [47], these high humidity are predominant in Florida coastal areas. The wetting of salt is also an issue, because the salt particles increase in size, and the rainfall will remove some of the aerosol chloride salts [47] from the concrete surface.

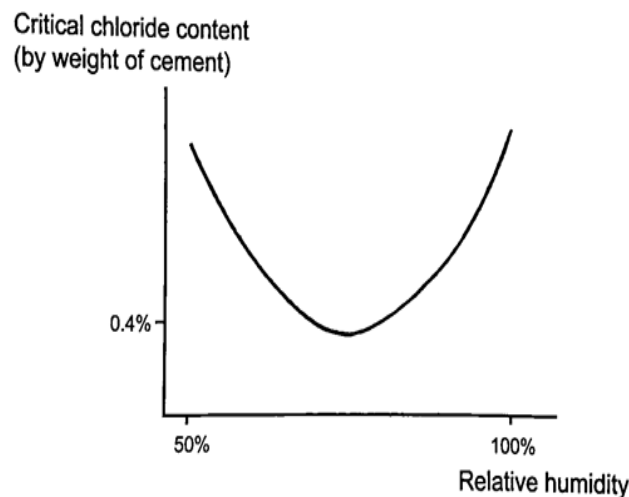


Figure 2-3: Graph showing the relation of humidity and chloride content [48]

In Figure 2-3 above, the graph shows the effect of relative humidity on the critical chloride content in concrete. At the range of about 60% to 80%, the critical level is decreased significantly, whereas corrosion could initiate with less amount of chloride.

Chloride deposition refers to the amount of chloride that can be deposited onto a specific area from the atmosphere for a given amount of time [49]. Generated by breaking waves in the surf zone, the marine aerosols that are produced contain particles of chlorides and other minerals. These aerosols are released into the air, and their mechanism of transport is influenced by wind speed [44]. Closer to the sea shore, these particles are larger and more congregated [44]. Transported by the wind, these particles can travel inland. Relative humidity also influences the marine aerosol particles, in that a decrease in humidity leads to a more concentrated aerosol [50].

Research suggests that these particles settle after certain distances from the sea and are dependent on wind speed and direction [44, 51]. This indicates that concrete structures closer to the sea shore receive a higher concentration of salt particles in the atmosphere than structures further away from the shore [44, 52, 53]. The amount of salt that can be deposited via marine

aerosols in the atmosphere is a function of distance from the sea, along with wind direction and precipitation patterns. The relationship of the chloride deposition rate with the effect of marine aerosol from several different regions is displayed below in Figure 2-4, as a function of the distance from the sea [41].

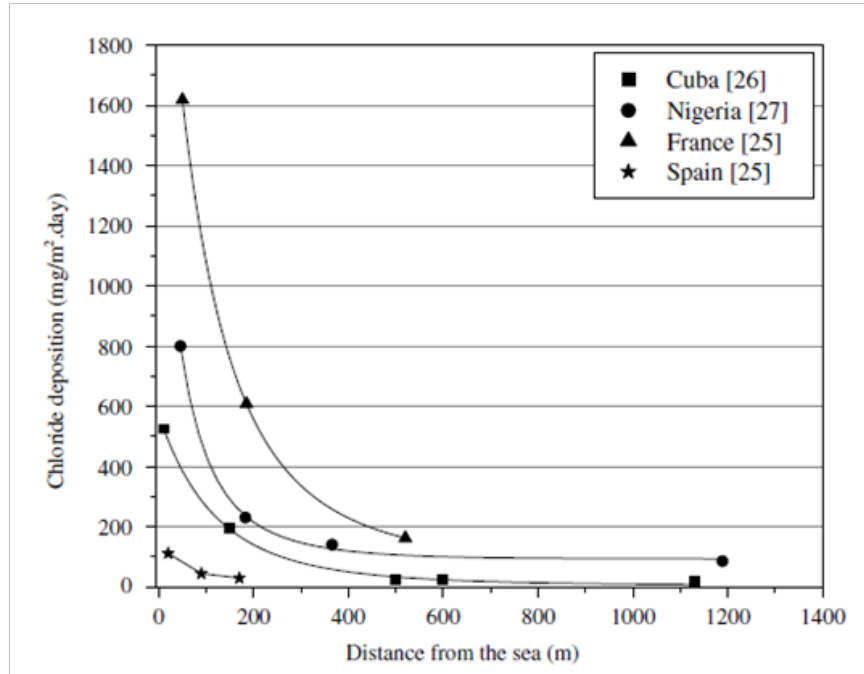


Figure 2-4: Studies of chloride deposition as a function of distance [41]

The plot shows how the chloride deposition may vary as a function of distance from the sea as the environmental parameters change. In areas where there are stronger winds, the marine aerosol particles are able to cover larger distances. The plot also shows that for each region, there is a sharp decline in chloride deposition within the first couple hundred meters.

There have been previous studies which have used a device called the Wet Candle, to measure the amount of the chlorides in the atmosphere through marine aerosols. The device collects the chlorides, of which can be quantified, and related to the environment. The Wet Candle has been used to show the potential amount of chlorides in the atmosphere that could accumulate into the concrete.

Meira has proposed a relationship in which the average amount of totals chlorides accumulated into the concrete after a given amount of time can be related to the environmental parameters, and to the deposition of chlorides accumulated by the wet candle device from the marine aerosol in the atmosphere. According to Meira, the average total amount of chloride accumulated increases with the square root of time [41]. By expressing the increasing total amount of chloride as a function of the square root of time, a relationship was developed in order to determine the effect of the distance from the sea (See, Figure 2-5). As the data for each sample was plotted, a trend could be seen in which the influence of concrete porosity and the water to cement ratios were evident [41] (not shown in here).

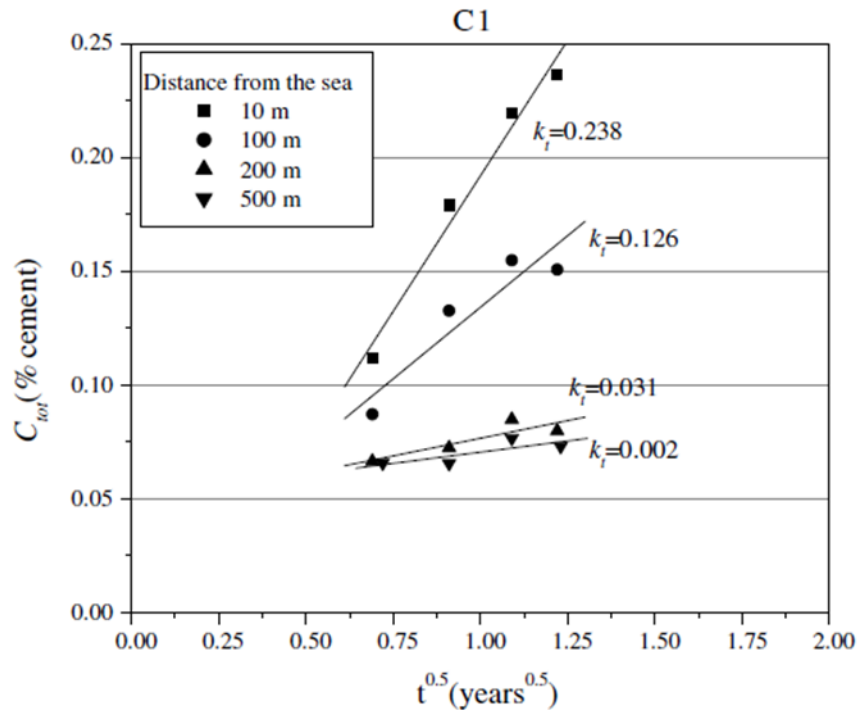


Figure 2-5: The relationship between total chloride amount and time [41]

In Figure 2-5, the total amount of chlorides accumulated ( $C_{tot}$  in % cement) on C1 specimens [41] over a given amount of time; with the  $C_{tot}$  values shown as a function of time<sup>0.5</sup>. The plot shows  $C_{tot}$  values obtained after four exposure times for samples at four different distances from the sea. The coefficient  $k_t$  is the slope fitted to each data series (i.e., each trend line), and relates the exposure time with the  $C_{tot}$  (amount of chloride that penetrated over a given period of time) [41].

## 2.9 Chloride Saturation of Concrete

The type of concrete, porosity and permeability of the concrete would likely dictate how much chloride will be needed to saturate it. On the other hand the amount of chloride available in the solution (or in the marine aerosol particles) would dictate the potential maximum concentration that could be present in the concrete pore solution. For samples fully immersed it could be assumed that there is no chloride build up after sometime.

## 2.10 Controlled Degree of Water Saturation on Diffusion

The transport properties of test specimens can be affected by the amount of pore water in concrete [54]. Studies have demonstrated that the degree of water saturation is a very important factor in the transport of ions in porous media [55] and in the transport of chloride ions into partially saturated concrete [56]. Mathematical models describing the diffusion of chloride and its dependences on the moisture content and relative humidity have been proposed since 1993 [57-61].

Test methods were not reported until Climent et al., developed an experimental procedure by exposing the surface of non-saturated concrete samples with controlled water contents to interact with the gaseous hydrogen chloride (HCl) produced from the combustion of PVC and then returning the specimens to controlled moisture condition for the transport of chloride ion [62,63]. The chloride profiles were fitted to a solution of Fick's 2nd law of diffusion with an instantaneous plane source. In parallel with Climent's work, Guimaraes and Climent investigated chloride diffusion through partially saturated Portland cement paste and mortar specimens by employing an alternate method [64]. The test samples with relevant water saturation degrees are first conditioned.

After some time, solid sodium chloride (NaCl) finely grinded is placed on the exposure surface and then housed with plastic wrap and vacuum for the duration of the diffusion experiment. The chloride profiles obtained after the test are fitted to the error function solution of Fick's 2nd law of diffusion. The test method employed by Nielsen and Geiker is different [20]. Portland cement mortar specimens are conditioned to reach the targeted relative humidity and contaminated by immersing in a high concentration of sodium chloride (NaCl) solution for a limited exposure time followed by a drying process until the initial weight of specimen is obtained. Subsequently, the specimens are returned to the conditioned room for diffusion. After obtaining chloride profiles, a composite theory and Powers' model are combined for estimating the diffusion coefficient as a function of the specimen moisture content.

The next few paragraphs briefly describe the results of work by Climent et al. and de Vera et al. [62,63]. As indicated above the method consists on testing chloride transport in unsaturated concrete by exposure to the gaseous products of the combustion of PVC. Chlorides can be introduced to the specimen while the specimen is in contact with this hydrogen chloride byproduct [62,63]. Two mixes of concrete cylinders were prepared for Climent's three year experiment. These cylinders measured 20 cm in length and 10 cm in diameter. The two concrete mixes cast were named H-25 and H-35 and had water to cement ratios of 0.6 and 0.5 respectively. H-35 also had 1.4 kg/m<sup>3</sup> of plasticizer in the mix while H-25 had none added.

Equation 8 is used to find the saturation degree (SD) which is a number between 0 and 1 (100 if reported as percentage) that describes the proportion of the concrete sample that is in a saturated condition.

$$SD = \frac{(m_{wet} - m_{dry})}{m_{dry}} * \frac{100}{A} \quad (8)$$

Where,

SD= saturation degree

$m_{wet}$  = mass of partially saturated concrete [kg]

$m_{dry}$  = mass of dry concrete [kg]

A = absorption as determined from a porosity test [65]

Values of  $D_{app}$  for H-35 measured by Climent were similar to those of H-25, but were slightly lower than values calculated for H-25. This was attributed by Climent and co-workers to the fact that H-35 has a lower porosity and a more refined pore network than that of H-25 [62,63].

Figure 2-6 shows that the diffusivity of H-25 samples increased just over two orders of magnitude as the saturation fraction was increased from 0.4 to 0.8.

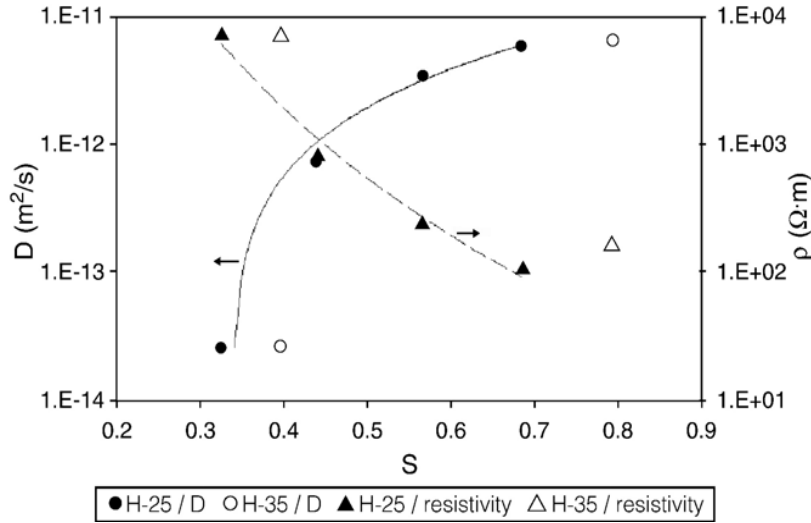


Figure 2-6: Diffusivity and resistivity vs. saturation [63]

Figure 2-7 demonstrates the exponential increase in concrete diffusivity as saturation degree increases. At 50% saturation, diffusion occurs at a rate of  $2 \times 10^{-12} \text{ m}^2/\text{s}$ . At 100% saturation, one value was measured at  $14 \times 10^{-12} \text{ m}^2/\text{s}$ .

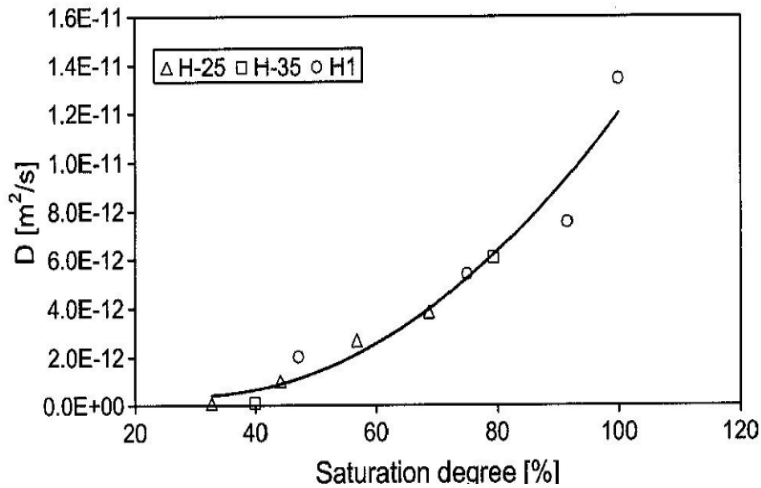


Figure 2-7: Diffusivity vs. saturation degree [63]

A chapter in this report presents an experimental study on the chloride diffusivity through partially saturated high performance mature concrete and the effect of mortar content/concrete surface condition on the diffusion. A test method similar to that proposed by Guimaraes et al. was used [64]. Four different degrees of water saturation relevant to Florida were investigated. It is expected that the outcome from this study will provide insight on the chloride diffusion properties and contribute the base of knowledge of chloride diffusivity through non-saturated high performance concrete.

## 2.11 Chloride Binding

The total amount of chlorides presented in the concrete can be divided into two groups, the amount of chlorides that are chemically and physically bounded and the free chlorides dissolved in the pore solution [66]. Also, it has been reported that the time to corrosion initiation can be delayed by the chloride binding capacity of concrete in two ways: The penetration of chloride ingress is decreased because when the binding capacity is high, there is less amount of chloride in the pore solution that can be transported. At the same time, free chlorides (chloride ions dissolved in the pore solution) are assumed to be able to initiate active corrosion once they exceed a certain critical concentration. Moreover, the total amount of chlorides is assumed to be a function of the chloride binding capacity [67].

Under natural, non-accelerated exposure, some chlorides move freely through the pore solution while others react with the cement phases as they travel into the concrete [23]. These chlorides that undergo the reaction have become bound within the cement and no longer pose a threat to the reinforcement steel. The quantities of chlorides which become bound vary significantly between different concrete chemistries. Binding capacity also depends on the type of cement, admixtures, composition of pore solution, and temperature, and type of exposure. The non-steady state diffusion coefficient  $D_{nss}$  refers to the total amount of chlorides and is expressed as the weight per unit volume of concrete after exposure.  $D_{nss}$  is calculated from experiments performed on concrete experiencing accelerated transport via an electric field. Thus there is not sufficient time for the portion of the chlorides (or just a small amount) that under normal conditions would have bound to be combined [23].

The chemically and physically bounded chlorides depend on different factors such as the type of cement, cementitious materials, mineral admixtures, temperature, and composition of the pore solution [23]. This last one is very important since having the presence of other ions in the pore solution can have an effect on the process of chloride binding since other ions such as hydroxide ions can compete for the binding site with the chloride ions [68]. Furthermore, the chloride binding capacity is also known to be determined by the process of how the chloride ions ingress into the concrete. For instance, if the chloride ions were added when the concrete mix was fresh, then the process of hydration can be highly affected [67]. Another important factor is carbonation; having concrete structures exposed to air (rich in  $\text{CO}_2$  and low humidity) and to chloride content caused a reduction in the surface area making the pore wall inert to chloride binding [69]. However, carbonation is also known to be able to release bound chlorides. For the most part carbonation is not an issue for the bridges and other structures exposed in Florida marine environment.

Many studies have been performed in order to better understand the relationship between free and total chloride. Mohammed and Hamada found that there is a higher binding capacity in concrete composed of calcium aluminate cement; also, this study confirmed that pozzolanic admixtures can increase the binding capacity [70].

## 2.12 Chloride Profiles

Knowing the total amount of chloride ions in the concrete at different depths is important because with this information the apparent diffusion and the rate of penetration can be calculated. Chloride profiles are used to show the chloride content distribution of a specimen as a function of depth after exposure for a certain time [67]. The chloride content at the concrete surface is expected to be higher and as the depth increases the amount of total chloride ions is significantly lower. Figure 2-8 represents the chloride profiles for two different mixes of concrete that have high and low binding capacity [67]. The curve of the concrete with low binding capacity shows how the amount of bound chlorides is low which causes an increment in the transport rate of chloride ions that will be able to initiate active corrosion [71]. The chloride profiles do not always follow the typical shape shown in the figure below. In fact, sometimes the maximum chloride concentration value is found at other layers rather than at the surface. This can be caused by different factors such as carbonation, presence of ions other than chloride, evaporation and water movement of the chlorides on the surface, and the skin effect.

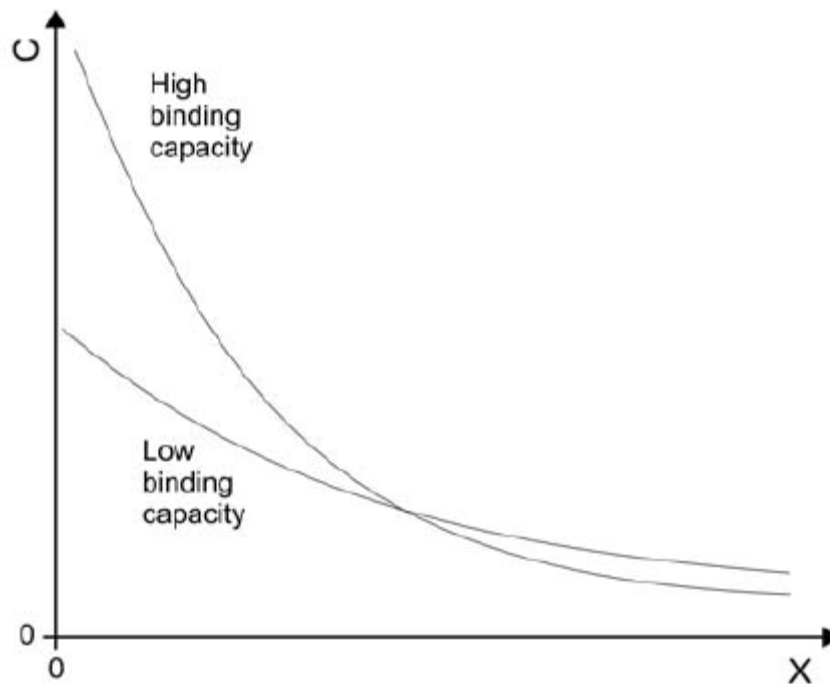


Figure 2-8: Chloride profiles for two different compositions of concrete exposed for the same time [67]

## 2.13 Existing Test Methods used in this Project

The following test methods and standard have been developed over past years and were performed as prescribed but in some instances slightly modified.

### **2.13.1 Resistivity Measurement**

- Florida Department of Transportation (FDOT), Florida method of test For concrete resistivity as an electrical Indicator of its permeability, FM5-578; January 27, 2004 [72].
- American Association of State Highway Transportation Officials, Standard test method for surface resistivity indication of concrete's ability to resist chloride ion penetration. ASSHTO Designation: TP95-11, AASHTO Provisional Standards, Washington D.C.; June 2010 [73].

### **2.13.2 Density, Absorption, and Voids in Hardened Concrete**

- American Society for Testing of Materials, Standard test method for density, absorption, and voids in hardened concrete, ASTM C 642-06, Annual Book of ASTM Standards, 2006 [65].

### **2.13.3 Rapid Chloride Migration Test (RCMT)**

- Nordtest Method, Chloride migration coefficient from non-steady-state migration experiment, NT Build 492, Nordtest, Espoo, Finland, Proj. 1388-98, 1999 [74].

### **2.13.4 Bulk Diffusion**

- Concrete, Hardened: Accelerated Chloride Penetration (Nordtest Method NT Build 443) [75]
- Standard Test Method for Determining the Apparent Chloride Diffusion Coefficient of Cementitious Mixture by Bulk Diffusion (ASTM C1556-04 ) [76]

The Nordtest bulk diffusion test is a modification of another test developed to address the deficiencies of the salt ponding test to measure diffusion [76]. The test was established as the Nordtest bulk diffusion test (NT Build 443) [75] and consists of calculating the diffusion without taking into account the effects from absorptions and wicking. The test consists of having cylindrical specimens cured for 28 days (sometimes the curing time is longer), cut in half and coated in a polymer/epoxy; then only one face is exposed to a 16.5% NaCl by wt% solution for a period of time of at least 35 days (see figure 5). This is done in order to allow natural transport of the chloride ions through one saturated surface. The projects performed by FDOT-SMO/FAU have a typical duration in the chloride solution of one year immersed and also the chloride concentration varies, e.g., 16.5% or 3% NaCl. After this exposure period is completed, the specimens are removed, cut, sliced and pulverized; chloride concentration analyses are then performed with the powder obtained at different depths of the specimens.

### **2.13.5 Wet Candle Test**

- American Society for Testing of Materials, Standard test method for determining the atmospheric chloride deposition rate by wet candle method, ASTM G 140-02, Annual Book of ASTM Standards, 2002 [49].

### **2.13.6 Chloride Content Analysis**

- The chloride content of both concrete powder and atmospheric chloride deposition are obtained in accordance with FDOT method with slightly modification: “Florida Method of Test for Determining Low-Level of Chloride in Concrete and Raw Materials, FM5-16” [77].
- Besides the total chloride content, the free chloride content was measured on selected specimens exposed to bulk diffusion in accordance to RILEM/AFREM test procedures [78]

## **2.14 Conclusions from Literature Review**

As indicated at the beginning of this chapter this is not a comprehensive review and it is intended to provide background for the type of tests and analysis performed in this investigation. Although a significant amount of research has been carried out in recent years, there are still a number of issues that are not well understood. The aim of the current research is to fill some of these knowledge gaps.

### 3 Experimental Program

#### 3.1 Introduction

This chapter describes concrete compositions and geometries of the investigated specimens. Other sections describe the type of tests performed and the environmental exposures. This section also describes the concrete mixture compositions for both new and old specimens.

#### 3.2 New Specimens

##### 3.2.1 Concrete Mix Prepared

Table 3-1 details the concrete mixtures that were selected by the Florida Department of Transportation and FAU for the set called in here DCL. These concrete mixtures were cast at the Florida Department of Transportation State Materials Office in Gainesville, FL. The water to cementitious ratio has a range of 0.35 to 0.47 and the coarse and fine aggregate were Florida limestone #57 and Florida river sand, respectively. Type I/II cement was used for all the mixes. The mix DCL10 was prepared three times because the entrained air was significantly higher than the target amount. An air-entrained chemical admixture was used to control air distribution in concrete. Water reducing and super plasticizer chemical admixtures were used to allow the design of low w/cm concrete and to control the plastic properties of the concrete.

Table 3-1: DCL concrete mix detail

Mix	Cast Date	Cementitious Content	Cement Content	20% FA	8%SF	50% Slag	Fine agg.	Coarse agg.	w/cm ratio
		(kg/m <sup>3</sup> )							
DCL1	12/7/2011	390	312	78	0	0	1062	653	0.35
DCL2	9/22/2011	390	312	78	0	0	949	721	0.41
DCL3	10/19/2011	390	312	78	0	0	918	697	0.47
DCL4	12/21/2011	390	312	78	31	0	1062	653	0.35
DCL5	12/21/2011	390	312	78	31	0	949	721	0.41
DCL6	10/26/2011	390	312	78	31	0	918	697	0.47
DCL7	12/14/2011	390	195	0	0	195	1062	653	0.35
DCL8	11/22/2011	390	195	0	0	195	949	721	0.41
DCL9	11/2/2011	390	195	0	0	195	918	697	0.47
DCL10	9/28/2011	335	268	67	0	0	765	1007	0.41
DCL10a	10/12/2011	335	268	67	0	0	765	1007	0.41
DCL10b	11/16/2011	335	268	67	0	0	765	1007	0.41
DCL11	11/9/2011	279	223	56	0	0	765	1009	0.41

### 3.2.2 Concrete Mixes for Specimens at FAU Prepared Previously

The concrete mix designs for specimens prepared previously are listed in Table 3-2. Class F FA and SF were used in some of the mixes. Three mix designs were included with w/cm of 0.40. The coarse aggregate was #67 (check) Florida limestone and the fine aggregate used was silica sand.

Table 3-2: Mix detail

Mix No.	Cement	Coarse agg.	Cement (kg/m <sup>3</sup> )	FA (kg/m <sup>3</sup> )	Water		Fine agg.	Coarse agg.
					SF (kg/m <sup>3</sup> )	(kg/m <sup>3</sup> )	SSD (kg/m <sup>3</sup> )	SSD (kg/m <sup>3</sup> )
1C1	type I/II	Limestone	390	-		156	734	996
1C2	type I/II	Limestone	312	78		156	734	996
1C3	type I/II	Limestone	281	78	31	156	734	996

### 3.2.3 Additional Concrete Mixes for Specimens at SMO

Tables 3-3 and 3-4 document the mixture proportions used in the mixes for specimen exposed at SMO. All concrete mixes used either # 57 or # 67 gradation crushed Florida limestone. Silica sand was used as the fine aggregate. When specified, silica fume used was in slurry form. The water to total cementitious materials ratio (w/cm) was as indicated in the table (typically 0.37). An air-entrained chemical admixture was used to control air distribution in concrete. Water reducing and super plasticizer chemical admixtures were used to allow the design of low w/cm concrete and to control the plastic properties of the concrete.

Table 3-3: Concrete mix detail for tidal simulation specimens exposed at SMO

Sample Name	Design Components (kg/m <sup>3</sup> )				Water	Coarse Aggregate	Fine Aggregate	w/cm
	Cement	Superfine Fly Ash	Silica Fume	cm*				
OPC	390.4	NA	NA	390.4	160.1	852.3	864.8	0.41
7% SF	390.4	NA	46.1	436.5	139.1	948.4	744.4	0.33
11% SF	390.4	NA	72.4	462.8	131.4	948.4	704.5	0.3
15% SF	390.4	NA	98.7	489.1	153.2	948.4	685.8	0.34
SFFA - 15%	379.2	66.9	n/a	446.1	165.0	983.7	650.2	0.37
SFFA - 20%	356.9	89.2	n/a	446.1	165.0	991.8	643.8	0.37
SFFA - 25%	334.6	111.5	n/a	446.1	165.0	983.9	637.7	0.37

\*cm – cementitious materials

Table 3-4: Concrete used on specimens exposed partially immersed at SMO

Sample Name	Design Components (kg/m <sup>3</sup> )						
	Cement	Fly Ash	Cementitious material	Water	Fine Aggregate	Coarse Aggregate	w/cm
10% Fly Ash	401.5	44.6	446.1	165.0	677.8	992.0	0.37
20% Fly Ash	356.9	89.2	446.1	165.0	657.9	990.9	0.37
20% Fly Ash + CI**	356.9	89.2	446.1	165.0	657.9	990.9	0.37
30% Fly Ash	312.3	133.8	446.1	165.0	642.6	993.0	0.37
40% Fly Ash	267.7	178.5	446.1	165.0	621.8	991.4	0.37

Note: Specimens with CI were prepared with 8 lbs/cyd

Table 3-5: Details of concrete specimens

Mix Name	Cast Date	Geometries		
		G1a (22"x7"x4.75")	G2 (12"X12"X3")	G3 (d=4",L=8")
		No.	No.	No.
DCL1	12/7/2011	4	3	51
DCL2	9/22/2011	6	3	51
DCL3	10/19/2011	8	3	51
DCL4	12/21/2011	4	3	51
DCL5	12/21/2011	4	3	51
DCL6	10/26/2011	8	3	51
DCL7	12/14/2011	4	3	51
DCL8	11/22/2011	4	3	51
DCL9	11/2/2011	8	3	51
DCL10	9/28/2011	6	3	51
DCL10a	10/12/2011	6	3	51
DCL10b	11/16/2011	6	3	51
DCL11	11/9/2011	6	3	51

### 3.3 Specimen Geometry

#### 3.3.1 New Specimens

Three types of geometries were prepared, concrete blocks 55.9 cm × 17.8 cm × 12 cm (22 in × 7 in × 4.75 in) (named below G1a), 30 cm × 30 cm × 7.5 cm (12 in × 12 in × 3 in) G2 blocks and cylinders 10 cm diameter by 20 cm long (4 in diameter × 8 in - G3). The details on the number of specimens and cast dates are listed in Table 3-5. All of these samples were cast at the Florida

Department of Transportation State Materials Office in Gainesville, FL. The mixes were cast during the fall of 2011 (Between September and December).

G1a and G2 blocks as well as G3 concrete cylinders were removed from the mold after one day. The specimens were cured in a fog room for seven to fourteen days before transport from the cast site to FAU. G1a and G2 samples were then exposed to laboratory humidity for about 14 days (up to 21 days) before exposure to the different environments.

G3 cylinders were subjected to four different curing schedules. Table 3-6 shows the four curing scenarios that were used in this project for cylinders transported to FAU. Six cylinders from each group were cured at room temperature and high humidity for 14 days, then cured in elevated temperature (~36° C) immersed in calcium hydroxide solution for 14 days, then the cylinders were transferred to room temperature, high humidity storage. Nine cylinders from each group were cured at room temperature and high humidity for 14 days, cured in elevated temperature immersed in calcium hydroxide solution for 28 days, and then they were transferred to room temperature, high humidity storage. Six cylinders from each group were cured at room temperature and high humidity for 14 days, in elevated temperature immersed in calcium hydroxide solution for 77 days, and then they were transferred to room temperature, high humidity storage. Fifteen cylinders spent their entire curing period in room temperature, high humidity storage. Additional cylinders from the (three cylinders) first and (nine cylinders) fourth group remained at FDOT/SMO for compressive strength, early surface resistivity, and bulk diffusion testing. Curing at SMO was slightly different; a fog room was used for room temperature curing, and the elevated temperature cure took place in a high humidity (>95% RH) and elevated temperature chamber (~36° C). Cylinders from groups DCL2 and DCL10, transported to FAU, spent one extra week in room temperature storage upon their arrival at SeaTech before transferring them to the elevated temperature environment.

Table 3-6: DCL cylinder (G3) curing scenarios

Cylinder #	Curing Period
1 to 6	14RT/14ET/RT
7 to 15	14RT/28ET/RT
16 to 21	14RT/77ET/RT
22 to 36	RT

Elevated temperature curing at FDOT is performed differently than at FAU. FDOT keeps its cylinders in a high moisture, elevated temperature chamber. At FAU, accelerated curing occurs with cylinders fully immersed in calcium hydroxide solution with the containers in a temperature-controlled room (36-38°C). The solution periodically needs to be replenished to maintain the fully immersed conditions. After elevated temperature curing exposure, the cylinders were stored in high humidity at laboratory temperature.

### 3.3.2 Geometry of Specimens Previously Prepared and Exposed at FAU

These included two geometries G0 (24" × 7" × 10"), and G4 (12" × 12" × 6"). A third geometry G1 (24" × 7" × 4.75") was obtained by segmenting G0 specimens. G1 specimens were obtained by cutting G0 specimens into half along the 10 in side. G4 specimens were segmented along one of the 12" width sides resulting in 2 specimens of 12" × 6" × 5.75" each. The specimen geometry details are described in Table 3-7 and Table 3-8.

Table 3-7: Details of concrete mixes G0 and G1

Mix Name	Pozzolan	Cast Date	w/cm ratio	G0*	G1	Specimen Name
				No.	No.	
1C2	20% FA	7/2009	0.41	2	5	FA1, FA2, FA3, FA4, FA5, FA6, FA7
1C3	20% FA+8%SF	10/6/2009	0.41	2	2	SF1, SF2, SF3, SF4

Note these specimens were prepared with coarse aggregate #57

\* G0 specimens not segmented contained two #4 rebars

Table 3-8: Details of concrete mix G4

Mix Name	Pozzolan	Cast Date	w/cm ratio	G4	Specimen Name
				No.	
1C1	OPC only	3/3/2008	0.41	4	1A1A, 1A1B, 1A2A, 1A2B, 1A3A, 1A3B, 1A4A, 1A4B
1C2	20% FA	8/19/2008	0.41	2	2A1A, 2A1B
1C3	20% FA + 8%SF	10/26/2009	0.41	4	3A1A, 3A1B, 3A2A, 3A2B, 3A3A, 3A3B, 3A4A, 3A4B
1C1	OPC(FA top)	8/19/2008	0.41	2	2C1A, 2C1B
1C2	20% FA	6/2/2008	0.41	4	1E1A, 1E1B, 1E2A, 1E2B, 1E3A, 1E3B, 1E4A, 1E4B

G0 and G1 were cured at room temperature and high humidity storage for 15 days and this was followed by exposure to room temperature and laboratory humidity conditions. Selected specimens were subjected to wet cycles and cover with a plastic wrap. The specimens were subjected to various moisture conditions. G4 slabs were placed at room temperature and high humidity storage 60 days, and after transport to FAU the exposure was at room temperature and laboratory conditions, with periodic wet/dry during the next four months, and then to high moisture for eight months. After this the specimens were exposed to laboratory temperature and humidity. The specimens were between two and three and a half years old when the exposure described in here began.

### **3.3.3 Specimens Exposed at SMO**

Both groups of specimens have been exposed to 3.5% NaCl solution for over 18 years. One group was exposed to simulated tidal exposure and the second group to constant immersion (lower than 10 cm)

#### **3.3.3.1 Tidal Simulation Specimens**

Each sample set consisted of three replicas. The basic specimen configuration is shown in Figure 3-1. The specimens made were reinforced concrete columns, 60.00 inches (152.4 cm) tall, 5.50 inches (14.0 cm) wide, and 3.50 inches (8.9 cm) thick. Each specimen was reinforced with two 1.3 cm diameter (#4) bars and cast with a minimum 1.75 inches (4.5 cm) of concrete cover. The first bar is a continuous piece of steel rebar from top to bottom preserving the chosen cover at the ends as well. One specimen per mix type was selected for coring to obtain chloride profiles and the apparent diffusion coefficient. One sample set was different from the rest. The OPC mixture was 10.50 inches (26.7 cm) wide in order to accommodate a bent-bar feature and still retain the 1.75 inches (4.5 cm) cover in all directions.

Most of the remaining samples exposed to tidal simulated environment have been tested for more than 18 years. Table 3-9 indicates cast date and age at which the samples were removed from the tank for coring.

Table 3-9 Tidal samples age at time of testing

Tidal Samples					
Sample Name	#	w/cm ratio	Cast Date	Date in Tank	Exposure Time (years)
OPC	2	0.41	9/12/1989	6/15/1990	21.3
7% SF	3	0.33	4/18/1989	1/15/1990	21.8
11% SF	3	0.30	4/25/1989	1/15/1990	21.8
15% SF	3	0.34	5/2/1989	1/15/1990	21.8
SFFA - 15%	2	0.37	5/4/1995	8/31/1995	16.2
SFFA - 20%	2	0.37	8/8/1995	2/23/1996	15.7
SFFA - 25%	1	0.37	1/2/1996	5/10/1996	15.5

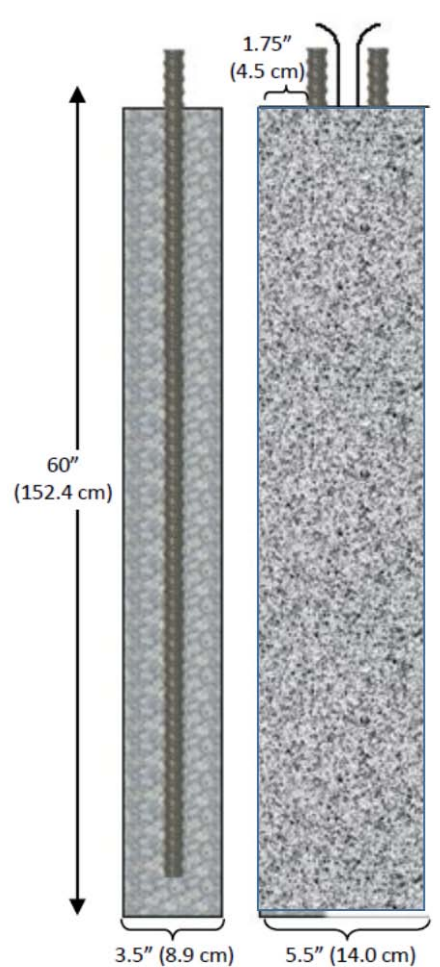


Figure 3-1: Specimen design used for tidal exposure

### 3.3.3.2 Exposure Tank Description at SMO

The exposure tank (Figure 3-2) is divided into two sections by a dividing wall in the middle. The tank is designed to simulate a high and low tide condition so that one side has water up to the high water level while the other has water up to the low water level. Every six hours, a pumping system moves the water from one section to the other. Each side gets two low tide cycles and two high tide cycles every twenty-four hours. The high tide level is set by an overflow hole in the dividing wall allowing water to flow into the low side. The low side water level is maintained by a technician who compensates for evaporation loss twice per week. Salt concentration is also checked twice per week using a salt portable salinity refractometer and adjusted as needed. The solution used was 3.5% NaCl. Figure 3-3 shows the actual tank with some of the samples.

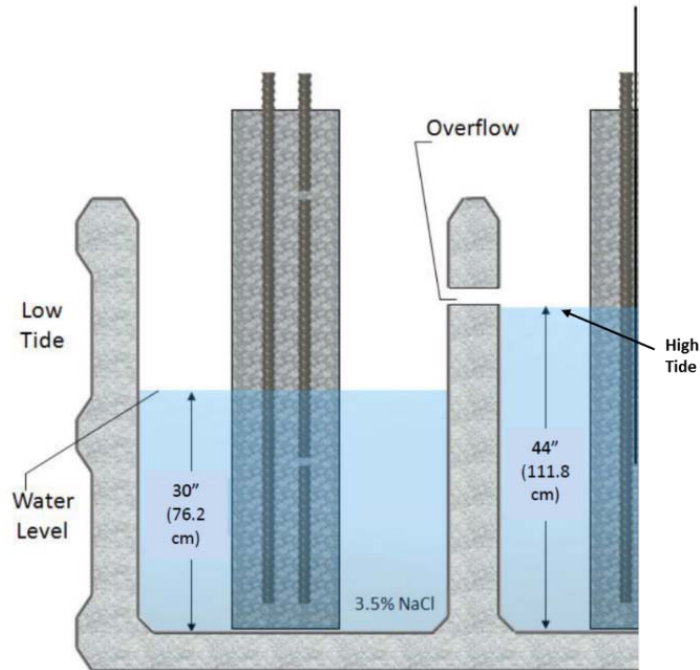


Figure 3-2: Diagram of tank used for tidal exposure simulation



Figure 3-3: Tidal simulated samples at SMO

The specimens were cored at 0.4 m (below water), 0.9 m (above low tide), 1.07 (just below high tide), 1.22 m (10 cm above high tide), and 1.34 m. The picture below (Figure 3-4) shows the elevations at which cores were obtained on one of the selected columns (shown units in Figure 3-4 are in inches).



Figure 3-4: Cored location on specimens subjected to tidal exposure at SMO

### 3.3.3.3 Partially Immersed Specimen

Each sample set consisted of three replicas. The specimens made were reinforced concrete columns, 21.0 inches (53.34 cm) tall, 5.25 inches (13.34 cm) wide, and 4.0 inches (10.16 cm) thick. Each specimen was reinforced with two 1.3 cm diameter (#4) bars and cast with a minimum 1.75 inches (4.5 cm) of concrete cover. The bottom 4 inches were immersed all the

time in 3.5% NaCl solution. Figure 3-5 shows a picture of the specimens while they were exposed. Most of the remaining samples exposed to partially immersed exposure have been tested for more than 18 years. Table 3-10 indicates cast date, transfer to tank date and age at which the samples were removed from the tank for coring.

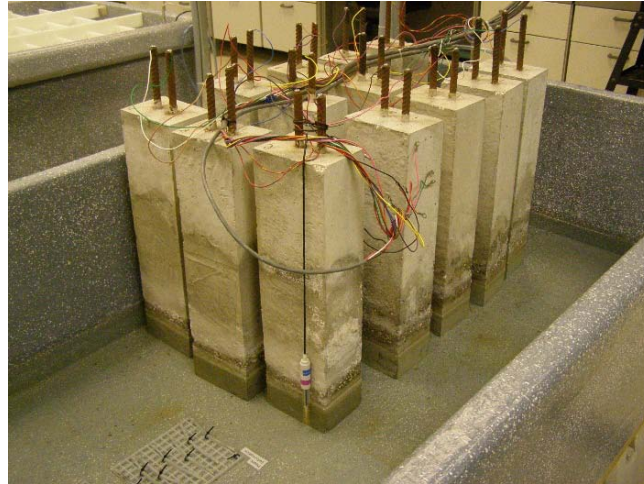


Figure 3-5: Partial immersion samples at SMO

The specimens were cored at 0.07 m (3" and below water line), 0.22 m (~10 cm above water line), and 0.34 m (13.5"). Figure 3-6 shows the elevations at which these specimens were cored (shown units are in inches)



Figure 3-6: Cored location on specimens subjected to partial immersion at SMO

Table 3-10: Age at coring of partially immersed samples

Sample Name	#	Constant Depth of 4"			Exposure Time (years)
		W/C Ratio	Cast Date	Date in Tank	
10% Fly Ash	2	0.37	12/14/1993	12/23/1993	20.39
20% Fly Ash	2	0.37	1/12/1994	1/24/1994	20.30
20% Fly Ash + Cl <sup>-</sup> **	3	0.37	8/23/1994	NA	about 17
30% Fly Ash	3	0.37	1/19/1994	2/1/1994	20.28
40% Fly Ash	3	0.37	2/8/1994	2/22/1994	20.22

### 3.4 Water Sealant Application on Specimens Exposed at FAU

Selected specimens for outdoor exposure were coated with a water sealant to minimize chloride penetration from those faces. The coring/milling took place from the non-coated faces. Table 3-11 shows the samples coated with Thoroseal water sealant and exposure environments.

Table 3-11: Specimens sides on which Thoroseal was applied

Samples	Exposure Environments	Coated Sides
G1a blocks	Barge	Four sides
	Tidal simulation	No water sealant
	Splash simulation	No water sealant
G2 slabs	Atmospheric	Five sides
G4 blocks	Atmospheric	Four/five sides

G0 and G1 blocks were left over from a previous experiment and thus had cured for a long enough period that applying water sealant was deemed unnecessary. G0 blocks were used for tidal simulation and placed in the barge (partial immersed outdoor simulation). G1 blocks were placed in the barge. The cores would be obtained far enough from the edge of the sample that 1-D transport can be assumed from the segmented section. It was assumed that chloride penetration from the edges of the specimen would not be large enough to cause a significant increase in concentration at the cored locations.

G1a blocks that were placed on the barge were coated on four sides with Thoroseal water sealant. Application of Thoroseal is discussed in the following section. Two sides were left uncoated so that chloride penetration can occur on those sides. The sides which were not coated were those which measured 22" × 7." G1a blocks used in the tidal simulation and splash simulation carried out indoors did not receive water sealant.

G2 slabs were coated on five sides and cut before being subjected to atmospheric exposure. The samples were placed at three locations. These specimens were subsequently cut 6" from the end of the slab, creating two slabs measuring 12" × 5.75" × 3". One side was left uncoated so that chloride penetration could occur on one side. In some cases, the exposed faces after the cut were not coated. The uncoated side exposed to chlorides measured 12" × 5.75".

G4 blocks were old stock samples that were cast in three different concrete mixes all with w/cm ratios of 0.41. Each of these blocks was coated on four/five sides with Thoroseal, and cut into two pieces. After being cut, these blocks measured 12" × 6" × 5.75". Additional details of these samples and exposure scenarios before segmenting them can be found in a FDOT report [4].

Concrete should be cool and damp before the coating is applied. Samples used in the experiment were stored outdoors under shelter for 24 hours before Thoroseal application. A mixing solution was prepared by mixing one part Acryl 60 with three parts tap water. For a 50-kg bag of Thoroseal cementitious sealant, 22.7 L of mixing solution is required. An amount of Thoroseal appropriate for the amount of blocks being coated was selected. This solution was then mixed gradually with Thoroseal powder using a slow speed drill and a mixing paddle. Once properly blended, the Thoroseal had a lump-free consistency. Pot life is 60-90 minutes at 21° C. The mixture is allowed to sit for 10 minutes, stirred again, and applied. The first coating was thoroughly worked into the substrate (faces of the concrete sample being coated) to completely fill any voids or surface imperfections in the concrete surface. A second coat was applied after 24 hours. The same procedure was observed 24 hours later when the samples were coated the second time. A photograph of a G4 block that underwent this sealing process is shown in Figure 3-7. The uncoated surface was directly exposed to chloride deposition.



Figure 3-7: Thoroseal-coated G4 specimen

### 3.5 Indoor and Outdoor Exposure: Partially Immersed Specimens

In addition to the cylinders described above, concrete blocks were prepared with DCL mixes. The concrete blocks per mix have a dimension of 55.9 cm × 17.8 cm x 12. cm. Table 3-12 represents the number of cylinders per mix exposed to three simulated field conditions: Tidal, Splash, and Barge.

Table 3-12: Number of cylinders per mix exposed to simulated field conditions

Mix	Exposure Conditions		
	Tidal	Splash	Barge
DCL1	2	2	0
DCL2	2	2	2
DCL3	2	2	2
DCL4	2	2	0
DCL5	2	2	0
DCL6	2	2	2
DCL7	2	2	0
DCL8	2	2	0
DCL9	2	2	2
DCL10	2	2	0
DCL10a	2	2	2
DCL10b	2	2	2
DCL11	2	2	2

#### 3.5.1 Tidal Simulation

The tidal simulation tanks measure 40'' × 16'' × 22.5''. Table 3-13 shows the concrete mixes for the tidal simulation.

Table 3-13: Concrete mixes for tidal simulation

Concrete Mixes	Geometries	Numbers
DCL1, DCL2, DCL3, DCL4, DCL5, DCL6, DCL7, DCL8, DCL9, DCL10, DCL10a, DCL10b, DCL11	G1a (22'' × 7'' × 4.75'')	Two per mix
FA6, FA7	G0 (24'' × 7'' × 10'')	Two per mix

Each tank holds one G0 block and 12 G1a blocks while allowing 1” of space between the samples as listed in Table 3-13. The experiment began with one G0 block and three G1a blocks in each tank. One tank was filled with sea water until the lower 7” of the blocks were immersed and the other tank was filled with sea water until the lower 14” of the blocks were immersed. Every 12 hours tidal change is simulated (period of time is controlled by using analog timers) by pumping water from the tank with the greatest amount of water to the tank with the least amount of water. The pump is stopped when the tank that is receiving water has reached a height of 14” on the blocks via a float-switch. Figure 3-8 shows the waterlines on samples that are in opposite tidal simulation tanks.

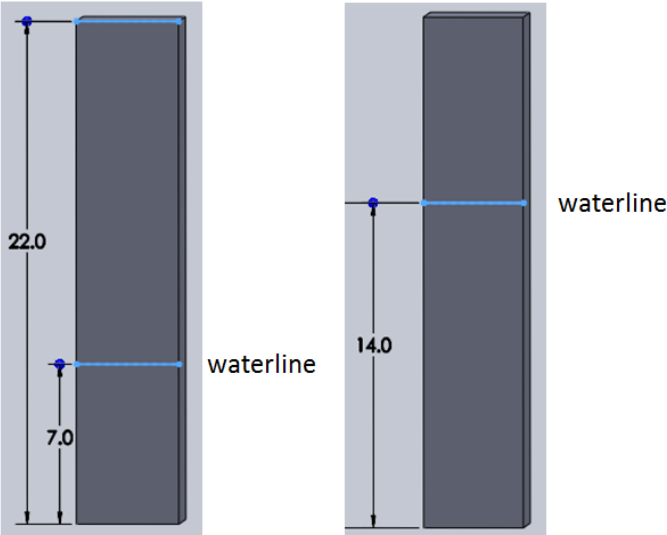


Figure 3-8: Tidal simulation exposure conditions

The float/bobber shown in Figure 3-9 is the component of the tidal simulation that indicates the water height and causes fluid transfer to stop. Blocks were added every two weeks after they had been cured for either three or four weeks depending on the concrete mix.



Figure 3-9: Tidal simulation (low tide seawater height = 7")

After all blocks had been received, two blocks from each mix were placed in the tidal simulation tank as the blocks arrived at SeaTech. Two times per day, seawater is pumped from the fullest to the least full tank. Figure 3-10 is another view of the tidal simulation that shows how the blocks were configured. As water was added, the water height was adjusted to account for the displacement caused by the new blocks.



Figure 3-10: Tidal simulation

### 3.5.2 Splash Simulation

Table 3-14 shows concrete mixes for splash simulation in 100% sea water and 10% seawater.

Table 3-14: Concrete mixes for splash simulation

Seawater	Concrete Mixes	Numbers
100%	DCL1, DCL2, DCL3, DCL4, DCL5, DCL6, DCL7, DCL8, DCL9, DCL10, DCL10a, DCL10b, DCL11	Two per mix
10%	DCL3, DCL6, DCL9	Two per mix

In the splash simulation, G1a blocks receive 10 minutes per day of constant spray on a line 14” above the bottom of the blocks. Each of splash simulation tanks is 22.5” long, 23.5” high, and 17.5” wide and holds six samples while allowing one inch of separation between the exposure faces. A Plexiglass guard was installed on each tank to prevent splash from reaching above the selected line. Figure 3-11 shows the waterline at 4.5” and the splash guard is located 14” above the base of the block.

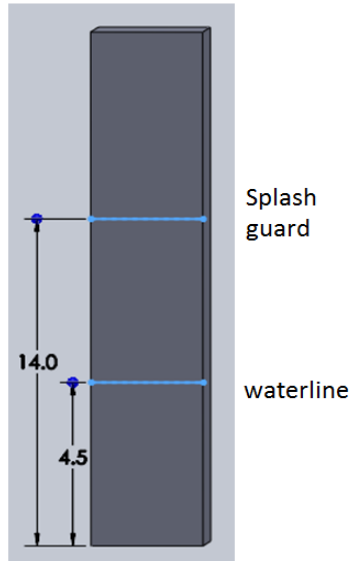


Figure 3-11: Splash simulation block

The containers were left slightly ajar to keep the moisture content of the upper third of the blocks stable. This was done to prevent a high moisture content at the upper region of the blocks. Typically about 2" of wetness was visible above the splash guard immediately after each spray simulation. Two concrete blocks per each groups DCL1 to 11 (except DCL10) underwent the splash simulation with seawater. Additionally, three block groups (DCL3, DCL6 and DCL9) had samples sprayed with a solution made up of 90% tap water and 10% seawater which is equivalent to chloride concentration of brackish water in some areas (3.5 g/L). Periodically the water level was adjusted, about once every month the seawater was replaced. Figure 3-12 shows the apparatus used to spray the blocks which underwent the splash simulation. A water pump was attached to a timer which was set to provide power to the pump for one 10 minutes period per day. Sprinkler nozzles were attached to the top of an apparatus made of PVC to spray water at a line 12" measured from the bottom of the blocks. Each nozzle sprays a steady jet of water 180° and four jets were needed to three blocks on each side of one container. Therefore eight total jets are attached to spray blocks on either side of the container.



Figure 3-12: Splash simulation

### 3.5.3 Partial Immersion Exposure: Barge Scenario

Concrete mixes for exposure are shown in Table 3-15. Blocks (two blocks per mix) were exposed on the barge. The barge is pictured in Figure 3-13 with all of the blocks one third immersed. The barge was built to be capable of remaining stable and above water with adequate support for 2000 lbs. of concrete. (Barge construction details can be found in a MS Thesis [79]) The floats prevent the tide from affecting the samples, so only permanent immersion and splash/atmospheric exposure are simulated by this exposure. Another requirement was to provide a minimum of 1” of space between samples. Samples measuring 24” × 7” × 10” were positioned with the 10” exposed face of the block facing the north. Samples measuring 22” × 7” × 5” were positioned with the 5” exposed face of the block facing the east.

Table 3-15: Concrete mixes for barge

Concrete Mixes	Geometries	Numbers
DCL2, DCL3, DCL6, DCL9, DCL10, DCL10a, DCL10b, DCL11	G1a	Two per mix
FA1, FA2, FA3, FA4, FA5, SF1, SF2, SF3, SF4	G0 and G1	At least two per mix

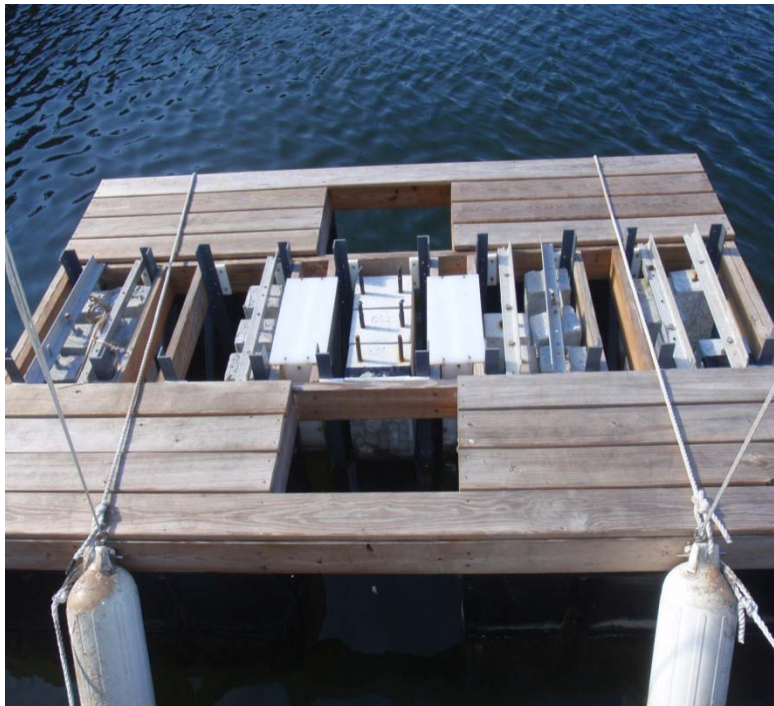


Figure 3-13: Barge scenario

For specimens placed in the barge, splash and tidal simulations, concrete cores were obtained at six, ten and eighteen months. The cores were milled and the powder obtained was subjected to the chloride concentration analysis (process is explained in the next section). The cores were milled from both sides for those exposed in the barge and tidal exposure and only one side (the splash side) for those subjected to splash (for more information about the locations where core sample were taken and the diameter of the cores refer to Appendix A). Figure 3-25 shows how the milling process is performed; to secure the samples, the cores were placed between two pieces of wood. For the first set of samples (six months of exposure), the target thickness of the first and second layer was 2 mm while the remaining layers were 4 mm. The group of samples cored after 10 and 18 months of exposure was milled with a first layer of 2 mm and the other layers were 3 mm thick.

### 3.6 Atmospheric Exposure

#### 3.6.1 Exposure Locations

The prepared concrete samples were placed at three different locations at SeaTech in Dania Beach, FL. Each location contained samples of the same concrete mix design. In Figure 3-14 below, a satellite image shows the three locations of the concrete samples, labeled by the leaders containing letters A, B, and E. Letter A represents the fence location, where the sample names are designated with the ‘-a’ suffix. Letter B refers to the west location, where the sample names are designated with the ‘-b’ suffix. Letter E represents the east location, where the sample names are labeled with the ‘-e’ suffix. (i.e., the name DC2b would represent mix design DC2 at the west (b) location).

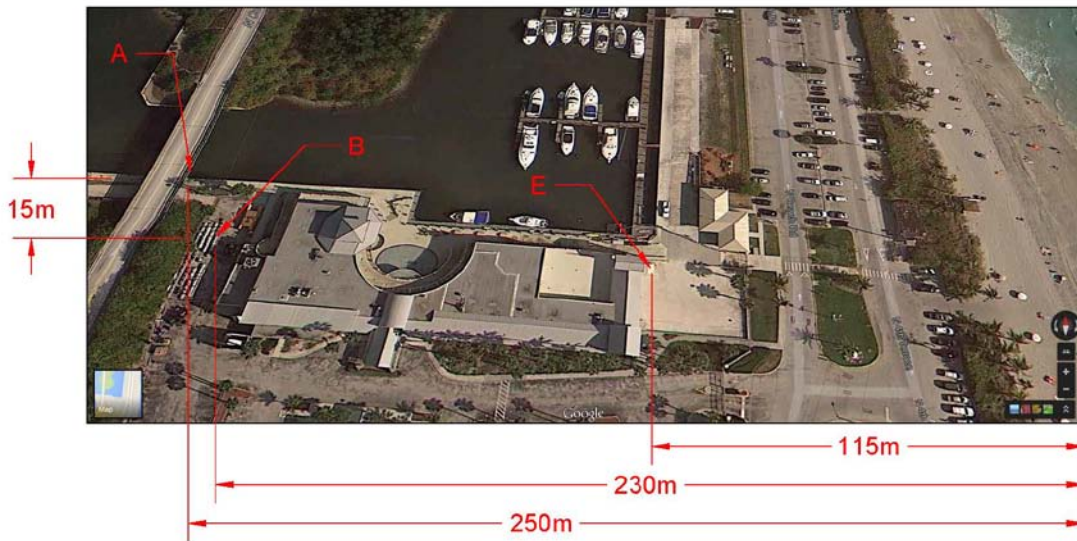


Figure 3-14: Satellite image of SeaTech showing locations of the concrete samples

The image in Figure 3-14 also shows the approximate distances from the sea to each sample location. The east location is about 115 m from the sea; the west location about 230 m; and the

fence location about 250 m. The fence samples are placed at the fence along the Intracoastal Waterway (ICW) and the Dania Beach marina. The west samples are about 15 m south from the ICW and the east samples are also about 15 m south from the marina. The SeaTech building is located between the east and west locations, which may prevent some wind from reaching certain concrete samples depending on the wind direction.

Figures 3-15, 3-16 and 3-17 show the three atmospheric exposure locations. Table 3-16 shows concrete blocks identifiers for these exposure sites.



East site Exposure



Look east – Atlantic Sea

Figure 3-15: East property exposure



Figure 3-16: West property: away from the fence

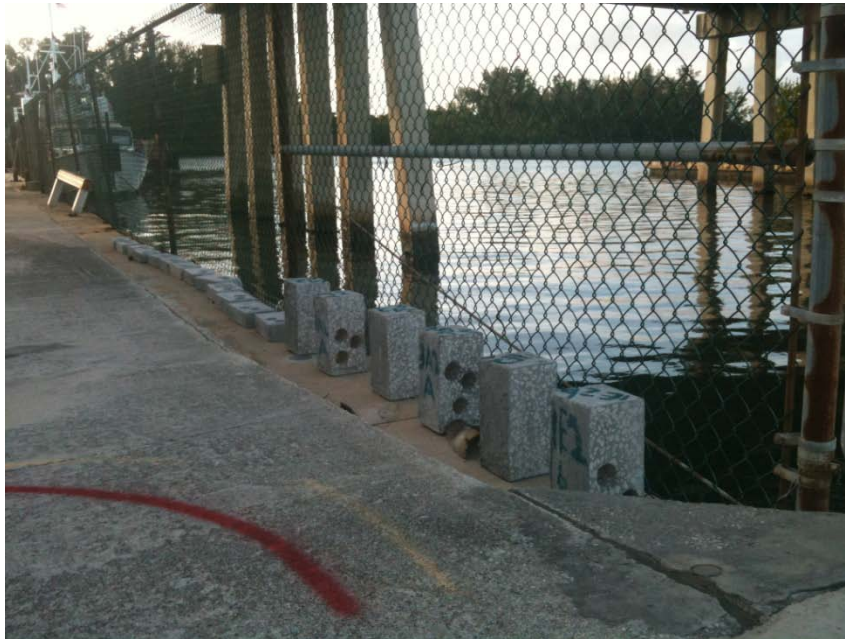


Figure 3-17: West property: adjacent to the fence

Table 3-16: Concrete mixes for atmospheric exposure

Locations	Concrete mixes	Geometries	No.
<b>East property</b>	DCL1, DCL2, DCL3, DCL4, DCL5, DCL6, DCL7, DCL8, DCL9, DCL10, DCL10a, DCL10b, DCL11	G2	2
	3A4, 2C2, 2A2	G4	2
<b>West property</b>	DCL1, DCL2, DCL3, DCL4, DCL5, DCL6, DCL7, DCL8, DCL9, DCL10, DCL10a, DCL10b, DCL11	G2	3
	2A2, 1E1, 1E3, 1E4, 3A1, 3A3, 1A1, 1A3, 1A4,2C1	G4	2
<b>West property – adjacent to Fence</b>	DCL1, DCL2, DCL3, DCL4, DCL5, DCL6, DCL7, DCL8, DCL9, DCL10, DCL10a, DCL10b, DCL11	G2	1
	1A2, 1E2, 3A2	G4	2

### 3.6.2 G2 Slabs

G2 slabs were exposed outside at three locations at Seatech beginning in October of 2011. G2 slabs were oriented with the exposure side (side that measures 12” × 5.75”) facing east for those placed on Seatech eastern site and facing-up for the other two locations. Figure 3-18 shows that slabs were oriented with the exposure side facing towards the sea (east) at the location on the east property.

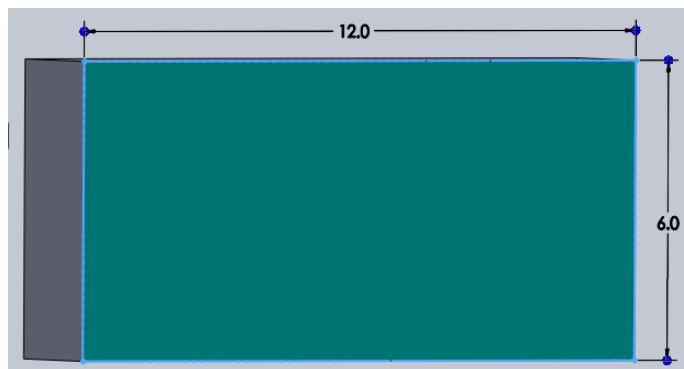


Figure 3-18: G2 – east property -horizontally oriented with exposure side eastward

Slabs placed on the west property and adjacent to the intracoastal waterway (fence) were all horizontally oriented with the exposure side facing the sky as seen in Figure 3-19. An exposure schedule for all mixes of G2 slabs is available in Appendix B.

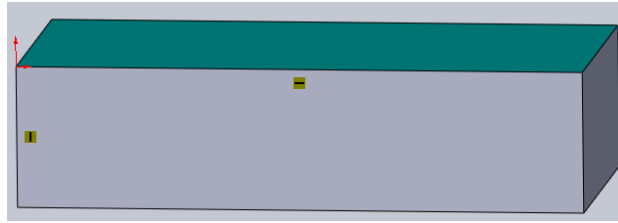


Figure 3-19: G2 – west property and fence adjacent – horizontally oriented with exposure side skyward

### 3.6.3 G4 Slabs

All G4 slabs were exposed to the atmosphere beginning on 10/14/2011. Some slabs were placed on the rack on the west property oriented vertically as seen in Figure 3-20 with the exposure side facing the east. Some of the slabs were placed adjacent to the fence at the intracoastal waterway and were also oriented vertically with the exposure side facing the east.

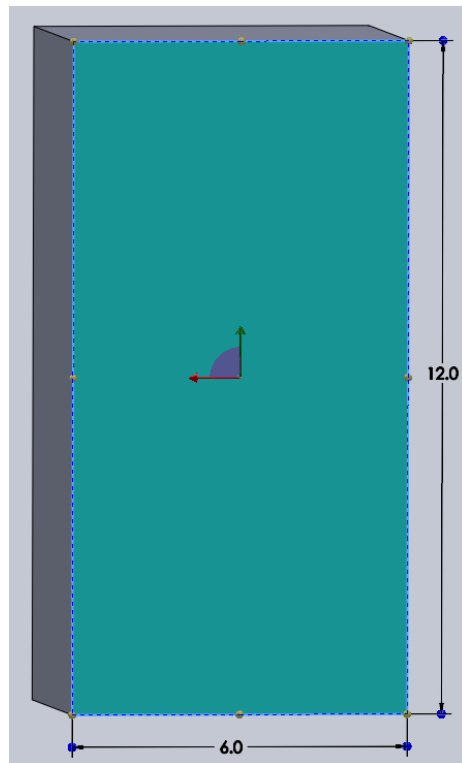


Figure 3-20: G4 – west property and fence adjacent – vertically oriented with exposure side eastward

Some slabs that were placed on the rack on the west property were oriented with the exposure side facing the sky as shown in Figure 3-21.



Figure 3-21: G4 – west property – horizontally oriented with exposure side skyward

Some slabs were placed on the east property and were oriented horizontally as shown in Figure 3-22 with the exposure side facing the east.



Figure 3-22: G4 – east property – horizontally oriented with exposure side eastward

### 3.7 Milling

Milling was performed for G4 (see Figure 3-23) and some G2 blocks after six months of exposure in preparation for titration. Each of the blocks in G4 was previously cut in half and both halves were exposed next to each other at the same location.



Figure 3-23: G4 slab (milling performed once)

One of these halves was milled for each block to act as a representative sample for that mix under those exposure conditions. The exposed blocks were milled along the same edge for all samples. Milling began at the bottom for vertically oriented samples and on the left for horizontally oriented samples. A section was marked at least ½ inch away from the edge of the concrete for the initial sample. Paper was set down to collect powder that fell during milling. The drill was turned on and the bit was put in contact with the surface of the sample and locked in place. Then a ½-mm strip was milled, and the powder was brushed off and collected. This step was repeated four times to reach 2 mm (in some cases additional layers were milled). After completing the analysis of the first six months, it was found that this method produced contamination from the top to lower layer, thus it was abandoned. Instead, the blocks were cored and then milled.

The powder was collected in a vial which was labeled, weighed, and set aside for titration. These steps were repeated at least four more times to reach a depth of 10 mm. The orientation of the strip selected for milling depended upon the orientation of the block. Figure 3-24 shows an example of the milled area on a G4 slab.

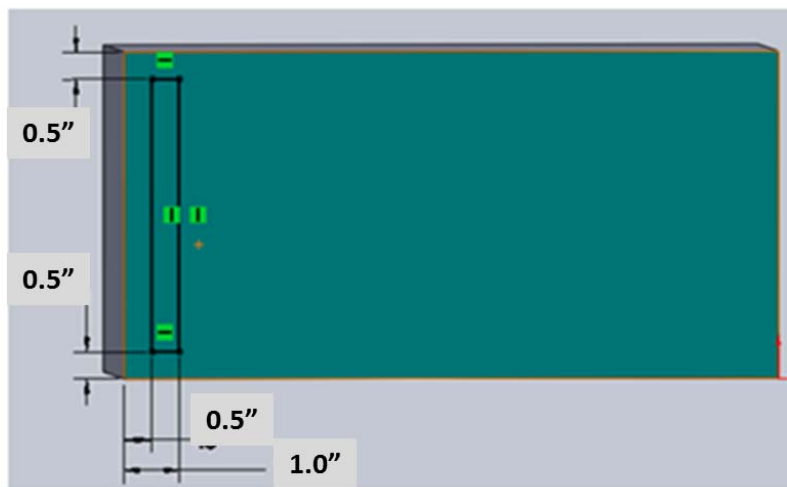


Figure 3-24: Typical milling of G4 slabs

The milling procedure on G2 and G4 slabs was changed for the 10-month profiles (actually some of the G2 slabs were not milled at six months). Instead of milling the slab directly, one 2” diameter core sample was obtained at least 1” away from the milled area. That cylinder was then milled into six ~2 mm layers. For four of the G2 slabs, the 6-month profile was found by taking a core 1” from the edge of the sample (DCL1, 4, 5, and 7).

### 3.8 Coring and Milling

Core samples 2” and 1.5” in nominal diameter were taken from blocks that were too large to be secured in the vice used for milling (G0, G1, and G1a). For G1 and G1a blocks deployed on the barge, core samples were taken along a center line 3” above the base of the block (permanently immersed section), 3” from the top of the block, 1” above the water line, and one more in

between the top and waterline spots. Coring configurations are available in Appendix A for the barge, splash, and tidal simulations. Table 3-17 shows the four elevations where these blocks were cored measured in inches from the base of the block to the center of gravity of the core sample.

Table 3-17: Core sampling elevations on blocks

Exposure Location	A	B	C	D
Barge	2.8	12.3	15.4	18.1
Tidal	1.8	8.3	12.8	18.0
Splash	2.3	6.3	12.3	18.0

Coring of block samples took place after  $180 \pm 2$  days of exposure and at  $300 \pm 2$  days. Milling of the core samples extracted typically was performed less than 14 days after coring. Milling was planned similar to how it was described in the previous section. Cylinders were placed in two wood pieces with half-circle cut out to accommodate the sample as shown in Figure 3-25. Then the work piece was secured in a vice attached to the drill press table. Slices that were 2 mm thick were taken off the core samples measuring 2" in diameter. Core samples taken after six months of exposure measured 1.5" in diameter and the first two layers milled measured 3 mm while the deeper layers were 4 mm. As slices were taken they were marked set aside to be broken into powder before titration could begin.

All the cores taken after ten month of exposure were 2" in nominal diameter. The first layer of these samples measured 2 mm while all subsequent layers measured 3 mm for the samples from the barge, tidal, and splash simulations. Atmospherically exposed specimens were milled in six 2 mm layers.



Figure 3-25: Milling setup for 2" diameter cylinder

### 3.9 Bulk Diffusion

#### 3.9.1 Exposure in 3% and 16.5% NaCl

Bulk diffusion tests were performed according to NT Build 443[75] with a one-year exposure period at FDOT. Each cylinder was cut in half and coated as per NT Build 443. Rather than using a single exposure solution, two solutions with different NaCl content were used. Of the two slices from each specimen, all the bottom halves were exposed to 16.5% NaCl solution (~3.1 M NaCl) and all the top slices were exposed to 3% NaCl solution (~0.52 M NaCl). Figure 3.26 shows the exposure tank and specimens exposed in NaCl solution. Three curing conditions were tested: 28 day high humidity room temperature curing (NC curing), 14 days high humidity room temperature and 14 days elevated temperature at high humidity (AC curing), and high humidity room temperature curing until the resistivity measured at room temperature reached the resistivity of those AC cured (NC=AC). Four mixtures were also tested after exposure to fog room curing for more than 28 days but before NC=AC, and these are identified in the results as NC<AC. Three concrete cylinders per curing regime selected. Once the specimens reached one year of exposure the samples was sliced in 0.635 cm thick layers and then pulverized for chloride analysis.



Figure 3-26: Bulk diffusion exposure

An additional cylinder per mix was selected for bulk diffusion in both solutions after the specimen was more than 700 days of age. These cylinders were from those cured 14RT/77ET/RT. The top halves were immersed in the 16.5% NaCl and the bottom halves to 3% NaCl solution. The exposure duration was between 102 days and 145 days.

### 3.9.2 Bulk Diffusion in Low Chloride Concentration (0.6% NaCl)

The test method was similar to Nordtest Method NT Build 443[75]. However, the concentration of NaCl solution was 0.6% NaCl (i.e., 6.1 g NaCl per liter or approx. 0.1 M NaCl), significantly smaller than that specified in NT Build 443. From this point on the concentration will be referred as 0.1 M NaCl. Two exposure durations were investigated 220 days and 400 days. The top side was used for 220 days exposure. Cylinders Nos. 5, 13, 20 and No. 31 of each mix were used for the bulk diffusion test, one per curing condition. Only the bottom sides of specimens 20 and 31 were terminated at 400 days of exposure. Specimens 5 and 13 continue to be exposed in 0.1 M NaCl.

#### 3.9.2.1 Conditioning for Specimens Immersed in 0.1 M NaCl

The selected cylinders were 180 days when this test began. The last 30 days the cylinders were immersed in water. Before testing, all these cylinders were immersed in water for 30 days (approx.) at an age of 150 days from casting. Then each cylinder was cut into two pieces (identified as portion A, B), which were the bottom section and top section of each cylinder, respectively (see Figure 3-27). Each section had the same length with the cuts perpendicular to the cylinder axis. All concrete portions after cutting were re-immersed in a saturated  $\text{Ca}(\text{OH})_2$  solution at room temperature ( $21^\circ\text{C}$ ) until fully saturated (see Figure 3-28) or reaching 175 days of age.



Figure 3-27: Saw cut of concrete cylinder



Figure 3-28: Specimens placed in the container with  $\text{Ca}(\text{OH})_2$  solution

The test specimens were surface dried with paper towel and then nature dried in laboratory environment for 20 minutes and were coated with epoxy Sikadur<sup>®</sup> 32 (Figure 3-29). After 24 hours, the coated test specimens were placed in the container with  $\text{Ca}(\text{OH})_2$  solution again until day 180.



Figure 3-29: Test specimens coated with Sikadur 32

### 3.9.2.2 Exposure and Diffusion

An aqueous NaCl solution is prepared with 6.1 grams of NaCl per liter (i.e., 0.6% NaCl or approx. 0.1 M NaCl). The solution was replaced once a week during the first three months. After that, the NaCl liquid was replaced once every two weeks due to the concentration remaining almost constant within those two weeks.

Before the first immersion the coated specimens were surface dried with paper towels and then were immersed in the saline solution (Figure 3-30). As indicated above, concrete cylinders were 10.2 cm diameter by 20.32 cm long. Figure 3-27 shows how the cylinders were then cut in half and coated with epoxy, except for the cut face. There were two different exposure times; the first one was 220 days (all four curing regimes) and the second exposure time was 400 days and only 14RT/77ET/RT and RT cured cylinders were selected. Upon reaching the target age, the specimens were then removed and the epoxy layer cut off. The specimens were then milled. Seven layers were marked (2-3 mm depth) on each cylinder and concrete powder was collected by milling. To obtain chloride concentrations, chloride titrations were performed to each layer. From these concentrations, chloride profiles were obtained and used to calculate the chloride diffusion coefficient through Fick's Second Law.



Figure 3-30: Bulk diffusion in 0.1 M NaCl

### 3.9.3 Chloride Diffusion on Concrete Under Controlled Partial Saturation

#### 3.9.3.1 Test Method

Neither ASTM nor Nordtest has developed a test method for chloride diffusivity through partially saturated concrete. Here a test method similar to the one proposed by Guimaraes et al. [64] was used. Table 3-19 shows the selected concrete cylinders mixes (G3) used.

Table 3-18: Concrete cylinders (G3) for study

Concrete mix	No.	Curing period
DC1	26, 27	RT
DC2	9, 10, 11, 12	14RT/28ET/RT
	25, 26, 27, 29	RT
DC3	26, 27	RT
DC10b	26, 27	RT
DC11	26, 27	RT

Five concrete mixes (out of the 13 prepared) were selected for this research effort. DCL1, DCL2, DCL3 had 20% Fly Ash (FA) as cementitious replacement by mass and the water to cementitious (w/cm) ratio ranged between 0.35 to 0.47 (see Table 1). DCL10b and DCL11 also contained had 20% Fly Ash (FA) as cementitious replacement by mass but with lower cementitious content (Table 3-20) and w/cm of 0.41. Type I/II cement was used for all the mixes. The coarse aggregate and fine aggregate were Florida limestone and Florida silica sand, respectively. Table 3-20 shows the details of the concrete mixes prepared for the present study.

Three cylinders from each mix DCL1, DCL3, DCL10b, DCL11 cured in RT were used for studying chloride diffusion under non-saturated and saturated conditions. Also four cylinders from mix DCL2 exposed in RT and another three cylinders from the same mix cured in 14RT/28ET/RT were used for this study. In addition, one cylinder per mix corresponding to the different sets described above were tested for measuring the bulk density, water absorption and porosity (see Section 3.9.3.4).

Table 3-19: Details of concrete mixes for present study

Mix name	Cementitious content	Cement content	20%FA	Fine agg.	Coarse agg.	FA	w/cm ratio
	(kg/m <sup>3</sup> )	(%)					
DCL1	390	312	78	1062	653	20	0.35
DCL2	390	312	78	949	721	20	0.41
DCL3	390	312	78	918	697	20	0.47
DCL10b	335	268	67	765	1007	20	0.41
DCL11	279	223	56	765	1009	20	0.41

### 3.9.3.2 Preparation and Conditioning of Specimens with Known Moisture

For saturated diffusion test, the concrete cylinders selected from each mix DCL1, DCL2, DCL3, DCL10b, DCL11 cured in RT were immersed at the same time as those used for bulk density, water absorption and porosity. These cylinders remained immersed until an age of 560 days. Each cylinder was cut into four pieces (identified as portion A, B, C, D), which were the bottom section, two middle sections, and top section of each cylinder, respectively. Each section had the same length with the cuts perpendicular to the cylinder axis. The exposed surface for layers A and D was the mortar surface (A mold surface and D trowel surface). In addition, half of the mortar surface was removed with a wet saw on sections A and D's. This was done in order to investigate the effect of mortar layers on the chloride diffusion. An epoxy paint was applied at the interface to avoid transport at the step side. Section C was also used for fully saturated exposure. All specimens were then re-immersed in saturated Ca(OH)<sub>2</sub> solution at room temperature (21°C) until fully saturated and getting the stable mass. Portion B were not used for this study (see Table 3-21).

For non-saturated diffusion test, the concrete cylinders selected were immersed at the same time as those used for bulk density, water absorption and porosity. These cylinders remained immersed until an age of 220 days and then were cut into three sections. The procedure for

cutting cylinders was the same than that previously described. All concrete portions after cutting were re-immersed in a saturated  $\text{Ca}(\text{OH})_2$  solution until fully saturated, which usually took about two additional days. Three water saturation degrees were investigated: 70%, 80% and 90%. There were 24 concrete sections obtained by cutting the two cylinders per each mix: DCL1, DCL3, DCL10b and DCL11. The specimens were randomly/arbitrary assigned to one of the three degrees of water saturation (See Table 3-21). There were 18 concrete portions (sections) A, B, C obtained by cutting the six cylinders from mix DCL2. Half of these sections were obtained by cutting cylinders cured in RT and the other half from cylinders cured 14RT/28HT/LH, respectively. One full cylinder (three sections) was stabilized to each of the three water saturation degrees. For the other mixes, only two sections were exposed to each degree of water saturation. Table 3-21 lists the targeted degree of water saturation and their corresponding concrete sections. The targeted degree of water saturation was obtained by drying the specimens in an oven at a temperature range from 40 to 47°C until they achieved the target mass ( $m_{SD}$ ) and is determined by the following equation[64]:

$$SD = \left( \frac{m_{SD} - m_{dry}}{m_{dry}} \right) * \frac{10000}{A} \quad (9)$$

Where

$SD$  = target degree of water saturation (%)

$m_{SD}$  = mass of the specimen for the targeted water saturation degree (grams)

$m_{dry}$  = dry mass of the specimen (grams)

$A$  = the water absorption (%).

Once the targeted degree of water saturation was obtained, the specimens were allowed to homogenize their moisture content. Each specimen was isolated by wrapping it with three layers of plastic wrap and then housed in plastic vacuum bags for 35 days to 42 days. A manual vacuum pump was used to remove as much air as possible. During the stabilization period, the mass of the specimens was monitored, and vacuum was performed once per week to ensure that the  $m_{SD}$  of each specimen remained the same.

Table 3-20: Degree of water saturation (SD) and concrete sections

Targeted SD(%)	DCL1 (RT)	DCL2 (RT)	DCL2 (14RT/28ET/RT)	DCL3 (RT)	DCL10b (RT)	DCL11 (RT)
70	C(2)	A,B,C	A,B,C	A(2)	B(2)	A,C
80	B(2)	A,B,C	A,B,C	C(2)	A(2)	B,C
90	A(2)	A,B,C	A,B,C	B(2)	C(2)	A,B
100*	A,C,D	A,D	A,C,D	A,C,D	A,C,D	A,C,D

\*100 SD(%) were 5 cm thick slices

### 3.9.3.3 Diffusion Exposure under Fix SD

For the fully saturated test, the portion A, C and D were used. A one inch slice of pvc pipe (with internal diameter identical to the concrete cylinder diameter) was attached to the test surface of each specimen and a marine grade epoxy used to glue it. After the epoxy dried (12 hours), these specimens were re-immersed into the solution until fully saturated again. Thereafter, the tested surfaces were dried with paper towels. Immediately, finely ground solid sodium chloride (passing #100 sieve) was used as the chloride source and placed on the tested surface of each specimen. For the portion A, the tested surface was on the bottom mold surface which is a smooth face with mortar layer. For the portion C, the exposed surface was the cut surface between portion C and D. For the portion D, the exposed was the top surface (trowel) during casting. After placing the solid NaCl, the specimens were partly immersed saturated  $\text{Ca}(\text{OH})_2$  solution in purposely manufactured boxes which were sealed and vacuumed twice a week to remove air. The diffusion time were 10 – 28 days which were longer than those used by Guimaraes et al. [64].

For the non-saturated tested exposures, after the described conditioning (moisture homogenization) period, all vacuum bags and plastic layers were removed and the mass of the specimens were recorded. Immediately, finely ground solid sodium chloride (passing #100 sieve) was used as the chloride source and placed on the tested surface of each specimen. For sections A (bottom), the tested surface was on the bottom mold surface (i.e., smooth face with mortar layer). For the middle portion B, the exposed surface was the cut surface between portions A and B. Finally, for the section C, the exposed surface was the cut surface between portions B and C. Coarse aggregate and mortar were exposed to NaCl for portions B and C. After placing the solid NaCl, each specimen was isolated by wrapping with four layers of plastic wrap and placing this arrangement into vacuum bags, and then a manual vacuum pump was used to remove air as much as possible. During the diffusion exposure period, the mass of each specimen was monitored, and vacuum was performed periodically. The diffusion times for 70%, 80%, 90% of the degree of water saturation were 103-130 days, 74-102 days, and 46-69 days, respectively. These exposure durations were at least twice those used by Guimaraes et al. [64]. After the diffusion exposure periods, all vacuum bags and plastic layers were removed, and the NaCl footprint on the top of the specimen was marked. Any remaining NaCl was removed as much as possible without scraping the concrete, and the tested surface of the specimen was then carefully cleaned with compressed air. An octagon shape was marked on the top surface, and vertical cuts were made to minimize edge effects, similar to what was done for bulk diffusion specimens.

For all specimens, the concrete powder was obtained by milling the material in layers parallel to the exposed surface. The first (1st) layer thickness typically was 1mm. The target thickness of the 2nd, 3rd, 4th, 5th and 6th layers was 2mm. In some cases a seventh (7th) layer was obtained, depending on the chloride concentration of the 6th layer. Chloride concentrations were obtained via a total chloride method in accordance with a slightly modified FDOT method [77]. The profiles were fitted to Fick's second law to obtain the apparent diffusion coefficients.

Two cylinders from each mix, DLC1, DCL3, DCL10b, DCL11, cured in RT were used for studying chloride diffusion under non-saturated conditions. Also, three cylinders from mix

DCL2 exposed in RT and another three cylinders from the same mix cured in 14RT/28ET/RT were used for this study. In addition, one cylinder per mix was tested to measure the bulk density, water absorption and porosity (see the results section). As indicated above one cylinder per mix from those cured at RT was used to investigate the diffusion under 100% SD with the top and bottom side of the cylinder exposed. The cover mortar was removed from half of the surface, see Figure 3-31.



Figure 3-31: Specimen for 100% SD with and without mortar layer

#### **3.9.3.4 Bulk Density and Water Absorption of Specimens**

As described above, one cylinder from each mix DLC1, DCL2, DCL3, DCL10b, DCL11 cured in RT and one cylinder from DCL2 cured in 14RT/28ET/RT were used for determining their bulk densities, water absorptions and porosity.

Before testing, all these cylinders were immersed in water for 30 days (approx.) at an age of 150 days from casting. Each cylinder was cut into three pieces (identified as portion A, B, C), which were the bottom section, middle section and top section of each cylinder, respectively. Each section had the same length with the cuts perpendicular to the cylinder axis. All specimens were then re-immersed in saturated  $\text{Ca}(\text{OH})_2$  solution at room temperature ( $21^\circ\text{C}$ ). After reaching full saturation, bulk density and water absorption of these specimens was performed in accordance with ASTM C 642- 06 [65]. The maximum temperature used to dry the specimens was  $60^\circ\text{C}$  as to minimize microstructure changes. The absorption results were used to calculate the target mass for the desired degree of water saturation and also to control/monitor each specimen mass during the non-saturated diffusion test.

### **3.10 Other Tests**

#### **3.10.1 Surface Resistivity of Concrete**

Surface resistivity measurements were initially scheduled to take place every 14 days on three cylinders from each curing group for each mix. Occasionally measurements were not taken exactly 14 days apart due to scheduling conflicts. Once the concrete reached one year of age the measurements were performed about once a month. The surface resistivity measurements were taken on each cylinder (90 degrees apart) and these values were recorded and the average calculated and corrected for finite geometry [72]. Temperature was also measured each time

measurements were performed to normalize all readings to a reference temperature of 21° C during data processing [80] while the specimens were immersed in limewater and exposed in the elevated temperature room. This report include values up-to at least 800 days of age.

The average surface resistivity value was obtained after each set of readings (i.e., the values reported by the meter). This average was then divided by a geometric constant value to obtain the resistivity normalized with respect to geometry. The geometric constant value that was used when measuring cylinders is 2.64 for a probe spacing of 5 cm. The resistivity with respect to geometry was then normalized with respect to temperature by applying procedure described in journal paper[80].

### 3.10.2 Rapid Chloride Migration Test (RCMT)

RCM test was carried out as per NT Build 492 [74]. (Slightly modified see below) For each mix, cylinders (G3) were selected that underwent RMT at 91-100 days, 365 days, 1.5 and 2 years of age. Past day ~90 all cylinders were cured in a high humidity chamber, and if selected for RMT the cylinder was immersed in water for at least 30 days before performing the RCM (this was done instead of using a vacuum pump to saturate the concrete). Table 3-22 shows concrete cylinders and ages for RCMT.

Table 3-21: Concrete cylinders and ages for RCMT

Cyl. No.	Mix													Curing	
	1	2	3	4	5	6	7	8	9	10	10a	10b	11		
3	2 yr													14RT/14ET/RT	
4	1 yr														
6	91-100 day														
8	NA	1 yr	NA											14RT/28ET/RT	
10	1.5 yr	NA	1.5 yr												
11	1 yr	NA	1 yr												
14	91-100 day														
15	91-100 day										NA	91-100 day			
16	2 yr													14RT/77ET/RT	
18	1.5 yr														
19	1 yr														
21	91-100 day														
28	1.5 yr									NA	1.5 yr				RT
30	2yr	1 yr	2 yr							NA	1 yr	2yr			
32		NA								NA					
33	1 yr	NA		1 yr					NA		1 yr				
34		NA							NA						
35	91-100 day														
36	1.5 yr														

Note: RT Cylinders at 2 year for DCL2-23, DCL3-24, DCL10a-25 and 26, none for DCL10

Before performing the cut, surface resistivity measurements were taken on each cylinder designated for RMT at room temperature. The average resistivity was calculated and geometry correction applied.

Then the center was marked and the cylinders were labeled with permanent marker so that all cylinder sections were identifiable after cutting. Next, the cylinders were placed in calcium hydroxide solution for 24-72 hours. The cylinders were first cut in half, dried with a towel, and 50 mm was measured in each direction from the cut. The locations were marked, cut, measured, and placed in calcium hydroxide solution until the migration test would begin (one to three days later).

The resistivity of the 5 cm thick samples was taken using two metal plates that were connected to the four leads of the resistivity meter as per the two point method. The sample rests between the plates and the resistivity can then be measured. The samples were placed in rubber rings and introduced to aquariums containing 10% sodium chloride solution (1.71 M) as shown in Figure 3-32. Each specimen had a stainless steel plate directly beneath the sample. The top of each sample was covered in 0.3 M NaOH solution and the temperature of the solution was measured before and towards the end of the test. Another stainless steel mesh was placed on top of each sample and the current was measured with a 30 V potential difference applied across the sample. Based on this initial measured current and the resistivity of the sample, a potential and duration for the test were selected according to Nordtest 492 [74].

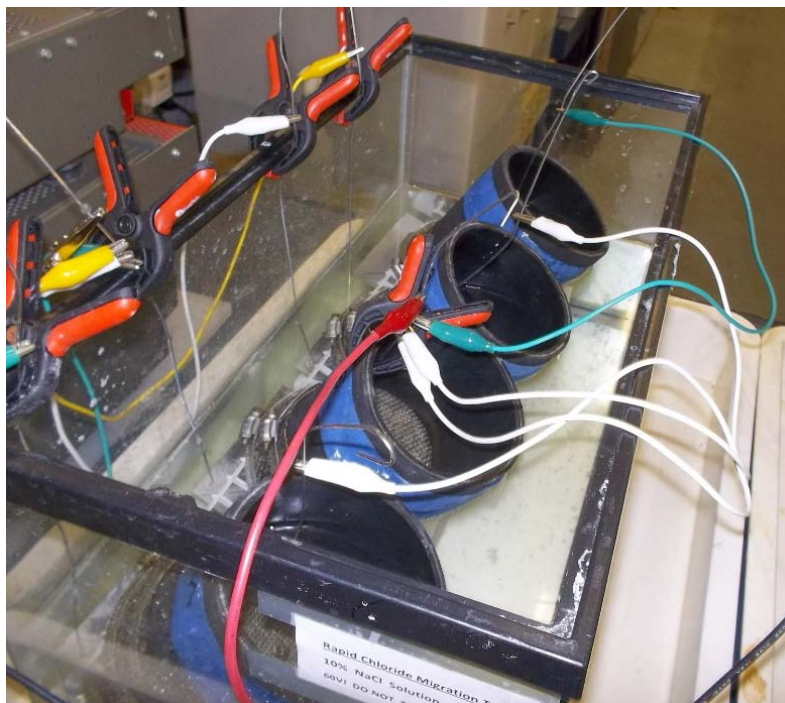


Figure 3-32: RMT setup [74]

After the period of time with the applied potential; the concrete slices were removed from the rubber and broken from the non-exposure side. Silver nitrate solution (0.1N) was sprayed and this exposed the chlorides trapped within the concrete (indicated by a change in color) and calipers were then used to measure the penetration depth at seven locations on each sample. Using this information a non-steady state migration coefficient was derived for each cylinder according to the method described in the standard.

### 3.10.3 Wet Candle Test

This test was performed in accordance ASTM G 140-02 [49]/ISO9225 [81]. The wet candle method was used to determine chloride deposition from seawater spray at outdoor exposure. The wet candle pictured in Figure 3-33 was used as an environmental indicator to preview chloride accumulation tendencies into concrete. It consists of a fabric-wrapped test-tube in which the fabric was kept wet with reagent water (30% glycerol/water solution) inside the flask. The wet fabric acted as a collector for chloride particulates. Particles of salt or spray were trapped by the wet fabric and retained. Monthly, a quantitative determination of the chloride collected by the fabric was made and a new fabric was exposed. Titrations were performed to determine chloride concentration of the solution.

Relative humidity and temperature data was collected to assist in data analysis. Wet candles were placed at the following sites: on the east property, the west property, and on the barge adjacent to the block samples. A sampling period of one month was used. Longer time periods can be a problem because the water in the beaker must not be allowed to dry up. It is important to protect the wet candle from rain water with a cover above it. In order to compensate for the high evaporation potential of the environment, bottles contained a 30% glycerol solution per ISO/DIS 9225 recommendations when ambient temperature exceeds 25° C.



Figure 3-33: Wet candle apparatus

### 3.10.4 Chloride Analysis of Concrete Powders

Total chloride concentrations were determined following FDOT FM-5-516 [77] slightly modified. The water soluble (Free) chloride was measured on selected specimens tested for bulk diffusion following AFREM-RILEM [78] method.

### 3.10.5 Porosity

Porosity was measured once specimens reached 180 days, one year, and 1.5 years of age. For those tested at 180 days, Section 3.9.3.4 describes how the concrete cylinder specimens were sliced in three pieces and how the porosity was measured. For the other two instances, the concrete cylinders were sliced into four slices of the same length. The center slices were subjected to the RCMT tests as described in section 3.10.2. The top and bottom slices were subjected to porosity test according to ASTM C642[65]. Because all the specimens were cured in high humidity and then immersed for at least 30 days before performing the porosity test (specimens were already water-saturated or close to), the test procedure in ASTM C642 was slightly modified as follows:

- 1: Measure the saturated, surface-dried mass  $C$ .
- 2: Measure the apparent weight in water  $D$ .
- 3: Measure the oven-dry mass ( $A$ ) at the time when the difference between the last two successive weight values is less than 0.5 % of the lowest value obtained.
- 4: Calculate the volume of permeable voids % =  $(C-A)/(C-D)$ .

To avoid the evaporation of the gel water, the temperature in the oven was adjusted to 60°C - 70°C rather than using the temperature range indicated in ASTM C642 (100°C - 110°C)[65]. The porosity value for each cylinder was the average of the top and bottom slices.

## 4 Experimental Results

The following table contains the physical properties measured on the thirteen mixes. It includes the density values, 28 day surface resistivity (as read from the meter with 3.8 cm spacing), 28 day compression strength results, and the initial chloride concentration done on a cylinder per mix at 28 days.

Table 4-1: Mix properties

Mix	Density (kg/m <sup>3</sup> )	Slump (m)	Air (%)	Unit Weight (kg/m <sup>3</sup> )	Mix Temp (°F)	Initial Chloride (kg/m <sup>3</sup> )	SR 28 day RT (kOhm-cm)	Compression (N/m <sup>2</sup> )
<b>DCL1</b>	2242.29	0.07	7	2193	73	0.08	13.8	5.302E+07
<b>DCL2</b>	2220.54	0.06	3.5	2255	76	0.16	9.9	5.102E+07
<b>DCL3</b>	2186.97	0.21	2.2	2239	75	0.09	7.7	4.178E+07
<b>DCL4</b>	2232.56	0.18	9.4	2109	72	0.12	45.0	4.992E+07
<b>DCL5</b>	2210.05	0.08	4.5	2207	72	0.10	34.0	5.516E+07
<b>DCL6</b>	2178.45	0.10	1.9	2243	74	0.11	24.7	5.171E+07
<b>DCL7</b>	2246.90	0.20	2.8	2274	72	0.08	24.8	6.136E+07
<b>DCL8</b>	2224.00	0.07	4.5	2227	72	0.08	22.6	5.364E+07
<b>DCL9</b>	2191.10	0.21	4.5	2192	73	0.11	17.2	4.406E+07
<b>DCL10</b>	2246.21	0.14	13	2041	75	0.08	11.7	2.875E+07
<b>DCL10a</b>	2246.24	0.15	9.5	2115	75	0.12	11.5	3.689E+07
<b>DCL10b</b>	2244.46	0.08	5.6	2216	73	0.09	9.6	4.964E+07
<b>DCL11</b>	2248.84	0.07	4	2270	72	0.18	10.8	5.143E+07

### 4.1 Resistivity

Figure 4-1 presents the average concrete resistivity values for specimens cured at RT. The top row corresponds to the plots of the resistivity for the DCL1, DCL2, DCL3, DCL4, DCL5, and DCL6; on the bottom row, the plots represent the resistivity of DCL7, DCL8, DCL9, DCL10, DCL10b and DCL11. As seen on the figure, the group of specimens with a composition of 20%FA+8%SF (DCL4, DCL5, and DCL6) had higher resistivity values than the other mixes. On the other hand, DCL7, DCL8, and DCL9 appeared to have consistently lower resistivity values. Also, specimens with low w/cm ratio (0.35) had a higher resistivity when compared to the mixes with a w/cm ratio of 0.41, and 0.47; as would be expected. For instance, DC1 had a resistivity range between 6.5 kohm-cm to 45 kohm-cm while DCL2 had a resistivity range of 7 kohm-cm to 29 kohm-cm.

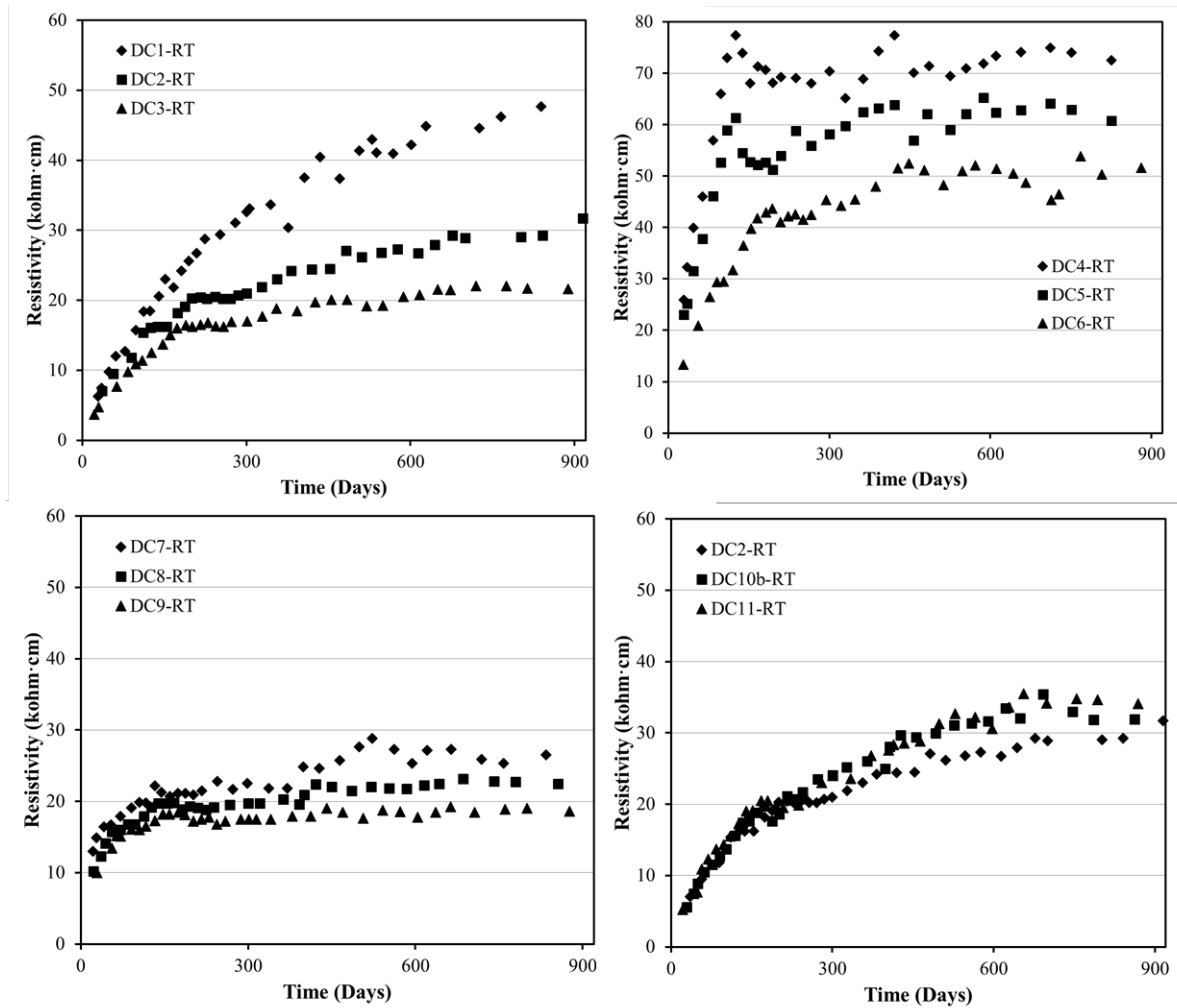


Figure 4-1: Resistivity for DCL specimens cured at RT vs. time

Figures 4-2, 4-3 and 4-4 show the resistivity of DCL1, DCL4, DCL7 (G3 specimens) cured at the four curing regimes: 14RT/14ET/RT, 14RT/28ET/RT, 14RT/77ET/RT, RT, respectively. The w/cm ratio of cylinders from DCL1, DCL4, and DCL7 is 0.35. This is the lowest w/cm investigated, hence it corresponds to the highest resistivity values measured when compared to the values from higher w/cm samples.

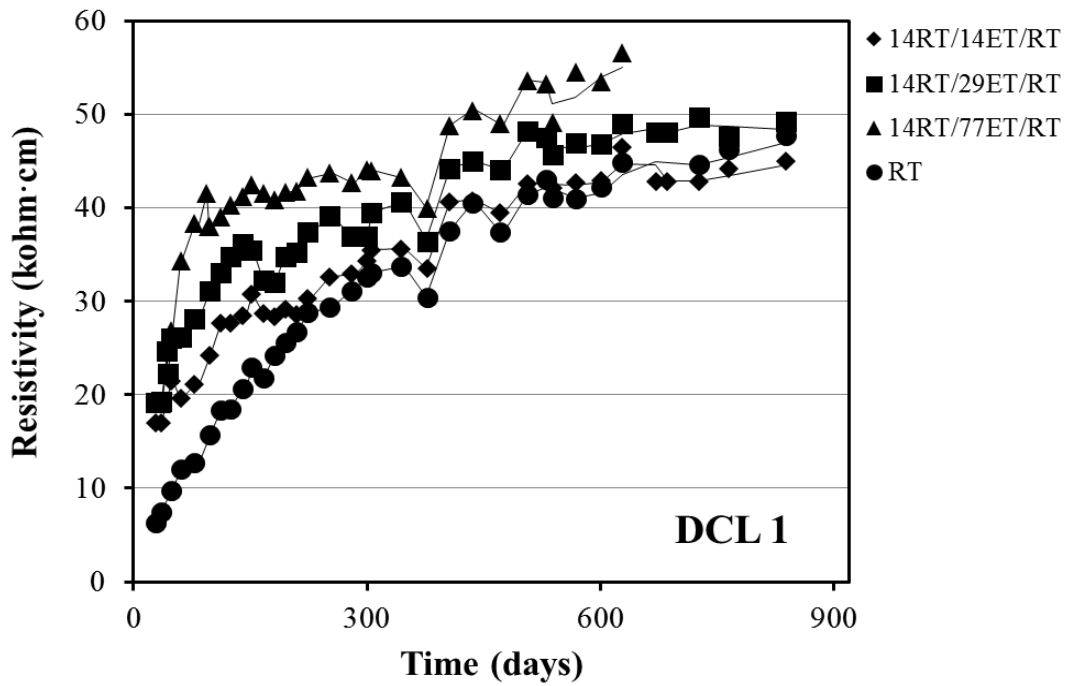


Figure 4-2: DCL1 resistivity

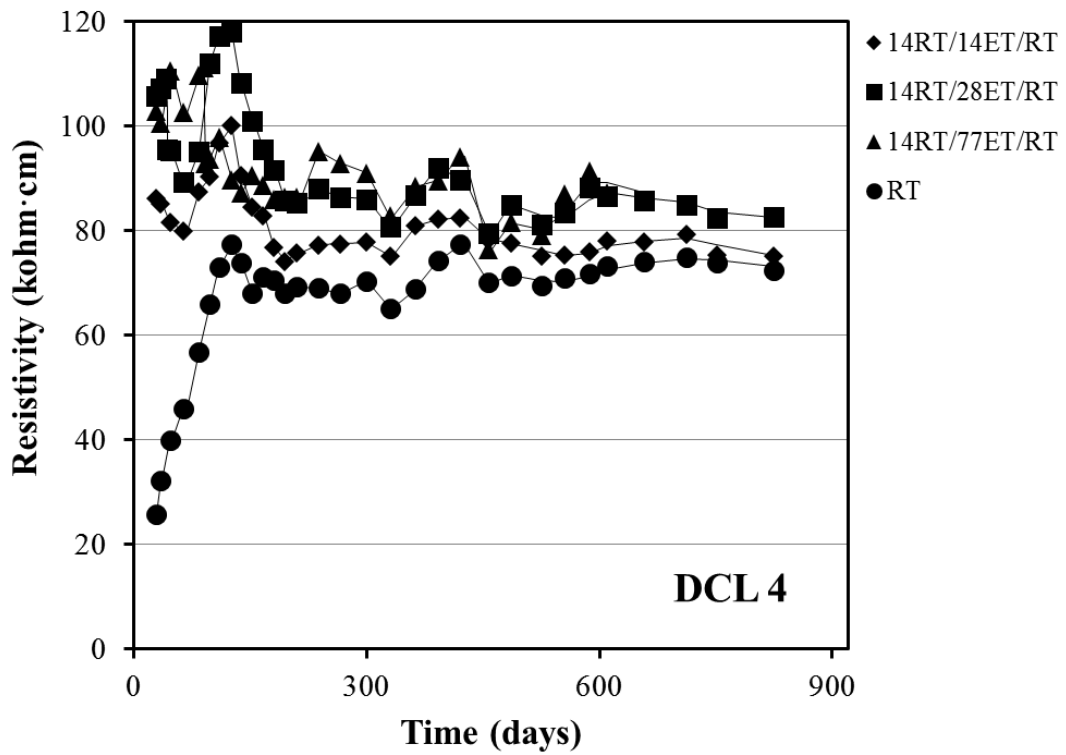


Figure 4-3: DCL4 resistivity

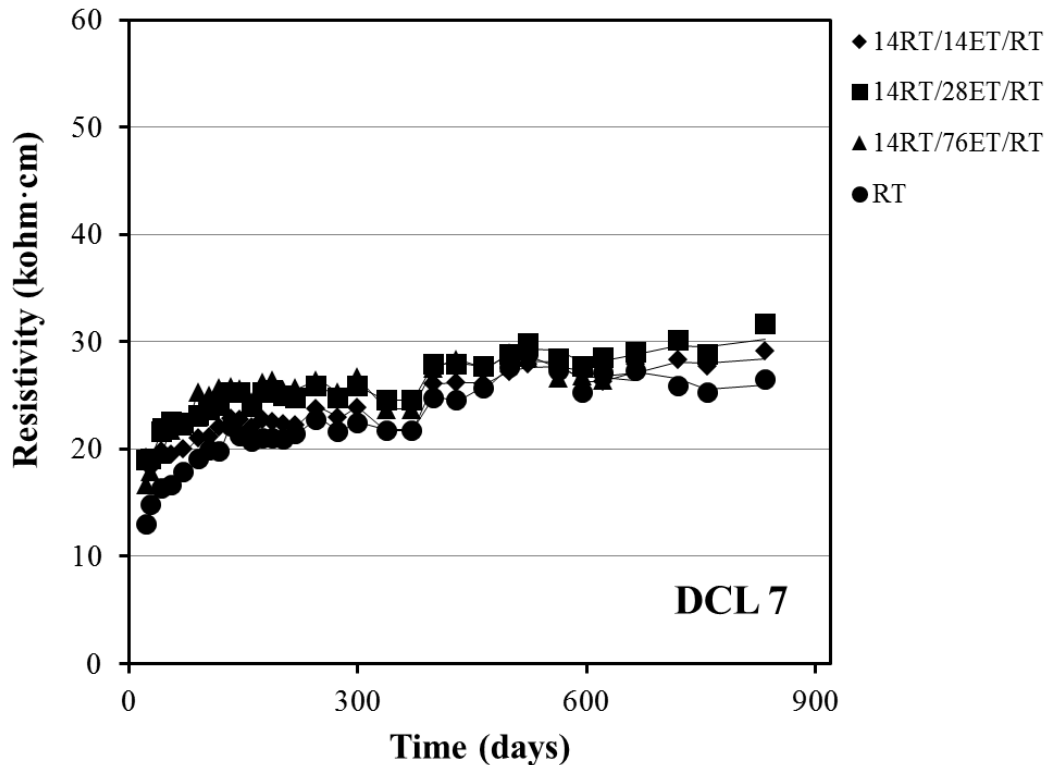


Figure 4-4: DCL7 resistivity

Cylinders from DCL1 contained 20% FA (Figure 4-2). The resistivity of these cylinders increased with time spent curing at the elevated temperature room. Also, there was a measured increase in resistivity as the cylinders aged for all curing regimes, once exposed at room temperature and high humidity.

DCL4 cylinders contained 20% FA + 8% SF. The silica fume incorporated into DCL4 resulted in concrete of greater than twice the resistivity of the samples from DCL1. The resistivity of the DCL4 cylinders from all 4 curing regimes increased as the specimens aged, up-to day ~125. In subsequent measurements taken resistivity values leveled off. Cylinders cured at elevated temperature for the longest period of time were found to have a higher resistivity than those that left the accelerated cure earlier on. Once the specimens were transferred to high humidity and lab temperature, the measured resistivity value dropped below the values of the cylinders that left elevated temperature after 28 days. Two factors might explain this unexpected observation. The temperature normalized resistivity value should have been lower than the one predicted by the used equation, however this drop in resistivity is also observed on the 14RT/28ET/RT series. A more likely explanation for the increase in resistivity observed on the 14RT/28ET/RT is that the high humidity was not maintained (i.e., it was lower) until about day 125 which allowed the concrete to have a lower saturation degree and hence a higher resistivity. Once this trend was identified the humidity was increased again, by having more periodic water sprays into the storage container. The relative humidity was better controlled since then and hence resulting in more stable resistivity trends.

DCL7 cylinders contained 50% slag and were found to have a consistently lower resistivity than the DCL1 concrete cylinders (20% FA) as the cylinders aged. For DCL7 specimens the resistivity increased with age up to about 140 days then values leveled off, past day 300 a small increase in resistivity was observed. Cylinders containing 50% slag appear to be affected less by changing curing conditions than the cylinders containing 20% fly ash or 20% fly ash + 8% silica fume.

Only typical results were evaluated in this section but all mixes and curing regimes were measured and processed periodically. The results are used to interpret the significance of the calculated apparent diffusion coefficients described in the discussion section. Appendix C contains the resistivity evolution vs. time for the four curing regimes for mixtures other than DCL1, DCL4 and DCL7.

Figure 4-5 shows the resistivity values measured on concrete cylinders cured under the four different regimes upon reaching 300 days. DCL1, 2, and 3 cylinders cured at elevated temperature for 77 days, measured on average 34 % higher resistivity than those which were cured at room temperature. After 300 days DCL4, 5, and 6 cylinders followed the same pattern as DCL1, 2, and 3. However, what is not shown in Figure 4-5 is that after being removed from elevated temperature near day 90, cylinders from DCL4 and 6 which cured in elevated temperature for 28 days (14RT/28ET/RT) measured a higher resistivity than those which cured for 77 days at elevated temperature (14RT/77ET/RT). The moisture content was increased within the room temperature storage chambers. By day 200, the 14RT/77ET/RT cylinders were measuring higher than the other groups as should be expected for cylinders cured under that regime. DCL7, 8, and 9 cylinders followed the same pattern of w/cm ratios as DCL1, 2, and 3. The w/cm ratio and the curing condition had less influence on the resistivity values than was the case for the other mixes. DCL10, 10a, 10b, and 11 were composed of 20% fly ash and had w/cm ratios of 0.41. The cementitious content was lower for DCL11 and had resistivity values that were comparable to those from DCL10.

The w/cm ratio influences the effect of concrete curing on resistivity. The cylinders with a lower w/cm ratio were found to have the greatest difference in resistivity between the cylinders placed under an accelerated curing regime and those which were not. Those cylinders cured at RT in general had the lowest resistivity when compared to the same mix and other curing regimes. Cylinders that spent more time curing at elevated temperature measured higher resistivity than those that spent less time at elevated temperature. By day 300, cylinders from DCL3 that cured for 28 days at ET and those that cured for 77 days at ET had a difference of only ~0.1 kohm-cm. All the samples composed of 50% slag (DCL7, 8, and 9) had lower resistivity than those containing different admixtures and also a lower average change due to changing the curing regime than the mixes containing the other admixtures.

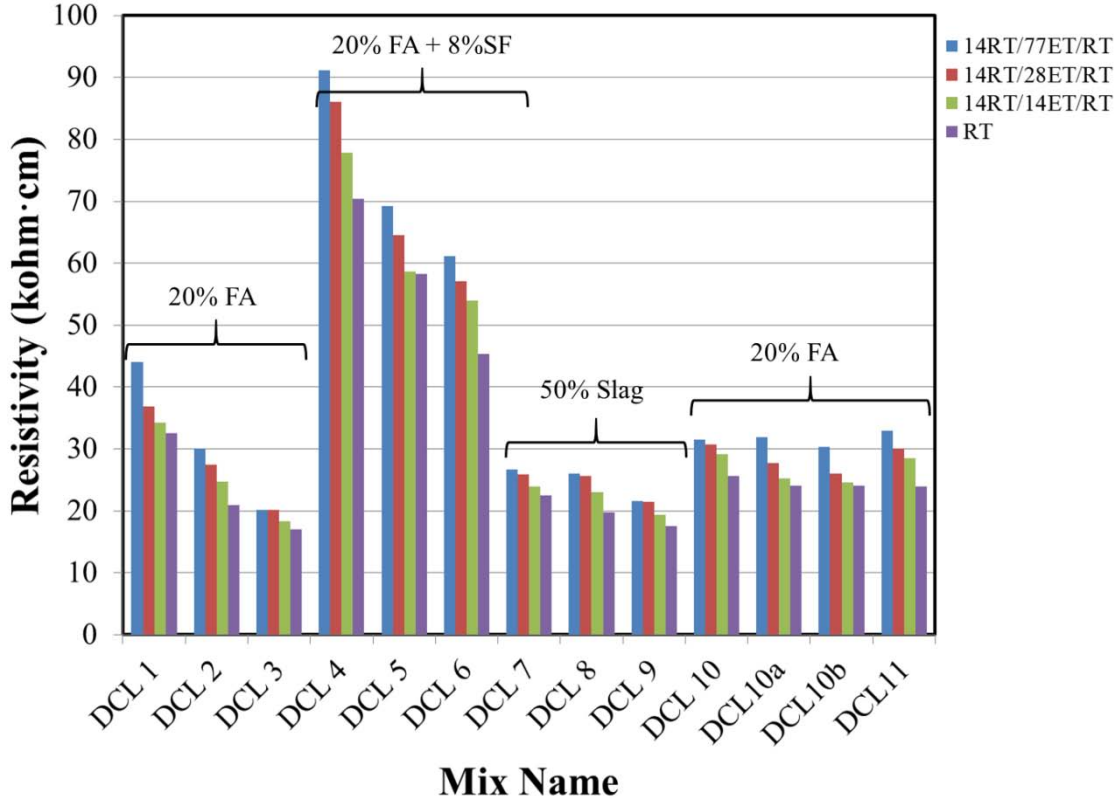


Figure 4-5: G3 specimens resistivity after 300 days

#### 4.2 Rapid Chloride Migration Coefficients (RCMT)

The RCMT test was performed on the cylinders at 91-100 days, 365 days, 540 and 730 days of age as per NT Build 492 [74], respectively. The  $D_{nssm}$  for each specimen was calculated by using the following equation:

$$D_{nssm} = \frac{0.0239(273+T)L}{(U-2)t} \left[ x_d - 0.0238 \sqrt{\frac{(273+T)Lx_d}{U-2}} \right] \quad (10)$$

Where:

$D_{nssm}$  = non-steady-state migration coefficient [ $\times 10^{-12}$  m<sup>2</sup>/s]

$U$  = voltage applied [V]

$T$  = average of initial and final temperatures of anolyte solution [°C]

$L$  = specimen thickness [mm]

$x_d$  = penetration depth of chloride [mm, obtained by measuring

$t$  = test duration [hour]

Each concrete cylinder had two center slices which underwent RCMT. Results of RCMT test and the corresponding 21 °C resistivity values measured before performing RCMT tests are listed in Tables 4-2, 4-3, 4-4, in which the  $D_{nssm}$  values shown are the average of the two center slices per specimen tested performed at the indicated ages. Similarly one data point for each tested concrete cylinder is shown in the plots. Figure 4-6 shows the  $D_{nssm}$  values vs. resistivity values

grouped per age at the time of testing. Figures 4-7, 4-8, 4-9 and 4-10 show the non-steady-state migration coefficient ( $D_{nssm}$ ) vs. resistivity for different grouping for the four base mixture groups per supplementary cementitious type or cementitious content as well as the concrete age at the time of testing.

Table 4-2: RMT performed on specimens at 90 to 100 days

Specimen ID	$\rho_{21}$ kohm-cm	$D_{nssm}$ ( $10^{-12}$ m <sup>2</sup> /s)	Specimen ID	$\rho_{21}$ kohm-cm	$D_{nssm}$ ( $10^{-12}$ m <sup>2</sup> /s)
DCL 1-6	24.5	4.8	DCL 7-6	21.9	4.1
DCL 1-14	27.6	4.2	DCL 7-14	25.5	3.4
DCL 1-15	29.5	5.5	DCL 7-15	24.3	3.1
DCL 1-21	36.8	2.9	DCL 7-21	24.2	2.9
DCL 1-35	16.8	6.4	DCL 7-35	19.0	5.6
DCL 1-36	15.2	6.6	DCL 7-36	21.6	5.7
DCL 2-6	18.1	7.2	DCL 8-6	22.1	4.8
DCL 2-14	21.9	6.4	DCL 8-14	21.2	6.2
DCL 2-15	21.9	5.5	DCL 8-15	22.6	4.0
DCL 2-21	30.3	4.0	DCL 8-21	22.5	3.0
DCL 2-35	12.5	7.8	DCL 8-35	18.1	6.2
DCL 2-36	12.5	5.7	DCL 8-36	17.0	5.6
DCL 3-6	13.7	7.2	DCL 9-6	18.2	4.5
DCL 3-14	15.5	6.3	DCL 9-14	18.6	4.3
DCL 3-15	14.9	6.4	DCL 9-15	19.8	3.8
DCL 3-21	19.5	4.5	DCL 9-21	18.8	3.4
DCL 3-35	10.8	8.2	DCL 9-35	14.6	4.3
DCL 3-36	10.7	9.3	DCL 9-36	14.6	4.2
DCL 4-6	88.6	2.2	DCL 10-6	20.7	7.9
DCL 4-14	85.4	1.9	DCL 10-14	23.9	5.8
DCL 4-15	82.3	1.7	DCL 10-15	22.3	6.5
DCL 4-21	92.9	1.0	DCL 10-21	29.0	5.9
DCL 4-35	72.2	2.4	DCL 10-35	14.0	10.1
DCL 4-36	64.5	2.3	DCL 10-36	15.0	8.1
DCL 5-6	70.0	1.9	DCL 10a-6	22.6	6.5
DCL 5-14	68.1	1.6	DCL 10a-14	22.5	6.1
DCL 5-15	72.2	1.7	DCL 10a-15	23.6	8.8
DCL 5-21	66.8	0.9	DCL 10a-21	30.8	4.7
DCL 5-35	48.6	2.3	DCL 10a-35	13.6	9.3
DCL 5-36	68.0	2.6	DCL 10a-36	14.1	12.4
DCL 6-6	42.5	3.8	DCL 10b-6	19.6	6.5
DCL 6-14	50.3	3.3	DCL 10b-14	20.7	5.0
DCL 6-15	51.5	3.5	DCL 10b-15	21.8	4.0
DCL 6-21	63.7	2.2	DCL 10b-21	26.4	3.9
DCL 6-35	28.7	4.5	DCL 10b-35	14.2	6.7
DCL 6-36	31.0	5.2	DCL 10b-36	12.8	7.0
DCL 11-21	29.8	4.0	DCL 11-6	22.1	4.6
DCL 11-35	13.0	7.3	DCL 11-14	24.4	5.9
DCL 11-36	13.1	7.4	DCL 11-15	24.7	5.6



Table 4-4: RMT performed on specimens after 1.5 years and 2 years of age

RMT 1.5 yrs			RMT 2 yrs		
Specimen ID	$\rho_{21}$ kohm·cm	Dnssm ( $10^{-12}$ m <sup>2</sup> /s)	Speciment ID	$\rho_{21}$ kohm·cm	Dnssm ( $10^{-12}$ m <sup>2</sup> /s)
DCL1-10	50.8	1.5	DCL1-3	53.8	1.5
DCL1-18	54.9	2.9	DCL1-16	61.6	1.5
DCL1-28	40.0	2.0	DCL1-30	49.2	1.5
			DCL1-32	53.8	1.8
DCL2-18	38.1	1.6	DCL2-3	39.6	1.9
DCL2-24	33.1	1.7	DCL2-16	40.3	2.3
			DCL2-23	36.7	2.3
DCL3-10	26.8	3.3	DCL3-3	24.1	2.3
DCL3-18	24.3	3.6	DCL3-16	23.0	2.4
DCL3-28	25.4	3.5	DC3-24	23.1	2.5
DCL4-10	96.6	1.3	DC4-3	91.5	1.6
DCL4-18	96.9	1.5	DC4-16	101.0	1.0
DCL4-28	88.0	1.1	DC4-30	89.4	1.4
			DC4-32	95.6	1.6
DCL5-10	72.8	1.2	DC5-3	64.1	1.3
DCL5-18	77.5	1.3	DC5-16	70.8	1.0
DCL5-28	71.7	1.4	DC5-30	75.7	1.3
			DC5-32	76.7	1.3
DCL6-10	66.6	1.3	DC6-3	66.1	1.6
DCL6-18	69.9	1.2	DC6-16	65.2	1.3
DCL6-28	55.0	1.8	DC6-30	52.8	1.5
			DC6-32	51.5	1.4
DCL7-10	29.0	3.0	DC7-3	32.0	1.8
DCL7-18	29.3	3.3	DC7-16	31.4	1.6
DCL7-28	27.2	2.2	DC7-30	29.8	1.5
			DC7-32	31.3	2.0
DCL8-10	27.2	3.1	DC8-3	28.7	1.9
DCL8-18	27.1	2.2	DC8-16	30.8	1.8
DCL8-28	23.6	2.5	DC8-30	24.4	2.7
			DC8-32	24.6	2.2
DCL9-10	24.8	2.4	DC9-3	23.6	2.4
DCL9-18	21.7	2.7	DC9-16	24.1	2.3
DCL9-28	17.3	2.4	DC9-30	19.6	2.9
			DC9-32	20.1	2.7
DCL10-10	37.5	2.0	DC10-3	39.4	2.3
DCL10-18	34.0	2.2	DC10-16	41.8	2.4
			DC10a-3	38.4	2.2
			DC10a-16	38.5	2.1
			DC10a-25	34.0	2.5
			DC10a-26	36.7	2.7
DCL10b-10	34.9	2.6	DC10b-3	38.0	2.9
DCL10b-18	33.5	2.6	DC10b-16	37.8	2.6
DCL10b-28	34.5	3.2	DC10b-30	35.0	2.5
			DC10b-32	33.7	3.1
DCL11-10	37.7	1.3	DC11-3	39.4	3.0
DCL11-18	36.2	1.9	DC11-16	37.0	2.0
DCL11-28	33.9	1.7	DC11-30	39.5	2.8
			DC11-32	38.4	2.0

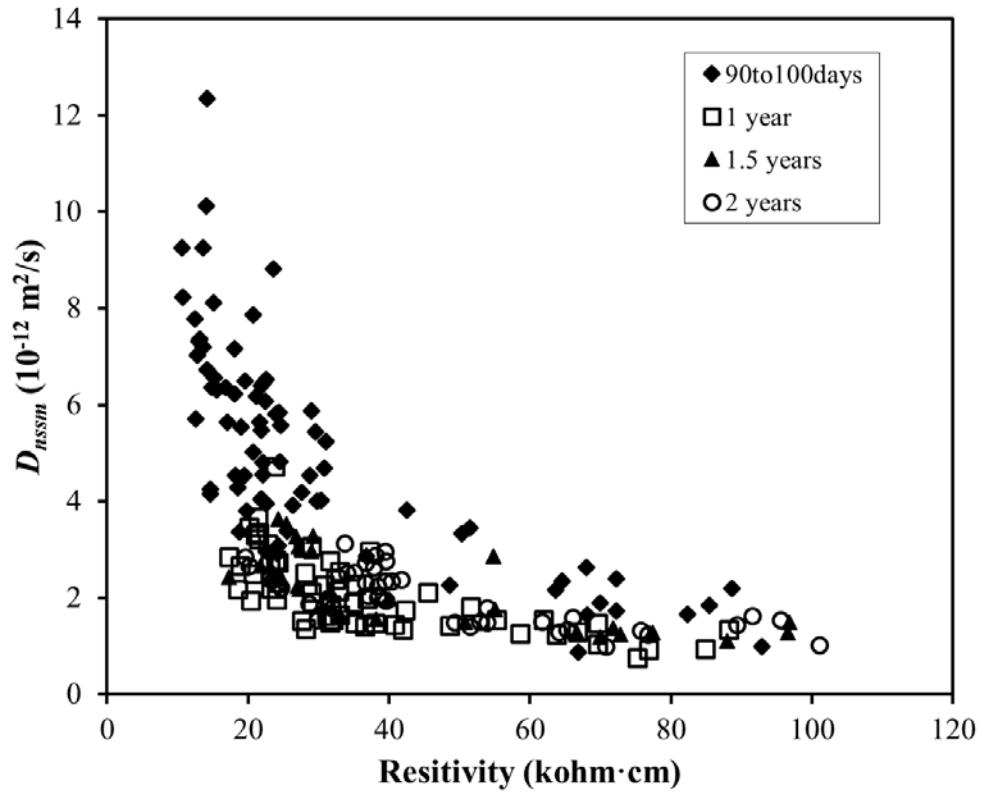


Figure 4-6:  $D_{nssm}$  vs. resistivity grouped by age at time of testing

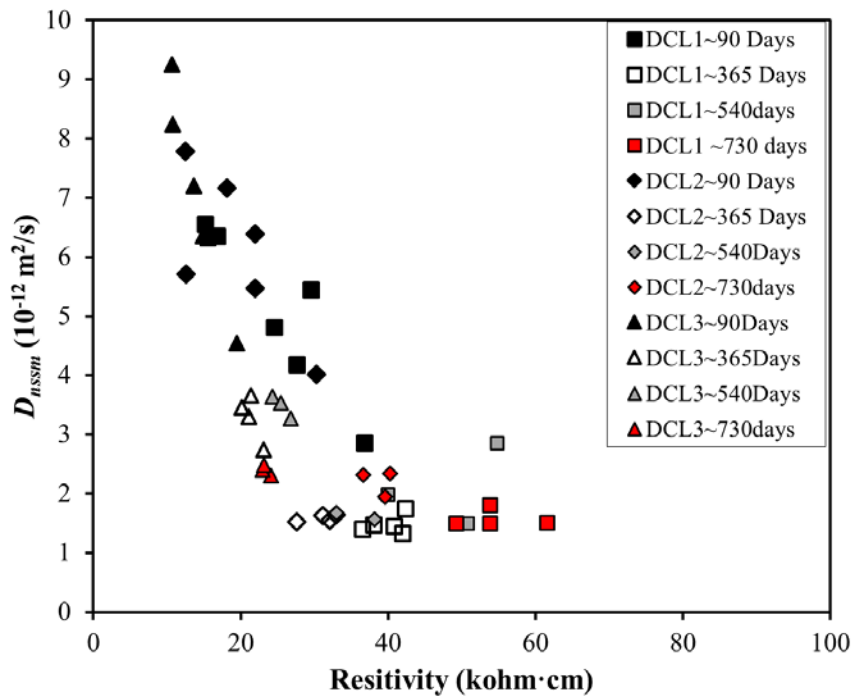


Figure 4-7: DCL1, DCL2 and DCL3  $D_{nssm}$  vs. resistivity

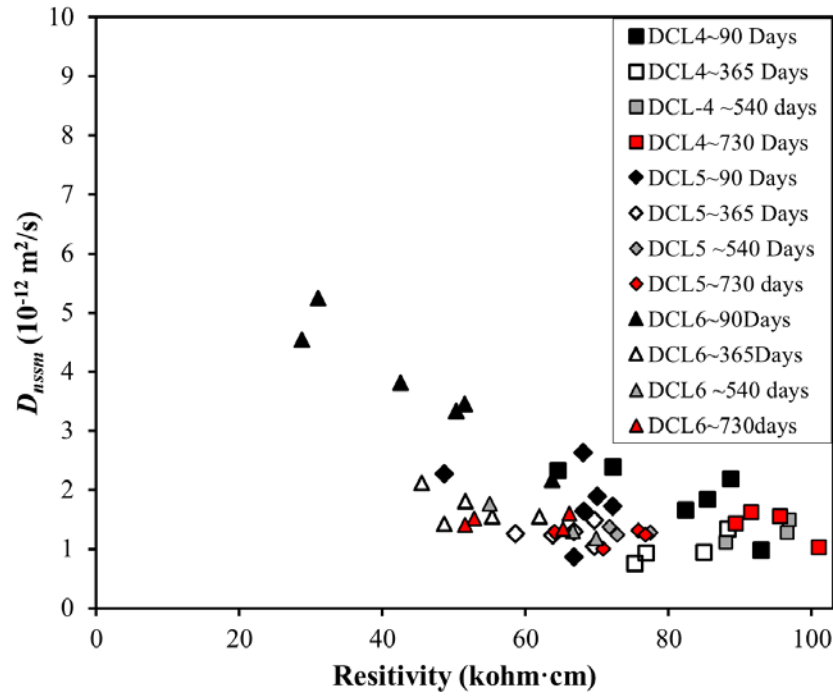


Figure 4-8: DCL4, DCL5, and DCL6  $D_{nssm}$  vs. resistivity

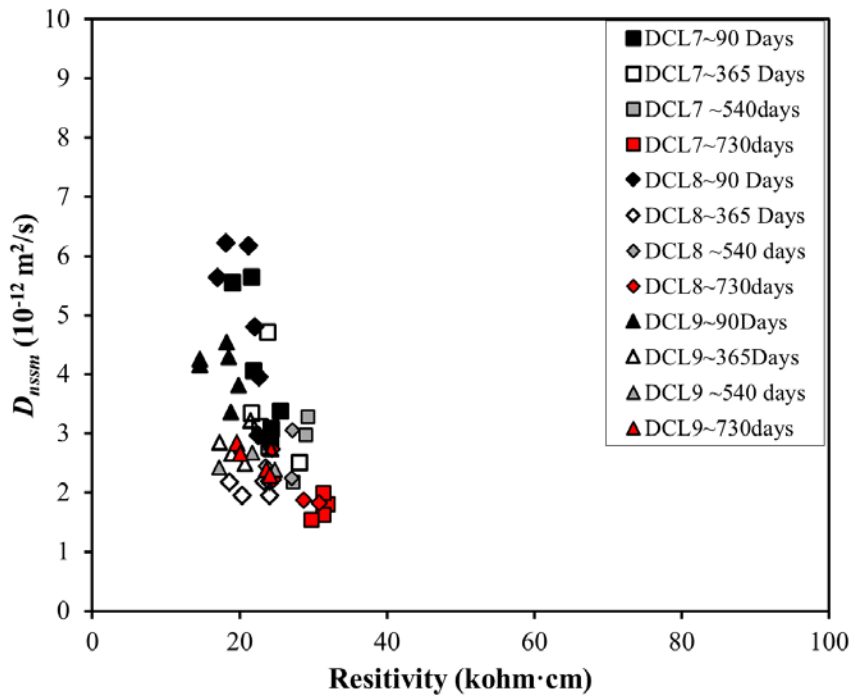


Figure 4-9: DCL7, DCL8, and DCL9  $D_{nssm}$  vs. resistivity

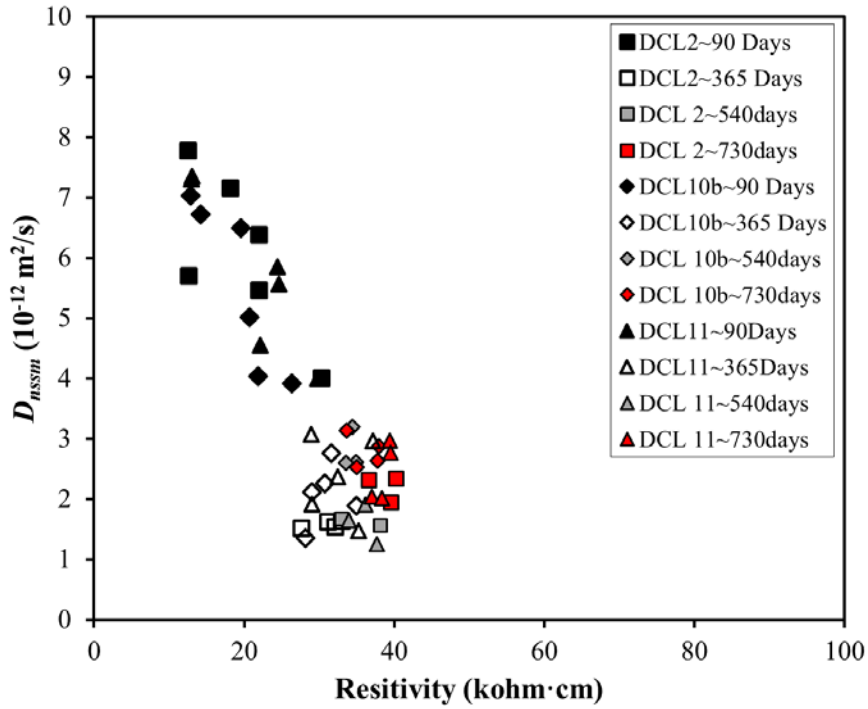


Figure 4-10: DCL2, DCL10b, and DCL11  $D_{nssm}$  vs. resistivity

### 4.3 Porosity

Cylinder slices were subjected to porosity test according to ASTM C642 [65] at 180 days, 365 and approximately 540 days of age. Table 4-5 shows the porosity measured for the top and bottom slices, the average porosity per cylinder and the corresponding resistivity (if available) value measured just before the porosity test. In general specimens with lower w/cm had the lower porosity values. There was a modest effect due to the various curing regimes used.

Table 4-5: Porosity measured at various ages on specimens of groups DCL1 to DCL6

Days	Specimen ID	Porosity by Volume			Resistivity kohm·cm
		Top	Bottom	Average	
180	DC1-12	5.2	5.5	5.4	39.4
	DC1-29	5.6	5.5	5.5	23.3
	DC1-15	7.0	5.5	6.2	29.5
	DC1-36	6.4	6.2	6.3	15.2
360	DC1-4	5.4	4.8	5.1	42.3
	DC1-11	5.3	4.4	4.9	40.8
	DC1-19	4.6	4.1	4.3	42.0
	DC1-33	4.9	5.7	5.3	38.0
	DC1-34	4.7	4.8	4.8	36.5
540	DC1-10	6.1	5.1	5.6	50.8
	DC1-18	6.3	5.2	5.7	54.9
	DC1-28	7.2	5.8	6.5	40.0
180	DC2-12	7.7	6.6	7.2	28.6
	DC2-29	7.8	7.9	7.8	22.6
360	DC2-4	6.4	5.6	6.0	33.0
	DC2-8	6.4	4.7	5.6	31.2
	DC2-19	6.0	4.9	5.5	32.1
	DC2-30	6.2	5.2	5.7	27.6
540	DC2-18	8.0	6.1	7.0	38.1
	DC2-24	7.7	7.1	7.4	33.1
180	DC3-12	10.5	8.5	9.5	19.1
	DC3-29	10.5	9.8	10.2	14.5
360	DC3-4	8.8	7.2	8.0	21.1
	DC3-11	8.9	6.0	7.4	21.4
	DC3-19	9.0	6.5	7.8	23.1
	DC3-30	8.9	7.3	8.1	20.1
540	DC3-10	10.8	8.6	9.7	26.8
	DC3-18	10.9	8.2	9.5	24.3
	DC3-28	10.3	8.9	9.6	25.4
Days	Specimen ID	Porosity by Volume			Resistivity kohm·cm
		Top	Bottom	Average	
180	DC4-12	5.7	6.0	5.8	95.7
	DC4-29	5.4	5.9	5.6	75.0
	DC4-15	6.8	7.1	6.9	
	DC4-36	6.8	7.0	6.9	
360	DC4-4	8.4	7.3	7.8	75.2
	DC4-11	7.7	7.3	7.5	84.9
	DC4-19	7.2	6.3	6.7	88.2
	DC1-34	4.7	4.8	4.8	36.5
540	DC1-10	6.1	5.1	5.6	50.8
	DC4-18	6.2	6.3	6.3	96.9
	DC4-28	7.4	7.4	7.4	88.0
180	DC5-12	5.9	6.2	6.1	65.7
	DC5-29	5.7	6.2	5.9	51.5
	DC5-15	7.2	5.9	6.5	
	DC5-36	7.2	7.1	7.2	
360	DC5-4	6.9	6.2	6.6	69.6
	DC5-11	6.8	6.2	6.5	63.8
	DC5-19	6.3	6.1	6.2	69.6
	DC5-33	8.2	7.0	7.6	66.7
	DC5-34	7.5	6.7	7.1	58.5
540	DC5-10	6.5	6.3	6.4	72.8
	DC5-18	7.1	6.2	6.7	77.5
	DC5-28	6.4	6.4	6.4	71.7
180	DC6-12	5.9	5.5	5.7	60.3
	DC6-29	6.2	5.9	6.0	35.4
360	DC6-4	8.3	7.2	7.8	51.5
	DC6-11	7.7	7.1	7.4	55.3
	DC6-19	7.5	6.4	6.9	61.9
	DC6-33	8.1	7.5	7.8	48.6
540	DC6-34	7.9	6.9	7.4	45.4
	DC6-10	8.1	7.1	7.6	66.6
400	DC6-18	7.3	6.7	7.0	69.9
	DC6-28	8.1	7.5	7.8	55.0

Table 4-6: Porosity measured at various ages on specimens of groups DCL7 to DCL11

Days	Specimen ID	Porosity by Volume			Resistivity kohm·cm
		Top	Bottom	Average	
180	DC7-12	5.7	6.0	5.8	23.8
	DC7-29	6.3	5.8	6.1	23.9
	DC7-15	6.6	5.6	6.1	
	DC7-36	8.0	6.3	7.2	
360	DC7-4	7.6	6.2	6.9	23.8
	DC7-11	6.8	6.5	6.6	23.9
	DC7-19	7.9	6.1	7.0	28.0
	DC7-33	8.0	7.0	7.5	22.8
540	DC7-34	8.2	7.0	7.6	21.6
	DC7-10	6.6	5.7	6.2	29.0
	DC7-18	7.3	5.5	6.4	29.3
810	DC7-28	7.6	6.1	6.9	27.2
	DC8-12	6.2	6.1	6.2	25.1
	DC8-29	6.9	6.5	6.7	20.0
1080	DC8-15	6.8	6.2	6.5	
	DC8-36	8.3	7.3	7.8	
	DC8-4	6.8	5.5	6.1	23.3
	DC8-11	6.8	5.1	6.0	24.1
1350	DC8-19	6.3	5.3	5.8	24.1
	DC8-33	7.4	6.1	6.7	20.4
	DC8-34	7.0	5.8	6.4	18.6
1620	DC8-10	7.4	6.2	6.8	27.2
	DC8-18	6.6	5.5	6.1	27.1
	DC8-28	7.2	5.9	6.5	23.6
1890	DC9-12	7.2	6.9	7.1	24.6
	DC9-29	7.2	6.3	6.7	15.6
	DC9-15	9.1	7.0	8.0	
	DC9-36	12.0	7.0	9.5	
2160	DC9-4	9.8	8.6	9.2	21.5
	DC9-11	9.5	7.8	8.7	24.2
	DC9-19	8.9	7.9	8.4	20.7
	DC9-33	11.5	7.3	9.4	17.3
	DC9-34	10.1	8.2	9.1	18.9
2430	DC9-10	9.3	7.6	8.5	24.8
	DC9-18	9.3	6.8	8.0	21.7
2700	DC9-28	9.6	8.3	8.9	17.3
Days	Specimen ID	Porosity by Volume			Resistivity kohm·cm
		Top	Bottom	Average	
180	DC10-12	9.0	7.2	8.1	23.9
	DC10-15	6.4	5.4	5.9	22.3
	DC10-36	6.5	6.7	6.6	15.0
360	DC10-4	7.9	6.5	7.2	31.6
	DC10-11	7.6	6.7	7.2	31.7
	DC10-19	6.8	6.0	6.4	37.0
540	DC10-10	9.0	8.5	8.7	37.5
	DC10-18	7.7	7.5	7.6	34.0
810	DC10a-12	5.4	5.3	5.4	27.7
	DC10a-29	7.0	6.5	6.7	20.0
1080	DC10a-4	6.9	6.0	6.4	32.9
	DC10a-11	6.3	5.4	5.9	33.0
	DC10a-19	6.0	5.3	5.6	35.3
	DC10a-30	7.4	6.6	7.0	27.9
1350	DC10b-12	8.5	8.9	8.7	20.1
	DC10b-29	9.5	9.6	9.5	19.3
	DC10b-15	9.5	7.9	8.7	
	DC10b-36	8.8	9.3	9.1	
1620	DC10b-4	8.3	8.6	8.5	30.8
	DC10b-11	10.0	7.8	8.9	31.6
	DC10b-19	9.7	7.5	8.6	35.0
	DC10b-33	8.2	8.4	8.3	28.2
	DC10b-34	8.6	7.8	8.2	29.0
1890	DC10b-10	8.1	6.6	7.3	34.9
	DC10b-18	7.9	6.8	7.3	33.5
	DC10b-28	9.4	7.4	8.4	34.5
2160	DC11-12	7.6	7.9	7.7	31.1
	DC11-29	8.5	7.5	8.0	20.2
	DC11-15	6.4	4.3	5.3	
	DC11-36	6.5	5.5	6.0	
2430	DC11-4	8.4	7.0	7.7	35.2
	DC11-11	8.2	6.9	7.5	32.5
	DC11-19	7.6	6.3	6.9	37.2
	DC11-33	8.4	6.7	7.5	29.1
2700	DC11-34	8.2	7.0	7.6	29.0
	DC11-10	6.7	6.0	6.4	37.7
3060	DC11-18	7.2	6.5	6.9	36.2
	DC11-28	7.8	5.9	6.8	33.9

#### 4.4 Profiles after Bulk Diffusion and Fully Immersed Locations

##### 4.4.1 Specimens Exposed to Low Concentration of Sodium Chloride Solution (0.1M NaCl)

Figure 4-11 represents the typical chloride concentration profiles as a function of depth obtained for specimens DCL1, DCL2 and DCL3 after 220 days and 400 days of exposure time. The top row corresponds to the profiles for specimens cured 14 days at room temperature, 77 days in elevated temperature, and the remaining time in room temperature (14RT/77ET/RT); the bottom

row shows specimens cured at room temperature (RT) all the time. These mixes had the same concrete mix composition but different w/cm, 0.35, 0.41, and 0.47.

The chloride concentration profiles showed that as the w/cm ratio increased, the chloride ions had higher concentration at the layer closest to the surface. For instance, the chloride concentration of DCL3 increased proportionally with the depth compared to the curve produced by the chloride concentration values on DCL1 at 14RT/77ET/RT curing condition. Also, specimens cured at RT were expected to have chloride profiles with higher concentration than for the other curing regime; however, this was only observed in specimen of mix DCL1 at 220 days of exposure time. It is speculated that this was due to the 180 days of curing before exposing these specimens to chloride solution.

In general, the concentration profiles measured at 220 days of exposure showed higher concentrations than those measured at 400 days. This difference might partially be explained by the bottom half of the concrete cylinders being used for those exposed for 400 days. Better compaction and denser concrete has been reported for the bottom half than for the top half. The lower chloride for the first layer might be the results of having a somewhat lower NaCl concentration solution when the specimens were exposed for 400 days. Another possible reason is that the silver/silver sulfate electrode was old and probably not functioning correctly when the measurements at 220 days were done. For most cases there were just modest differences in the curves shapes when comparing with the other profiles of the same mix. The profiles after 400 days of exposure showed that the chloride penetrated farther in than those obtained at 220 days.

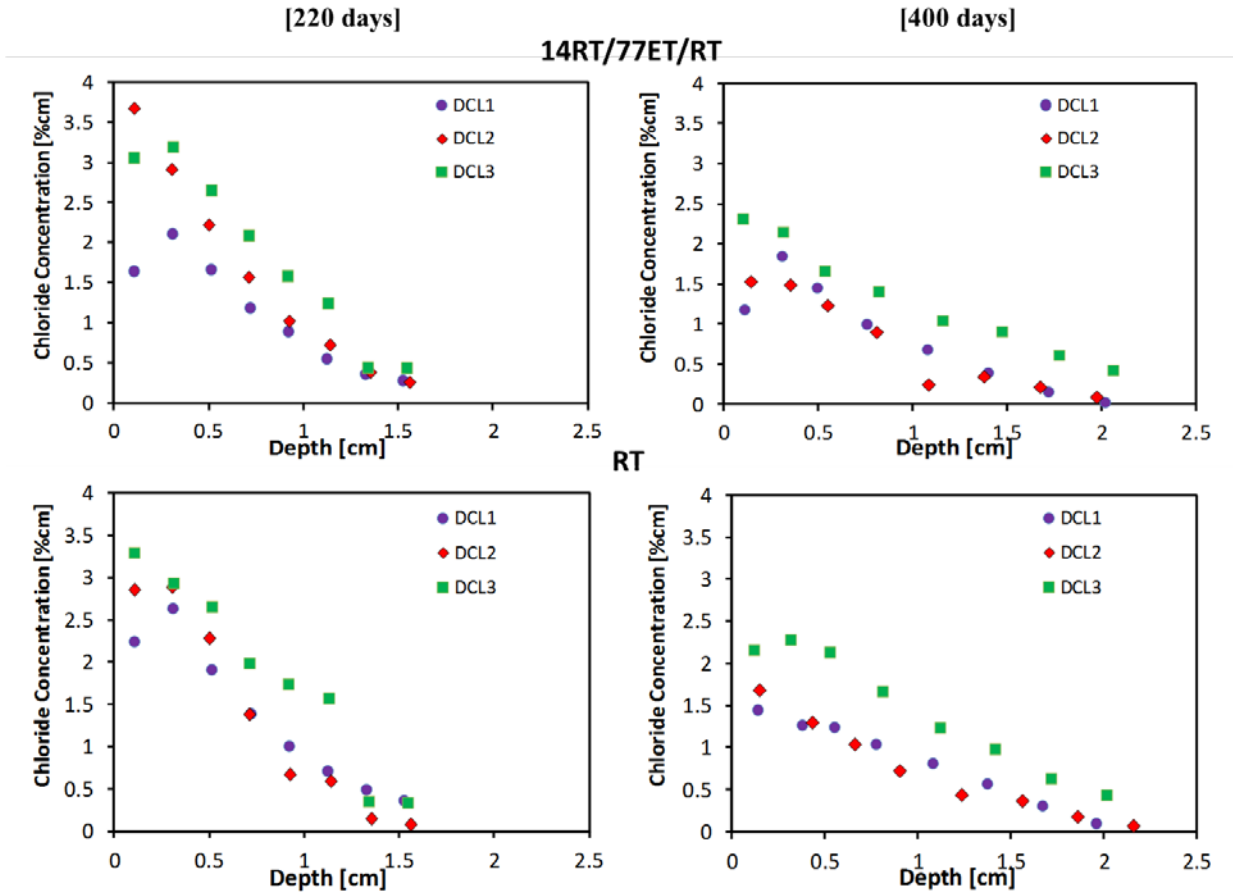


Figure 4-11: DCL1, 2 and 3 specimens exposed to 0.1M NaCl solution at 220 and 400 days cured at 14RT/77ET/RT and RT vs. depth

Figure 4-12 shows the typical chloride concentration measured for DCL3, DCL6, and DCL9 after 220 and 400 days of exposure to 4 curing conditions and 2 curing conditions respectively. These specimens had different concrete mix compositions and the same w/cm ratio (0.47). The plots located on the top row of the figure correspond to the DCL3 sample which has a composition of 20% FA. The second row of plots shows the sets of specimen DCL6 with a composition of 20% FA+8% SF. The third row has the profiles for DCL9 specimen made of 50% Slag. The chloride profile of DCL3 showed the higher amount of chloride penetration compared to the other mixes at 220 days and 400 days of exposure time.

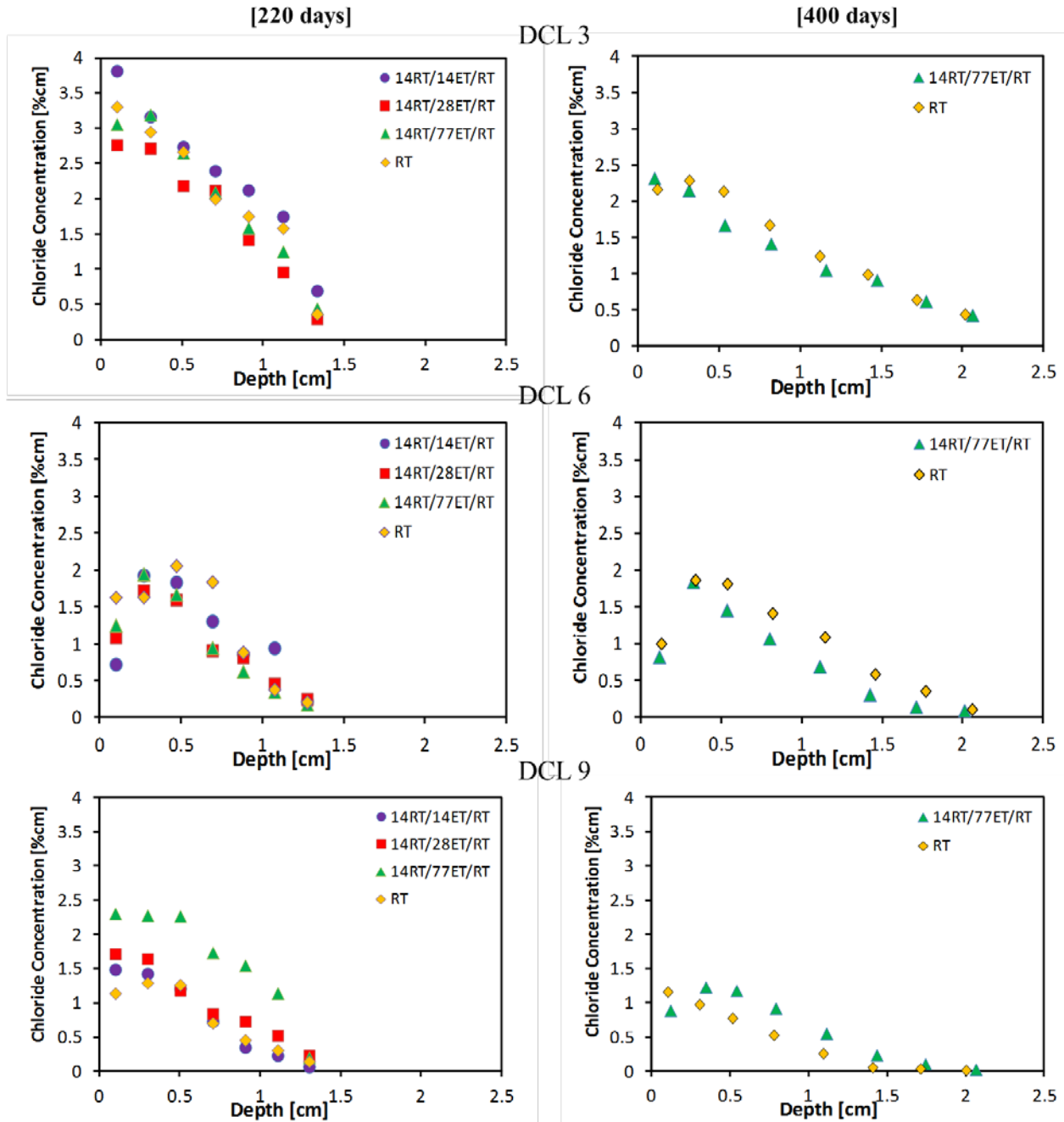


Figure 4-12: DCL3, 6, and 9 specimens exposed to 0.1M NaCl solution at 220 and 400 days vs. depth

As expected, the chloride concentration distribution curves for the mixes had almost the same shape in both of the exposure times. However, as seen in Figure 4-12, the concentrations closer to the surface were slightly lower at 400 days; DCL6 was the specimen with very similar values for the chloride concentration of the layer closer to the surface at 220 and 400 days. Furthermore, for any given mix, exposing the specimens to accelerating curing regimes only had a modest effect on the profiles shape and chloride concentration. Although, every concrete mix was

exposed to the same solution, the concentration of the first layer varied significantly (i.e., it depended on the mixture composition, w/cm and porosity). The chloride concentration profiles for the other DCL specimens exposed to low sodium chloride concentration solution can be found in Appendix D.

Additionally, Tables 4-7 and 4-8 present the surface concentrations calculated from the fittings and the chloride concentration at the first layer measured during the chloride analysis for all mixes at 220 and 400 days. There was modest decrease in the  $C_S$  amount between the chloride concentration for DCL1, DCL4 and DCL7 specimens at all of the curing conditions except when DCL4 was cured at room temperature; these three groups had the same w/cm ratio but different mix concrete compositions. In the case of the mixes with the highest w/cm ratio investigated, the  $C_S$  at 220 days on DC3 ranges between 4 to 3.7 %cm, on DC6 ranges between 3.1 to 2.8 %cm and on DCL9 ranges between 2.9 to 1.9 %cm. After 400 days of exposure, the  $C_S$  decreased on DCL3 and DCL6 to 2.5 %cm and ranged between 1.4 to 1.8 %cm on DCL9. Furthermore, in some cases the concentrations calculated through fitting were significantly larger than the concentrations measured at the first layer. For instance, when DCL10 was exposed at 220 days and cured at 14RT/14ET/RT, the calculated  $C_S$  value was 5.30 %cm and the measured  $C_S$  of the first layer was 1.60 %cm. The large difference is due to the fact that one or two layers needed to be removed on these profiles to achieve a good fit. When comparing the  $C_S$  obtained at 220 and 400 days for the two curing conditions selected, the only specimens that had an increment on their values were DCL4, DCL5, DCL10a, and DCL11. The DCL10 specimen was not investigated for the room temperature (RT) curing condition.

Table 4-7: Chloride concentration at surface and first layer for specimens exposed at 220 days

Mix	Concentration at surface [%cm] (from fitting )				Concentration at first layer [%cm] (measured )			
	Curing condition				Curing condition			
	14RT/14ET/RT	14RT/28ET/RT	14RT/77ET/RT	RT	14RT/14ET/RT	14RT/28ET/RT	14RT/77ET/RT	RT
<b>DCL1</b>	2.92	2.52	2.23	2.86	2.43	2.20	1.65	2.25
<b>DCL2</b>	4.08	2.98	3.14	3.61	3.68	2.61	2.73	2.87
<b>DCL3</b>	4.00	3.29	3.69	3.70	3.81	2.76	3.06	3.30
<b>DCL4</b>	2.02	2.91*	1.98	1.93	1.70	1.03	1.51	1.46
<b>DCL5</b>	1.36	1.41	1.04	1.35	1.10	1.08	0.84	1.03
<b>DCL6</b>	2.80*	2.56*	3.05*	2.81*	0.72	1.09	1.25	1.63
<b>DCL7</b>	1.43	1.48	1.60	1.64	1.25	1.36	1.52	1.58
<b>DCL8</b>	1.97*	1.75	1.63	2.18	1.73	1.54	1.41	1.93
<b>DCL9</b>	1.87	2.02	2.88	1.54	1.49	1.72	2.31	1.14
<b>DCL10</b>	5.30*	5.10*	5.31*	N/A	1.60	1.94	1.87	N/A
<b>DCL10a</b>	3.16	3.50	3.22	4.27*	2.48	2.50	2.40	1.82
<b>DCL10b</b>	2.51	2.62	1.89	1.93	1.96	2.03	1.58	1.48
<b>DCL11</b>	2.37	1.84	2.33	2.14	2.01	1.77	1.69	1.60

\*First layer removed at fitting

Table 4-8: Chloride concentration at surface and first layer for specimens exposed at 400 days

Mix	Concentration at surface [%cm] (from fitting )		Concentration at first layer [%cm] (measured )	
	Curing Condition		Curing Condition	
	14RT/77ET/RT	RT	14RT/77ET/RT	RT
DCL1	2.44*	1.68	1.19	1.45
DCL2	1.90	1.88	1.53	1.69
DCL3	2.44	2.59	2.32	2.16
DCL4	2.38	2.56*	1.87	0.68
DCL5	1.31	1.33	1.20	1.05
DCL6	2.52*	2.56*	0.82	1.00
DCL7	0.81	0.77	0.73	0.67
DCL8	0.88	2.02	0.77	1.62
DCL9	1.82*	1.34	0.89	1.17
DCL10	3.46	N/A	2.18	N/A
DCL10a	3.35	3.06	2.22	2.56
DCL10b	0.88	1.88*	0.77	1.23
DCL11	2.61*	3.01*	0.89	1.12

\*First layer removed at fitting

#### 4.4.2 Specimens Exposed to High Concentration of Sodium Chloride Solutions (3% and 16.5% NaCl)

Figure 4-13 corresponds to the averaged chloride concentrations profiles measured for the DCL1, DCL2 and DCL3 group of specimens that were immersed in high concentration of NaCl solution for one year. The graphs on the right side present the average chloride concentration values for the specimens exposed to 16.5% NaCl solution (bottom half of the cylinder). On the left side, the plots present the results of the average chloride profiles found when the specimens were exposed to 3% NaCl solution (top side). The curing regimes selected were NC on the first row, AC on the second row, and NC=AC on the third row of the figure. It is apparent that the chloride concentrations were significantly higher in the bottom side of the specimens compared to the top sections; this was expected since the top sides were exposed to a lower chloride concentration solution. When looking at the curing regimens, DCL2 had higher chloride concentration values when cured at normal conditions. Also, DCL2 specimen, cured at NC and exposed to 16.5% NaCl solution, had a slightly higher chloride concentration as the depth increased compared to AC and NC=AC curing conditions of the same mix. On the case of DCL1 and DCL3, the chloride distribution values were comparable when exposed at NC and AC in 16.5% and 3% NaCl solution. However, the chloride profiles for the DC3 cured at NC=AC in both sodium chloride concentration solutions were slightly higher compared to the other specimens. As seen on these profiles, the w/cm ratio seems to play an important role as to how much chloride penetrates each layer. In fact, the chloride ions in the DCL3 mix, with w/cm ratio of 0.47, were reaching higher levels farther in compared to DCL1 mix, with a w/cm ratio of 0.35 when cured at NC=AC. For instance, at a depth of 0.95 cm (in 16.5% NaCl), the chloride concentration was 4.2 %cm for DC3 and 1.98 %cm for DCL1.

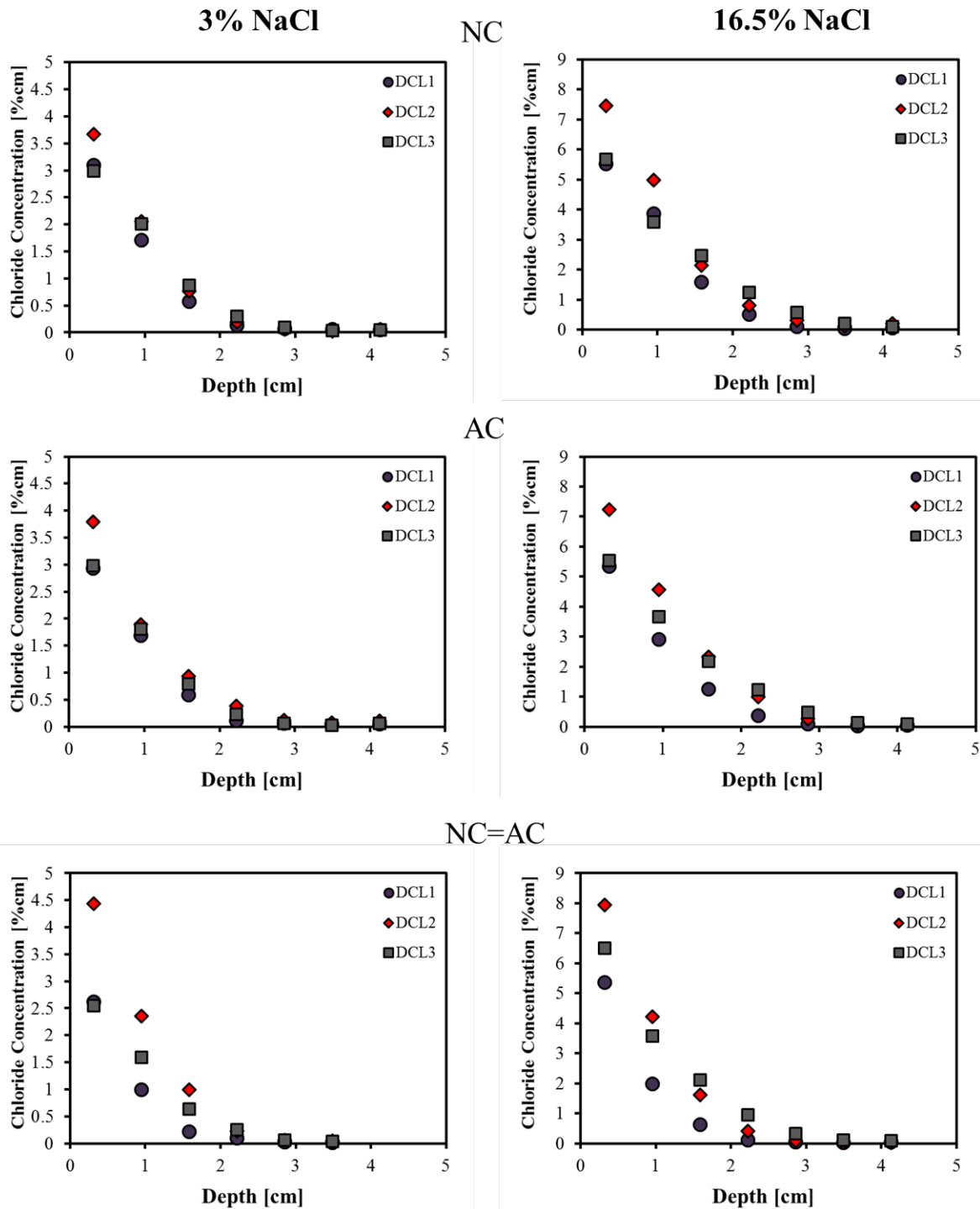


Figure 4-13: DCL1, 2, and 3 - Average chloride concentrations vs. depth

The average chloride profiles for DCL3, DCL6 and DCL9 exposed to 3% (on the left side) and 16.5% (on the right side) NaCl concentration solutions for one year are shown in Figure 4-14. The curing conditions investigated are NC, AC, and NC=AC for all of the concrete mixes.

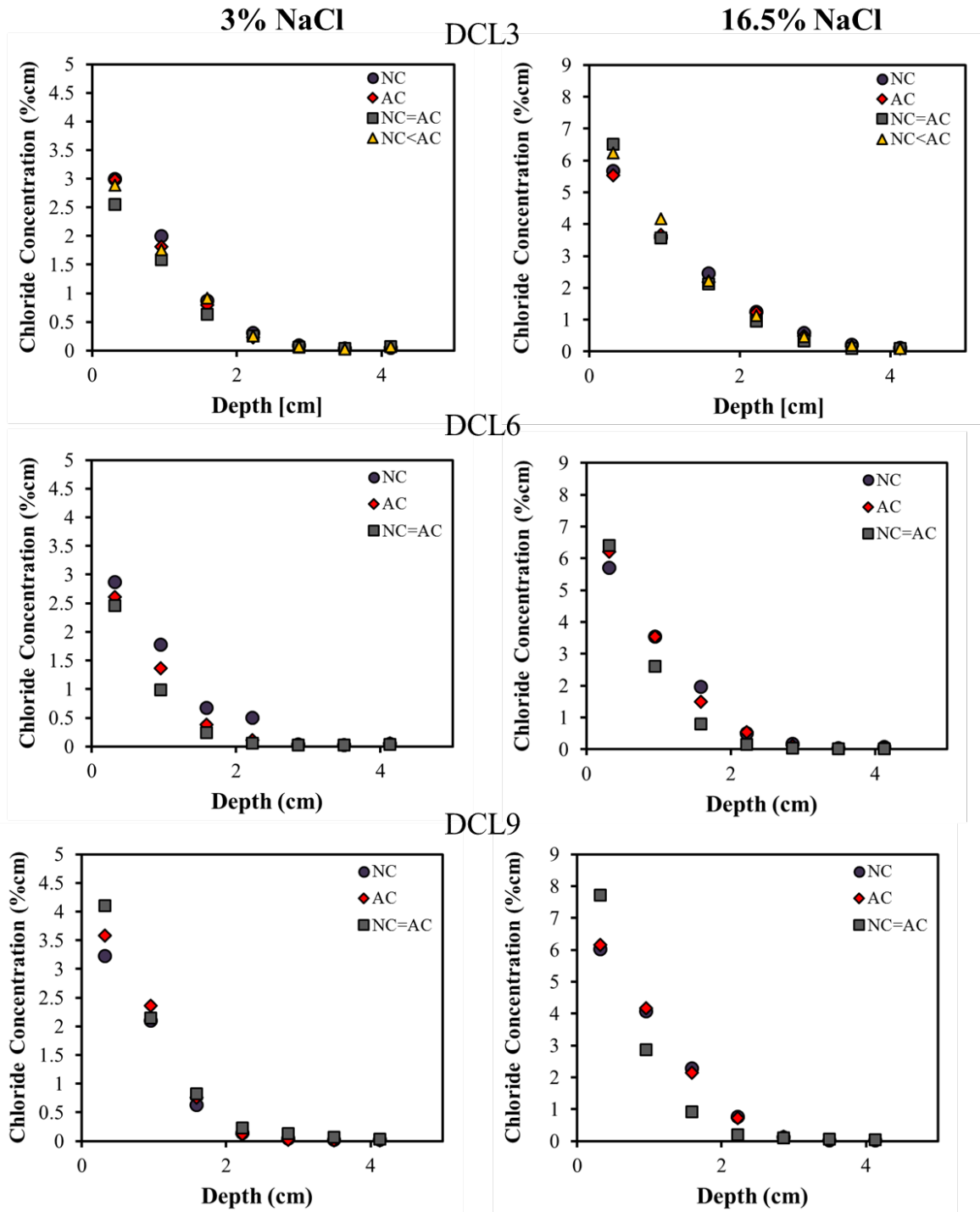


Figure 4-14: DCL3, 6, and 9 - Average chloride concentrations vs. depth

The chloride ions on DCL3 specimen reached very similar values as the depth increased when cured at the three conditions and exposed to 3% NaCl solution. On DCL6, profiles corresponding to NC curing condition showed the highest concentration when exposed to 3% NaCl solution; however, when it was exposed to 16.5% NaCl solution, the chloride ions reached higher

concentrations when cured at accelerated conditions. Comparing the chloride concentration values obtained for the three mixes cured at NC=AC, it can be seen that the highest concentration was obtained for DCL9 when exposed to both sodium chloride solutions. For instance, the chloride at the first layer at one year and exposed to 16.5% NaCl on DCL9 was 7.7 %cm, on DCL6 was 6.4 %cm and on DCL3 was 6.3 %cm. In general, the concentration measured when the specimens were exposed to 16.5% NaCl solution showed higher concentrations as the depth increased compared to those measured when exposed to 3% NaCl solution.

Tables 4-9 and Table 4-10 show the average chloride concentration calculated at the surface and measured at the first layer for all of the DCL mixes exposed to 16.5% NaCl and 3% NaCl solutions respectively. These  $C_S$  fitted values were calculated including all the layers. When comparing the specimens with a composition of 20% FA, DCL2 had the highest calculated and measured  $C_S$  values for the NC, AC, and NC=AC curing regimes in both NaCl solutions. The group of specimens with a composition of 20% FA+8% SF had a calculated  $C_S$  that ranged between 6.8 and 8.9 %cm when they were immersed in 16.5% NaCl solution and between 3.5 and 4.5 %cm when immersed in 3% NaCl solution. Additionally, the specimens composed of 20% FA had a higher calculated  $C_S$  when compared to the other group of concrete mixes. In fact, the calculated  $C_S$  for DCL10, DCL10a, DCL10b, and DCL11 had a range of 7 to 10 %cm. The standard deviation for the calculated and measured  $C_S$  values for all the mixes immersed in the two sodium chloride solutions showed the dispersion of the values obtained for each cylinder from the average value shown in the tables. For example, the observed the average standard deviation for the DCL5 sample was AC cured in 16.5% NaCl was 0.27 %cm for the calculated  $C_S$  at the surface and 0.14 %cm for the measured  $C_S$  at the first layer. Appendix E contains the chloride profiles for each of the cylinders tested in 3% and 16.5% NaCl.

Table 4-9: Chloride concentration at surface and at first layers for DCL mixes exposed to 16.5% NaCl solution

Mix	Curing Condition	Average Concentration at surface (%cm) (from fitting)	Standard Deviation (%cm)	Average Concentration at first layer (%cm) (measured)	Standard Deviation (%cm)
<b>DCL1</b>	NC	7.0	0.68	5.5	0.15
	AC	6.8	0.31	5.4	0.73
	NC=AC	7.5	1.37	5.4	0.49
<b>DCL2</b>	NC	9.4	0.89	7.4	0.69
	AC	8.9	1.05	7.2	0.83
	NC<AC	6.7	0.25	5.6	0.12
	NC=AC	10.2	1.65	7.9	1.22
<b>DCL3</b>	NC	6.6	0.39	5.6	0.31
	AC	6.5	0.28	5.5	0.23
	NC<AC	7.5	0.60	6.2	0.44
	NC=AC	7.8	1.02	6.5	0.74
<b>DCL4</b>	NC	7.1	0.88	5.2	0.61
	AC	7.2	0.28	5.2	0.31
	NC=AC	7.9	0.00	5.2	0.18
<b>DCL5</b>	NC	6.8	0.23	5.2	0.16
	AC	7.1	0.27	5.5	0.14
	NC=AC	8.9	0.37	5.8	0.11
<b>DCL6</b>	NC	7.1	0.09	5.7	0.04
	AC	7.8	0.44	6.2	0.38
	NC=AC	8.8	0.19	6.4	0.19
<b>DCL7</b>	NC	6.9	0.19	5.6	0.23
	AC	6.7	0.62	5.4	0.37
	NC=AC	8.0	0.12	6.3	0.22
<b>DCL8</b>	NC	8.0	0.15	6.3	0.13
	AC	7.23	0.29	5.7	0.19
	NC=AC	9.41	0.54	6.9	0.42
<b>DCL9</b>	NC	7.4	0.02	6.0	0.05
	AC	7.7	0.48	6.1	0.29
	NC=AC	10.8	0.63	7.7	0.52
<b>DCL10</b>	NC	10.6	0.89	8.7	1.02
	AC	7.7	1.05	6.3	0.34
	NC<AC	9.9	0.25	6.3	1.43
	NC=AC	9.9	1.65	7.9	0.34
<b>DCL10a</b>	NC	8.3	0.29	6.9	0.28
	AC	7.8	0.41	6.4	0.32
	NC<AC	8.7	0.48	7.1	0.42
	NC=AC	9.6	1.45	7.5	0.99
<b>DCL10b</b>	NC	6.7	0.26	6.2	0.36
	AC	7.5	0.72	5.8	0.49
	NC=AC	7.5	0.39	6.1	0.31
<b>DCL11</b>	NC	8.1	0.34	6.8	0.32
	AC	7.1	0.31	5.9	0.35
	NC=AC	7.9	0.32	6.5	0.24

Table 4-10: Chloride concentration at surface and at first layers for DCL mixes exposed to 3% NaCl solution

Mix	Curing Condition	Average Concentration at surface (%cm) (from fitting)	Standard Deviation (%cm)	Average Concentration at first layer (%cm) (measured)	Standard Deviation (%cm)
<b>DCL1</b>	NC	4.0	0.07	3.1	0.04
	AC	3.9	0.58	2.9	0.40
	NC=AC	3.7	0.46	2.6	0.23
<b>DCL2</b>	NC	4.7	0.13	3.7	0.08
	AC	4.7	0.73	3.8	0.67
	NC<AC	4.8	0.27	3.7	0.25
	NC=AC	5.7	0.57	4.4	0.40
<b>DCL3</b>	NC	3.8	0.16	3.0	0.14
	AC	3.8	0.39	3.0	0.25
	NC<AC	3.6	0.62	2.9	0.50
	NC=AC	3.3	0.13	2.5	0.10
<b>DCL4</b>	NC	3.7	0.14	2.7	0.10
	AC	4.0	0.32	2.8	0.06
	NC=AC	4.5	0.55	2.7	0.13
<b>DCL5</b>	NC	3.6	0.25	2.7	0.16
	AC	3.8	0.33	2.7	0.23
	NC=AC	4.5	0.24	2.8	0.11
<b>DCL6</b>	NC	3.5	0.16	2.8	0.29
	AC	3.5	0.10	2.6	0.08
	NC=AC	3.4	0.64	2.5	0.14
<b>DCL7</b>	NC	3.8	0.16	2.90	0.15
	AC	3.5	0.09	2.62	0.07
	NC=AC	3.8	0.10	2.84	0.05
<b>DCL8</b>	NC	4.0	0.12	3.1	0.09
	AC	4.0	0.22	2.9	0.14
	NC=AC	4.4	0.04	3.3	0.17
<b>DCL9</b>	NC	4.23	0.26	3.2	0.16
	AC	4.67	0.23	3.6	0.23
	NC=AC	5.5	0.98	4.1	0.57
<b>DCL10</b>	NC	4.1	0.13	3.3	0.30
	AC	4.7	0.73	3.7	0.35
	NC<AC	6.1	0.25	4.8	0.40
	NC=AC	3.3	0.57	3.9	0.34
<b>DCL10a</b>	NC	4.4	0.28	3.6	0.33
	AC	4.6	0.33	3.8	0.37
	NC<AC	4.3	0.49	3.5	0.59
	NC=AC	4.9	0.26	3.6	0.36
<b>DCL10b</b>	NC	3.8	0.26	2.8	0.56
	AC	3.3	0.42	2.9	0.13
	NC=AC	3.3	0.10	3.5	0.13
<b>DCL11</b>	NC	4.0	0.51	3.1	0.40
	AC	3.9	0.35	3.2	0.19
	NC=AC	3.7	0.11	2.8	0.10

### 4.4.3 Specimen Exposed to Simulated Field Conditions

#### 4.4.3.1 Tidal Simulation

Figure 4-15 shows profiles for DCL3, DCL6, and DCL9 after six, ten, and 18 months of exposure time to the tidal simulation. These three mixes have different concrete compositions and the higher w/cm ratio studied. As mentioned earlier, the two sides of the concrete blocks for all of these mixes were exposed to this simulation. Therefore, as expected, the amounts of chloride ions were almost the same in both sides of the blocks for all of the specimens. Also, it is apparent that the concentration at the first layer varied with the concrete mix composition and the exposure time. For instance, the  $C_s$  at six months on DCL3 was about 1.5 %cm in both sides, on DCL6 ranged from 0.7 to 1.2 %cm, and on DCL9 ranged from 0.9 to 1.9 %cm. At 10 months of exposure, the  $C_s$  on DCL3 ranged from 1.5 to 1.9 %cm, on DCL6 was 1.2 %cm in both sides and on DCL9 ranged from 1.8 to 2.7 %cm. Finally, when the specimens were exposed for 18 months the  $C_s$  value on DCL3 was 1.7 %cm, on DCL6 ranged from 0.8 to 1.2 %cm and on DCL9 ranged from 2.8 to 3.2 %cm. In general, the concentration profiles measured at 18 months of exposure showed higher concentrations than those measured at ten and six months. The specimen made of 20%FA + 8% SF (DCL6) showed an overall lower chloride concentration when exposed to 6, 10, and 18 months compared to the other mix compositions. DCL9 specimen showed a considerable increment on the chloride ions amount between the second and third exposure times. The chloride ions closest to the surface appear to move farther up as the exposure time increased. Additionally, the concentration profiles at six, ten, and 18 months for specimens DCL3 followed similar patterns.

The chloride concentrations calculated at the surface and measured at the first layer for all of the mixes exposed to the tidal simulation at six, ten, and 18 months are presented on Table 4-11. When comparing the mixes with a w/cm ratio of 0.35 and different concrete compositions, it is apparent that the specimen made of 50% slag (DCL7) had an overall higher chloride concentration at the surface values as the time of exposure increased. As seen on Table 4-11, the average  $C_s$  calculated at 18 months on DCL7 was 3.3 %cm, on DCL4 was 2.34 %cm, and on DCL1 was 3.14 %cm. This was also seen on the group of specimens with a w/cm ratio of 0.41 since the concrete with a mix composition of 50% slag (DCL8) had an average higher  $C_s$  than the other two mixes (DCL2 and DCL5) for the three exposure times. On DCL8, the average  $C_s$  calculated at 18 months was 3.62 %cm;  $C_s$  on DCL5 was 2.41 %cm and on DCL2 was 2.3 %cm at 18 months. In general, the specimen that had the smallest amount of chloride ions at the surface was DCL6 with a composition of 20% FA+8% SF and a w/cm ratio of 0.47.

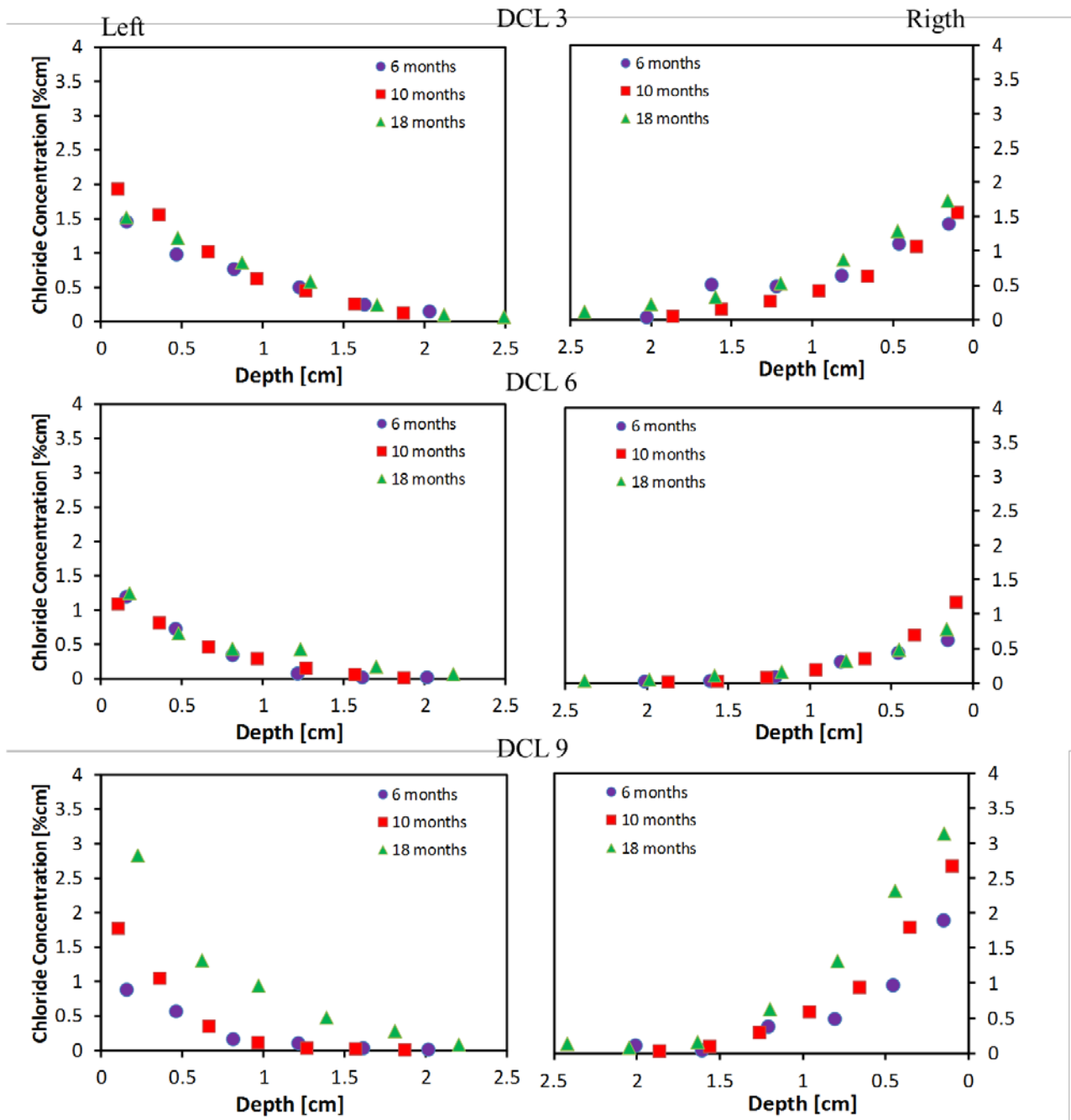


Figure 4-15: DCL3, 6, and 9 - Tidal simulation chloride concentration vs. depth (left and right)

Table 4-11: Chloride concentration at surface and at first layer for DCL mixes exposed to tidal simulation for 6, 10, 18 months

Mix	Side	Concentration at surface (%cm) (from fitting)			Concentration at first layer (%cm) (measured)		
		6 Months	10 Months	18 Months	6 Months	10 Months	18 Months
DCL1	R	2.80	2.80	3.79	3.55	2.75	3.59
	L	3.94	2.84	2.50	2.53	2.55	3.46
DCL2	R	2.31	3.29	2.23	1.03	3.11	1.00
	L	1.16	3.05	2.37	2.28	3.01	1.43
DCL3	R	1.60	1.77	3.43	1.40	1.56	1.73
	L	1.65	2.23	0.81	1.45	1.93	1.51
DCL4	R	2.09	4.73	2.65	1.70	4.30	2.29
	L	2.29	5.22	2.13	1.95	4.51	2.31
DCL5	R	2.19	2.35	2.34	1.75	1.95	2.18
	L	3.00	2.72	2.47	2.40	2.36	2.10
DCL6	R	0.78	1.41	0.89	0.62	1.18	0.79
	L	1.55	1.29	1.31	1.20	1.10	1.24
DCL7	R	5.41	5.33	3.09	4.46	4.85	3.15
	L	2.26	5.30	3.56	2.00	4.90	3.18
DCL8	R	3.28	3.34	3.38	2.61	2.79	3.10
	L	3.40	3.92	3.87	2.59	3.15	3.12
DCL9	R	2.34	3.14	3.69	1.90	2.67	3.14
	L	1.17	2.25	3.42	0.88	1.77	2.82
DCL10a	R	1.31	3.69	2.51	1.12	3.55	2.56
	L	1.86	3.57	0.99	1.36	3.28	2.61
DCL10b	R	3.06	5.22	3.68	2.60	5.04	3.86
	L	2.38	3.88	2.58	2.49	3.73	3.58
DCL11	R	1.53	1.82	2.69	1.40	1.76	2.32
	L	1.46	1.71	2.80	1.35	1.73	2.53

#### 4.4.3.2 Splash Simulation

The chloride concentration profiles for DCL3, DCL6, and DCL9 mixes exposed to six, ten, and 18 months are presented on Figure 4-16. The concentration profiles for specimens sprayed with a solution of 10% seawater/ 90% tap water are plotted on the right side and with 100% seawater are on the left side. The specimen with a composition of 20% FA (DCL3) showed higher amount of chloride concentrations when it was exposed to 100% seawater at six, ten, and 18 months in comparison with the results showed for the other solution. However, this was not seen on the other two specimens (DCL6 and DCL9) where the concentrations reached higher values when the mixes were sprayed with a solution of 10% seawater and 90% tap water. For instance, the  $C_S$  at 18 months on DCL6 was 0.8 %cm and 0.4 %cm when sprayed with low and high seawater concentrations respectively. DCL9 had a steady distribution of chloride ions as the exposure time increased when exposed to 100% seawater; this was also observed on DCL6; however, the concentration at the first two layers were slightly higher than the values obtained on DCL9. On DCL3 exposed to 100% seawater, there was a significant increment on the concentration values measured after 18 months of exposure; the  $C_S$  value measured for this specimen was 4.9 %cm at 18 months and 3.3 %cm at 10 months. Typically, the longer the exposure time, the higher chloride concentration levels were reached. This might be a result of not having the appropriate solution concentration in the tanks.

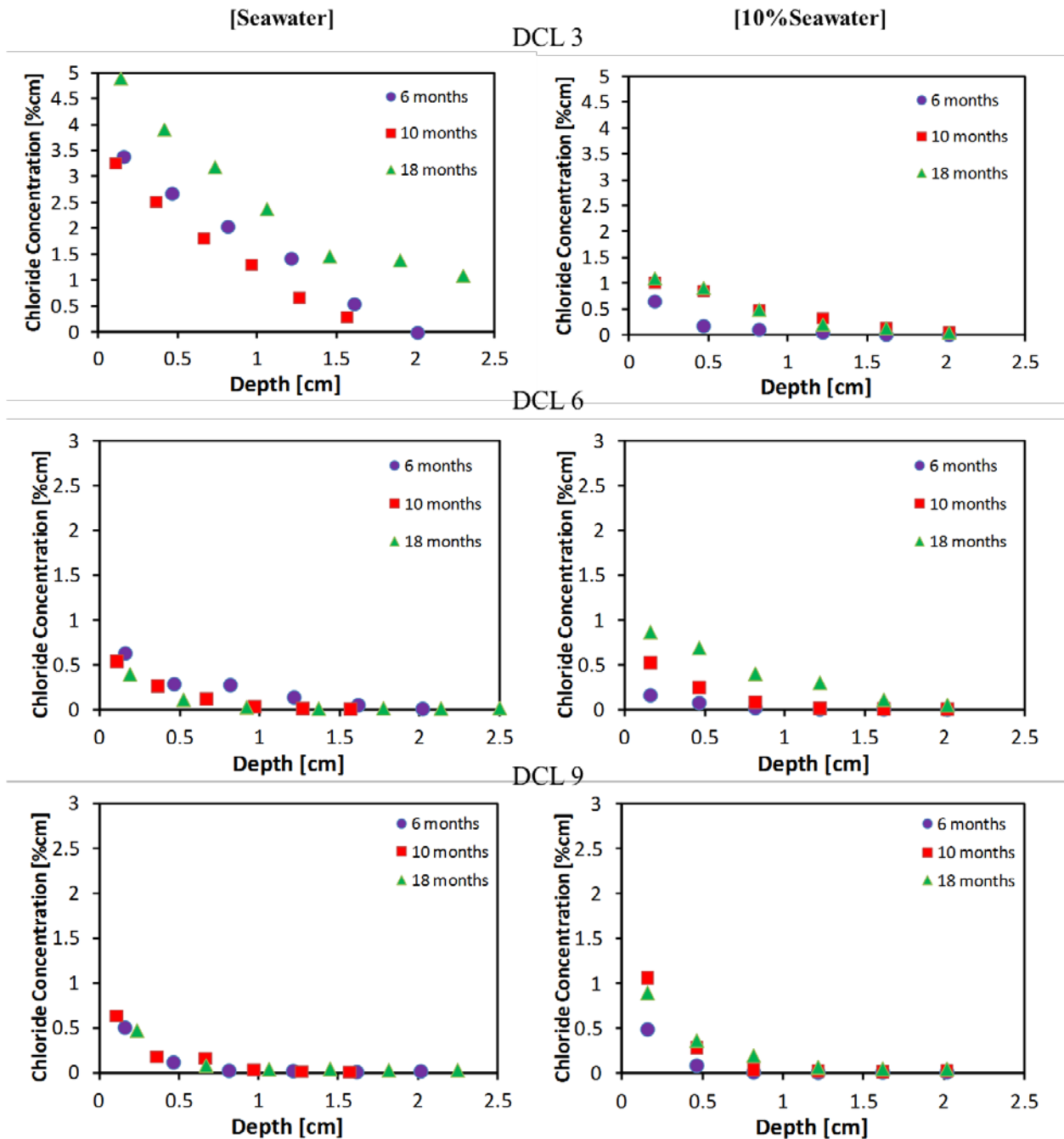


Figure 4-16: DCL3, 6, and 9- Splash simulation chloride concentration vs. depth.

Table 4-12 has the values for the chloride concentration calculated at the surface and measured at the first layer for specimens exposed to the splash simulation for six, ten, and 18 months. On the bottom part of the table, the values for the three mixes exposed to 90% tap water/10% seawater are presented. After 18 months of exposure, the calculated chloride concentration at the surface and the measured at the first layer of DCL3 showed the highest values (5.04 %cm and 4.91 %cm respectively) when compared to the other profiles. On the other hand, the profile that showed the

smallest calculated and measured  $C_S$  at 18 months was DCL6 with values of 0.64 %cm 0.40 %cm. However, when observing the average  $C_S$  calculated at the three periods of exposure, the mix with a composition of 20% FA and a w/cm ratio of 0.41, DCL11, reached the smallest value (0.63 %cm) while DCL6 had an average of 0.68 %cm followed by DCL9 with a value of 0.86 %cm.

Table 4-12: Chloride concentration at surface at first layers for DCL mixes exposed to splash simulation for 6, 10, 18 months

Mix	Concentration at surface (%cm) (from fitting)			Concentration at first layer (%cm) (measured)		
	6 Months	10 Months	18 Months	6 Months	10 Months	18 Months
<b>100% Seawater</b>						
DCL1	1.54	1.58	2.36	1.13	1.34	1.91
DCL2	1.27	2.06	1.05	1.10	1.81	0.90
DCL3	3.60	3.76	5.04	3.40	3.33	4.91
DCL4	2.13	2.12	2.50	1.65	1.71	2.13
DCL5	0.53	2.05	3.11	0.38	1.63	2.52
DCL6	0.72	0.69	0.64	0.64	0.54	0.40
DCL7	2.53	1.91	2.29	1.88	0.68	1.75
DCL8	2.13	2.68	1.75	1.66	2.16	1.50
DCL9	0.87	0.87	0.85	0.51	0.64	0.48
DCL10a	1.81	2.84	1.81	1.59	2.67	1.68
DCL10b	2.42	3.09	1.77	2.10	2.84	1.92
DCL11	0.44	0.63	0.80	0.30	0.44	0.53
<b>90% Tap water/10% Seawater</b>						
DCL3	1.02	1.25	1.29	0.66	1.02	1.10
DCL6	0.24	0.70	1.02	0.16	0.53	0.87
DCL9	0.90	0.42	1.15	0.49	1.07	0.89

#### 4.4.3.3 Barge Exposure

Figure 4-17 presents the chloride profiles obtained from selected concrete mixes (DCL3, 6 and 9) exposed on the barge simulation for six, ten, and 18 months. The chloride analysis was performed to both sides of the concrete blocks. As seen on Figure 4-17, the specimen with a composition of 50% Slag (DCL9) showed overall highest chloride concentrations when exposed at 6, 10 and 18 months; also, the first layer of the profiles of this mix measured a %cm of 4.4 on the left side and 3.8 on the right side. On DCL6, the highest concentration was obtained when the exposure time was 10 months and the chloride amounts for the other two periods of time were similar. For instance, the average  $C_S$  measured on DCL6 was 2.6 %cm at 10 months and 1.1 %cm at 6 and 18 months. For DCL3 specimen, there were discrepancies between the concentrations measured on both sides of the block. In fact, the values obtained on the left side were significantly larger as the depth increased at 10 and 18 months compared to the other side. For instance, DCL3 had a chloride concentration at 10 months on the first layer of 2.8 %cm on the left side of the block and 1.92 %cm on the right side. On the other hand, the chloride ion

distribution for DCL3 mix exposed at six months was almost the same for the left and right side of the concrete block. In general, the specimen that showed less resistance to chloride penetration for the three mixes presented on the figure was DCL9 with the same w/cm ratio as the other specimens but with a different mix composition.

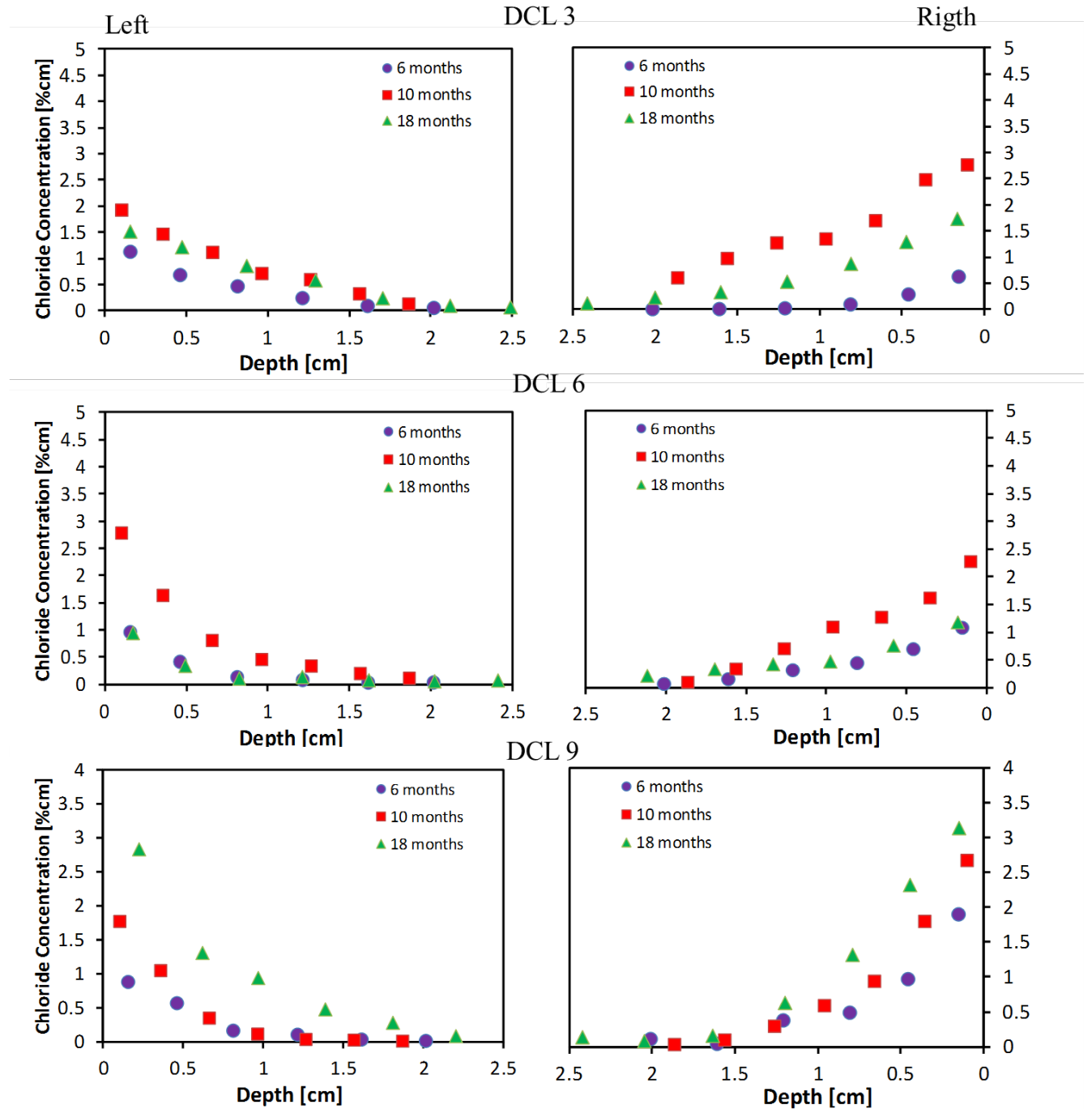


Figure 4-17: DCL3, 6, and 9 - Barge simulation chloride concentration vs. depth (left and right)

Table 4-13 shows the calculated chloride concentration at the surface and the measured chloride concentration at the first layer for the seven mixes exposed to the barge simulation at six, ten, and 18 months. At 18 months of exposure, the DCL6 profile showed the smallest calculated  $C_s$  (1.29 %cm) and a slightly smaller value for the measured chloride concentration at the first layer (1.06 %cm). The next specimen with a lower calculated  $C_s$  at 18 months corresponded to the DCL2 mix since it reached an average value of 2.25 %cm. The measurement at the right side of the DCL10a specimen at six months of exposure was not performed.

Table 4-13: Chloride concentration at surface and at first layers for DCL mixes exposed to barge simulation for 6, 10, 18 months

Mix	Side	Concentration at surface (%cm) (from fitting)			Concentration at first layer (%cm) (measured)		
		6 Months	10 Months	18 Months	6 Months	10 Months	18 Months
DCL2	R	1.6	1.4	2.68	1.41	1.10	2.69
	L	1.7	1.3	1.81	1.47	1.10	1.57
DCL3	R	0.9	3.0	2.89	0.63	2.76	1.73
	L	4.0	2.2	2.41	1.13	1.93	1.51
DCL6	R	1.2	2.5	1.22	1.10	2.28	1.18
	L	1.4	3.3	1.35	0.96	2.79	0.95
DCL9	R	3.4	4.3	4.37	2.55	3.73	3.77
	L	4.3	5.4	4.47	3.67	4.79	4.40
DCL10a	R	N/A	2.6	3.09	N/A	2.12	3.11
	L	1.5	2.4	2.36	1.41	2.34	2.36
DCL10b	R	1.9	2.3	3.18	2.50	2.18	2.99
	L	1.7	1.8	2.53	1.62	1.81	2.46
DCL11	R	2.1	3.0	2.95	1.34	1.73	2.80
	L	1.9	2.8	2.43	1.86	2.81	2.58

## 4.5 Free Chlorides Concentration Profiles

### 4.5.1 Specimens Exposed to Low Concentration of Sodium Chloride Solution (0.1M NaCl)

As explained above, the AFREM [78] method of chloride analysis was also performed to calculate the amount of free chloride presented on the different mixes investigated (this was done only on selected specimens). Figure 4-18 presents the distribution of free and total chloride ions for DCL1, DCL2, and DCL3 at 400 days of exposure time to 0.1M NaCl solution and on specimens cured at 14RT/77ET/RT. The labels of the profiles are the name of the mix followed by the letter f (free) or t (total) corresponding to the type of chloride ions illustrated. When comparing the amount of free chloride concentration on the specimen, it is apparent that DCL2 mix with a w/cm ratio of 0.41 had the lowest value as the depth increased. On the other hand, DCL1 and DCL3 had similar free chloride concentration values for the 6 layers measured. However, this was not seen on the case of total chloride concentration where DCL3 mix reached higher values than the other two samples. Also, the free and total  $C_s$  values measured were 0.43 %cm and 2.31 %cm on DCL3, 0.26 %cm and 1.53 %cm on DCL2, and 0.45 %cm and 1.2 %cm on DCL1 respectively.

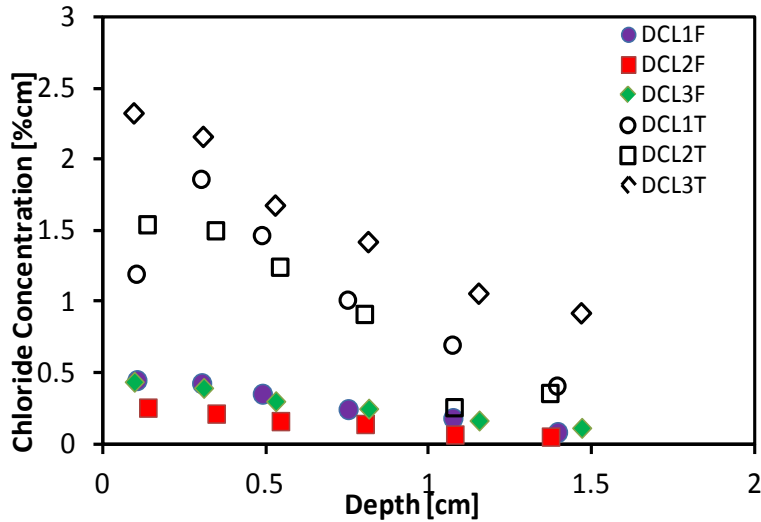


Figure 4-18: DCL1, 2, and 3 Free and total chloride concentration vs. depth (400 days in 0.1M)

Figure 4-19 shows the relation between the amount of free and total chloride concentrations and the composition of the mixes with the highest w/cm ratio (DCL3, DCL6, and DCL9). The results showed that the mix with a composition of 20% FA (DCL3) had the greater bound chloride content. Also, the free chloride ions content was relatively low in these three mixes and it slowly decreased as the depth increased. On DCL9, the free  $C_s$  value was 0.27 %cm, on DCL6 was 0.35 %cm, and on DCL3 was almost 0.5 %cm; however, the total  $C_s$  value was 0.89 %cm on DCL9, 0.82 %cm on DCL6, and 2.31 %cm on DCL3. The total-chlorides profiles for DCL6 and DCL9 show the skin effect trend, and also on the corresponding free-chloride profiles.

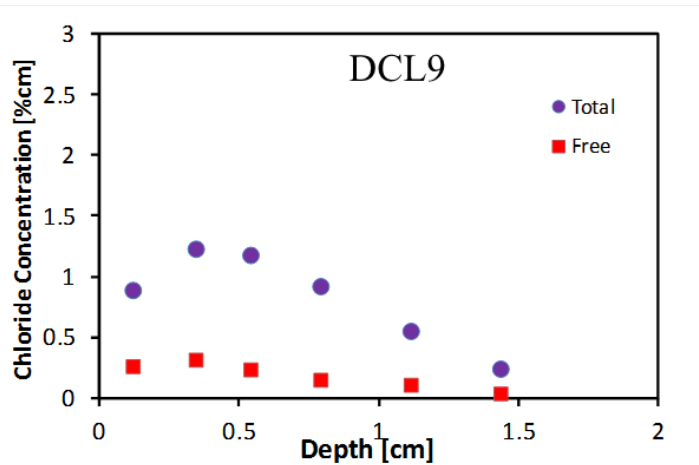
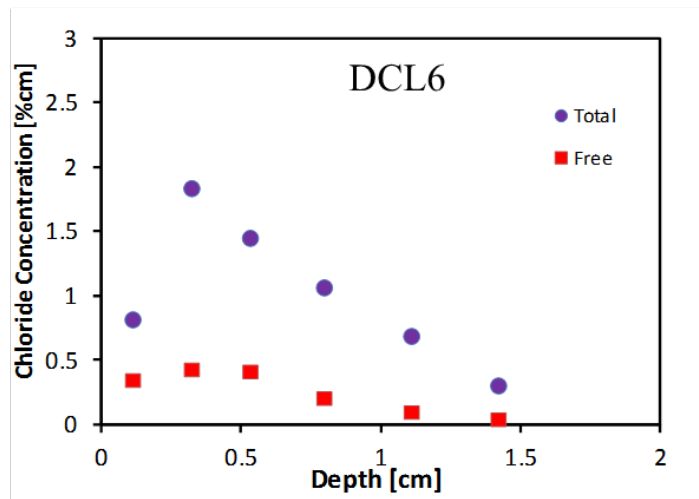
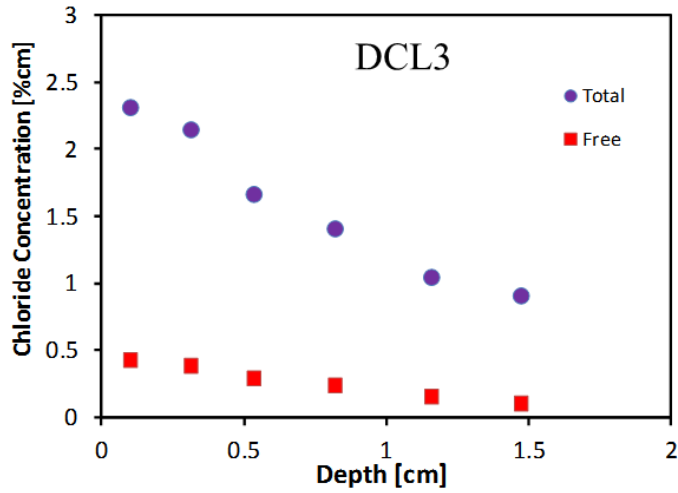


Figure 4-19: DCL3, 6, and 9 Free and total chloride concentration vs. depth (400 days in 0.1M)

The free and total chloride concentration calculated at the surface and measured at the first layer for the 13 mixes exposed at 14RT/77ET/RT and immersed in 0.1M NaCl for 400 days can be

seen on Table 4-14. As marked on the table, the first layer for some of the specimens was removed in order to be able to calculate the  $C_s$  values by using Fick's second law. The specimen that showed the smallest content of free chloride ions at the surface was DCL7 with a value of 0.10 %cm. On the other hand, 1.11 %cm was the highest free  $C_s$  value calculated on the specimen with 20% FA (DCL10) with intermediate cementitious and a w/cm ratio of 0.41. In general, the amount of total chloride is significantly larger than the free when it was calculated at the surface and measured at the first layer in all of the mixes.

Table 4-14: Free and total chloride concentration at surface and at first layer for DCL mixes exposed to 0.1M NaCl solution for 400 days

Mix	Concentration at surface (%cm) (from fitting)		Concentration at first layer (%cm) (measured)	
	Free	Total	Free	Total
<b>DCL1</b>	0.56*	2.44*	0.44	1.19
<b>DCL2</b>	0.29	1.90	0.25	1.53
<b>DCL3</b>	0.47	2.44	0.43	2.32
<b>DCL4</b>	0.77*	2.38	0.49	1.87
<b>DCL5</b>	0.37	1.31	0.32	1.20
<b>DCL6</b>	0.68*	2.52*	0.35	0.82
<b>DCL7</b>	0.10	0.81	0.09	0.73
<b>DCL8</b>	0.31*	0.88	0.19	0.77
<b>DCL9</b>	0.54*	1.82*	0.27	0.89
<b>DCL10</b>	1.11	3.46	0.93	2.18
<b>DCL10a</b>	1.03	3.35	0.94	2.22
<b>DCL10b</b>	0.17	0.88	0.22	0.77
<b>DCL11</b>	0.67*	2.61*	0.31	0.89

\*First layer removed at fitting

#### 4.5.2 Specimens Exposed to High Concentrations of Sodium Chloride Solutions (3% and 16.5% NaCl)

Figure 4-20 illustrates the amount of total and free chloride found in specimens DCL1, DCL2, and DCL3 which have a composition of 20% FA and different w/cm ratios. The letters F and T found after the name of the mixes in the plots indicates the chloride concentration (F= free and T=total). The plots located on the right side represent the mixes exposed to 16.5% NaCl solution and on the left side the mixes exposed to 3% NaCl. Also, the curing conditions presented on this figure are NC=AC on the top row and AC on the bottom row. As expected, the amount of total

chloride ions is higher than the free ones for these mixes when cured at both curing regimes and exposed to both sodium chloride concentration solutions. In addition, it can also be seen that the  $C_S$  of free chloride ions measured for the three mixes cured at NC=AC and exposed to 3% NaCl were 1.1 %cm on DCL1, 1.4 %cm on DCL2 and DCL3. However, there was a modest increment on the free  $C_S$  values when the curing condition was AC; for instance, the  $C_S$  on DCL1 was 1.5 %cm, 1.9 %cm on DCL2, and it remained at 1.4 %cm on DCL3. On the other hand, when the mixes were exposed to a higher NaCl concentration solution, the free  $C_S$  values increased significantly between curing conditions. In fact, at AC curing regimen, the %cm of free  $C_S$  on DCL1 was 3.6, on DCL2 4.6, and on DCL3 2.3 while the free  $C_S$  values measured at NC=AC were 2.5 %cm, 2.9 %cm, and 2.5% on DCL, DCL2, and DCL3 respectively. Additionally, it is apparent that the w/cm ratio clearly affects the chloride ion penetration and bounding process since there is a significant dispersion on the amount of free and total chloride ions between the three mixes when they were exposed to 16.5% NaCl solution and cured at AC.

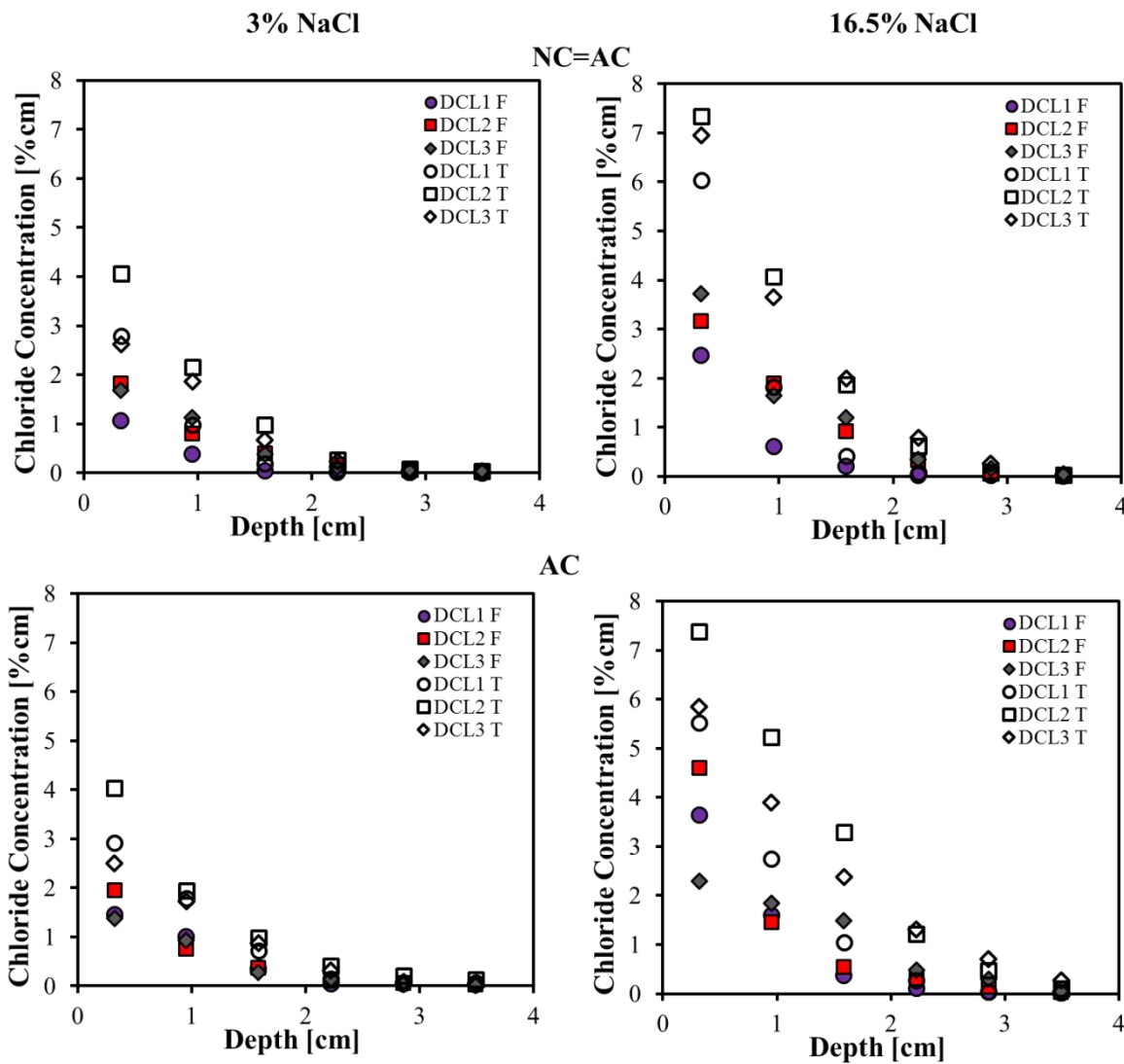


Figure 4-20: DCL1, 2, and 3: free and total chloride concentration vs. depth

Figure 4-21 presents the profiles for DCL3 and DCL6 after one year of exposure to high concentration of sodium chloride solutions at three different curing regimens (NC, AC, NC=AC). These two mixes have the highest w/cm ratio investigated; DCL9 mix also had a w/cm ratio of 0.47 but the chloride analysis was not performed on time for this study. The free chloride ion distribution on DCL3 was slightly low when the mix was cured at NC and exposed to 3% and 16.5% NaCl solutions. Also, when exposed to 3% NaCl, the amount of total  $C_s$  measured was about twice that of what the free for DCL3 at NC, AC, and NC=AC; for example, the free and total  $C_s$  for this specimen at AC were 1.38 %cm and 2.95 %cm respectively. On DCL6, the lower amount of free chloride ions was obtained when the mix was cured at NC=AC compared to the other curing conditions. The free  $C_s$  measured on DCL6 at AC were 1.51 %cm when immersed in 3% NaCl and 2.96 %cm in 16.5% NaCl; on the other hand, the total  $C_s$  for this specimen at these conditions were 2.64 %cm and 6.61 %cm respectively; it is apparent that as the concentration of the NaCl solution increased, there amount of the free and total  $C_s$  values also increased.

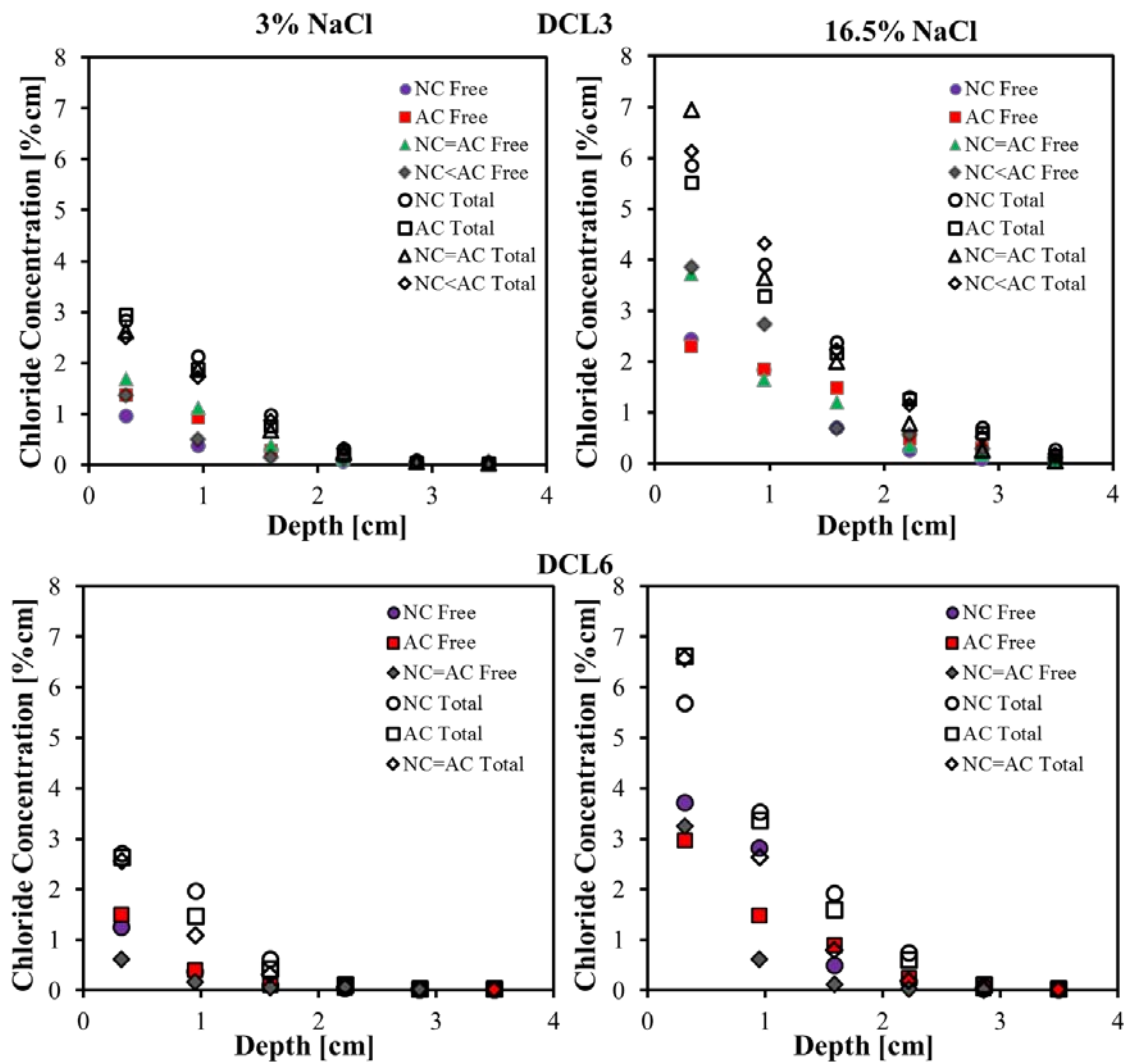


Figure 4-21: DCL3 and 6: free and total chloride concentration vs. depth

As seen in Tables 4-15 and 4-16, the amount of free chloride ions at the surface for specimens exposed to 3% NaCl was significantly smaller compared to the ones exposed to 16.5% NaCl. Also, the concentration profiles measured at the first layer and calculated at the surface from fitting were similar. In general, when immersed in 3% NaCl, the mix that reached the largest amounts of free  $C_S$  was DCL10a with values of 3.78 %cm and 3.38 %cm at NC and AC respectively. This was also seen when the NaCl solution had a higher concentration (16.5% NaCl) since 7.14 %cm was the value obtained for free  $C_S$  on DCL9 at NC curing regimen. The specimen made of 20%FA+8%SF (DCL5) showed the lowest overall free  $C_S$  content (1.5 %cm) in comparison with the other mixes where the specimens were immersed in 3% NaCl for 1 year. However, the specimen with a composition of 20%FA and higher w/cm ratio (0.47) had the smallest amount of free calculated  $C_S$  when exposed to 16.5% NaCl. In fact, the average free  $C_S$  on DLC3 was about 2.70 %cm followed by DCL4 which obtained average free chloride content at the surface of 2.73 %cm.

Table 4-15: Free and total chloride concentration at surface and at first layer for DCL mixes exposed to 3% NaCl solution for 1 year

Mix	Concentration at surface (%cm) (from fitting)						Concentration at first layer (%cm) (measured)					
	Free			Total			Free			Total		
	NC	AC	NC=AC	NC	AC	NC=AC	NC	AC	NC=AC	NC	AC	NC=AC
DCL1	0.89	1.89	1.56	3.98	3.74	4.01	0.71	1.46	1.07	3.05	2.93	2.78
DCL2	1.67	2.60	2.16	4.87	5.02	4.83	1.23	1.96	1.41	3.74	4.03	3.83
DCL3	1.20	1.77	1.88	3.59	3.76	3.11	0.96	1.37	1.36	2.84	2.94	2.49
DCL4	1.72	1.18	1.11	3.59	4.22	5.16	1.19	0.79	0.49	2.72	5.43	2.86
DCL5	1.03	1.25	1.17	3.43	4.10	4.44	0.76	0.88	0.66	2.61	2.52	2.74
DCL6	1.84	2.31	0.96	3.56	3.47	3.49	1.25	1.51	0.62	2.72	2.64	2.56
DCL7	1.20	1.02	1.19	3.96	3.42	3.71	0.72	0.63	0.70	3.06	2.62	2.78
DCL8	1.66	1.22	0.88	3.92	4.07	4.48	1.07	0.66	0.54	3.20	2.89	3.32
DCL9	1.98	2.83	1.47	4.45	4.86	4.73	1.23	1.72	0.90	3.38	3.75	3.65
DCL10a	3.78	3.38	2.28	4.56	4.55	3.78	2.65	2.62	1.79	3.60	3.78	3.50
DCL10b	1.39	1.48	0.91	3.88	3.24	3.49	2.32	1.14	0.69	2.81	2.98	2.57
DCL11	0.39	2.28	1.81	4.22	4.11	3.53	0.91	1.83	1.19	3.09	3.18	2.84

Table 4-16: Free and total chloride concentration at surface and at first layer for DCL mixes exposed to 16.5% NaCl solution for 1 year

Mix	Concentration at surface (%cm) (from fitting)						Concentration at first layer (%cm) (measured)					
	Free			Total			Free			Total		
	NC	AC	NC=AC	NC	AC	NC=AC	NC	AC	NC=AC	NC	AC	NC=AC
<b>DCL1</b>	4.71	5.19	4.92	7.66	7.19	8.93	3.02	3.77	3.01	5.91	5.53	6.03
<b>DCL2</b>	4.10	6.55	3.27	8.94	9.25	7.01	3.28	4.60	2.89	7.38	7.45	5.70
<b>DCL3</b>	3.11	2.81	3.88	6.85	6.37	7.42	2.43	2.29	3.85	5.85	5.52	6.13
<b>DCL4</b>	2.70	3.16	3.20	7.41	7.19	7.93	1.86	2.30	1.90	9.59	5.21	4.97
<b>DCL5</b>	3.82	3.30	5.14	6.78	6.82	8.55	2.80	2.44	2.76	5.16	5.47	5.43
<b>DCL6</b>	4.99	3.67	5.44	6.98	8.32	9.00	3.72	2.96	3.25	5.68	6.61	6.57
<b>DCL7</b>	2.83	2.78	3.08	7.14	7.11	8.12	1.98	1.89	2.15	5.81	5.66	6.41
<b>DCL8</b>	4.69	3.24	3.63	7.85	6.90	9.03	3.16	1.97	2.11	6.39	5.47	6.50
<b>DCL9</b>	4.75	4.66	4.74	7.43	7.88	10.21	3.52	3.17	2.94	5.97	6.35	7.68
<b>DCL10a</b>	7.14	5.42	6.20	8.63	8.15	8.48	5.88	4.46	4.70	6.89	6.44	7.08
<b>DCL10b</b>	3.59	2.97	3.11	8.44	6.86	7.71	2.88	2.25	2.32	6.17	5.85	6.02
<b>DCL11</b>	4.47	3.99	4.93	7.69	7.47	7.37	3.23	3.70	3.78	6.79	5.87	6.45

#### 4.6 Nomenclature for Specimens Partially Immersed at Elevations above Water

The following sections will discuss the results for specimens subjected to the simulated partially immersed conditions. Most of the results will refer to the elevations above water (previous sections have presented the results for the elevation below water all the time and compared these to the results from Bulk Diffusion tests).

The tidal environment was investigated indoors using fresh seawater rather than sodium chloride solution. In this simulation, Coring on the concrete blocks was carried out at elevations 4.4, 21, 32.4 and 45.7 cm (1.8”, 8.3”, 12.8”, and 18”) from the base of the block, and these locations were identified by A, B, C, and D, respectively, with “A” being the lowest elevation on the block (see Figure 4-22).

Core samples were taken after six, ten and 18 months of exposure. Cores obtained after ten months of exposures were obtained from the same blocks from which the six-month sample were obtained. A third coring took place at 18 months of age on the second specimen. This second block remains under exposure for future testing. Immediately after the six-month sampling, the holes resulting from the coring were filled using concrete (a similar procedure was followed after the 18-months coring). Cores were measured, placed in a vice, and milled to specified depths. Concrete powder was collected from between five and eight layers from the exposure faces of the cores. Chloride analysis via a slightly modified FDOT method [77] was then performed (smaller mass). Core samples taken after six months of exposure measured 3.8 cm (1.5”) in nominal diameter. The first two layers milled had a target thickness of 3 mm while the deeper layers target thickness was 4 mm. After each layer, the cylinder was measured and the powder was placed in a vial which was labeled and set aside for titration. Core samples taken after ten months of exposure measured 5 cm (2”) in nominal diameter. At the 10-month interval, the first layer target thickness was 2 mm while the deeper layers were 3 mm (thinner layers were possible because the cores had a larger diameter). Typically, at least 1 gram was used for each chloride

analysis performed in duplicate. The chloride concentration values shown below are the average of these two measured values. The concentration values are reported in %cm.

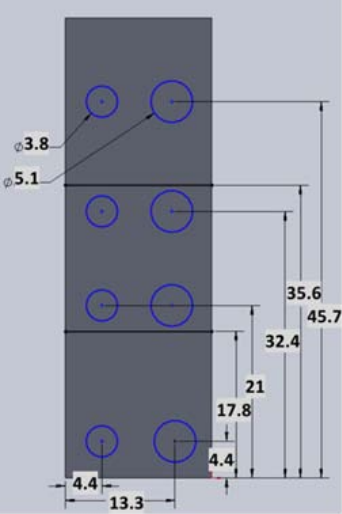


Figure 4-22: Locations of coring for specimens subjected to tidal simulation (in cm)

#### 4.6.1 Tidal Exposure Chloride Concentration Profiles

Figure 4-23, Figure 4-24 and Figure 4-25 shows profiles for DCL3, DCL6 and DCL9 respectively, after six, ten, and eighteen months of exposure time to the tidal simulation for elevations B and C (i.e., both obtained within the tidal region). These three mixes have different concrete compositions and the higher w/cm ratio studied (0.47).

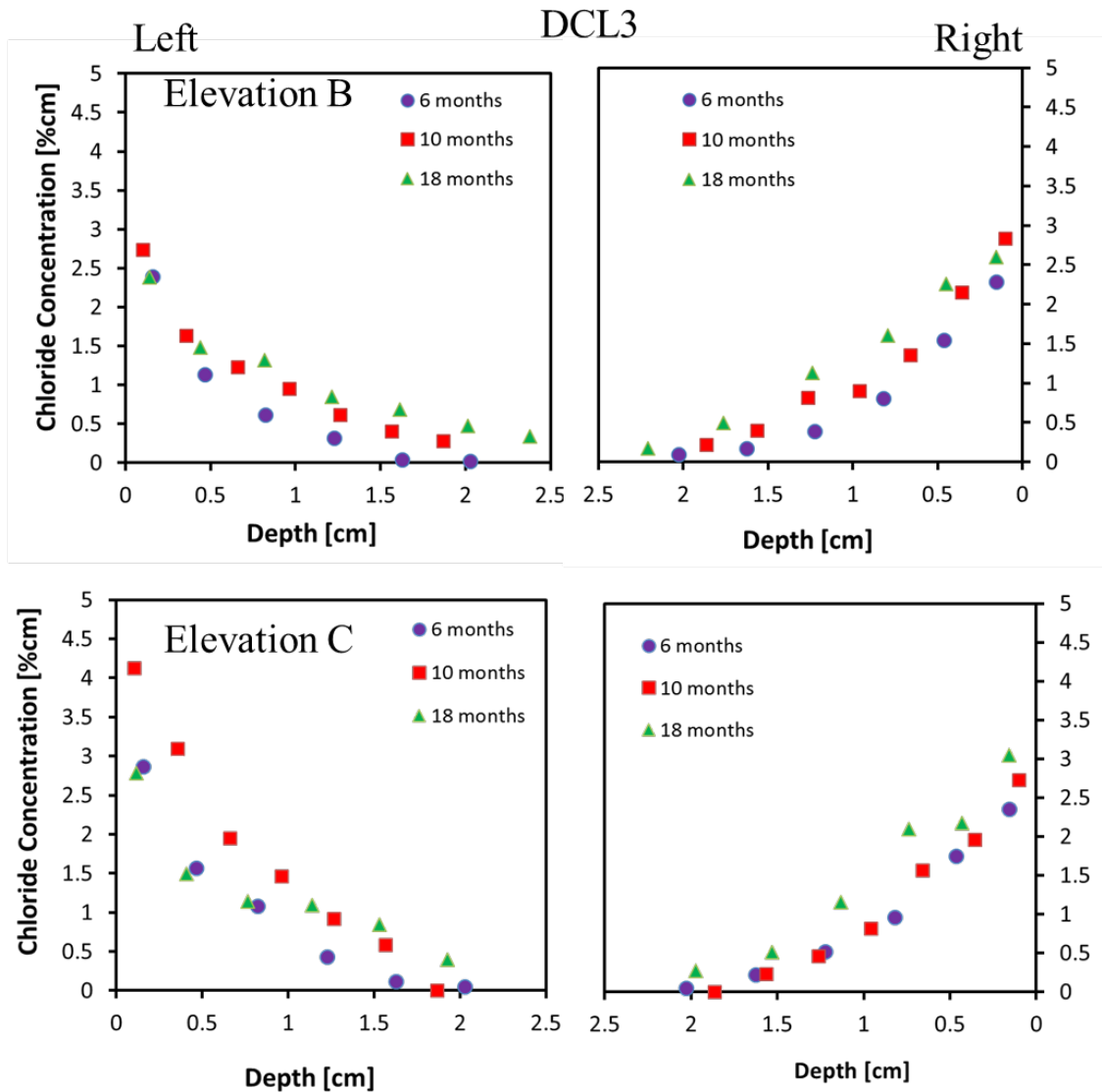


Figure 4-23: DCL3- Tidal simulation chloride concentration vs. depth (elevations B and C)

It is apparent that concrete mix composition plays an important role as to how much chloride penetrates at the different elevations. As mentioned earlier, the two sides of the concrete blocks for all of these mixes were exposed to this simulation. Similar to what was observed at elevation A (elevation below water), the amount of chloride observed at elevation B (just above water) were almost the same in both sides of the blocks for most specimens, but not all of them. The chloride profiles at elevation C were not always the same in both sides. For some specimens one side was the bottom mold face during casting, and likely had better compaction than the opposite side. However, for most specimens both sides were mold vertical sides. Also, it is apparent that the concentration at the first layer (and also at other depths) varied with the concrete mix composition and the exposure time. For instance, the concentration of the first layer at six months on DCL3 elevation B was about 2.5 %cm (1.5 %cm elevation A) in both sides, on DCL6

ranged from 1.0 to 1.25 %cm, and on DCL9 ranged from 1.2 to 2.5 %cm (elevation A 0.9 to 1.9 %cm). At 10 months of exposure, the concentration of the first layer at elevation B on DCL3 was approximately 2.7 %cm (elevation A was 1.5 to 1.9 %cm), on DCL6 was 1.5 to 1.7 %cm and on DCL9 ranged from 2 to 3.5 %cm (elevation A range from 1.8 to 2.7 %cm). Finally, when the specimens were exposed for 18 months the  $C_S$  value on DCL3 ranged was 2.4 %cm on both sides (2.4 %cm concentration is somewhat smaller than for ten months, but the 18 months profile was obtained from a different specimen), on DCL6 ranged from 1.8 to 2.3 %cm and on DCL9 ranged from 2.5 to 4.3 %cm. In general, the concentration profiles measured at 18 months of exposure showed higher concentrations than those measured at 10 and six months. Similar trends were observed at elevation C, but higher concentrations were usually observed. The specimen made of 20%FA + 8% SF (DCL6) showed an overall lower chloride concentration when exposed to 6, 10, and 18 months compared to the other mix compositions. DCL9 specimen showed a considerable increase on the chloride ions amount between the second and third exposure times. The chloride concentration on the layer closest to the surface appears to continue to increase as the exposure time was longer. Additionally, the concentration profiles at six, ten, and 18 months for specimens DCL3 followed similar patterns. A distinctive separation was observed for DCL6 and DCL9 chloride concentration profiles as time progressed. On DCL3 and DCL9, profiles corresponding to elevation C showed the highest concentrations at six months and 10 months (comparable concentrations), and at 18 months the DCL9 left side was the highest. Wetting and drying (due to the tidal exposure) is the reason that the profiles with the higher concentrations were observed at elevation C (followed by those at elevation B) than at the immersed region (elevation A).

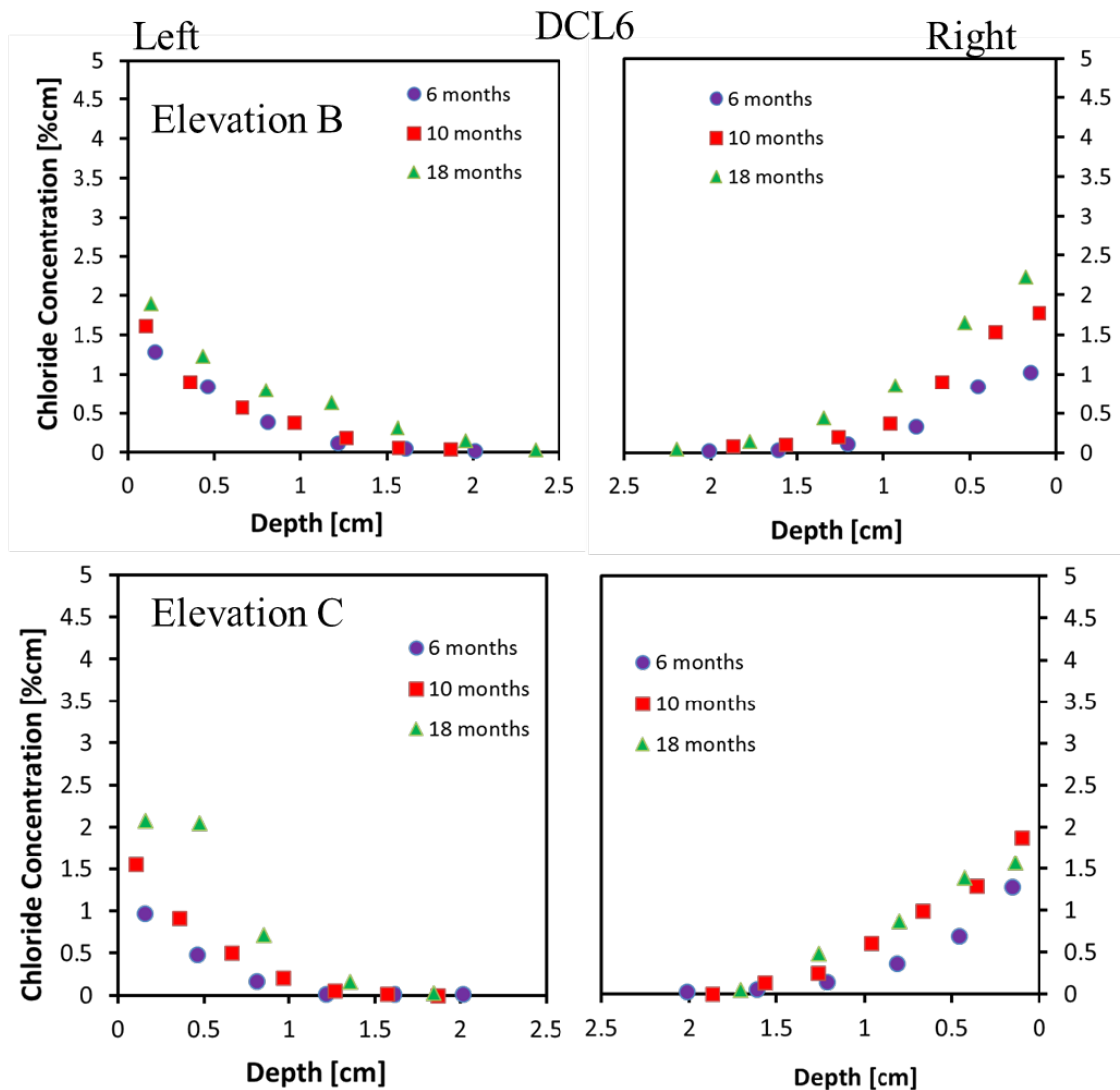


Figure 4-24: DCL6 - Tidal simulation chloride concentration vs. depth (elevations B and C)

Figure 4-26 show the chloride profiles for elevation D (above the high tide line) obtained at 6, 10 and 18 months for mixtures DCL3, DCL6 and DCL9. At six months for all three mixes the highest elevation had the lowest  $C_s$ , and was lower than 0.4 %cm (when compared to the profiles of elevations A, B and C). This was expected as at this elevation the chlorides are due to deposition of seawater spray particles (due to tank fill-up, but very little splash occurs), and to moisture gradient from the immersed portion to the higher portion of the concrete prism. In general, the concentration profiles measured at 10 months of exposure showed higher concentrations than those measured at six months, and those at 18 months showed higher concentration than those measured at 10 months. When looking at of the profiles measured at 10 months on DCL9 at the highest elevation and right side (red squares), the first two layers showed similar concentration than that measured on the core obtained just below the high water line elevation. One possible scenario is that this specimen might have been located on the side where the seawater was periodically refreshed and that sometimes the seawater might have wetted the

surface. Alternatively, the longer exposure time might have allowed the chlorides close to the surface to reach farther up (i.e., elevation D) due to moisture gradient and capillary suction. This was not observed on DCL3 specimen, but somewhat similar pattern was observed on DCL6 specimen. After 10 months the profiles on DCL6 at the various elevations were higher than those measured at six months, but the corresponding concentration only increased by a modest amount when compared to DCL3 and DCL9 profiles. The maximum chloride concentration within a given profile was not observed on the first layer for all profiles obtained at 18 months, i.e., the skin effect was observed. Recall that the profiles for 18 months of exposure were obtained from the second specimen, and this might in part explain why the concentrations were no always larger than concentrations measured at 10 months.

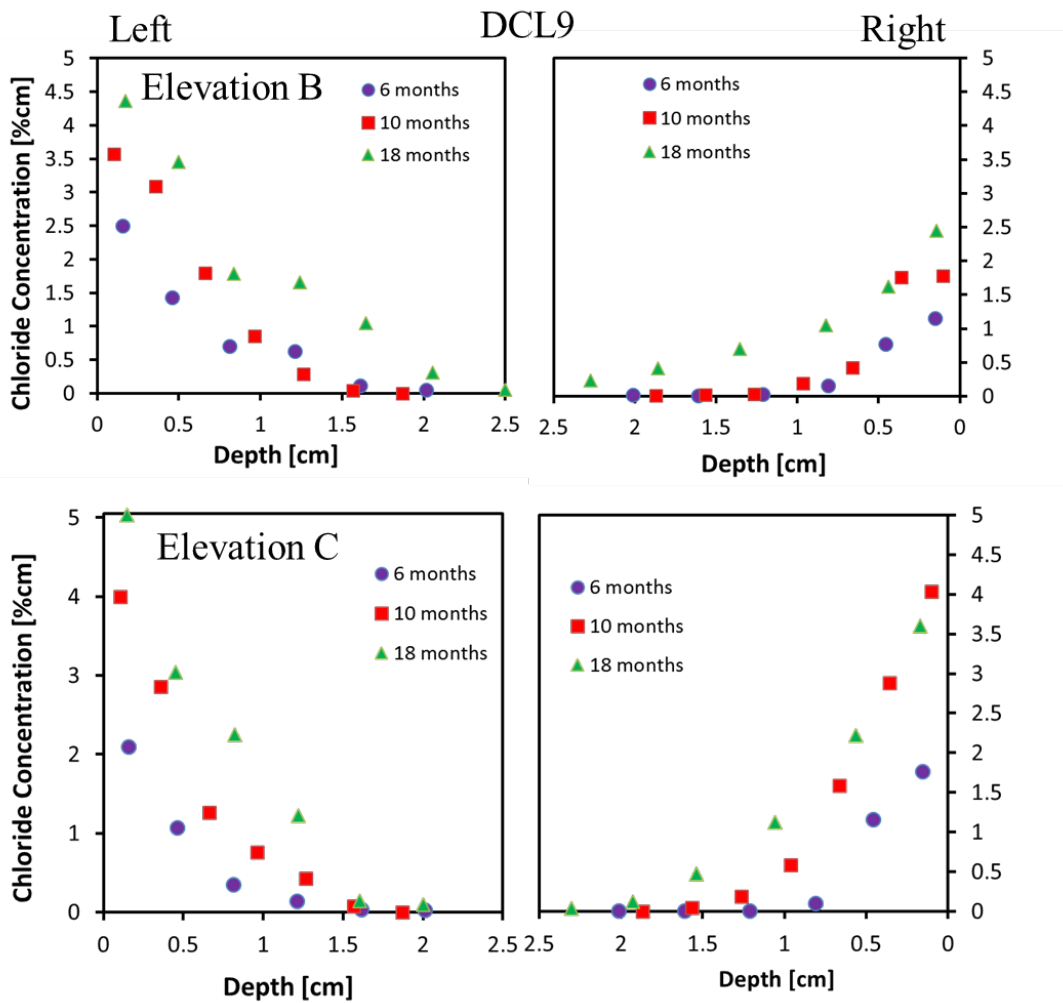


Figure 4-25:DCL9- Tidal simulation chloride concentration vs. depth (elevations B and C)

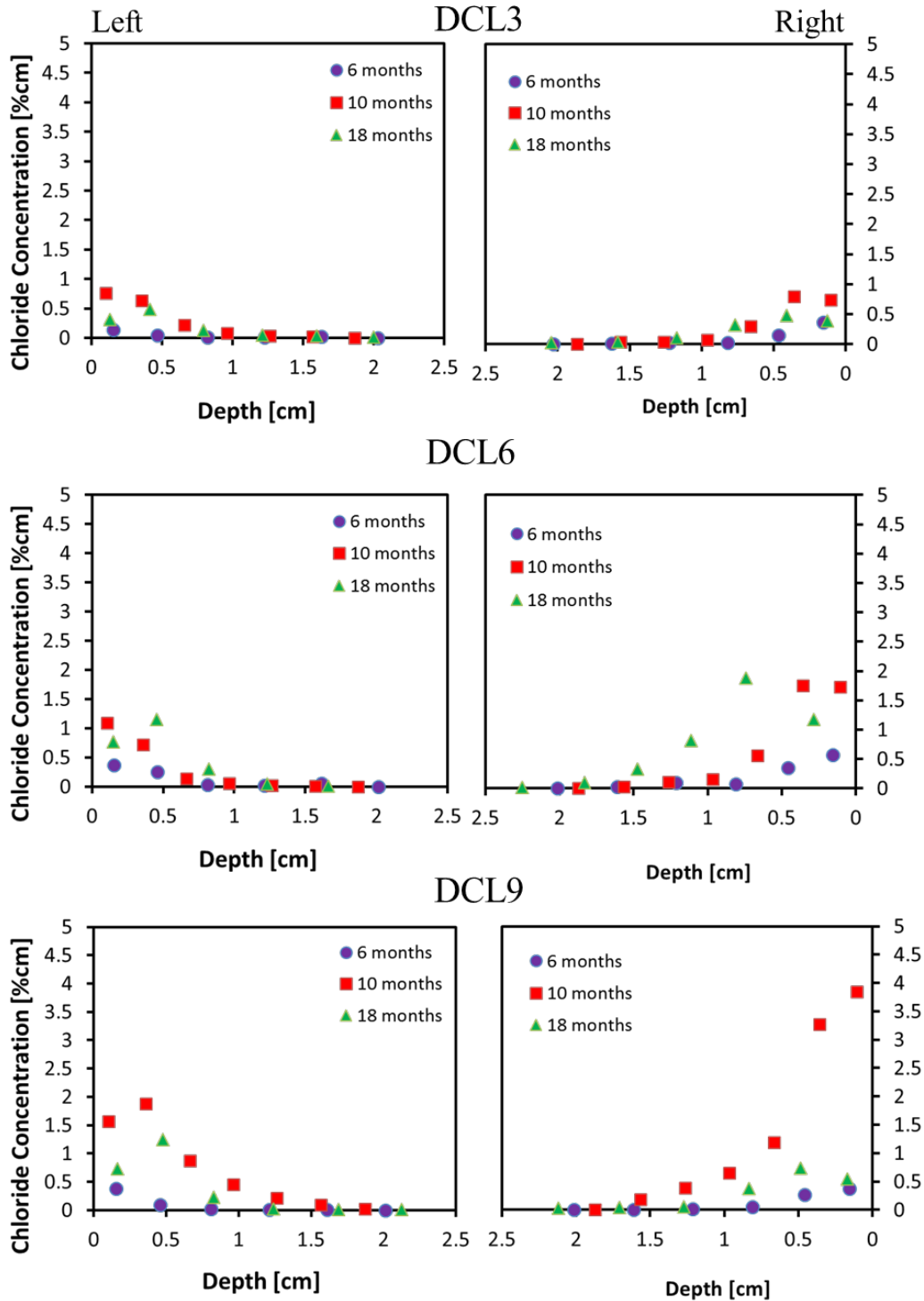


Figure 4-26: DCL3, 6 and 9- Tidal chloride profiles (elevation D)

Appendix F includes the profiles at the four elevations for the mixes not described in here (i.e., DCL1, DCL2, DCL4, DCL5, DCL7, DCL8, DCL10a, DCL10b, DCL11, and FA). FA specimens were cored only after six and ten months of exposure.

#### 4.6.2 Tidal Exposure: Chloride Surface Concentration Calculated and First Layer

The chloride concentrations calculated at the surface from the fittings done to obtain the apparent diffusivity and the concentration measured at the first layer for all of the mixes exposed to the tidal simulation at six, ten, and 18 months are presented on Table 4-17 (elevation B), Table 4-18 (elevation C) and Table 4-19 (elevation D). When comparing the measured concentration at elevation B and C for mixes with a w/cm ratio of 0.35 and different concrete compositions, it was observed that the concentration typically increased from six to ten months, but not always increase from 10 to 18 months. As seen on the table, the average  $C_S$  measured for elevation C at 18 months on DCL7 was 3.3 and 2.6 %cm, on DCL4 was 2.3 and 2 %cm, and on DCL1 was 3.05 and 1.84 %cm. When comparing the measured  $C_S$  for the group of specimens with a w/cm ratio of 0.41 the concrete with a mix composition of 50% slag (DCL8) had an average higher  $C_S$  than the other two mixes (DCL2 and DCL5) for the three exposure times. On DCL8, elevation C the  $C_S$  measured at 18 months was 5.9 and 5.2 %cm;  $C_S$  on DCL5 was 2.27 and 2.44 %cm and on DCL2 was 1.3 and 2.09 %cm.

Table 4-17: Concentration at the surface and first layer (Tidal Exposure Elevation B)

Mix	Side	Concentration at surface (%cm) (from fitting)			Concentration at first layer (%cm) (measured)		
		6 Months	10 Months	18 Months	6 Months	10 Months	18 Months
DCL1	R	1.65	5.37	2.21	1.35	3.28	3.59
	L	2.72	4.08	1.66	2.20	1.86	1.53
DCL2	R	1.85	2.01	1.15	1.60	1.83	0.73
	L	0.94	2.09	1.21	0.72	2.53	0.85
DCL3	R	3.04	3.35	1.72	2.39	2.74	2.39
	L	2.82	2.85	1.92	2.28	2.84	2.60
DCL4	R	2.62	3.16	2.38	1.93	4.14	2.07
	L	1.77	4.86	2.13	1.47	4.01	2.31
DCL5	R	3.07	4.69	2.68	2.50	2.19	2.15
	L	2.64	2.69	2.44	2.06	2.33	2.13
DCL6	R	1.67	4.69	2.12	1.29	1.61	1.89
	L	1.37	1.83	2.67	1.03	1.78	2.22
DCL7	R	1.52	2.21	2.05	1.22	1.99	1.58
	L	3.56	2.40	1.78	2.67	3.79	1.56
DCL8	R	4.20	4.24	4.96	3.41	4.69	4.31
	L	4.85	5.44	5.12	4.11	3.99	3.92
DCL9	R	3.00	4.86	4.91	2.50	3.57	4.37
	L	1.59	4.46	2.50	1.16	1.78	2.45
DCL10a	R	2.91	5.81	2.72	2.44	2.41	2.49
	L	3.75	2.54	2.68	3.39	3.26	2.57
DCL10b	R	2.64	3.46	3.68	2.26	3.27	3.55
	L	3.38	3.50	3.29	3.19	5.06	2.92
DCL11	R	1.31	5.74	2.56	1.13	2.86	2.51
	L	1.77	3.03	2.28	1.43	2.25	2.05

Table 4-18: Concentration at the surface and first layer (Tidal Exposure Elevation C)

Mix	Side	Concentration at surface (%cm) (from fitting)			Concentration at first layer (%cm) (measured)		
		6 Months	10 Months	18 Months	6 Months	10 Months	18 Months
<b>DCL1</b>	R	1.62	3.50	3.34	2.20	2.72	3.05
	L	2.05	3.75	2.37	1.16	3.10	1.84
<b>DCL2</b>	R	0.79	2.25	1.87	0.66	1.80	1.33
	L	0.38	1.67	2.87	0.21	1.32	2.09
<b>DCL3</b>	R	3.46	4.63	2.33	2.86	4.13	2.78
	L	2.90	3.14	2.97	2.35	2.73	3.05
<b>DCL4</b>	R	3.79	5.26	2.85	2.76	4.33	2.30
	L	2.36	4.64	2.62	1.69	4.29	2.01
<b>DCL5</b>	R	2.40	2.85	2.73	1.90	2.37	2.27
	L	2.35	3.38	2.93	1.88	2.89	2.44
<b>DCL6</b>	R	1.33	1.89	1.91	0.97	1.56	1.56
	L	1.63	2.14	2.03	1.28	1.87	1.68
<b>DCL7</b>	R	2.45	2.24	3.57	1.88	2.45	3.26
	L	3.74	6.27	2.87	2.90	5.61	2.59
<b>DCL8</b>	R	4.24	5.73	6.20	3.26	4.78	5.23
	L	5.03	5.38	7.49	3.69	4.84	5.98
<b>DCL9</b>	R	2.84	4.82	5.61	2.10	4.00	5.03
	L	2.57	4.93	4.17	1.76	4.04	3.59
<b>DCL10a</b>	R	2.65	3.95	1.64	2.71	3.38	1.44
	L	3.01	4.31	2.98	2.19	3.83	2.84
<b>DCL10b</b>	R	2.85	4.65	4.97	2.52	4.22	4.99
	L	4.37	5.85	4.25	3.74	5.52	3.62
<b>DCL11</b>	R	1.36	2.67	2.99	1.02	2.48	2.87
	L	2.09	1.95	2.15	1.79	2.80	1.91

Table 4-19: Concentration at the surface and first layer (Tidal Exposure Elevation D)

Mix	Side	Concentration at surface (%cm) (from fitting)			Concentration at first layer (%cm) (measured)		
		6 Months	10 Months	18 Months	6 Months	10 Months	18 Months
<b>DCL1</b>	R	0.66	1.02	1.70	0.48	0.69	1.13
	L	0.72	0.59	1.28	0.37	0.44	0.91
<b>DCL2</b>	R	0.49	1.03	0.81	0.10	0.83	0.88
	L	0.28	1.26	3.05	0.14	0.97	1.97
<b>DCL3</b>	R	0.24	0.98	2.57	0.14	0.76	0.39
	L	0.53	1.88	2.33	0.36	0.74	0.31
<b>DCL4</b>	R	0.47	7.27	1.73	0.24	5.42	1.26
	L	2.87	4.42	1.18	2.10	3.38	2.01
<b>DCL5</b>	R	1.77	3.61	2.73	1.36	2.91	2.95
	L	0.47	6.66	2.93	0.31	5.49	4.60
<b>DCL6</b>	R	0.53	1.44	3.43	0.38	1.09	0.76
	L	0.77	4.35	4.02	0.57	1.73	1.71
<b>DCL7</b>	R	0.53	0.65	1.58	0.29	0.58	1.01
	L	1.15	1.56	2.35	0.66	1.35	0.81
<b>DCL8</b>	R	1.93	2.14	1.50	1.40	1.69	1.81
	L	1.93	0.70	1.10	1.34	0.47	0.82
<b>DCL9</b>	R	0.64	3.41	1.58	0.38	1.57	0.73
	L	1.58	4.85	5.28	0.38	3.84	0.54
<b>DCL10a</b>	R	0.17	0.80	2.63	0.12	0.65	2.08
	L	0.10	1.39	3.43	0.08	1.17	2.87
<b>DCL10b</b>	R	1.30	1.96	0.69	0.94	1.18	0.43
	L	0.35	0.70	0.56	0.19	0.61	0.42
<b>DCL11</b>	R	0.42	1.31	1.40	0.31	1.10	1.12
	L	0.98	3.19	1.18	0.73	1.74	1.05

### 4.6.3 Splash Exposure Chloride Concentration Profiles

In this section, profiles obtained after exposure to simulated splash with seawater and 10% seawater will be presented. The figures show profiles obtained at elevations: B, C and D (elevation A was described above). Figure 4-27 show profiles obtained for mixture DCL3 after six, ten and eighteen months of exposure. Similarly, Figure 4-28 and Figure 4-29 show the profiles obtained for mixtures DCL6 and DCL9. On each of these figures; the plots on the left column shows the profiles on specimens exposed to seawater, and those on the right column those exposed to 10% seawater. For splash exposure only one side was subjected to the seawater (or 10% seawater) spray, unfortunately there was no control as to which face was exposed to the spray. Also, the sprinkler head used to simulate the splash sometime clogged and thus delivered less amount of spray that intended. Additionally, profiles for 18 months exposure were obtained from a second specimen, and the second specimen's exposure side might have been the mold side whereas the first specimen had the trowel side exposed. These factors and concrete composition combined to have the variety of concentrations observed. The largest concentration as a function of depth was observed on specimens of mixture DCL3 exposed to seawater, followed by DCL9 and the one with lesser chloride penetration was DCL6. On mixtures DCL6 and DCL9 the profiles with the larger chloride concentration and penetration were observed on elevation D. For DCL3 the profiles for elevations B, C, D were similar at any given age for those exposed to seawater. Significantly smaller amounts of chlorides were found on specimens exposed to 10% seawater, as would be expected. Profiles for specimens of the other mixtures exposed to seawater only can be found in Appendix G.

### 4.6.4 Splash Exposure: Chloride Surface Concentration Calculated and First Layer

The chloride concentrations calculated at the surface from the fittings done to obtain the apparent diffusivity and the concentration measured at the first layer for all of the mixes exposed to the splash simulation at six, ten, and 18 months are presented on Table 4-20 (elevation B), Table 4-21 (elevation C) and Table 4-22 (elevation D), for both those exposed to seawater and 10% seawater. In general the concentration at elevation D was the largest for any given mix, as would be expected as this elevation is the closest to where the spray took place every day. The measured concentration on layer one ( $C_s$ ) at 18 months was observed on DCL5 (4.4 %cm), and was followed by DCL3 (2.96 %cm). Diluting the seawater allowed to achieve significant lower concentrations, at 18 months and elevation D the  $C_s$  measured ranged between 1.48 %cm (DCL9) and 1.73 %cm (DCL6).

### DCL3 - Splash

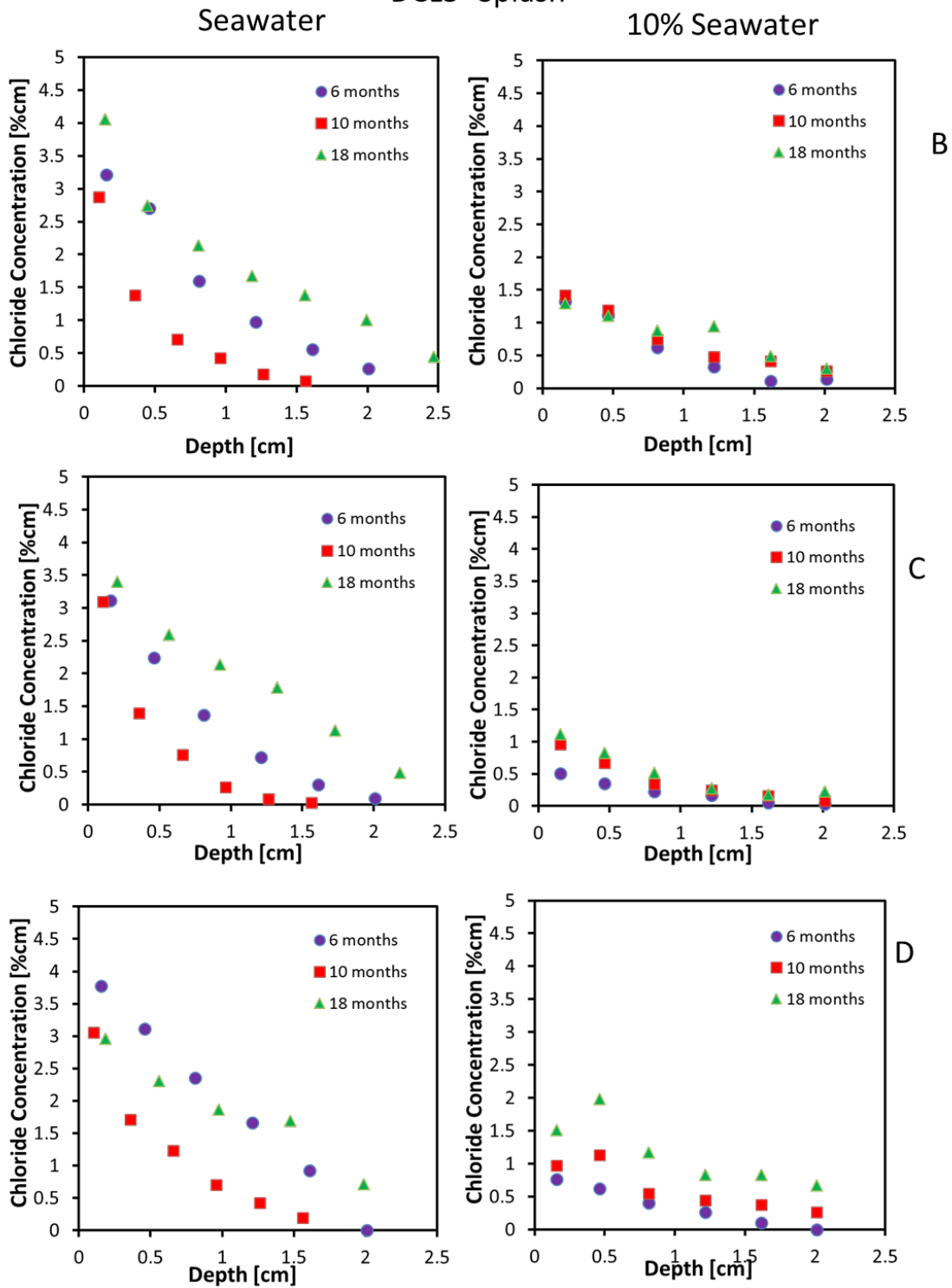


Figure 4-27: Chloride profiles for DCL3 splash exposure (elevations B, C, and D)

DCL6 -Splash

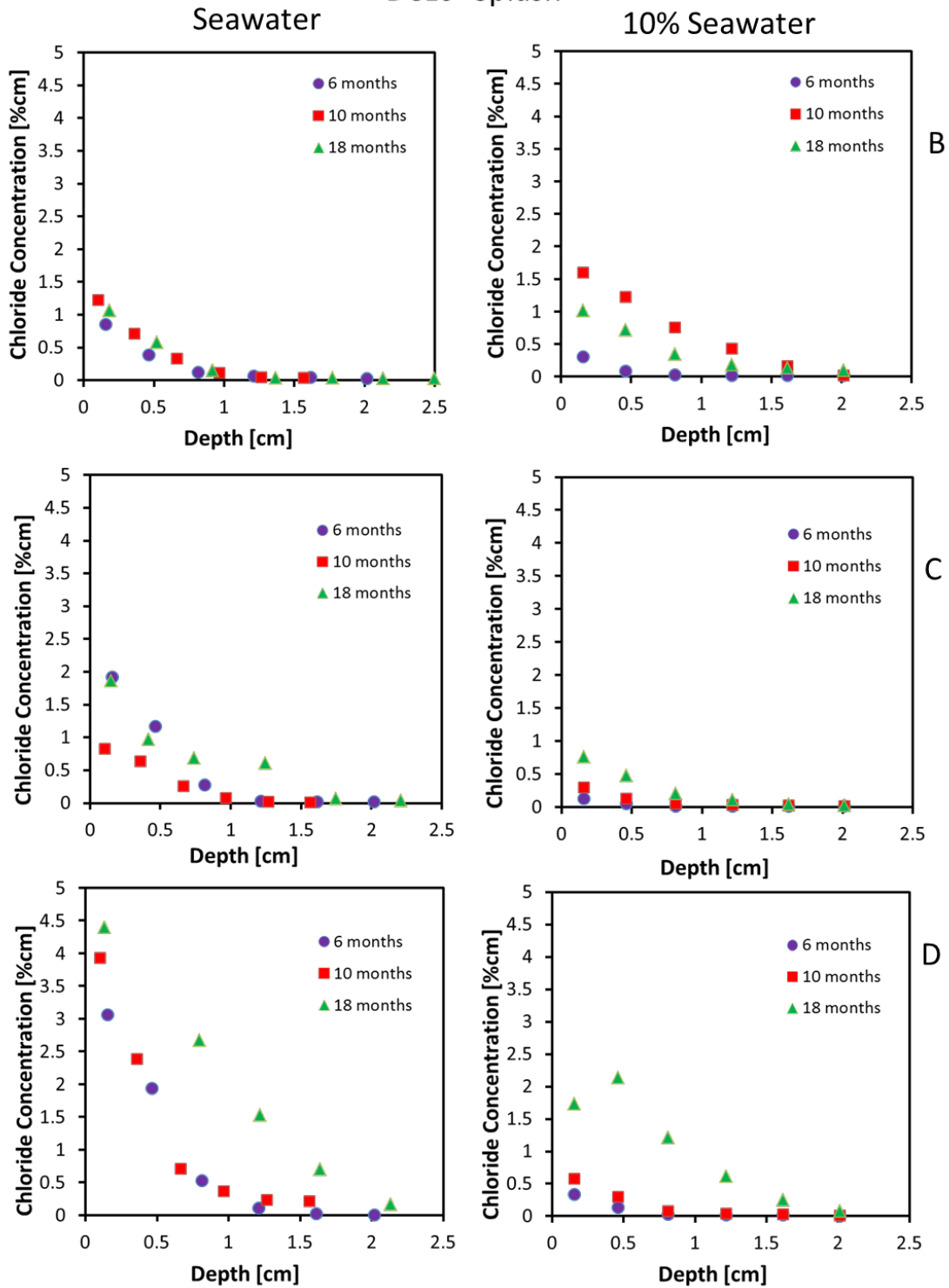


Figure 4-28: Chloride profiles for DCL6 splash exposure (elevations B, C, and D)

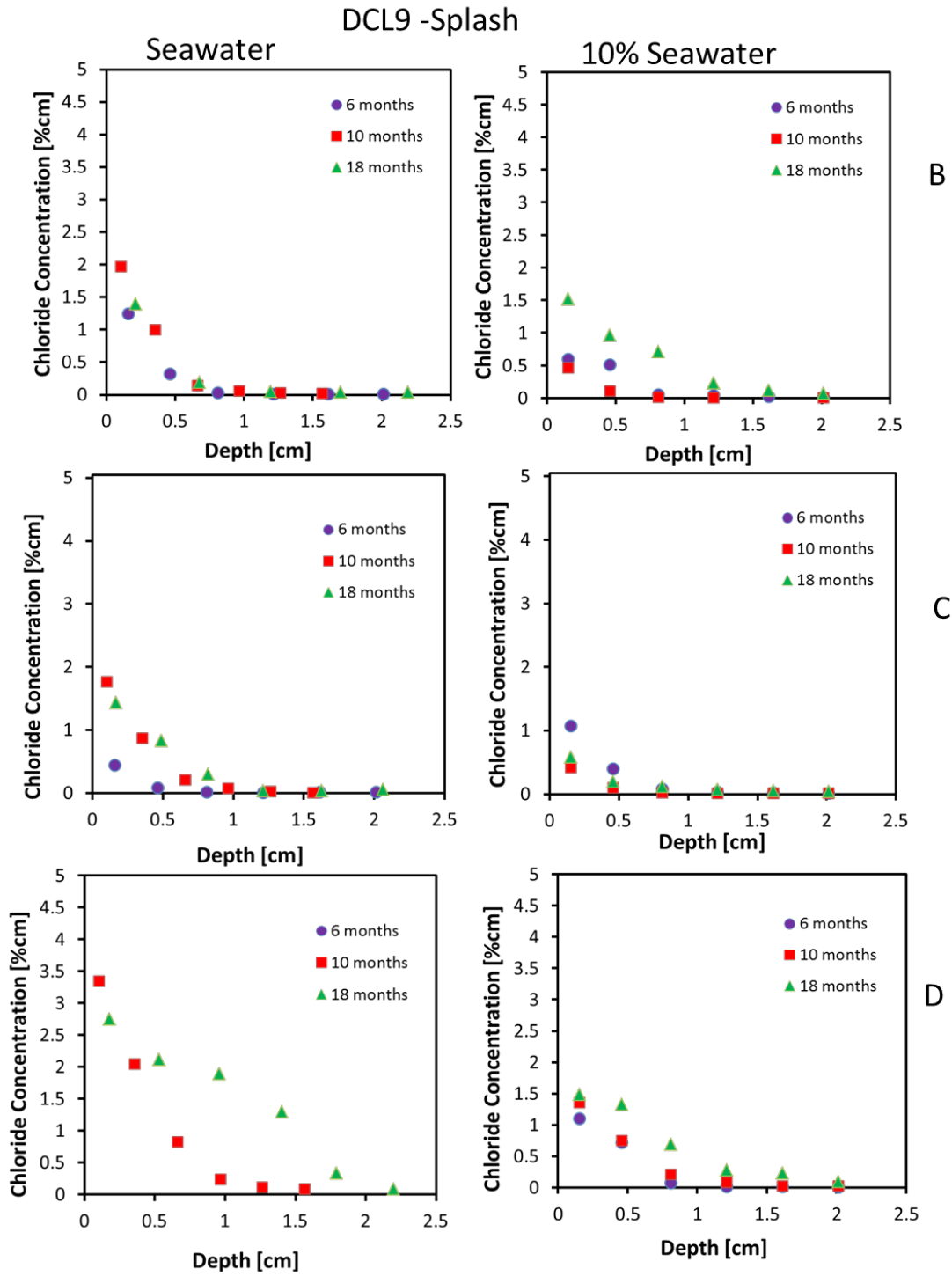


Figure 4-29: Chloride profiles for DCL9 splash exposure (elevations B, C, and D)

Table 4-20: Concentration at the surface and first layer (Splash Exposure - Elevation B)

Mix	Concentration at surface (%cm) (from fitting)			Concentration at first layer (%cm) (measured)		
	6 Months	10 Months	18 Months	6 Months	10 Months	18 Months
	<b>100% Seawater</b>					
DCL1	1.93	2.41	2.81	1.39	1.96	2.64
DCL2	1.68	2.25	2.03	1.23	1.80	1.76
DCL3	3.92	3.45	3.99	3.22	2.87	4.05
DCL4	2.96	2.74	2.17	2.26	2.13	1.67
DCL5	2.53	3.70	2.08	2.03	3.17	1.77
DCL6	0.13	1.52	1.34	0.08	1.22	1.06
DCL7	3.25	4.35	2.83	2.50	3.94	2.57
DCL8	3.23	4.89	4.54	2.99	4.47	3.88
DCL9	2.07	2.63	2.46	1.24	1.97	1.40
DCL10a	1.76	2.37	2.10	1.49	2.08	1.93
DCL10b	1.13	4.64	3.59	1.72	4.21	3.83
DCL11	0.81	2.08	1.41	0.55	1.82	1.22
<b>90% Tap water/10% Seawater</b>						
DCL3	1.66	1.63	1.42	1.32	1.42	1.30
DCL6	0.51	1.93	1.18	0.31	1.60	1.02
DCL9	0.58	0.73	1.71	0.59	0.47	1.52

Table 4-21: Concentration at the surface and first layer (Splash Exposure - Elevation C)

Mix	Concentration at surface (%cm) (from fitting)			Concentration at first layer (%cm) (measured)		
	6 Months	10 Months	18 Months	6 Months	10 Months	18 Months
	<b>100% Seawater</b>					
DCL1	2.24	2.41	2.78	1.71	2.02	2.38
DCL2	2.24	2.55	1.96	1.75	2.21	1.51
DCL3	3.78	3.82	3.74	3.11	3.09	3.40
DCL4	2.35	2.62	2.00	1.82	2.11	1.44
DCL5	1.82	1.91	1.77	1.35	1.67	1.37
DCL6	2.66	1.07	1.93	1.92	0.83	1.86
DCL7	3.47	4.24	3.47	2.91	3.49	2.91
DCL8	3.46	4.72	3.52	2.73	3.97	3.01
DCL9	0.83	2.33	1.88	0.45	1.77	1.45
DCL10a	3.41	3.43	3.25	3.04	2.97	2.76
DCL10b	3.32	4.11	2.98	2.70	1.90	2.97
DCL11	0.44	1.71	2.03	0.26	1.45	1.50
<b>90% Tap water/10% Seawater</b>						
DCL3	0.60	1.12	1.24	0.51	0.96	1.11
DCL6	0.21	0.40	0.93	0.13	0.30	0.76
DCL9	1.60	0.65	0.79	1.07	0.42	0.58

Table 4-22: Concentration at the surface and first layer (Splash Exposure - Elevation D)

Mix	Concentration at surface (%cm) (from fitting)			Concentration at first layer (%cm) (measured)		
	6 Months	10 Months	18 Months	6 Months	10 Months	18 Months
	100% Seawater					
DCL1	1.98	2.07	1.72	1.50	1.74	1.68
DCL2	3.29	2.33	2.75	2.37	2.00	2.44
DCL3	4.40	3.39	3.26	3.77	3.06	2.96
DCL4	2.96	2.91	3.36	2.20	2.39	2.84
DCL5	2.43	3.75	3.31	2.01	2.99	2.83
DCL6	4.19	4.99	5.66	3.06	3.93	4.39
DCL7	3.94	3.48	2.69	3.08	2.93	2.37
DCL8	0.81	1.40	2.82	0.55	1.00	2.21
DCL9	0.06	4.18	3.16	0.04	3.34	2.75
DCL10a	4.17	4.21	3.40	3.60	3.82	2.57
DCL10b	0.50	2.40	1.86	0.38	1.90	1.69
DCL11	1.65	2.00	2.03	1.29	1.82	1.80
90% Tap water/10% Seawater						
DCL3	0.93	1.49	1.84	0.77	0.97	1.51
DCL6	0.51	0.77	3.48	0.34	0.58	1.73
DCL9	1.58	1.76	1.80	1.10	1.36	1.48

#### 4.6.5 Chloride Concentration Profiles of Specimens Exposed at the Barge

The concrete blocks on the barge have a portion of the specimen always immersed, but the blocks are not subjected to natural tides. The portion above water are exposed to chloride deposition from seawater spray (from the ocean) and from intracoastal water spray. Depending on the location within the barge, some specimens are also exposed to waves (splash) that might be generated by boat traffic. Thus, the portion above the water was not exposed to the same amounts of chlorides on all specimens. Figure 4-30, Figure 4-31 and Figure 4-32 show the profiles at 6, 10 and 18 months of exposure (elevations B, C and D) on specimens of mixtures DCL3, DCL6 and DCL9 respectively. In general, the profiles with the largest concentration were observed at elevation B. The plots show on the left column one of the sides and on the right column the profiles obtained from the opposite side. As time progressed additional amount of chlorides were able to penetrate. On specimens DCL3 and DCL6; as the elevation increased the chloride concentration observed along the profiles for a given age decreased, (i.e., B > C > D). The chloride concentration observed on the first layer at elevation C and D increased for longer exposure periods. The skin effect was observed on DCL3 at 18 months on elevation C right side and elevation D on the left side, and on DCL6 at elevation D right side. The profiles for DCL9 at elevations C and D showed significant larger chloride concentrations. As it was stated above, this might be due to the location of the specimen within the barge and to some extent to the mixture composition. At elevation C the chloride of the first layer reached concentrations as high as 5 %cm.

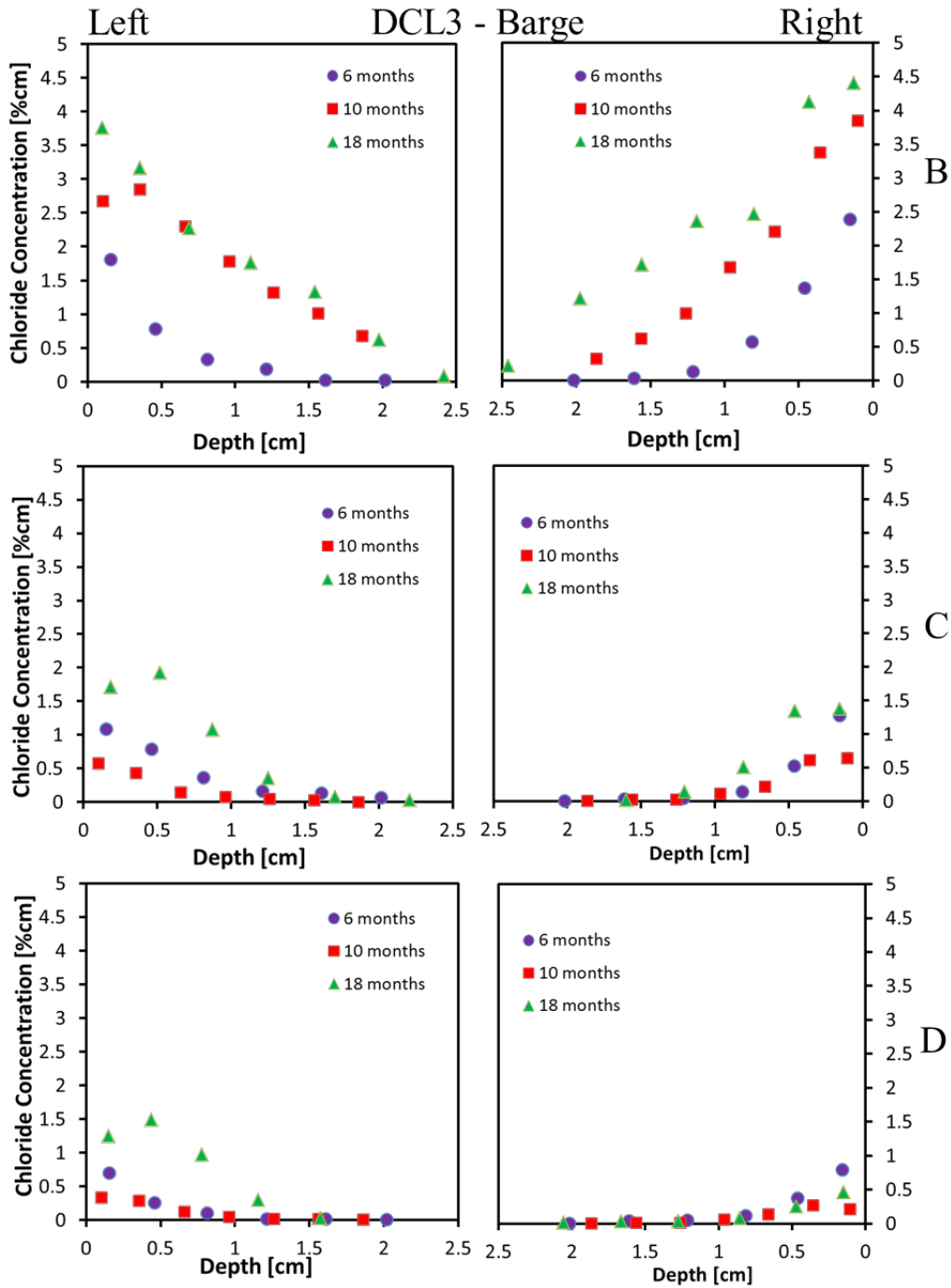


Figure 4-30: Chloride profiles for DCL3 Barge exposure (elevations B, C, and D)

Figure 4-33, Figure 4-34, and Figure 4-35 show the profiles at 6, 10 and 18 months of exposure (elevations B, C and D) on specimens of mixtures DCL2, DCL10b and DCL11 respectively. The three mixtures contain 20%FA and w/cm of 0.41, but different cementitious content. The profiles showed higher concentration on specimens of DCL10b mixture, followed by DCL11 and the lower concentration were observed on DCL2. However, these three specimens appear to have been placed on sites with higher chloride access. When comparing profiles on Figure 4-33

(DCL2) and Figure 4-30 (DCL3) the concentration at the higher elevations (C and D) are significantly larger on DCL2 than DCL3, although DCL2 has a w/cm of 0.41 and DCL3 w/cm=0.47.

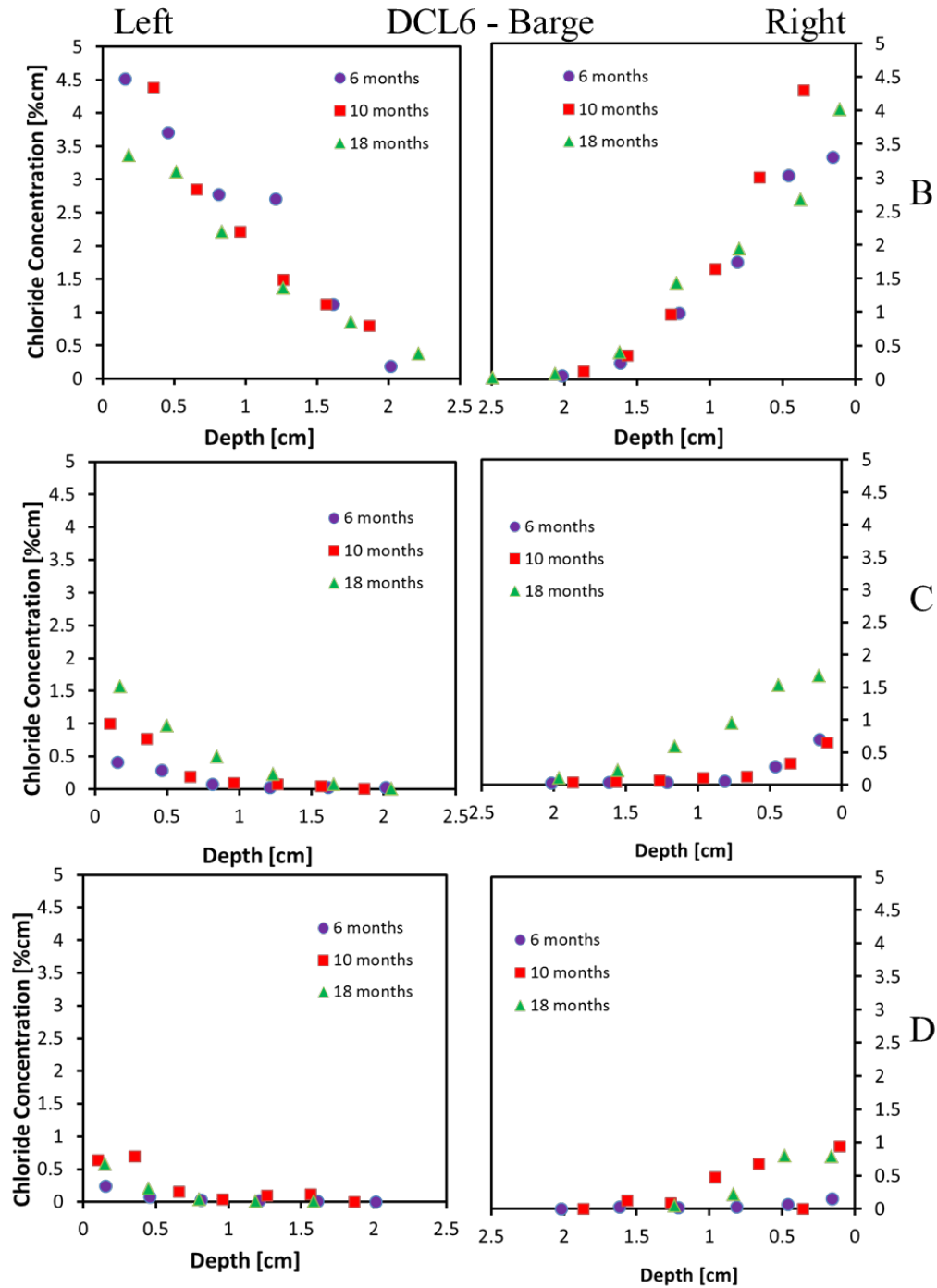


Figure 4-31: Chloride profiles for DCL6 Barge exposure (elevations B, C, and D)

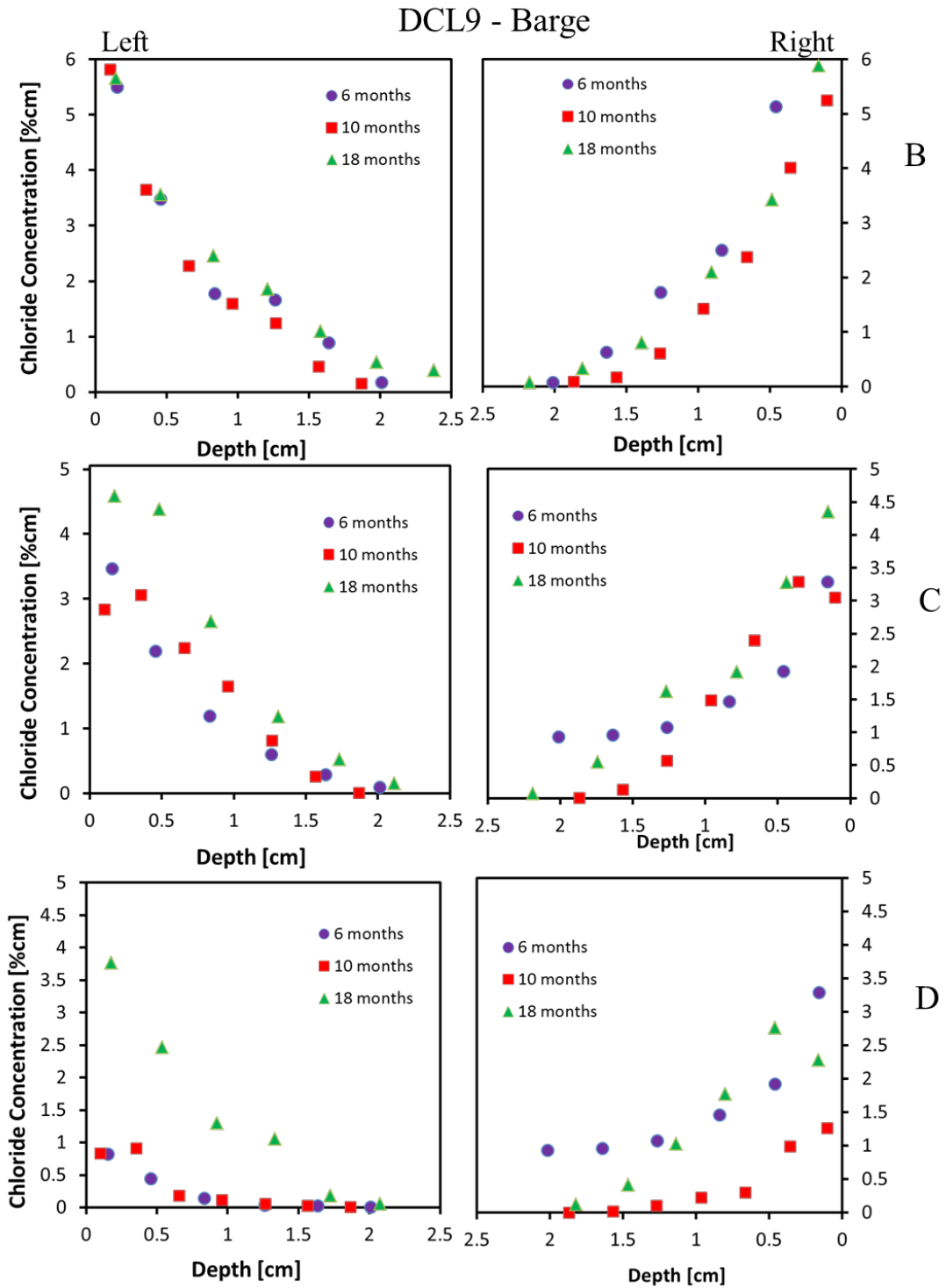


Figure 4-32: Chloride profiles for DCL9 Barge exposure (elevations B, C, and D)

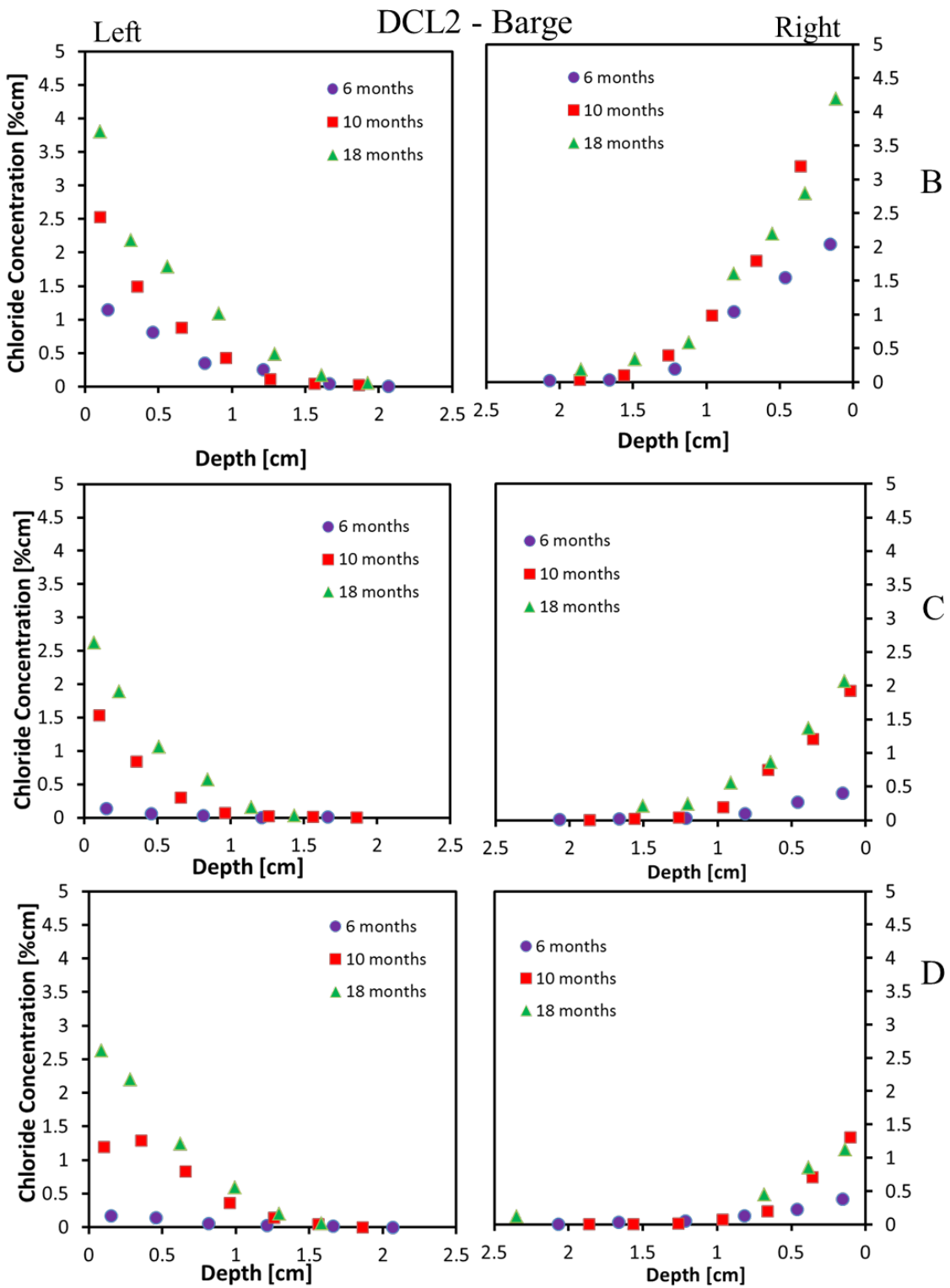


Figure 4-33: Chloride profiles for DCL2 Barge exposure (elevations B, C, and D)

### DCL10b - Barge

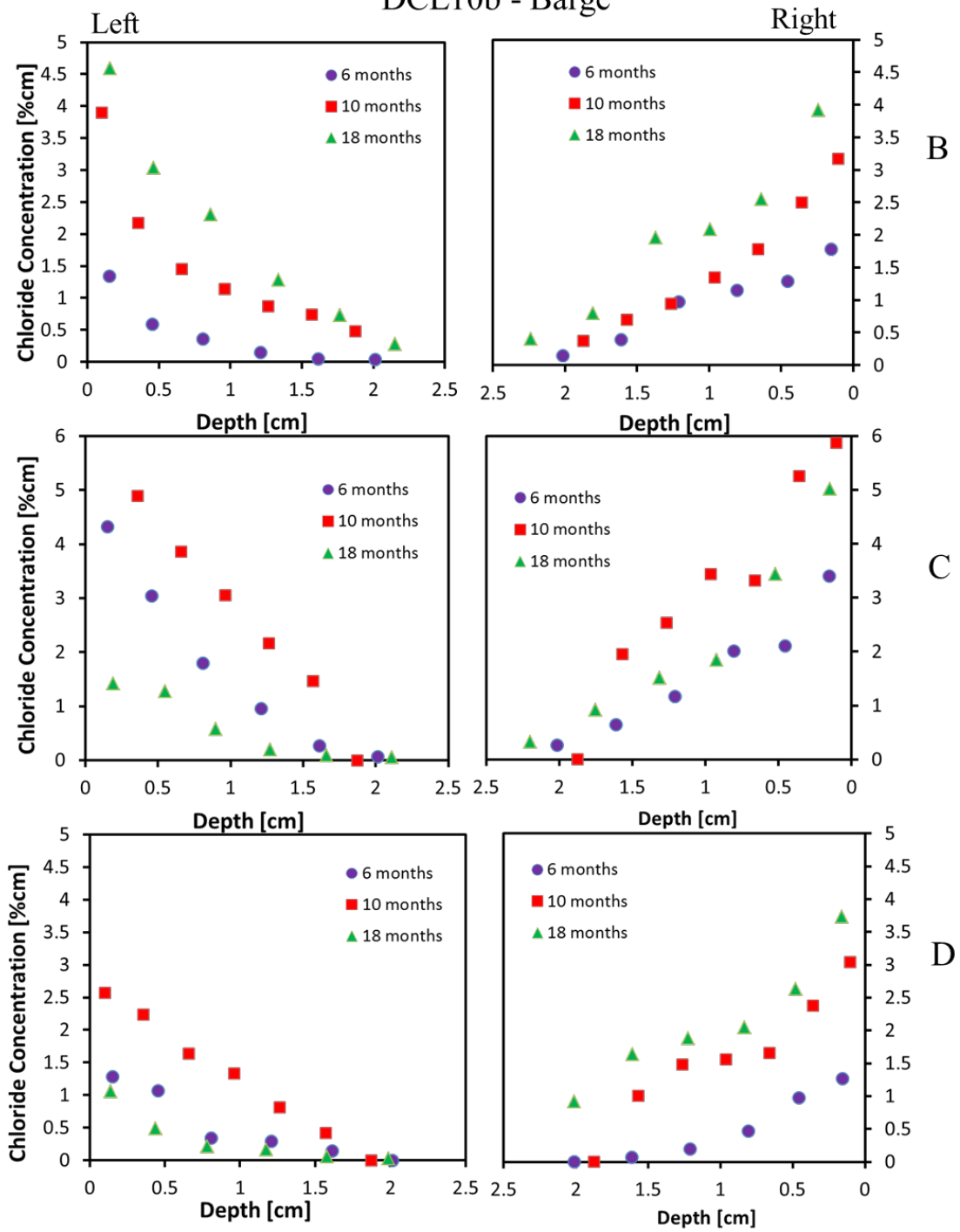


Figure 4-34: Chloride profiles for DCL10b Barge exposure (elevations B, C, and D)

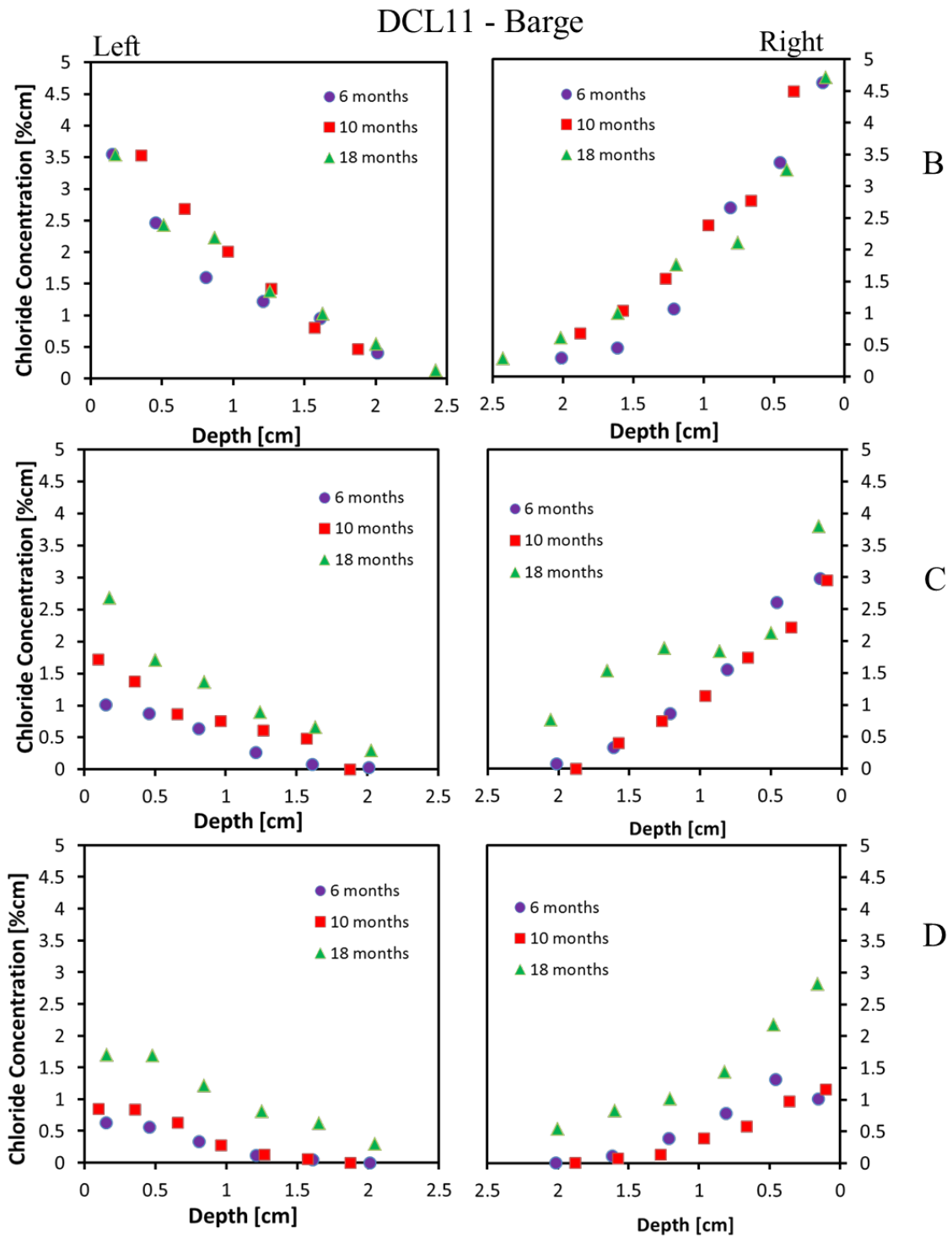


Figure 4-35: Chloride profiles for DCL11 Barge exposure (elevations B, C, and D)

The profiles for specimens of group G0/G1 were also obtained after six, ten and 18 months. Appendix H contains the profiles for each of the four elevations for specimens of group SF and FA.

#### 4.7 Barge Exposure: Chloride Surface Concentration Calculated and First Layer

The chloride concentrations calculated at the surface from the fittings done to obtain the apparent diffusivity and the concentration measured at the first layer for all of the mixes exposed to the barge simulation at six, ten, and 18 months are presented on Table 4-23 (elevation B), Table 4-24 (elevation C) and Table 4-25 (elevation D), Typically the largest concentration was observed at elevation B (when compared to concentrations at elevation C and D), and the smallest concentration was measured at elevation D. At 18 months of exposure the concentration of the first layer at elevation B ranged between 3.3 %cm (DCL6) and 5.88 %cm (DCL9), whereas at elevation C it ranged between 1.24 %cm (DCL10a) and 5.02 %cm (DCL10b). The location of the specimens within the barge allowed some of the specimens to have easier access to chloride particulates than others. For example, specimens located facing the boat traffic were likely more prone to splash. For elevation D the smallest concentration was 0.46 %cm (DCL3) and as large as 4.58 %cm (DCL9). Eight of the measured concentration at 18 months of the first layer at elevation D was equal or less than 1.5 %cm.

Table 4-23: Fitted concentration at the surface and first layer (Barge Exposure - Elevation B)

Mix	Side	Concentration at surface (%cm) (from fitting)			Concentration at first layer (%cm) (measured)		
		6 Months	10 Months	18 Months	6 Months	10 Months	18 Months
<b>DCL2</b>	R	1.41	2.95	3.91	0.40	2.53	3.80
	L	2.58	5.85	4.54	0.17	5.04	4.20
<b>DCL3</b>	R	2.45	3.70	3.94	1.08	2.67	3.75
	L	3.14	4.51	4.39	1.28	3.85	4.40
<b>DCL6</b>	R	5.42	6.58	3.99	4.52	6.10	3.36
	L	4.36	7.27	4.15	3.30	6.34	4.01
<b>DCL9</b>	R	6.22	6.39	5.88	5.50	5.82	5.65
	L	8.47	6.26	6.66	6.97	5.24	5.88
<b>DCL10a</b>	R	N/A	5.54	5.72	N/A	4.85	5.59
	L	0.72	5.31	4.31	2.94	5.05	3.98
<b>DCL10b</b>	R	1.68	3.84	3.18	1.78	3.17	4.59
	L	1.97	3.41	2.53	1.34	3.89	3.92
<b>DCL11</b>	R	3.80	5.71	4.79	4.63	5.81	3.55
	L	5.44	6.20	2.84	3.55	5.58	4.71

Table 4-24: Fitted concentration at the surface and first layer (Barge Exposure - Elevation C)

Mix	Side	Concentration at surface (%cm) (from fitting)			Concentration at first layer (%cm) (measured)		
		6 Months	10 Months	18 Months	6 Months	10 Months	18 Months
<b>DCL2</b>	R	0.20	1.93	2.82	0.40	1.92	2.62
	L	0.53	2.30	2.39	0.14	1.54	2.07
<b>DCL3</b>	R	1.36	0.73	2.34	1.28	0.64	1.71
	L	1.85	1.39	1.81	1.08	0.57	1.37
<b>DCL6</b>	R	1.04	1.30	2.72	0.40	0.64	2.01
	L	0.55	0.81	1.87	0.70	0.99	1.56
<b>DCL9</b>	R	4.19	4.68	5.73	3.29	3.05	4.58
	L	3.24	5.43	4.77	3.47	2.83	4.35
<b>DCL10a</b>	R	N/A	2.72	2.30	N/A	2.22	2.11
	L	3.45	2.71	1.57	0.57	2.22	1.24
<b>DCL10b</b>	R	5.15	6.56	1.86	3.40	5.87	1.42
	L	3.67	6.27	5.46	1.28	6.10	5.02
<b>DCL11</b>	R	1.48	1.79	3.53	2.98	2.95	2.67
	L	3.69	3.22	2.84	1.01	1.71	3.79

Table 4-25: Concentration at the surface and first layer (Barge Exposure - Elevation D)

Mix	Side	Concentration at surface (%cm) (from fitting)			Concentration at first layer (%cm) (measured)		
		6 Months	10 Months	18 Months	6 Months	10 Months	18 Months
<b>DCL2</b>	R	0.27	1.58	2.89	0.17	1.19	2.63
	L	0.48	1.67	1.34	0.38	1.30	1.12
<b>DCL3</b>	R	1.02	0.43	2.73	0.70	0.33	1.25
	L	1.10	0.30	0.58	0.79	0.21	0.46
<b>DCL6</b>	R	0.39	0.88	0.84	0.24	0.63	0.58
	L	0.22	1.14	1.07	0.15	0.94	0.78
<b>DCL9</b>	R	1.11	2.90	4.60	0.82	0.83	4.58
	L	1.95	1.60	1.31	1.46	1.26	2.27
<b>DCL10a</b>	R	N/A	1.02	0.66	N/A	0.77	0.50
	L	0.52	1.56	1.84	0.34	1.28	1.50
<b>DCL10b</b>	R	1.61	2.91	1.30	1.27	2.57	1.06
	L	1.58	3.05	2.68	1.28	3.04	3.73
<b>DCL11</b>	R	0.79	1.38	3.02	1.01	1.16	1.69
	L	1.44	1.36	2.00	0.63	0.85	2.81

## 4.8 Specimens Exposed to 70%, 80%, 90%, and 100% SD

### 4.8.1 Absorption of Specimens

Table 4-26 shows the measured absorption. These results were used to calculate and control/monitor the degree of water saturation weights for the non-saturated diffusion test.

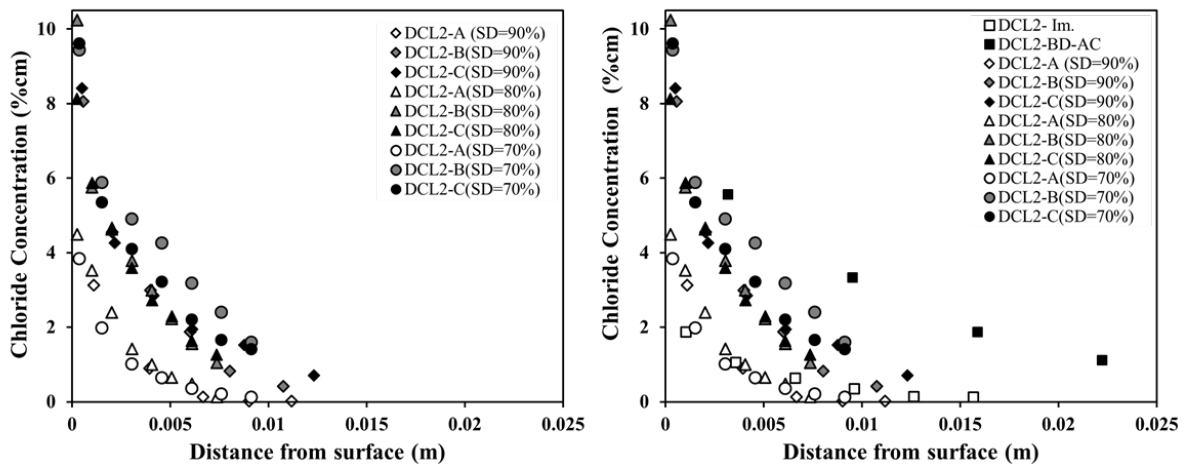
Table 4-26: Absorption of specimens (%)

Sections	DCL1 (RT)	DCL2 (RT)	DCL2 (14/28ET/RT)	DCL3 (RT)	DCL10b (RT)	DCL11 (RT)
A	2.44	3.58	2.97	4.45	4.44	3.33
B	2.86	3.59	3.51	4.98	4.98	4.17
C	2.52	3.55	3.48	5.04	4.53	3.89

#### 4.8.2 Chloride Concentration Profiles

Figure 4-36 shows the chloride profiles obtained from DCL2 specimens after non-saturated exposure to 70%, 80% and 90% degree of water saturation. The diffusion time is 105 days, 74 days and 46 days, respectively. Figure 4-36 (a) on the left shows concentration profiles for specimens DCL2 cured in 14RT/28ET/RT. Figure 4-36 (b) on the right shows concentration profiles for RT cured specimens. It also shows the chloride profiles of two fully saturated DCL2 (100% degree of water saturation - immersed) specimens part of a different section of this study. One profile was obtained from parallel bulk diffusion test on DCL2 RT cured for 130 days and then exposed to a solution with 15% NaCl solution for 365 days (DCL2-BD) as well as the chloride profile of DCL2 which was cured in RT and then immersed in seawater at an age of 70 days for 300 days (DCL2-Im) [79]. DCL2-Im exposed face was the mold surface for the simulated tidal exposure. Here the degrees of water saturation of DCL2-BD and DCL2-Im are 100% (actually fully immersed). The chloride concentrations obtained from portions A and DCL2 –Im are significantly lower than the concentrations obtained from portions B, C and DCL2-BD, regardless of curing type and degree of saturation. These results are in agreement with FDOT past experience in which cored specimens from the field (with cover concrete) had significantly lower  $D_{app}$  than  $D_{app}$  from laboratory bulk diffusion tested specimens of comparable ages. Others have attributed the difference in chloride profiles to skin effect. In [84] the authors verified that chloride profiles through concrete cover are lower than that on profiles from the cored inner portion; and this was explained by carbonation of cover concrete which reduces the porosity of concrete cover and makes the passage of chlorides more difficult, leading to lower chloride diffusion coefficients. In our investigation such carbonation was not present; however, FA pozzolanic reaction would likely start sooner at the cover concrete than at inner portions. In the present study, the thin mortar layer where the salt was deposited on portion A and the concrete cover directly in contact with solution on specimen DCL2-Im might have resulted in lower porosity and slower chloride transport. See section comparing 100% degree of saturation with and without mortar layer. It is also clear that the chloride concentrations profiles from sections A are almost identical for profiles corresponding to 80% and 90% degree of saturation and slightly lower for the profile obtained after exposure to 70% degree of saturation. Although the exposure time is different the concentration profiles are similar which suggest that the degree of water saturation plays a key role in the chloride diffusion. For concrete sections B cured in 14RT/28ET/RT with 80% and 90% of the degree of water saturation, the chloride concentrations are similar, but higher chloride content is observed in concrete section B with a 70% of the degree of water saturation. This might be attributed to the longer exposure time. Similar observation could be made from profiles of portions C. The chlorides penetrated less on those specimens subjected to 14RT/28ET/RT cured than on those specimens cured RT when

comparing same exposure conditions, but was a modest difference. This might be due to the mature age in which the diffusion exposure began (>220 days)



(a) 14RT/28ET/RT

(b) RT, immersed and bulk diffusion

Figure 4-36: Measured chloride profiles for DCL2

It is also apparent that chloride profile of DCL2-BD in Figure 4-36 (b) is generally higher than those of other specimens. The causes for this might be associated with the exposed surface (cut surface) and longer exposure time. In addition, it can be also observed that the chloride concentration of the first layer was significantly higher than that of the second layer on portions B and C, a more modest difference is observed when comparing the concentration of the first two layers on portions A. Because of this, the diffusion coefficient was computed both with the concentration of all layers and with the first layer omitted. The latter is a common practice when a skin effect is observed in experimentally obtained chloride profiles.

Figure 4-37 shows the chloride concentration profiles obtained on concrete specimens from three different mixes. The profiles correspond to specimens exposed with 80% degree of water saturation. Figure 4-37 (a) shows profiles from mixes DCL1, DCL2 and DCL3. Recall that the w/cm ratios for DCL1, DCL2, and DCL3 are 0.37, 0.41 and 0.47 respectively. It can be observed that chloride profiles that correspond to DCL3 have the highest chloride concentrations while the profiles for DCL1 have the lowest chloride concentrations. The chloride concentration of DCL2 is in between the former two profiles. The cause for this is associated with the w/cm ratio. It should be noticed that DCL3 and DCL1 have the same diffusion time (90 days) and DCL2's time is 74 days.

Figure 4-37 (b) shows that chloride concentration profiles of different concrete sections with the same w/cm ratio (w/cm=0.41) but different cementitious amount. The profiles trends indicate that the chloride contents of sections B and C are higher than those in section A. The causes for this might be attributed to the FA pozzolanic reaction taking place earlier at the thin mortar layer as discussed above. The exposure time for DCL2, DCL10b and DCL11 are 74 days, 92 days and

102 days, respectively. The cementitious amount does not appear to have a significant effect on how much chloride penetrated into the concrete.

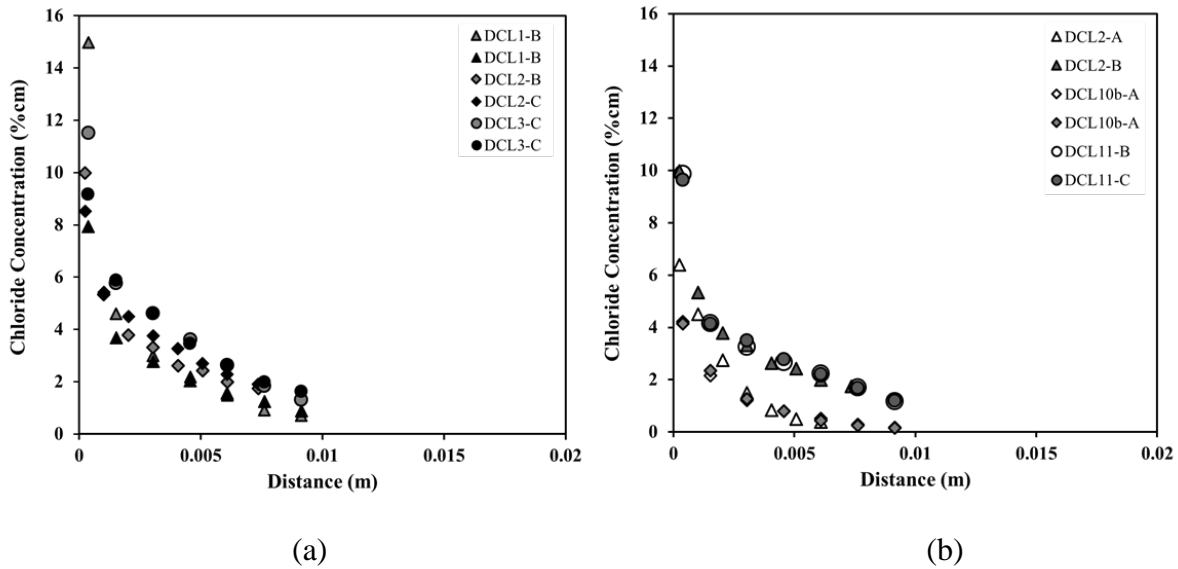


Figure 4-37: Chloride profiles for DCL1, DC2, DC3, DC10b and DCL11 with SD =80%

#### 4.8.3 Effect of Mortar on the Chloride Diffusion (100% Degree of Saturation)

The results shown in Fig. 4.36 and Fig. 4.37 above have indicated that the chloride concentrations obtained from portions A are significantly lower than the concentrations obtained from portions B and C, and it might be attributed to the effect of mortar layer. In this section, these are further discussed.

Figure 4-38 shows the chloride concentration profiles of DCL1, DCL2, DCL3, DCL10b and DCL11 cured in RT up to day 560 and then exposed to finely grounded salt at 100% degree of water saturation. Recall that top and bottom surface were exposed with the mortar layer and with the mortar layer removed.

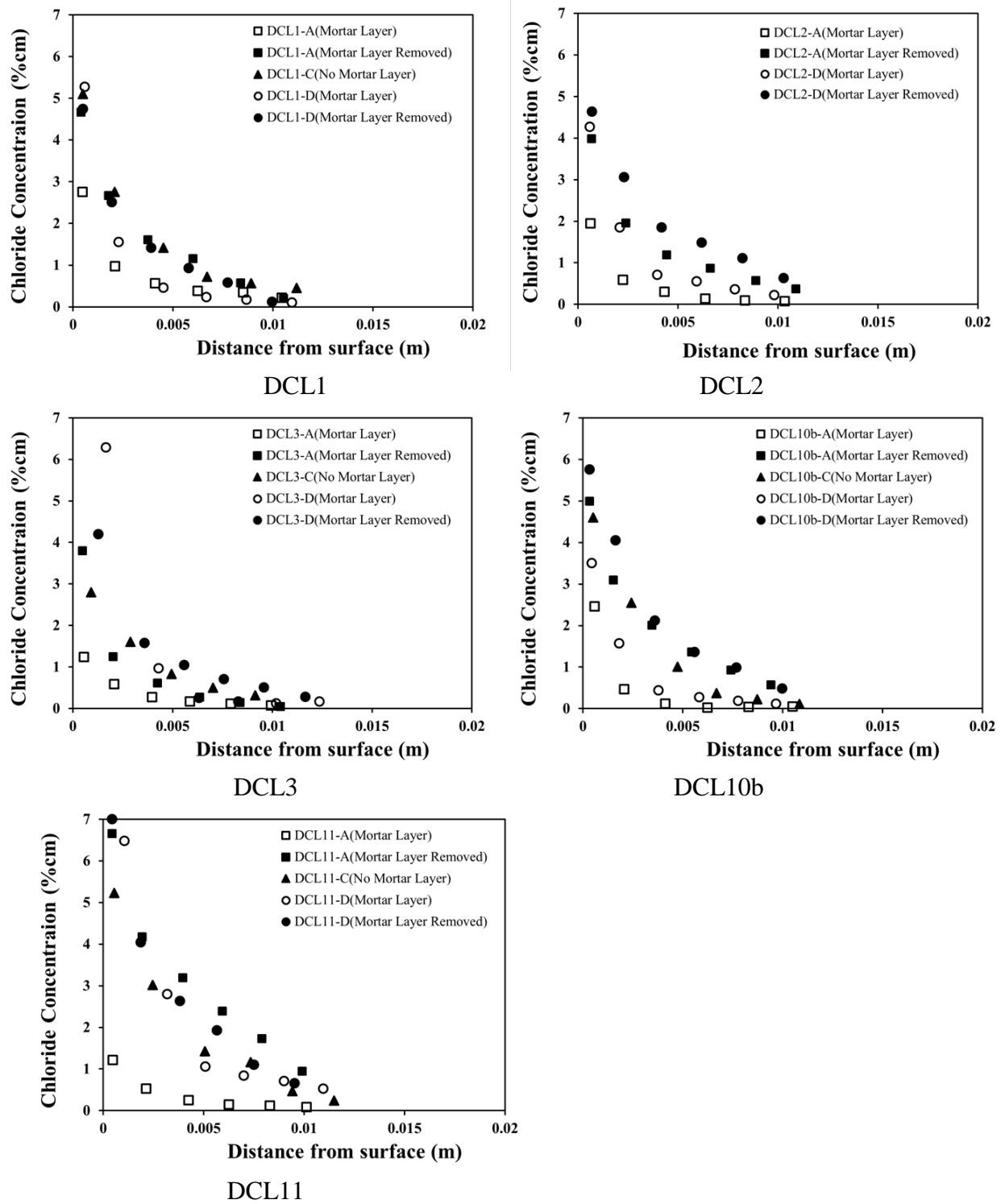


Figure 4-38: Chloride profiles from DCL1, DC2, DC3, DC10b and DCL11 cured in RT with SD =100% under the conditions of exposed surface with and without mortar layers

It is observed in Figure 4-38 (a) that the chloride concentrations obtained from the concrete portions DCL1-A with mortar layer and DCL1-D with mortar layer are generally lower than those obtained from the concrete portions DCL1-A with the mortar layer removed, DCL1-C without mortar layer and DCL1-D with mortar layer removed, regardless of the concrete section. Similarly, this trend is also observed for the chloride profiles obtained on concrete sections for mixtures DCL2, DCL10b and DCL11 as shown in Figure 4-38 (b), (d) and (e), respectively. There is a slight difference for concrete section DCL3-D with the mortar layer. Figure 4-38 (c) shows that the chloride concentrations closer to the surface for DCL3-D with mortar layer is higher than that from the DCL3-D with mortar layer removed, and might be due to the higher  $w/cm$  on this concrete mixture (0.47). As before the chloride profile obtained from DCL3-A with mortar layer are lower than that obtained from DCL3-A with the mortar layer removed and DCL3-C without mortar layer.

#### 4.8.4 Chloride Surface Concentration

Tables 4-27 and Table 4-28 show the chloride surface concentration obtained by measuring the 1st layer, the calculated  $C_s$  value using all chloride profile layers and the calculated  $C_s$  with the first layer removed. From Tables 4-27 and Table 4-28 it can be seen that the calculated  $C_s$  obtained with all the layers are generally closer to the measured concentration than the  $C_s$  obtained after removing the 1st depth chloride data. However, a better fit is achieved if the 1st layer is removed for most profiles. Comparing  $C_s$  values of DCL2 sections A, B, C cured in 14RT/28ET/RT in Table 4-33 for a given  $SD$ , it is apparent that the measured  $C_s$  of section A is generally lower than the  $C_s$  for sections B and C, which may be attributed to the mortar layer on the section A and the causes have been discussed previously.

Table 4-27: Chloride surface contents of DCL2 cured in 14RT/28ET/RT

SD(%)	Specimen	Curing regime	Chloride surface concentration (% cm)		
			From profile		Calculated
			Measured 1st layer	All depth	
90	DCL2-A	14RT/28ET/RT	3.24	4.49	5.35
	DCL2-B	14RT/28ET/RT	8.35	8.66	6.62
	DCL2-C	14RT/28ET/RT	8.71	8.69	5.42
80	DCL2-A	14RT/28ET/RT	4.49	4.72	4.55
	DCL2-B	14RT/28ET/RT	10.25	9.58	6.79
	DCL2-C	14RT/28ET/RT	8.14	8.10	6.78
70	DCL2-A	14RT/28ET/RT	3.83	4.10	2.80
	DCL2-B	14RT/28ET/RT	9.44	8.66	7.06
	DCL2-C	14RT/28ET/RT	9.61	8.82	6.37

The results from Table 4-28 show that the calculated  $C_s$  values of DCL2-A are lower than the  $C_s$  values of DCL1-A after removing the 1st layer when  $SD=90\%$ , whereas the calculated  $C_s$  values are comparable for DCL2-B and DCL3-B after removing the first layer. The calculated  $C_s$  value of DCL2-C and DC10b-C are almost the same when  $SD=90\%$ . The calculated  $C_s$  value of DCL2-A is lower than those in DCL11-A at the same  $SD$ . These trends are also observed when  $SD=70\%$  and  $SD=80\%$  except for DCL11-C. The  $C_s$  values measured and calculated for

specimens exposed to SD=100% are shown in Table 4-29. The test exposure was shorter, thus the concentration measured was in many instances smaller than that measured on lower %SD investigated. Fitted values with all layers as expected were larger than those measured at measured for layer one.

Table 4-28: Chloride surface contents of DCL1, DCL2, DCL3, DCL10b and DCL11 in RT

SD(%)	Specimen	Curing regime	Chloride surface concentration (% cm)		
			From profile	Calculated	Calculated
			Measured 1st layer	All depth	1st depth removed
90.00	DCL1-A1	RT	4.53	5.01	3.80
	DCL1-A1	RT	5.32	6.00	4.38
	DCL2-A	RT	4.76	6.38	2.81
	DCL2-B	RT	9.57	10.60	7.98
	DCL2-C	RT	7.38	7.69	6.10
	DCL3-B1	RT	13.66	12.44	7.18
	DCL3-B2	RT	9.29	9.44	8.38
	DCL10b-C1	RT	10.98	10.03	6.94
	DCL10b-C2	RT	9.96	9.46	7.14
	DCL11-A1	RT	5.43	5.94	4.26
	DCL11-A2	RT	9.84	9.49	7.22
80.00	DCL1-B1	RT	14.98	18.19	5.71
	DCL1-B2	RT	7.93	7.24	4.34
	DCL2-A	RT	6.40	6.78	6.26
	DCL2-B	RT	9.99	8.37	5.52
	DCL2-C	RT	8.53	7.42	5.92
	DCL3-C1	RT	11.52	10.39	7.01
	DCL3-C2	RT	9.17	8.58	6.94
	DCL10b-A1	RT	4.93	5.11	3.33
	DCL10b-A2	RT	4.84	5.10	3.82
	DCL11-B	RT	13.83	12.05	6.72
	DCL11-C	RT	13.51	11.70	6.89
70.00	DCL1-C1	RT	10.91	10.40	6.62
	DCL1-C2	RT	6.54	6.73	6.20
	DCL2-A	RT	5.21	5.75	3.79
	DCL2-B	RT	10.33	9.72	6.64
	DCL2-C	RT	12.61	10.55	6.16
	DCL3-A1	RT	5.55	5.86	4.54
	DCL3-A2	RT	5.57	5.57	4.29
	DCL10b-B1	RT	7.63	7.85	7.23
	DCL10b-B1	RT	8.19	8.19	7.47
	DCL11-A	RT	6.21	6.21	4.54
	DCL11-C	RT	12.89	11.34	7.77

Table 4-29:  $C_S$  measured and Fitted for 100% SD

100% SD	Cs Chloride Concentration (%cm)		
	Measured	All Layers	1 Layer Removed
DC1-25A-M(1-6)	2.7	3.3	1.1
DC1-25A-X(1-6)	4.7	4.8	3.6
DC1-25-C(1-6)	5.1	5.3	3.6
DC1-25D-M(1-6)	5.3	7.0	2.8
DC1-25D-X(1-6)	4.7	4.9	3.5
DC2-25A-M(1-6)	1.9	2.5	0.9
DC2-25A-X(1-6)	4.0	4.0	2.4
DC2-28D-M(1-6)	4.3	5.0	2.7
DC2-28D-X(1-6)	4.6	4.6	3.7
DC3-25A-M(1-6)	1.2	1.4	0.9
DC3-25A-X(1-6)	3.8	4.7	2.0
DC3-25-C(1-6)	2.8	3.3	2.8
DC3-25D-M(1-6)	6.3	11.8	4.3
DC3-25D-X(1-6)	4.2	5.5	2.7
DC10b-25A-M(1-6)	2.5	3.6	1.2
DC10b-25A-X(1-6)	5.0	4.9	3.8
DC10b-25-C(1-6)	4.6	5.1	4.7
DC10b-25D-M(1-6)	3.5	4.2	3.2
DC10b-25D-X(1-6)	5.7	6.1	5.5
DC11-25A-M(1-6)	1.2	1.4	0.8
DC11-25A-X(1-6)	6.7	6.4	5.2
DC11-25-C(1-6)	5.2	5.5	4.5
DC11-25D-M(1-6)	6.5	8.3	4.5
DC11-25D-X(1-6)	7.0	7.0	5.4

#### 4.9 Marine Atmospheric Exposure Chloride Profiles

Samples from each DCL mix were exposed to the atmosphere at three locations and data was collected after six, ten, 12, 18, 24 and 28 months of exposure. After six months samples from mixes DCL2, 3, 6, 8, 9, 10, 10a, 10b, and 11 were placed in a vice and were milled to a depth of 1 cm. Upon reviewing the results it was realized that some of the profiles might have suffered contamination from the depths closer to the surface. Samples from DCL1, 4, 5, and 7 were cored

and the cores were subsequently milled to a depth of 1.2 cm. At and after the ten month sampling interval all samples were cored and milled to a depth of 1.2 cm (in some cases up to 2 cm depth). The chloride concentration was obtained for each milled depth. Typical results of chloride concentration profiles for DCL3 and 6 are found in Figure 4-39 and Figure 4-40.

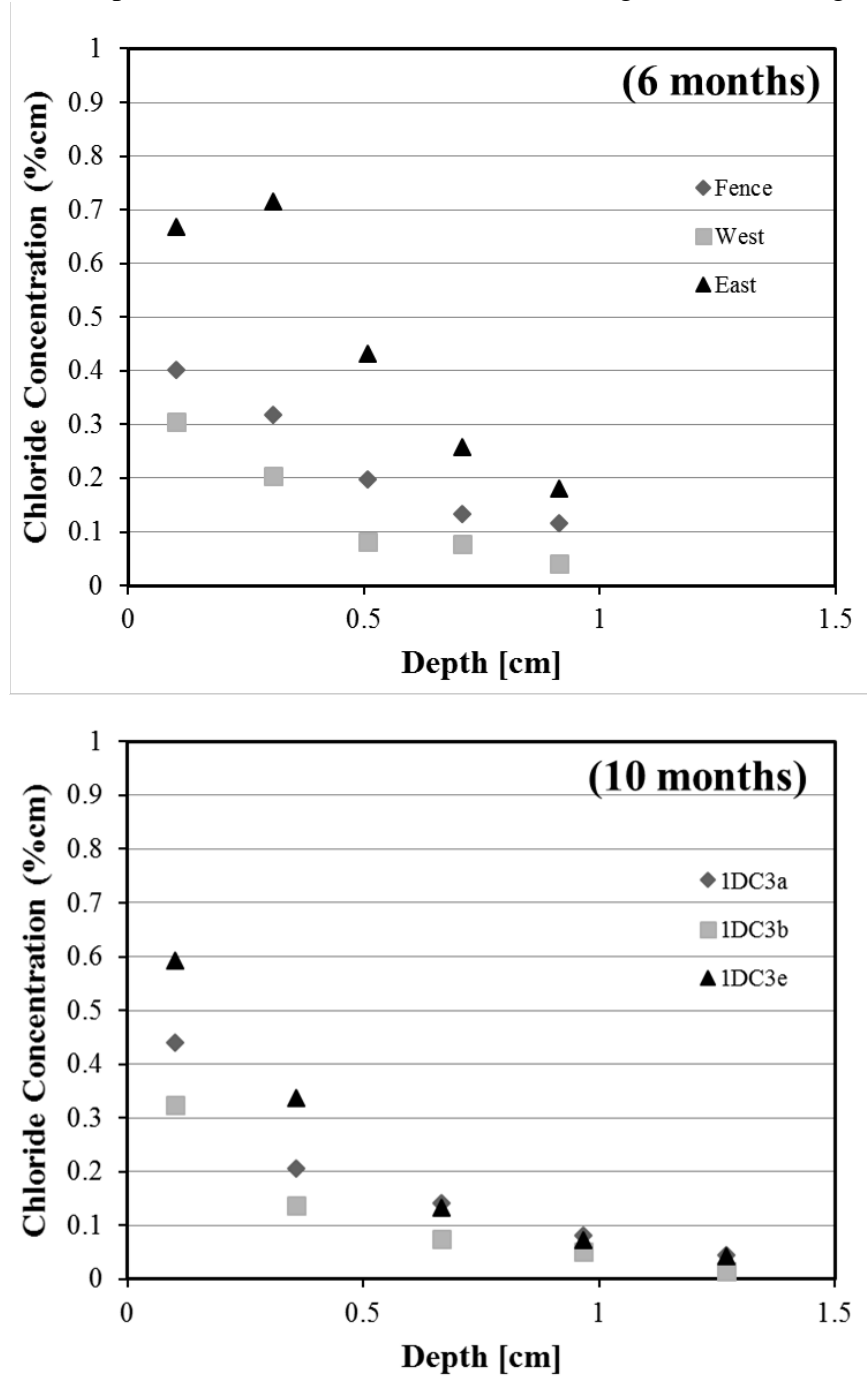


Figure 4-39: DCL3 Atmospheric simulation - chloride concentration vs. depth

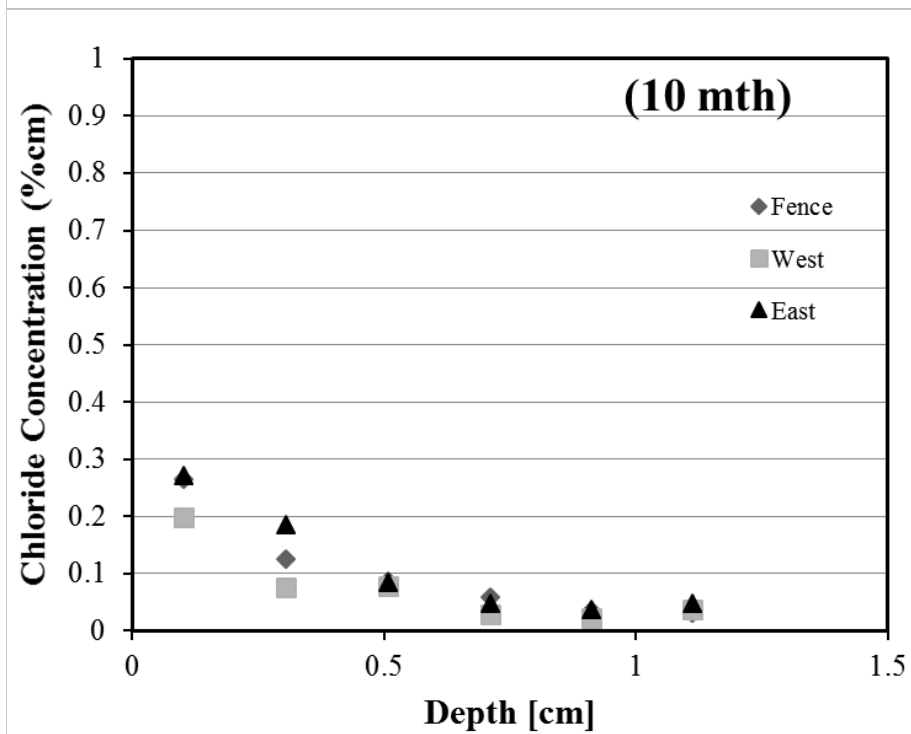
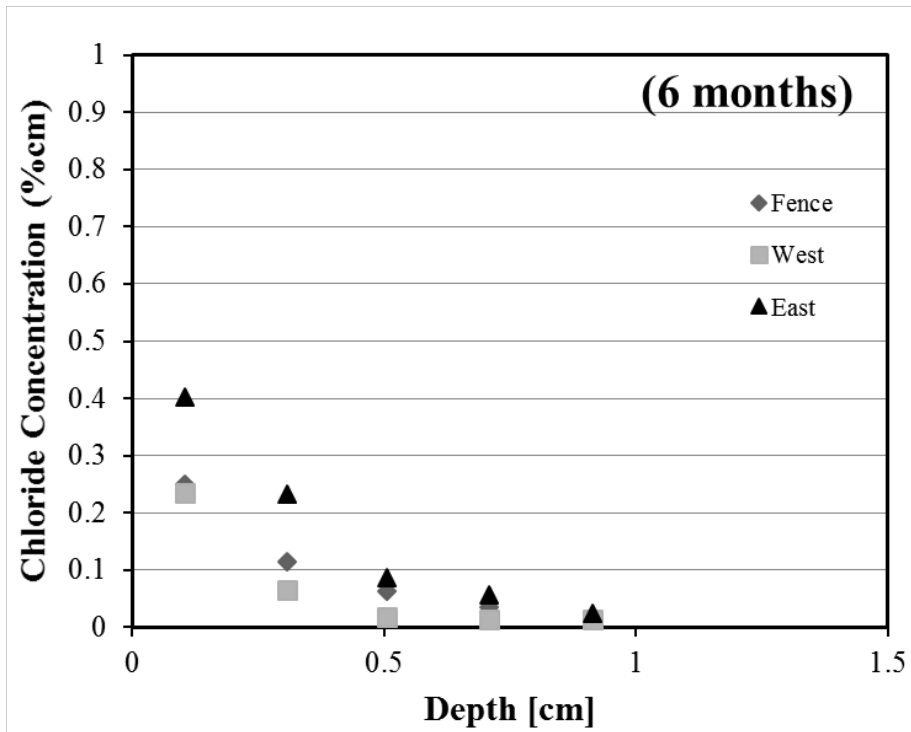


Figure 4-40: DCL9 Atmospheric simulation - chloride concentration vs. depth

In DCL3, the chloride concentration of the first layer was  $2.6 \text{ kg/m}^3$  for samples placed on the east property. Samples from DCL6 had a maximum chloride concentration of  $1.6 \text{ kg/m}^3$  for

samples placed on the east property. There was a decrease seen in total chlorides found in concrete samples from six to ten months for DCL3 and 9. The sampling procedure was changed from milling directly into the slab for the 6 month measurement to coring then milling for the ten month samples. The sampling procedure change should not have had an effect on the chloride profiles. Possible contamination from top to lower layer might have occurred on those milled directly from the slabs, however, that does not explain the reduction in concentration measured at the first layer at ten months when compared to six months. One possible explanation for the lower chloride concentration for layer 1 at 10 months is washout of some of the chlorides due to rain. Diffusivities were calculated for all concrete groups not just on the typical profiles shown here.

The following charts (shown in Figure 4-41, Figure 4-42, and Figure 4-43) display the chloride profiles that were obtained for the concrete samples DC1, DC2, and DC3, which were obtained for 24 months of exposure at their test locations. Note: “a” represents the samples placed at the fence location, “b” represents the west location, and “e” denotes the east location.

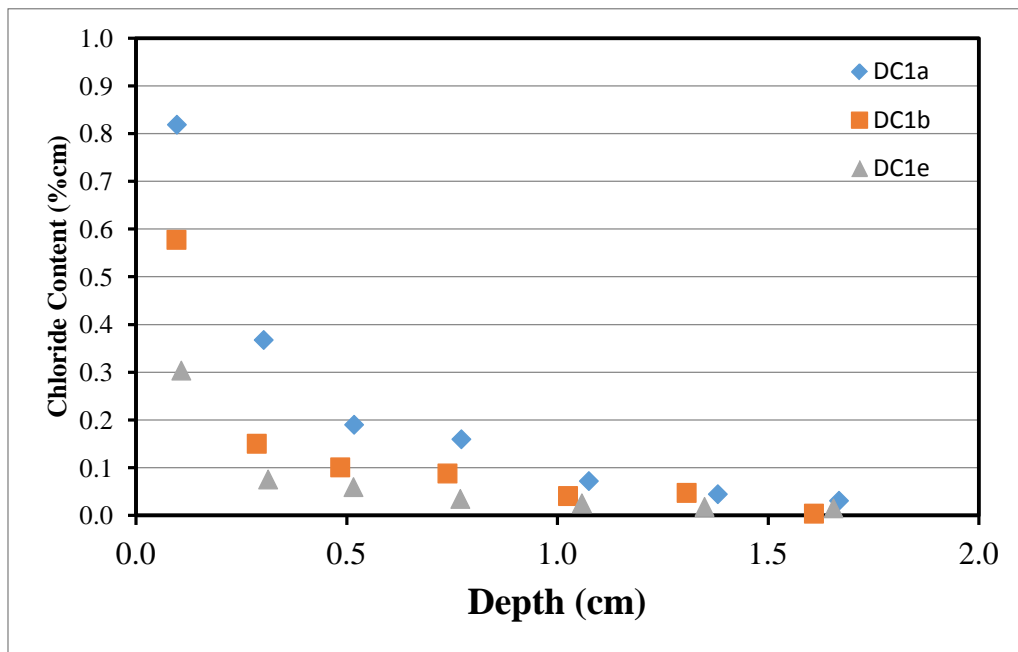


Figure 4-41: Chloride profile for DC1 after 24 months of exposure

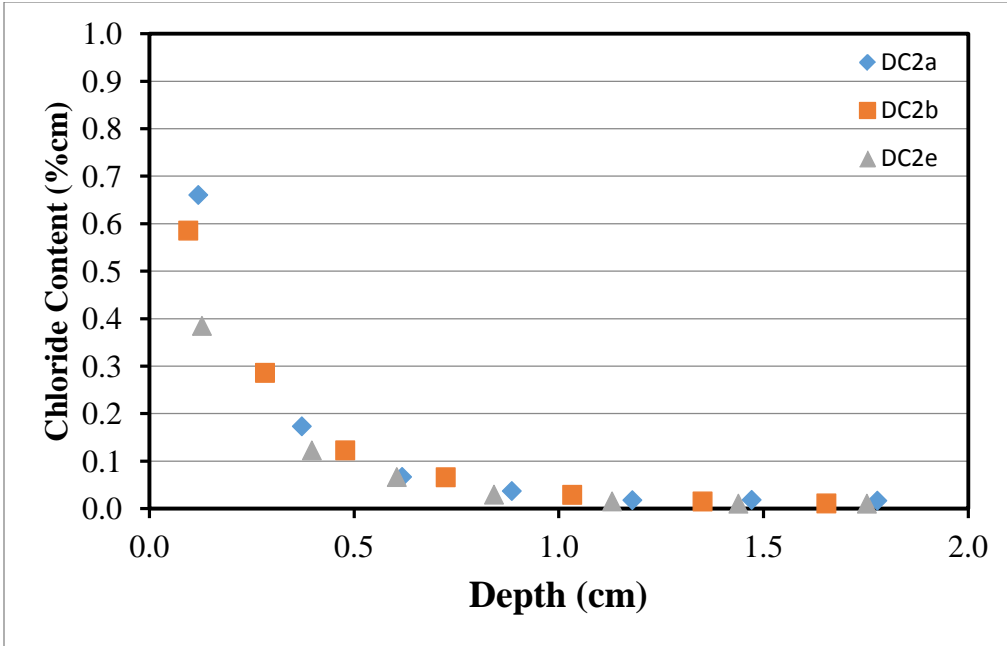


Figure 4-42: Chloride profile for DC2 after 24 months of exposure

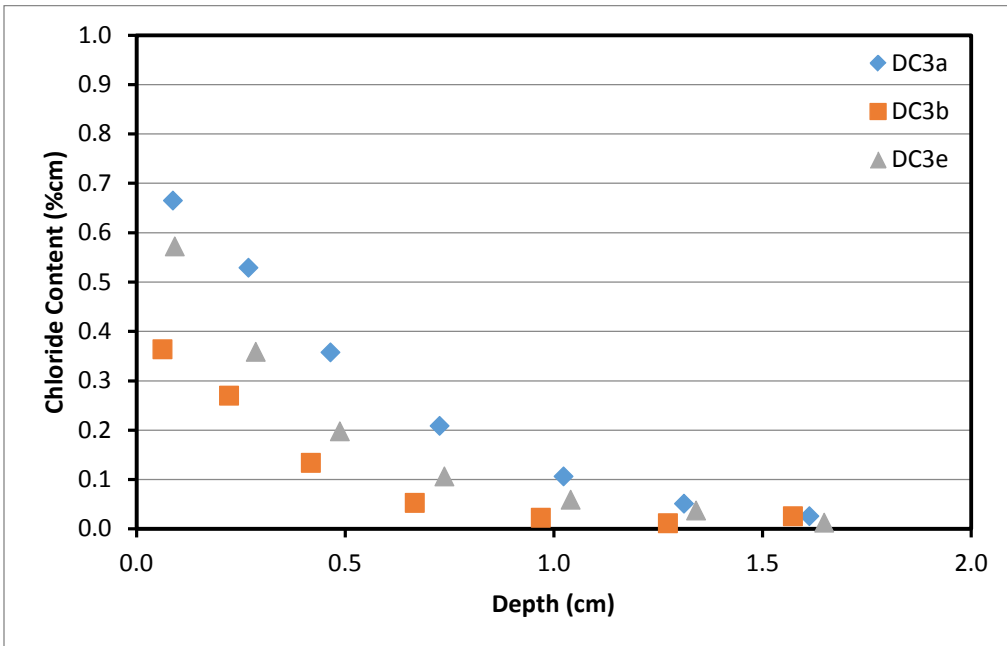


Figure 4-43: Chloride profile for DC3 after 24 months of exposure

In each case shown above, the samples located at the fence (“a”) have shown the highest amount of chlorides for the depth into the concrete. The samples at the fence location may have higher amounts of chloride in this scenario due to proximity to the Intracoastal Waterway. It is also interesting to note that in many cases, the concrete samples at the west location contained higher amounts of chloride than the samples at the east location. The samples at the west locations are

farther from the sea than the east samples, and also have a building blocking much of the easterly winds.

The orientation of the samples may provide reasoning for this observation, as the west samples are oriented with the exposure surface vertical, facing the sky, whereas the east samples are oriented horizontal, facing the east. The chlorides from the marine aerosol particles may be able to deposit on the vertical concrete samples and therefore penetrate into the concrete with greater frequency, size, and amount, than on the horizontal samples. In regards to the effect of distance from the sea, it may be more beneficial to investigate the fence and west samples with respect to the Intracoastal Waterway; a difference of only a few meters.

The three mixes, DC1, DC2, and DC3, all contained 20% fly ash, but with varying water to cementitious ratios. Therefore, it is beneficial to represent the same results, comparing the water to cementitious ratios from a particular location to better visualize the differences. Figure 4-44 below displays the results of the three mixes located at the east location after being exposed to the environment for 24 months.

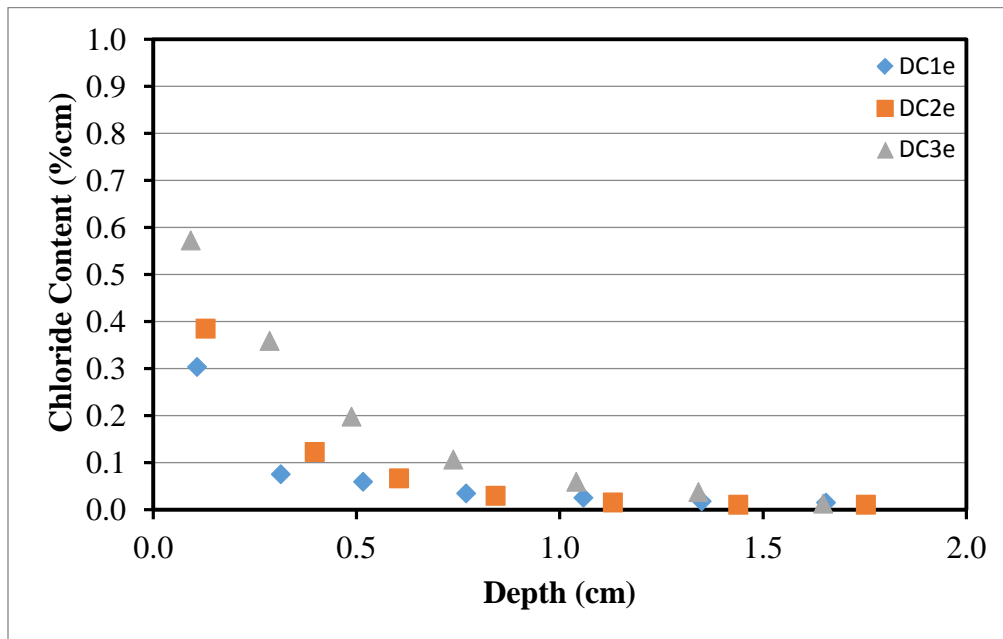


Figure 4-44: Chloride profiles at the east location after 24 months of exposure

The results shown in Figure 4-44 indicate that the DC3 mixture composition contained the highest amount of chlorides and that DC1 had the lowest. These results are in accordance with the theory that the rate of chloride diffusion is reduced with a lower water to cementitious ratio. The water to cementitious ratios for these samples are as follows: DC1 (0.35), DC2 (0.41), and DC3 (0.47). DC1, having the lowest water to cementitious ratio, showed the least amount of chlorides between this group at the east location, and DC3, having the highest water to cementitious ratio, also contained the highest amount of chlorides for the given set of profiles.

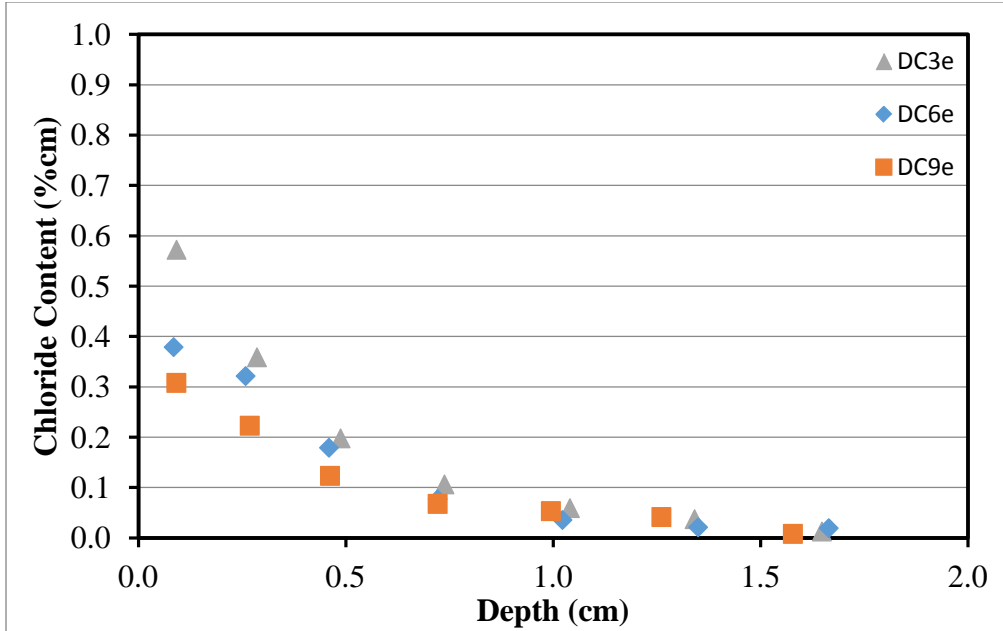


Figure 4-45: Chloride profiles comparing the different mix compositions after 24 months of exposure at the east location

The comparisons for the three different mix designs at the east location after 24 months of exposure are represented in Figure 4-45. The samples DC3, DC6, and DC9, all contain the same water to cementitious ratios, but were composed of different mix designs containing distinctive cementitious materials. DC3 contained 20% fly ash, DC6 contained 20% fly ash with 8% silica fume, and DC9 contained 50% slag. The chart in Figure 4-45 shows that the mixture containing the 50% slag (DC9) had the least amount of chloride for the given profile. The addition of the 8% silica fume to the 20% fly ash mixture indicated a lower amount of chlorides than the mix containing only fly ash in this particular case.

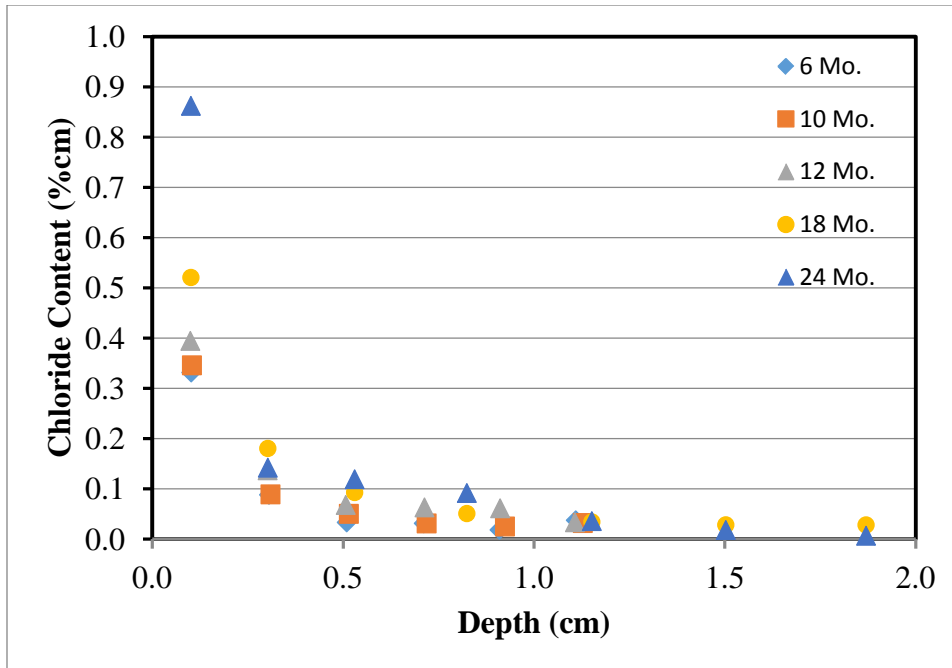


Figure 4-46: Chloride profiles for DC7e shown with time of exposure

The chloride profiles of each exposure period were overlaid on a plot to show the chloride content with respect to time. Figure 4-46 shows good results to how the theoretical chloride content should accumulate overtime. With each exposure period, the chloride concentration increased significantly in the first few layers indicating the accumulation of deposited chlorides on the concrete. The diffusivity can be visualized by observing the chloride content that actually diffused into the deeper layers. A very sharp decline with the first few layers (with depth) in the concentration of chlorides shows a low diffusivity; whereas a more gradual slope with higher chloride levels would indicate a higher diffusivity.

Specimens with geometry G4 were also exposed to marine atmosphere at the same locations and were cored after similar periods of time than those described for DCL specimens. Recall that these mixes have compositions 1C1, 1C2, and 1C3 (Table 3-2) and that the surface exposed was the one resulting after the cut, i.e., the aggregate is exposed (See Figure 3-23). Figure 4-47 shows a typical profile after 24 months of exposure. Chlorides penetrated deeper and a higher concentration on specimens exposed next to the fence and on the east site. 1C1 specimens have a lower Cs of the three groups, but also the larger concentration at the deeper layer. When comparing horizontal and vertical specimens exposed on the west site, those placed horizontally (skyward orientation) allowed a larger amount of chlorides to penetrate.

#### 4.10 Wet Candle Deposition

The wet candles were first deployed to collect data at the end of October 2011. Data has been collected and processed from the wet candles 28 times and results can be seen in Figure 4-48 and Figure 4-49. The values shown are converted to average (per exposure period) chloride deposited daily in  $\text{mg}/\text{m}^2$ . The chloride deposition data shown in these plots describe that the wet candles on the east property came into contact with the greatest quantity of chlorides.

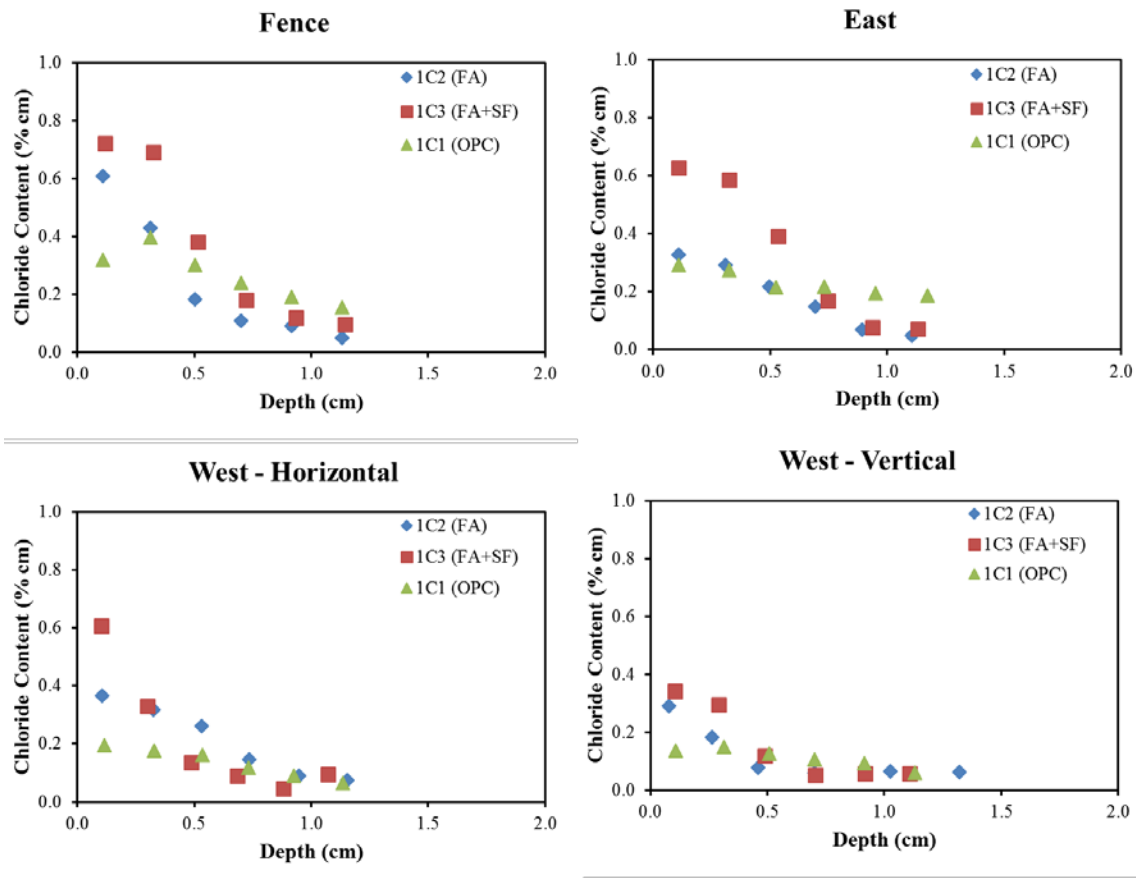


Figure 4-47: Profiles after 18 months of exposure on G4 specimens

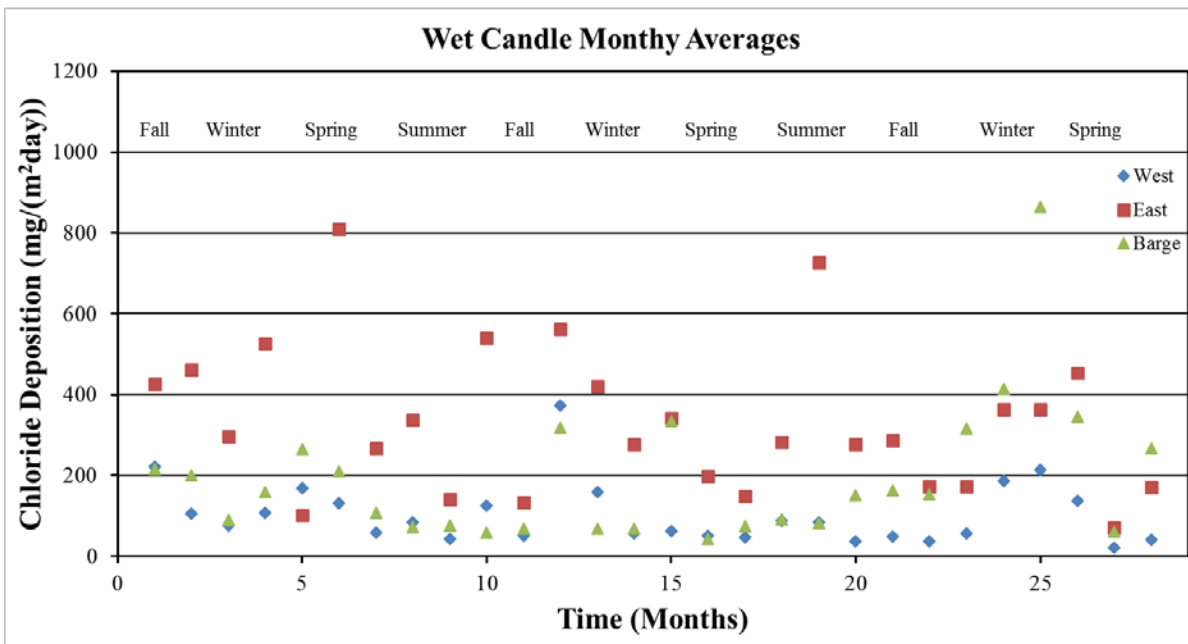


Figure 4-48: Average chloride deposition values measured at the three stations

Figure 4-49: Chloride deposition measured at each site per wet-candle setup

Table 4-30: Cumulative chloride deposition (in g/m<sup>2</sup>)

West	6 mo	10 months	12 months	18 months	24 months	28 months
<b>Group A</b>	25.56	36.20	45.71	58.68	71.35	90.72
<b>DC2</b>	24.85	34.47	43.23	59.28	68.44	86.75
<b>DC10</b>	24.85	34.47	43.23	59.28	68.44	86.75
<b>DC10a</b>	22.68	31.96	43.24	59.54	68.22	83.25
<b>DC3</b>	22.68	31.96	43.24	61.78	68.22	83.25
<b>DC6</b>	19.92	29.08	42.17	54.64	67.49	79.99
<b>DC9</b>	19.92	29.08	42.17	54.64	67.49	79.99
<b>DC11</b>	19.92	29.08	42.17	54.64	67.49	79.99
<b>DC10b</b>	19.54	31.16	41.93	54.02	69.96	79.26
<b>DC8</b>	19.54	31.16	41.93	54.02	69.96	79.26
<b>DC1</b>	18.98	35.09	41.02	52.72	72.68	77.27
<b>DC7</b>	18.98	35.09	41.02	52.72	72.68	77.27
<b>DC4</b>	18.51	36.23	40.78	52.32	72.57	76.62
<b>DC5</b>	18.51	36.23	40.78	52.32	72.57	76.62

East	6 mo	10 months	12 months	18 months	24 months	28 months
<b>Group A</b>	64.49	117.06	141.40	182.71	251.29	295.28
<b>DC2</b>	77.06	119.09	135.97	190.70	246.40	287.60
<b>DC10</b>	77.06	119.09	135.97	190.70	246.40	287.60
<b>DC10a</b>	78.69	116.12	136.57	215.07	246.03	281.37
<b>DC3</b>	78.69	116.12	136.57	230.44	246.03	281.37
<b>DC6</b>	75.96	111.12	136.46	198.24	244.58	276.17
<b>DC9</b>	75.96	111.12	136.46	198.24	244.58	276.17
<b>DC11</b>	75.96	111.12	136.46	198.24	244.58	276.17
<b>DC10b</b>	74.03	110.11	134.47	199.58	244.61	272.90
<b>DC8</b>	74.03	110.11	134.47	199.58	244.61	272.90
<b>DC1</b>	71.05	111.61	131.25	196.35	247.48	264.33
<b>DC7</b>	71.05	111.61	131.25	196.35	247.48	264.33
<b>DC4</b>	68.87	113.35	131.43	196.19	246.51	261.88
<b>DC5</b>	68.87	113.35	131.43	196.19	246.51	261.88

Barge	6 mo	10 months	12 months	18 months	24 months	28 months
<b>Group A</b>	35.18	48.39	56.29	74.82	102.18	162.89
<b>DC2</b>	35.09	45.58	53.68	76.24	102.94	159.02
<b>DC10</b>	35.09	45.58	53.68	76.24	102.94	159.02
<b>DC10a</b>	34.08	43.05	52.44	77.84	107.17	156.97
<b>DC3</b>	34.08	43.05	52.44	86.34	107.17	156.97
<b>DC6</b>	32.26	40.56	49.95	71.80	111.05	156.53
<b>DC9</b>	32.26	40.56	49.95	71.80	111.05	156.53
<b>DC11</b>	32.26	40.56	49.95	71.80	111.05	156.53
<b>DC10b</b>	30.39	40.82	47.96	70.42	124.47	159.13
<b>DC8</b>	30.39	40.82	47.96	70.42	124.47	159.13
<b>DC1</b>	27.84	41.42	45.32	69.41	136.37	155.39
<b>DC7</b>	27.84	41.42	45.32	69.41	136.37	155.39
<b>DC4</b>	27.65	41.13	46.87	70.42	137.53	156.81
<b>DC5</b>	27.65	41.13	46.87	70.42	137.53	156.81

Wet candles on the east property were deployed ~115 m from the Atlantic Ocean. The candles on the east property indicated a rate of deposition that was about twice that of the candles deployed on the west property. The candles deployed on the west property were located ~15 m from the Intracoastal waterway and ~230 m from the Atlantic Ocean. However there is a building between the ocean and these wet candles that prevents some of the chlorides from directly reaching them. Depending on the wind direction there might be some contribution of wind-blown chlorides particles from the Intracoastal waterway.

The wet candles on the barge received about half of the deposition of the east property wet candles. Exposed gauze on barge wet candles is located 1.5 m above the saltwater in the Intracoastal waterway and approximately ~235 m from the Atlantic Ocean. Wet candles on the barge on average did receive more chloride deposition than those on the west property. Boat traffic might be responsible for splash that produces a larger spread on the range of values measured on those placed on the barge.

Integrated deposition was calculated for the first six, ten, 12, 18, 24 and 28 months that each sample group was exposed. The integrated values were obtained using deposition on the wet candle at each site. Average monthly deposition was used in conjunction with the amount of days in each month that the samples were exposed to determine the chlorides available to be deposited into each concrete group. The deployment date was different depending on when the specimens were cast, transported to Seatech and after the application of the waterproofing mortar. The results of the cumulative potential chloride that could go into each concrete mixture can be found in Table 4-30 expressed in  $\text{g/m}^2$ .

#### **4.11 Specimens Subjected to Tidal Simulation for >18 Years: Chloride Profiles**

The cores were sliced at SMO. One column per each of the mixtures types described in Table 3-9 were selected for coring. Each layer was 0.635 cm (0.25 inches). The titrations for this set were made at SMO. Two profiles were obtained per core, i.e., the core was sliced from both ends.

Additionally, the chloride concentration at the center of the core was also determined from a 0.63 cm (0.25 inch) slice obtained from the center of the core. The obtained profiles at each elevation are shown in Figure 4-50 and Figure 4-51 for specimens with SFFA, SF and OPC respectively. Two profiles per elevation are shown along the thickness of the core, one on the left and one on the right. On each column the lowest  $C_5$  usually corresponded to those cores obtained at the highest location. A couple of exceptions took place for the right side of specimens with 20% and 25% superfine fly ash. The  $C_5$  for the second highest location was usually the largest  $C_5$  concentration since this location is just above the high tide mark, although for some cases the largest  $C_5$  was observed for the elevation just below the high tide mark (cored obtained 1.07 m from the bottom) Skin effect was observed at some elevations on cores from columns with superfine fly ash and on just a couple of profiles for those with silica fume (11%SF Left 0.9 m, i.e., low tide, and 15%SF Left 0.4 m, i.e., below water).



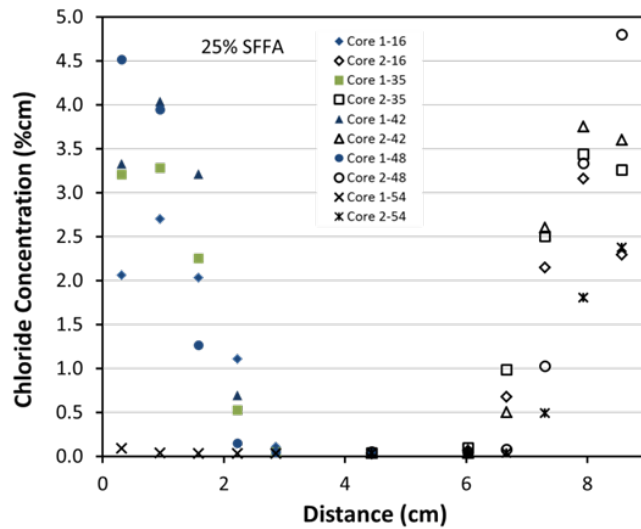
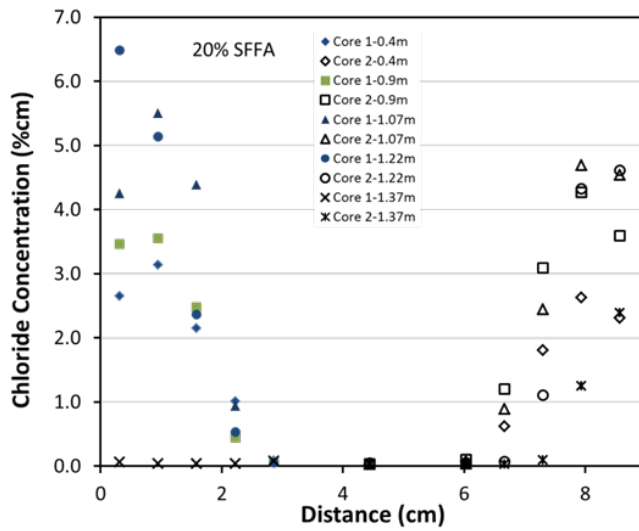
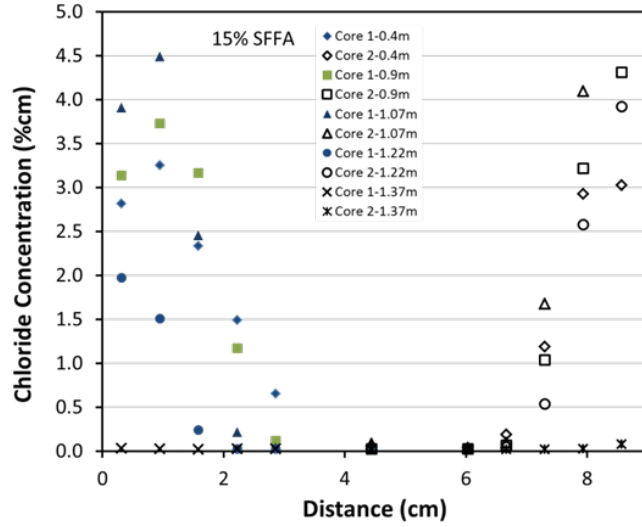


Figure 4-51: Profiles for specimens with superfine fly ash (SFFA)

In some cases the profile obtained at a given elevation was very different when comparing left side with right side profiles. Minor splash likely occurred while the solution was transferred from one tank to the other, this might account for some of the chlorides sometimes observed at the highest elevation. Also the location within the tank might have influenced how much back-splash took place. However, the main contributor to the differences in concentration from the left and right profiles observed for a given specimen and elevation is that the mold side (probably at the bottom) experienced better compaction than the opposite side; this was more evident on specimens with silica fume. For SFFA the chloride penetrated farther on the specimen containing 15% SFFA. In all instances a difference in the shape of the profile was found when comparing at a given elevation the left and right sides. This is likely due to one side being the mold side and the opposite the trowels face. The difference was more pronounced on specimens with SF than for specimens with SFFA. The skin effect (i.e., maximum  $C_s$  not for the layer closest to the surface) was obvious below water and the two tidal locations on both sides for SFFA specimens regardless of the % of SFFA. From these elevations, the  $C_{max}$  was observed on the second layer. Overall, the largest chloride concentration corresponded to elevation just below the high tide line. For 20% SFFA and 25% SFFA the largest concentration was found at the elevation just above the high tide (AHT) line.

For the column with OPC only, the elevation just above the high tide was where the profile with the higher concentration was found. The surface concentration at the highest elevation was somewhat comparable to the location above high tide; however, at fourth and fifth depths the chloride concentrations were lower. The concentration profiles show that at the center of the specimens the concentration ranged between nil and 2.5 %cm. For OPC the infinite 1D slab assumption does not hold anymore, see below for additional fitting done for this case. For the mix with only OPC the 3.5" sample width was no long enough to assume semi-infinite conditions. This was particularly obvious from the profiles corresponding to the two higher and the two lower elevations.

For some of the other compositions the concentration found at the center of the core was not the minimum concentration, (e.g., 15% SF 1.22 m left profile, and several of the OPC profiles) reinforcing the idea that the mortar layer and overall compaction on one side was better on one side than on the opposite side.

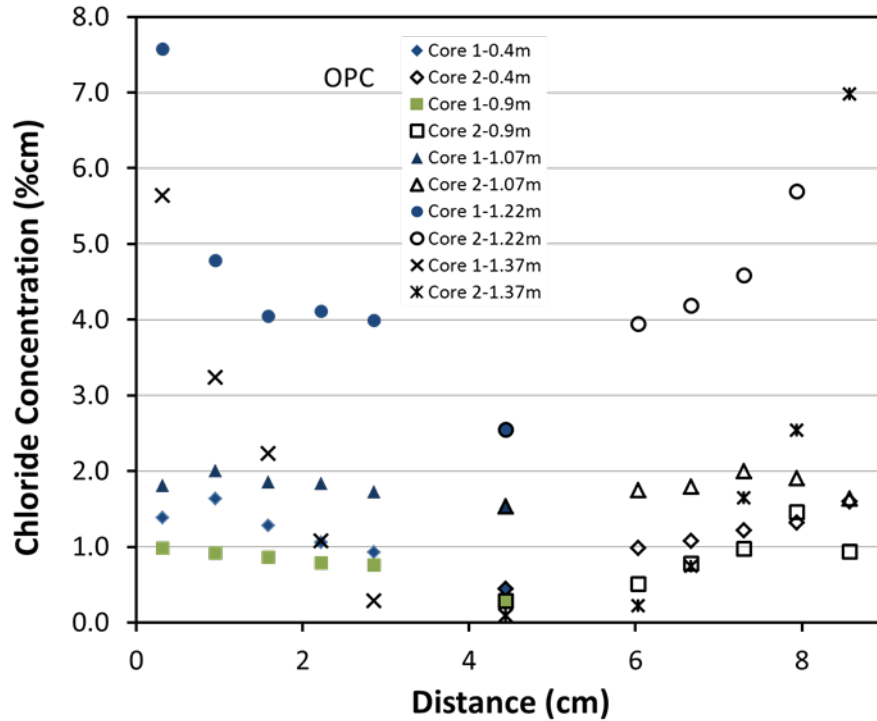


Figure 4-52: Profiles for specimen only with OPC as cementitious material

As observed on Figure 4-52, the concentration at the center was significantly greater than zero for four elevations (exception was 1.37 m elevation). Fitting using 1-D semi-infinite slab produces a  $D_{app}$  that could be significantly higher than actual  $D_{app}$  value, on the other hand if the fitting is done assuming  $C_o$  equals the concentration at the center this likely produces a  $D_{app}$  value that is likely smaller. Comsol was used to model scenarios that assumed a thickness as the one of the columns and the concentration at the surface based on the observed measured values for the first layer. Figure 4-53 shows the measured and fitted profiles computed by the numerical modeling. Using this approach the  $D_{app}$  values fitted are somewhat larger and close to the values obtained using the larger value for  $C_o$ . For example, for the location just below the high tide, the  $D_{app}$  obtained using infinite geometry gives  $D_{app} = 11.6 \times 10^{-12} \text{ m}^2/\text{s}$ , using a  $C_o$  value somewhat smaller than that measured at the center gives  $D_{app} = 0.6 \times 10^{-12} \text{ m}^2/\text{s}$ , and using finite geometry (modeling)  $D_{app} = 1.8 \times 10^{-12} \text{ m}^2/\text{s}$ . The values shown in the discussion section when describing  $D_{app}$  vs. elevation for OPC are those obtained with the modeling just described. Figure 4-53 also shows that the concentration calculated using  $D_{app}$  values of  $0.7 \times 10^{-12} \text{ m}^2/\text{s}$  at the elevation below water (0.4 m),  $0.8 \times 10^{-12} \text{ m}^2/\text{s}$  for elevation 1.22 m and  $0.17 \times 10^{-12} \text{ m}^2/\text{s}$  for 1.37 m.

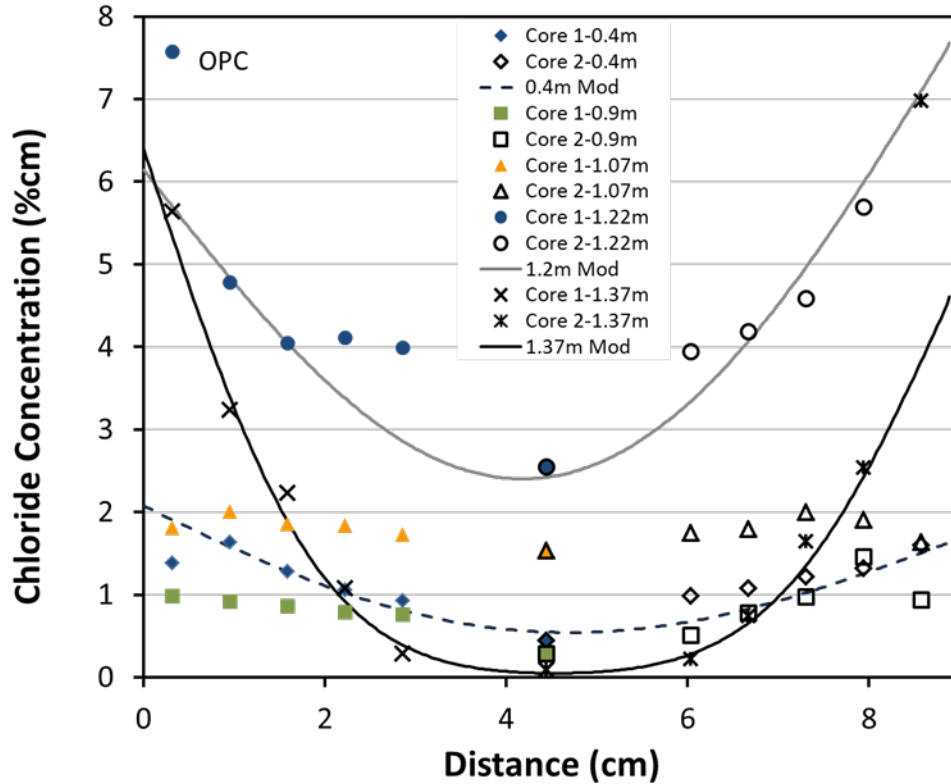


Figure 4-53: Measured and fitted profiles for specimen only with OPC

#### 4.12 Partial Immersion at SMO

Similar to what was described above for the specimens exposed to simulated tidal, cores were obtained in this case at three elevations on specimens partially immersed that contained various amounts of Fly Ash. One specimen per each of the mixtures types described in Table 3-10 was selected for coring. Each layer was 0.635 cm (0.25 inches) nominal thickness. The core slicing and titrations for this set were also made at SMO. Two profiles were obtained per core, i.e., the core was sliced from both ends, but in this case the core was 10.16 cm long. Additionally, the chloride concentration at the center of the core was also measured from a center slice.

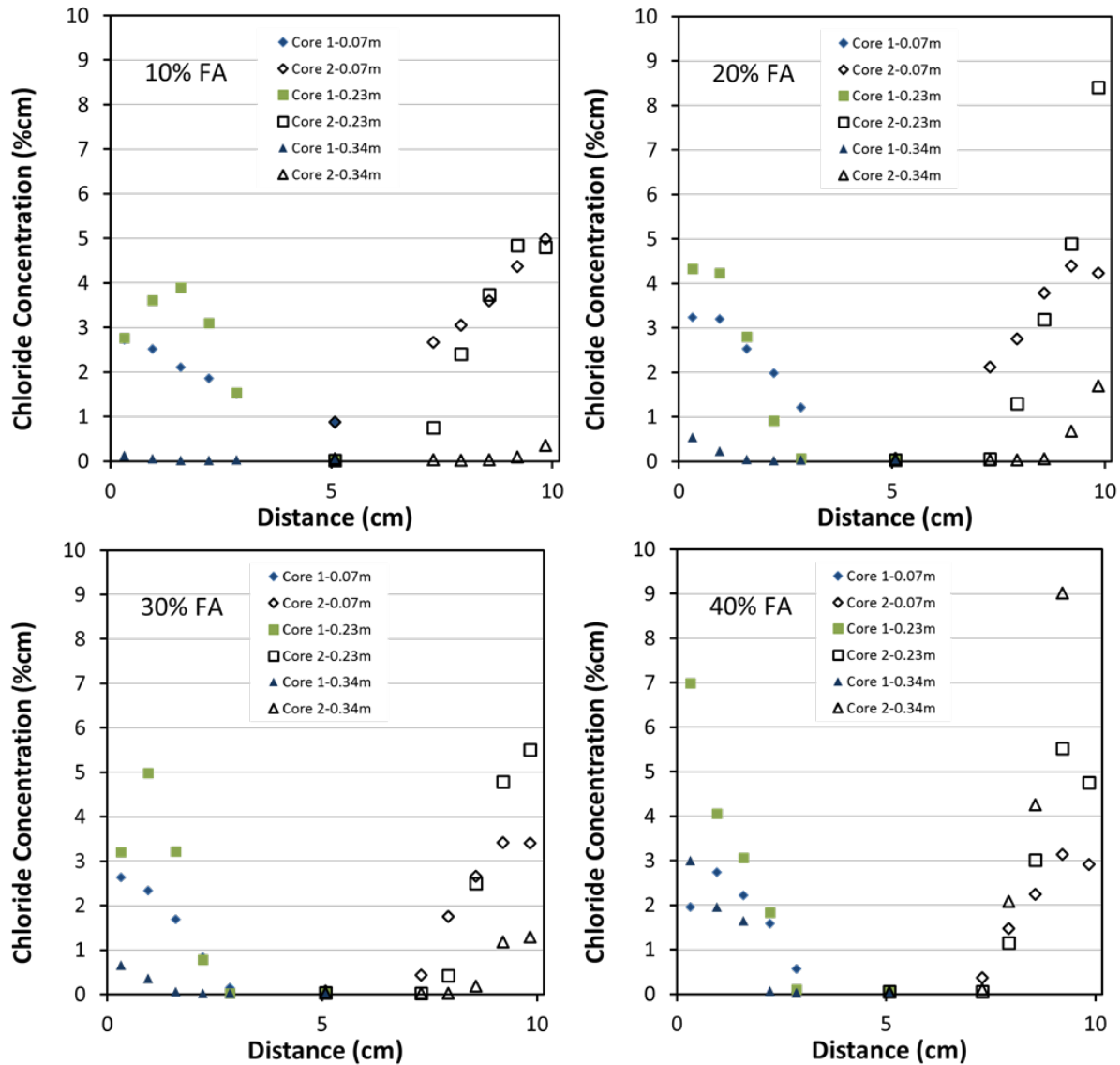


Figure 4-54: Profiles for specimens with FA (partial immersion)

Figure 4-54 show the chloride profiles measured. Profiles labeled as 0.07 m were obtained just below the water mark; those 0.23 were centered about 10 cm above the waterline. The profiles of these specimens indicate that only the 0.07 m elevation for specimen with 10% FA had a significant chloride concentration at the center, on the order of almost 1 %cm. When comparing profiles for 0.07 elevations the concrete with 30% showed the smaller concentration at the fifth depths, followed by specimens with 40%FA, %20FA and finally %10FA. For elevations above water; the chlorides have a combined transport of diffusion and capillary suction (closer to the surface). Moisture differential (both upwards and from the surface into the concrete) likely influenced the shape of the observed profiles.

The skin effect (i.e., largest concentration not at layer one) was observed on specimens collected at the elevation above the water (i.e., 0.23 m) in most instances. The skin effect was also

observed for some of the profiles corresponding to the permanent immersed elevation (0.07 m). The chloride concentration of the first layer reached a maximum of 14.5% percent cementitious (not shown) for the specimens with 40% FA at the top elevation and right side; the next largest  $C_s$  measured corresponded for the specimens with 20% at 0.23 m elevation ( $[Cl^-] \sim 8.2 \%cm$ ) and was also observed for the profile on the right side. In general, chlorides penetrated farther down on specimens with Fly ash than on specimens with superfine fly ash or those with silica fume.

## 5 Discussion

### 5.1 Aging Factor Using Resistivity

The measured resistivity values vs. time were used to calculate  $q$  values using Equation 11. The parameter  $t$  represents time in days and for this section  $q$  represents a unitless aging factor. This equation suggests that as the concrete hydration progresses and pore structure changes as concrete ages (due to cement hydration and if present by the pozzolanic reaction), the resistivity increases. The value of  $q$  is mix-dependent and it has been assumed to be constant for a given concrete if fully saturated (i.e., for permanently immersed specimens) [17,29,82]. Although specimens in this investigation were exposed to a high humidity environment, the specimens were likely not fully saturated. In most instances, a change in  $q$  was observed over time suggesting that reaction rate slows down after some period of time and this change in aging factor was mix dependent. In this section we describe two fittings with respect to  $t_0$  and  $t_1$ ; thus, two different  $q$  values,  $q_0$  and  $q_1$ , were obtained with respect to  $\rho_0$  and  $\rho_1$ .

$$\rho(t) = \rho_0(t/t_0)^q \quad (11)$$

Figure 5-1 shows examples of the fitted  $q$  values. Figure 5-1 shows that for DCL2 samples cured at room temperature, the initial time and resistivity were 36 days and 7.02 kohm-cm, respectively. These values were used as  $\rho_0$  and  $t_0$  until day 174 and an average value for  $q$  ( $q_0 = 0.63$ ) was used to draw the red fitted curve shown. Another  $q$  ( $q_1 = 0.39$ ) value was calculated for days 175-382 using as the initial time 174 days and a resistivity of 18.2 kohm-cm. The red line shows the calculated resistivity evolution using the fitted  $q$  values and extends to approx. 800 days. Past day 800 it appears that there is another transient. This trend has been reported in a recent publication for fully immersed specimens [17]. The red line segments were connected using the last projected resistivity value from the first segment as  $\rho_0$  when projecting the second segment of the curve.

The curve representing samples from DCL10 that were cured at room temperature had a second pivot point at 182 days. The average  $q_0$  value for the first 182 days was 0.69 and the average  $q_1$  value for days 183-376 was calculated to be 0.17. This represents a sharper change in direction than was seen in the curve for DCL2 RT. A third transient took place around day 700 for samples of this mixture.

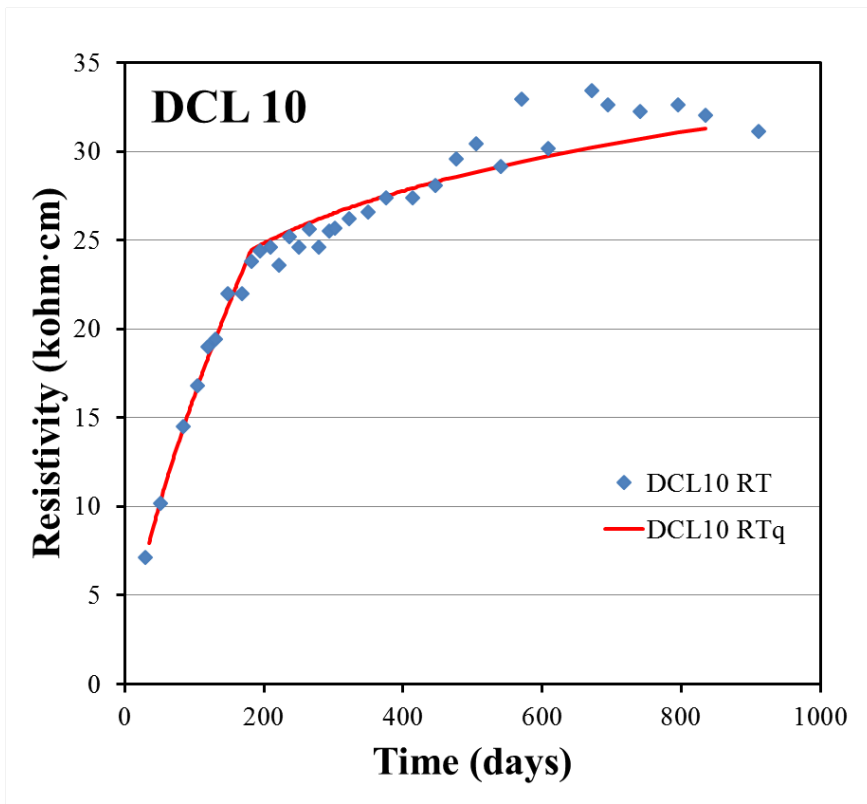
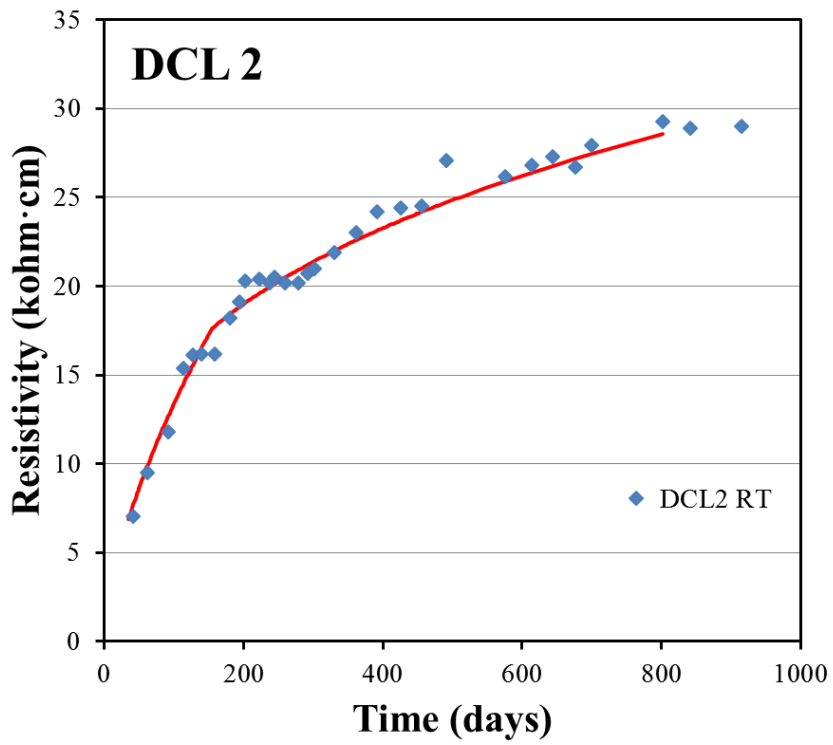


Figure 5-1: DCL2 and 10 - measured and projected resistivity using two aging factor values

Table 5-1 below shows the calculated aging factor values for cylinders cured at elevated temperature for 77 days (Table 5-1a) and those that were cured at room temperature (Table 5-1b). The tables also include the initial resistivity and initial time used to calculate the q value. In Table 5-1a, cylinders from DCL8 and 9 used one initial value as the results have maintained a constant trend.

Table 5-1: Aging factors q0 and q1 (14RT/77ET/RT)

(a)

Mix and Curing	q0	q1	$\rho_0$	t0	$\rho_1$	t1
DCL1 14RT/77ET/RT	0.57	0.11	19.0	29	40.3	124
DCL2 14RT/7ET/7RT/69ET/RT	0.63	0.09	17.0	42	28.7	98
DCL3 14RT/78ET/RT	0.74	0.11	6.6	22	18.3	84
DCL4 14RT/77ET/RT	N/A					
DCL5 14RT/77ET/RT	N/A					
DCL6 14RT/77ET/RT	0.45	0.04	37.4	28	57.8	77
DCL7 14RT/76ET/RT	0.27	0.18	16.7	22	22.2	71
DCL8 14RT/77ET/RT	0.12		19.1	23		
DCL9 14RT/77ET/RT	0.08		17.5	29		
DCL10 14RT/7ET/7RT/71ET/RT	0.71	0.09	16.0	36	29.2	84
DCL10a 14RT/77ET/RT	0.51	0.17	15.3	29	28.9	105
DCL10b 14RT/77ET/RT	0.50	0.13	14.9	29	27.2	92
DCL11 14RT/77ET/RT	0.23	0.24	22.0	57	28.3	126

(b)

Mix and Curing	q0	q1	$\rho_0$	t0	$\rho_1$	t1
DCL1 RT	0.77	0.35	6.3	29	28.8	224
DCL2 RT	0.63	0.39	7.0	36	18.2	174
DCL3 RT	0.69	0.34	4.7	30	15.0	161
DCL4 RT	0.81	0.13	25.9	29	68.1	153
DCL5 RT	0.60	0.13	23.0	29	46.1	84
DCL6 RT	0.64	0.24	13.3	28	39.8	154
DCL7 RT	0.20	0.18	14.9	28	19.1	91
DCL8 RT	0.47	0.16	10.2	23	15.7	56
DCL9 RT	0.48	0.11	10.0	29	16.1	91
DCL10 RT	0.69	0.17	7.1	30	23.8	182
DCL10a RT	0.65	0.44	6.2	29	19.5	168
DCL10b RT	0.76	0.66	5.6	29	15.6	119
DCL11 RT	0.68	0.20	5.2	22	19.0	140

## 5.2 Aging Factor (Using Resistivity) vs. Time

The aging factors of concrete specimens for the different mixes and curing regimes were calculated using Equation 6 with a reference age of 28 days ( $t_0$ ) and the corresponding concrete resistivity obtained at that age ( $\rho_0$ ). This is an alternative method to that presented in the previous section.

### 5.2.1 Aging Factor vs. Time for Specimens under RT Curing

Figure 5-2 shows the aging factors of specimens in groups DCL1, DCL2 and DCL3 with 20% fly ash and the three different w/cm ratios cured in room temperature (RT) all the time. Here  $t_0 = 28$  days. The y-axis shows the calculated aging factors ( $m$ ) values and the x-axis shows  $t - t_0$ , all values will be mentioned with respect to this axis. For the specimen in group DCL1, the  $m$  value started at 0.92 and gradually decayed to 0.67 by day 300 and appears to have reached a stable value of 0.6 by day 800. Similar transients were observed for DCL2 and DCL3 specimens, with  $m$  values as high 0.7 but by day 800 the  $m$  values for both mixtures was 0.45. Past day 500 there was very little difference between the aging factor of DCL2 and DCL3 groups. The terminal aging factor for DCL2 ( $m=0.45$ ) is somewhat lower than that recently reported ( $m=0.65$ ) on concrete with similar composition but smaller coarser aggregate (#89) and immersed in lime water while aging.

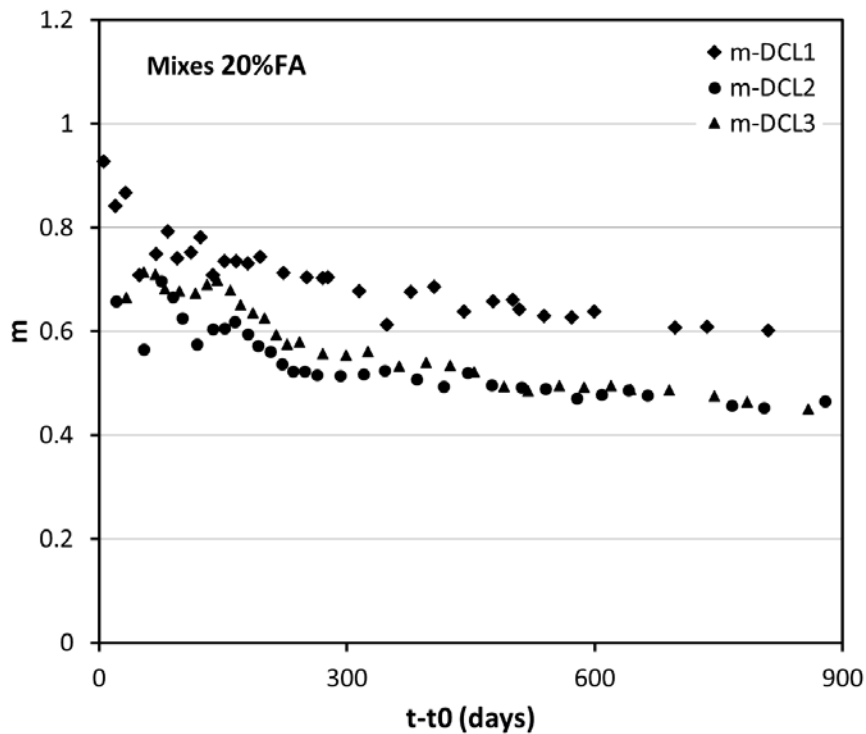


Figure 5-2: Aging factor for DCL1, 2 and 3 mixtures for specimens RT cured

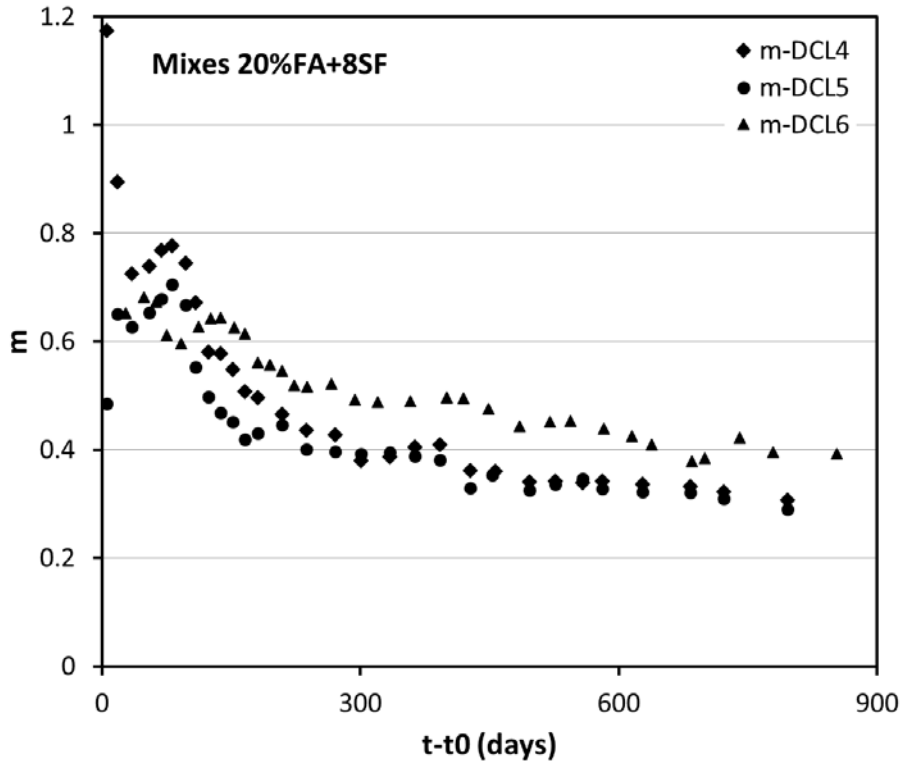


Figure 5-3: Aging factor for DCL4, 5 and 6 mixtures for specimens RT cured

Figure 5-3 shows the aging factor for specimens that contain both fly ash and silica fume. It can be observed that in this case the initial  $m$  value was larger than for specimens with fly ash and that the aging factor eventually decreased to values of 0.4 (DCL6) and 0.3 (DCL4 and DCL5). In this case the terminal  $m$  value was larger for the specimens with higher  $w/cm$  ratio. The transient is initially faster (likely due to mainly silica fume contribution and smaller contribution from continuing pozzolanic reaction, i.e., fly ash); later, the rate of change in  $m$  slows down considerably indicating that fly ash likely continues its pozzolanic reaction but at a significant slower rate. Eventually,  $m$  is expected to reach a plateau (terminal value). It is possible that at later times  $Ca(OH)_2$  might no longer be available, thus stifling the pozzolanic reaction. Figure 5-4 shows  $m$  values for specimens with Slag (i.e., DCL7, DCL8 and DCL9). Specimens with slag cement experience an even faster transient to terminal  $m$  values, which occurred as early as day 50 for DCL7, to 300 days for DCL8 and DCL9. The terminal  $m$  value for specimens with 50% slag was close to 0.2. This value compares well with the  $m$  value reported ( $m=0.26$  [86]) for specimens with 50% slag,  $w/cm$  0.41, cured immersed in lime water and #89 limestone.

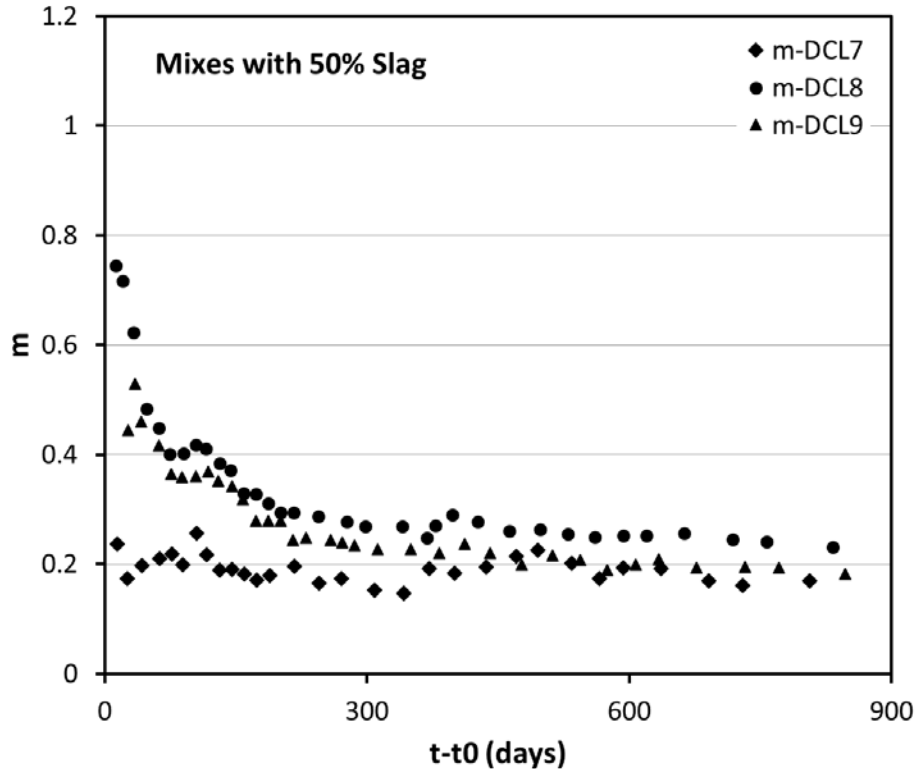


Figure 5-4: Aging factor for DCL7, 8, and 9 mixtures for specimens RT cured

### 5.2.2 Effect of Cementitious Material Content on Aging Factor vs. Time

Figure 5-5 shows the aging factor for RT cured specimens with various cementitious contents and same w/cm. Mixtures DCL10b and DCL11 contained smaller amounts of cementitious materials (i.e., the sum of cement and fly ash were 335 and 279 kg/m<sup>3</sup> respectively) than DCL2 (390 kg/m<sup>3</sup>). DCL2, DCL10b and DCL11 all have w/cm of 0.41. When comparing the transient on the aging factor it is apparent that the aging factor is somewhat higher for specimens with lower cementitious content. For over a year (between day 200 and 700) specimens of mixes DCL10b and DCL11 had an aging factor value of 0.6, and more recently decreased to values close to 0.51 (DCL10b) and 0.55 (DCL11).

The above described transients suggest that the m for diffusivity should also transient as well (and depends on concrete composition) when considering only changes in the microstructure. Additional contributions to the aging factor for diffusion (particularly for apparent diffusion coefficients) are due to the binding capacity of the concrete and changes in the chloride concentration in the solution, as well as environmental parameters (i.e., Temperature, RH to name a few) that might affect the transient.

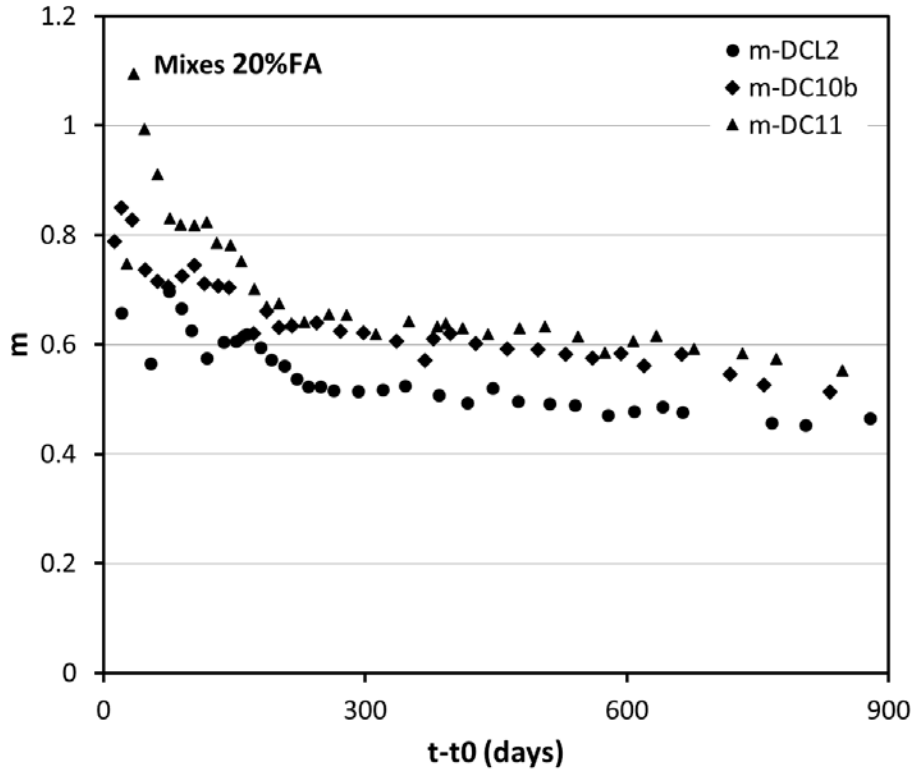


Figure 5-5: Aging factor for DCL2, DCL10b and DCL11 mixtures for specimens RT cured

More recently a method similar to the one used for maturity calculation of concrete (i.e., and hyperbolic equation) has been proposed by our group to predict the ultimate resistivity value and the resistivity rate of change [83]. This latter analysis was not performed but could be implemented if deemed necessary. See later section on  $D_{nssm}$  vs. resistivity section.

An alternative method to visualize how the resistivity evolves is to plot  $1/\text{resistivity}$  vs. time in log-log scale. For example see Figure 5-6 for the DCL2 resistivity values shown in Figure 5-2, but now it also includes the resistivity<sup>-1</sup> measured on specimens subjected to the other curing regimes. Appendix I contains  $1/\text{resistivity}$  vs. time plots for all mixes and various curing regimes.

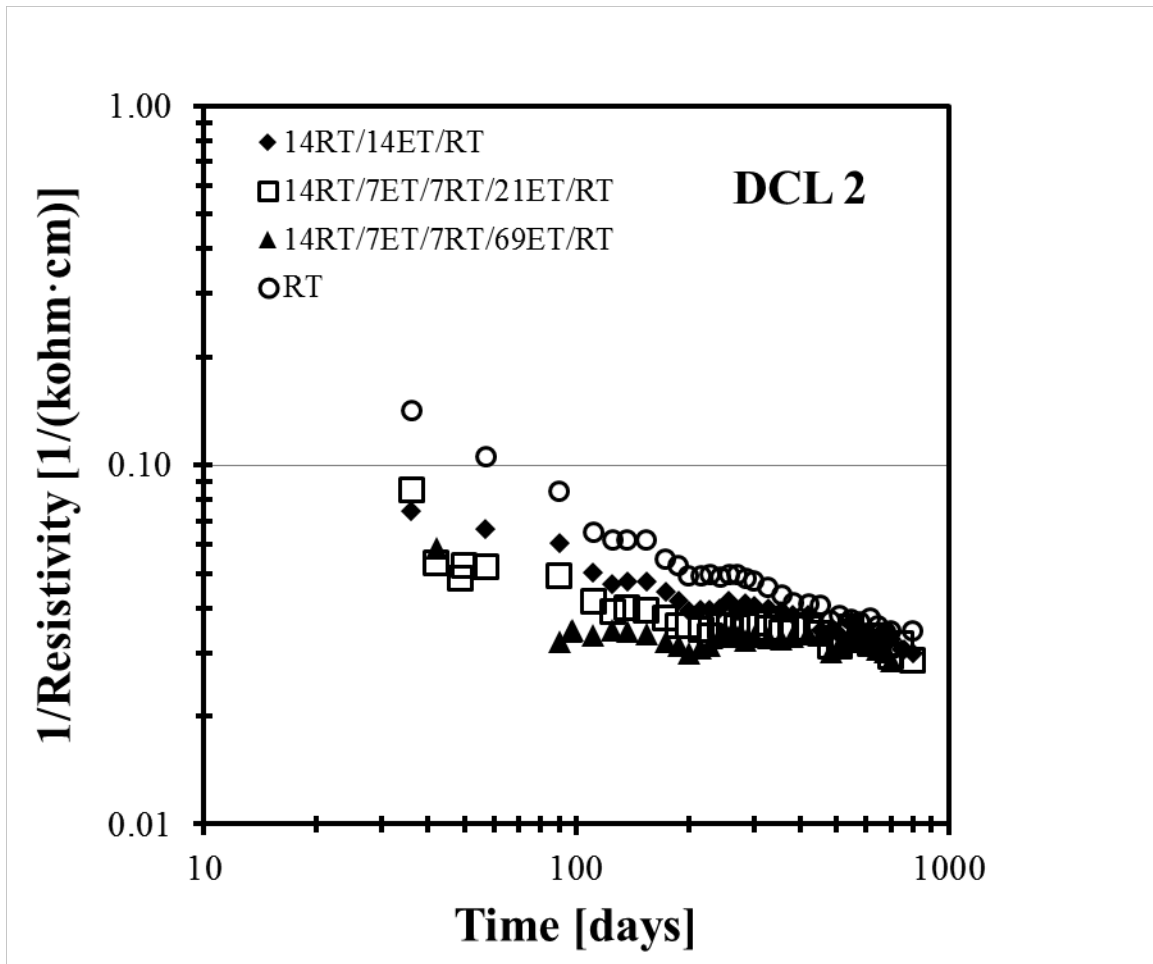


Figure 5-6: Evolution of the resistivity inverse in log-log scale

### 5.3 Resistivity vs. $D_{nssm}$

Non-steady state diffusion coefficients ( $D_{nssm}$ ) were calculated and the correlation between the coefficient and the resistivity of the sample was investigated. As indicated in the experimental section, rapid migration tests were performed at 90-100 days of age, 365 days, 540 days and 730 days of age.

When the results from all the mixes were plotted on the same graph for tests performed between 90-100 days of age, two distinct groups of data points became visible. A Pearson's R correlation coefficient was calculated for each of these groups and placed on Figure 5-7. Higher diffusion coefficients measured from DCL10 and 10a may be attributed to higher porosity of these samples due to the presence of a higher-than-designed-amount of entrained air.

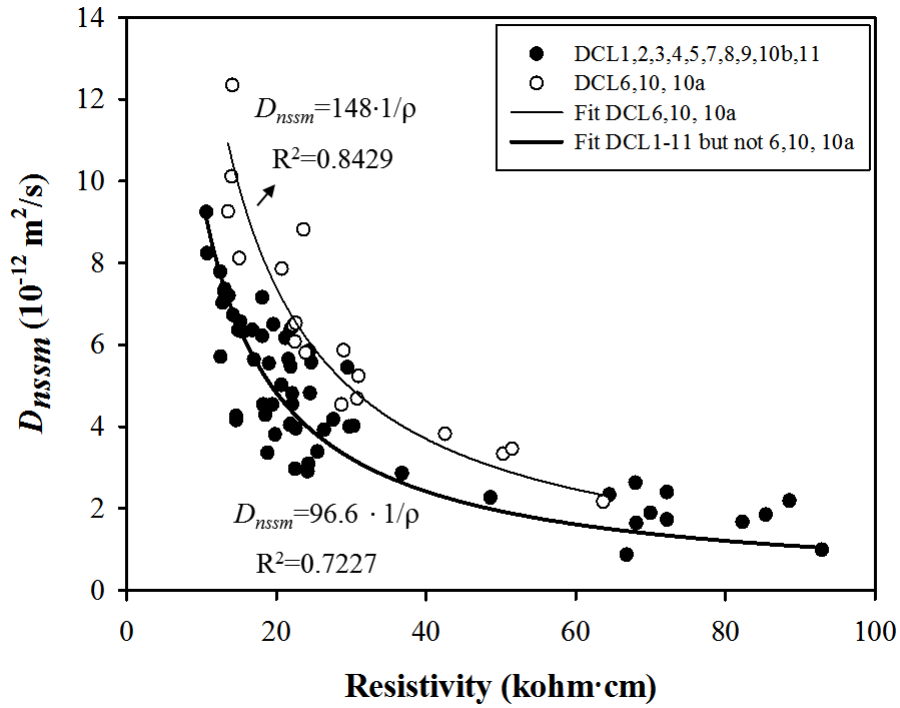


Figure 5-7:  $D_{nssm}$  vs. resistivity grouped per entrained air content (90 days values)

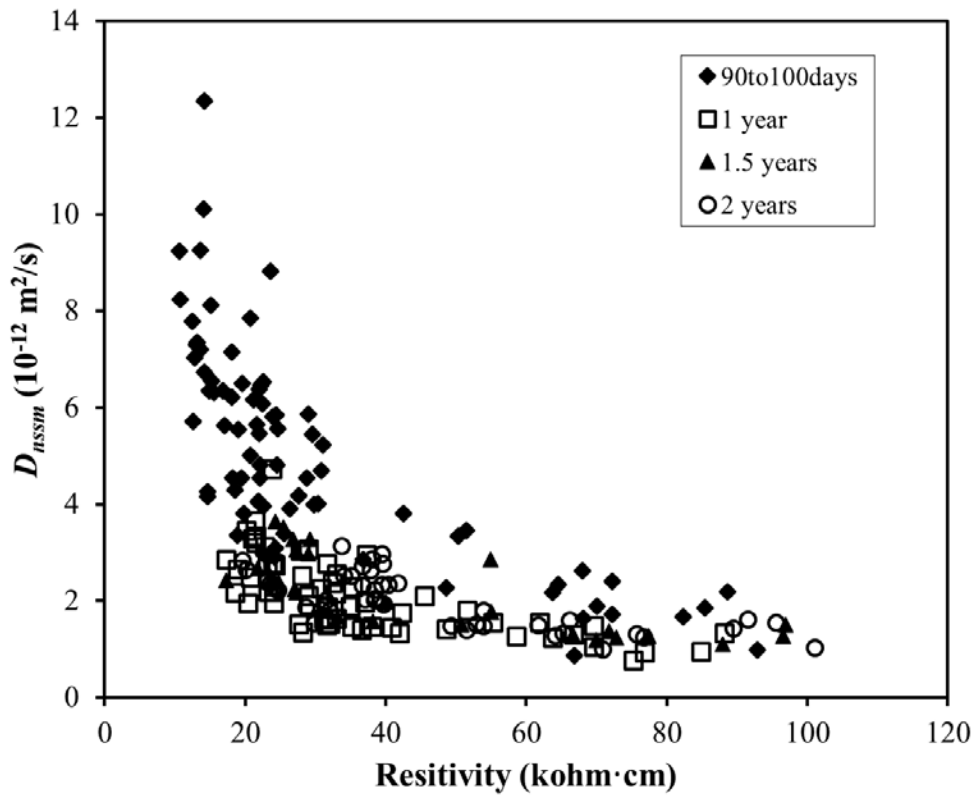


Figure 5-8:  $D_{nssm}$  vs. resistivity grouped per specimen age

Figure 5-8 shows  $D_{nssm}$  vs. resistivity grouped by the time that the RMT tests were performed, but not differentiating based on concrete composition. Figure 5-9 shows a correlation between  $D_{nssm}$  and resistivity including all collected values. The K value has been calculated for the following groupings: Groups 1 to 11 (all, and each time), and Group 1 to 9 (all and each time) see Table 5-2. It can be observed that the K value was significantly larger for the K value obtained at 90-100 days for both groups ( $K=106 \times 10^{-2} \text{ k}\Omega\text{-m}^3/\text{s}$ : DCL1 to11 and  $K= 97 \times 10^{-2} \text{ k}\Omega\text{-m}^3/\text{s}$ : DCL1 to 9). The K value including all the tests performed at different times were between 16 and 15 points smaller. The K value obtained for these groupings at 1 year or later ranged between  $61 \times 10^{-2} \text{ k}\Omega\text{-m}^3/\text{s}$  and  $72 \times 10^{-2} \text{ k}\Omega\text{-m}^3/\text{s}$ . The cementitious content appears to have a modest effect on the K value.

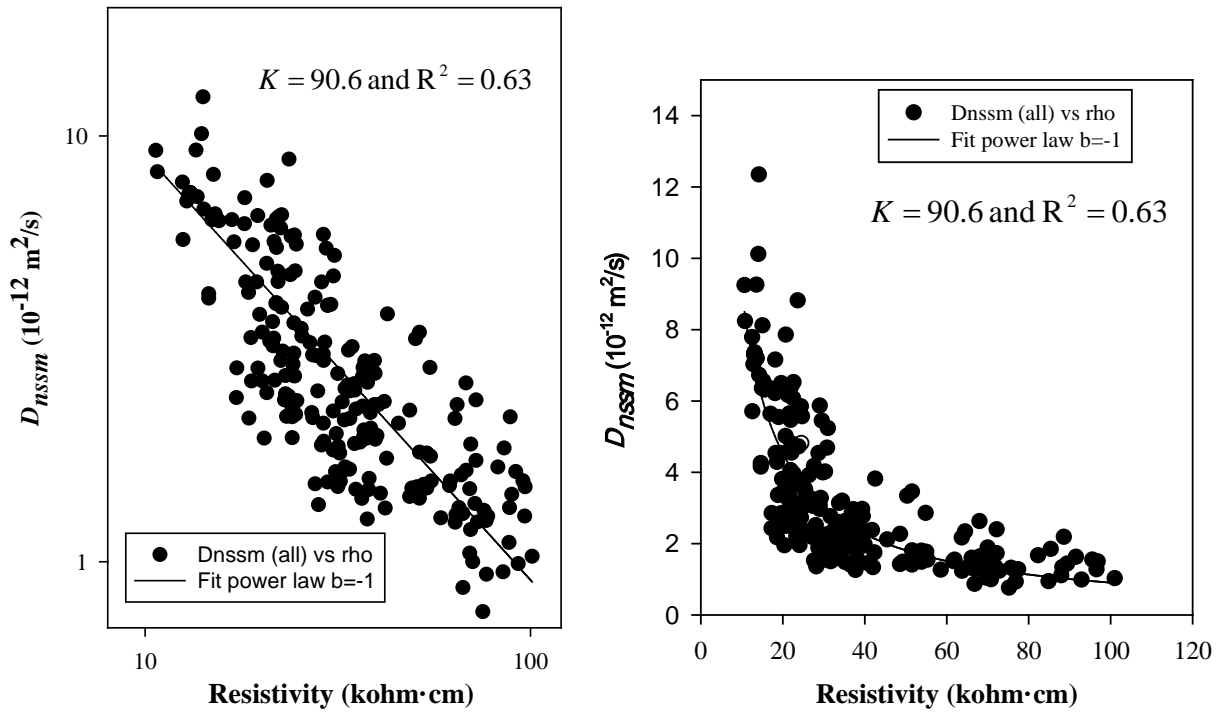


Figure 5-9: Correlations that include all values log-log on the left and linear-linear on the right

Table 5-2: K values as per Nernst-Einstein (units in  $10^{-2}$  kohm·m<sup>3</sup>/s) equation obtained at different ages

		K	R	R <sup>2</sup>
DCL-1 to DCL-11	90 to 100 days	106.1	0.768	0.590
	1 year	63.7	0.674	0.454
	1.5 year	72.4	0.537	0.288
	2 year	70.4	0.000	0.000
	All	90.6	0.797	0.635

DCL1 to DCL9	90 to 100 days	96.8	0.832	0.693
	1 year	61.7	0.746	0.557
	1.5 years	71.2	0.565	0.319
	2 years	62.4	0.374	0.139
	All	81.5	0.798	0.630

Table 5-3 shows the K values for cases grouped by cementitious type (e.g., DCL1, DCL2 and DCL3 for specimens with 20% FA). The K values were larger for specimens with fly ash and silica fume, followed by those with fly ash and finally the smaller K values were those observed for specimens only with Slag. The difference between K values obtained on younger (90-100 days) concrete specimens and the K values on specimens older than 1 year were again significant. The K values were in-between as would be expected when the  $D_{nssm}$  measured at all ages for these subgroups. The K values appear to depend somewhat on the type of supplementary cementitious material used.

Table 5-3: K values grouped by SCM type (units in  $\times 10^{-2}$  kohm·m<sup>3</sup>/s) obtained at different ages.

			K	R	R <sup>2</sup>
20% FA	DCL1,	90 to 100 days	100.1	0.740	0.550
	DCL2,	1, 1.5 and 2 years	68.6	0.692	0.478
	DCL3	All	89.9	0.882	0.777

20% FA+ 8% SF	DCL4,	90 to 100 days	144.0	0.885	0.78
	DCL5,	1, 1.5 and 2 years	90.5	0.000	0.000
	DCL6	All	114.7	0.756	0.57

50% Slag	DCL7,	90 to 100 days	85.4	0.000	0.000
	DCL8,	1, 1.5 and 2 years	58.7	0.000	0.000
	DCL9	All	69.9	0.522	0.270

## 5.4 Apparent Diffusion Coefficient

### 5.4.1 Specimens Exposed to Low Concentration of Sodium Chloride Solution (0.1M NaCl)

Table 5-4 shows the calculated chloride diffusion coefficient values of concrete exposed to 0.1 M NaCl solution for 220 and 400 days. After 220 days of exposure, it can be seen that the chloride diffusivity values were higher in DLC10 group of specimens than the  $D_{app}$  values found for the other specimens. The specimens made of 20%FA and 8%SF and with a 0.41 w/cm ratio (DCL5) showed the lowest  $D_{app}$  values when cured at 14RT/28ET/RT and exposed to 0.1 M NaCl for 220 days. However, after 400 days of exposure time, the lowest  $D_{app}$  was found on DCL7 with a value of  $0.46 \times 10^{-12} \text{ m}^2/\text{s}$  and  $0.36 \times 10^{-12} \text{ m}^2/\text{s}$  for 14RT/77ET/RT and RT curing conditions. The highest value found for the chloride diffusion coefficient at 400 days of exposure was  $3.3 \times 10^{-12} \text{ m}^2/\text{s}$  for DCL10b when cured at 14RT/77ET/RT. In general, all mixes showed a decrease in the  $D_{app}$  values from the results obtained at 220 days to 400 days. For instance, DCL1 at RT had  $D_{app}$  values  $2.41 \times 10^{-12} \text{ m}^2/\text{s}$  at 220 days and  $1.99 \times 10^{-12} \text{ m}^2/\text{s}$  at 400 days of exposure time.

Table 5-4:  $D_{app}$  values for specimens exposed to 0.1M NaCl

Mix	Apparent Chloride Diffusivity ( $10^{-12} \text{ m}^2/\text{s}$ )						
	220 days of Exposure Time				400 days of Exposure Time		
	Curing Condition				Curing Condition		
	14RT/14ET/RT	14RT/28ET/RT	14RT/77ET/RT	RT	14RT/77ET/RT	RT	
DCL1	2.58	1.93	3.68	2.41	0.95	1.99	
DCL2	2.11	2.87	2.40	2.07	1.05	1.26	
DCL3	5.37	3.86	4.18	4.43	2.43	2.65	
DCL4	1.28	1.36	1.79	0.88	1.07	0.83	
DCL5	0.78	0.50	1.09	1.35	0.47	0.61	
DCL6	2.62	2.09	1.55	1.93	0.98	1.69	
DCL7	1.77	2.02	2.09	2.00	0.46	0.36	
DCL8	1.48	2.35	2.07	2.98	1.07	0.95	
DCL9	1.92	2.65	4.16	2.79	1.16	0.78	
DCL10	4.17	4.03	2.83	N/A	2.09	N/A	
DCL10a	4.12	5.13	6.21	3.69	2.87	3.16	
DCL10b	6.03	4.50	4.46	3.83	3.30	1.06	
DCL11	3.00	3.29	7.34	4.85	1.78	2.33	

### 5.4.2 Specimens Exposed to High Concentration of Sodium Chloride Solutions (3% and 16.5% NaCl)

The average apparent diffusivity values for the specimens exposed to 3% NaCl solution and 16.5% NaCl are shown in Tables 5-5 and 5-6, respectively (each value is the average of three values and these values can be found in Appendix J, except for curing condition 700 days RT). In general, the specimens exposed to the higher sodium chloride concentration solution reached slightly higher values for the apparent chloride diffusion coefficient. For cases in which  $D_{app}$  was calculated using all layers, DCL10 and DCL10b showed the greater values for  $D_{app}$  ( $5.51 \times 10^{-12} \text{ m}^2/\text{s}$  and  $5.41 \times 10^{-12} \text{ m}^2/\text{s}$ , respectively) when cured at accelerated conditions. Additionally,

when comparing the mix compositions, the group of specimens made of 20%FA+8%SF (DCL4, DCL5, and DCL6) showed the smaller apparent diffusion coefficients when they were immersed in both 3% and 16.5% NaCl solutions. Also, when exposed to 16.5% NaCl solution, DCL1, DCL2, DCL3, DCL4, DCL6, DCL10b, and DCL11 showed higher  $D_{app}$  values when cured at normal conditions than the other curing regimes. However, this was not observed on DCL1, DCL2, and DCL3 when the solution was 3% NaCl, since higher  $D_{app}$  values were calculated when cured at AC. Having higher  $D_{app}$  values does not necessarily mean that a larger amount of chlorides penetrated the specimens, as the corresponding measured  $C_s$  is also relevant.

Table 5-5: Average  $D_{app}$  diffusion values of concrete mixes exposed to 3% NaCl for 1 year  
All Layers

Mix	Average Apparent Chloride Diffusivity ( $10^{-12} \text{ m}^2/\text{s}$ )				
	Curing Condition				
	NC	AC	NC=AC	NC<AC	700 days RT
DCL1	1.98	2.11	1.18	N/A	0.95
DCL2	2.11	2.11	2.10	2.06	0.92
DCL3	2.90	2.93	3.10	2.85	1.87
DCL4	1.95	1.27	0.74	N/A	0.60
DCL5	2.01	1.30	0.84	N/A	0.42
DCL6	2.80	1.73	1.36	N/A	0.99
DCL7	2.01	1.81	1.53	N/A	1.36
DCL8	2.03	1.31	1.64	N/A	1.05
DCL9	2.28	2.33	2.45	N/A	1.31
DCL10	3.91	4.02	2.70	3.11	2.20
DCL10a	3.45	3.27	1.53	2.91	1.75
DCL10b	3.40	2.98	2.98	N/A	N/A
DCL11	4.06	3.07	2.10	N/A	N/A

Layer 1 removed for Selected Cases

Mix	Average Apparent Chloride Diffusivity ( $10^{-12} \text{ m}^2/\text{s}$ )				
	Curing Condition				
	NC	AC	NC=AC	NC<AC	700 days RT
DCL1	1.98	1.75	1.18	N/A	1.56
DCL2	1.89	2.66	1.91	2.06	1.55
DCL3	2.54	2.60	2.08	2.85	2.32
DCL4	0.90	0.88	0.74	N/A	1.01
DCL5	1.22	0.87	1.37	N/A	1.56
DCL6	2.51	1.33	1.39	N/A	0.84
DCL7	1.47	1.81	1.53	N/A	0.93
DCL8	1.96	1.11	1.64	N/A	1.23
DCL9	1.37	1.45	2.22	N/A	0.73
DCL10	3.28	2.97	1.73	2.33	0.97
DCL10a	3.09	2.83	1.53	2.75	1.38
DCL10b	2.74	2.41	1.72	N/A	N/A
DCL11	2.25	2.50	1.86	N/A	N/A

Table 5-6: Average  $D_{app}$  values of concrete mixes exposed to 16.5% NaCl for 1 year  
All Layers

Mix	Average Apparent Chloride Diffusivity ( $10^{-12} \text{ m}^2/\text{s}$ )				
	Curing Condition				
	NC	AC	NC=AC	NC<AC	700 days RT
DCL1	2.94	2.24	1.24	N/A	0.38
DCL2	3.41	3.20	2.04	3.19	0.79
DCL3	4.45	4.22	4.22	3.80	1.87
DCL4	1.58	1.39	0.93	N/A	0.36
DCL5	2.35	2.06	0.92	N/A	0.74
DCL6	2.99	2.40	1.24	N/A	1.05
DCL7	2.83	2.70	2.01	N/A	1.21
DCL8	2.27	2.32	1.44	N/A	0.87
DCL9	3.42	3.26	1.45	N/A	1.24
DCL10	4.75	5.51	2.99	3.87	0.95
DCL10a	4.54	3.72	2.06	3.47	0.70
DCL10b	5.06	5.41	3.23	N/A	1.82
DCL11	4.65	4.20	2.76	N/A	1.78

Layer 1 removed for selected cases

Mix	Average Apparent Chloride Diffusivity ( $10^{-12} \text{ m}^2/\text{s}$ )				
	Curing Condition				
	NC	AC	NC=AC	NC<AC	700 days RT
DCL1	2.06	2.04	1.24	N/A	1.55
DCL2	2.25	2.90	1.94	3.19	1.21
DCL3	4.73	4.05	3.47	3.61	2.06
DCL4	0.93	0.86	0.93	N/A	1.48
DCL5	1.53	1.63	0.87	N/A	2.91
DCL6	2.93	2.46	1.14	N/A	1.96
DCL7	2.60	2.70	2.41	N/A	1.69
DCL8	2.15	2.40	1.44	N/A	1.42
DCL9	2.59	2.47	1.45	N/A	2.33
DCL10	3.88	4.64	2.36	3.11	1.14
DCL10a	3.87	3.39	2.43	2.94	1.46
DCL10b	4.19	4.55	2.72	N/A	2.27
DCL11	4.11	3.73	2.65	N/A	1.72

An additional reduction in  $D_{app}$  values was observed on specimens cured at room temperatures for more than 700 days. (These specimens were not exposed for 1 year, rather between 105 and 145 days.) A better fit was usually obtained for  $D_{app}$  values upon removing the first layer, particularly for those specimens cured >700 days at room temperature. For the other curing conditions, removing the first layer was not always required; hence, the same values are shown on both tables.

### 5.4.3 Specimens Exposed to Simulated Field Conditions

#### 5.4.3.1 Tidal Simulation

Table 5-7 contains the apparent diffusivity values for the specimens exposed to the tidal simulation at elevation A. DCL4, DCL8, DCL9, DCL10a, and DCL11 were the specimen groups that had a modest increment on the  $D_{app}$  values after each six, ten, and 18 months of exposure time; for the rest of the mixes, the apparent diffusion coefficient value decreased as the exposure time increased. In general, after 18 months, the specimen that showed the lowest  $D_{app}$  was DCL6 with an average value of  $0.93 \times 10^{-12} \text{ m}^2/\text{s}$ . On the other hand,  $2.49 \times 10^{-12} \text{ m}^2/\text{s}$  was the highest  $D_{app}$  value calculated for DCL10b at 18 months.

Table 5-8, Table 5-9, and Table 5-10 contain the  $D_{app}$  values calculated at elevations B, C and D, respectively. Additionally, the chloride diffusivity values of DCL10b at elevations A and B are higher than those of all other concrete mixes at the same elevations, while at elevation C, the chloride diffusivity value of DCL1 is highest. The largest  $D_{app}$  at elevation D was observed on mix DCL11. In addition, it can also be seen that among all calculated chloride diffusivity values after six months of exposure, DCL10b mix has the maximum  $D_{app}$  value at elevation A ( $8.08 \times 10^{-12} \text{ m}^2/\text{s}$ ) and DCL2 has the minimum  $D_{app}$  value ( $0.15 \times 10^{-12} \text{ m}^2/\text{s}$ ) at elevation D. Incidentally, after six months of exposure, the  $D_{app}$  value of every mix was lowest at elevation D.

After ten months of exposure, the chloride diffusivity values of DCL2, DCL9 and DCL10b at elevation A are still higher than the  $D_{app}$  values for the other elevations (within each block). For the other mixes, the elevation at which the  $D_{app}$  was highest was different than after six months. For DCL1, it is at elevation A which was originally at elevation C. For DCL3 and DCL5, it is located at elevation B. The elevation with the largest chloride diffusivity value for DCL4, DCL6, DCL7, DCL8 and DCL11 is elevation 'C'. Incidentally, the largest chloride diffusivity value at elevation 'A' corresponds to mix DCL10b, which is the same as that after six months of exposure. At elevation B the chloride diffusivity value of DCL5 is highest and the chloride diffusivity values of DCL11 at elevations C and D (the same as that of six month exposure) are the largest. In addition, it can also be seen that among all the chloride diffusivity values, DCL5 has the maximum chloride diffusivity value at elevation B ( $3.57 \times 10^{-12} \text{ m}^2/\text{s}$ ) and DCL1 has the minimum chloride diffusivity value ( $0.205 \times 10^{-12} \text{ m}^2/\text{s}$ ) at elevation D.

Comparing the chloride diffusivity values of concrete mixes after six months' exposure with those after ten months' exposure, it is observed that such values of DCL1, DCL8 and DCL9 have decreased at all elevations. For DCL5, the chloride diffusivity values increase at elevations A and B and decrease at elevations C and D. The chloride diffusivity values of DCL4, DCL6, DCL7 and DCL11 at elevation C and those of DCL2, DCL3, DCL7, DCL10b and DCL11 at elevation D also increase. The chloride diffusivity values of these concrete mixes at other elevations decrease.

At 18 months most of the  $D_{app}$  values for all elevations decreased, or remained close to the  $D_{app}$  value observed after 10 months of exposure. From these results, it is demonstrated that the chloride diffusivity value of concrete is significantly dependent on the exposure elevation and exposure ages as the chloride concentration at the surface changes and the moisture content varies.

Table 5-7: Apparent diffusion values of concrete mixes at tidal simulation (Elevation A)

Mix	Side	Apparent chloride diffusivity ( $10^{-12} \text{ m}^2/\text{s}$ )		
		6 Months	10 Months	18 Months
DCL1	R	2.18	1.29	1.32
	L	2.28	1.10	1.05
DCL2	R	7.04	2.29	0.99
	L	4.32	1.25	0.72
DCL3	R	4.84	1.75	1.33
	L	4.19	0.67	1.57
DCL4	R	2.16	0.89	0.96
	L	2.01	1.14	0.90
DCL5	R	1.64	1.67	1.35
	L	1.73	0.68	0.96
DCL6	R	2.28	1.15	0.74
	L	1.35	0.91	0.98
DCL7	R	1.19	1.05	1.59
	L	2.34	0.52	0.62
DCL8	R	1.34	0.39	1.08
	L	0.97	0.94	1.25
DCL9	R	1.44	0.45	0.79
	L	1.21	1.34	0.75
DCL10a	R	2.91	1.04	2.25
	L	0.65	1.47	2.04
DCL10b	R	2.22	2.97	1.94
	L	8.08	1.60	2.49
DCL11	R	2.14	1.90	3.78
	L	3.81	N/A	6.58

Table 5-8: Apparent diffusion values of concrete mixes at tidal simulation (Elevation B)

Mix	Side	Apparent chloride diffusivity ( $10^{-12} \text{ m}^2/\text{s}$ )		
		6 Months	10 Months	18 Months
<b>DCL1</b>	R	1.28	0.32	0.56
	L	1.74	1.27	0.67
<b>DCL2</b>	R	1.89	0.69	0.23
	L	1.02	0.24	0.39
<b>DCL3</b>	R	1.23	1.86	2.19
	L	2.14	1.88	1.77
<b>DCL4</b>	R	0.74	0.81	0.78
	L	1.55	0.89	0.71
<b>DCL5</b>	R	1.66	0.78	0.67
	L	1.68	1.29	0.77
<b>DCL6</b>	R	1.55	0.91	3.20
	L	1.84	1.21	0.96
<b>DCL7</b>	R	1.33	0.42	0.25
	L	0.73	0.84	0.68
<b>DCL8</b>	R	1.63	0.62	0.87
	L	1.98	0.66	0.56
<b>DCL9</b>	R	1.88	1.18	1.43
	L	0.97	0.27	1.47
<b>DCL10a</b>	R	2.06	1.27	1.27
	L	6.20	1.93	1.85
<b>DCL10b</b>	R	3.77	1.97	2.01
	L	3.80	1.82	1.32
<b>DCL11</b>	R	3.08	0.92	1.92
	L	1.92	N/A	1.12

Table 5-9: Apparent diffusion values of concrete mixes at tidal simulation (Elevation C)

Mix	Side	Apparent chloride diffusivity ( $10^{-12} \text{ m}^2/\text{s}$ )		
		6 Months	10 Months	18 Months
<b>DCL1</b>	R	0.61	0.27	0.55
	L	3.76	0.43	0.32
<b>DCL2</b>	R	1.23	0.37	0.55
	L	0.22	0.56	1.01
<b>DCL3</b>	R	1.91	1.79	1.73
	L	2.63	1.56	1.42
<b>DCL4</b>	R	0.72	0.48	0.62
	L	0.68	0.97	0.26
<b>DCL5</b>	R	2.14	1.35	0.73
	L	2.69	0.83	0.70
<b>DCL6</b>	R	0.86	0.65	3.20
	L	1.36	1.47	0.96
<b>DCL7</b>	R	0.93	2.37	0.42
	L	0.95	0.62	0.63
<b>DCL8</b>	R	1.32	0.61	0.78
	L	0.77	0.81	0.58
<b>DCL9</b>	R	0.93	0.86	0.85
	L	0.74	0.84	0.92
<b>DCL10a</b>	R	1.23	0.48	0.65
	L	2.75	1.48	2.38
<b>DCL10b</b>	R	2.57	0.64	2.26
	L	2.24	1.57	1.13
<b>DCL11</b>	R	1.20	0.75	0.72
	L	1.65	N/A	1.74

Table 5-10: Apparent diffusion values of concrete mixes at tidal simulation (Elevation D)

Mix	Side	Apparent chloride diffusivity ( $10^{-12} \text{ m}^2/\text{s}$ )		
		6 Months	10 Months	18 Months
DCL1	R	0.60	0.13	0.12
	L	0.18	0.21	0.13
DCL2	R	0.04	0.58	0.10
	L	0.15	0.32	5.85
DCL3	R	0.26	0.69	0.22
	L	0.55	0.37	0.66
DCL4	R	0.17	0.22	0.14
	L	0.71	0.24	0.04
DCL5	R	0.85	0.50	0.75
	L	0.43	0.65	0.39
DCL6	R	0.80	0.42	0.23
	L	1.03	0.35	0.86
DCL7	R	0.21	0.55	0.11
	L	0.25	0.67	0.035
DCL8	R	0.74	0.36	0.54
	L	0.60	0.12	0.48
DCL9	R	0.29	0.70	0.17
	L	0.90	0.89	0.47
DCL10a	R	0.63	0.52	1.36
	L	0.63	0.78	2.01
DCL10b	R	0.74	3.13	0.15
	L	0.19	1.07	0.71
DCL11	R	0.72	0.98	0.68
	L	1.09	N/A	0.74

#### 5.4.3.2 Splash Simulation

Table 5-11, Table 5-12, Table 5-13 and Table 5-14 show the  $D_{app}$  calculated values at elevations A, B, C and D, respectively. Each table represents the apparent chloride diffusion coefficient for specimens exposed to splash simulation for six, ten, and 18 months. The  $D_{app}$  values decreased as the exposure time increased for DCL1, DCL2, DCL6, DCL9, and DCL11 for the immersed portion of the specimens (elevation A) that were sprayed with 100% seawater. For some specimens, the highest  $D_{app}$  value was found at 6 or 10 months of exposure time; for instance, DCL7 that the highest  $D_{app}$  value at 10 months ( $1.06 \times 10^{-12} \text{ m}^2/\text{s}$ ) and the lowest at 18 months ( $0.28 \times 10^{-12} \text{ m}^2/\text{s}$ ). As shown on the bottom of the table, the apparent coefficient values increased with time for specimens exposed to a lower seawater concentration (10% Seawater).

After six months' exposure, it can be observed that the chloride diffusion coefficient values of DCL2 and DCL6 at elevation A are higher than the chloride diffusivity values for the other elevations. For DCL4, DCL5, DCL8, DCL9 and DCL10b the chloride diffusion coefficient values at elevation B are highest compared to the other elevations. Whereas, for DCL1, DCL3 and DCL11, the  $D_{app}$  value at elevation D has the highest values of all the corresponding concretes exposed to the other elevations. It is also observed that the chloride diffusion coefficient values of DCL10b at elevations A and B are higher than those of all other concrete mixes at the same elevations, which coincide with what is observed for the tidal set-up. At elevations C and D, the chloride diffusion coefficient values of DCL3 are also higher than other concrete mixes at the same elevations. In addition, it can also be seen that among the chloride diffusivity values of all concrete mixes, DCL3 has the maximum chloride diffusion coefficient value at elevation D ( $6.09 \times 10^{-12} \text{ m}^2/\text{s}$ ). DCL9 has the minimum chloride diffusion coefficient value ( $0.19 \times 10^{-12} \text{ m}^2/\text{s}$ ) at the same elevation.

After ten months' exposure, the highest chloride diffusion coefficient values of DCL2, DCL8 and DCL11 remain at elevation A, B and D, respectively. However, the largest  $D_{app}$  value for the other concrete mixes changed location. The locations of the highest chloride diffusion coefficient values move to the elevation A for mixes DCL1, DCL3, DCL4, DCL7 and DCL10b. And the locations of the highest chloride diffusion coefficient values for blocks of mixes DCL5 and DCL6 is elevation C and for DCL9, the largest  $D_{app}$  is at elevation D. DCL11 has the maximum chloride diffusion coefficient value at elevation D ( $4.63 \times 10^{-12} \text{ m}^2/\text{s}$ ) after 10 months among the chloride diffusivity values of all concrete mixes, and the minimum chloride diffusion coefficient value ( $0.17 \times 10^{-12} \text{ m}^2/\text{s}$ ) at elevation A. By comparing the chloride diffusivity values at the two exposure times, it is observed that these values decreased for 77% of the cases. The chloride diffusion coefficient values of DCL1, DCL2, DCL3, DCL4, DCL6 and DCL8 at all elevations after ten months of exposure are lower than those obtained after six months. But the chloride diffusion coefficient values of DCL4 at elevations A and C and DCL6 at elevation A have increased. Such increase can also be seen on DCL9 (elevations C and D), DCL10b at elevation A, and DCL11 at elevations B, C and D. Again, the chloride diffusion coefficient value of concrete is strongly dependent on the exposure elevation and exposure time. One interesting observation is that the locations of the highest chloride diffusion coefficient values of DCL2 when exposed to tidal set-up and splash set-up are the same (elevation A) regardless of six or ten months of exposure .

After 18 months of exposure, the  $D_{app}$  values ranged between  $0.16$  and  $0.58 \times 10^{-12} \text{ m}^2/\text{s}$  (except for DCL3, DCL10a and DCL10b which were between  $1.38$  and  $2.6 \times 10^{-12} \text{ m}^2/\text{s}$ ). For elevation B and C, most  $D_{app}$  values were smaller than  $1 \times 10^{-12} \text{ m}^2/\text{s}$ , whereas at elevation D, the  $D_{app}$  values were usually larger with eight values being equal or greater than  $0.95 \times 10^{-12} \text{ m}^2/\text{s}$ .

Table 5-11:  $D_{app}$  values of concrete mixes exposed at splash simulation (elevation A)

Mix	Apparent chloride diffusivity ( $10^{-12} \text{ m}^2/\text{s}$ )		
	6 Months	10 Months	18 Months
	100% Seawater		
DCL1	0.67	0.52	0.41
DCL2	2.23	0.78	0.58
DCL3	12.30	1.86	2.63
DCL4	1.20	0.56	0.57
DCL5	0.80	0.85	0.27
DCL6	2.17	0.39	0.15
DCL7	0.72	1.06	0.28
DCL8	1.44	0.38	0.49
DCL9	0.30	0.21	0.16
DCL10a	2.55	1.05	1.38
DCL10b	2.73	3.08	2.41
DCL11	0.38	0.17	0.13
90% Tap water/10% Seawater			
DCL3	0.44	1.36	0.86
DCL6	0.58	0.31	1.24
DCL9	0.22	0.11	0.29

Table 5-12:  $D_{app}$  values of concrete mixes exposed at splash simulation (elevation B)

Mix	Apparent chloride diffusivity ( $10^{-12} \text{ m}^2/\text{s}$ )		
	6 Months	10 Months	18 Months
	100% Seawater		
DCL1	0.64	0.37	1.06
DCL2	0.86	0.37	0.45
DCL3	3.82	0.51	2.45
DCL4	1.28	0.40	0.33
DCL5	1.90	1.19	0.86
DCL6	0.74	0.54	0.26
DCL7	0.85	0.75	0.71
DCL8	2.79	0.81	0.74
DCL9	0.33	0.30	0.15
DCL10a	1.95	0.76	1.24
DCL10b	4.19	1.53	3.14
DCL11	0.47	0.53	0.56
90% Tap water/10% Seawater			
DCL3	3.06	2.03	4.32
DCL6	0.33	1.15	0.73
DCL9	1.09	0.11	0.77

Table 5-13:  $D_{app}$  values of concrete mixes exposed at splash simulation (elevation C)

Mix	Apparent chloride diffusivity ( $10^{-12} \text{ m}^2/\text{s}$ )		
	6 Months	10 Months	18 Months
	100% Seawater		
DCL1	0.96	0.49	0.38
DCL2	1.21	0.74	0.30
DCL3	2.75	0.43	2.80
DCL4	1.15	0.42	0.17
DCL5	1.04	1.31	0.28
DCL6	1.00	0.66	0.82
DCL7	1.43	0.36	0.34
DCL8	1.20	0.66	0.56
DCL9	0.23	0.32	0.37
DCL10a	2.46	1.38	0.71
DCL10b	1.51	1.18	1.22
DCL11	0.26	0.54	0.19
90% Tap water/10% Seawater			
DCL3	2.90	1.05	1.25
DCL6	0.37	0.25	0.50
DCL9	0.51	0.11	0.20

Table 5-14:  $D_{app}$  values of concrete mixes exposed at splash simulation (elevation D)

Mix	Apparent chloride diffusivity ( $10^{-12} \text{ m}^2/\text{s}$ )		
	6 Months	10 Months	18 Months
	100% Seawater		
DCL1	3.82	0.50	0.25
DCL2	0.49	0.66	0.77
DCL3	0.77	1.06	3.04
DCL4	3.82	0.50	0.86
DCL5	0.49	1.27	1.15
DCL6	0.77	0.49	1.40
DCL7	3.82	0.87	0.71
DCL8	0.49	0.17	0.87
DCL9	0.77	0.54	2.05
DCL10a	3.82	1.17	1.57
DCL10b	0.49	1.03	2.07
DCL11	0.77	4.63	2.57
90% Tap water/10% Seawater			
DCL3	3.82	1.79	4.49
DCL6	0.49	0.32	0.81
DCL9	0.77	0.38	0.95

### 5.4.3.3 Barge Simulation

The apparent diffusion coefficient values for specimens exposed to the barge simulation for six, ten, and 18 months are shown in Table 5-15 (elevation A), Table 5-16 (elevation B), Table 5-17 (elevation C), and Table 5-18 (elevation D). In general, the  $D_{app}$  values for these specimens reached lower values for longer exposure times. For elevation A, DCL6 right side was the mix that showed the lowest  $D_{app}$  with a value of  $0.2 \times 10^{-12} \text{ m}^2/\text{s}$  followed by DCL2 which was the mix that showed the second lowest apparent diffusivity value ( $0.75 \times 10^{-12}$ ) at 18 months when compared to the other mixes. On the other hand, the specimen with the same mix composition as DCL2 but a w/cm ratio of 0.47 (DCL3) showed the overall highest  $D_{app}$  value ( $3.04 \times 10^{-12}$ ) after 18 months.

After six months' exposure, it can be observed that the chloride diffusion coefficient values of DCL2 and DCL3 at elevation A are higher than the chloride diffusion coefficient values at the other elevations for each block. The highest chloride diffusion coefficient values are at elevation B for DCL6, DCL10b and DCL11, whereas the highest  $D_{app}$  is at elevation C for DCL9 block. It is also seen that DCL2 has the maximum overall chloride diffusion coefficient value ( $8.58 \times 10^{-12} \text{ m}^2/\text{s}$ ) at elevation A and DCL6 has the minimum chloride diffusion coefficient value ( $0.445 \times 10^{-12} \text{ m}^2/\text{s}$ ) at elevation D.

After ten months' exposure, the highest chloride diffusion coefficient value remains at elevation A for DCL3, but the highest  $D_{app}$  for DCL9 and DCL11 is now at elevation C. DCL2, DCL6 and DCL10b have the highest  $D_{app}$  at elevation D. After 10 months of exposure, the maximum chloride diffusion coefficient value ( $4.72 \times 10^{-12} \text{ m}^2/\text{s}$ ) is for DCL10b at elevation D and DCL9 has the minimum chloride diffusion coefficient value ( $0.462 \times 10^{-12} \text{ m}^2/\text{s}$ ) at the same elevation. At elevations C and D, the chloride source is mainly due to splash from boat traffic and spray airborne particles from the sea or intracoastal water, but can also be washed out by rain events.

After eighteen months' exposure, six of the seven concrete mixtures (at least one side) had a  $D_{app}$  value greater than  $1.3 \times 10^{-12} \text{ m}^2/\text{s}$  for elevations A and B. For elevation C, the  $D_{app}$  values range between 0.38 and  $1.66 \times 10^{-12} \text{ m}^2/\text{s}$ , and at elevation D, mixture DCL2 to DCL9  $D_{app}$  values ranged between 0.14 and  $0.85 \times 10^{-12} \text{ m}^2/\text{s}$ , one of the sides of DCL10a, DCL10b and DCL11 had  $D_{app}$  values greater than  $1 \times 10^{-12} \text{ m}^2/\text{s}$ .

Table 5-15:  $D_{app}$  values of concrete mixes at barge simulation (Elevation A)

Mix	Side	Apparent chloride diffusivity ( $10^{-12} \text{ m}^2/\text{s}$ )		
		6 Months	10 Months	18 Months
DCL2	R	8.58	0.27	0.73
	L	2.43	0.60	0.76
DCL3	R	0.74	4.26	1.65
	L	4.80	2.22	3.04
DCL6	R	3.04	2.06	2.01
	L	0.72	0.63	0.20
DCL9	R	0.85	1.57	0.77
	L	2.73	1.45	1.49
DCL10a	R	N/A	1.14	1.67
	L	1.57	1.10	2.21
DCL10b	R	1.51	2.38	1.47
	L	4.34	2.96	1.84
DCL11	R	2.55	2.57	1.87
	L	4.48	1.97	2.33

Table 5-16:  $D_{app}$  values of concrete mixes at barge simulation (Elevation B)

Mix	Side	Apparent chloride diffusivity ( $10^{-12} \text{ m}^2/\text{s}$ )		
		6 Months	10 Months	18 Months
DCL2	R	1.98	0.74	0.61
	L	2.31	0.85	0.65
DCL3	R	0.84	3.90	2.06
	L	1.21	2.20	2.88
DCL6	R	5.62	1.80	2.00
	L	2.88	1.10	1.22
DCL9	R	3.03	1.30	1.32
	L	2.67	1.20	0.77
DCL10a	R	N/A	1.60	1.59
	L	4.72	1.50	2.20
DCL10b	R	1.05	1.70	1.38
	L	6.07	2.60	2.10
DCL11	R	4.67	2.00	1.52
	L	3.31	2.20	1.98

Table 5-17:  $D_{app}$  values of concrete mixes at barge simulation (Elevation C)

Mix	Side	Apparent chloride diffusivity ( $10^{-12} \text{ m}^2/\text{s}$ )		
		6 Months	10 Months	18 Months
<b>DCL2</b>	R	0.44	0.41	0.38
	L	1.24	0.71	0.55
<b>DCL3</b>	R	2.03	0.61	1.16
	L	0.62	0.40	0.67
<b>DCL6</b>	R	0.54	0.48	0.76
	L	0.98	0.36	1.10
<b>DCL9</b>	R	2.16	1.70	1.28
	L	6.83	1.30	1.28
<b>DCL10a</b>	R	N/A	0.47	1.66
	L	1.51	0.55	0.45
<b>DCL10b</b>	R	2.49	3.30	0.86
	L	4.54	4.40	1.32
<b>DCL11</b>	R	3.08	3.00	3.16
	L	3.10	2.10	1.56

Table 5-18:  $D_{app}$  values of concrete mixes at barge simulation (Elevation D)

Mix	Side	Apparent chloride diffusivity ( $10^{-12} \text{ m}^2/\text{s}$ )		
		6 Months	10 Months	18 Months
<b>DCL2</b>	R	1.25	1.50	0.60
	L	1.31	0.37	0.56
<b>DCL3</b>	R	0.56	0.92	0.60
	L	0.79	1.80	0.33
<b>DCL6</b>	R	0.36	0.67	0.14
	L	0.45	3.10	0.60
<b>DCL9</b>	R	0.93	0.22	0.27
	L	0.97	0.71	0.85
<b>DCL10a</b>	R	N/A	0.24	1.18
	L	0.39	0.38	0.30
<b>DCL10b</b>	R	2.12	2.70	0.30
	L	2.06	4.70	3.35
<b>DCL11</b>	R	2.47	1.10	1.82
	L	4.14	1.40	2.50

## 5.5 Comparison of Apparent Diffusivity Coefficient (Free vs. Total)

### 5.5.1 Specimens Exposed to Low Concentration of Sodium Chloride Solution (0.1M NaCl)

The apparent diffusivity values considering the presence of free and total chloride ions on specimens when cured at 14RT/77RT/RT and exposed to 0.1M NaCl for 400 days are shown in Table 5-19. In general, the  $D_{app}$  values obtained for the total chloride content were higher than when only the free chloride content was studied. For instance, the mixes made of 20% FA and 8% SF had a total  $D_{app}$  value 44% higher than the free  $D_{app}$  for DCL4, 59% for DCL5, and 35% for DCL6. However, this was not seen in all of the mixes; in the case of DCL7, the diffusivity rate for free chloride ions was significantly higher ( $0.72 \times 10^{-12} \text{ m}^2/\text{s}$ ) than the one for the total chloride ions ( $0.46 \times 10^{-12} \text{ m}^2/\text{s}$ ). The highest total and free  $D_{app}$  were  $3.3 \times 10^{-12} \text{ m}^2/\text{s}$  and  $1.77 \times 10^{-12} \text{ m}^2/\text{s}$  obtained on the mixtures DCL10b and DCL10a with a cementitious content of  $335 \text{ kg/m}^3$  (and cement content of  $268 \text{ kg/m}^3$ ). On the other hand, the transport of free chloride ions into concrete seemed to be relatively slow ( $0.192 \times 10^{-12} \text{ m}^2/\text{s}$ ) on the DCL5 mix with a w/cm ratio of 0.41 in comparison with the results obtained on the other mixes.

Table 5-19: Apparent diffusivity for free and total chloride analyses for DCL mixes exposed to 0.1M NaCl solution for 400 days

Mix	Apparent Chloride Diffusivity ( $10^{-12} \text{ m}^2/\text{s}$ )	
	Free	Total
DCL1	0.95	0.95
DCL2	0.83	1.05
DCL3	1.41	2.43
DCL4	0.60	1.07
DCL5	0.19	0.47
DCL6	0.64	0.98
DCL7	0.72	0.46
DCL8	0.73	1.07
DCL9	0.70	1.16
DCL10	1.34	2.09
DCL10a	1.77	3.16
DCL10b	1.43	3.30
DCL11	1.63	1.78

### 5.5.2 Specimens Exposed to High Concentrations of Sodium Chloride Solutions (3% and 16.5% NaCl)

The apparent diffusivity coefficient for specimens cured at NC, AC, NC=AC, and NC<AC and immersed in 3% and 16.5% of NaCl solutions for 365 days are illustrated on Table 5-20 and Table 5-21, respectively. When the specimens were cured at NC and exposed to 3% NaCl solution, the chloride transport of total chloride ions into concrete was faster than that of the free

chloride transport for almost all of the mixes. For instance, the total  $D_{app}$  for DCL7 was  $2.14 \times 10^{-12} \text{ m}^2/\text{s}$  while the free  $D_{app}$  value was  $0.57 \times 10^{-12} \text{ m}^2/\text{s}$ . However, DCL1, which has the same w/cm ratio as DCL7 (0.41) had a slightly higher free  $D_{app}$  ( $2.42 \times 10^{-12} \text{ m}^2/\text{s}$ ) than total  $D_{app}$  ( $1.88 \times 10^{-12} \text{ m}^2/\text{s}$ ). In the case of having mixes cured at NC=AC curing condition and immersed in 3% NaCl solution, all of the mixes had higher total  $D_{app}$  than free  $D_{app}$ . In fact, the highest difference between the diffusivity rate for free and total chloride ions was obtained on the specimens of the DCL9 mix. The  $D_{app\_total}$  value for this sample was almost 84% higher than the  $D_{app\_free}$ . In general, there was a modest difference between the free and total chloride penetration rate for some of the mixes cured at AC and exposed to 3% NaCl. For example, this was seen on DCL1, DCL3, DCL4, DCL5, DCL10a, and DCL10b.

Moreover, the specimen that showed an overall higher resistance to the chloride penetration in both cases (free and total) was DCL4. The  $D_{app}$  values for DCL4 were  $0.26 \times 10^{-12} \text{ m}^2/\text{s}$  and  $0.54 \times 10^{-12} \text{ m}^2/\text{s}$  for free and total, respectively, when cured at NC=AC.

Table 5-20: Apparent diffusivity for free and total chloride analyses for DCL mixes exposed to 3% NaCl solution for 365 days

Mix	Apparent Chloride Diffusivity ( $10^{-12} \text{ m}^2/\text{s}$ )							
	Curing Condition							
	NC		AC		NC=AC		NC<AC	
	Free	Total	Free	Total	Free	Total	Free	Total
<b>DCL1</b>	2.42	1.88	2.49	2.39	0.97	1.48	N/A	N/A
<b>DCL2</b>	2.49	2.08	1.47	2.21	1.8	2.2	0.78	2.25
<b>DCL3</b>	1.88	3.35	2.43	2.55	2.47	2.8	1.19	3.28
<b>DCL4</b>	1.02	1.92	0.85	0.88	0.26	0.54	N/A	N/A
<b>DCL5</b>	1.80	2.16	1.13	1.26	0.46	0.74	N/A	N/A
<b>DCL6</b>	0.88	2.55	0.77	1.91	0.72	1.32	N/A	N/A
<b>DCL7</b>	0.57	2.14	0.6	1.87	0.53	1.59	N/A	N/A
<b>DCL8</b>	0.73	1.86	0.41	1.18	0.6	1.47	N/A	N/A
<b>DCL9</b>	0.64	2.03	0.6	2.28	0.71	4.33	N/A	N/A
<b>DCL10a</b>	0.98	4.71	2.08	2.78	2.00	1.61	2.52	3.20
<b>DCL10b</b>	1.87	3.49	2.05	2.60	2.03	2.84	N/A	N/A
<b>DCL11</b>	1.55	3.4	2.43	3.38	0.77	2.42	N/A	N/A

As mentioned earlier, Table 5-21 represents the information of the apparent diffusivity coefficients of the free and total chloride ions when the mixes were exposed to 16.5% NaCl solution for 365 days. In the case of NC curing condition, DCL2 had the highest diffusivity rate for both free and total chloride ions ( $4.32 \times 10^{-12} \text{ m}^2/\text{s}$  and  $4.21 \times 10^{-12} \text{ m}^2/\text{s}$ , respectively) when compared to the other mixes. On the other hand, when cured at the same regime, DCL1 had the lowest diffusivity coefficient of free chloride ions with a value of  $0.24 \times 10^{-12} \text{ m}^2/\text{s}$ . DCL3 was the mix that had the highest free and total  $D_{app}$  values when it was cured at accelerated

conditions with calculated values of  $5.72 \times 10^{-12} \text{ m}^2/\text{s}$  for free and  $4.24 \times 10^{-12} \text{ m}^2/\text{s}$  for total. In general, the lowest  $D_{app}$  value for this curing condition corresponded to the mixes with 50% Slag (DCL7, DCL8, and DCL9) compared to the other two base compositions. Also, the normal to accelerated (i.e., NC=AC) curing condition was the regimen that had an overall lowest  $D_{app}$  value for both free and total ions. The group with the smallest diffusivity coefficient and NC=AC curing corresponded to the mixes with 20% FA and 8% SF in comparison to the other mixes. For instance, DCL5 had a free  $D_{app}$  value of  $0.39 \times 10^{-12} \text{ m}^2/\text{s}$  while DCL2 (with the same w/cm ratio is 0.41) obtained a value of  $2.75 \times 10^{-12} \text{ m}^2/\text{s}$ .

Table 5-21: Apparent diffusivity for free and total chloride analyses for DCL mixes exposed to 16.5% NaCl solution for 365 days

Mix	Apparent Chloride Diffusivity ( $10^{-12} \text{ m}^2/\text{s}$ )							
	Curing Condition							
	NC		AC		NC=AC		NC<AC	
	Free	Total	Free	Total	Free	Total	Free	Total
<b>DCL1</b>	0.24	2.52	1.32	1.86	0.62	1.40	N/A	N/A
<b>DCL2</b>	4.32	4.21	1.06	2.73	2.75	2.38	3.18	2.78
<b>DCL3</b>	3.05	4.53	5.72	4.24	2.41	2.59	2.77	3.95
<b>DCL4</b>	1.01	1.26	1.46	1.77	0.55	0.79	N/A	N/A
<b>DCL5</b>	1.35	2.06	1.62	2.44	0.39	0.83	N/A	N/A
<b>DCL6</b>	2.30	3.12	2.40	2.22	0.57	1.36	N/A	N/A
<b>DCL7</b>	1.04	2.68	0.92	2.29	1.02	2.07	N/A	N/A
<b>DCL8</b>	0.86	2.82	0.57	2.56	0.52	1.34	N/A	N/A
<b>DCL9</b>	1.43	3.36	0.92	2.69	0.76	1.82	N/A	N/A
<b>DCL10a</b>	2.28	3.55	2.41	2.78	1.38	1.94	1.42	3.35
<b>DCL10b</b>	2.53	4.22	3.19	5.74	1.41	2.69	N/A	N/A
<b>DCL11</b>	3.05	3.88	2.28	4.85	2.15	2.85	N/A	N/A

## 5.6 Additional $D_{app}$ Analysis for Cores Obtained at Elevation A or from Bulk Diffusion

### 5.6.1 Effect of w/cm Ratio on Specimens Exposed to 0.1 M NaCl

In Figure 5-10 the apparent diffusion coefficient is plotted against water-cement ratio on the specimens made of 20% Fly Ash (top row) and 50% Slag (bottom row). The results showed that having a w/cm ratio of 0.47 increases the  $D_{app}$  values; additionally, when the 20% FA specimens were cured at RT and exposed for 400 days, the  $D_{app}$  for 0.41 w/cm mix was 1/3 of the value obtained for 0.35 w/cm ratio specimen; however, the value at 0.47 w/cm ratio was almost twice that of  $D_{app}$  at 0.41 w/cm. A similar w/cm ratio effect was found on same mixes with 20% FA+8% SF for exposure time and exposure regime. The effect of the w/cm ratio has been explained in different studies by knowing that the porosity is mainly dependent on the w/cm, so having low w/cm ratio creates a microstructure with less connected pores.[84] However, as

explained by Hassan in his dissertation, there is a limitation to how low the w/cm ratio can be in order to show an improvement on the apparent diffusion coefficient value.[85] This refers to the results obtained when using supplementary cementitious admixtures such as Slag causing a significant reduction on the  $D_{app}$  value. This can be seen when looking at the results for 50% Slag mixes, where the  $D_{app}$  increased almost 63% from the specimen with 0.35 w/cm to 0.41 w/cm ratio but then it was reduced by 20% at a 0.47 w/cm ratio. In the case of having specimens exposed to low concentration of NaCl solutions, it was apparent that as the w/cm ratio increased, the  $D_{app}$  values also increased for all of the mixes. For instance,  $D_{app}$  on 20% FA mix increased 5% from 0.35 to 0.41 w/cm ratio and then 28% from 0.41 to 0.47 w/cm ratio.

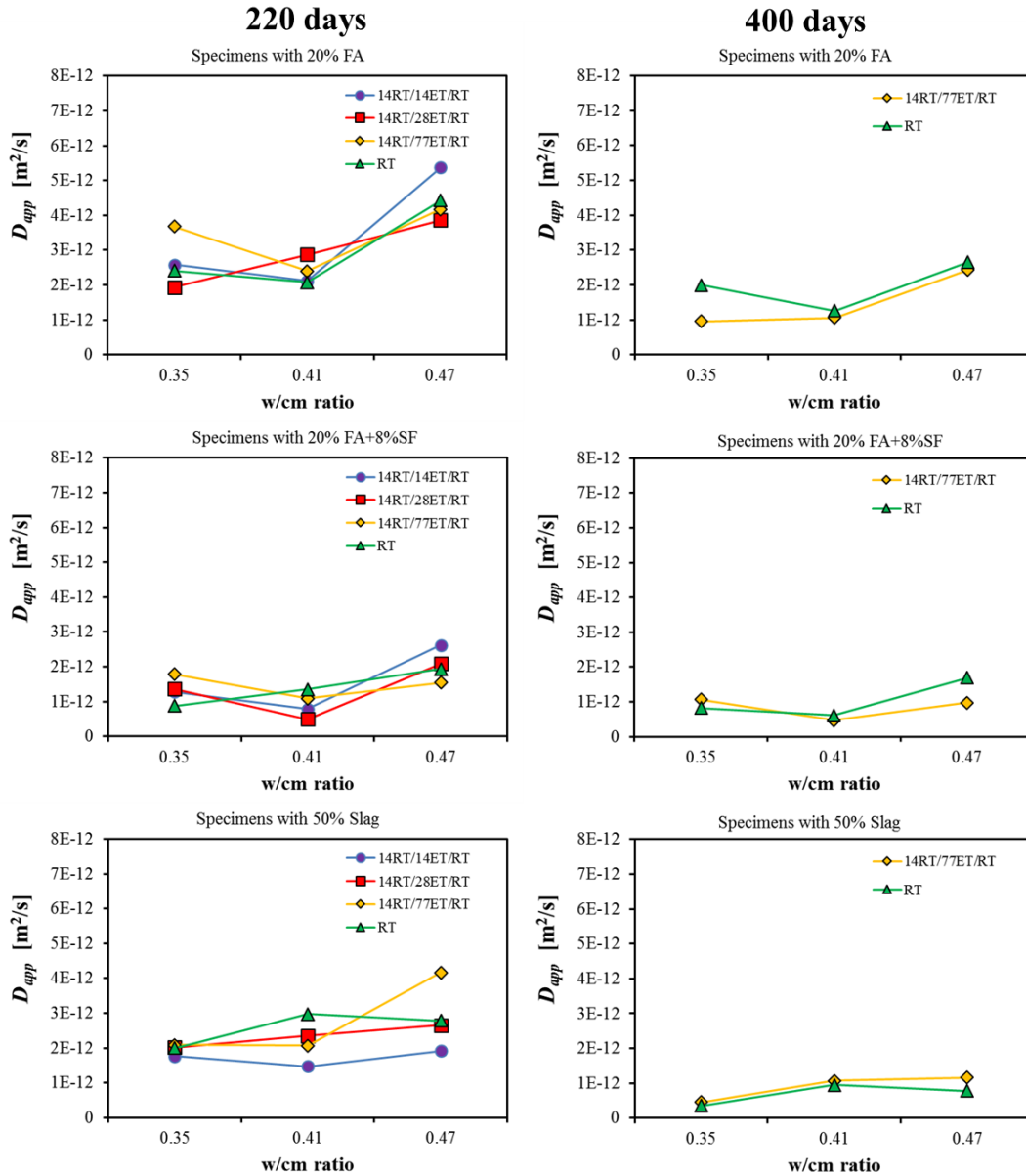


Figure 5-10: Relationship between apparent diffusion coefficient and w/cm ratio

The calculated and measured chloride concentration values at the surface and at the first layer for DCL1, DCL2, and DCL3 are plotted in Figure 5-11. When comparing the values for the concentration obtained at the first layer during the titration process (measured) and at the surface from fitting (calculated), they were very similar for these three mixes. In general, DCL3 specimen with the higher w/cm ratio presented the higher measured chloride concentration value compared to that of the other specimens (3.8 %cm) at 220 days. On the other hand, the DCL1 specimen had the lowest  $C_s$  when cured at the 4 curing regimes when exposed for 220 and 400 days. When looking at the curing regimens, the mixes had a lower value for  $C_s$  at 220 days when cured at 14RT/77ET/RT followed by 14RT/28ET/RT.

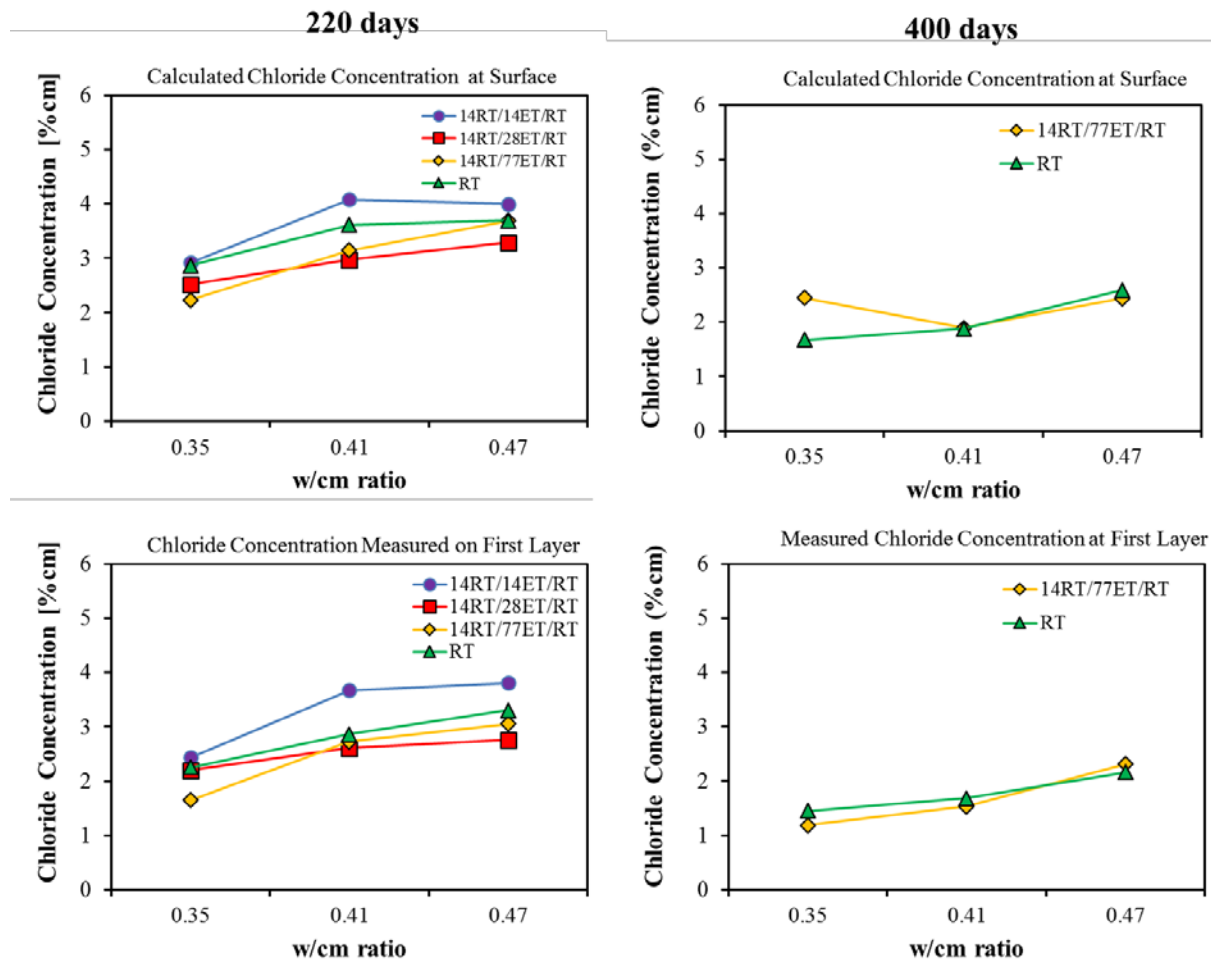


Figure 5-11: DCL1, 2 and 3 Calculated and measured chloride concentration vs. w/cm ratio

### 5.6.2 Effect of Supplementary Cementitious Material Type Based on Specimens Exposed to 3% or 16.5% NaCl

To illustrate the effect of the type cementitious material used on the apparent diffusion coefficient, the  $D_{app}$  value obtained for mixes with 20% FA, 20% FA + 8% SF and 50% Slag were plotted on Figure 5-12. These three mixes had the same w/cm ratio (0.47) and were

exposed to NC, AC, and NC=AC curing conditions in 3% and 16.5% NaCl. The plots for the same mixes exposed to a lower sodium chloride concentration solution are presented on Appendix K. The results showed that the specimen with 20% FA (DCL3) reached higher values of  $D_{app}$  in all of the curing conditions than the other two mixes.

Furthermore, when comparing these results to the ones found in a similar study performed by Presuel-Moreno the  $D_{app}$  values found for specimens made of 20% FA and with a w/cm ratio of 0.41, the  $D_{app}$  values were slightly smaller [86]. For instance, during this investigation, the  $D_{app}$  found at NC=AC was  $3.1 \times 10^{-12} \text{ m/s}^2$  and on the other study a specimen with similar composition and exposure conditions had a  $D_{app}$  of  $1.52 \times 10^{-12} \text{ m/s}^2$ . This can be a result of having a specimen with higher w/cm ratio (0.47); also, the age at which the specimens were exposed to the NaCl solutions might have caused a variation on the measured  $D_{app}$ . Additionally, adding silica fume in the composition of the concrete appeared to contribute to the reduction of  $D_{app}$  since it was consistently lower in the specimen made of 20% FA + 8% SF (DCL6), especially under accelerated curing conditions. In the case of having a mix with 50% Slag, the  $D_{app}$  values were relatively low when exposed to high NaCl solution but it clearly showed the lowest apparent diffusion coefficient when cured at RT and immersed in low NaCl solution for 400 days with a value of  $0.78 \times 10^{-12} \text{ (m/s}^2)$  (see Appendix K). It is important to highlight that the use of Slag in concrete mixes has been reported to greatly improve the performance of the concrete by reducing the chloride ions diffusion rate from an early age [13, 85, 86].

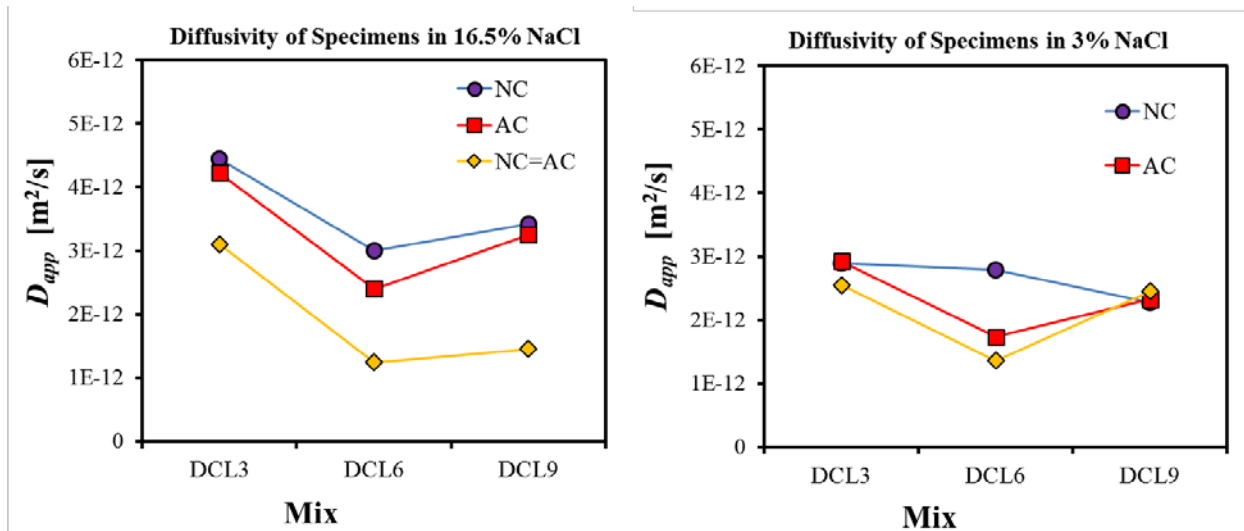


Figure 5-12: Relationship between average apparent chloride coefficient and type of cementitious material

### 5.6.3 Effect of Sodium Chloride Concentration Solution and w/cm

The effect of the concentration of the NaCl solution on the apparent diffusivity coefficient for specimens with 20% FA and 20% FA + 8% SF and cured at NC is shown in Figure 5-13. On DCL1, DCL2 and DCL3, the results showed that when the specimens were exposed to 16.5% NaCl solution (the higher concentration used during this investigation) for one year, there was a slight increase on  $D_{app}$  as the w/cm increased; however, this was not seen in all of the cases. In

fact, as reported in *Chloride Penetration into Concrete with Lightweight Aggregates* the concentration of NaCl solution seems to have an insignificant effect on the calculated diffusion coefficients [13]. This can be seen on the apparent diffusivity plot of specimens with 20% FA + 8% SF where the  $D_{app}$  was very similar for these three mixes when immersed in 16.5% NaCl and 3% NaCl for one year, respectively.

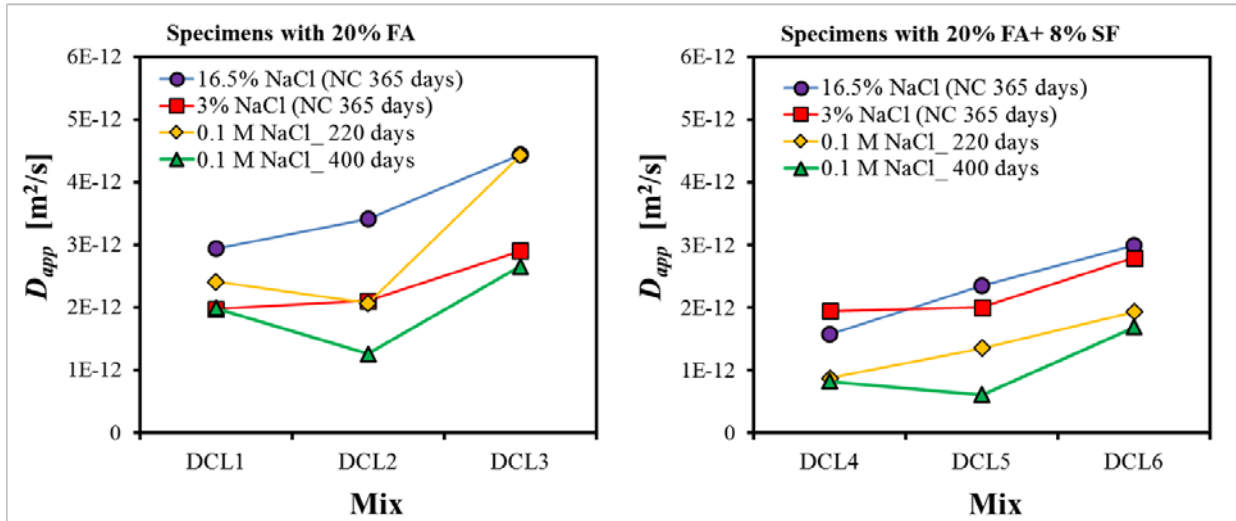


Figure 5-13: Relationship between apparent diffusivity and NaCl concentration solution

As mentioned previously, the surface chloride content  $C_s$  was also calculated by regression analysis. Figure 5-14 shows the effect of the concentration of the NaCl solution on the calculated  $C_s$  and measured chloride concentration on the first layer. The values plotted for the case of 16.5% and 3% NaCl solutions are the average value of the three cylinders considered and for 0.1M NaCl solution are the typical values obtained. The results showed that even though the concentrations of the NaCl solution used were not relevant on  $D_{app}$ , they seemed to have an important effect on  $C_s$  for all of the cases and mixes considered. For instance, the  $C_s$  on specimens exposed to 16.5% NaCl solution for one year was significantly greater than when exposed to lower solutions with lower NaCl content. However, in the case of evaluating the measured chloride content at the first layer it is important to note that the thickness considered for the specimens exposed to high concentrations of NaCl was larger (6.35 mm) than the one used for low concentrations (2-3 mm).

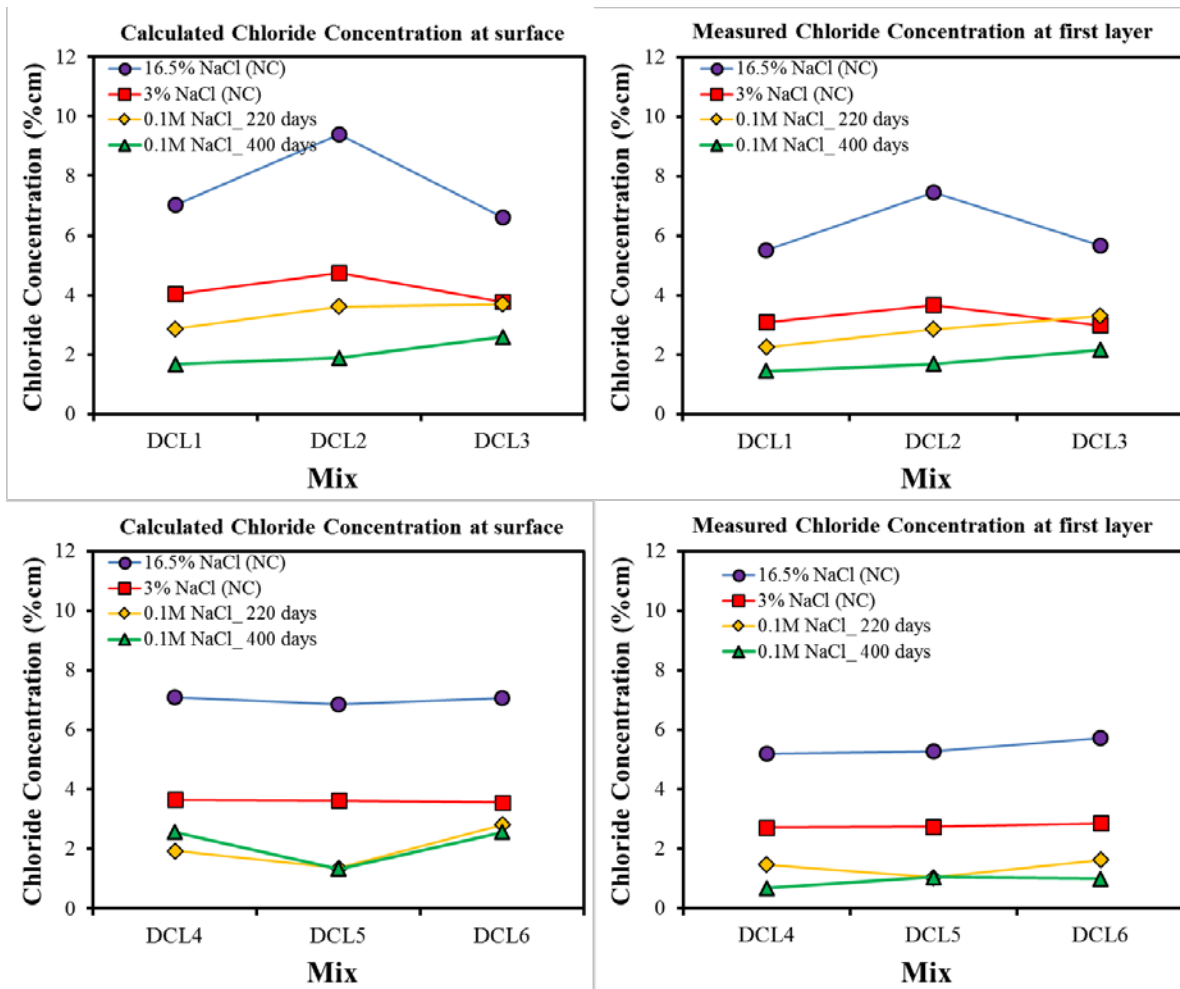
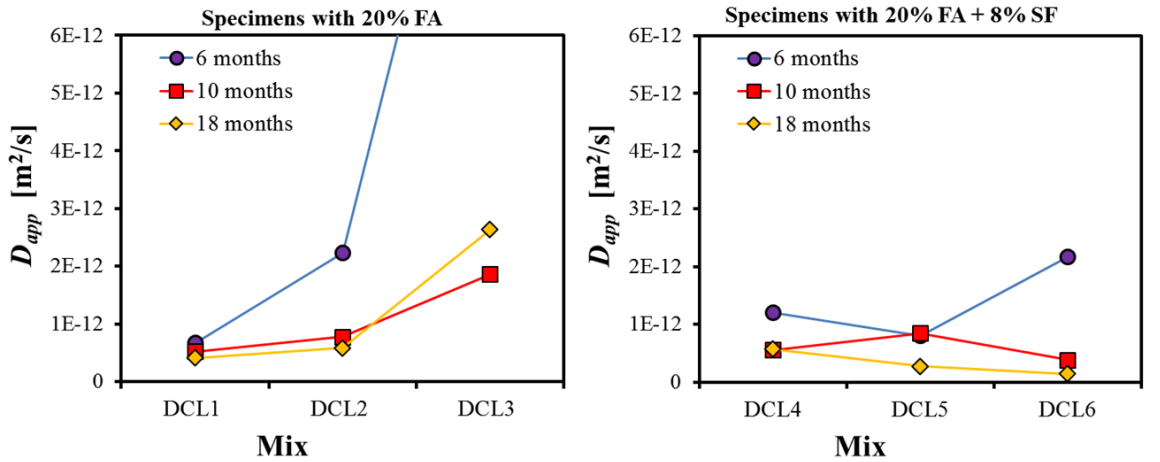


Figure 5-14: Relationship between calculated and measured chloride concentration and NaCl concentration solutions

### 5.6.4 Effect of Exposure Time

The effect of the exposure time on the apparent diffusion coefficient for specimens exposed to seawater in splash (top row) and in tidal (bottom row) simulated conditions are plotted in Figure 5-15. This study showed that after 10 months the rate of diffusion seemed to get stable for the specimens exposed to simulated conditions. In fact, independently on the concrete composition, there was not too much variation on the calculated  $D_{app}$  on specimens between 10 and 18 months of exposure time. This was also seen for the case of mixes with 50% Slag where the apparent diffusion coefficient was very constant especially on the mixes with the lowest w/cm ratio (0.35) (refer to Appendix L for the plot).

## Splash



## Tidal

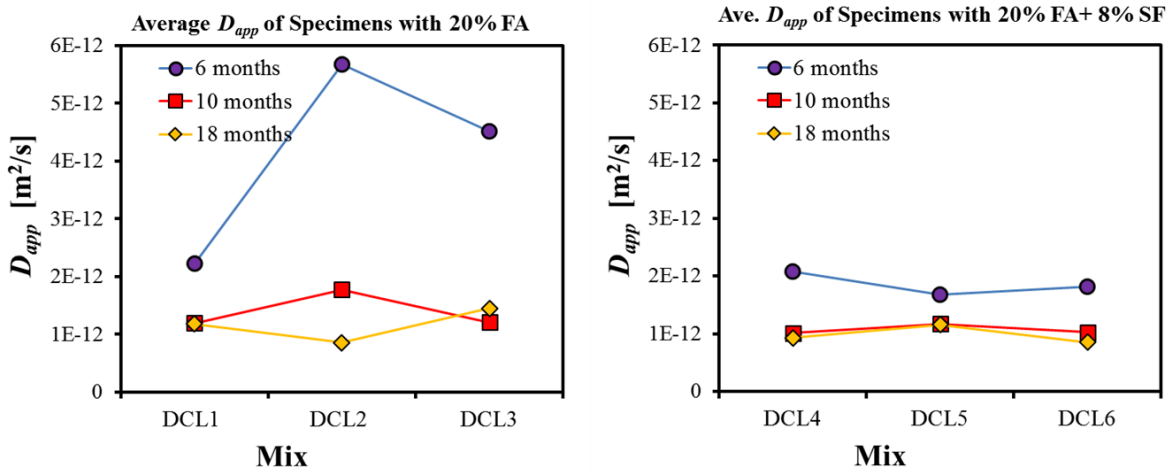


Figure 5-15: Relationship between apparent coefficient and exposure time

### 5.6.5 Effect of Exposure Condition

Figure 5-16 represents the effect of the different exposure conditions on specimens with 20%FA and different w/cm on the calculated  $D_{app}$  values. It is important to note that the specimens exposed to tidal and splash effects were exposed to fresh seawater and the specimens immersed in the barge were exposed to intracoastal water; while for the other cases presented the solution used was NaCl at different concentrations. It is apparent that the lowest  $D_{app}$  values were found on specimens exposed to seawater in splash conditions for all of these three mixes (DCL1, DCL2, DCL3). Also,  $D_{app}$  for tidal simulated exposure seemed to be higher than in splash; these differences in the  $D_{app}$  values might be caused by the evaporation present on the tidal scenario since the tanks were not covered and the concentration was higher for some periods of time. Also, for these scenarios, there were not significant changes when the exposure time increased; however, in a study performed in the UK with specimens of an age range from 5 to 10 years and exposed to tidal zones, it was found that mixes with a low w/cm ratio and a composition of fly ash and slag had a continuing reduction in  $D_{app}$  [87].

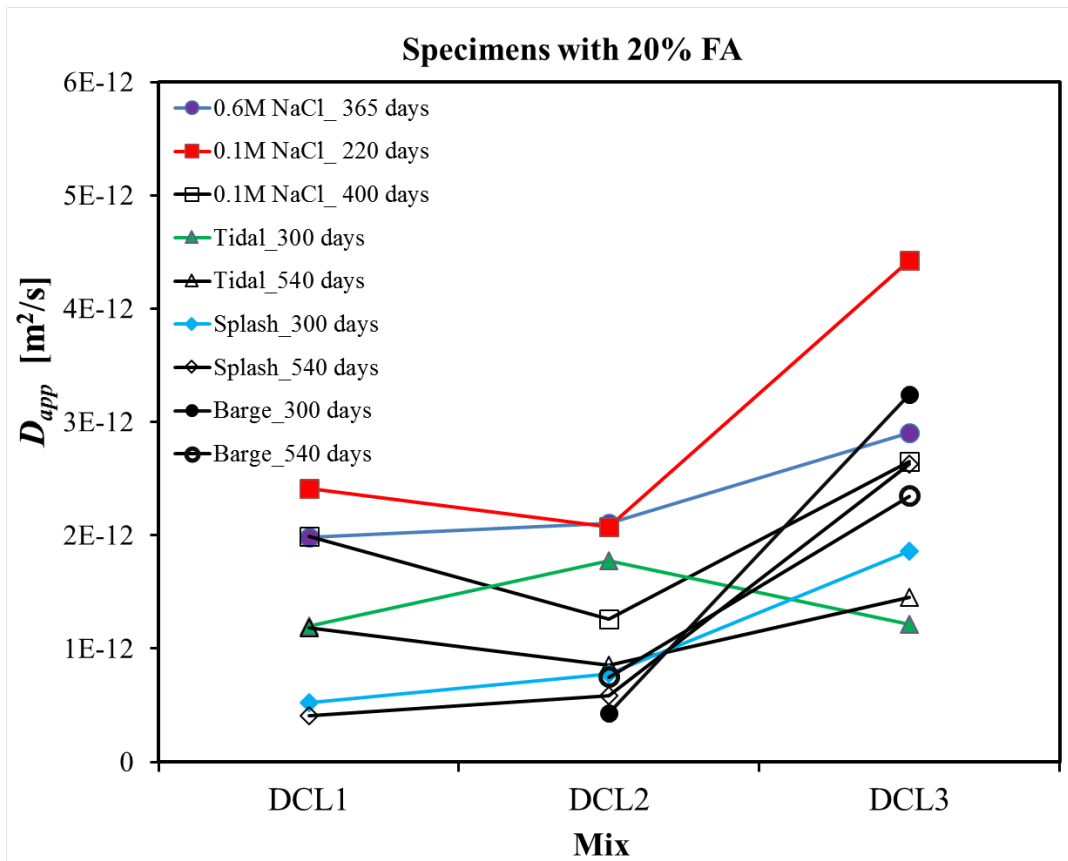


Figure 5-16: Relationship between  $D_{app}$  and w/cm for various exposure conditions

Figure 5-17 shows the relationship between calculated  $D_{app}$  values on specimens with 0.47 w/cm and different compositions after the different exposures. DCL6 and DCL9 specimens exposed to the splash simulated environment after 540 days showed the lower  $D_{app}$  values.

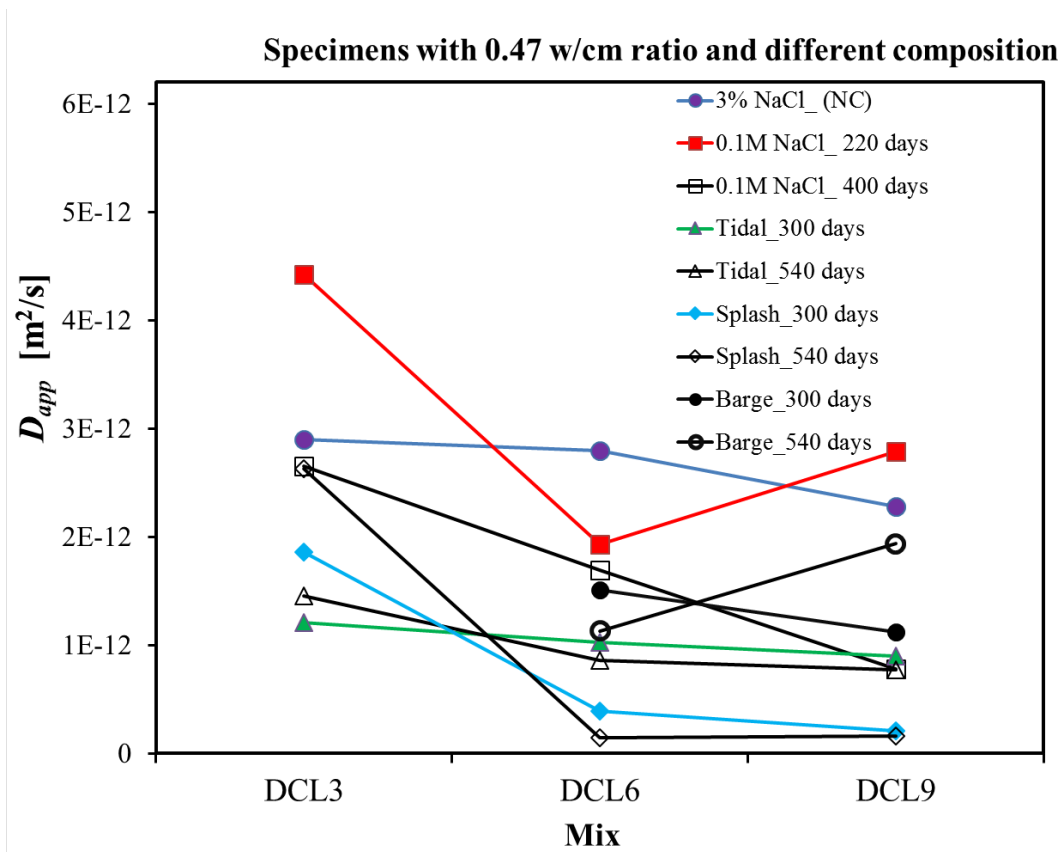


Figure 5-17: Relationship between apparent diffusion coefficient and exposure conditions (0.47 w/cm and different compositions)

Figure 5-18 represents the apparent diffusivity calculated for specimens with 20% FA and a w/cm ratio of 0.41 but different cementitious and cement amount.  $D_{app}$  value was smaller on DCL2 for the majority of the cases compared to the other specimens that had lower cement and cementitious content. The diffusivity was significantly lower when the exposure time increased when the specimens were exposed to NaCl solution. For instance, the  $D_{app}$  value for DCL10b when exposed at 0.1M NaCl for 220 days was  $5.3 \times 10^{-12} \text{ m}^2/\text{s}$  and then this value decreased almost 80% when it was calculated for an exposure time of 400 days. The  $D_{app}$  value obtained for splash simulation on specimens DCL11 and DCL10b were almost the same as for DCL2 for 540 days.

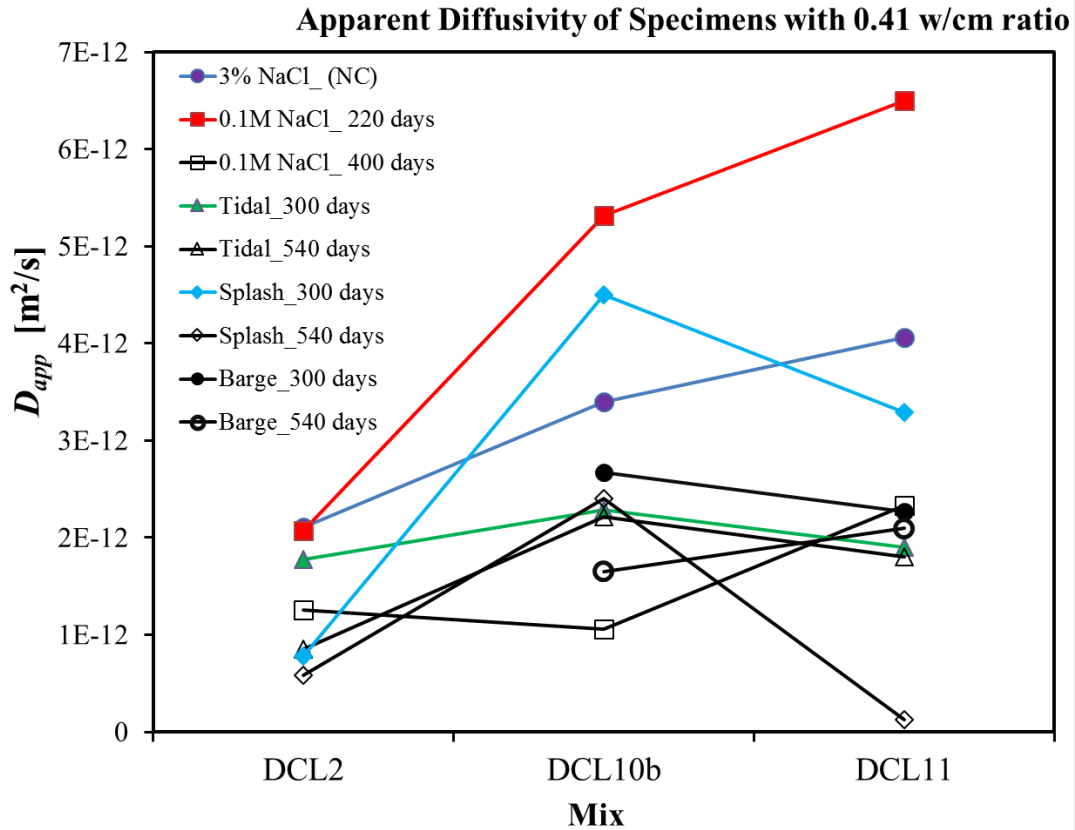


Figure 5-18: Relationship between apparent diffusion coefficient and exposure conditions (0.41 w/cm with 20% FA and different cementitious amount)

Figure 5-19 shows the chloride concentration measured on the first layer and the  $C_s$  calculated at the surface for the specimens with different composition (20% FA, 20% FA +8% SF, and 50% SF). The  $C_s$  measured values were slightly lower than the fitted calculated  $C_s$ ; a reason for this is that the measured values are the average over the thickness of the first layer while the calculated  $C_s$  is the projected value at the surface from the fitted profile. Additionally,  $C_s$  reached higher values when the mixes DCL3 and DCL6 were immersed in 3% NaCl solution by comparison to what was found in the other exposure conditions shown. In general, the results showed that exposing the specimens to the barge simulated condition increased the amount of the total chloride content at the surface compared to the tidal scenario. As documented in other studies, the presence of sulfate ions likely reduced the ability of the binding capacity of the concrete, and also reduces the diffusion of the chloride ions due to the formations of new compounds [85]. Thus, this could be the cause of having high  $C_s$  amounts at the barge scenario where the sulfate content in the intracoastal waterway solution might be lower compared to the content in seawater.

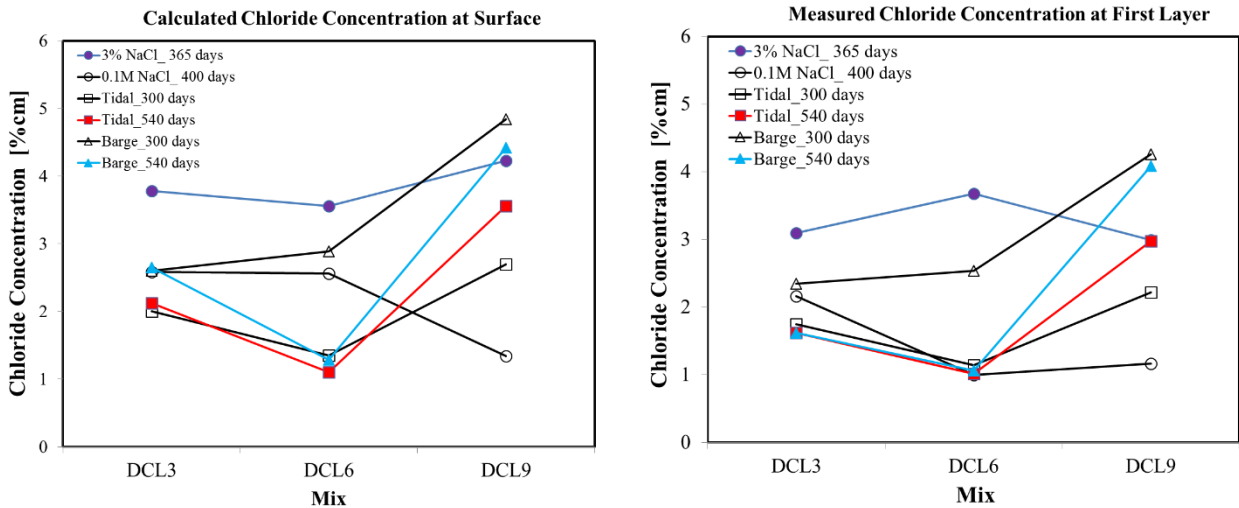


Figure 5-19: DCL3, 6, and 9 Calculated and measured chloride concentration at the surface and first layer

## 5.7 Specimens Subjected to Tidal Simulation for >18 Years at SMO

### 5.7.1 $D_{app}$ vs. Elevation

Figure 5-20 shows the  $D_{app}$  calculated values vs. elevation for specimens with superfine fly ash obtained from each profile, similarly for specimens with silica fume Figure 5-21 shows the  $D_{app}$  calculated values vs. elevation. These elevations reflect the elevations at which the cores were obtained. Figure 5-22 shows the average  $D_{app}$  values for elevation and all specimens. Those for OPC were obtained using a finite geometry and Fick's second Law.

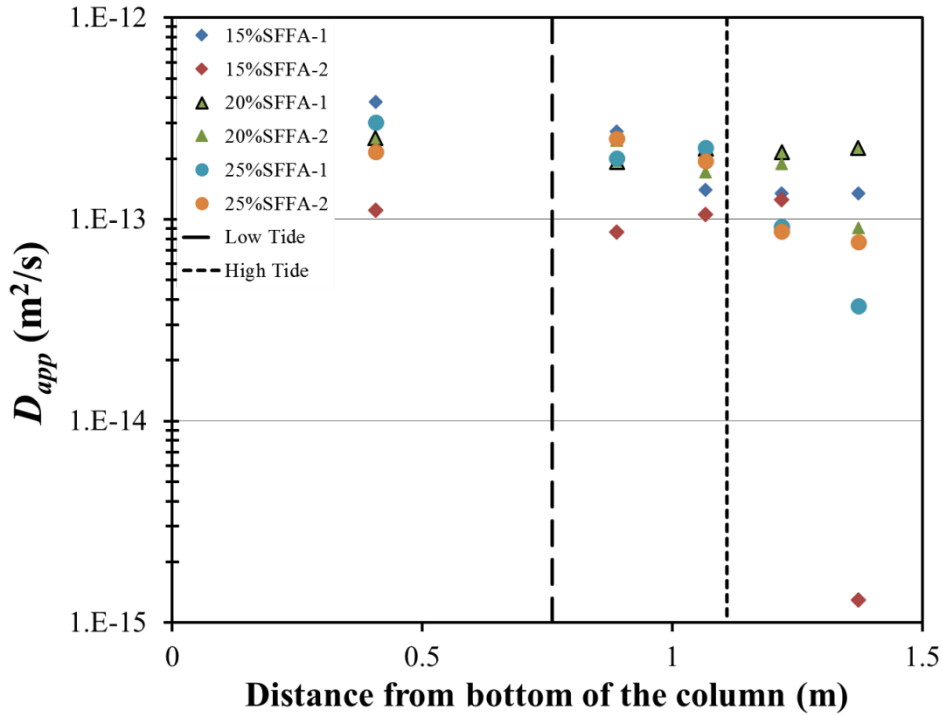


Figure 5-20:  $D_{app}$  vs. elevation for specimens with superfine fly ash

The  $D_{app}$  values on specimens with superfine fly ash ranged from  $0.4 \times 10^{-12} m^2/s$  to  $0.04 \times 10^{-12} m^2/s$ , with one value that was as little as  $0.001 \times 10^{-12} m^2/s$ . The  $D_{app}$  values tended to be smaller for the two elevations above the high tide mark. Similar trends were observed on specimens with silica fume, but in some cases, the largest  $D_{app}$  value was observed at locations within the tide marks. Figure 5-22 shows the average  $D_{app}$  values; it is clear that the larger  $D_{app}$  values were observed for specimens with only OPC. Recall that this specimen has a w/cm of 0.4, whereas, for all other specimens the value was  $< 0.37$  w/cm. The decay of the  $D_{app}$  values as the elevation increased is easier to observe when reviewing the figure with the average the  $D_{app}$  values.

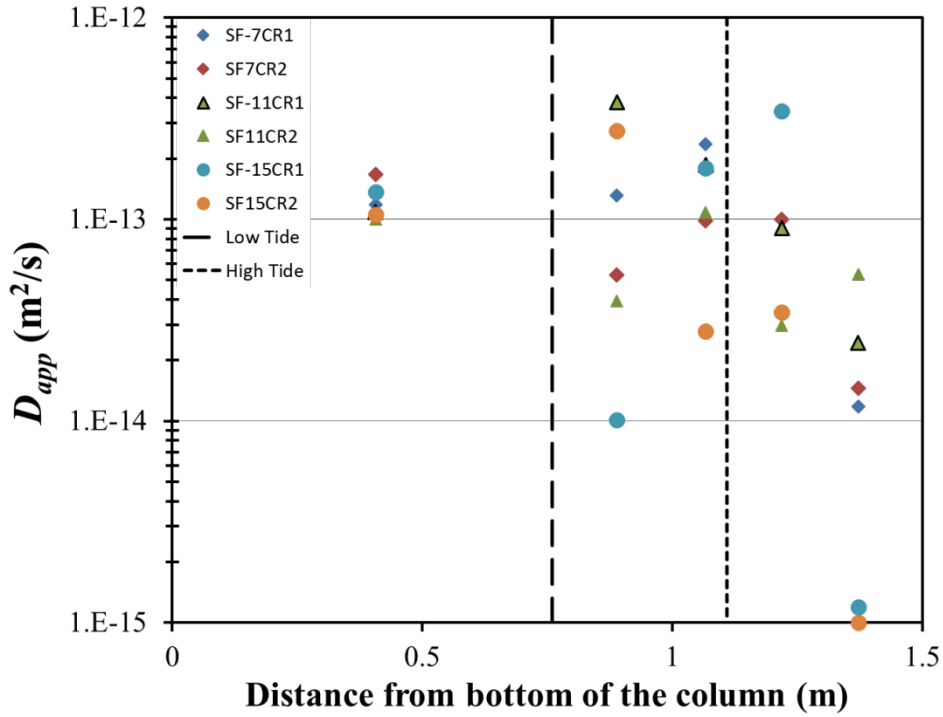


Figure 5-21:  $D_{app}$  vs. elevation for specimens with silica fume

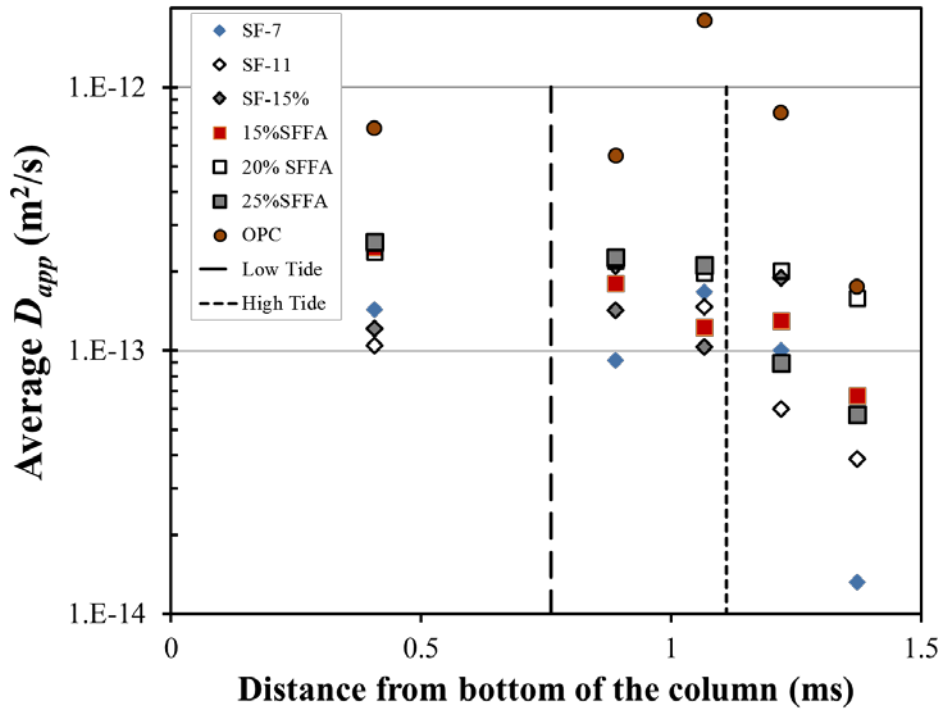


Figure 5-22: Average  $D_{app}$  vs. elevation computed for specimens exposed to tidal simulation

The following two figures show the calculated  $D_{app}$  values as a function of elevation. Figure 5-23 contains the values calculated for each profile, whereas Figure 5-24 shows the average  $D_{app}$

from the two profiles calculated for a given elevation. For profiles that showed the skin effect, those layers were not included in the fitting. It is evident that the calculated  $D_{app}$  decreased as the elevation increased. It is likely that this is due to the lower moisture level at these elevations. (Moreover, the transport as mentioned before is not simple diffusion.)

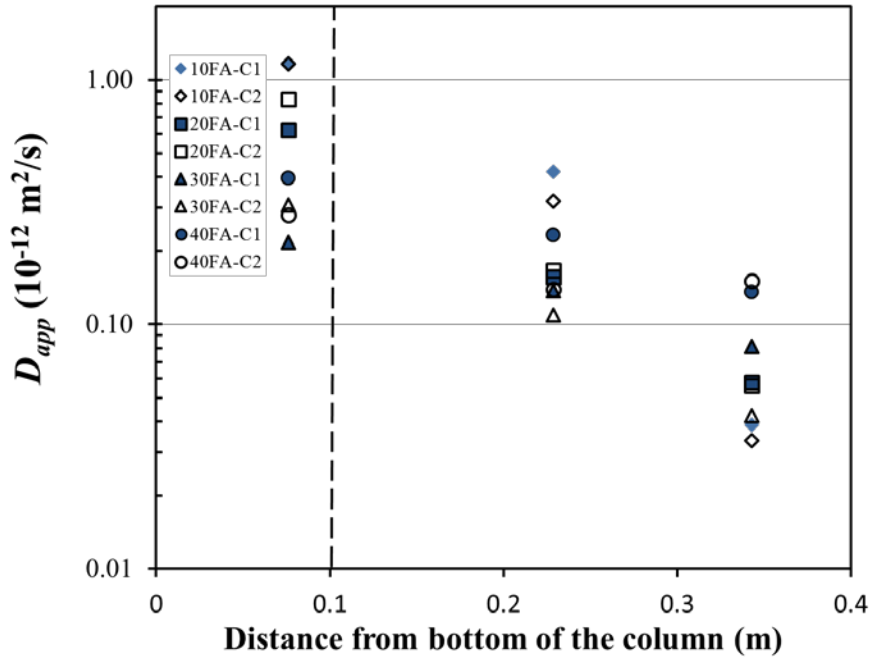


Figure 5-23:  $D_{app}$  vs. elevation calculate for each side on specimens with Fly Ash

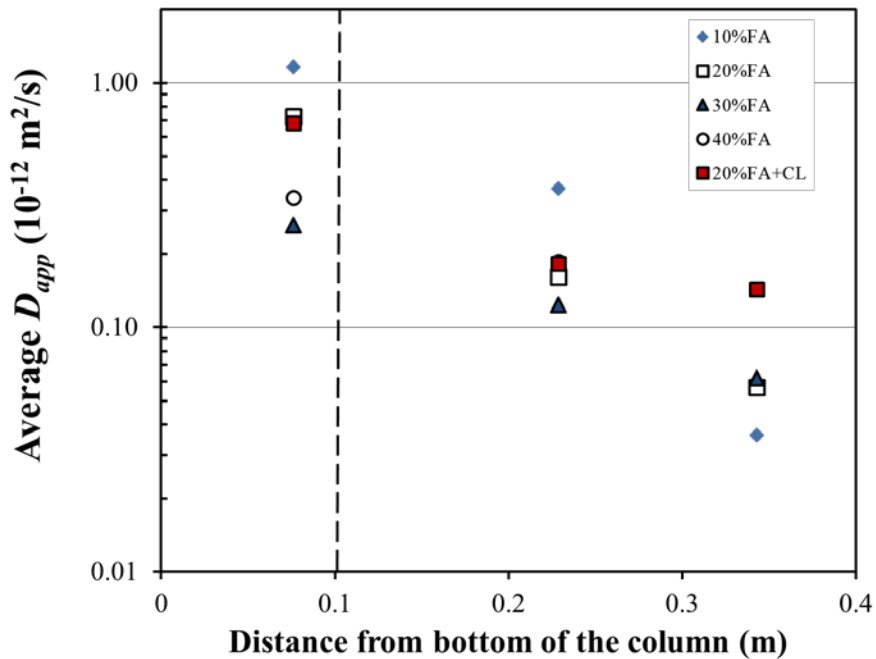


Figure 5-24: Average  $D_{app}$  vs. elevation on specimens with Fly Ash

Recently some researchers have been suggesting to re-zero the x-axis where  $C_{max}$  is located, and to re-calculate the  $D_{app}$ . This new  $D_{app}$  value then could be used for predictions of performance (the cover layer needs to also be reduced by the thickness of the layers removed). These types of  $D_{app}$  values were calculated and Table 5-22 shows a comparison of the  $D_{app}$  calculated after just removing layer(s) vs.  $D_{app}$  calculated after removing layers and re-setting the origin for the x-axis. The last two columns indicate the percent difference between these pairs of values; the  $D_{app}$  was smaller after re-setting the x-axis and  $D_{app}$  was smaller by 17% to up-to 48%. Cells shown with the same  $D_{app}$  values for both columns did not experience the skin effect, but were included in here to calculate the average reduction at a given elevation. It can be observed that the skin effect took place at all levels on specimens with 30% FA and 40% FA. All calculated  $D_{app}$  values after the re-zeroing was done were smaller; the calculated values ranged between 0.7 and  $0.02 \times 10^{-12} \text{ m}^2/\text{s}$ , whereas, before they ranged between 0.83 and  $0.05 \times 10^{-12} \text{ m}^2/\text{s}$ . The  $D_{app}$  values depended on elevation, moisture content and concrete composition.

Table 5-22:  $D_{app}$  values with and without re-zeroing

		$D_{app} (10^{-12} \text{ m}^2/\text{s})$						
	Elevation (m)	Side	Layers Removed		Re-zero on x-axis		Percent Difference	
				Average		Average		
10%FA	0.23	L	0.42	0.37	0.27	0.26	36.6	30.7
		R	0.32		0.24		23.0	
20%FA	0.07	L	0.62	0.73	0.51	0.60	18.7	18.2
		R	0.83		0.69		17.8	
	0.23	L	0.16	0.16	0.11	0.11	28.9	28.6
		R	0.17		0.12		28.2	
30%FA	0.07	L	0.22	0.26	0.16	0.20	26.0	24.4
		R	0.31		0.24		23.2	
	0.23	L	0.14	0.12	0.10	0.08	30.3	31.3
		R	0.11		0.07		32.6	
	0.34	L	0.08	0.06	0.08	0.05		16.6
		R	0.04		0.02		48.4	
40%FA	0.07	L	0.40	0.34	0.31	0.26	21.5	22.4
		R	0.28		0.21		23.7	
	0.23	L	0.23	0.19	0.17	0.14	25.4	26.9
		R	0.14		0.10		29.5	
	0.34	L	0.14	0.14	0.09	0.12	31.7	15.0
		R	0.15		0.15			

## 5.8 Chloride Binding Capacity

Figure 5-25 illustrates the relationship between free and total chloride content of specimens with 20%FA and with w/cm ratios of 0.35, 0.41, and 0.47 which were exposed to 3% and 16.5% NaCl for 1 year. As done in previous studies, linear relationships were obtained when plotting the data obtained for free vs. total chloride concentration when the specimens were cured at NC, NC=AC, and AC. Binding capacity of the specimens was also calculated using equation 12 in terms of percentage with the following equation:[71]

$$P_{cb} = \frac{[(C_t - C_f) * 100]}{C_t} \quad (12)$$

Where,

$P_{cb}$  = Percentage binding capacity [%]

$C_f$  = Free chloride content [% cm]

$C_t$  = Total chloride content [% cm]

Table 5-23: DCL1, 2, and 3 Chloride binding capacity when cured at NC, AC, NC=AC and exposed to high concentration of NaCl solution

Mix	Curing Condition	Linear Relationship	Correlation Coefficient (R)	Percentage Chloride Binding Capacity ( $P_{cb}$ )
<b>0.6M NaCl Solution</b>				
<b>DCL1</b>	NC	$C_f = 0.2405C_t$	0.973	75.95%
	AC	$C_f = 0.5145C_t$	0.995	48.55%
	NC=AC	$C_f = 0.3833C_t$	0.998	61.67%
<b>DCL2</b>	NC	$C_f = 0.3656C_t$	0.947	63.47%
	AC	$C_f = 0.4616C_t$	0.984	53.84%
	NC=AC	$C_f = 0.3180C_t$	0.900	68.20%
<b>DCL3</b>	NC	$C_f = 0.2792C_t$	0.837	72.08%
	AC	$C_f = 0.4688C_t$	0.994	53.12%
	NC=AC	$C_f = 0.4401C_t$	0.853	55.99%
<b>2.8M NaCl Solution</b>				
<b>DCL1</b>	NC	$C_f = 0.3767C_t$	0.734	62.33%
	AC	$C_f = 0.6527C_t$	0.987	34.73%
	NC=AC	$C_f = 0.4854C_t$	0.996	51.46%
<b>DCL2</b>	NC	$C_f = 0.4642C_t$	0.988	53.58%
	AC	$C_f = 0.5269C_t$	0.900	47.31%
	NC=AC	$C_f = 0.4874C_t$	0.854	51.26%
<b>DCL3</b>	NC	$C_f = 0.4077C_t$	0.947	59.23%
	AC	$C_f = 0.4740C_t$	0.905	52.60%
	NC=AC	$C_f = 0.6009C_t$	0.958	39.91%

The chloride binding capacity determined for these specimens is presented on Table 5-23. As seen on Figure 5-25, when the specimens were cured at accelerated conditions and immersed in 3% and 16.5% NaCl solutions, the binding capacity of the specimens was lower than when cured

in the other regimes for these three mixes. Also, the highest percentage of chloride binding capacity was obtained on DCL1 when it was cured at NC and immersed in 3% NaCl with a value of 75.95%.

These results confirmed what previous research reported; for instance, Sumaranwanich and Tangtermsirikul affirmed that the chloride binding capacity of cement-fly ash cementitious was dependent on the curing and the chloride exposure periods [88].

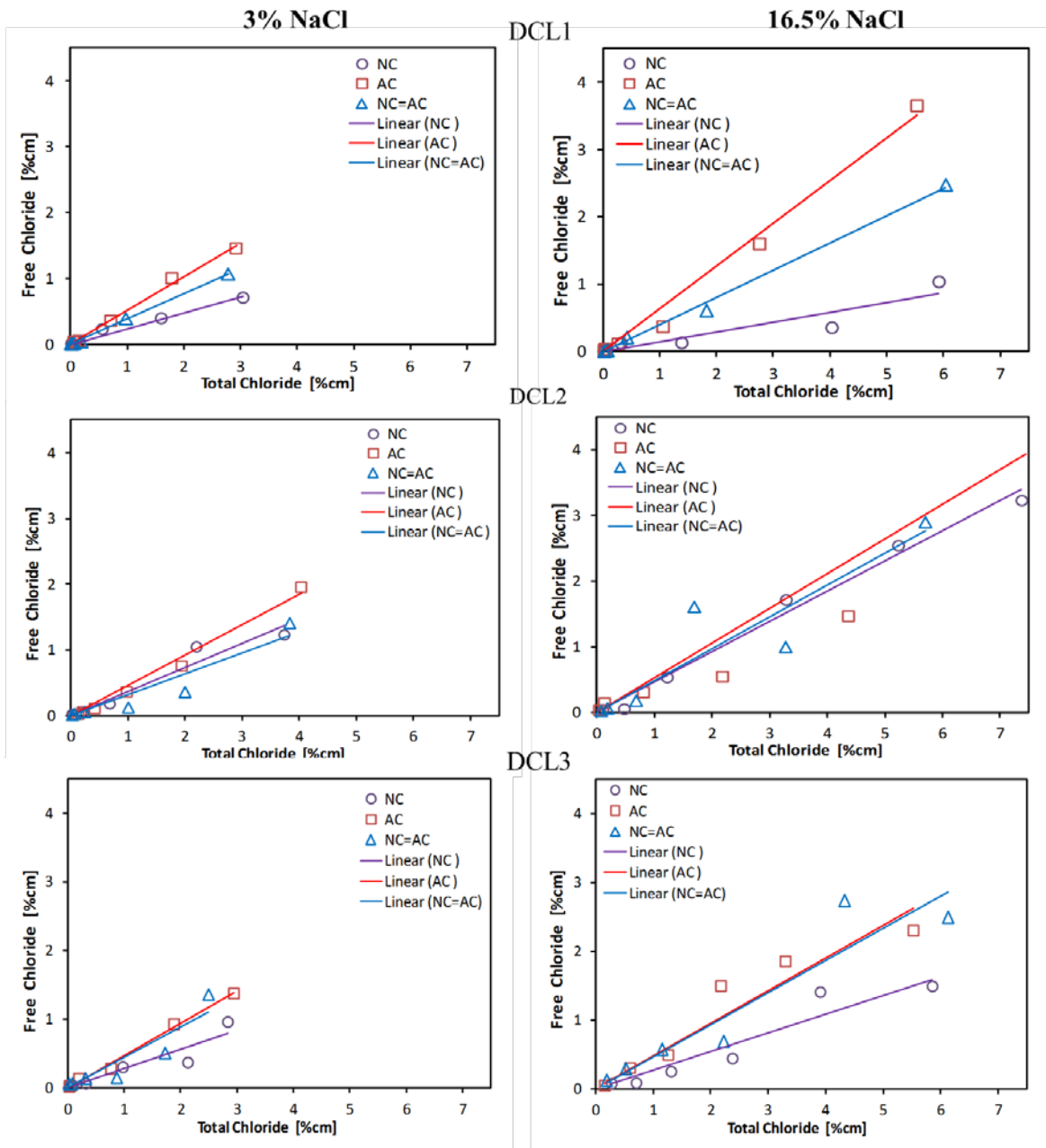


Figure 5-25: Relationship between free and total chloride content of DCL1, 2, and 3

Note that as proposed by Mohammed and Hamada, the bound chloride content can be also calculated by subtracting the free chloride content from both sides of the linear equations (i.e.,  $C_t - C_f$ ) [70].

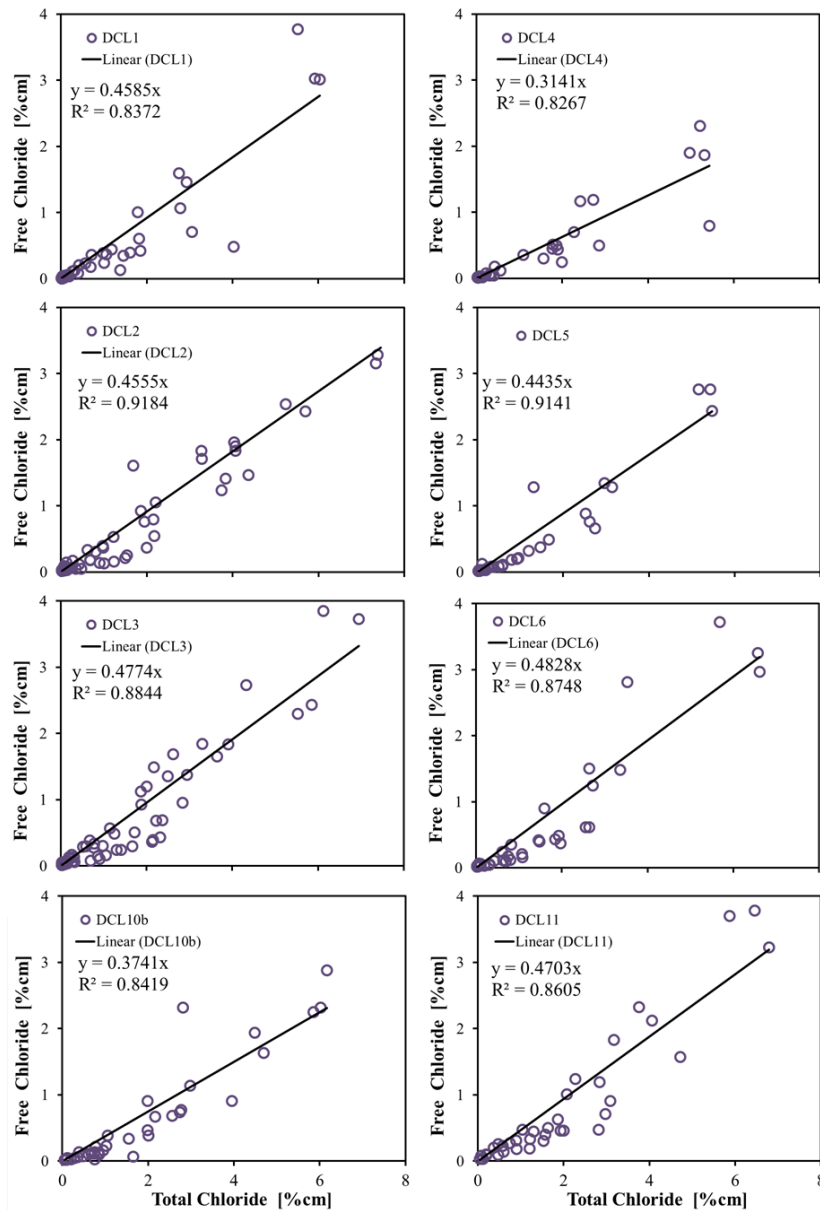


Figure 5-26: DCL1, DCL2, DCI3, DCL4, DCL5, DCL6, DCL10b, and DCL11 Relationship between free and total chloride content

Also, when analyzing effect of the sodium chloride concentration solutions on the amount of bound chloride content, it had been found that the bound chloride concentration increased with the chloride ion concentration of the solution [89, 90]. However, this relationship was not observed during this study; for example, DCL1 had a chloride binding capacity of 76% and 63% when exposed to 3% and 16.5% NaCl solutions, respectively.

Figure 5-26 represents the linear relationship between free and total chloride concentrations of DCL1, DCL2, DCL3, DCL4, DCL5, DCL6, DCL10b, and DCL11 (DCL7, DCL8, DCL9, and DCL10a can be found in Appendix M). The data plotted corresponds to the chloride analyses done when the specimens were cured at 14RT/77ET/RT and exposed to 0.1M NaCl solution for 400 days, as well as when they were cured at NC, AC, and NC=AC and exposed to both 3% and 16.5% NaCl solutions for one year.

As reported on other research and as seen on Table 5-25, having larger amounts of FA in the concrete composition appeared to modestly increase the  $P_{cb}$  values [71]. For example, DCL2 with a composition of 78 kg/m<sup>3</sup> of FA had a binding capacity of 54.45% while DCL11 with a composition of 56 kg/m<sup>3</sup> FA had a binding capacity of 52.97%; both of these mixes had a w/cm ratio of 0.41. However, DCL10b with a composition of 70 kg/m<sup>3</sup> of FA had a binding capacity of 62.59%. In addition, the presence of silica fume in concrete mixes has been related to the reduction on the bound chloride content even in mixes with a low w/cm ratio [90]; however, this was not seen in the case of DCL4 (with a composition of 20%FA+8%SF) that had a binding capacity of 68.5% which is higher than 54.1 % binding capacity found on DCL1 (with a composition of 20%FA). Also, as presented on *A Model for Predicting Time-Dependent Chloride Binding Capacity of Cement-Fly Ash Cementitious System*, the physically bound and total chloride content increases as the w/cm ratio decreases [80]. When considering the effect of the water to cementitious ratio on the percentage chloride binding capacity, it can be seen that the  $P_{cb}$  did not have a significant variation between the three different w/cm ratios investigated. This was also previously found in a study where  $P_{cb}$  of different concrete mixes exposed for over seven years was determined [71].

Table 5-24: Chloride binding capacity for all DCL mixes

Mix	Linear Relationship	Correlation Coefficient (R)	Percentage Chloride Binding Capacity ( $P_{cb}$ )
DCL1	$C_f=0.4585C_t$	0.8372	54.15%
DCL2	$C_f=0.4555C_t$	0.9184	54.45%
DCL3	$C_f=0.4474C_t$	0.8844	52.26%
DCL4	$C_f=0.3141C_t$	0.8267	68.59%
DCL5	$C_f=0.4435C_t$	0.9141	55.65%
DCL6	$C_f=0.4828C_t$	0.8748	51.72%
DCL7	$C_f=0.2818C_t$	0.9077	71.82%
DCL8	$C_f=0.3142C_t$	0.8184	68.58%
DCL9	$C_f=0.3733C_t$	0.8116	62.67%
DCL10b	$C_f=0.3741C_t$	0.8419	62.59%
DCL11	$C_f=0.4703C_t$	0.8605	52.97%

## 5.9 Correlation between Apparent Diffusivity and Equivalent Resistivity

The equivalent resistivity can be determined by integrating the measured resistivity values between the initial resistivity and final resistivity values to find the area under the curve and applying equation 13 (see Figure 5-27 after [91]). In this study the inverse of the measured resistivity values for each mixture were used to obtain the equivalent resistivity values. The resistivity values were measured as the concrete aged on companion cylinders for all of the DCL mixes on specimens cured at RT and 14RT/14ET/RT. The resistivity values corresponded to the exposure ages in 0.1M NaCl, as well as, when cured at NC, AC, and NC=AC immersed in 3% and 16.5% NaCl. Refer to Appendix N to see the equivalent resistivity values for each mix. Some specimens were cured for more than 700 days (14RT/77ET/RT) before performing bulk diffusion. For these specimens the resistivity measured just before starting the bulk diffusion test was assumed to be representative of the equivalent resistivity. The resistivity changes at a very slow rate past 700 days (see 1/resistivity vs. time plots in Appendix I)

$$\rho_{equivalent} = \frac{S}{t_f - t_i} \quad (13)$$

Where,

$\rho_{equivalent}$  = equivalent resistivity [kohm·cm],

$t_f$  = final time [days],

$t_i$  = initial time [days],

$S$  = area under the curve [cm<sup>2</sup>]

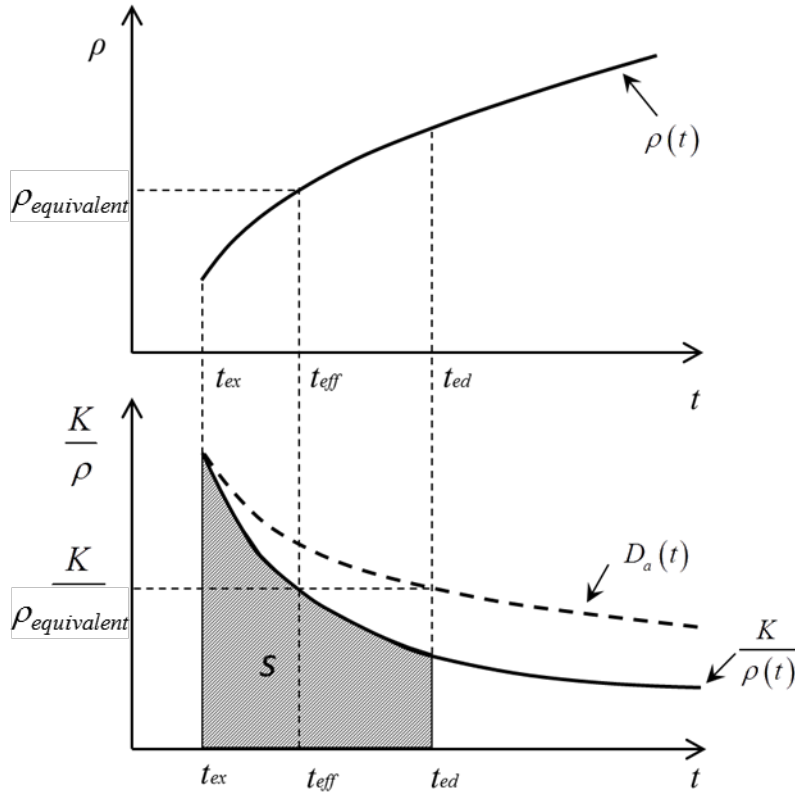


Figure 5-27: Equivalent resistivity curve [91]

The top plot on Figure 5-28 illustrates the correlation found between  $D_{app}$  and equivalent resistivity for all of the mixes cured at the conditions described above. The bottom plot shows the range of the resistivity values measured from the initial to the final time having as a reference the calculated equivalent resistivity values. The initial and final resistivity measured values are indicated by the error bars. In general, there was a large variation of the initial and final resistivity values on the calculated equivalent resistivity values for the different cases investigated. Also, as seen on the bottom plot, for most cases the calculated  $\rho_{equivalent}$  values seemed to be closer to the measured  $\rho_{final}$  than to the initial values. The range was also smaller for those that were cured longer (i.e., started with larger  $\rho_{initial}$ ). Symbols shown with no range correspond to cylinders cured for more than 700 days before the bulk diffusion started.

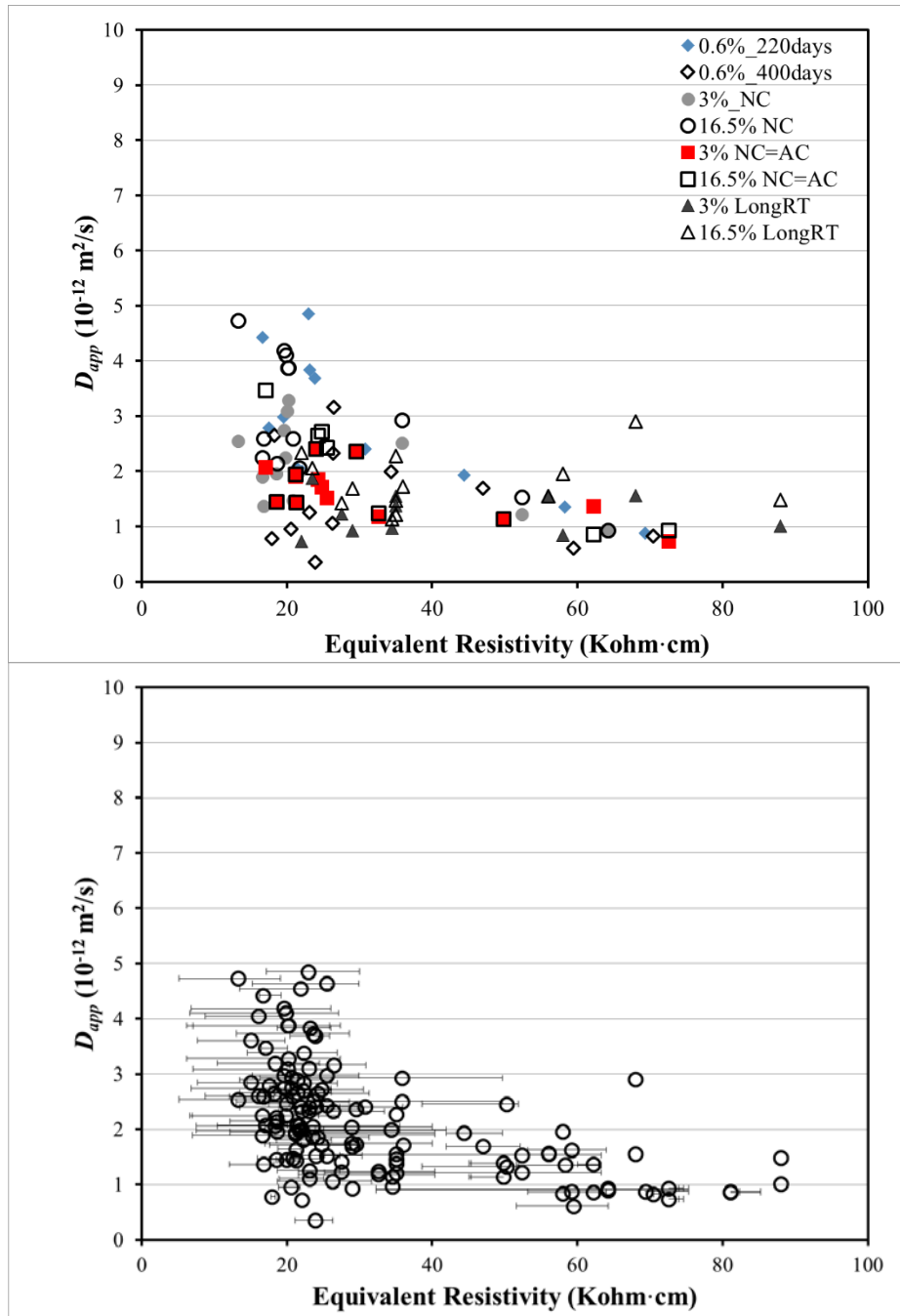


Figure 5-28: Correlation of apparent diffusivity and equivalent resistivity

Figure 5-29 presents the individual plots for each curing condition considered when analyzing the correlation between  $D_{app}$  and  $\rho_{equivalent}$ . For instance, the specimens cured at NC and immersed in 16.5% NaCl solution, mostly reached higher  $D_{app}$  calculated values (up to  $5.06 \times 10^{-12} \text{ m}^2/\text{s}$ ) when the equivalent resistivity was lower (about 20 kohm-cm) than the ones cured at other conditions. This behavior was also seen when the specimens were cured at the same curing regime but exposed to 3% NaCl; however, the apparent diffusivity values were slightly lower as the equivalent resistivity value calculated increased. This can be explained by having the

specimens exposed to a lower sodium chloride concentration. Additionally, the mixes cured at RT (NC) and immersed in the lowest NaCl concentration (0.1M) for 220 days had similar correlation between  $D_{app}$  and equivalent resistivity to the ones previously explained.

It is important to note that when the specimens were exposed to longer periods of time, there was more variation on the equivalent resistivity calculated. Furthermore, the chloride concentration solution appeared to play an important role on the  $D_{app}$  as the time increased. When the mixes were exposed for 400 days, the  $D_{app}$  significantly decreased when compared to 220  $D_{app}$  values. Results on Figure 5-29 also indicated that the  $D_{app}$  was reduced by having specimens cured for additional time (e.g., NC=AC and LongRT), since, as explained in a previous research, additional hydration takes place on specimens cured longer [86].

Figure 5-30 shows the  $D_{app}$  vs. equivalent resistivity with the values grouped by mix and type of cementitious material. For example, as seen on the DCL4, DCL5, and DCL6 plot, there was an effect of the water to cementitious ratio on the correlation between  $D_{app}$  and  $\rho_{equivalent}$ . In fact, as the w/cm ratio decreased, the  $D_{app}$  values also decreased and  $\rho_{equivalent}$  increased (this was not as obvious for the other two groups). The cause for this might be that there is more porosity on the concrete with higher w/cm ratio causing an increment on  $D_{app}$ .

Table 5-25: Correlation between apparent diffusivity and equivalent resistivity

Cases Investigated	K ( $10^{-2}$ kohm·m <sup>3</sup> /s)	Person Coefficient (R)
All	52.3	0.49
20%FA (DCL1, 2, and 3)	48.7	0.70
20%FA+8%SF (DCL4, 5, and 6)	81.2	0.61
50% Slag (DCL7, 8, and 9)	37.2	0.29
RT180_400 in 0.6%	36.7	0.00
NC in 3%	42.1	0.00
NC=AC in 3%	41.1	0.00
Long RT in 3%	38.5	0.00
NC in 16.5%	60.5	0.59
NC=AC in 16.5%	50.3	0.65
Long RT in 16.5%	56.6	0.00

Table 5-25 represents the values calculated for the K constant by using the Nernst Einstein Equation to fit the values described above. The specimens with 20% FA+ 8% SF had the highest K value (81.2); on the other hand, specimens with 50% Slag had the lowest K value (37.2). Also, the correlation between  $D_{app}$  and  $\rho_{equivalent}$  was represented by the correlation coefficient (R) and as seen on Table 5-25. It was high for specimens with silica fume and fly ash. Also, when the specimens were exposed to 16.5% NaCl and cured NC and NC=AC the correlation was 0.59 and 0.65, respectively. The correlation coefficient was not determined for the other cases (i.e., R=0).

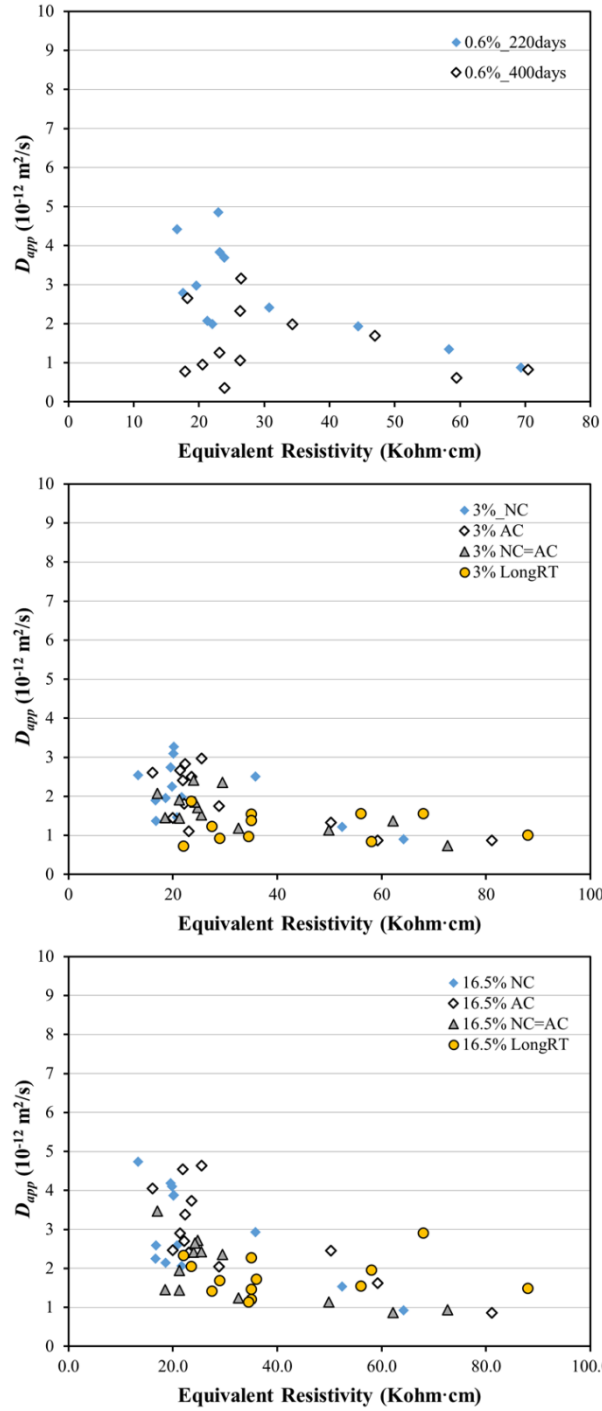


Figure 5-29: Correlation between  $D_{app}$  and equivalent resistivity for specimens exposed to different curing conditions

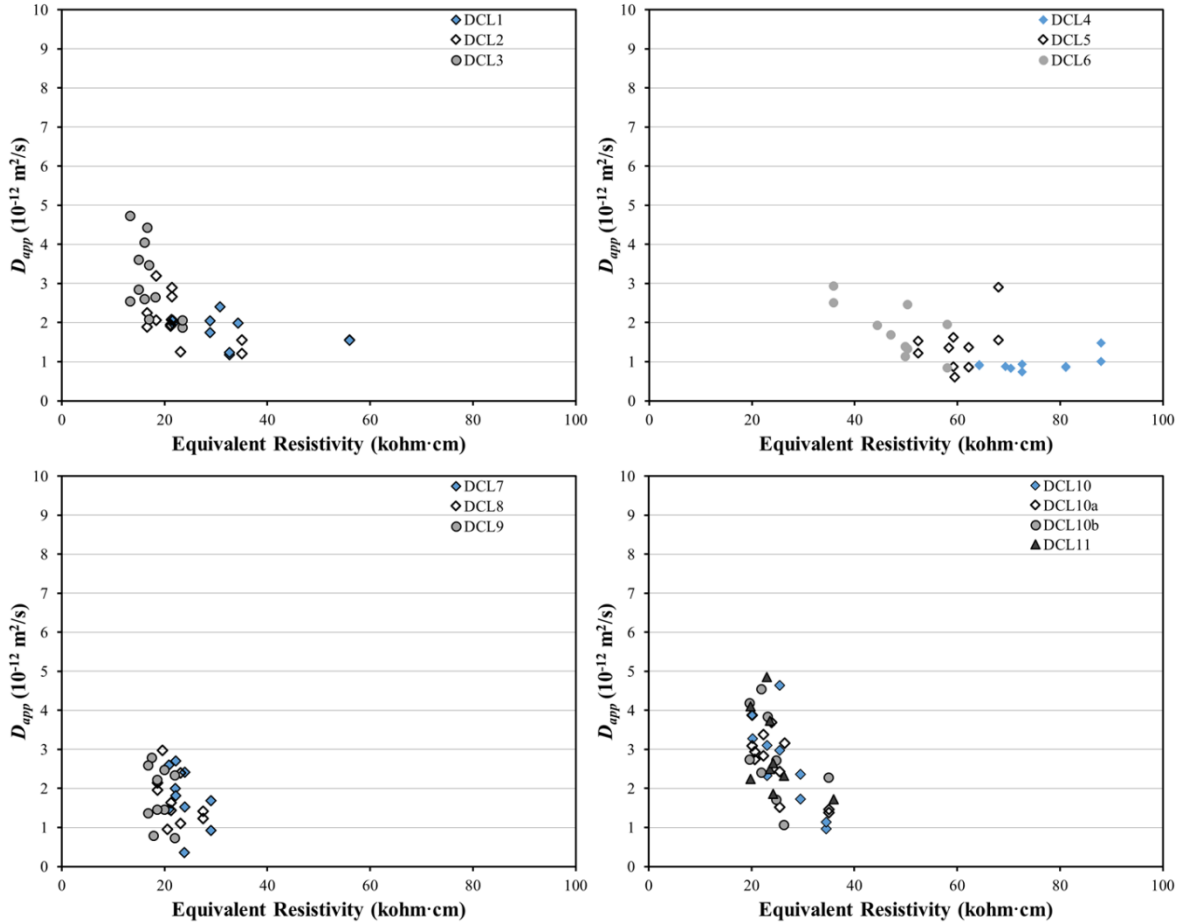


Figure 5-30: Correlation between  $D_{app}$  and equivalent resistivity (specimens grouped by mix)

### 5.10 $D_{app}$ of Specimens Exposed to 70%, 80%, 90%, and 100% Saturation Degree

The fit to each profile produces  $D_{app}$  and  $C_s$  values.  $D_{app}$  is the calculated apparent diffusion coefficient value over the exposure period [18]. A better fitting was obtained (i.e., better  $R^2$ ) for most profiles by removing the chloride concentration measured for the first layer. Figures 5-31, 5-32 and 5-33 show the fitted  $D_{app}$  values obtained after removing the 1st layer. The x-axis displays the target degree of water saturation and the y-axis displays the calculated  $D_{app}$  values.

Figure 5-31 shows  $D_{app}$  chloride coefficients of DCL2 with different degrees of water saturation and two different curing regimes. It can be observed that the chloride diffusivities of concrete sections A are generally lower than those for concrete sections B and C for a given curing regime and degree of water saturation. The  $D_{app}$  value of DCL2-Im-RT with cover concrete is slightly less than that of DCL2-BD-RT (100% degree of water saturation - immersion); however, the ages and exposure duration might have affected the measured  $D_{app}$ . Almost occluded is the  $D_{app}$  value obtained for section A with mortar at 100% SD and was slightly larger than the  $D_{app}$  value BD-RT. For DCL2 cured at 14RT/28ET/RT, the  $D_{app}$  value of section A hardly changed when the SD varied from 70% to 80%. A gradual increase in the  $D_{app}$  value is observed when the degree of water saturation (SD) is increased from 80% to 90%.

A similar trend is also observed on sections B and C, but a greater increase in  $D_{app}$  values is observed from 80% SD to 90% SD. For DCL2 cured at RT, the  $D_{app}$  value of section A gradually increased as the SD went from 80% to 100%. Comparable  $D_{app}$  values were observed for both 80% SD and 70% SD. The  $D_{app}$  value of section C-RT increased when SD increased from 70% to 80% and shows a  $D_{app}$  value plateau when the SD ranged from 80% to 90%; however, it increased significantly when SD increased to 100%. The  $D_{app}$  value measured on section B (RT) is influenced greatly by the SD when SD increased from 70% to 90%.

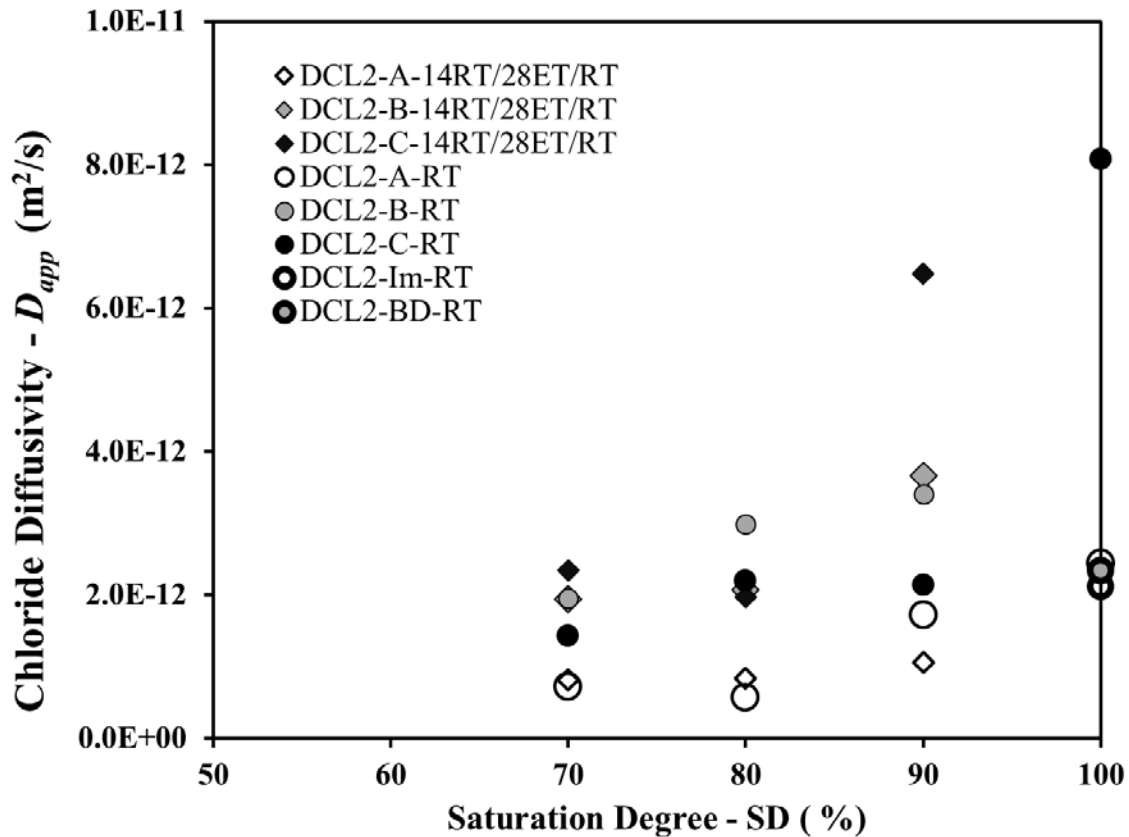


Figure 5-31: Chloride diffusivity of DCL2 specimens vs. SD

Figure 5-32 shows the  $D_{app}$  values of DCL1, DCL2 and DCL3 cured in RT and exposed under different degrees of water saturation. Similar to the results described above, the  $D_{app}$  values of concrete sections A are generally lower than those in concrete sections B and C for a given curing regime and given degree of water saturation. Except for 100% SD, when the trend was reversed for DCL1 and DCL3. (However, if the mortar layer is removed the  $D_{app}$  is larger. The next section discusses  $D_{app}$  of specimens with mortar vs.  $D_{app}$  of specimens with mortar removed.) The w/cm ratio has a modest effect on the chloride diffusivity in the present study. The  $D_{app}$  value of DCL1-A at 100% SD is greater than the  $D_{app}$  values of both DCL2-A and DCL3-A at 100% SD. The  $D_{app}$  value of DCL1-A at 90% SD is lower than the  $D_{app}$  values of

DCL2-A at 90% SD. Furthermore, at 80% SD, the  $D_{app}$  value of DCL1-B is also less than that of DCL2-B.

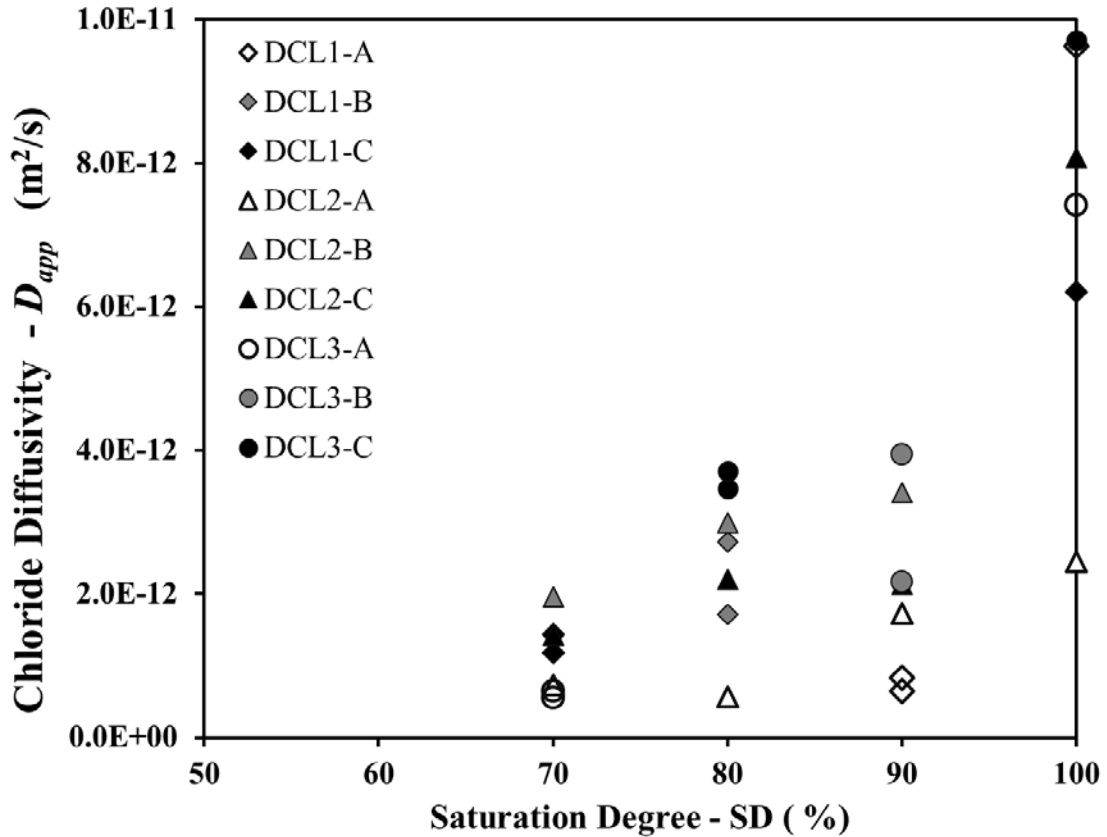


Figure 5-32: Chloride diffusivity of DCL1, DCL2, DCL3 specimens cured in RT vs. SD

Figure 5-33 shows the chloride coefficients of DCL2, DCL10b and DCL11 cured in RT for the different degrees of water saturation. Once more, the  $D_{app}$  values of concrete sections A are generally lower than the  $D_{app}$  values in concrete sections B and C for a given curing regime and given degree of water saturation. It is observed that  $D_{app}$  values ( $1.34 \times 10^{-12} m^2/s$  and  $1.11 \times 10^{-12} m^2/s$ ) of DCL10b-A are higher than the  $D_{app}$  value ( $0.56 \times 10^{-12} m^2/s$ ) for DCL2-A at 80% degree of water saturation. It is also seen that the  $D_{app}$  value ( $2.94 \times 10^{-12} m^2/s$ ) of DCL11-C is higher than the  $D_{app}$  value ( $1.43 \times 10^{-12} m^2/s$ ) for DCL2-C at 70% degree of water saturation. The cause for this observation could be associated with the different cementitious content. Somewhat similar results can also be obtained by comparing the  $D_{app}$  value of DCL2-C with that of DCL11-C at 70% degree of water saturation. However, when comparing the  $D_{app}$  value of DCL11-A ( $8.58 \times 10^{-13} m^2/s$ ) with the  $D_{app}$  value for DCL2-A ( $1.72 \times 10^{-12} m^2/s$ ) at 90% degree of water saturation, the latter is larger than the former which is different from that described above. It is also observed that the  $D_{app}$  value of both DCL11-A ( $4.18 \times 10^{-12} m^2/s$ ) and DCL10b-A ( $2.4 \times 10^{-12} m^2/s$ ) are larger than the  $D_{app}$  of DCL2-A ( $1.08 \times 10^{-12} m^2/s$ ) at 100% SD. A similar trend was observed when comparing the  $D_{app}$  for sections C and 100% SD, but the values were higher. Therefore, the effect of cementitious amount on the chloride diffusivity is complicated for a given degree of water saturation and it should be further investigated.

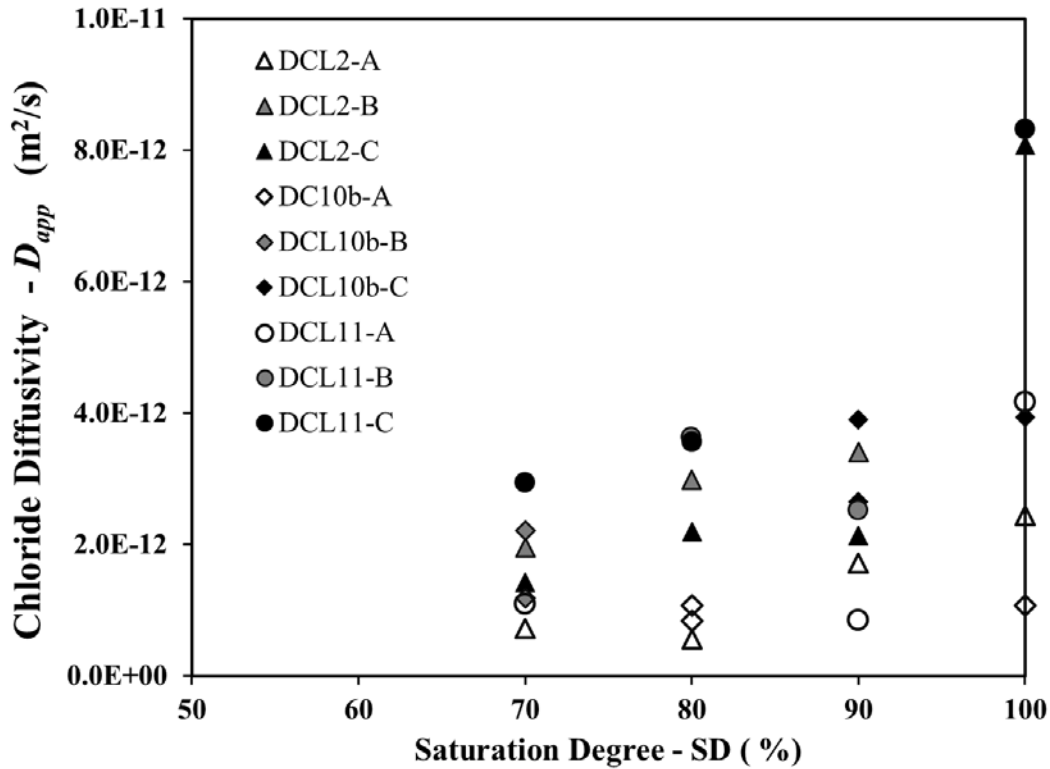


Figure 5-33: Chloride diffusivity of DCL2, DCL10b, DCL11 cured in RT vs. SD

Olsoon and co-authors [92] recently proposed a model that predicts  $D_{app}$  as SD is increased based on conductivity measurements. The model was based on measurements on ordinary Portland cement mortars and the degree of hydration of the binder was assumed to be 70% (0.38 w/cm) and 90% (0.53 w/cm). The  $D_{app}$  values were found to double when the SD increased from 72% to 91%. Guimaraes and co-authors[64] reported that the  $D_{app}$  values of concrete mixes with a content of 12% fly ash increased when the SD is increased and the  $D_{app}$  values of some mixes increased only slightly or reached a plateau in a range of SD between 75% and 100% on mortars and concretes with high w/cm ratios.

### 5.10.1 Effect of Mortar Layer on $D_{app}$ for Sections Exposed in 100% SD

Table 5-26 shows the  $D_{app}$  values calculated with all layers and with the concentration closest to the surface removed (1 layer removed). In most instances, the  $D_{app}$  values increased once the first layer was removed, and the calculated  $C_S$  decreased.

The table also shows the values for a given section A or D with mortar and with the mortar layer removed. The  $D_{app}$  value was usually smaller for those with the mortar layer. Figure 5-34 shows a bar plot of the  $D_{app}$  values calculated with 1 layer removed (see right column in Table 5-26). Figure 5-32 shows the chloride diffusivities of DCL1, DCL2, DCL3, DCL10b and DCL11 cured in RT and exposed at 100% degree of water saturation, comparing the  $D_{app}$  values under

conditions of exposed surface with mortar layers and without mortar layers. In general, the chloride diffusivity of concrete portions with mortar layers are generally lower than those without mortar layers.

Table 5-26: Apparent diffusivity for specimens exposed to 100% SD

	$D_{app}$ ( $10^{-12}$ m <sup>2</sup> /s)	
	All Layers	1 Layer Removed
DC1-25A-M(1-6)	0.84	9.63
DC1-25A-X(1-6)	3.70	5.89
DC1-25-C(1-6)	3.00	6.21
DC1-25D-M(1-6)	0.46	2.21
DC1-25D-X(1-6)	2.95	5.38
DC2-25A-M(1-6)	0.43	2.45
DC2-25A-X(1-6)	2.67	8.41
DC2-28D-M(1-6)	0.93	3.07
DC2-28D-X(1-6)	5.49	8.08
DC3-25A-M(1-6)	3.23	7.41
DC3-25A-X(1-6)	1.45	6.60
DC3-25-C(1-6)	7.63	9.72
DC3-25D-M(1-6)	1.85	3.86
DC3-25D-X(1-6)	7.34	19.46
DC10b-25A-M(1-6)	0.29	1.08
DC10b-25A-X(1-6)	5.58	8.69
DC10b-25-C(1-6)	3.50	3.94
DC10b-25D-M(1-6)	1.22	1.86
DC10b-25D-X(1-6)	5.69	6.83
DC11-25A-M(1-6)	1.53	4.18
DC11-25A-X(1-6)	11.32	16.69
DC11-25-C(1-6)	6.06	8.33
DC11-25D-M(1-6)	2.88	7.35
DC11-25D-X(1-6)	6.36	9.88

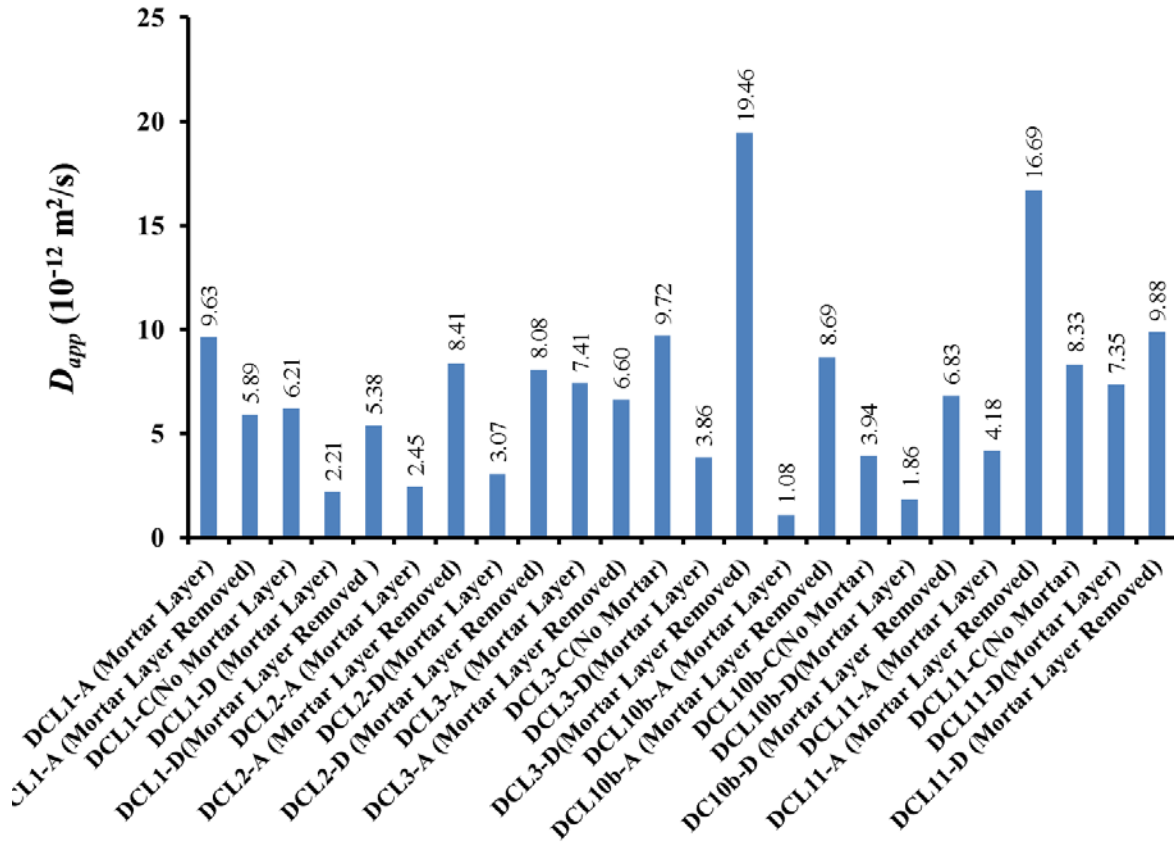


Figure 5-34:  $D_{app}$  for specimens in 100% SD during exposure

### 5.11 $D_{app}$ for Specimen Exposure Outdoors to Marine Atmosphere

Figure 5-35 shows the calculated  $D_{app}$  values vs.  $\text{time}^{0.5}$  grouped per mixture type for DCL1, DCL2, DCL3, DCL4, DCL5 and DCL6 for specimens exposed at the three locations. Recall that –a indicates those specimens exposed next to the fence, –b are specimens exposed at the west site and –e indicate specimens exposed at the east site (115 m from the ocean). DCL2 and DCL3 experienced a monotonic decrease in the  $D_{app}$  values with time as it is usually reported for specimens with fly ash; however, this trend was not obvious for specimens from DCL1 group which had the lowest w/cm ratio. The  $D_{app}$  values for specimens exposed on the east site with mixtures with fly ash and silica fume (DCL4, DCL5 and DCL6) show the expected decay. This trend was not as steep for those exposed at the west site. For some of the  $D_{app}$  calculations it was necessary to remove the first layer to achieve a good fit, but for most, this was not necessary, suggesting that diffusion is likely the predominant transport mode. As these specimens are exposed outdoors, the concrete is not saturated and the moisture content closer to the exposed surface will likely experience greater moisture transients. Wet during rain events or during the early mornings if the dew is significantly high; on the other hand, during the dry season this region likely is drier. These events might explain some of the variations in  $D_{app}$  vs. time.

The  $D_{app}$  values shown in this section were significantly smaller than those reported under 70% or 80% SD (on specimens with 20% FA, i.e., DCL1, DCL2, DCL3, DCL10a, DC10b and

DCL11). The smaller  $D_{app}$  values observed under controlled moisture conditions were for DCL2-A (i.e., mold face)  $0.7 \times 10^{-12} \text{ m}^2/\text{s}$  and  $0.5 \times 10^{-12} \text{ m}^2/\text{s}$  for 70% and 80% SD. One possible explanation is that the chloride concentration is significantly different (a slow build up for those under the marine atmosphere), and another is that the mold face was the side exposed for all specimens subjected to the marine atmosphere. Moreover, the test durations were significantly longer for those under marine atmospheric exposure. Appendix O shows typical environmental conditions as a function of time for relative humidity, temperature, precipitation, predominant wind direction (from the weather station at the Ft. Lauderdale, Florida, airport).

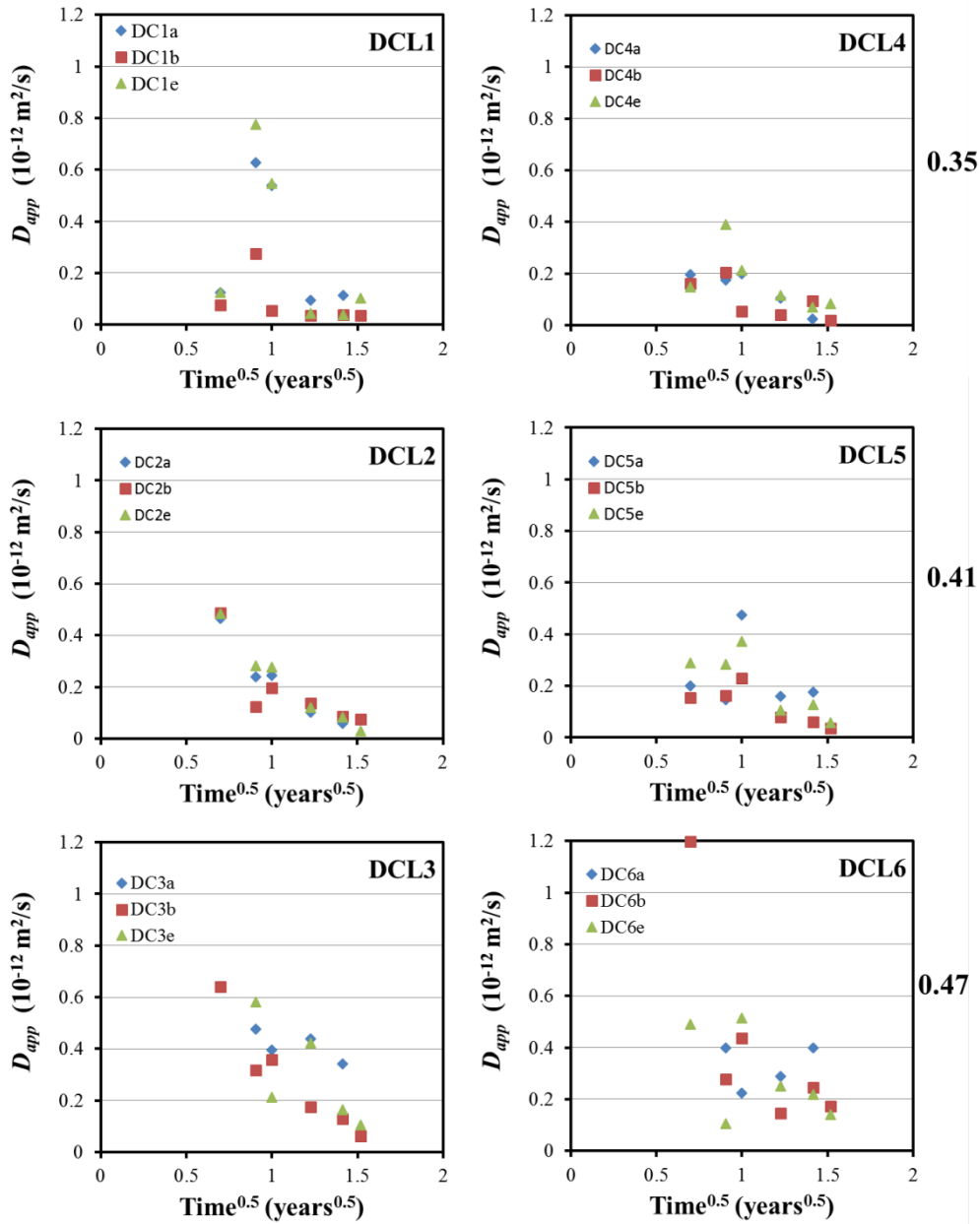


Figure 5-35:  $D_{app}$  vs. time marine atmosphere exposure (DCL1 to DCL6)

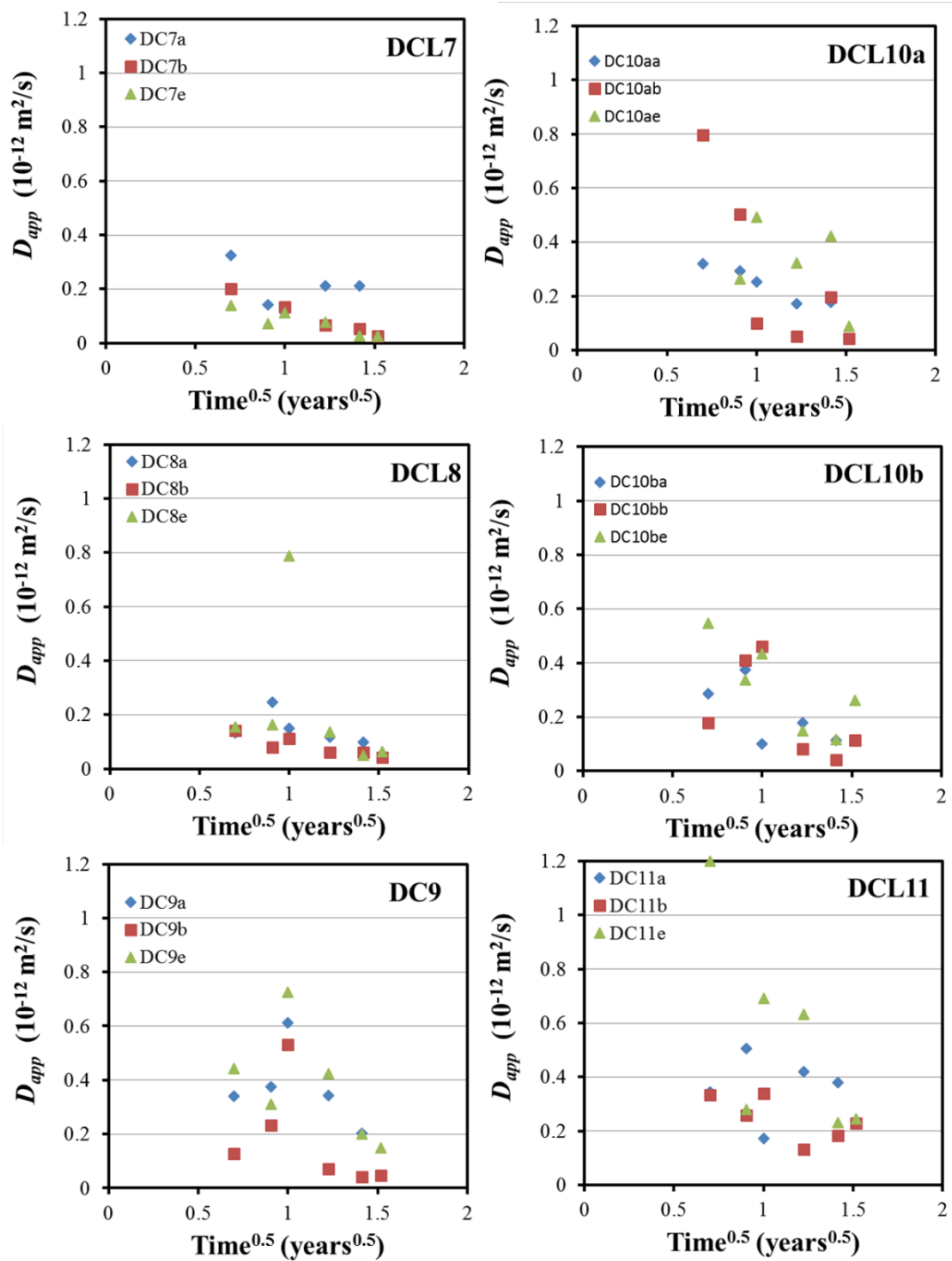


Figure 5-36:  $D_{app}$  vs. time marine atmosphere exposure (DCL7 to DCL11)

Figure 5.36 shows the  $D_{app}$  vs. time for specimens of mixtures DCL7 to DCL11. DCL7, DCL8 and DCL9 contain 50% slag as cementitious material. The magnitude of  $D_{app}$  was small from the beginning on specimens DCL7 and CL8 regardless of where the specimens were located during the outdoor atmospheric exposure. The DCL10a, DCL10b and DCL11 contain 20% fly ash with

a w/cm of 0.41, but a lower cementitious content than DCL2. The  $D_{app}$  for these specimens appear to follow a reduction in  $D_{app}$  value for each location with time, but with different reduction rates. Also, there was significantly more scatter on the calculated  $D_{app}$  values for these three mixtures.

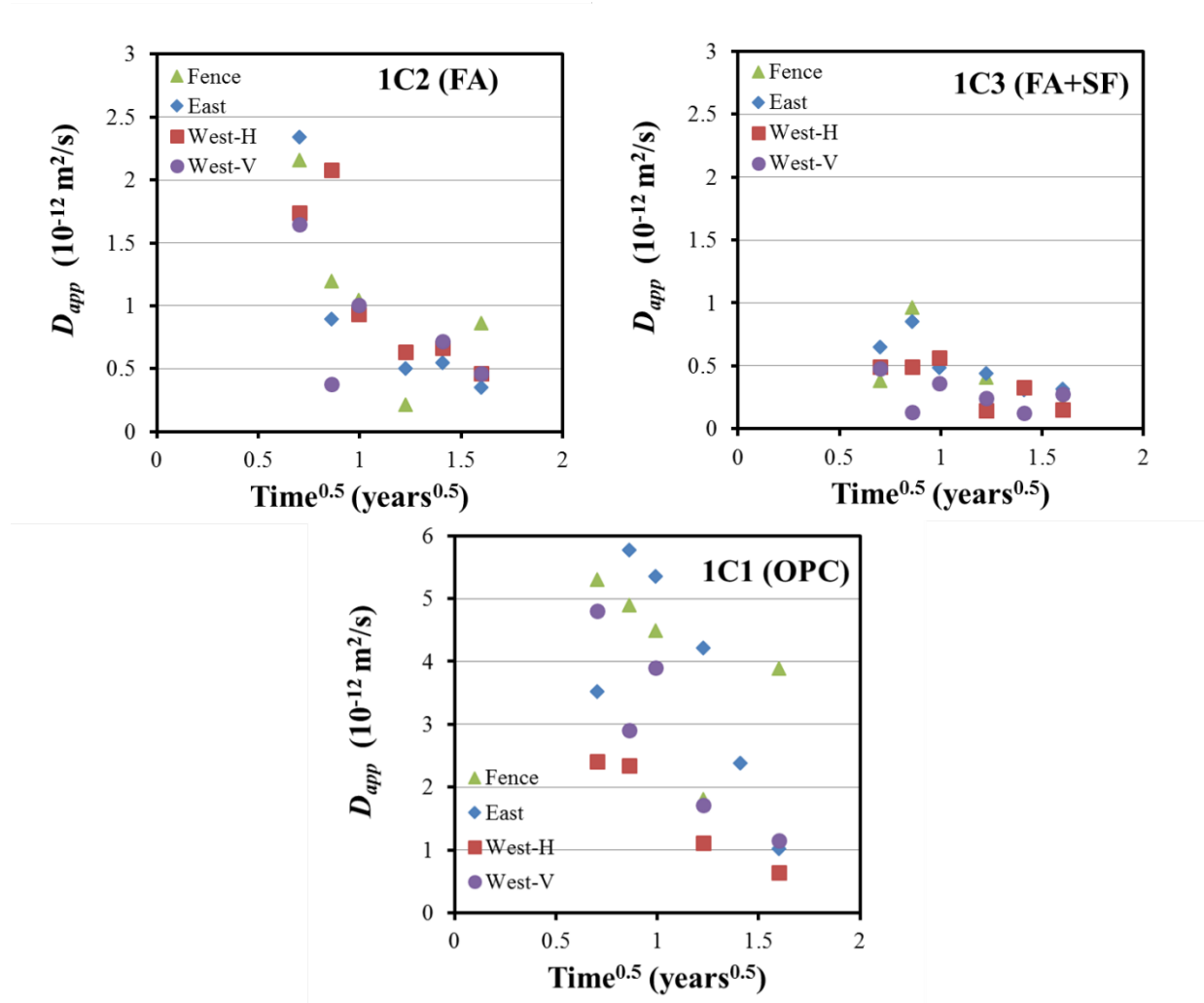


Figure 5-37:  $D_{app}$  vs. time marine atmosphere exposure (1C1, 1C2, and 1C3)

Figure 5-37 shows the  $D_{app}$  vs. time for specimens of mixes 1C1, 1C2, and 1C3. These specimens were exposed at the three outdoor locations, but those on the west site were exposed both horizontally and vertically. Larger  $D_{app}$  values were observed on 1C1 specimens oriented vertically than were on those oriented horizontally. Note the larger magnitude of the  $D_{app}$  values (i.e., different y-axis scale) on the plots shown in Figure 5-37. These larger  $D_{app}$  values might be in part be due to the fact that the surface exposed did not have the mortar layer and that the coarse aggregate size was smaller on 1C specimens.  $D_{app}$  values for 1C2 and 1C3 can be compared with  $D_{app}$  values for DCL2 and DCL5, respectively. The  $D_{app}$  values for 1C2 and 1C3 were larger than those observed on DCL2 and DCL5, respectively.

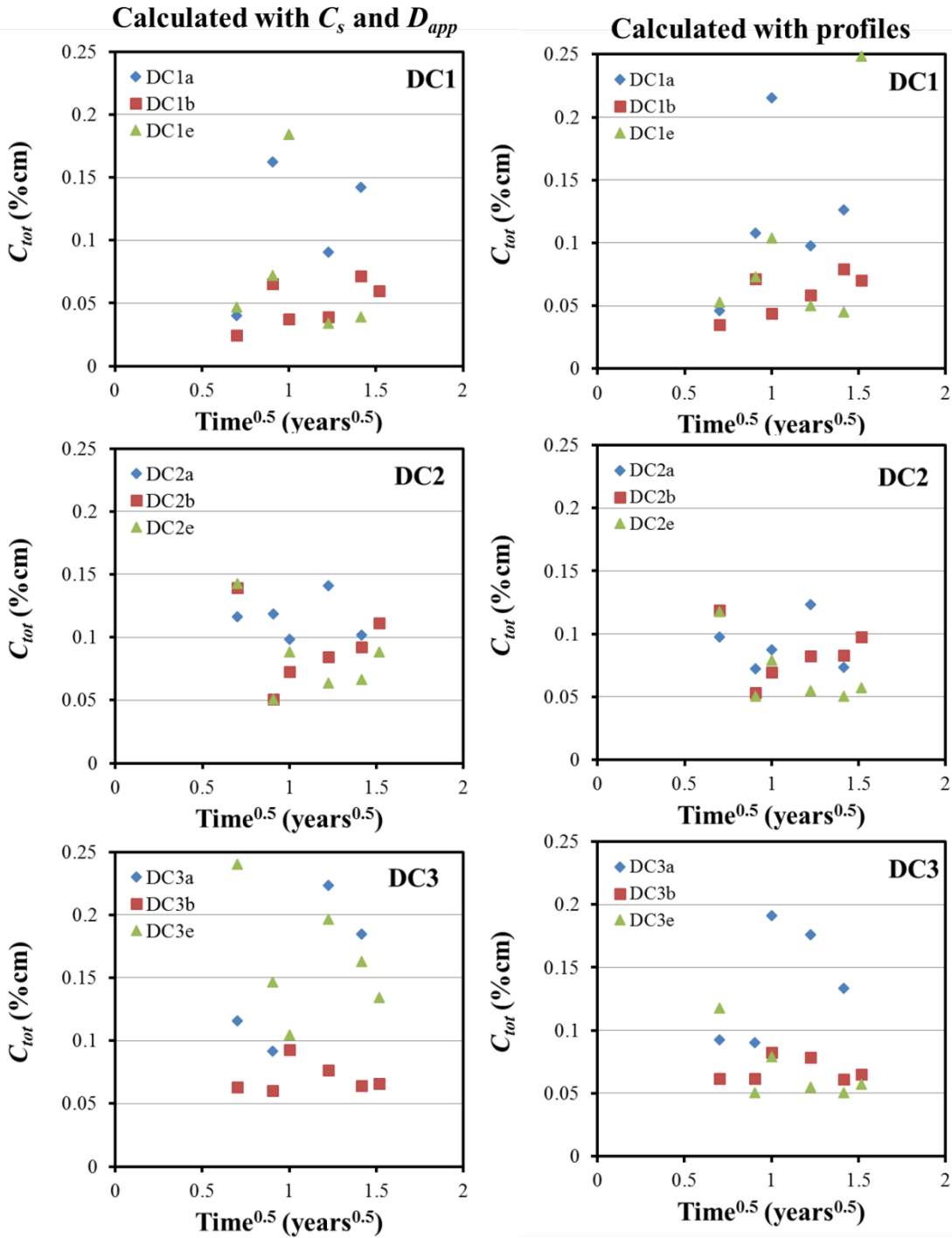


Figure 5-38:  $C_{tot}$  vs. time for specimens with 20%FA (DCL1, DCL2 and DCL3)

### $C_{tot}$ vs. time

The amount of chlorides that penetrated the concrete specimens exposed to the marine atmosphere over a given exposure time (named in here  $C_{tot}$ ) was calculated in two different ways: a) integrating the area under the curve using the calculated  $D_{app}$  and  $C_s$ , and b) by

integrating the measured profiles (i.e., the sum of the measured concentration multiplied by the thickness of the corresponding layer). Since the chloride did not penetrate to a significant depth, in most instances, the values were similar. Most of the fits were performed assuming that the initial concentration in the concrete was nil, but in some cases a small concentration was assumed ( $\sim 0.026\%$  cm). Figure 5-38 shows the  $C_{tot}$  values vs. time at the different location for mixtures DCL1, DCL2 and DCL3. On the left, are the  $C_{tot}$  values obtained using the calculated  $D_{app}$  and  $C_S$  values, and on the right, using the measured profiles. When comparing  $C_{tot}$  vs. time for a given site location, in general, the  $C_{tot}$  values are larger for those with higher  $w/cm$ .

On DC1 and DCL3 there is a spike on the  $C_{tot}$  values observed after ten and 12 months of exposure. It is believed that this sudden increase in  $C_{tot}$  value is in part due to a tropical storm that took place late October 2012. Figure 5-39 shows a picture with the specimens located next to the fence. The picture shows the specimens partially flooded due to a combination of storm surge and high tide. These spikes are more pronounced on –a specimens (fence location), but it also appeared on some of the specimens located on the east site (not related to the flooding, but higher winds during the week of the storm). It is also believed that rain events periodically washed-out some of the chlorides because the  $C_{tot}$  returned to lower values subsequently.

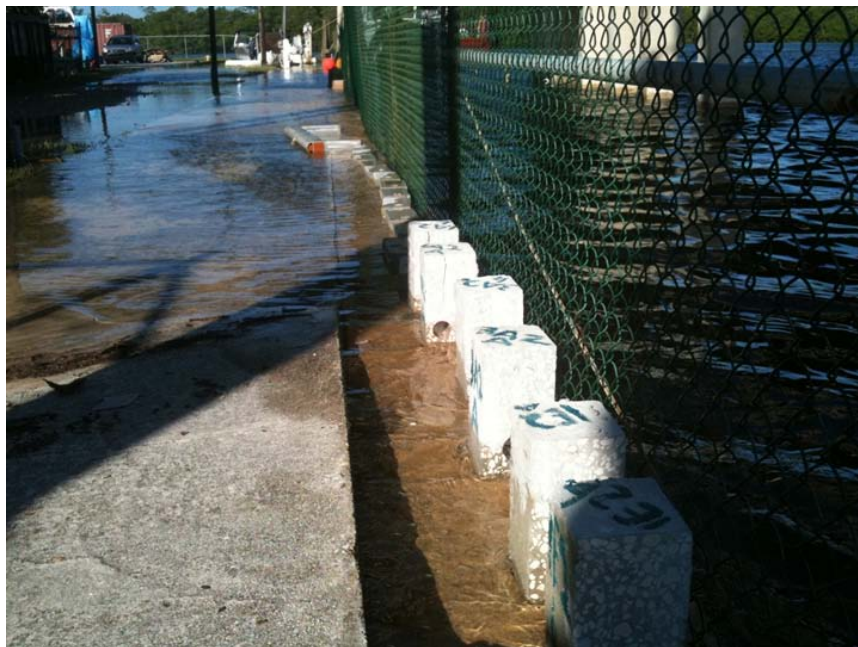


Figure 5-39: Storm surge during high tide at fence site (Fall 2012)

Figure 5-40 shows the  $C_{tot}$  values (using method b) vs. time for specimens of mixtures DCL4, DCL5, DCL6, DCL7, DCL8 and DCL9. After the six-month exposure, the  $C_{tot}$  only increased moderately as time passed, indicating that for concrete with either slag (DCL7 to DCL9) or with fly ash and silica fume (DCL4 to DCL6), the  $k_t$  values that would be fitted would be very small if the  $C_{tot}$  obtained after six months were subtracted. In general, specimens located next to the fence showed the higher  $C_{tot}$  values. A spike in the calculated  $C_{tot}$  value was observed for some mixtures after ten and 12 months of exposure and might be influenced by the event described above; in addition, the higher chloride deposited due to faster winds during the summer/fall

seasons. For specimens located at the east and west sites, most  $C_{tot}$  values were below 0.1 %cm, and for some mixes the  $C_{tot}$  values remained around 0.05 %cm. Similar trends can be observed on Figure 5-41. This figure shows the  $C_{tot}$  values (using method b) vs. time for specimens of mixtures DCL10, DCL10a, DCL10b, and DCL11.

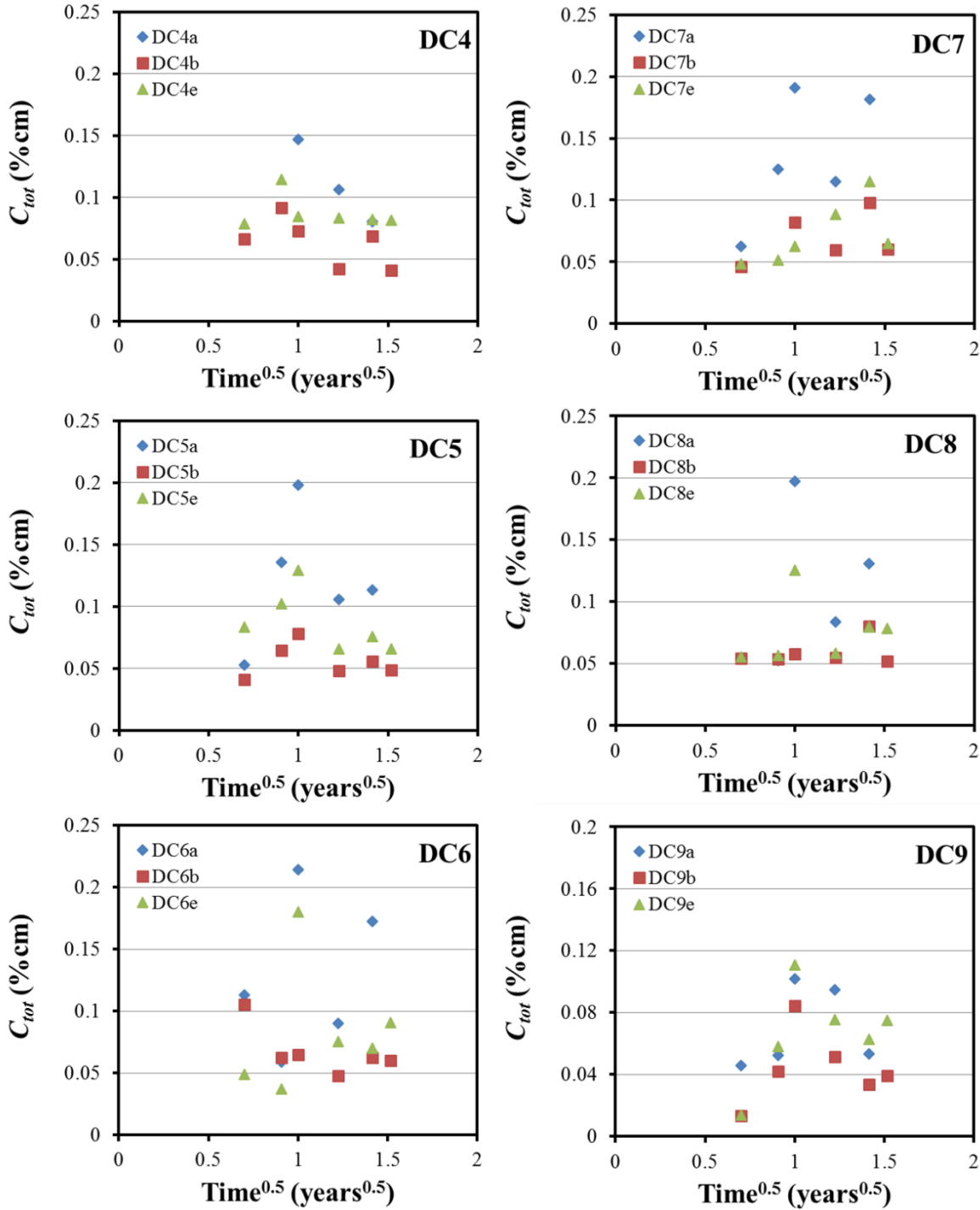


Figure 5-40:  $C_{tot}$  values vs. time for DCL4 to DCL9

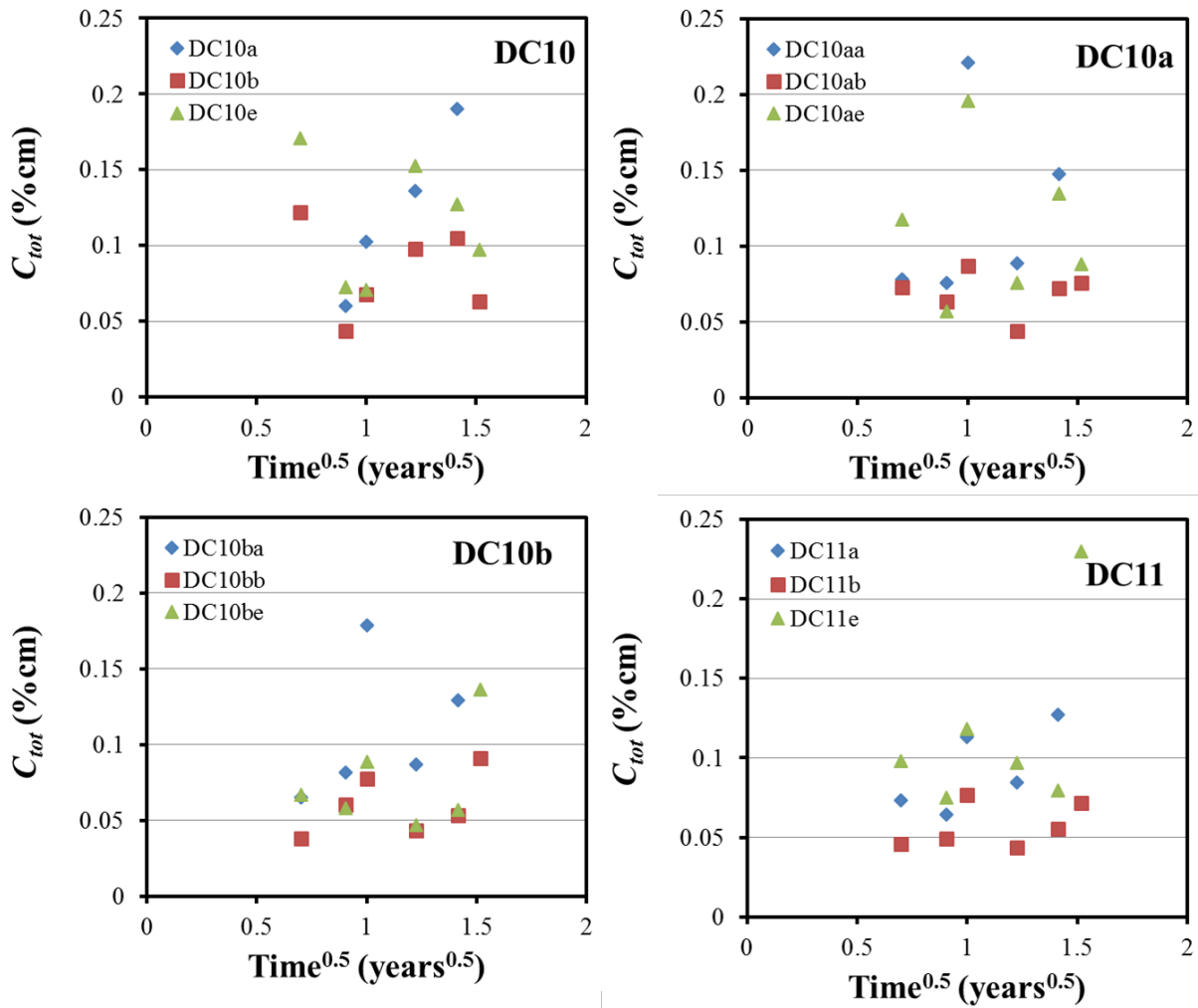


Figure 5-41:  $C_{tot}$  values vs. time for DCL10, 10a, 10b, and DCL11

Figure 5-42 show the  $C_{tot}$  values (using method b) vs. time for specimens of mixtures 1C1 (OPC), 1C2 (FA) and 1C3 (FA+SF). At the west site, the specimens were exposed with both horizontal and vertical orientation. It is apparent that those facing skyward (horizontal) had higher  $C_{tot}$  values, regardless of the duration of the exposure period. For these samples, those exposed next to the fence were also exposed vertically. Almost twice as many chlorides penetrated these specimens when compared to similar mixes of DCL mixes (1C2 vs. DCL2 and 1C3 vs. DCL5).

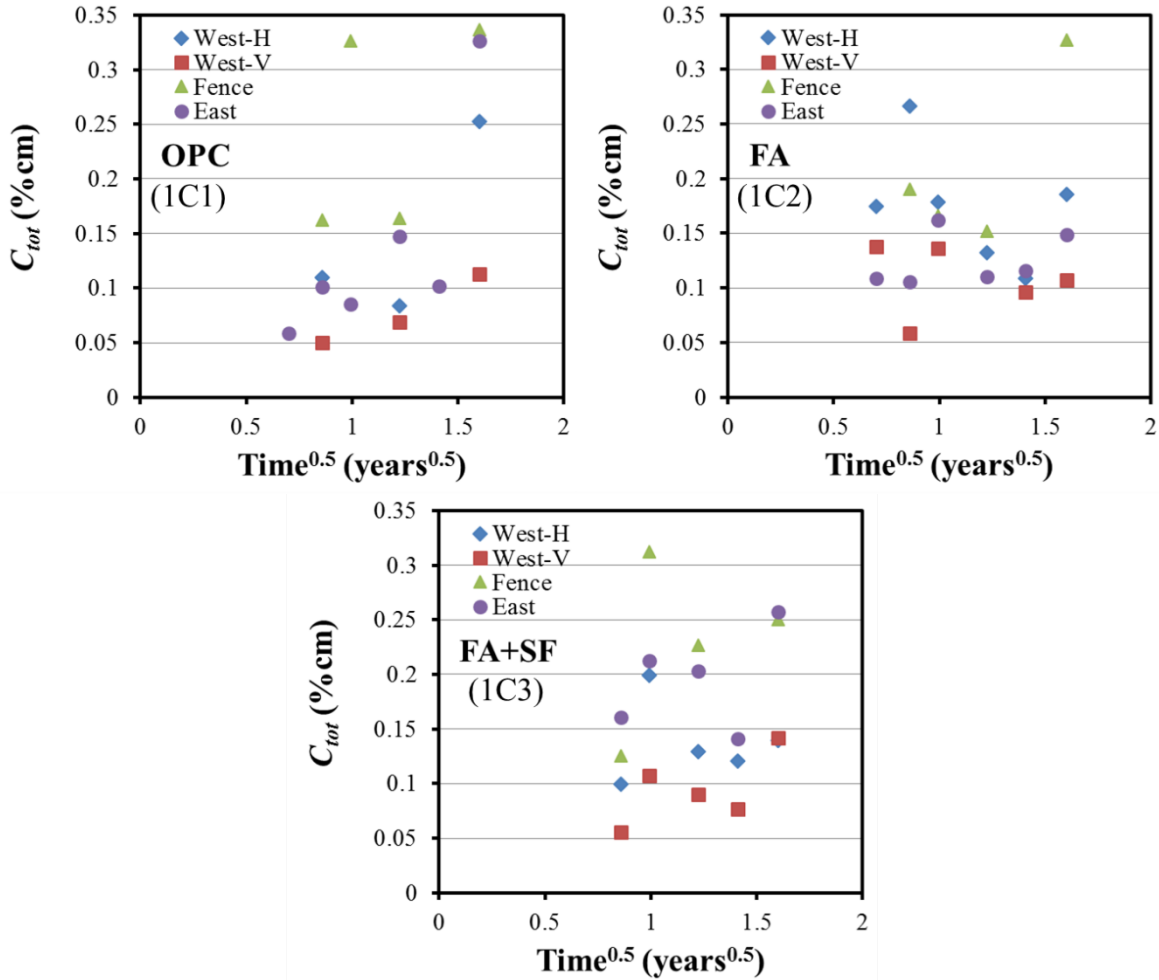


Figure 5-42:  $C_{tot}$  values vs. time calculated for 1C1, 1C2, and 1C3 (older specimens)

Table 5-27 shows  $k_t$  values calculated for specimens of 1C1, 1C2, 1C3 mixtures and Table 5-28 shows the  $k_t$  values calculated for DCL specimens. The  $k_t$  values are calculated by assuming that at time zero  $C_{tot}$  was zero, i.e., initial concentration  $C_0=0$ . A linear relationship ( $C_{tot}$  vs.  $\text{time}^{0.5}$ ) is assumed, using the relationship that Meira proposed,  $C_{tot} = C_0 + k_t \cdot \sqrt{t}$ . As it can be observed on Figure 5-38, 5-40, 5-41 and 5-42 and briefly described above, a linear fit is not always good for all cases, due to the  $C_{tot}$  values plateau observed after longer exposure periods. Nevertheless, the  $k_t$  values allow us to compare the rate of chloride penetration for the different exposure sites and mix compositions. 1C type of specimens are exposed at the west site both horizontally and vertically; the  $k_t$  values for those specimens oriented horizontally are larger (up to twice as much) as that observed on those exposed vertically.

Table 5-27:  $k_t$  values calculated for specimens with 1C1, 1C2, 1C3 mixtures

	Fence	East	West-H	West-V
1C1(OPC)	0.208	0.128	0.125	0.064
1C2 (FA)	0.179	0.138	0.105	0.087
1C3 (FA+SF)	0.189	0.156	0.107	0.077

Table 5-28:  $k_t$  values calculated for DCL specimens

	100 m East	200 m West	200 m Fence
DCL1	0.088	0.052	0.111
DCL2	0.054	0.070	0.082
DCL3	0.054	0.057	0.127
DCL4	0.072	0.051	0.119
DCL5	0.070	0.046	0.112
DCL6	0.071	0.054	0.121
DCL7	0.071	0.087	0.128
DCL8	0.064	0.050	0.098
DCL9	0.058	0.037	0.064
DCL10a	0.092	0.058	0.114
DCL10b	0.066	0.053	0.101
DCL11	0.084	0.048	0.087
Average	0.070	0.055	0.105

Table 5-29:  $k_t$  values reported by Meira[41]

	10 m	100 m	200 m
C3	0.103	0.061	0.017
C6	0.120	0.051	0.008

Table 5-29 shows the  $k_t$  values reported by Meira[41] for mixtures with the closest w/cm to those investigated in here (i.e., in Meira's study, 0.5 w/cm, and those of DCL3, DCL6 and DCL9 with 0.47 w/cm). The  $k_t$  values reported by Meira for specimens at 10 m from the sea ranged between 0.103 and 0.120; in this study,  $k_t$  values for specimens next to the fence range between 0.127 and 0.121 for DCL3 and DCL6 respectively, suggesting that some of the spray particles originated from the intracoastal water, and not only from the sea.  $k_t$  values for specimens at the east site (115 m) can be compared with  $k_t$  values for specimens at 100 m from the sea [41]; the  $k_t$  values are 0.054 (DCL3) and 0.071 (DCL6), whereas for C3 and C6 specimens, the  $k_t$  values ranged between 0.051 and 0.061, i.e., the  $k_t$  values are similar. The  $k_t$  values for specimens at the west site (200 m from the sea) for DCL specimens range between 0.054 and 0.057 and are significantly larger than the 0.017 and 0.008 reported by Meira. The larger  $k_t$  values for specimens of DCL group are also influenced by the larger average wind velocity at Dania Beach.

The  $k_t$  values for DCL specimens that would be associated with those with a steeper slope were close to 0.13 and these larger values corresponded to specimens at the fence site. Moreover, the larger  $k_t$  values ranged between 0.05 and 0.10, and the smaller ones ranged between 0.035 and

0.05. The smallest  $k_t$  value reported by Meira was 0.05 at 100 m and 0.008 at 200 m for a concrete with 0.5 w/cm ratio.

### Relationship between $C_{tot}$ and $D_{ac}$

The relationship between the total amount of chlorides that accumulated into the concrete after a given exposure time ( $C_{tot}$ ) and the total chloride deposited ( $D_{ac}$ ) over the same period (in  $\text{g/m}^2$ ) from the marine aerosols on the wet candles are discussed in this section. The accumulated deposition ( $D_{ac}$ ) over a given exposure period is the sum of the monthly chloride depositions from the wet candles that correspond to each sample during the coinciding exposure periods. (See Table 4-30 for  $D_{ac}$  values) The plots in Figure 5-43 present the typical relationship observed between the amount of chlorides that potentially could be deposited onto the concrete and the amount that actually penetrated and accumulated in each concrete specimen.

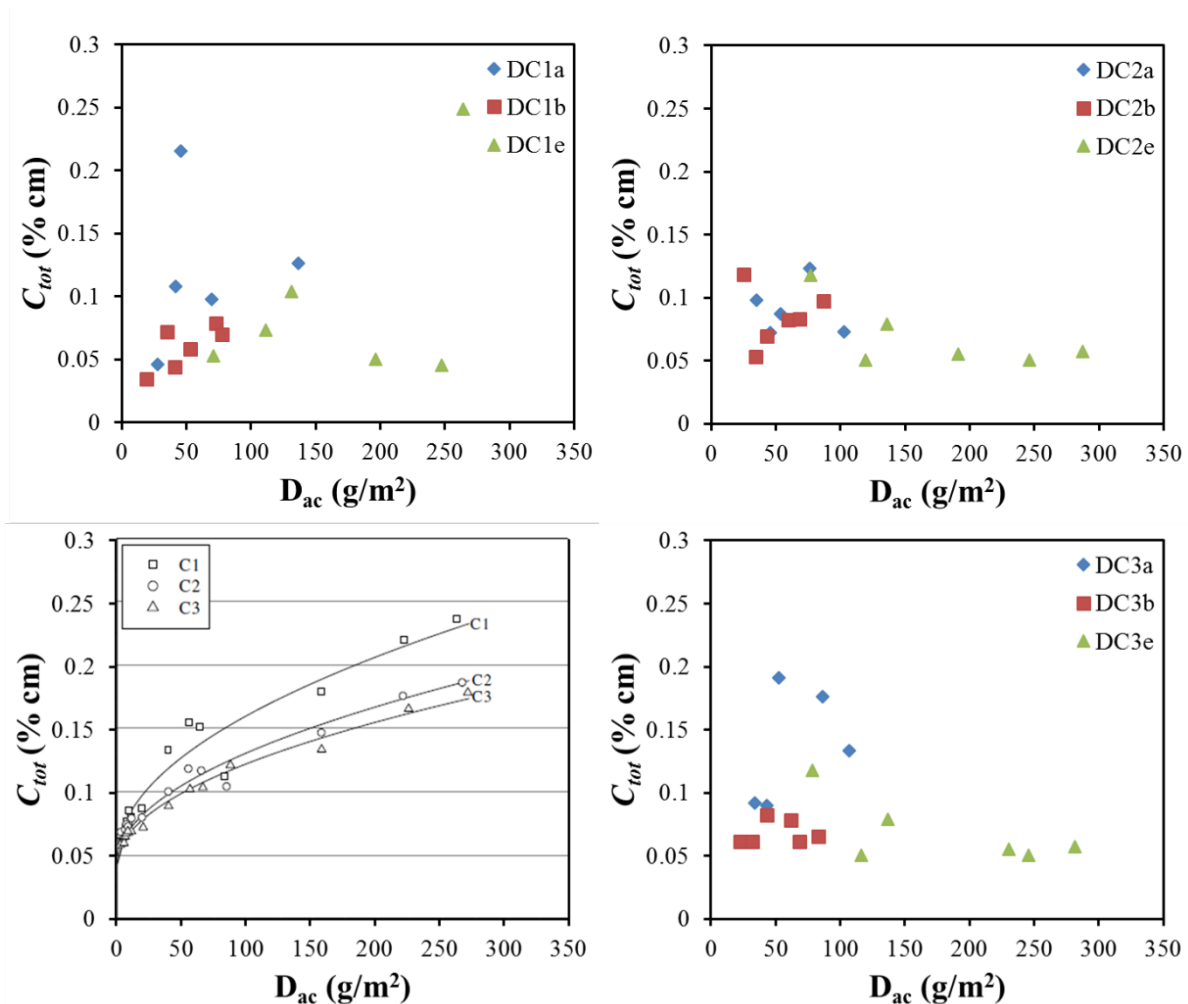


Figure 5-43:  $C_{tot}$  vs.  $D_{ac}$  for DCL1, DCL2, and DCL3 and C1, C2, C3 [41]

Specimens exposed on the east site (DCL1e, DCL2e, DCL3e) that had  $D_{ac}$  values greater than  $150 \text{ g/m}^2$  did not have  $C_{tot}$  values as large as those observed on C1, C2 and C3 specimens from

Meira's study; and the difference is likely due to the location of the two type of specimens. Those from the Meira study were 10 m from the sea, whereas DCL1e, DCL2e and DCL3e were located at 100 m from the sea. It should also be noted that the nonlinear relationship showed a decreasing rate of change in the accumulated chloride content into the concrete as the total chloride deposited into the wet candles increased. This could be indicative of the fact that the chloride penetration into the concrete slows as the accumulated chloride deposition increases, but it is also influenced by the distance from the sea. The fact that rate decreased, as the chloride accumulation increased, could be a result of a minimizing difference in the chloride concentration gradient; therefore, slowing down the rate of apparent diffusivity as shown above.

Meira also proposed a relation between  $C_{tot}$  vs.  $D_{ac}$  (obtained from the wet candles),  $C_{tot} = C_0 + k_d \cdot \sqrt{D_{ac}}$ . The  $k_d$  value represents the rate of chloride deposition as an environmental indicator. In a similar manner in which  $k_t$  values are calculated with respect to time<sup>0.5</sup>, the  $k_d$  value represents the slope of the line when plotted vs.  $D_{ac}^{0.5}$ . The  $k_d$  values might be a useful variable in selecting an optimal concrete design based on the chloride deposition from the marine atmosphere. The  $k_d$  values are calculated using the  $C_{tot}$  results discussed in the previous section vs. the corresponding  $D_{ac}^{0.5}$  values. Note: Similar to what was done when calculating  $k_t$  values,  $C_0$  was also assumed to be equal to zero. The  $k_d$  values are thought to suggest a representation of the rate of chloride accumulation in the concrete as per the amount of chlorides deposited from the marine aerosols over the time period that the samples were exposed to the environment. The results of the calculated  $k_d$  values are shown in Table 5-30.

Table 5-30:  $k_d$  values calculated for DCL and 1C specimens

Cementitious Type	w/cm	Mix	Fence	East	West
20% FA	0.35	<b>DC1</b>	0.0146	0.0050	0.0086
	0.41	<b>DC2</b>	0.0113	0.0048	0.0113
	0.47	<b>DC3</b>	0.0171	0.0047	0.0093
20% FA + 8% SF	0.35	<b>DC4</b>	0.0154	0.0065	0.0086
	0.41	<b>DC5</b>	0.0146	0.0063	0.0078
	0.47	<b>DC6</b>	0.0167	0.0063	0.0090
Slag	0.35	<b>DC7</b>	0.0172	0.0062	0.0148
	0.41	<b>DC8</b>	0.0132	0.0057	0.0083
	0.47	<b>DC9</b>	0.0088	0.0051	0.0063
Average $K_d$ per location			0.0143	0.0056	0.0093
Accumulated Deposition at 28 months (g/m <sup>2</sup> ):			156	276	81

Cementitious type	w/cm	Mix	Fence	East	West-H	West-V
OPC		<b>1C1</b>	0.0267	0.0112	0.0199	0.0102
FA	0.41	<b>1C2</b>	0.0232	0.0093	0.0224	0.0140
FA+SF		<b>1C3</b>	0.0240	0.0138	0.0174	0.0124
Accumulated Deposition at 31 months(g/m <sup>2</sup> ):			174.1	302.5	92.4	92.4

Table 5-31 shows  $k_d$  values reported by Meira for concrete specimens with 0.5 w/cm. The average  $k_d$  value for DCL specimens exposed at the east side is 0.0056, and is smaller than the  $k_d$  value for C6 (0.0069) from Meira's study. On the other had the  $k_d$  value for DCL from specimens at the west (0.0093) and fence site (0.0143). All  $k_d$  values for 1C specimens were larger than 0.01 regardless of location. The maximum  $k_d$  value observed was 0.0267 for 1C1 specimens (OPC mix) located next to the fence, and this  $k_d$  values is almost 4 times that of  $k_d$  value for C6 (OPC mix) from Meira's study.

Table 5-31:  $k_d$  values reported by Meira[41]

Cement type	w/cm	Mix	Overall $k_d$ using 4 locations
25% pozzolan	0.50	<b>C3</b>	0.0080
OPC	0.50	<b>C6</b>	0.0069

Finally, the average chloride deposition at 115 m (east site) was 320 mg/(m<sup>2</sup>day); at the fence, it was 188 mg/(m<sup>2</sup>day), and at the west site (230 m) it was 97 mg/(m<sup>2</sup>day). These average deposition values are larger than those reported by Meira.

Through observations and results obtained by the wet candle, there is strong evidence supporting the claim that wind speed and direction affect the marine aerosols in the marine atmosphere and the amount of chloride particles that could be deposited into the concrete specimens. By referring to the wet candle results in the results section and the historical climatic data provided in appendix O, some inferences can be made.

With respect to relative humidity, the historical data provides a record that the relative humidity for the area at which the testing occurred was between the range of 60 to 80%, which is the range at which capillary sorption and diffusion is most prevalent, as discussed in the literature review. As a result, it is probable that capillary sorption is heavily affected by wetting and drying cycles in the surface layers, and the inner layers are affected through diffusion. This may account for some of the profiles in which the first layer contained fewer chlorides than in the second layer.

By observing the precipitation patterns, the seasons with the highest rainfall generally resulted in lower values of chlorides, which may provide evidence of the washout effect in the concrete profiles. The mean monthly temperatures were also higher than those in the coastal Brazilian region, which could suggest higher rates of diffusion, although the apparent diffusivities were not compared.

## 6 Compilation of Previous Field Visits and New Field Visits

There are several reports of projects sponsored by FDOT in which diffusivity values have been reported, but not all of them are in the same units. In addition, the FDOT state materials office had a number of profiles that have not been previously published.

Table 6-1: List of sites visited by SMO not previously published

Bridge #	In Service date	Visit date	Age at Visit (yr)	Location	Elevation	$D_{app}$ ( $10^{-12} \text{ m}^2/\text{s}$ )	Fitted $C_s$ $\text{kg/m}^3$
30148	7/1/1969	6/2/2004	35	Bent 18 Pile 3 EF	0' AHT	0.26	35.4
100300	7/1/1975	11/2/2005	30	Pile 271-3 North Face 10" from corner	1 AHT	15.10	14.5
105504	7/1/1926	6/23/2009	83	Pier 9 EF	0.5' above marine growth	0.81	15.1
105504	7/1/1926	6/23/2009	83	Pier 6 Cap	7.6' above marine growth	0.07	2.5
120084	7/1/1976	3/26/2001	25	Footer	4' AHT	1.38	2.2
120084	7/1/1976	3/26/2001	25	Footer	6" AHT	1.91	2.3
139003	7/1/1966 7/1/1993 redone	6/10/2009	43	Pile 11-3	2' AHT	0.75	13.4
139003	7/1/1966 7/1/1993 redone	6/10/2009	43	Pile 6-3	2' AHT	3.12	16.2
150189	7/1/1986	7/13/1994	8	Pier 15 Nothbound North Face	3' AHT	0.31	20.8
150189	7/1/1986	7/13/1994	8	Pier 30 South Bound North Face North of channel	3' above high tide	0.31	23.1
150189	7/1/1986	7/13/1994	8	Pier 30 South Bound North Face North of channel	1' above high tide	1.13	18.6
150189	7/1/1986	7/13/1994	8	Pier 1 North North Face	6'10" above high tide	0.41	35.4
150189	7/1/1986	2/2/1997	11	Pier 117-2	6' above high tide	0.08	24.3
150189	7/1/1986	2/2/1997	11	Pier 106-1	3' above high tide	0.14	25.4
150189	7/1/1986	2/2/1997	11	Pier 116	3' above high tide	0.24	22.2
150189	7/1/1986	4/3/1997	11	Pier 155	18' above high tide	0.06	5.2
150189	7/1/1986	4/3/1997	11	Pier 151	19' Above high tide	0.08	4.9
150189	7/1/1986	4/3/1997	11	Pier 126-1	60' Above high tide	0.05	3.2
159008	7/1/1966 7/1/1993 redone	6/10/2009	16	Pile 2-2	2' AHT	0.60	12.8
340014	7/1/1964	6/14/2003	39	NW BH Pile 1	2' AHT	1.48	12.8
340053	1974	2010	36	bent 15, pile cap	5 foot above the tide	0.91	2.8
340053	1974	2010	36	bent 6, pile cap	5 foot above the tide	0.13	2.7
700081	7/1/1971	7/28/2008	37	Pile 8	6" AHT	2.34	5.3
700174	7/1/1978	6/1/2011	33	footer Pier 20	21" above marine growth	2.49	11.0
700174	7/1/1978	6/1/2011	33	Crash Wall Pier 14	12" above marine growth	4.53	10.4

Table 6.1 Continued

Bridge #	In Service date	Visit date	Age at Visit (yr)	Location	Elevation	$D_{app}$ ( $10^{-12}$ m <sup>2</sup> /s)	Fitted $C_s$ kg/m <sup>3</sup>
700181	1985	2011	26	Crashwall Pier 15	14" above marine growth	0.93	9.6
700181	1985	2011	26	footer Pier 13	19" above marine growth	5.63	10.3
720053	1972	2011	39	Pile 8-2	4' AHT	0.04	0.6
720053	1972	2011	39	Pile 4-8	1' AHT	0.15	10.6
720053	1972	2010	38	Pile 8-4	1' AHT	0.13	7.1
720053	1972	2010	38	Pile 10-2	4' AHT	0.01	1.2
720053	1972	2010	38	at mean high tide	Mean HT	0.33	4.6
720053	1972	2010	38	Pile Crashwall	Mean HT	0.52	7.1
720336	7/1/1967	5/24/2004	37	Bent 9 Pile 6 EF	0' AHT	1.28	23.9
870660	7/1/1929	6/8/2010	81	West Pier NF	36" AHT	3.42	1.6
870660	7/1/1929	6/8/2010	81	East Pier EF	60" AHT	1.60	4.7
870660	7/1/1929	6/8/2010	81	East Pier EF	60" AHT	1.54	2.0
880050	7/1/1967	1/15/2010	43	Pile 3-4	1' AHT	3.65	14.2
880051	7/1/1967	9/29/2009	42	Pile 18-5 EF	1' AHT	0.45	11.0
880051	7/1/1967	1/15/2010	43	Pile 18-5	1' AHT	0.40	11.2
880052	7/1/1967	9/22/2009	42	Pile 4-3 EF	1' AHT	1.07	5.9
900086	7/1/1978	7/29/2003	25	Bent 2 Pile 2 WF	1' AHT	3.50	10.2
900086	7/1/1978	7/29/2003	25	Bent 3 Pile 2 SF	1' AHT	7.38	20.3
900125	7/1/1985	7/29/2003	18	Bent 8 Pile 1 SF	0' AHT	1.12	18.2

Table 6-1 contains the calculated  $D_{app}$  values for those profiles provided by the state materials office that had not been published before. Table 6-1 also contains the bridge number, elevation,  $D_{app}$ , and calculated  $C_s$ . The units of the last two columns are in m<sup>2</sup>/s ( $\times 10^{-12}$ ) and kg/m<sup>3</sup> for  $D_{app}$  and  $C_s$ , respectively. Appendix N contains a table that compiles the  $D_{app}$  values from various previous projects [93-99]. The table includes the bridge number, year of service and year when the visit took place, age at the time of the visit, location if available, elevation either with respect to high tide (ATH) or with respect to the top of the marine growth (MG) in meters, and finally the  $D_{app}$  values in m<sup>2</sup>/s ( $\times 10^{-12}$ ).

Several bridges were selected for an additional visit. In some cases, this was a second visit; whereas, for other bridges, this was a third visit. The bridges were selected from those structures built after 1990 which had been visited at least once before. Cores were also obtained from the Key Royale bridge by coring the fender piles (this bridge contains six different concrete mixtures). The cores were 5 cm nominal diameter. The cores were either milled or sliced. Four cores total from two components were obtained from the Sunshine Skyway bridge from locations at high elevation. Table 6-1 shows the list details of when the cores were obtained and exposure time for fender piles of the Key Royale bridge. A recent report includes additional details [99], in here the  $D_{app}$  vs. elevation for both trips will be discussed and compared with the results from the other visited sites. Table 6-3 shows the details for the bridges visited during fall 2013. This table includes bridge number, bent and pile, the elevation with respect to the marine growth and also the  $D_{app}$  value calculated from the obtained profiles. The observed  $D_{app}$  values were as high as  $4.6 \times 10^{-12}$  m<sup>2</sup>/s and as little as  $0.02 \times 10^{-12}$  m<sup>2</sup>/s.

Table 6-2: Dates at which the fender piles were deployed and cored

	Pile Driven on	Coring 1	Coring 2	Coring 1	Coring 2	Trip1 Label	Trip 2 Label
				Exposure Years	Exposure Years		
OPC	9/7/2006	4/15/2009	4/4/2012	2.61	5.58	45	FP1
FA+UFA	9/7/2006	4/15/2009	12/1/2011	2.61	5.24	44	FP2
FA	9/7/2006	4/15/2009	12/1/2011	2.61	5.24	43	FP3
FA+SF	1/15/2007	4/15/2009	11/30/2011	2.25	4.88	42	FP4
FA+BFS	1/15/2007	4/15/2009	11/30/2011	2.25	4.88	41	FP5
FA+MET	1/15/2007	4/15/2009	11/30/2011	2.25	4.88	40	FP6

Note: OPC top cored on 12/1/2011

Table 6-3: List of bridges visited during 2013 including  $D_{app}$  values

Bridge	Construction Year	Age (years)	Bent	Pile	ID	Elevation from MG (m)	Face	W to A (m)	Core Length [cm]	Resistivity Kohm-cm	Dapp (m <sup>2</sup> /s) ×10 <sup>-12</sup>
150243	2001	12	10	1	A	0.30	W	0.27	5.4	3.3	3.01
			10	1	B	0.86			5.9	8.7	0.46
			10	1	C	1.46			5.6	9.1	1.03
150243	2001	12	8	1	A	0.28	W	0.25	6.5	5.0	4.64
			8	1	B	0.64			5.1	11.0	0.66
			8	1	C	1.24			5.6	10.4	0.39
150243	2001	12	11	2	A	0.25	E	0.18	8.9	3.9	2.79
			11	2	B	1.09			5.4	5.2	
			11	2	C	1.68			5.0	5.1	1.71
700203	1999	14	5	15	A	-0.03	W	0.18	4.9	15.3	0.23
			5	15	B	0.61			5.2	18.2	0.05
			5	15	C	1.52			6.7	20.6	0.03
700203	1999	14	5	14	A	-0.03	E	0.18	8.1	17.7	0.42
			5	14	B	0.61			8.0	12.9	0.03
			5	14	C	1.52			6.3	26.3	0.02
700203	1999	14	4	15	A	-0.03	W	0.18	6.3	18.2	0.12
			4	15	B	0.61			5.4	20.4	0.03
			4	15	C	1.52			6.1	20.2	0.03
890145	2005	8	W	10	A	0.28	S	0.28	6.8	8.9	0.44
890150	2007	6		10	A	0.28	S	0.28	7.3	35.3	0.21
124115	2007	6	B	2	A	-0.05	E	0.25	6.4	5.9	0.83
490003	2003	10	20	T	A	-0.25	N	0.30	5.2	19.0	0.68
			20	T	B	0.56			5.1	23.2	0.34
			20	T	C	1.42			5.6	25.2	0.16
490003	2003	10	36	T	A	-0.22	SE	0.27	4.4	19.7	0.18
			36	T	B	0.61			6.2	34.4	0.15
			36	T	C	1.52			5.5	50.2	0.07
490003	2003	10	60	T	A	-0.38	S	0.33	5.2	18.5	0.43
			60	T	B	0.61			4.5	18.1	0.13
			60	T	C	1.52			3.9	29.2	0.06

## 6.1 Chloride Profiles

Figure 6-1 shows the concentration profiles for the four cores obtained from the Sunshine Skyway bridge during a visit that took place in 2011. The cores corresponding to these profiles were obtained from the trestle cap at elevations of about 8 m AHT at an age of 25 years. Figure 6-2 shows a diagram from where the cores were obtained. Chlorides reached this location due to seawater spray particles or from wash out that might have occurred during rain events from the road or from the passing vehicles. Three of the profiles show skin effect (i.e., lower concentration on the first two/three layers than the maximum concentration of the profile; these layers were removed to obtain the calculated  $D_{app}$  value).

The chloride profiles for bridges visited during 2013 where cores were obtained only at a low elevation are shown in Figure 6-3. Figure 6-4 shows the chloride profiles obtained for the three testing piles cored at the St. George bridge (this is the third visit from which cores have been obtained at this site). Profiles from pile 20 show skin effect but not the profiles from pile 60. These piles are subjected to direct exposure of ocean water (channel between the island and land).

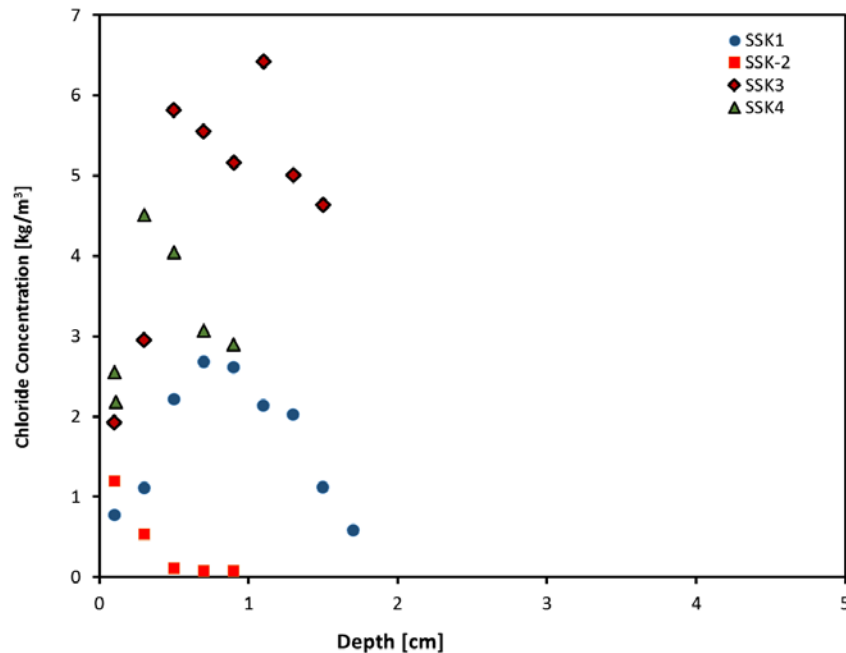


Figure 6-1: Chloride profiles obtained at sound locations (Sunshine Skyway bridge)

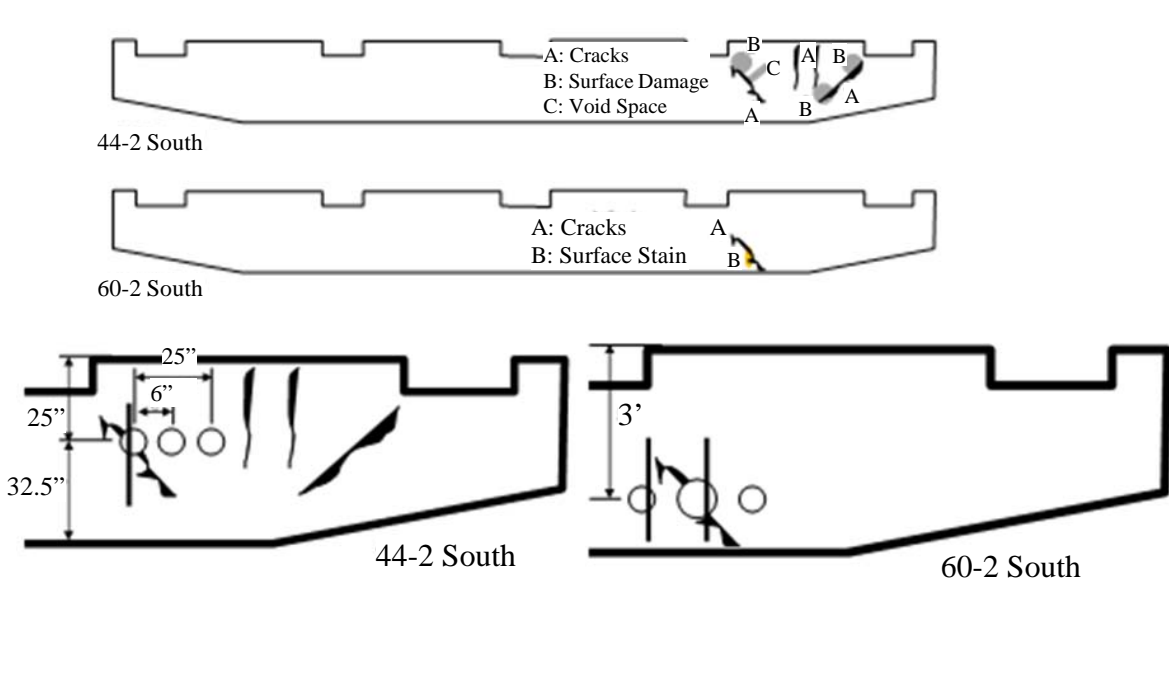


Figure 6-2: Location at which cores were obtained south face of trestle caps on pier 44 and 60

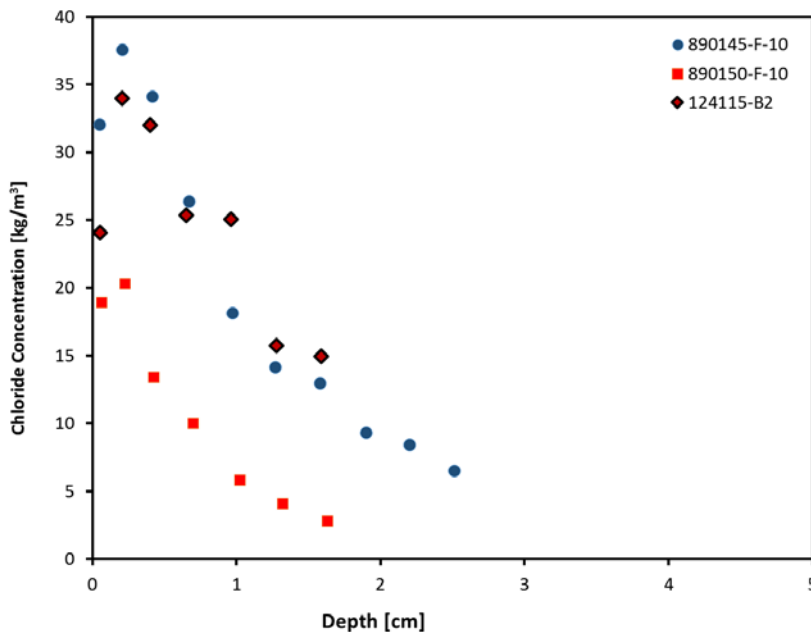


Figure 6-3: Chloride profiles obtained from elevation close to the MG

Figure 6-5 shows selected chloride profiles from the cores obtained during the visit to bridge #700203 Turkey Creek bridge (south Florida east coast). This bridge is located on the intracoastal side; each profile was obtained from a different elevation. Refer to Table 6-3 for the corresponding elevations. Figure 6-6 shows selected chloride profiles from the cores obtained during the visit to #150243 Bounces Pass bridge located in the Tampa Bay area. Note that from the profiles shown on Figures 6-3, Figure 6-4, Figure 6-5 and Figure 6-6 the profiles obtained

from cores for elevations B and C from Turkey Creek showed the lower concentration. This is likely in part due to its location, concrete composition and limited to small boat traffic.

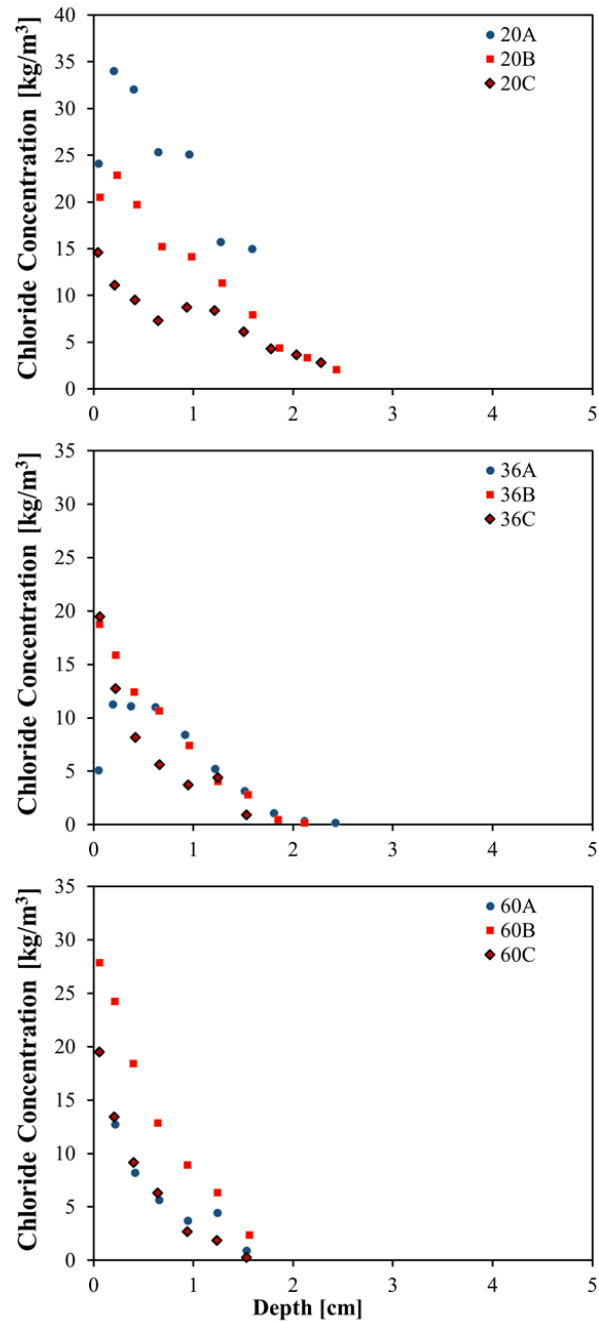


Figure 6-4: Profiles obtained from test piles at St. George bridge (#490100)

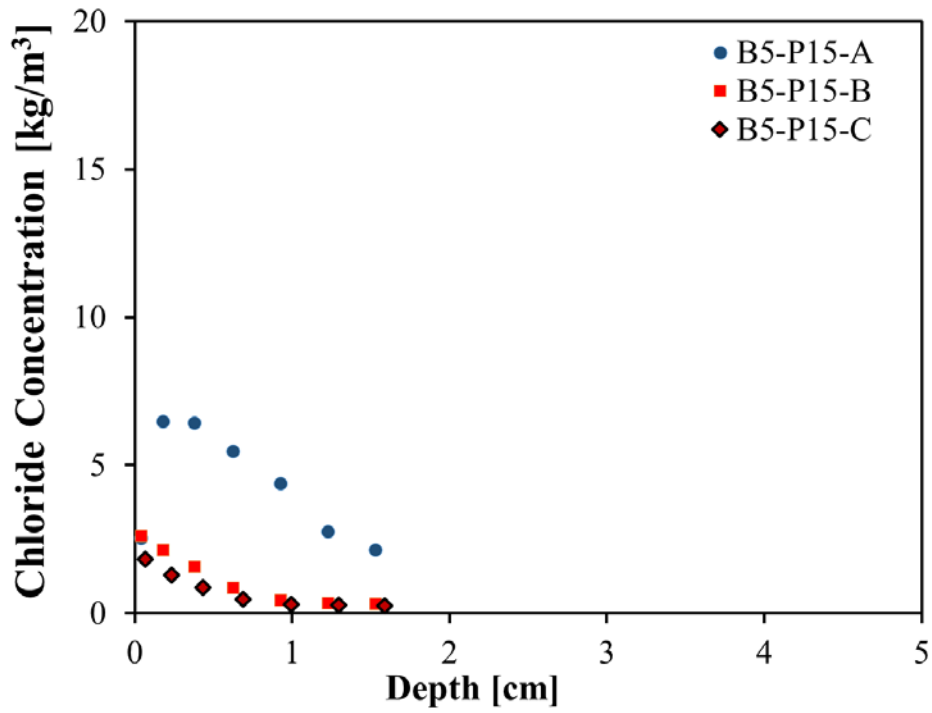


Figure 6-5: Typical profiles obtained at Turkey Creek #700203 bridge (three elevations)

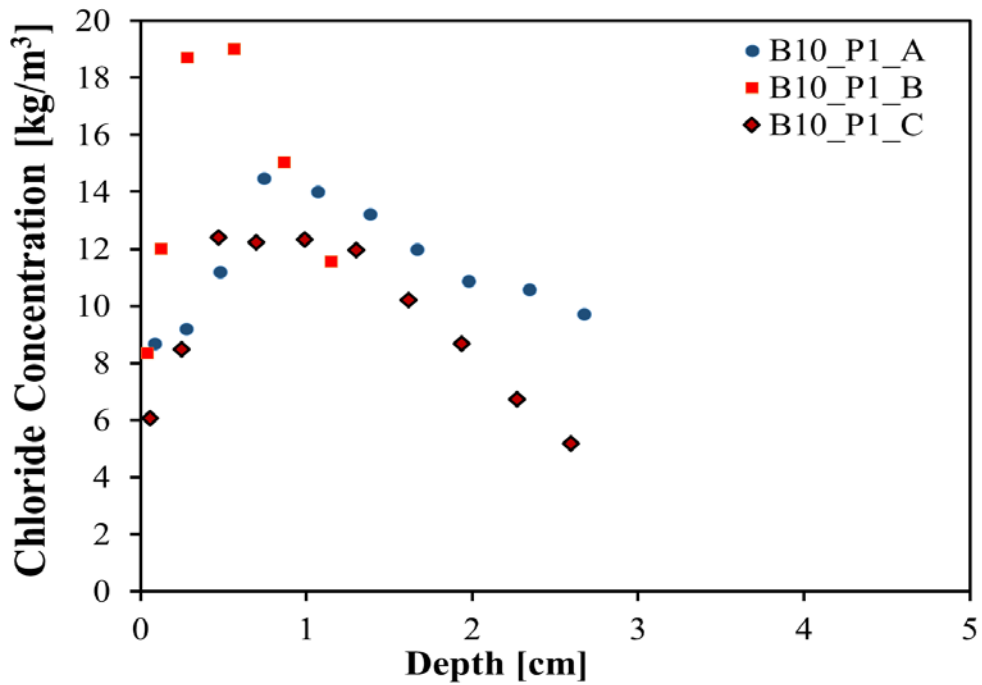


Figure 6-6: Typical profiles obtained at Bounces Pass bridge (#150243)

## 6.2 $D_{app}$ vs. Elevation

Figure 6-7 shows the  $D_{app}$  calculated values vs. elevation obtained from fitting profiles on profiles from both visits to the Key Royale bridge. The x-axis shows the elevations at which the cores were obtained.  $D_{app}$  values are shown for both the recently reported visit and from a previous visit. The values obtained at higher elevations appear to suggest lower  $D_{app}$  values at these locations. However, at these higher elevations, the moisture content is likely lower. Moreover, the chloride at the surface was lower for the  $D_{app}$  values corresponding to the higher elevations [86].

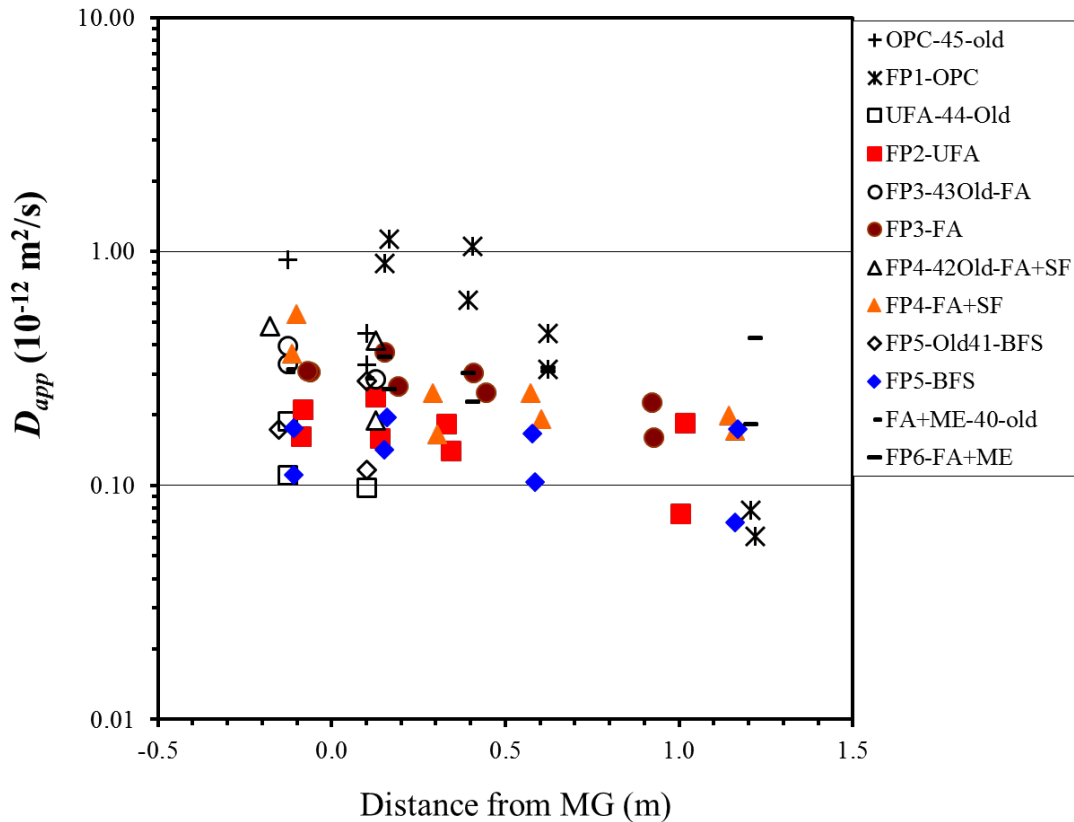


Figure 6-7:  $D_{app}$  vs. elevation Key Royale bridge

Incidentally, there was no significant reduction on the  $D_{app}$  values when comparing the  $D_{app}$  obtained after 2 and 5 years of exposure for the  $D_{app}$  calculated values from cores obtained at the lower elevations.

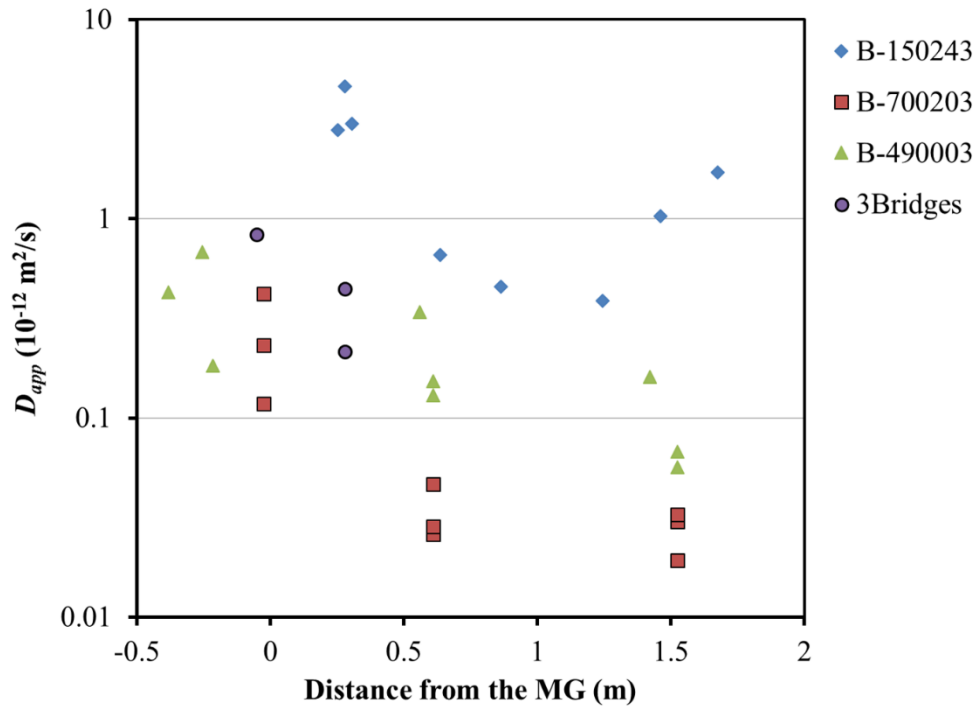


Figure 6-8:  $D_{app}$  vs. elevation for bridges visited during 2013

Figure 6-8 shows the  $D_{app}$  vs. elevation obtained from profiles gathered during the field visits performed in 2013. Similar to what was observed for the KRB, the  $D_{app}$  values were lower at the higher elevation when comparing the  $D_{app}$  values calculated for a given bridge. The data values also show that the  $D_{app}$  values spread over less than an order of magnitude at a given elevation from the same bridge. Besides different environmental conditions (micro-climate), the concrete composition might be somewhat different. For locations as bridge 700203 (Turkey Creek) or Key Royale where there is no direct exposure to the ocean water, the splash zone is mainly due to boat traffic. Thus, the apparent diffusivity at elevations as low as 0.5 m above the marine growth can be significantly lower than that observed at the marine growth elevation (or within the tidal region). Figure 6-9 shows the  $D_{app}$  values vs. elevation from the recent and previous visit (note that cores during the previous visit were obtained closer to the MG). In general, there is no significant difference in the  $D_{app}$  values calculated from the previous visit and the currently reported visit.

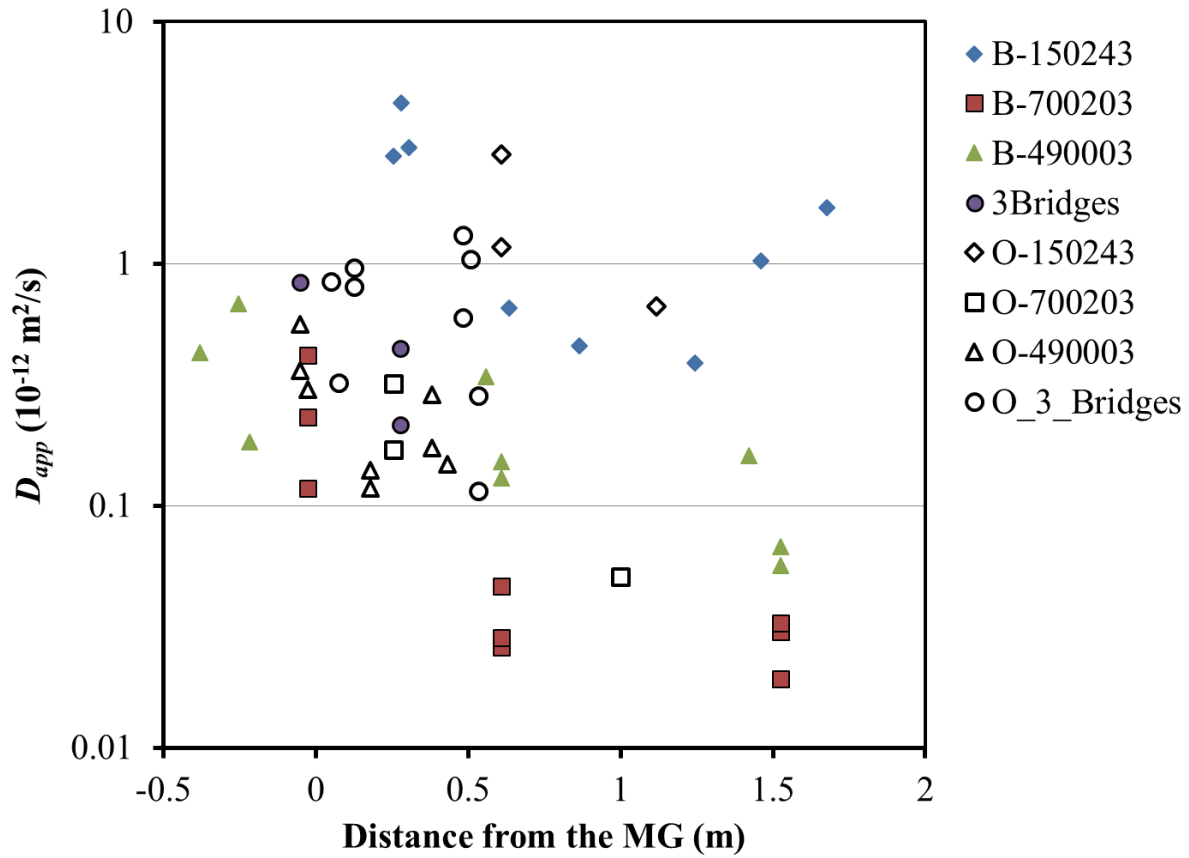


Figure 6-9:  $D_{app}$  vs. elevation for bridges visited fall 2013 and before (empty symbols)

### 6.3 $D_{app}$ values from cores obtained at elevations higher than 2 m

Table 6-4 lists the cores obtained at elevations  $> 2$  m AHT and the corresponding  $D_{app}$  obtained. At most of these elevations the moisture content likely is low, unless exposed directly to constant ocean seawater spray. Those visited in 2011 were part of this project and the cores were obtained from the trestle cap (piers 44 and 60 of the Sunshine Skyway bridge) at an estimated elevation of 8 meters above the high tide. The c next to some of the apparent diffusivity values indicate if the core was obtained from a location with visible cracks.

Table 6-4: List of cores obtained at elevations > 2 m

Bridge #	Construction Year	Visited	Age (years)	Elevation AHT (m)	Dapp (m <sup>2</sup> /s) ×10 <sup>-12</sup>	
170158	1986	1992	6	2.06	0.041	
860466	1989	1992	3	2.06	1.676	
150189	7/1/1986	7/13/1994	8	2.08	0.380	
874664	1985	1993	8	2.08	0.450	
930349	1982	1993	11	2.08	6.95	
150169	1986	1993	7	2.13	0.245	
870606	1983	1992	9	2.16	0.920	
874663	1985	1993	8	2.21	0.368	
10058	1980	1992	12	2.29	0.204	
874664	1985	1993	8	2.31	2.044	
130132	1985	1991	6	2.34	0.879	
890107	1987	1993	6	2.34	1.574	
170158	1986	1992	6	2.41	6.133	
150189	1986	1993	7	2.44	0.082	
900017	1983	1988	5	2.44	1.82	
150189	1986	1993	7	2.54	0.838	
10092	1983	1992	9	2.64	0.756	
570082	1979	1992	13	2.72	0.879	
150189	1986	1993	7	2.74	0.348	
490031	1988	1992	4	2.90	19.627	
870607	1983	1992	9	3.00	1.002	
150189	1986	1993	7	3.25	0.532	
150189	1985	1996	11	5.49	0.090	
150189	1985	1996	11	5.49	0.062	
150189	7/1/1986	4/3/1997	11	5.49	0.057	
150189	1985	1996	11	5.79	0.201	
150189	1985	1996	11	5.79	0.089	
150189	1985	1996	11	5.79	0.106	
150189	7/1/1986	4/3/1997	11	5.79	0.077	
150189	1985	2011	26	8.00	0.240	
150189	1985	2011	26	8.00	0.004	
150189	1985	2011	26	8.00	0.055	c
150189	1985	2011	26	8.00	0.747	
150189	1985	2011	26	8.00	0.083	
150188	1985	1996	11	18.29	0.049	
150189	7/1/1986	4/3/1997	11	18.29	0.052	
150188	1985	1996	11	18.29	0.226	c
150188	1985	1996	11	18.29	0.057	c
150188	1985	1996	11	18.29	0.064	c
150188	1985	1996	11	36.58	0.149	c

### 6.4 $D_{app}$ vs. Resistivity

Figure 6-10 shows the correlation between resistivity and  $D_{app}$  from values obtained on cores used for chloride profiles. All resistivity values reported in here were obtained using the two point method. The values circled in red corresponds to locations where the moisture content in the concrete was low (thus, the lower  $D_{app}$  values observed than if the concrete were to have been fully saturated), but the resistivity at the different elevations was not as different. This small difference in resistivity might be in part to the wet coring used that increased the moisture of the concrete but likely did not affect (or minorly affected) the chloride distribution. The plot on the right also includes the  $D_{app}$  and resistivity values (for those cores for which wet-resistivity was measured) for cores from the Key Royale bridge identifying the mixture type.

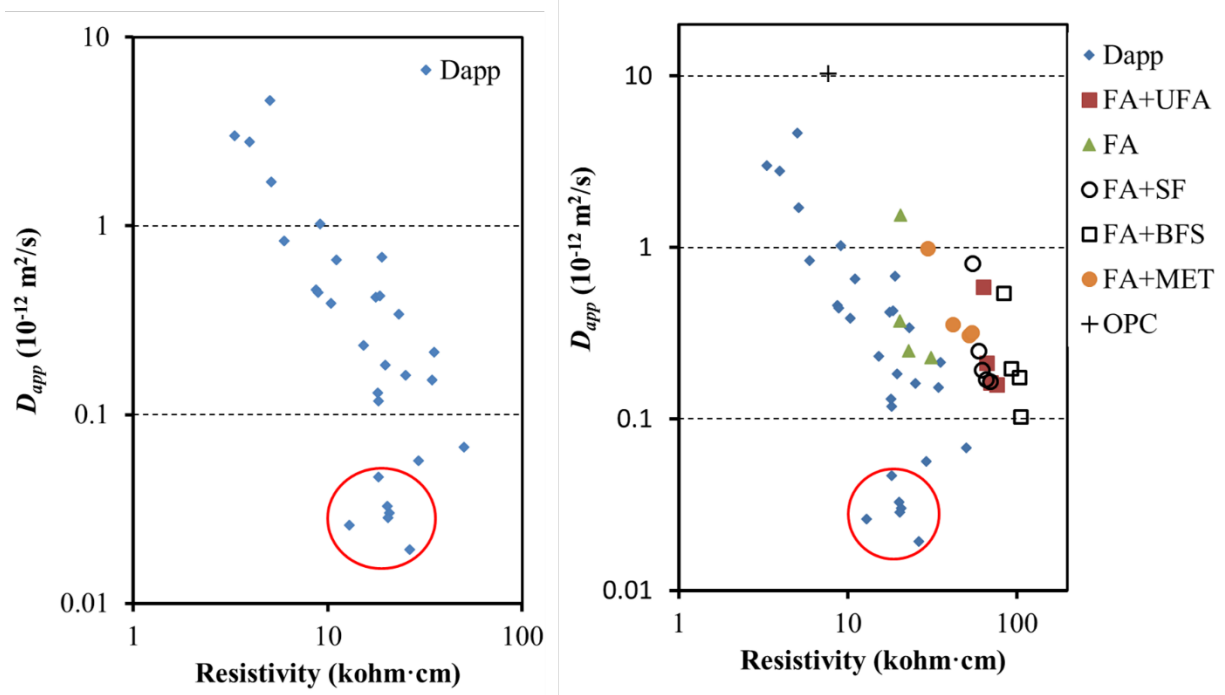


Figure 6-10:  $D_{app}$  vs. resistivity (field results)

## 7 Conclusions

### Specimens exposed under controlled degree of saturation

- The chloride diffusivity is affected by the degree of water saturation, curing regime, and w/cm ratio. The effect of cementitious content on the  $D_{app}$  values appears to be small.
- Chloride diffusivity appears to be slightly dependent on curing regime (only tested on DCL2).
- Measured chloride surface concentration ( $C_S$ ) values of concrete with mortar cover layer are generally lower than the  $C_S$  measured on concrete specimens without such layer.

### Specimens exposed to marine atmosphere

- The diffusivity values measured by fitting Fick's second law were significantly smaller than those obtained under controlled SD. Longer tests' duration and significantly lower chloride at the surface might explain the difference in the observed  $D_{app}$  values. Additionally, the moisture content of exposed outdoor specimens was not uniform over time.
- $C_{tot}$ ,  $k_t$ , and  $k_d$  values were calculated and compared with those previously reported. Location and orientation of the sample affected the observed  $D_{app}$ ,  $C_{tot}$ ,  $k_t$ , and  $k_d$  values.

### Aging factor from resistivity

- Specimens with slag and fly ash + silica fume react more quickly during curing, which results in the resistivity increasing more quickly than on specimens with only fly ash.
- Slag samples had the lowest aging factor ( $q$ ) values.
- The aging factor was calculated as a function of time from resistivity measurements on DCL specimens. The aging factor was found to change with time and to reach terminal values after 300 to 700 days.

### $D_{nssm}$ vs. resistivity

- Rapid migration tests (RMT) showed a strong correlation between the  $D_{nssm}$  and concrete resistivity. Samples with a 0.47 w/cm ratio and composed of 20% FA (DCL3) were found to have the lowest average resistivity after 90 days (14.2 kohm·cm) and one of the highest average  $D_{nssm}$  value at  $7 \times 10^{-12}$  m<sup>2</sup>/s. Cylinders from DCL10a, however, measured the highest  $D_{nssm}$  value ( $\sim 12 \times 10^{-12}$  m<sup>2</sup>/s) which could be attributed to the high amount of entrained air within the specimens of this mix.

- K values were calculated. K values obtained using test values after 90-100 days were significantly larger than the K value obtained from RMT tests after one, 1.5 and two years of exposure.
- Composition also affects the K value calculated.

$D_{app}$  values after bulk diffusion and full immersion

- The chloride concentration at the surface was dependent on the concentration of the NaCl solution for all of the mixes. In fact, the chloride concentration at the surface was reduced when silica fume was added into the mix for specimens exposed to 3% and 16.5% NaCl solutions compared to the other mixes.
- Concrete mixes with slag appeared to have lower surface concentration when exposed to a low concentration of NaCl solution compared to the other two compositions investigated. Also, the skin effect was present on specimens exposed to 0.1M NaCl.
- Specimens exposed to simulated field conditions had a lower surface concentration when exposed on the barge followed by the results obtained for those exposed to the splash scenario. 20% FA + 8% SF mixes showed the lowest surface concentration values when exposed on the barge in comparison with the other mixes.
- $D_{app}$  values for mixes with 20% fly ash and a water-to-cementitious ratio of 0.47 decreased 85% from 6 to 10 months and 41% from 10 to 18 months of exposure time when exposed to the splash simulated exposure.
- On the tidal simulation, the exposure time had a significant effect on the  $D_{app}$  values for specimens with fly ash mixes and a water-to-cementitious ratio of 0.41. After 10 months of exposure, the apparent diffusivity was reduced by 68% (compared to six months) and 52% after 18 months.
- The correlation between free and total chloride amount was presented. The chloride binding capacity calculated was greater on specimens composed of slag and lower w/cm with a percentage chloride binding capacity ( $P_{cb}$ ) of 71.82% when compared with the other mixes. The minimum  $P_{cb}$  was 51.7% on DCL6 mix with fly ash and silica fume and w/cm of 0.47.
- In most of the cases, mixes designed with higher water-to-cementitious ratio had higher apparent diffusion coefficients compared to those with low w/cm ratio.  $D_{app}$  values for 20% fly ash mixes exposed to 3% NaCl for 1 year and cured at normal conditions increased almost 28% as the water-to-cementitious ratio increased from 0.41 to 0.47.
- The amount of w/cm ratio appeared to have a modest effect on the binding capacity.
- $D_{app}$  calculated had a range of values ( $0.74 \times 10^{-12}$  to  $3 \times 10^{-12}$  m<sup>2</sup>/s) at high equivalent resistivity values (35 to 76 kohm-cm) for concrete compositions of 20% FA + 8% SF.

- $D_{app}$  decreased and equivalent resistivity increased as w/cm ratio decreased for mixes with 20% FA + 8% SF. This was also observed on the other compositions.
- The best correlation between  $D_{app}$  and equivalent resistivity was calculated for specimens with 20% fly ash, while specimens with 50% slag had the lowest R correlation between these two parameters. Mixes with 20% FA + 8% SF showed the highest typical K value compared to the other two compositions investigated.

Simulated tidal exposure or partially immersed for a long time at SMO:

- The  $D_{app}$  values were calculated from profiles of cores obtained from specimens exposed for 18 years at SMO to tidal exposure. The cores were obtained at five elevations and profiles from both core ends. The  $D_{app}$  values for cores for specimens with admixtures (either superfine fly ash or silica fume) were significantly smaller than from the specimen with OPC.  
Below water:  $D_{app}$  values were  $0.1 \times 10^{-12}$  and  $0.3 \times 10^{-12}$  m<sup>2</sup>/s, but for OPC mix the  $D_{app}$  value was  $0.7 \times 10^{-12}$  m<sup>2</sup>/s.  
At elevations of low tide and below high tide:  $D_{app}$  values ranged between  $0.1 \times 10^{-12}$  and  $0.3 \times 10^{-12}$  m<sup>2</sup>/s, but  $D_{app}$  values for OPC mix was between 0.6 and  $2 \times 10^{-12}$  m<sup>2</sup>/s.  
At the elevation farther from the high tide mark, the  $D_{app}$  values ranged between 0.01 and  $0.2 \times 10^{-12}$  m<sup>2</sup>/s, with most values  $< 0.07 \times 10^{-12}$  m<sup>2</sup>/s.
- The  $D_{app}$  values were calculated from profiles of cores obtained from specimens exposed for >20 year to partial immersion conditions. The cores were obtained at three elevations and profiles from both core ends. These specimens contained 10 to 40% fly ash.  
Below water:  $D_{app}$  values were  $0.25 \times 10^{-12}$  m<sup>2</sup>/s for specimens with 30% and 40% FA,  $0.7 \times 10^{-12}$  on specimens with 20% FA and  $1.1 \times 10^{-12}$  m<sup>2</sup>/s on specimens with 10% FA. This trend remained for elevations above water. For the elevation 25 cm above the water mark,  $D_{app}$  values ranged between 0.04 and  $0.15 \times 10^{-12}$  m<sup>2</sup>/s.

$D_{app}$  values at 18 months on specimens exposed to simulated tidal, splash and partially immersed. The  $D_{app}$  values from both ends of a core were usually different.

- Tidal: At elevations above low tide and below high tide marks, the  $D_{app}$  values ranged between 0.2 and  $3.2 \times 10^{-12}$  m<sup>2</sup>/s. The larger  $D_{app}$  values were observed on specimens with 0.47 w/cm. At the elevations above high tide, the  $D_{app}$  values ranged between 0.04 and  $0.86 \times 10^{-12}$  m<sup>2</sup>/s.
- Splash: At all elevations, the  $D_{app}$  values ranged between 0.15 and  $3.0 \times 10^{-12}$  m<sup>2</sup>/s.
- Barge: At elevations above water, the  $D_{app}$  values ranged between 0.14 and  $2.8 \times 10^{-12}$  m<sup>2</sup>/s. The largest  $D_{app}$  value at the higher elevation was  $0.85 \times 10^{-12}$  m<sup>2</sup>/s.

Field work

- The  $D_{app}$  values ranged between 0.02 and  $4.0 \times 10^{-12}$  m<sup>2</sup>/s. The  $D_{app}$  values from cores obtained at the higher elevations were smaller.

## References

1. Clear, K.C., "Time to corrosion of reinforcing steel in concrete slab," Vol.3. Report No. FHWA-RD-76-70. Federal Highway Administration; 1986.
2. Funahashi, M., "Predicting corrosion free service life of a concrete structure in a chloride environment," ACI Materials Journal; Vol.87, pp. 581-587; 1990.
3. Hooton, R.D.; Geiker, M.R.; Bentz, E.C., "Effects of curing on chloride ingress and implications on service life," ACI Materials Journal; Vol. 99: pp. 201-2066, 2002.
4. Presuel-Moreno F., "Characterization of new and old concrete structures using surface resistivity measurements," Contract Number BD 546-08, FDOT Final Report; Boca Raton, FL: Florida Atlantic University, 2010.
5. Tang, L.; and Gulikers, J., "On the mathematics of time-dependent apparent chloride diffusion coefficient in concrete," Cement and Concrete Research, V. 37, pp. 589-595; 2007.
6. Mangat, P.S.; and Molloy, B.T., "Prediction of long term chloride concentration in concrete", Materials and Structures, V. 27, pp. 338-346; 1994.
7. Stanish, K.; and Thomas, M., "The use of bulk diffusion tests to establish time-dependent concrete chloride diffusion coefficients," Cement and Concrete Research, V.33, pp. 55-62; 2003.
8. Thomas, M D.A.; and Bamforth P.B., "Modeling chloride diffusion in concrete – Effect of fly ash and slag", Cement and Concrete Research, Vol. 29, pp. 487-495, 1999.
9. Gjørsv, O.E.; Vennesland, Ø.; and El-Busaidy, A. H. S., "Electrical resistivity of concrete in the oceans", Offshore Technology Conference: Houston, TX, pp. 581-588, 1977
10. Buenfeld, N.R.; and Newman, J.B., "The permeability of concrete in a marine environment," Magazine of Concrete Research, V.36, No.127, pp. 67-80, 1984
11. Justnes, H.; Weerd, K.D.; Geiker M., "Chloride binding in concrete exposed to seawater and salt solutions", in Concrete under Severe Conditions, Eds. Li Z.J.; Sun W, et al., RILEM Proceeding PRO84, pp. 647-659; 2013.
12. Maage, M.; Helland, S.; Carlsen, J. E.; and Selmer A.S., "Practical non-steady state chloride transport as a part of a model for predicting the initiation period," in 1st RILEM International Workshop on Chloride Penetration into Concrete; Eds: L.-O. Nilsson and J.-P. Ollivier; pp. 398 – 406; 1995.
13. Maage, M.; Helland. S.; and Carlsen. J. E., "Chloride penetration into concrete with lightweight aggregates," EuroLightCon Project Report BE96-3942, 1999.
14. Isaksen, H. R.; Liestoel, G. ; Giaever, N. A. ; Kompen, R., "Development of a chloride-resistant concrete" in 2nd International Conference: Concrete Under Severe Conditions, E & FN Spon , London; pp. 1893-1903; 1998.

15. Markeset G.; and Skjølvold O., "Time dependent chloride diffusion coefficient - field studies of concrete exposed to marine environment in Norway," in 2nd International Symposium on Service Life Design for Infrastructures; Editor(s): K. van Breugel, Guang Ye, Yong Yuan; RILEM Proceeding PRO070, pp. 83 – 90; 2010.
16. Ehlen, M.A.; Thomas, M.D.A.; and Bentz, E.C., "Life-365 service life prediction model™ Version 2.0," Concrete International, V. 31, No.5, pp. 41-46; 2009.
17. Presuel-Moreno, F.; Wu, Y-Y.; and Liu, Y., "Effect of curing regime on concrete resistivity and aging factor over time". Journal of Construction and Building Materials. 48: pp. 874-882; 2013.
18. Hall, C., "Water sorptivity in mortars and concrete: A review," Magazine of Concrete Research Vol. 41, No 147, pp. 51-61, 1989.
19. Wilson, M.A.; Hoff, W.D.; and Hall, C., "Water movement in porous building materials- absorption from a small cylinder cavity," Building and Environment, Vol. 26, pp. 143-152, 1991.
20. Nielson E.P.; and Geiker M R., "Chloride diffusion in partially saturated cementitious materials", Cement and Concrete Research, Vol. 33 pp. 133-138, 2003
21. Crank, J., 'The mathematics of diffusion', 2nd Ed (Clarendon, Oxford); 1975.
22. Rey, D. E., "Chloride penetration in high-performance concrete in florida marine bridges," Tampa: FL, University of South Florida. Ms Thesis; 2002.
23. Andrade, C., "Concepts on the chloride diffusion coefficient," Third International RILEM Workshop on Testing and Modeling the Chloride Ingress into Concrete. pp. 3-17; 2002.
24. Liu, Y., "accelerated curing of concrete with high volume pozzolans-resistivity, diffusivity and compressive strength," Boca Raton, FL: Florida Atlantic University, Ph.D.Dissertation, 2012.
25. Tang, L.; and Gulikers, J.; "Chloride diffusivity in high strength concrete at different ages," Nordic Concrete Research Publication, No. 11, pp.162-171, 1992.
26. Bamforth, P.B.; and Price W.F., "Factors influencing chloride ingress into marine structures," In: Dhir RK, Jones MR, editors. Concrete 2000; pp. 1105–18, 1993
27. Bentz, E.C.; Evans, C.M.; and Thomas M.D.A., "Chloride diffusion modeling for marine exposed concretes," In: Corrosion of reinforcement in concrete construction, Page C.L.; Bamforth, P.B.; and Figg, J.W., Editors. Cambridge,UK: The Royal Society of Chemistry Publication; pp. 136-145, 1996.
28. Mangat, P.; and Molloy, B., "Prediction of long term chloride concentration in concrete," Material and Structures, Vol. 27, pp. 338-346, 1994.
29. Andrade, C.; Castellote, M.; and d'Andrea, R., "Measurement of ageing effect on chloride diffusion coefficients in cementitious matrices," Journal of Nuclear Materials.412: pp. 209-216, 2011.
30. Zhang, T.; and Gjørsv, O. E., "Effect of chloride source concentration on chloride diffusivity in concrete," ACI Materials Journal, Vol. 102, pp. 295-298, 2005.

31. Castellote, M.; Andrade, C.; Alonso, C., "Measurement of the steady and non-steady-state chloride diffusion coefficients in a migration test by means of monitoring the conductivity in the anolyte chamber: Comparison with nature diffusion tests," *Cement and Concrete Research*, Vol. 31, pp. 1411-1420, 2001.
32. Arsenault, J.; Bigas, J.-P.; and Olliver, J.-P., "Determination of chloride diffusion coefficient using two different steady state methods: Influence of concentration gradient", *Proceedings of International Workshop on Chloride Penetration into Concrete*, L. O. Nilsson and J.P. Oliver eds, RIELM pp. 150-160, 1997.
33. Gilleece, P.R.V., "Effect of concentration on the accelerated chloride ion migration test for modified concretes", in *Proceedings of International Workshop on Chloride Penetration into Concrete*, L. O. Nilsson and J.P. Oliver eds, RIELM pp. 161-167, 1997.
34. Florida Department of Transportation. Florida Method of Test For Determining Low-Level of Chloride in Concrete and Raw Materials, FM5-16 , State of Florida Department of Transportation, May 13, 2009.
35. Pack, S-W.; Jung, M.-S.; Song, H-W.; Kim, S-H; Ann, K.Y., "Prediction of time dependent chloride transport in concrete structures exposed to a marine environment", *Cement and Concrete Research*, Vol. 40 pp. 302-312, 2010.
36. Uji, K.; Matsuoka, Y.; and Maruya T., "Formulation of an equation for surface chloride content of concrete due to permeation of chloride, corrosion of reinforcement in concrete", *Elsevier Applied Science*, pp. 258-267, 1990.
37. Song, H-W.; Lee, C-H.; and An K.Y., "Factors influencing chloride transport in concrete structures exposed to marine environments", *Cement and Concrete Research*, Vol.30 pp. 113-121, 2008
38. Ann K.Y.; Ahn, J.H.; and Ryou, S.S., "The important of chloride content at the concrete surface in assessing the time to corrosion of steel in concrete structures", *Construction and Building Materials*, Vol.23 pp. 239-245.
39. Andrade, C.; Diaz, J.M.; and Alonso; C., "Mathematical modeling of a concrete surface "skin effect" on diffusion in chloride contaminated media", *Advanced Cement-Based Materials*, Vol. 6 pp. 39-44, 1997.
40. Meira, G R.; Andrade, C.; Alonso, C.; Boral, J.C.; Padilha, M., "Durability of concrete structures in marine atmosphere zones – the use of chloride deposition rate on the wet candle as an environmental indicator," *Cement and Concrete Composites*, Vol. 32 pp. 427-435, 2010.
41. Meira, G.R.; Andrade, C.; Padaratz I.J.; Alonso, C.; and Borba Jr., J.C., "Chloride penetration into concrete structures in the marine atmosphere zone - Relationship between deposition of chlorides on the wet candle and chlorides accumulated into concrete," *Cement and Concrete Composites*, no. 29, pp. 667-676, 2007
42. McKay, W.A.; Garland, J.A.; Livesly, D.; Halliwell, C. M.; and Walker, M. I., "The characteristics of the shore-line sea spray aerosol and the landward transfer of radionuclide discharged to coastal sea water," *Atmospheric Environment*, vol. 28, pp. 3299-3309, 1994.

43. Erickson, D. J.; Merrill, J. T.; and Duce, R. A., "Seasonal estimates of global atmospheric sea-salt distributions," *Journal of Geophysical Research*, vol. 91, pp. 1067-1072, 1986.
44. Fitzgerald, J. W., "Marine aerosols: A review," *Atmospheric Environment*, vol. 25A, pp. 533-45, 1991.
45. Poulsen, E.; and Mejlbro, L., "Diffusion of chloride in concrete: theory and application" (*Modern Concrete Technology*), vol. 14, New York: Taylor and Francis Group, 2006.
46. Gustafsson, M. E.; and Franzen, L. G., "Dry deposition and concentration of marine aerosols in a coastal area, SW Sweden," *Atmospheric Environment*, vol. 30, no. 6, pp. 977-989, 1996.
47. Meira, G. R.; Andrade, M. C.; Padaratz, I. J.; Alonso, M. C.; and Borba Jr, J. C., "Measurements and modelling of marine salt transportation and deposition in a tropical region in Brazil," *Atmospheric Environment*, no. 40, pp. 5596 - 5607, 2006.
48. M. G. Richardson, "Fundamentals of Durable Reinforced Concrete (*Modern Concrete Technology*)," vol. 11, New York: Taylor and Francis Group, 2002.
49. ASTM G 140-02, ASTM International, "Standard Test Method for Determining Atmospheric Chloride Deposition rate by Wet Candle Method," ASTM International, West Conshohocken, 2002.
50. Cole, I.S.; Paterson, D.A.; and Ganther, W.D., "Holistic model for atmospheric corrosion. Part I - Theoretical framework for production, transportation and deposition of marine salts," *Corrosion Engineering and Science Technology*, vol. 38, pp. 129-134, 2003
51. Feliu, S.; Morcillo, M.; and Chico, B., "Effect of distance from sea on atmospheric corrosion rate," *Corrosion*, vol. 55, no. 9, pp. 883-891, 1999.
52. Meira, G. R.; Padaratz, I. J.; Alonso, C.; and Andrade, C., "Effect of distance from the sea on chloride aggressiveness in concrete structures in Brazilian coastal site," *Materiais de Construção*, vol. 53, pp. 179-188, 2003.
53. Meira, G.R.; Andrade, C.; Padaratz, I.J.; Alonso, C.; and Borba Jr, J. C., "Sea-salt model to marine atmosphere environment," in *Proceedings of the international conference "fib symposium structural concrete and time"*, La Plata, 2005
54. Parrot, L.J., "Moisture conditioning and transport properties of concrete test specimens," *Materials and Structures* 27(8) pp. 460-468, 1994.
55. Martys, N.S., "Diffusion in partially-saturated porous materials," *Materials and Structures* 32(8) pp. 555-562, 1999.
56. Chatterji, S., "On the non-applicability of unmodified Fick's law to ion transport through cement based materials," *Proceedings of the 1st International Workshop on Chloride Penetration Into Concrete*, RIELM Publication, Saint-Rémy-lès-Chevreuse, France, pp. 64-73, 1997.
57. Saetta, A.V., Scotta, R.V., Vitaliani, R.V., 'Analysis of chloride diffusion into partially saturated concrete', *ACI Mater Journal* 90(5) pp. 441-451, 1993.
58. Swaddiwudhipong, S., Wong, S.F., Wee, T.H., Lee, S.L., 'Chloride ingress in partially and fully saturated concretes', *Concrete Science and Engineering* 2(5) pp. 17-31, 2000.

59. Samson, E., Marchand, J., Snyder, K.A., Beaudoin, J.J., “Modelling ion and fluid transport in unsaturated cement systems in isothermal conditions,” *Cement and Concrete Research* 35(1) pp. 141–153, 2005.
60. Oh, B.H., Jang, S.Y., “Effects of material and environmental parameters on chloride penetration profiles in concrete structures,” *Cement and Concrete Research* 37(1) pp. 47–53, 2007.
61. Nguyen, T.Q., Petkovic', J., Dangla, P., Baroghel-Bouny, V., “Modelling of coupled ion and moisture transport in porous building materials,” *Construction and Build Materials* 22(11) pp. 2185–2195, 2008.
62. Climent, M.A., de Vera, G., Lopez, J.F., Viqueira, E., Andrade, C., ‘A test method for measuring chloride diffusion coefficients through nonsaturated concrete. Part I: The instantaneous plane source diffusion case’, *Cement and Concrete Research* 32(7) pp. 1113-1123, 2002.
63. de Vera, G., Climent, M.A., Viqueira, E., Anton, C., Andrade, C., ‘A test method for measuring chloride diffusion coefficients through nonsaturated concrete. Part II: The instantaneous plane source diffusion case with chloride binding consideration’, *Cement and Concrete Research* 37(5) pp. 714-724, 2007.
64. Guimaraes, A.T.C.; Climent, M.A.; de Vera, G.; Vicente, F.J.; Rodrigues, F.T.; Andrade, C., “Determination of chloride diffusivity through partially saturated Portland concrete by a simplified procedure”, *Construction and Building Materials* 25(2) pp. 785-790, 2011.
65. ASTM C 642-06, “Standard test method for density, absorption, and voids in hardened concrete,” American Society for Testing of Materials, Annual Book of ASTM Standards, 2006.
66. Gjorv, O.E., *Durability Design of Concrete Structures in Severe Environments*: Taylor and Francis; 2009.
67. Ferreira, R. M., “Probability based durability analysis of concrete structures in marine environment,” Guimaraes, Portugal: University of Minho. Ph.D. Dissertation, 2004.
68. Tang, L.; and Nilsson, L.O., “Chloride binding capacity and binding isotherms of opc pastes and mortars,” *Cement and Concrete Research*. 23(2): pp. 247-253, 1993.
69. Tuutti, K., “Corrosion of Steel in Concrete,” Swedish Cement and Concrete Research Institute. Stockholm, Sweden, 1982.
70. Mohammed, T.U., and Hamada, H., “Relationship between Total and Free Chloride Contents in Concrete,” *Cement and Concrete Research*. 33: pp. 1487-1490, 2003.
71. Cheewaket, T.; Jaturapitakkul, C.; and Chalee, W., “Long term performance of chloride binding capacity in fly ash concrete in a marine environment,” *Construction and Building Material*. 24: pp. 1352-1357, 2010.
72. FM5-578, “Florida method of test for concrete resistivity as an electrical Indicator of its permeability,” Florida Department of Transportation (FDOT); January 27, 2004.
73. ASSHTO TP95-11 “Standard test method for surface resistivity indication of concrete's ability to resist chloride ion penetration,” American Association of State Highway Transportation Officials, AASHTO Provisional Standards, Washington D.C.; June 2010.

74. NT Build 492 Nordtest Method, “Chloride migration coefficient from non-steady-state migration experiment,” Espoo, Finland, Proj. 1388-98, 1999.
75. NT Build 443 Nordtest Method, “Accelerated chloride penetration into hardened concrete,” Espoo, Finland, Proj. 1154-94, 1995.
76. ASTM C 1556-04, “Standard test method for determining the apparent chloride diffusion coefficient of cementitious mixtures by bulk diffusion,” American Society for Testing of Materials, Annual Book of ASTM Standards, 2006.
77. FM-5-516 FDOT, “Florida Method of Test for Determining Low-Levels of Chloride in Concrete and Raw Materials,” 2013.  
<http://www.dot.state.fl.us/statematerialsoffice/administration/resources/library/publications/fstm/methods/fm5-516.pdf>
78. Chaussadent, T.; and Arliguie G., “AFREM test procedures concerning chlorides in concrete: Extraction and titration methods,” *Materials and Structures*, Vol. 32, pp. 230 – 234, 1999.
79. Echevarria, V., “Concrete diffusivity and its correlation with chloride deposition rate on concrete exposed to marine environments,” Boca Raton: Florida Atlantic University. Master of Science Thesis; 2012.
80. Liu, Y.; and Presuel-Moreno F., “Normalization of temperature effect on concrete resistivity by a method using Arrhenius law,” Accepted for publication in *ACI Materials Journal* (2014) available online in the in-press area, 2014.
81. ISO-9225:2012 Corrosion of metals and alloys — Corrosivity of atmospheres — Measurement of environmental parameters affecting corrosivity of atmospheres, 2012.
82. Andrade, C., et al., “Chloride Aging Factor of Concrete Measured by Means of Resistivity”, in *International Conference on Durability of Building Materials*, Porto, Portugal, 2011.
83. Liu Y.; and Presuel-Moreno F., “Time-dependency of chloride diffusion coefficients in concrete by electrical resistivity method,” Submitted for publication to *Cement and Concrete Composites*, 2014.
84. Cascudo, O.; Carasek, H.; Yssorche-Cubaynes, M. P.; Lopes, A.N.; and Ollivier, J.P., “Evaluation of cover concrete by analysis of chloride diffusion coefficients,” *American Concrete Institute. SP-229*: pp. 135-150, 2005.
85. Hassan, Z.F.A., “Rapid assessment of the potential chloride resistance of structural concrete,” United Kingdom: University of Dundee, Ph.D. Dissertation, 2012.
86. Presuel-Moreno, F., Wu, Y.Y., Arias, W. and Liu, Y., “Analysis and Estimation of Service Life of Corrosion Prevention Materials Using Diffusion, Resistivity and Accelerated Curing for New Bridge Structures,” Final Report BDK79-977-02 (Volume 2: Accelerated Curing of Concrete with High Volume Pozzolans - Resistivity Diffusivity, and Compressive Strength); Boca Raton, FL: Florida Atlantic University, 2013.
87. Hoob, D.W., “Minimum requirements for durable concrete: British cement association,” 1998.

88. Sumaranwanich, T. and Tangtermsirikul, S., A Model for Predicting Time-Dependent Chloride Binding Capacity of Cement-Fly Ash Cementitious System. *Materials and Structures*, Vol 37: pp. 387-396, 2004.
89. Dhir, R.K.; El-Mohr, M.A.K.; and Dyer, T.D., "Chloride binding in ggbs concrete," *Cement and Concrete Research*. 26(12): pp. 1767-1773, 1996.
90. Delagrave, A.; Marchant, J.; Ollivier, J.P.; Julien, S.; and Hazrati, K., "Chloride binding capacity of various hydrated cement paste systems," *Advanced Cement Based Materials* Vol 6: pp. 28-35, 1997.
91. Liu Y.; Presuel-Moreno, F.; and Paredes M., "Determination of chloride diffusion coefficients in concrete by electrical resistivity method," Submitted for publication to *ACI Materials Journal*, 2014.
92. Olsson, N.; Baroghel-Bouny, V.; Nilsson, L. O.; and Thiery, M., "Non saturated ion diffusion in concrete – new laboratory measurements", In: *Proceedings of the International Congress on Durability of Concrete (ICDC 2012)*; Herald Justnes, Stefan Jacobsen, Eds. Trondheim, Norway, 2012.
93. Sagüés, A.A.; et al, *Corrosion of epoxy coated rebar in Florida bridges*, Final Report submitted to Florida Department of Transportation (Contract No 0510603), 1994.
94. Sagüés, A.A.; Kranc, S.C.; Yao, L.; Presuel-Moreno, F.; and Rey, D., Torres-Acosta A. "Corrosion Forecasting for 75-Year Durability Design of Reinforced Concrete," Final Report submitted to Florida Department of Transportation (Contract No. 0510805), 2001.
95. Sagüés, A.A.; and Lau, K., "Corrosion evaluation of Bridges with Epoxy-Coated Rebar," Final Report submitted to Florida Department of Transportation (Contract No. BD544-23), 2009.
96. Sagüés, A.A.; and Lau, K., "Corrosion of steel in locally deficient concrete," Final Report submitted to Florida Department of Transportation (Contract No. BD544-31), 2009.
97. Sagüés, A.A.; Lau, K.; and Yao, L., "Corrosion Performance of Concrete Cylinder Piles," Final Report submitted to Florida Department of Transportation (Contract No. BC353-10), 2005.
98. Hamilton, H.R.; Boyd, A.J.; and Vivas, E.A., "Permeability of concrete – comparison of conductive and diffusion methods," Final Report submitted to Florida Department of Transportation" (Contract No. BD536), 2007.
99. Presuel-Moreno, F., Wu, Y.Y., Arias, W., and Liu, Y., 'Analysis and estimation of service life of corrosion prevention materials using diffusion, resistivity and accelerated curing for new bridge structures,' Final Report BDK79-977-02 (Volume 1); Boca Raton, FL: Florida Atlantic University, 2013.

## Appendices

### Appendix A: Core Collection for Field Simulations

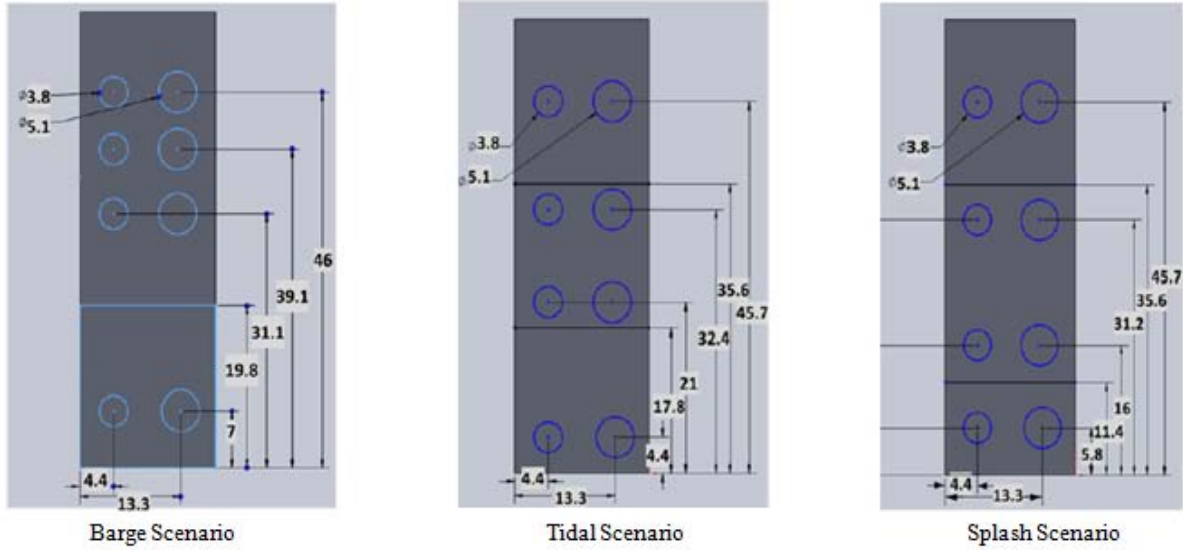


Figure A.1: Location at which cores were obtained

Note (units shown in here are in cm)

## Appendix B: Exposure Date and Coring Ages for G2 Specimens

Table B1: Age at which slabs exposed to marine atmosphere were cored

Sample	Exposure Date	6 Months	10 Months	12 Months	18 Months	24 Months	28 Months
DCL1	1/9/2012	0.49	0.74	0.99	1.50	1.98	2.25
DCL2	11/1/2011	0.49	0.82	0.99	1.50	1.94	2.33
DCL3	11/18/2011	0.49	0.82	0.99	1.70	1.95	2.30
DCL4	1/23/2012	0.49	0.74	0.99	1.50	1.96	2.25
DCL5	1/23/2012	0.49	0.74	0.99	1.50	1.96	2.25
DCL6	12/5/2011	0.49	0.82	0.99	1.50	1.95	2.28
DCL7	1/9/2012	0.49	0.74	0.99	1.50	1.98	2.25
DCL8	12/20/2011	0.49	0.82	0.99	1.50	1.96	2.28
DCL9	12/5/2011	0.49	0.82	0.99	1.50	1.95	2.28
DCL10	11/1/2011	0.49	0.82	0.99	1.50	1.95	2.33
DCL10a	11/18/2011	0.49	0.82	0.99	1.60	1.95	2.30
DCL10b	12/20/2011	0.49	0.82	0.99	1.50	1.96	2.28
DCL11	12/5/2011	0.49	0.82	0.99	1.50	1.95	2.28

## Appendix C: Resistivity vs. Time

Figure C.1: Resistivity vs. time for DCL2, 3, 5, 6, 8 and 9

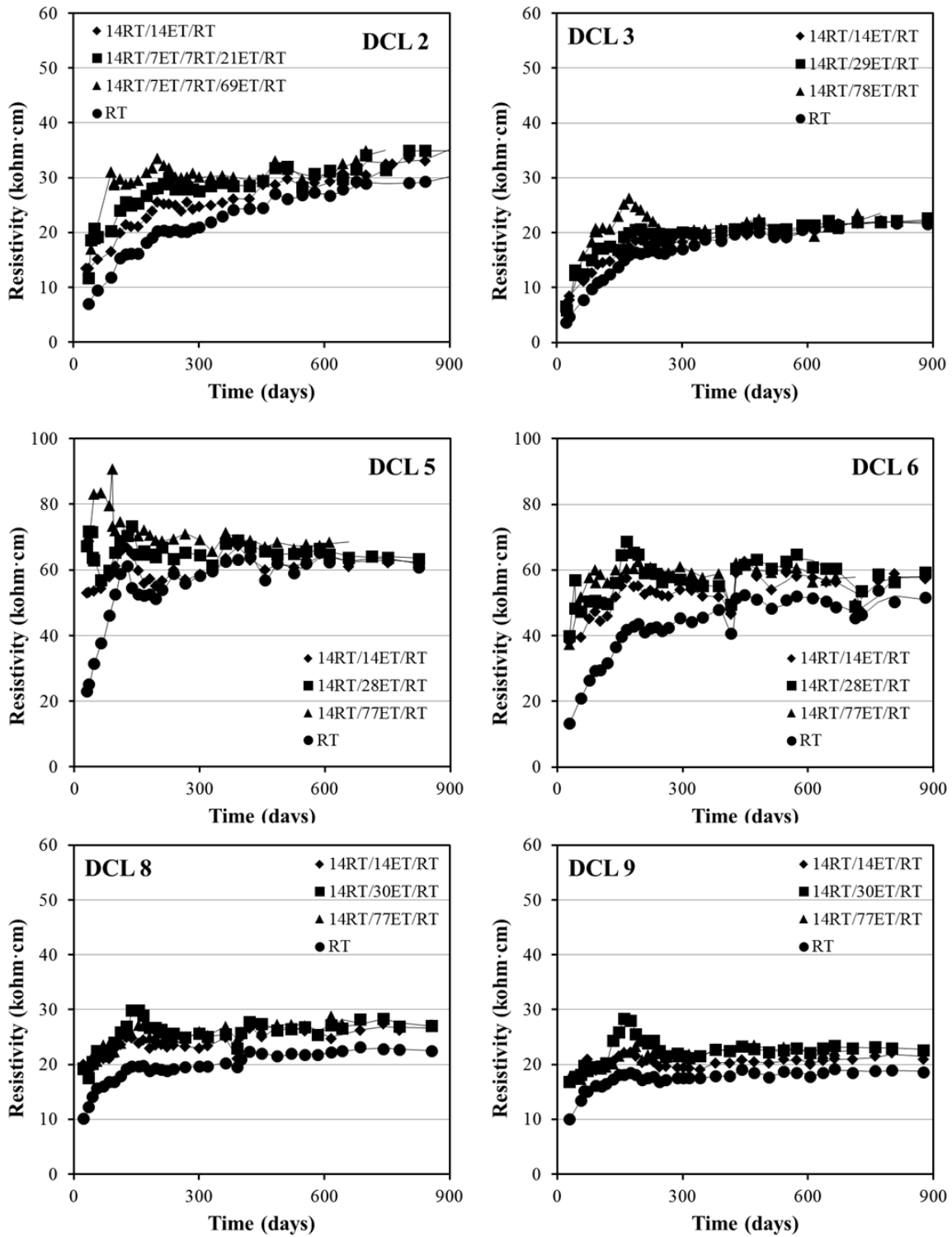
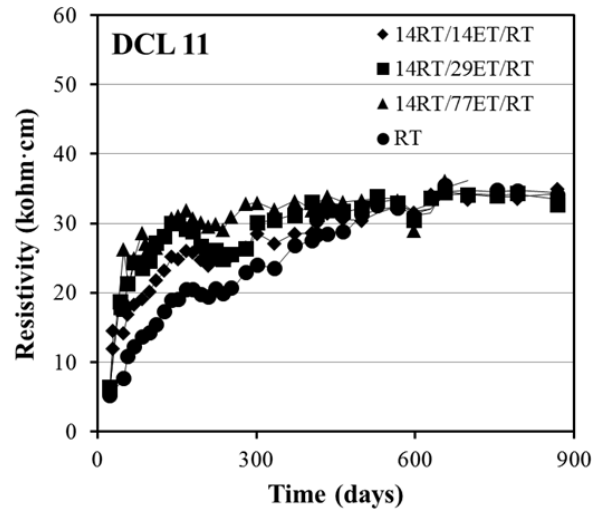
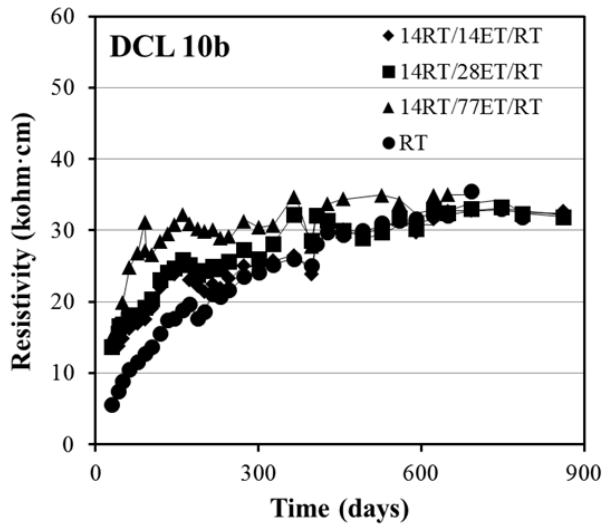
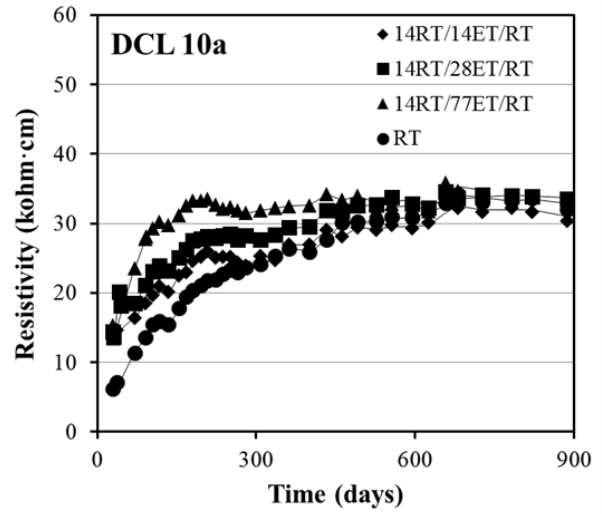
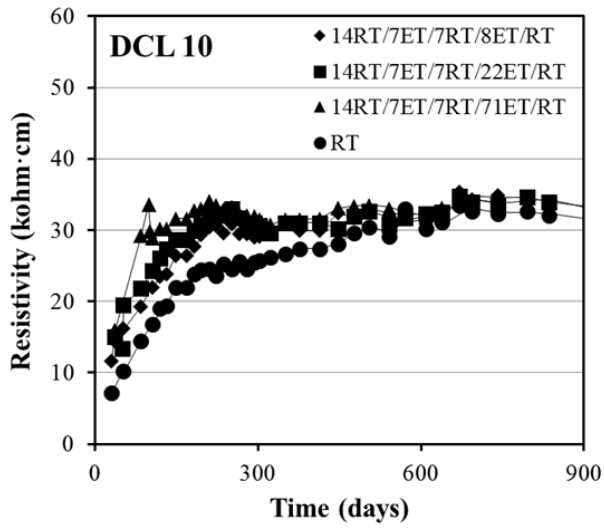


Figure C.2: Resistivity vs. time for DCL10, 10a, 10b, and 11



## Appendix D: DCL4, 5, 7, 8, 10a, 10b, and 11: Chloride Concentration for Specimens Exposed to 0.1M NaCl Solution vs. Depth

Figure D.1: Chloride profiles for specimens exposed in 0.1 M NaCl for 220 and 400 days (DCL4, 5, 7, 8, 10a, 10b, and 11)

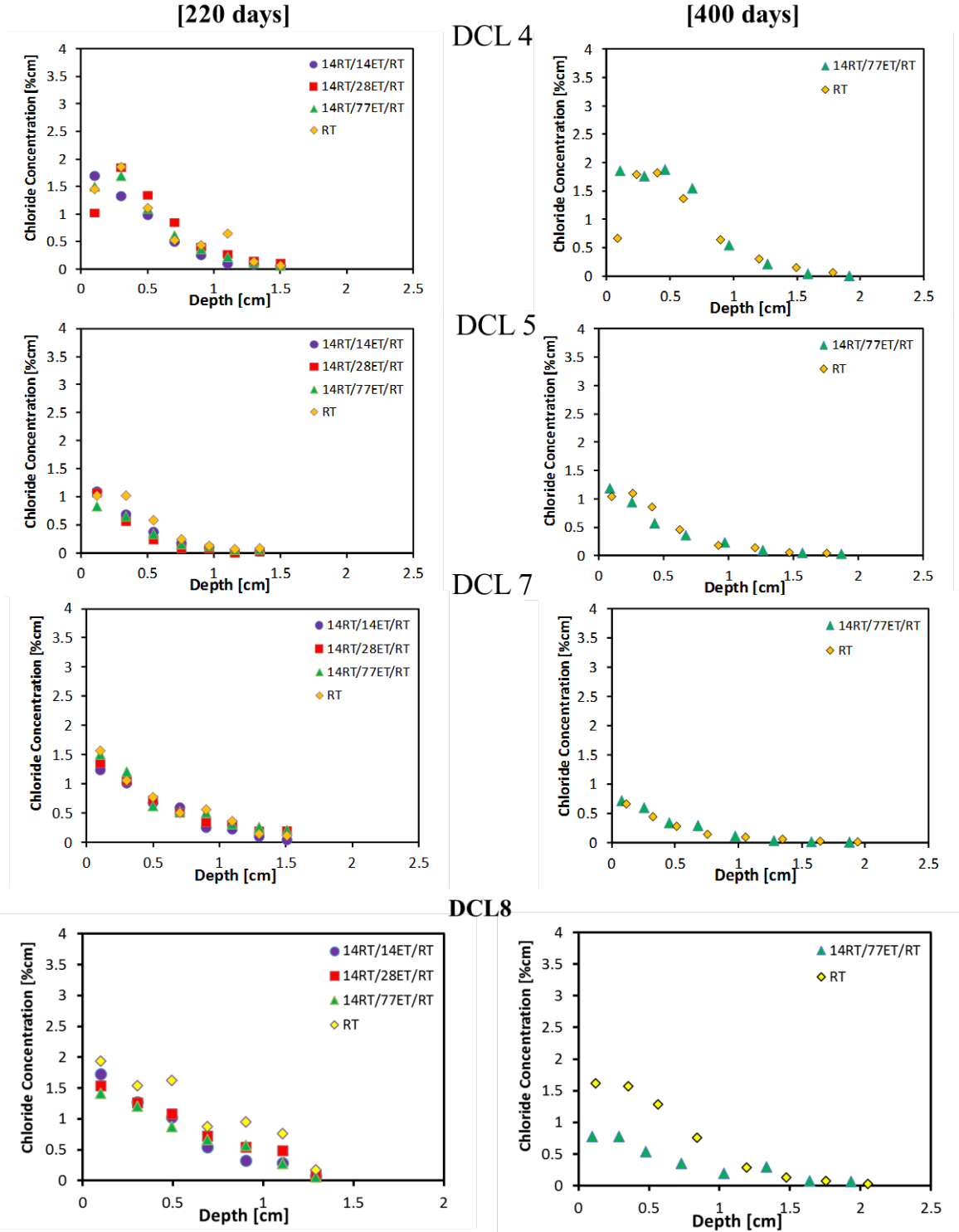
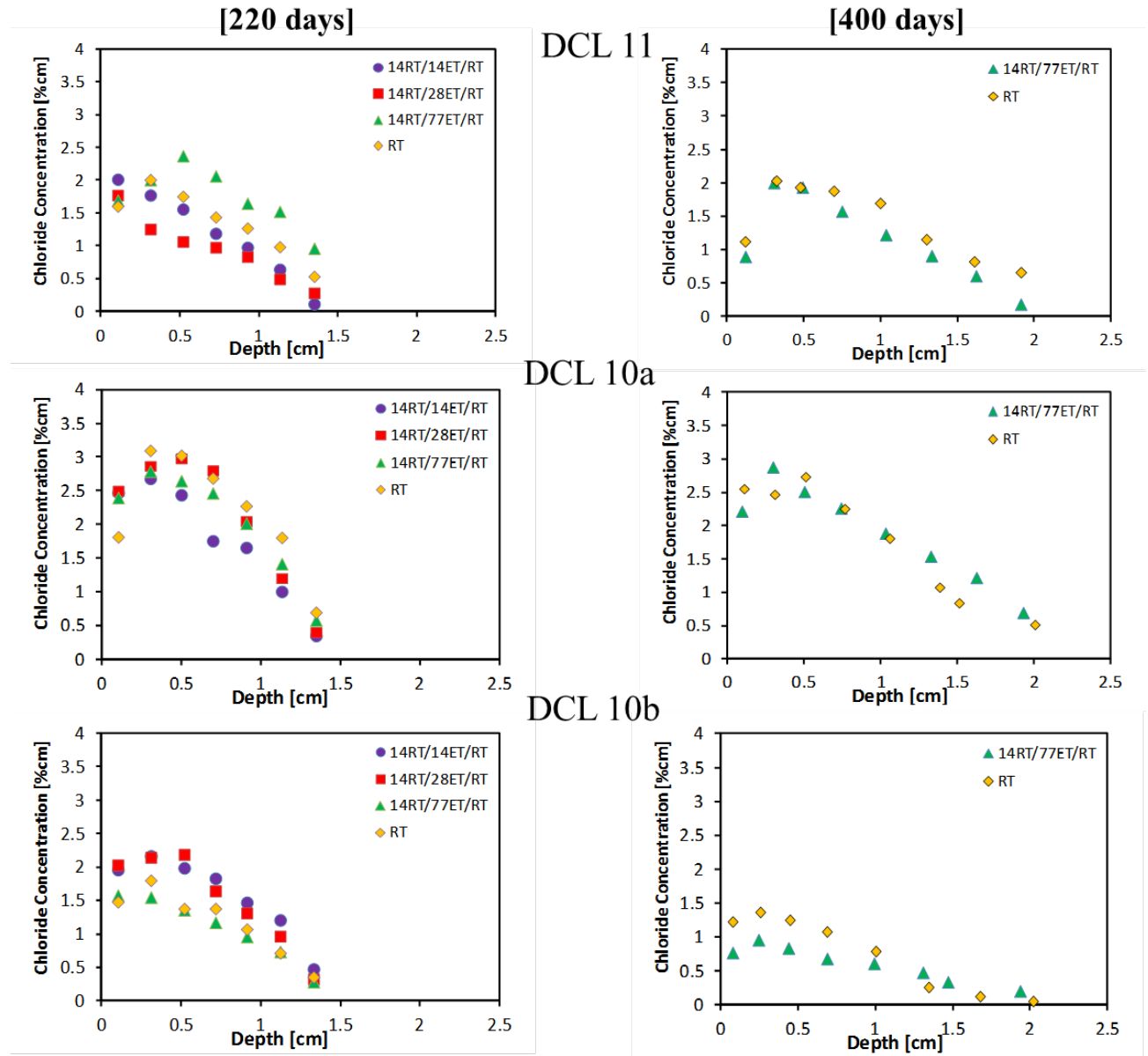


Figure D.1: Continued



## Appendix E: Chloride Profiles for Specimens Exposed to 3% and 16.5% NaCl Solutions

Figure E.1 Profiles of specimens exposed to bulk diffusion in 16.5% and 3% NaCl

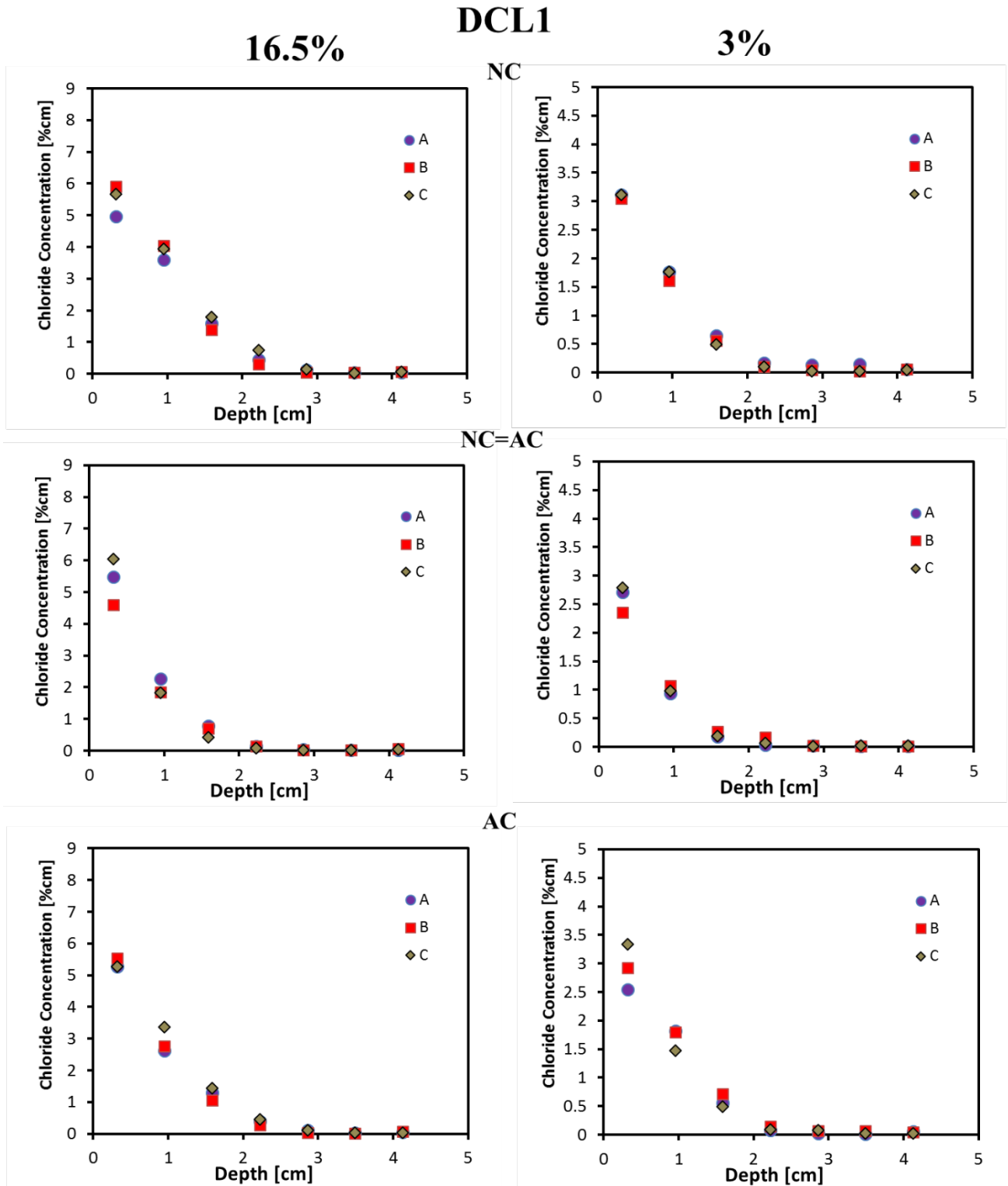


Figure E.1: Continued

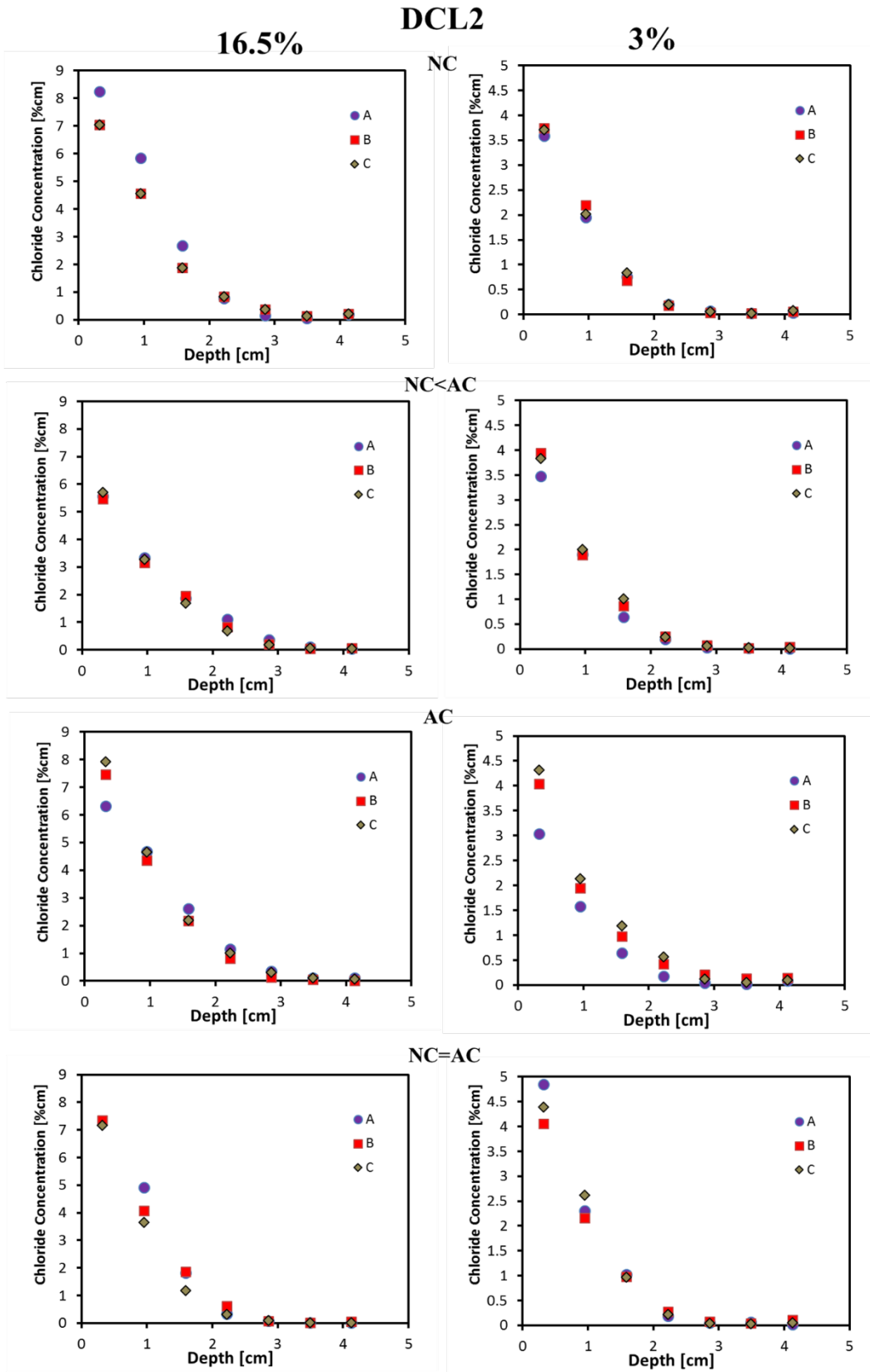


Figure E.1: Continued

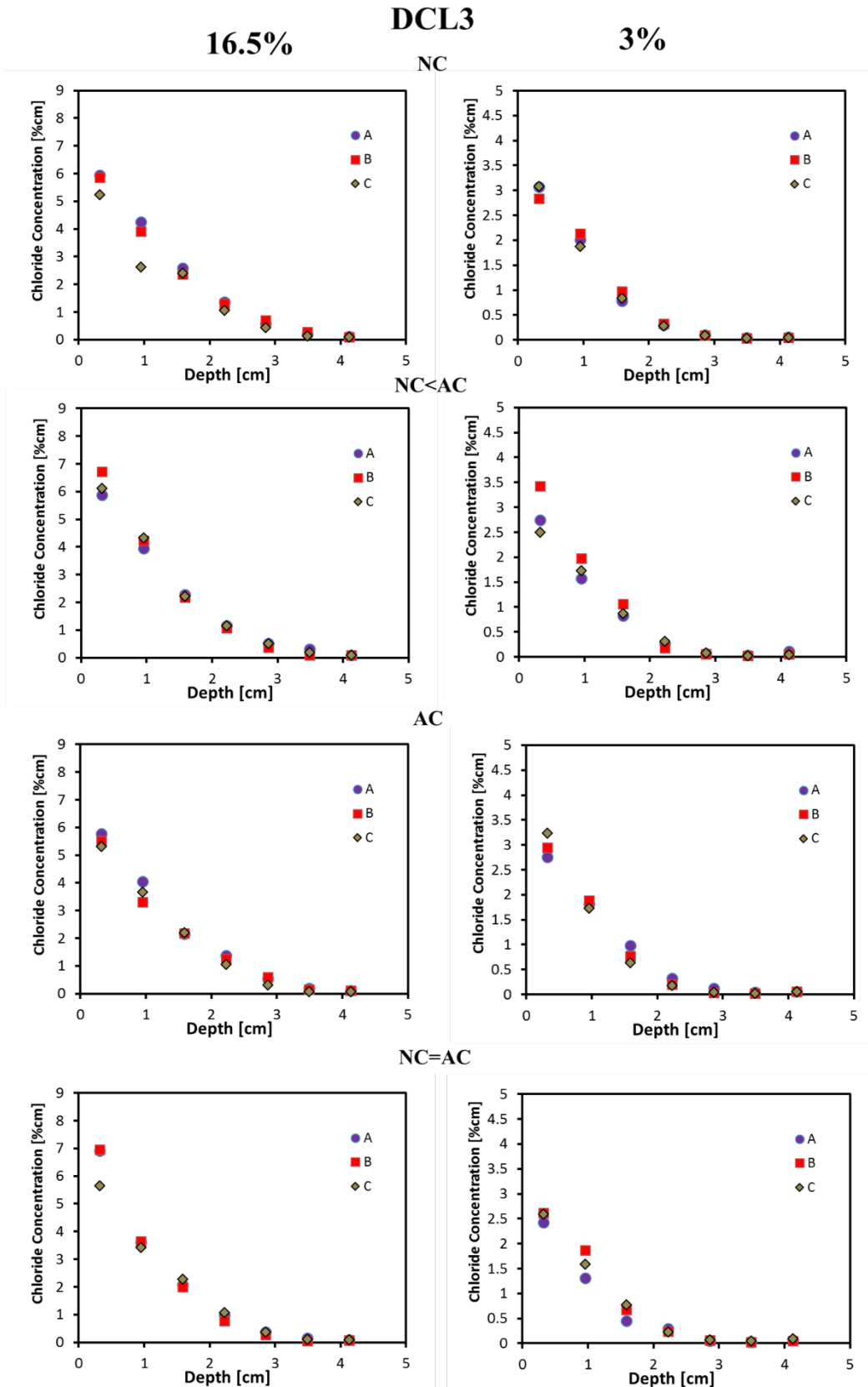


Figure E.1: Continued

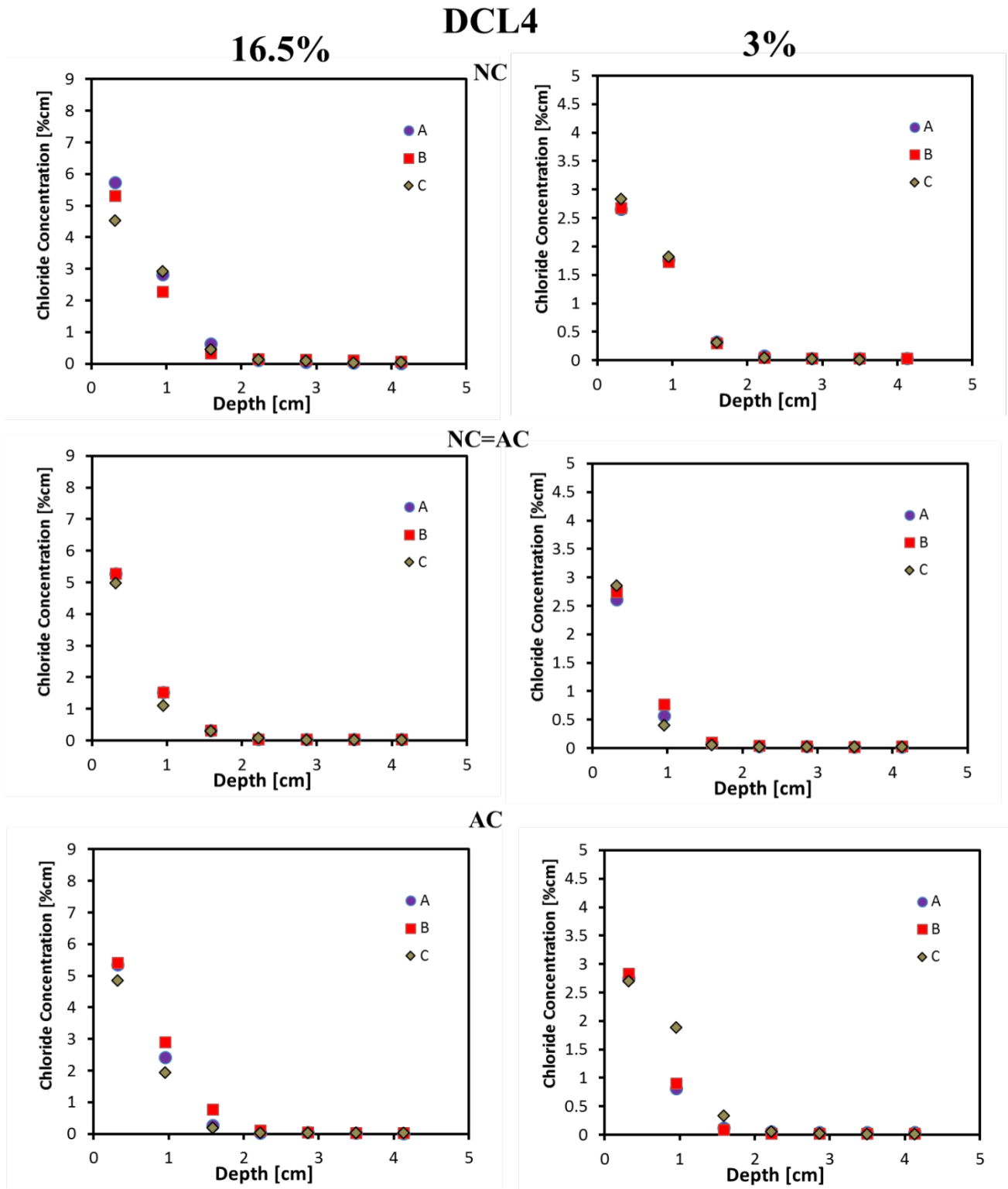


Figure E.1: Continued

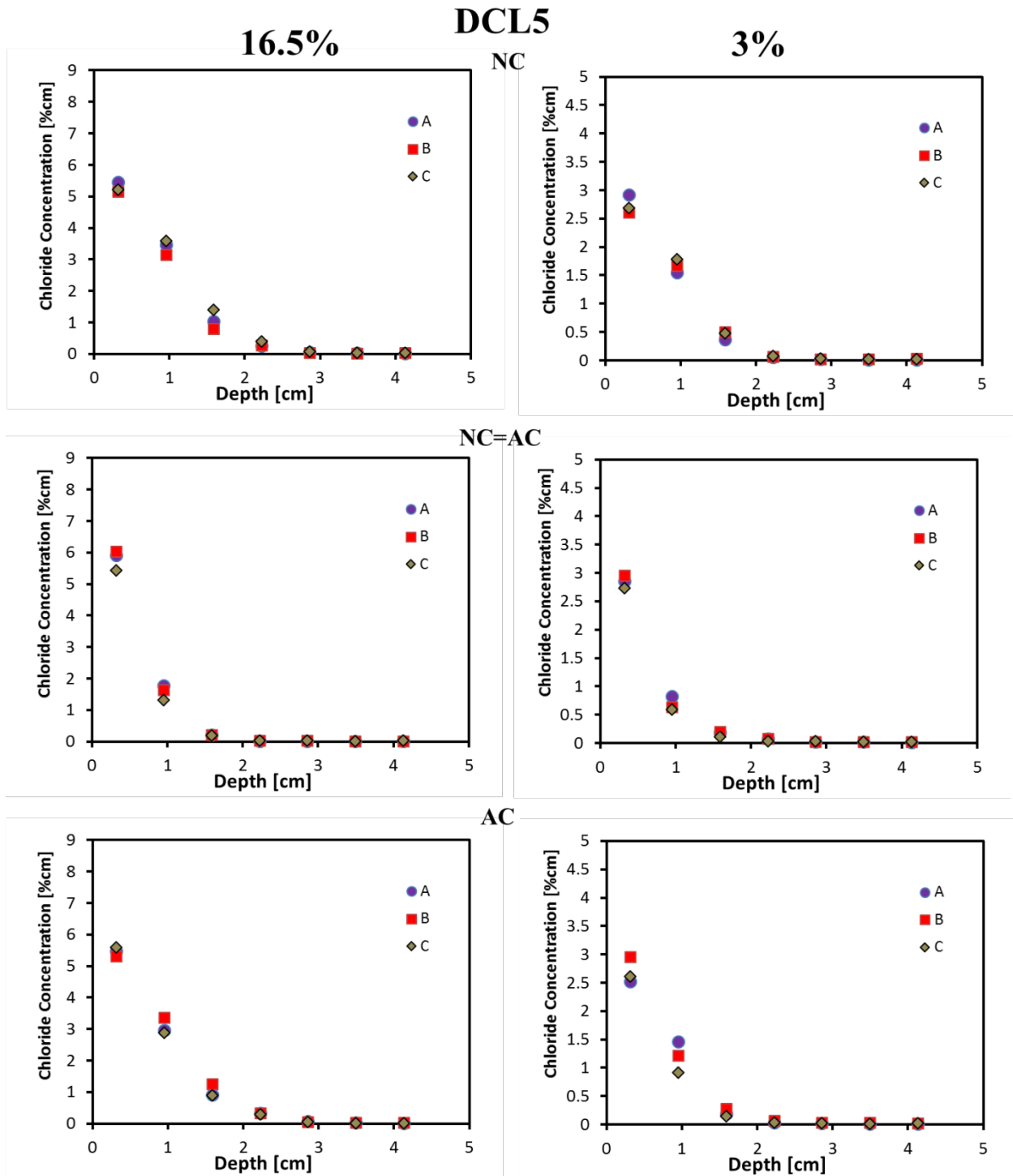


Figure E.1: Continued

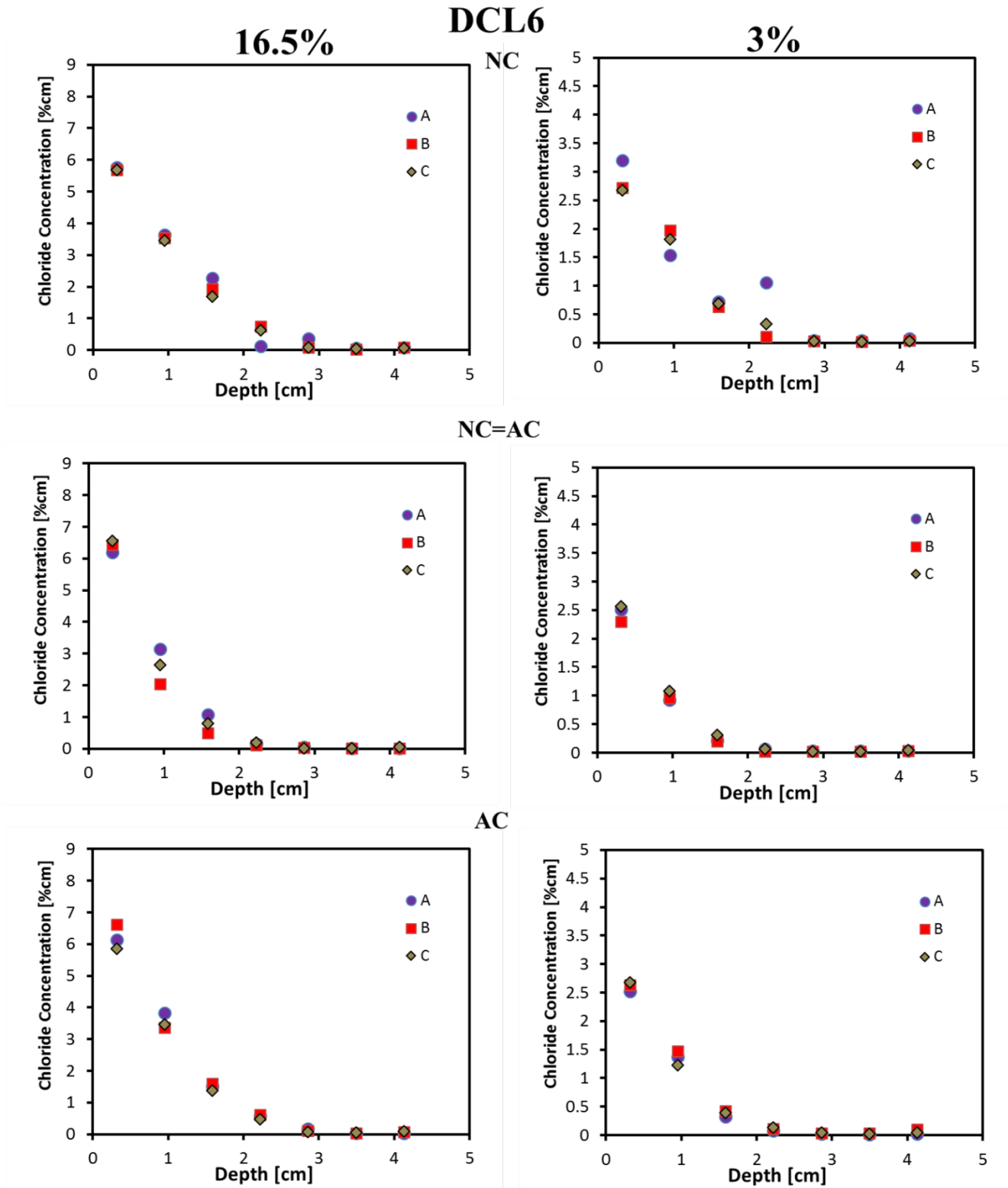


Figure E.1: Continued

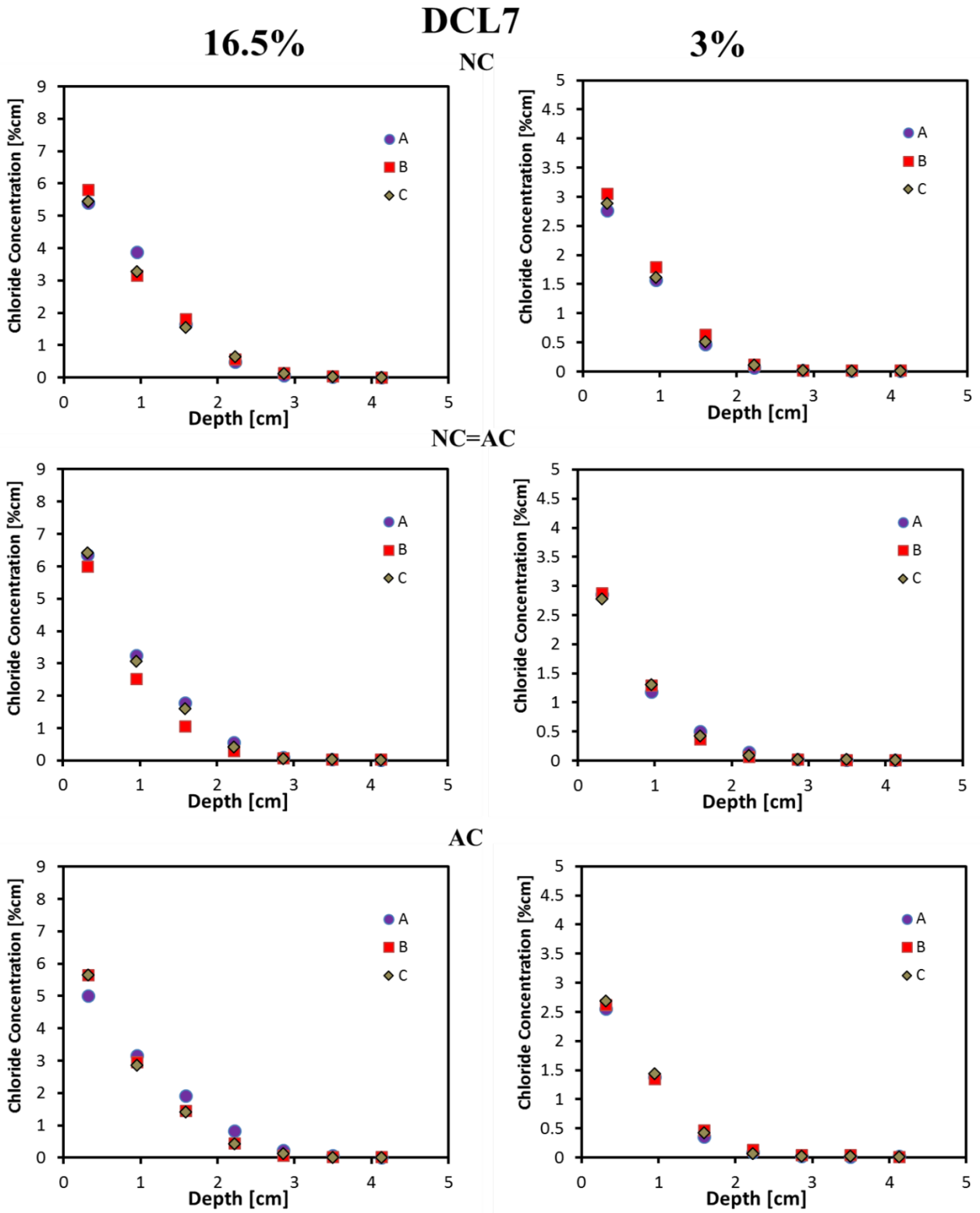


Figure E.1: Continued

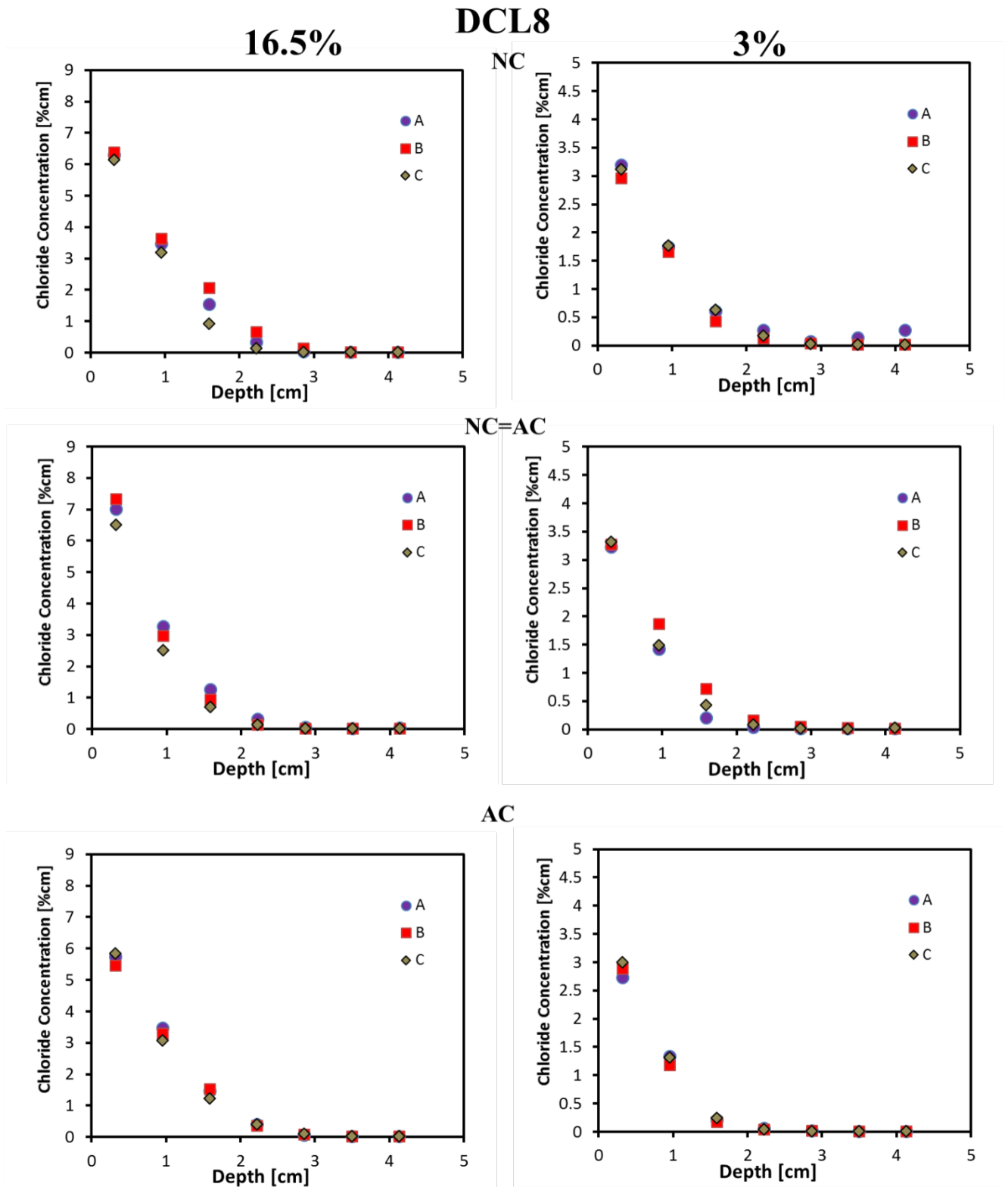


Figure E.1: Continued

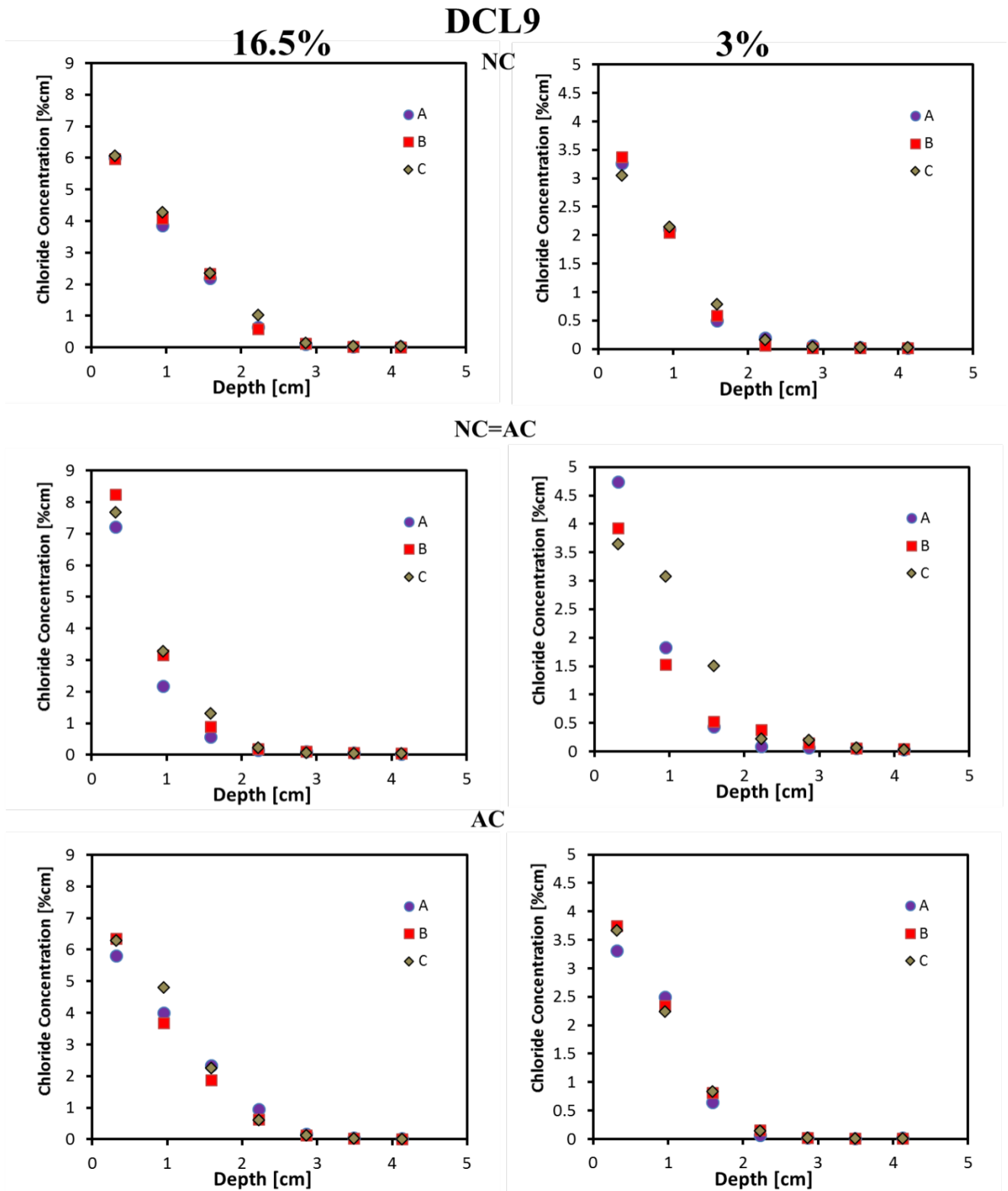


Figure E.1: Continued

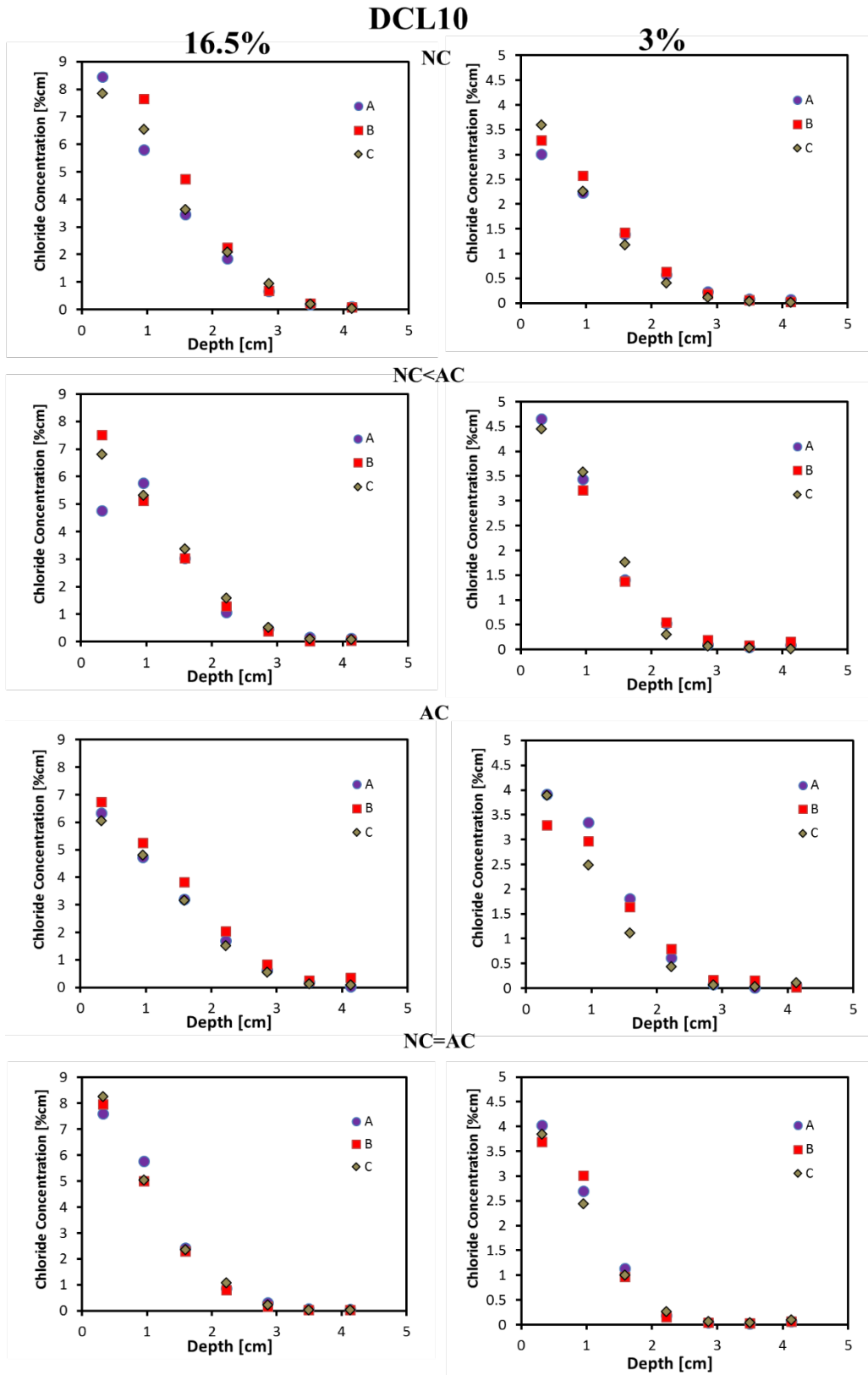


Figure E.1: Continued

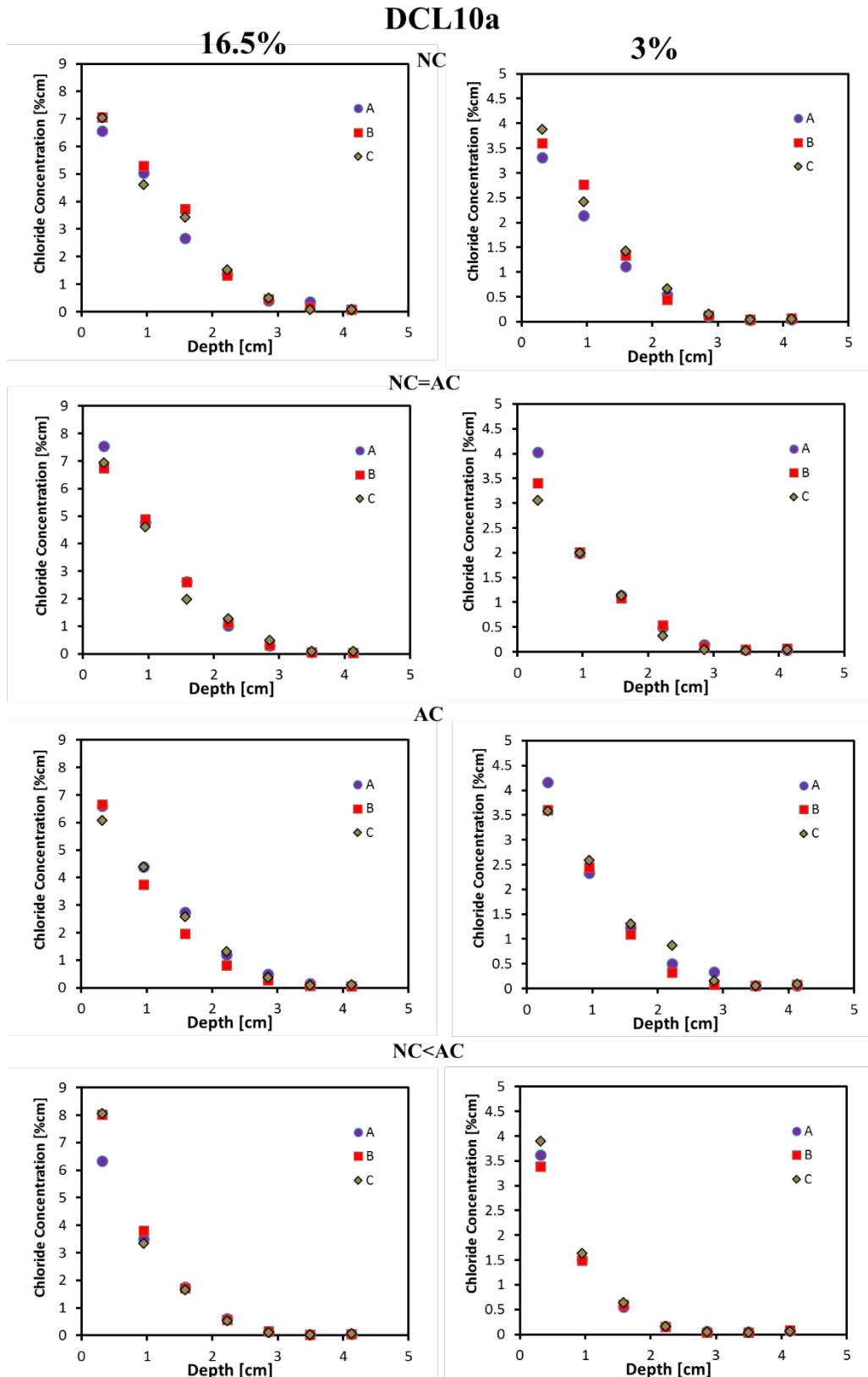


Figure E.1: Continued

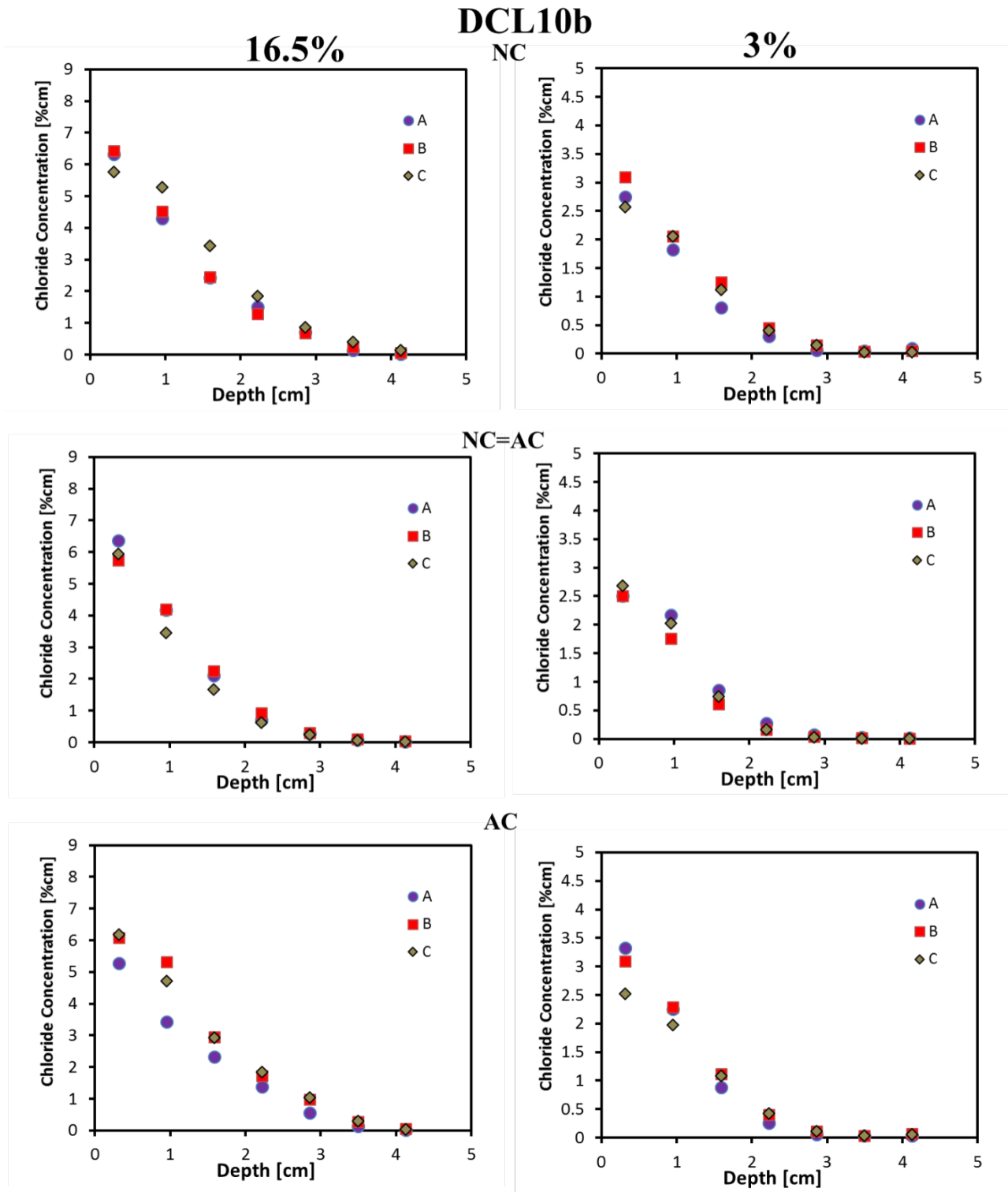
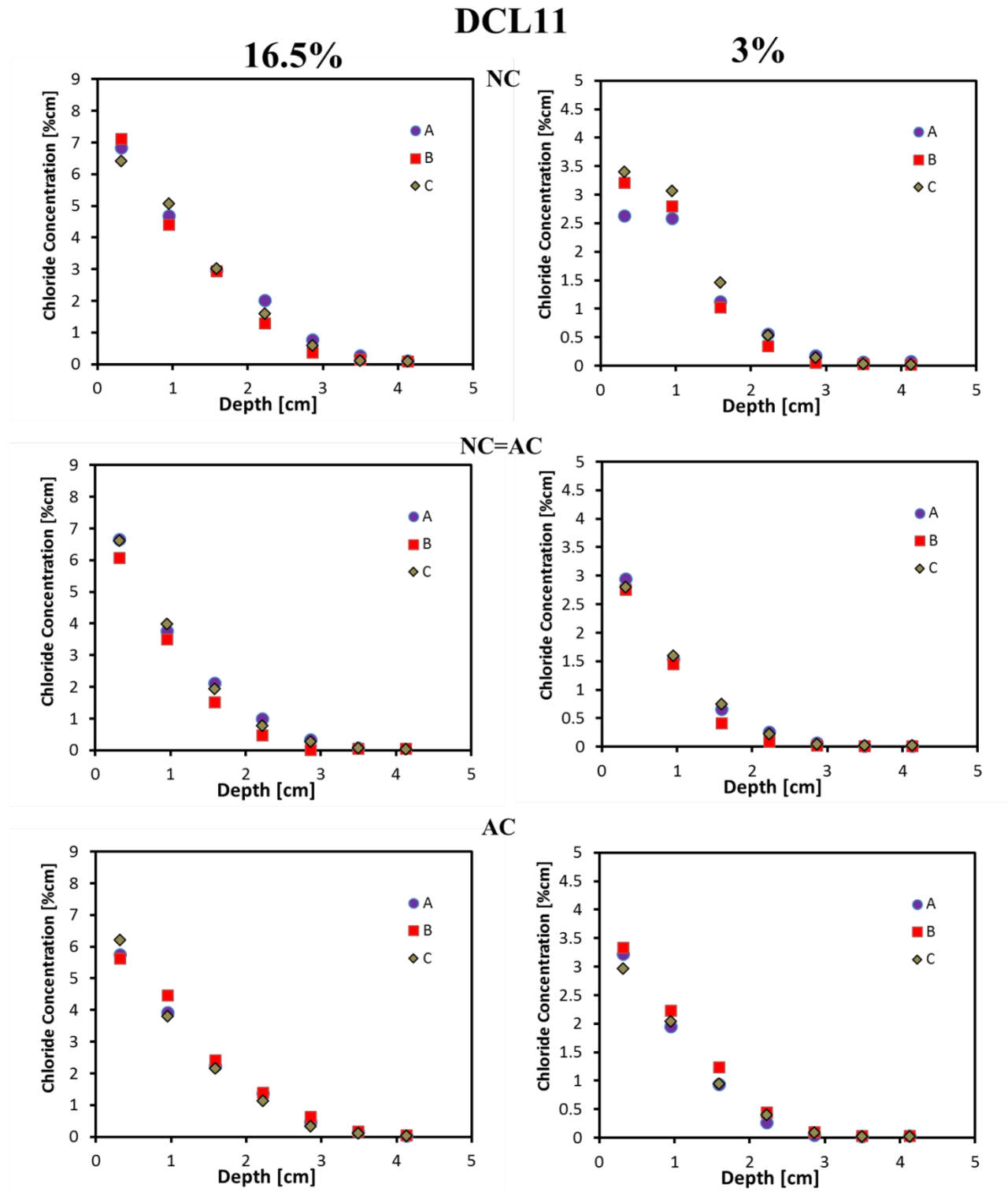


Figure E.1: Continued



### Appendix F: Chloride Profiles for Tidal Simulated Exposure

Figure F.1: Chloride profiles vs. elevation: Tidal simulation DCL1, 2, 4, 5, 7, 8, 10a, 10b, 11, and FA

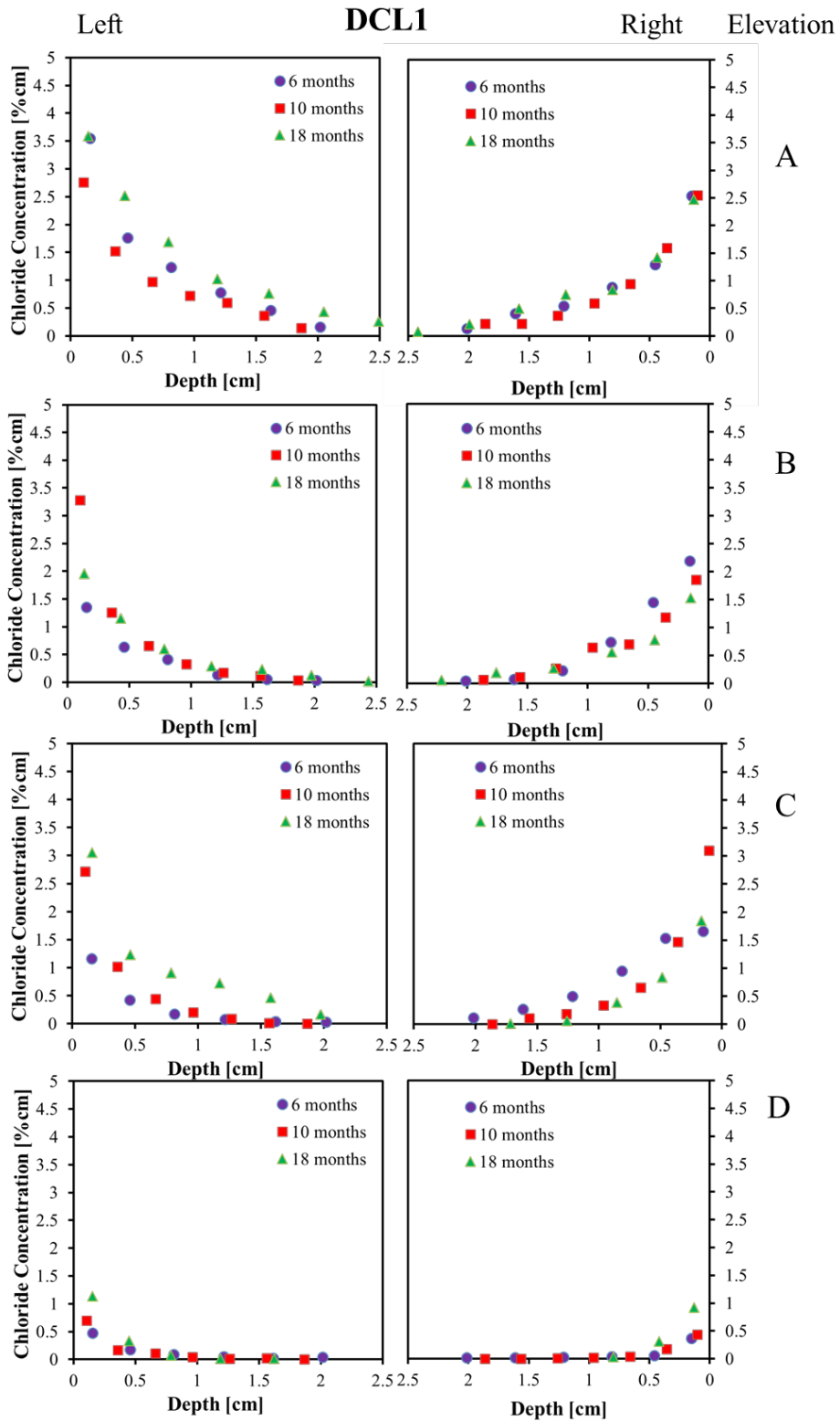








Figure F.1: Continued

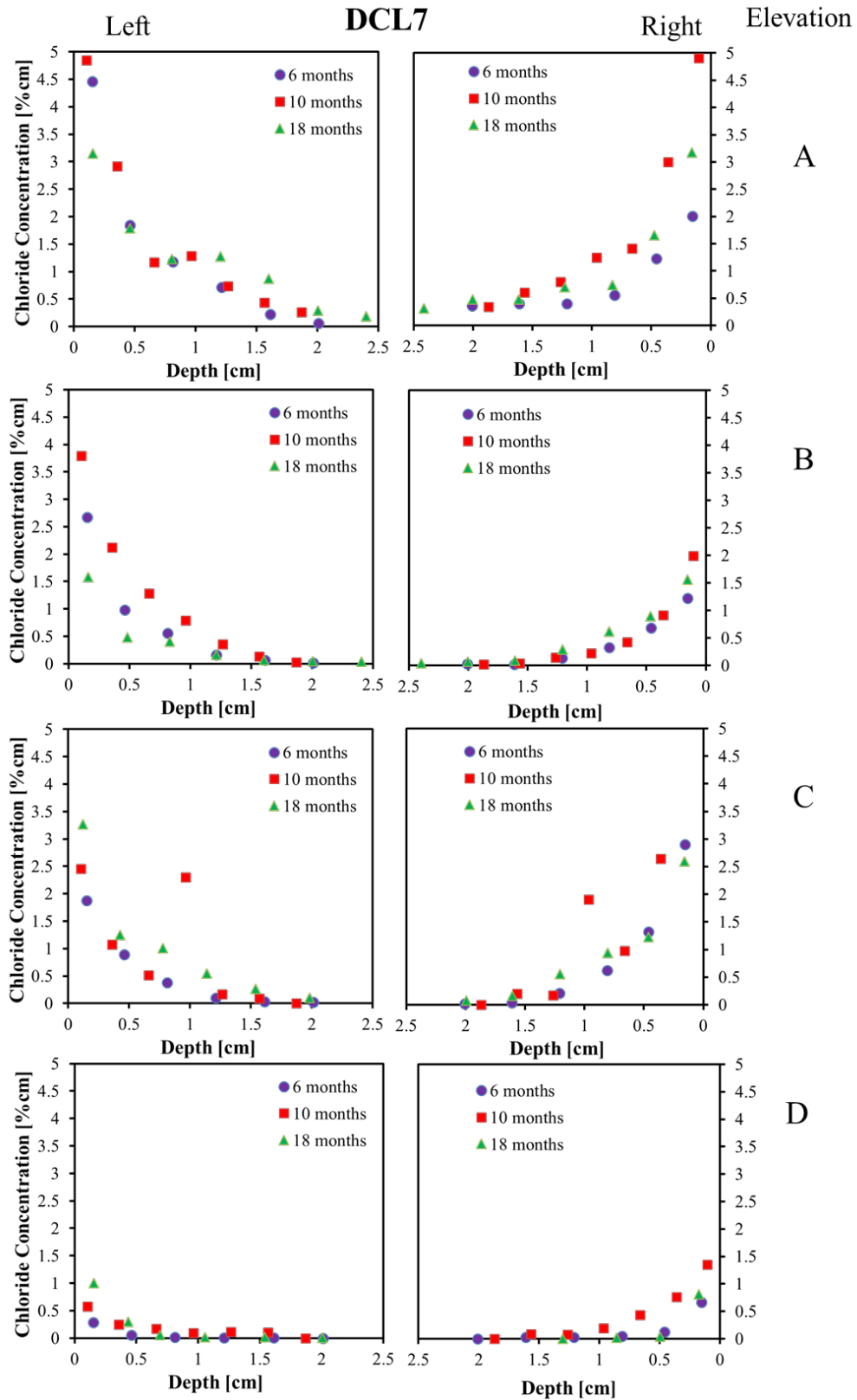




Figure F.1: Continued

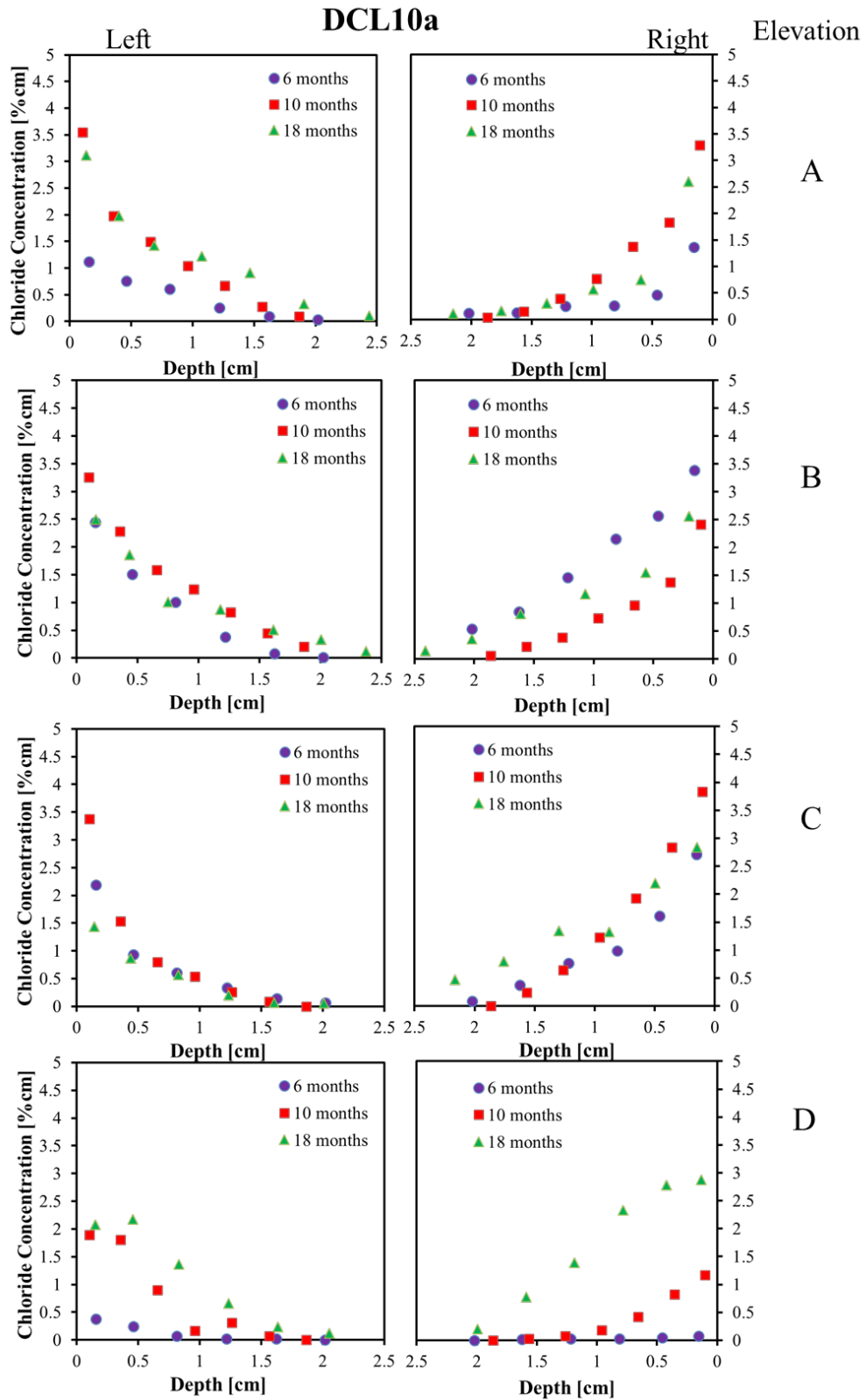


Figure F.1: Continued

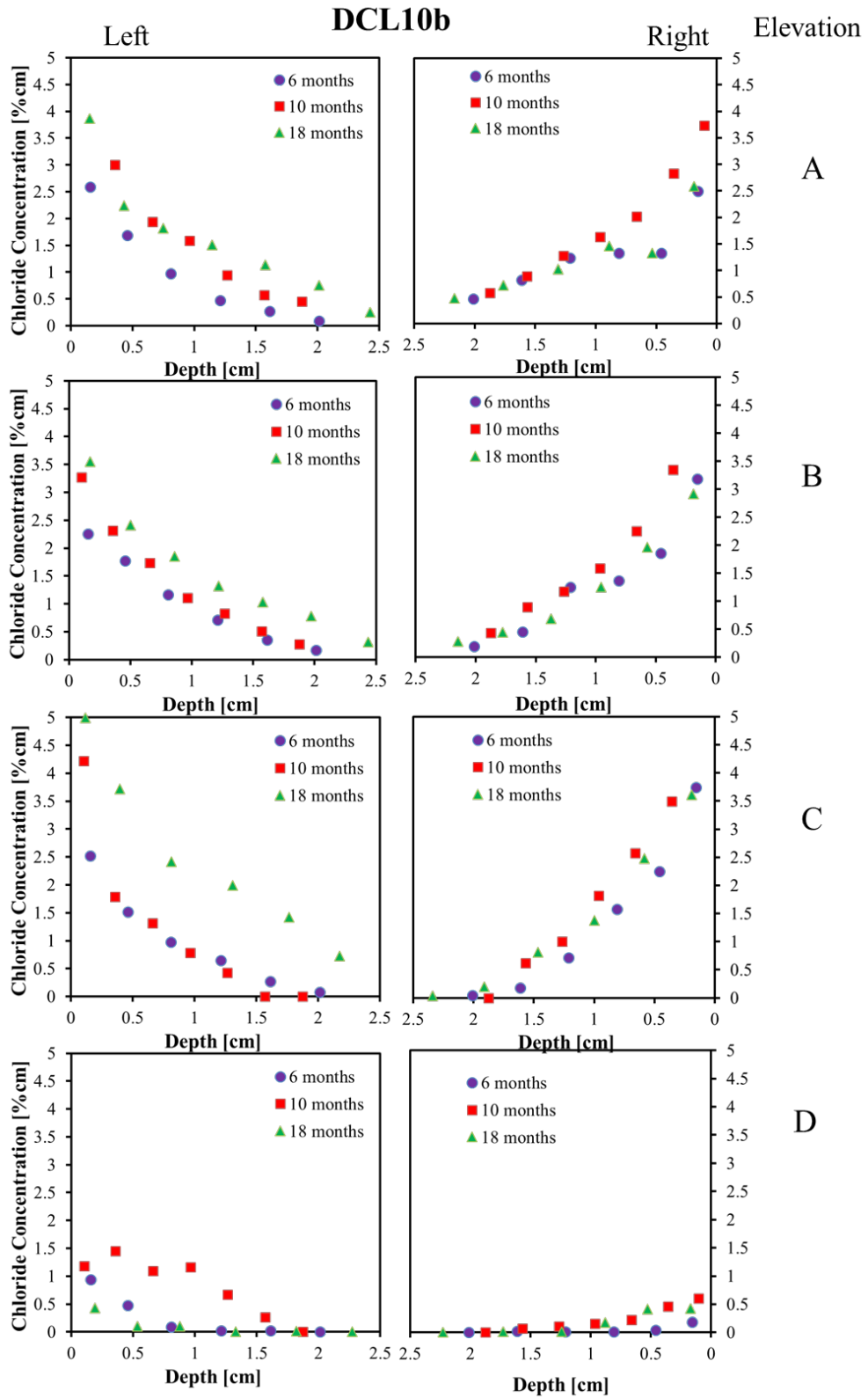
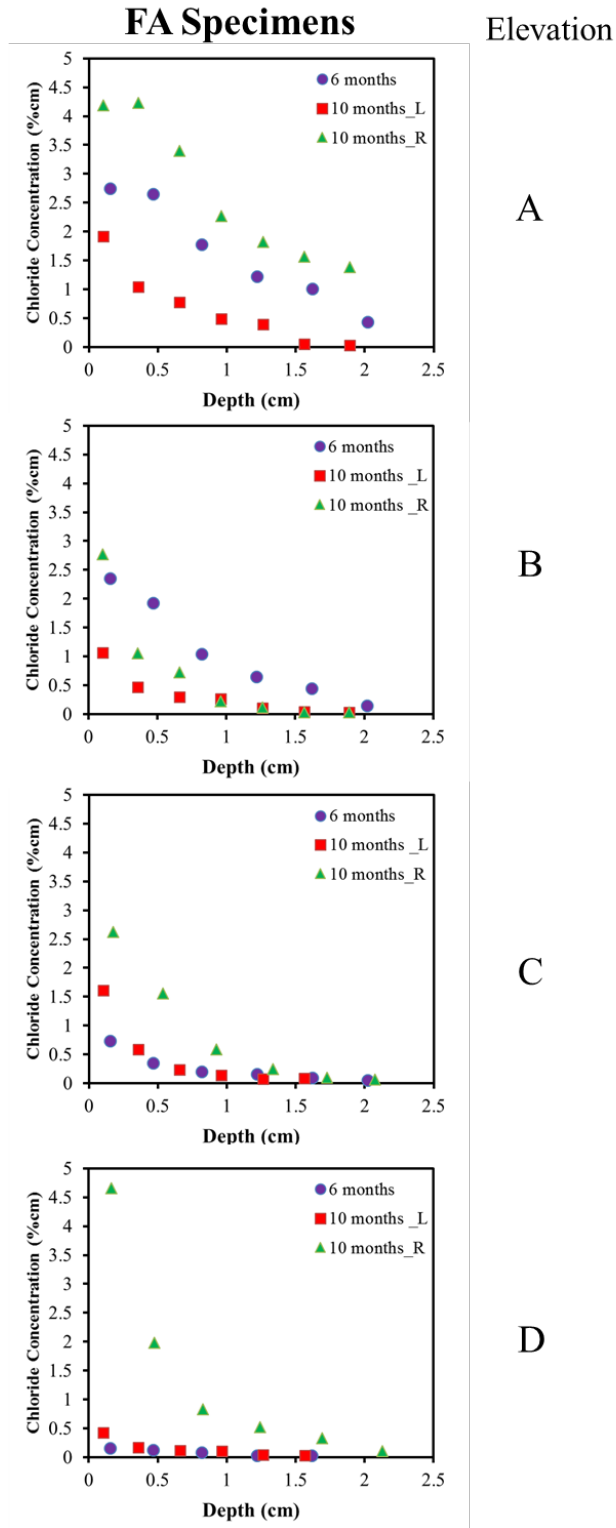




Figure F.1: Continued



## Appendix G: Chloride Profiles for Splash Simulated Exposure

Figure G.1: Chloride profiles vs. elevation: splash simulation DCL1, 2, 4, 5, 7, 8, 10b, and 11

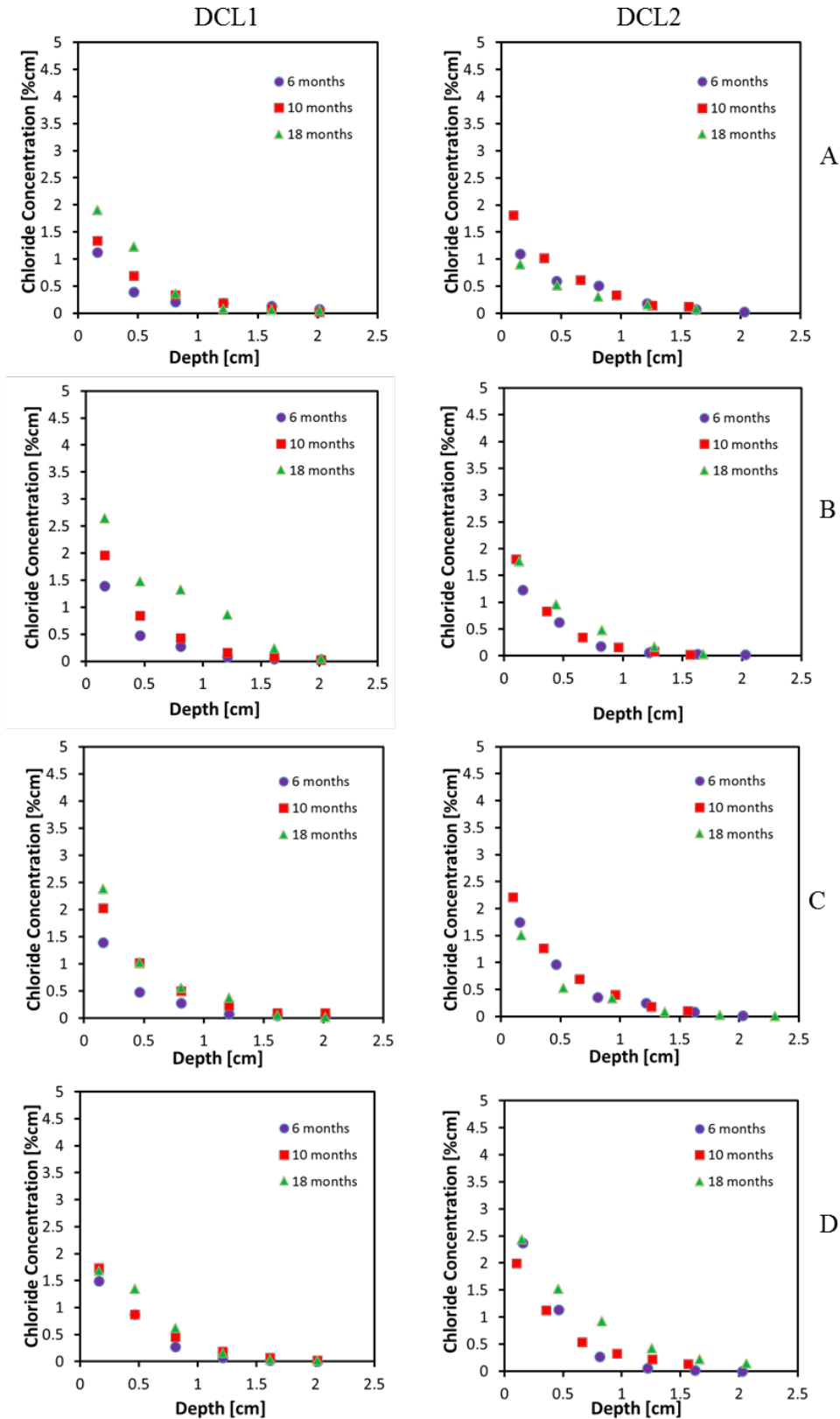


Figure G.1: Continued

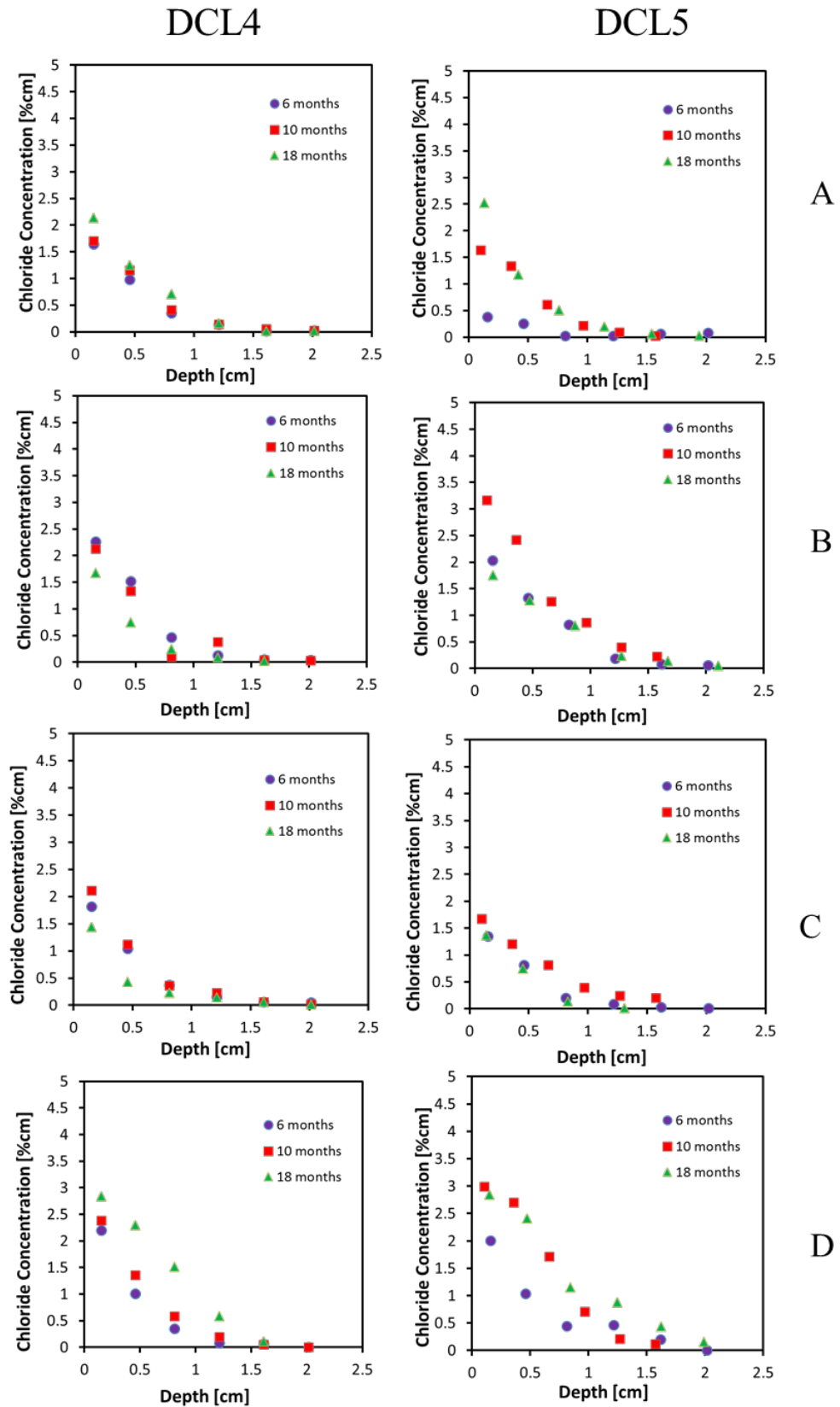


Figure G.1: Continued

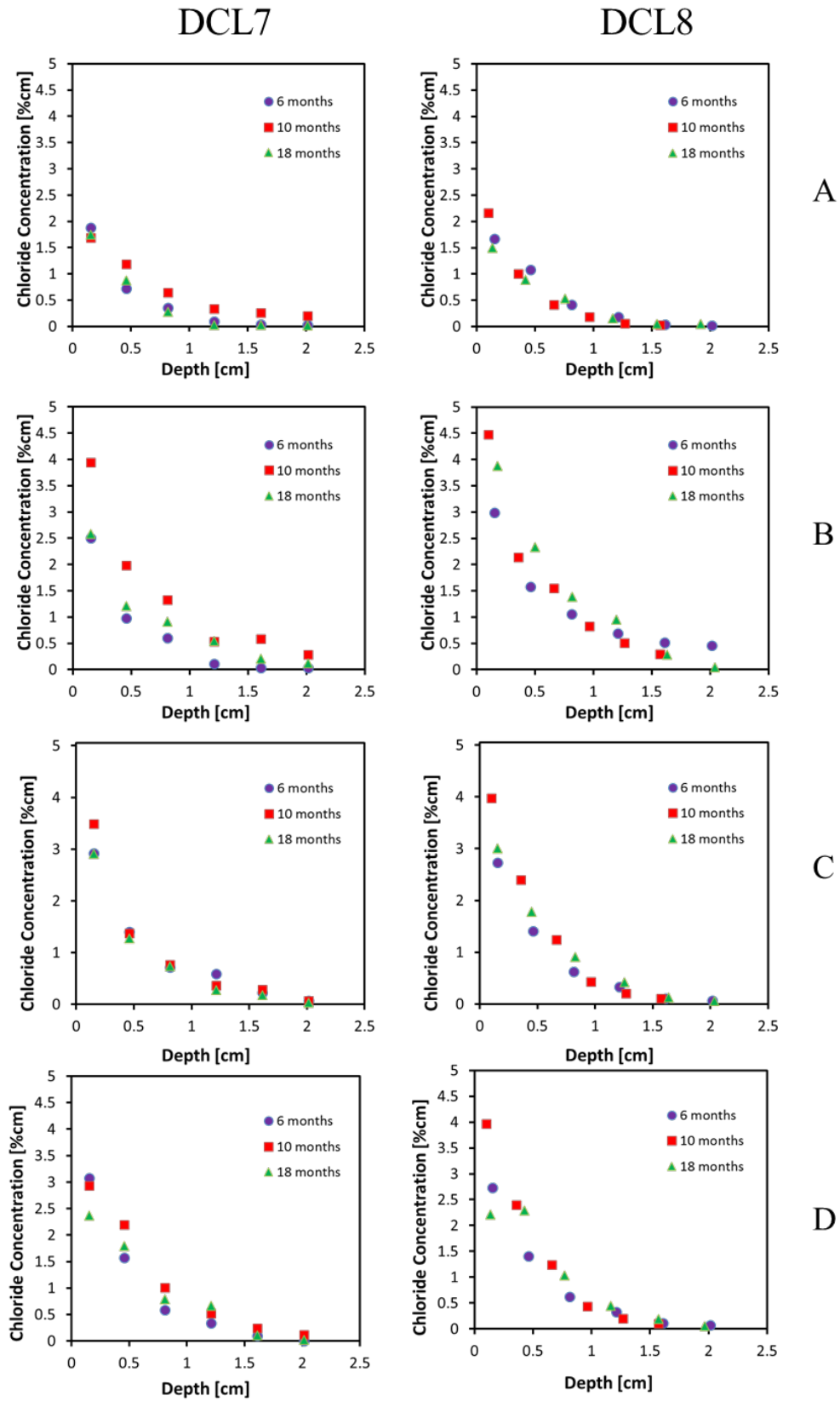
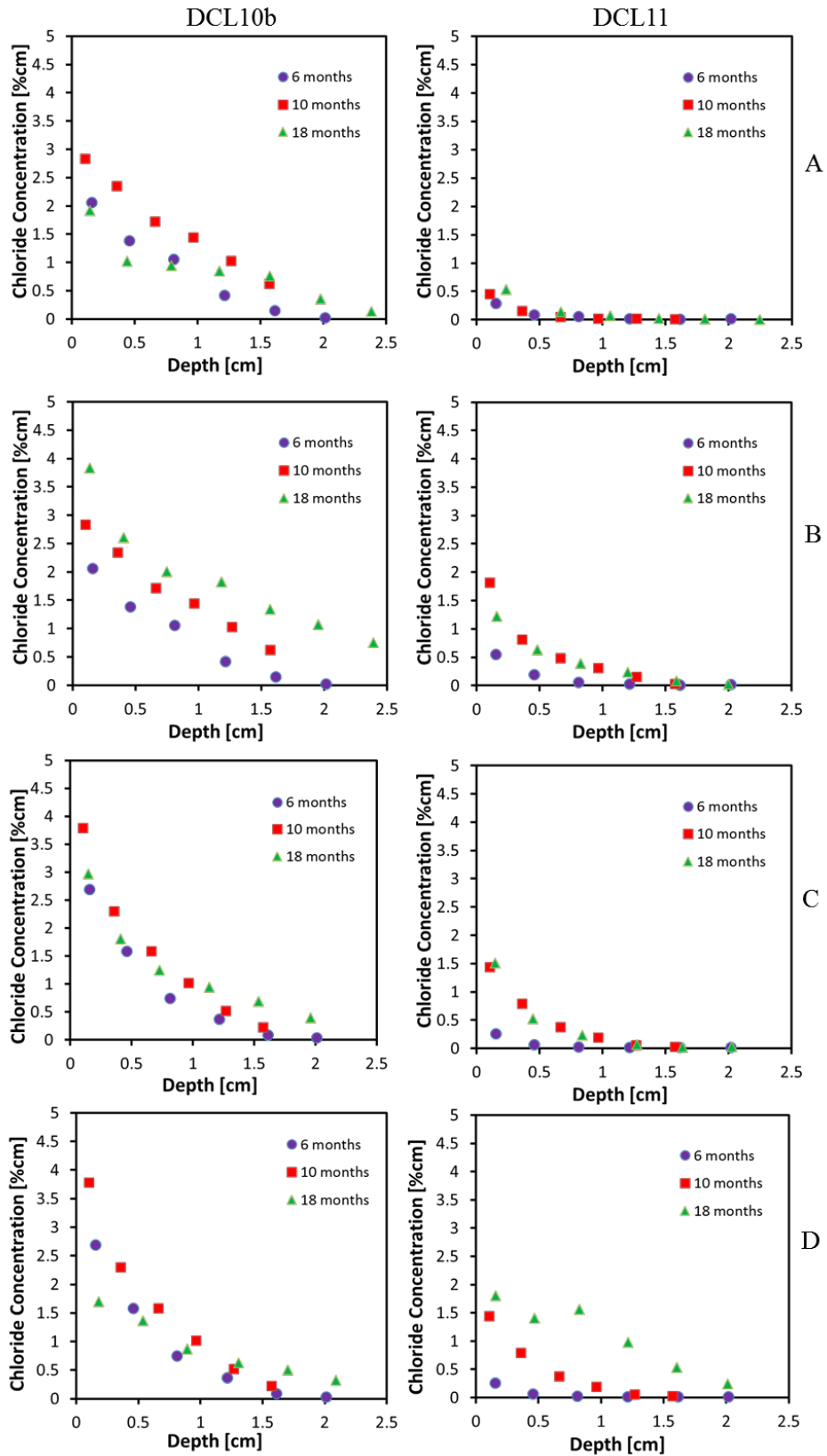


Figure G.1: Continued



## Appendix H: Chloride Profiles for Specimens Exposed at Barge

Figure H.1: Chloride profiles vs. elevation: barge simulation FA and FA+SF specimens

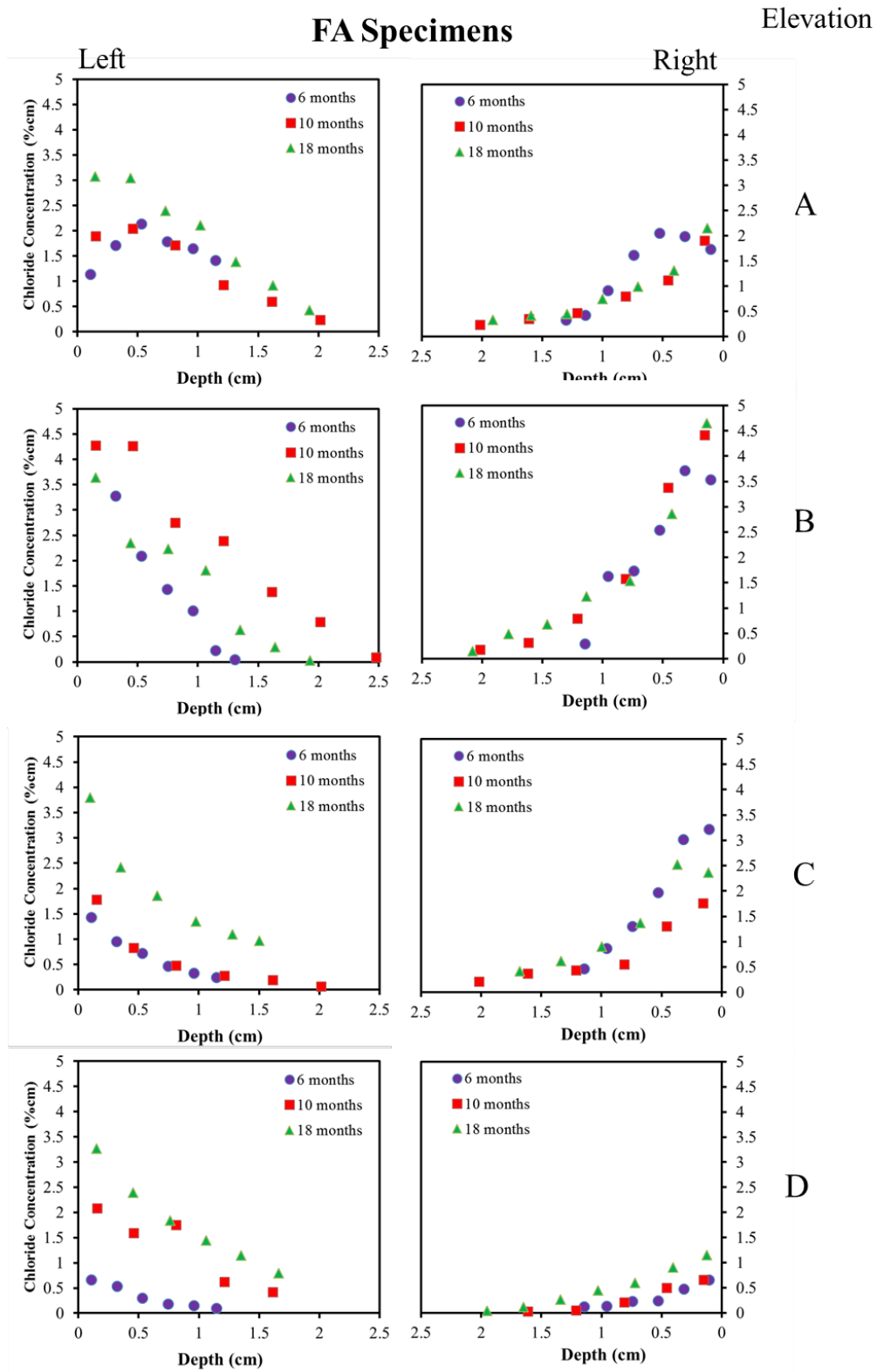
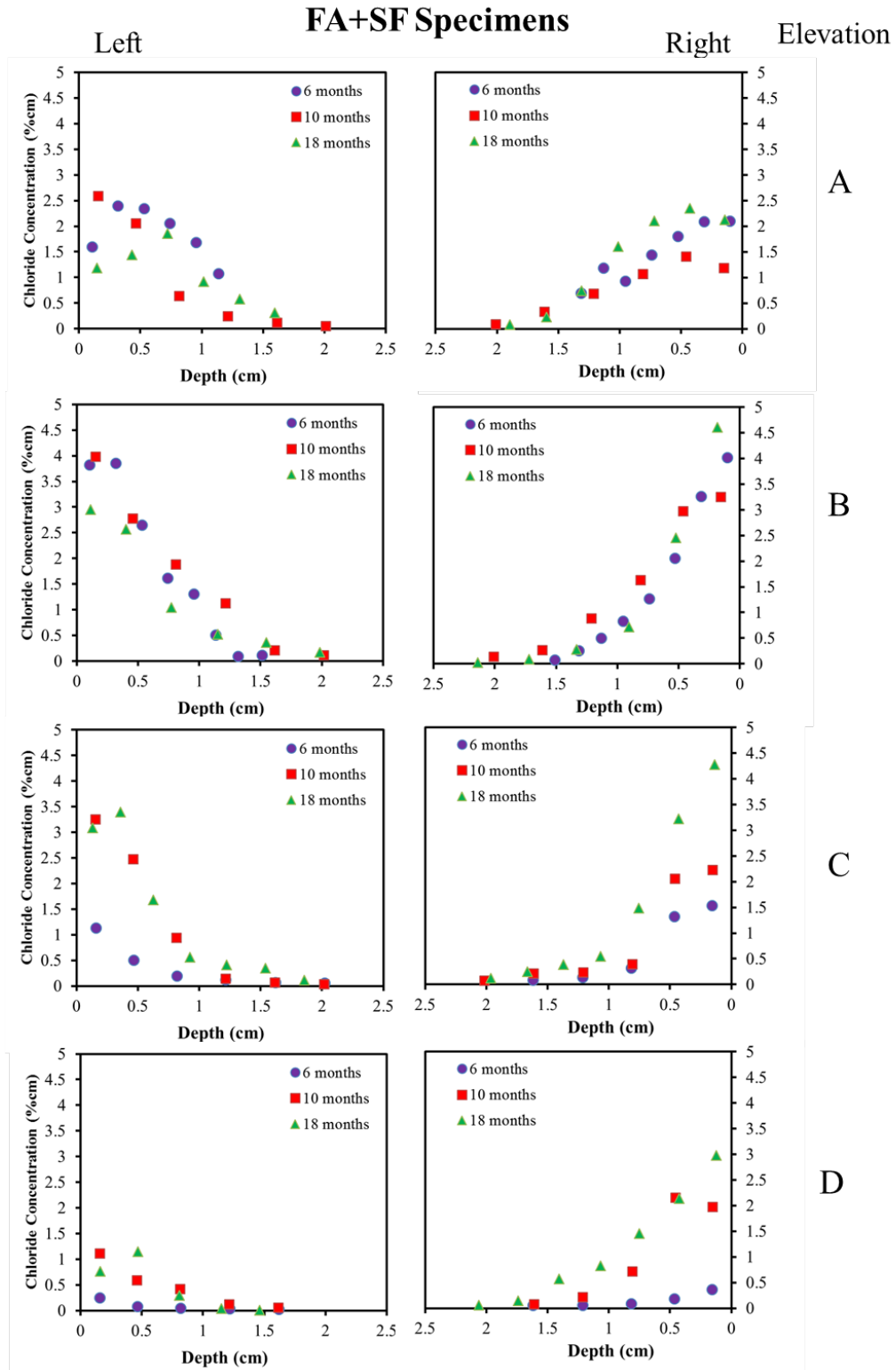


Figure H.1: Continued



## Appendix I: Inverse Resistivity vs. Time (Log-Log Scale)

Figure I.1: Conductivity (1/resistivity) vs. time for all mixtures

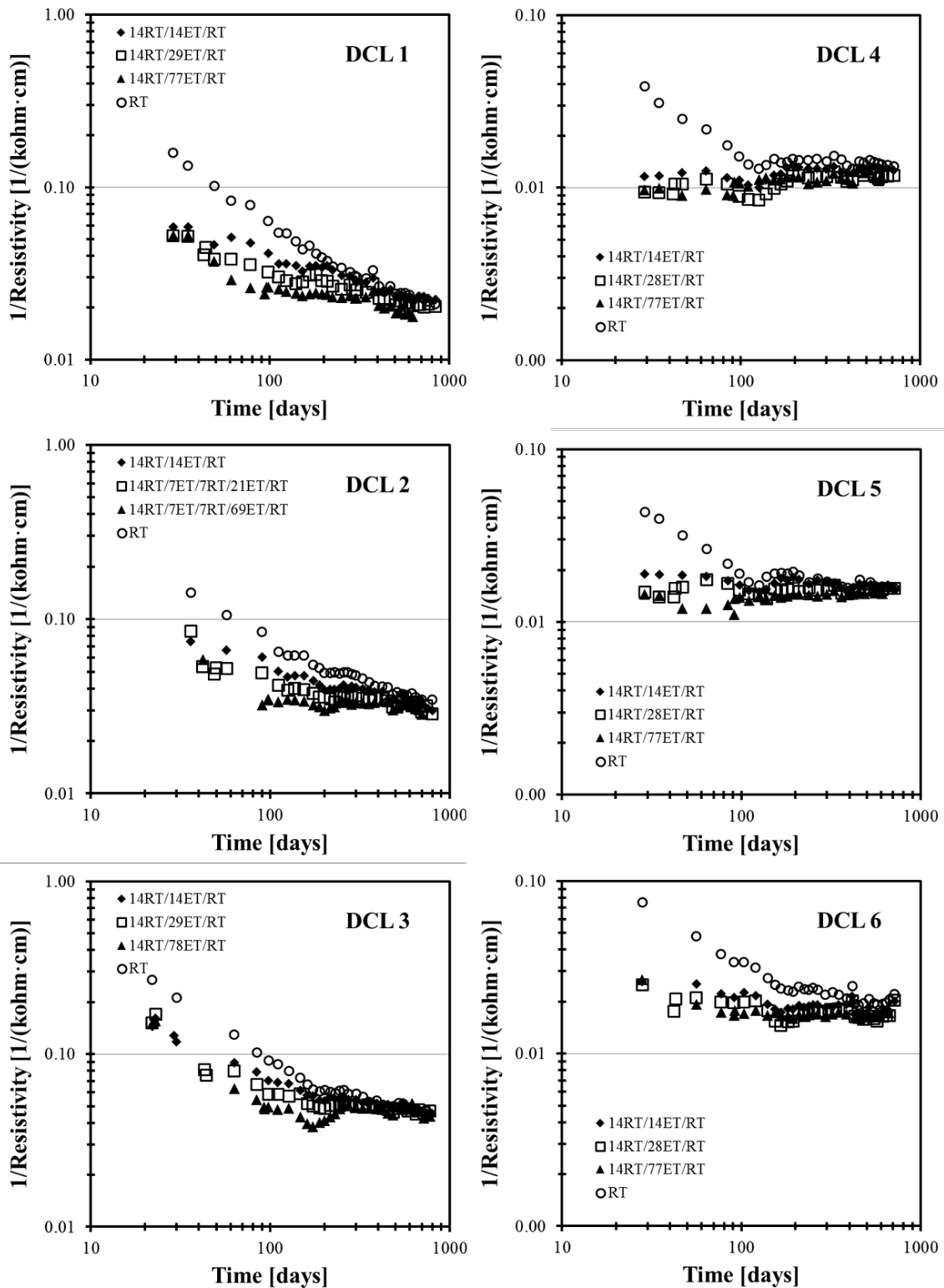
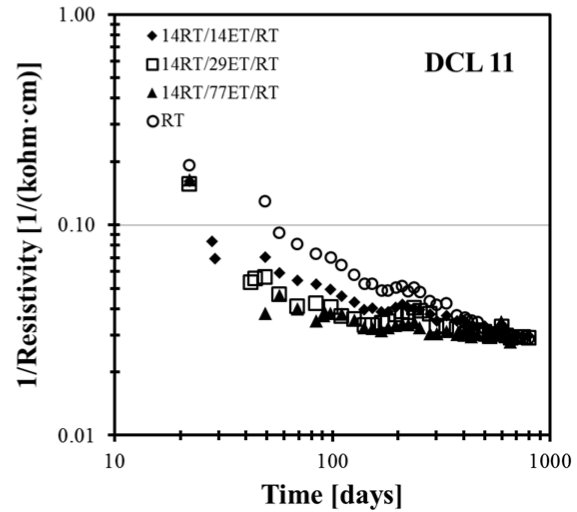
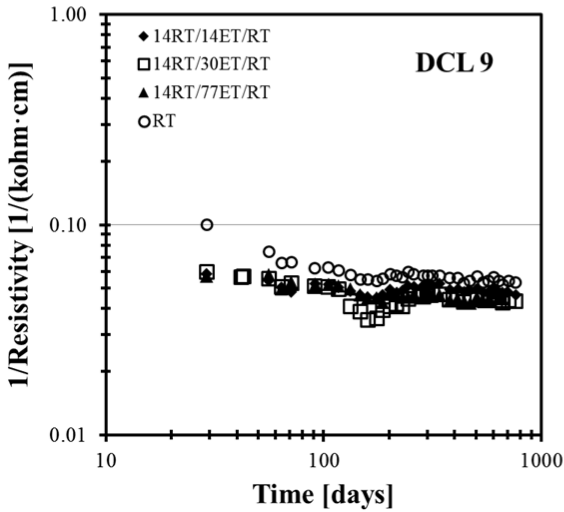
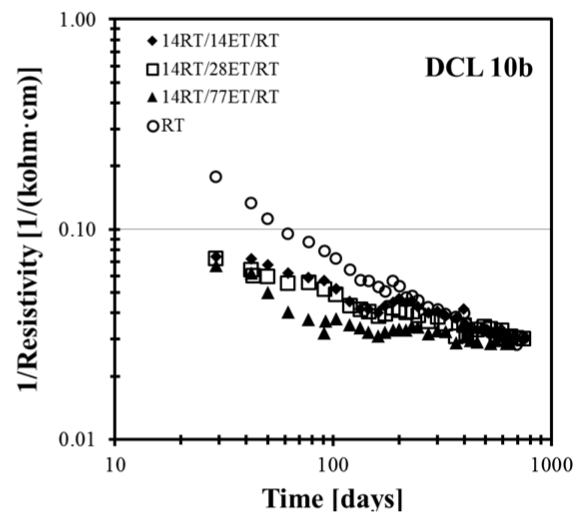
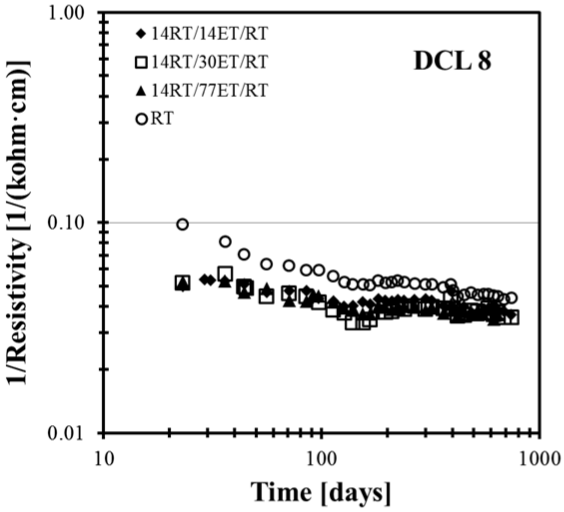
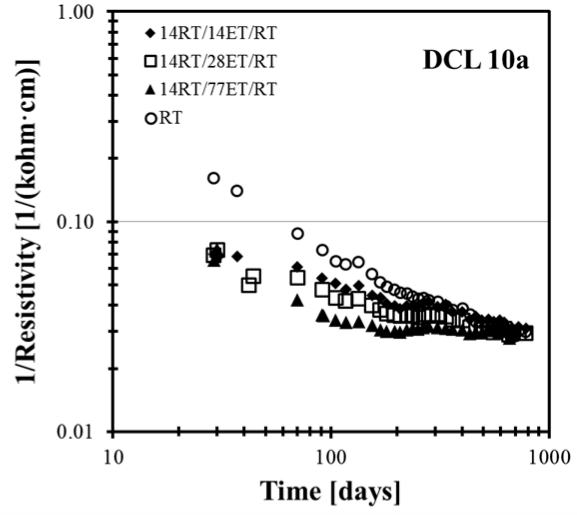
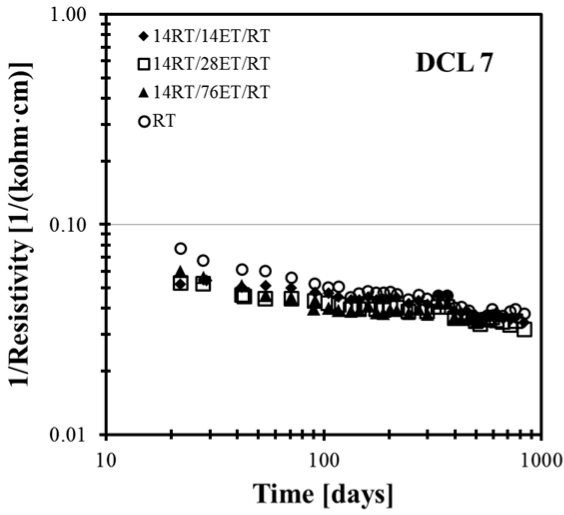


Figure I.1: Continued



**Appendix J: Apparent Diffusivity Coefficient of Specimens Exposed at SMO**

Table J.1:  $D_{app}$  for specimens exposed to bulk diffusion and RT cured for 28 days

Tops in 3.0% salinity / Bottoms 16.5% salinity									
28 day normal cure									
Mix #	Sample:	Location	Cast date:	Age:	Start date:	Exposure time:	End date:	Diffusion Coefficient - Chlorides (m <sup>2</sup> /sec):	Average:
DCL 02	(NC) A bot	Tank 1	9/22/2011	35	10/27/2011	364	10/25/2012	3.14E-12	3.41E-12
	(NC) B bot							4.205E-12	
	(NC) C bot							2.886E-12	
	(NC) A top	Tank 2	9/22/2011	35	10/27/2011	364	10/25/2012	2.097E-12	
	(NC) B top							2.079E-12	
	(NC) C top							2.143E-12	
DCL 10	(NC) A bot	Tank 1	9/28/2011	35	11/2/2011	364	10/31/2012	4.281E-12	4.749E-12
	(NC) B bot							4.774E-12	
	(NC) C bot							5.193E-12	
	(NC) A top	Tank 2	9/28/2011	35	11/2/2011	364	10/31/2012	4.447E-12	
	(NC) B top							3.02E-12	
	(NC) C top							4.248E-12	
DCL 10a	(NC) A bot	Tank 1	10/12/2011	35	11/16/2011	364	11/14/2012	4.341E-12	4.536E-12
	(NC) B bot							4.71E-12	
	(NC) C bot							4.556E-12	
	(NC) A top	Tank 2	10/12/2011	35	11/16/2011	364	11/14/2012	3.314E-12	
	(NC) B top							3.552E-12	
	(NC) C top							3.485E-12	
DCL 03	(NC) A bot	Tank 1	10/19/2011	35	11/23/2011	364	11/21/2012	4.65E-12	4.445E-12
	(NC) B bot							4.155E-12	
	(NC) C bot							4.53E-12	
	(NC) A top	Tank 2	10/19/2011	35	11/23/2011	364	11/21/2012	2.716E-12	
	(NC) B top							3.35E-12	
	(NC) C top							2.639E-12	
DCL 06	(NC) A bot	Tank 1	10/26/2011	35	11/30/2011	364	11/28/2012	3.07E-12	2.994E-12
	(NC) B bot							3.122E-12	
	(NC) C bot							2.791E-12	
	(NC) A top	Tank 2	10/26/2011	35	11/30/2011	364	11/28/2012	3.03E-12	
	(NC) B top							2.551E-12	
	(NC) C top							2.808E-12	
DCL 09	(NC) A bot	Tank 1	11/2/2011	35	12/7/2011	364	12/5/2012	3.191E-12	3.425E-12
	(NC) B bot							3.356E-12	
	(NC) C bot							3.727E-12	
	(NC) A top	Tank 2	11/2/2011	35	12/7/2011	364	12/5/2012	2.146E-12	
	(NC) B top							2.027E-12	
	(NC) C top							2.662E-12	
DCL 11	(NC) A bot	Tank 1	11/9/2011	35	12/14/2011	364	12/12/2012	4.951E-12	4.645E-12
	(NC) B bot							3.881E-12	
	(NC) C bot							5.104E-12	
	(NC) A top	Tank 2	11/9/2011	35	12/14/2011	364	12/12/2012	4.623E-12	
	(NC) B top							3.399E-12	
	(NC) C top							4.151E-12	

Table J.1: Continued

Tops in 3.0% salinity / Bottoms 16.5% salinity									
28 day normal cure									
Mix #	Sample:	Location	Cast date:	Age:	Start date:	Exposure time:	End date:	Diffusion Coefficient - Chlorides (m <sup>2</sup> /sec):	Average:
DCL 10b	(NC) A bot	Tank 1	11/16/2011	35	12/21/2011	364	12/19/2012	4.379E-12	5.06E-12
	(NC) B bot							4.224E-12	
	(NC) C bot							6.577E-12	
	(NC) A top	Tank 2	11/16/2011	35	12/21/2011	364	12/19/2012	2.687E-12	
	(NC) B top							3.487E-12	
	(NC) C top							4.033E-12	
DCL 08	(NC) A bot	Tank 1	11/22/2011	35	12/27/2011	364	12/25/2012	2.235E-12	2.265E-12
	(NC) B bot							2.822E-12	
	(NC) C bot							1.739E-12	
	(NC) A top	Tank 2	11/22/2011	35	12/27/2011	364	12/25/2012	2.107E-12	
	(NC) B top							1.856E-12	
	(NC) C top							2.119E-12	
DCL 01	(NC) A bot	Tank 1	12/7/2011	35	1/11/2012	364	1/9/2013	3.106E-12	2.945E-12
	(NC) B bot							2.525E-12	
	(NC) C bot							3.204E-12	
	(NC) A top	Tank 2	12/7/2011	35	1/11/2012	364	1/9/2013	2.159E-12	
	(NC) B top							1.883E-12	
	(NC) C top							1.898E-12	
DCL 07	(NC) A bot	Tank 1	12/14/2011	35	1/18/2012	364	1/16/2013	3.014E-12	2.827E-12
	(NC) B bot							2.684E-12	
	(NC) C bot							2.784E-12	
	(NC) A top	Tank 2	12/14/2011	35	1/18/2012	364	1/16/2013	1.929E-12	
	(NC) B top							2.138E-12	
	(NC) C top							1.953E-12	
DCL 04	(NC) A bot	Tank 1	12/21/2011	35	1/25/2012	364	1/23/2013	1.55E-12	1.58E-12
	(NC) B bot							1.258E-12	
	(NC) C bot							1.931E-12	
	(NC) A top	Tank 2	12/21/2011	35	1/25/2012	364	1/23/2013	2.018E-12	
	(NC) B top							1.924E-12	
	(NC) C top							1.911E-12	
DCL 05	(NC) A bot	Tank 1	12/21/2011	35	1/25/2012	364	1/23/2013	2.237E-12	2.347E-12
	(NC) B bot							2.056E-12	
	(NC) C bot							2.748E-12	
	(NC) A top	Tank 2	12/21/2011	35	1/25/2012	364	1/23/2013	1.669E-12	
	(NC) B top							2.164E-12	
	(NC) C top							2.199E-12	

Table J.2:  $D_{app}$  for specimens exposed to bulk diffusion and AC cured (14RT/14ET)

Tops in 3.0% salinity / Bottoms 16.5% salinity									
14 day normal / 14 day accelerated									
Mix #	Sample:	Location	Cast date:	Age:	Start date:	Exposure time:	End date:	Diffusion Coefficient - Chlorides (m <sup>2</sup> /sec):	Average:
DCL 02	(AC) A bot	Tank 1	9/22/2011	35	10/27/2011	364	10/25/2012	4.088E-12	3.202E-12
	(AC) B bot							2.729E-12	
	(AC) C bot							2.791E-12	
	(AC) A top	Tank 2	9/22/2011	35	10/27/2011	364	10/25/2012	2.016E-12	
	(AC) B top							2.214E-12	
	(AC) C top							2.475E-12	
DCL 10	(AC) A bot	Tank 1	9/28/2011	35	11/2/2011	364	10/31/2012	5.21E-12	5.512E-12
	(AC) B bot							5.235E-12	
	(AC) C bot							6.091E-12	
	(AC) A top	Tank 2	9/28/2011	35	11/2/2011	364	10/31/2012	2.829E-12	
	(AC) B top							4.259E-12	
	(AC) C top							4.981E-12	
DCL 10a	(AC) A bot	Tank 1	10/12/2011	35	11/16/2011	364	11/14/2012	4.052E-12	3.717E-12
	(AC) B bot							4.315E-12	
	(AC) C bot							2.784E-12	
	(AC) A top	Tank 2	10/12/2011	35	11/16/2011	364	11/14/2012	2.837E-12	
	(AC) B top							4.05E-12	
	(AC) C top							2.914E-12	
DCL 03	(AC) A bot	Tank 1	10/19/2011	35	11/23/2011	364	11/21/2012	4.236E-12	4.223E-12
	(AC) B bot							4.086E-12	
	(AC) C bot							4.348E-12	
	(AC) A top	Tank 2	10/19/2011	35	11/23/2011	364	11/21/2012	3.266E-12	
	(AC) B top							2.546E-12	
	(AC) C top							2E-12	
DCL 06	(AC) A bot	Tank 1	10/26/2011	35	11/30/2011	364	11/28/2012	2.585E-12	2.397E-12
	(AC) B bot							2.22E-12	
	(AC) C bot							2.387E-12	
	(AC) A top	Tank 2	10/26/2011	35	11/30/2011	364	11/28/2012	1.73E-12	
	(AC) B top							1.905E-12	
	(AC) C top							1.567E-12	
DCL 09	(AC) A bot	Tank 1	11/2/2011	35	12/7/2011	364	12/5/2012	3.712E-12	3.256E-12
	(AC) B bot							2.692E-12	
	(AC) C bot							3.363E-12	
	(AC) A top	Tank 2	11/2/2011	35	12/7/2011	364	12/5/2012	2.434E-12	
	(AC) B top							2.275E-12	
	(AC) C top							2.271E-12	

Table J.2: Continued

Tops in 3.0% salinity / Bottoms 16.5% salinity									
14 day normal / 14 day accelerated									
Mix #	Sample:	Location	Cast date:	Age:	Start date:	Exposure time:	End date:	Diffusion Coefficient - Chlorides (m <sup>2</sup> /sec):	Average:
DCL 11	(AC) A bot	Tank 1	11/9/2011	35	12/14/2011	364	12/12/2012	4.854E-12	4.205E-12
	(AC) B bot							4.281E-12	
	(AC) C bot							3.479E-12	
	(AC) A top	Tank 2	11/9/2011	35	12/14/2011	364	12/12/2012	2.642E-12	
	(AC) B top							3.383E-12	
	(AC) C top							3.175E-12	
DCL 10b	(AC) A bot	Tank 1	11/16/2011	35	12/21/2011	364	12/19/2012	4.746E-12	5.414E-12
	(AC) B bot							5.735E-12	
	(AC) C bot							5.761E-12	
	(AC) A top	Tank 2	11/16/2011	35	12/21/2011	364	12/19/2012	3.497E-12	
	(AC) B top							2.595E-12	
	(AC) C top							2.842E-12	
DCL 08	(AC) A bot	Tank 1	11/22/2011	35	12/27/2011	364	12/25/2012	2.481E-12	2.373E-12
	(AC) B bot							2.562E-12	
	(AC) C bot							2.076E-12	
	(AC) A top	Tank 2	11/22/2011	35	12/27/2011	364	12/25/2012	1.44E-12	
	(AC) B top							1.177E-12	
	(AC) C top							1.299E-12	
DCL 01	(AC) A bot	Tank 1	12/7/2011	35	1/11/2012	364	1/9/2013	2.159E-12	2.241E-12
	(AC) B bot							1.862E-12	
	(AC) C bot							2.702E-12	
	(AC) A top	Tank 2	12/7/2011	35	1/11/2012	364	1/9/2013	2.453E-12	
	(AC) B top							2.39E-12	
	(AC) C top							1.495E-12	
DCL 07	(AC) A bot	Tank 1	12/14/2011	35	1/18/2012	364	1/16/2013	3.593E-12	2.699E-12
	(AC) B bot							2.286E-12	
	(AC) C bot							2.219E-12	
	(AC) A top	Tank 2	12/14/2011	35	1/18/2012	364	1/16/2013	1.771E-12	
	(AC) B top							1.865E-12	
	(AC) C top							1.797E-12	
DCL 04	(AC) A bot	Tank 1	12/21/2011	35	1/25/2012	364	1/23/2013	1.282E-12	1.39E-12
	(AC) B bot							1.772E-12	
	(AC) C bot							1.117E-12	
	(AC) A top	Tank 2	12/21/2011	35	1/25/2012	364	1/23/2013	8.501E-13	
	(AC) B top							8.869E-13	
	(AC) C top							2.07E-12	
DCL 05	(AC) A bot	Tank 1	12/21/2011	35	1/25/2012	364	1/23/2013	1.937E-12	2.061E-12
	(AC) B bot							2.445E-12	
	(AC) C bot							1.801E-12	
	(AC) A top	Tank 2	12/21/2011	35	1/25/2012	364	1/23/2013	1.647E-12	
	(AC) B top							1.26E-12	
	(AC) C top							1.003E-12	

Table J.3:  $D_{app}$  for specimens exposed to bulk diffusion, RT cured until resistivity NC=AC

Tops in 3.0% salinity (Tank 2)/ Bottoms 16.5% salinity (Tank 1)										
normal cure = accelerated cure										
Mix #	Sample:	Location	Cast date:	Age:	Start date:	Exposure time:	End date:	Diffusion Coefficient - Chlorides (m <sup>2</sup> /sec):	Average:	
<b>DCL 02 (early)</b>	(N<A) A bot	Tank 1	9/22/2011	62	11/23/2011	364	11/21/2012	3.54E-12	3.19E-12	
	(N<A) B bot							3.24E-12		
	(N<A) C bot							2.79E-12		
	(N<A) A top	Tank 2	9/22/2011	62	11/23/2011	364	11/21/2012	1.99E-12		2.06E-12
	(N<A) B top							1.95E-12		
	(N<A) C top							2.25E-12		
<b>DCL 02 (replacement)</b>	(N=A) 32 bot	Tank 1	9/22/2011	130	1/30/2012	364	1/28/2013	1.94E-12	2.04E-12	
	(N=A) 33 bot							2.38E-12		
	(N=A) 34 bot							1.81E-12		
	(N=A) 32 top	Tank 2	9/22/2011	130	1/30/2012	364	1/28/2013	1.85E-12		2.10E-12
	(N=A) 33 top							2.20E-12		
	(N=A) 34 top							2.25E-12		
<b>DCL 10 (early)</b>	(N<A) A bot	Tank 1	9/28/2011	70	12/7/2011	364	12/5/2012	3.84E-12	3.87E-12	
	(N<A) B bot							2.89E-12		
	(N<A) C bot							4.87E-12		
	(N<A) A top	Tank 2	9/28/2011	70	12/7/2011	364	12/5/2012	3.16E-12		3.11E-12
	(N<A) B top							2.70E-12		
	(N<A) C top							3.46E-12		
<b>DCL 10 (replacement)</b>	(N=A) 32 bot	Tank 1	9/28/2011	147	2/22/2012	364	2/20/2013	3.32E-12	2.99E-12	
	(N=A) 33 bot							2.79E-12		
	(N=A) 34 bot							2.86E-12		
	(N=A) 32 top	Tank 2	9/28/2011	147	2/22/2012	364	2/20/2013	2.66E-12		2.70E-12
	(N=A) 33 top							2.86E-12		
	(N=A) 34 top							2.57E-12		
<b>DCL 10a (early)</b>	(N<A) A bot	Tank 1	10/12/2011	70	12/21/2011	364	12/19/2012	3.80E-12	3.47E-12	
	(N<A) B bot							3.26E-12		
	(N<A) C bot							3.35E-12		
	(N<A) A top	Tank 2	10/12/2011	70	12/21/2011	364	12/19/2012	2.47E-12		2.91E-12
	(N<A) B top							3.05E-12		
	(N<A) C top							3.20E-12		
<b>DCL 10a (replacement)</b>	(N=A) 32 bot	Tank 1	10/12/2011	162	3/22/2012	363	3/20/2013	1.94E-12	2.06E-12	
	(N=A) 33 bot							2.54E-12		
	(N=A) 34 bot							1.68E-12		
	(N=A) 32 top	Tank 2	10/12/2011	162	3/22/2012	363	3/20/2013	1.61E-12		1.53E-12
	(N=A) 33 top							1.46E-12		
	(N=A) 34 top							1.51E-12		

Table J.3: Continued

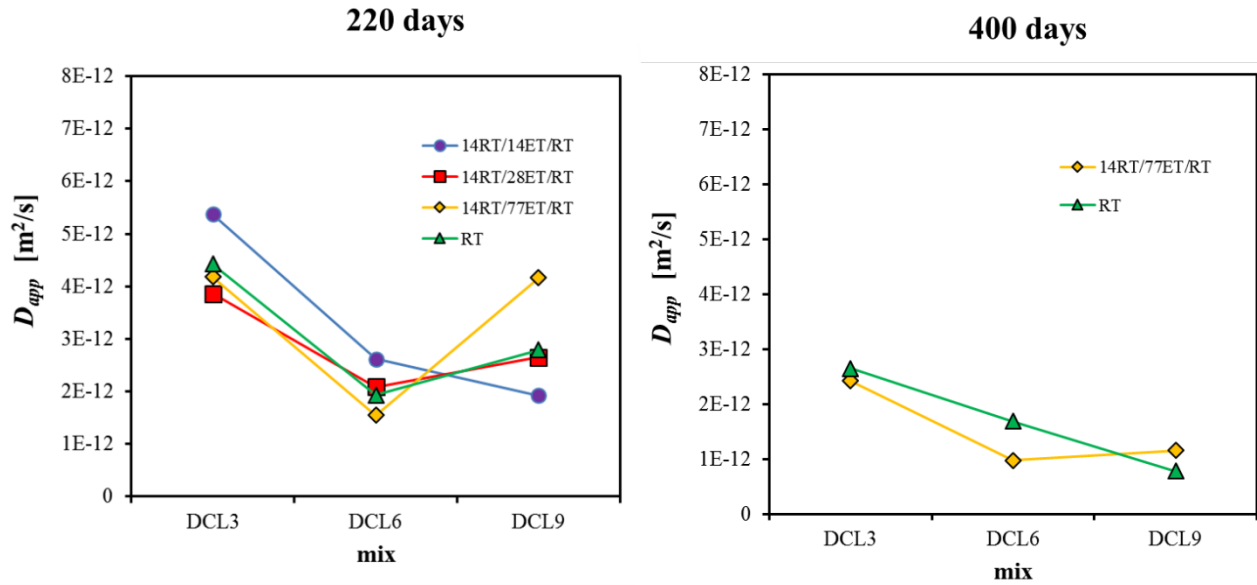
Tops in 3.0% salinity (Tank 2)/ Bottoms 16.5% salinity (Tank 1)									
normal cure = accelerated cure									
Mix #	Sample:	Location	Cast date:	Age:	Start date:	exposure time	End date:	Diffusion Coefficient - Chlorides (m <sup>2</sup> /sec):	Average:
<b>DCL 03 (early)</b>	(N<A) A bot	Tank 1	10/19/2011	61	12/19/2011	364	12/17/2012	4.14E-12	3.801E-12
	(N<A) B bot							3.32E-12	
	(N<A) C bot							3.95E-12	
	(N<A) A top	Tank 2	10/19/2011	61	12/19/2011	364	12/17/2012	2.69E-12	
	(N<A) B top							3.28E-12	
	(N<A) C top							2.57E-12	
<b>DCL 03 (replacement)</b>	(N=A) 32 bot	Tank 1	10/19/2011	117	2/13/2012	364	2/11/2013	2.59E-12	3.103E-12
	(N=A) 33 bot							2.84E-12	
	(N=A) 34 bot							3.88E-12	
	(N=A) 32 top	Tank 2	10/19/2011	117	2/13/2012	364	2/11/2013	2.12E-12	
	(N=A) 33 top							2.80E-12	
	(N=A) 34 top							2.74E-12	
<b>DCL 06</b>	(N=A) A bot	Tank 1	10/26/2011	341	10/1/2012	364	9/30/2013	1.11E-12	1.243E-12
	(N=A) B bot							1.25E-12	
	(N=A) C bot							1.36E-12	
	(N=A) A top	Tank 2	10/26/2011	341	10/1/2012	364	9/30/2013	1.80E-12	
	(N=A) B top							9.65E-13	
	(N=A) C top							1.32E-12	
<b>DCL 09</b>	(N=A) A bot	Tank 1	11/2/2011	488	3/4/2013	325	1/23/2014	1.09E-12	1.452E-12
	(N=A) B bot							1.45E-12	
	(N=A) C bot							1.82E-12	
	(N=A) A top	Tank 2	11/2/2011	488	3/4/2013	325	1/23/2014	1.40E-12	
	(N=A) B top							1.62E-12	
	(N=A) C top							4.33E-12	
<b>DCL 11</b>	(N=A) A bot	Tank 1	11/9/2011	134	3/22/2012	364	3/21/2013	3.05E-12	2.761E-12
	(N=A) B bot							2.38E-12	
	(N=A) C bot							2.85E-12	
	(N=A) A top	Tank 2	11/9/2011	134	3/22/2012	364	3/21/2013	2.12E-12	
	(N=A) B top							1.75E-12	
	(N=A) C top							2.42E-12	
<b>DCL 10b</b>	(N=A) A bot	Tank 1	11/16/2011	147	4/11/2012	364	4/10/2013	3.16E-12	3.225E-12
	(N=A) B bot							3.83E-12	
	(N=A) C bot							2.69E-12	
	(N=A) A top	Tank 2	11/16/2011	147	4/11/2012	364	4/10/2013	3.50E-12	
	(N=A) B top							2.60E-12	
	(N=A) C top							2.84E-12	

Table J.3: Continued

Tops in 3.0% salinity (Tank 2)/ Bottoms 16.5% salinity (Tank 1)										
normal cure = accelerated cure										
Mix #	Sample:	Location	Cast date:	Age:	Start date:	exposure time	End date:	Diffusion Coefficient - Chlorides (m <sup>2</sup> /sec):	Average:	
DCL 08	(N=A) A bot	Tank 1	11/22/2011	232	7/11/2012	364	7/10/2013	1.74E-12	1.44E-12	
	(N=A) B bot							1.34E-12		
	(N=A) C bot							1.24E-12		
	(N=A) A top	Tank 2	11/22/2011	232	7/11/2012	364	7/10/2013	1.27E-12		1.64E-12
	(N=A) B top							2.18E-12		
	(N=A) C top							1.47E-12		
DCL 01	(N=A) A bot	Tank 1	12/7/2011	145	4/30/2012	364	4/29/2013	1.41E-12	1.24E-12	
	(N=A) B bot							1.40E-12		
	(N=A) C bot							9.04E-13		
	(N=A) A top	Tank 2	12/7/2011	145	4/30/2012	364	4/29/2013	1.01E-12		1.18E-12
	(N=A) B top							1.48E-12		
	(N=A) C top							1.03E-12		
DCL 07	(N=A) A bot	Tank 1	12/14/2011	201	7/2/2012	364	7/1/2013	2.40E-12	2.01E-12	
	(N=A) B bot							1.57E-12		
	(N=A) C bot							2.07E-12		
	(N=A) A top	Tank 2	12/14/2011	201	7/2/2012	364	7/1/2013	1.53E-12		1.53E-12
	(N=A) B top							1.45E-12		
	(N=A) C top							1.59E-12		
DCL 04	(N=A) A bot	Tank 1	12/21/2011	439	3/4/2013	325	1/23/2014	1.00E-12	9.33E-13	
	(N=A) B bot							1.00E-12		
	(N=A) C bot							7.89E-13		
	(N=A) A top	Tank 2	12/21/2011	439	3/4/2013	325	1/23/2014	7.44E-13		7.40E-13
	(N=A) B top							9.39E-13		
	(N=A) C top							5.36E-13		
DCL 05	(N=A) A bot	Tank 1	12/21/2011	439	3/4/2013	325	1/23/2014	1.01E-12	9.19E-13	
	(N=A) B bot							9.17E-13		
	(N=A) C bot							8.30E-13		
	(N=A) A top	Tank 2	12/21/2011	439	3/4/2013	325	1/23/2014	1.01E-12		8.39E-13
	(N=A) B top							7.66E-13		
	(N=A) C top							7.45E-13		

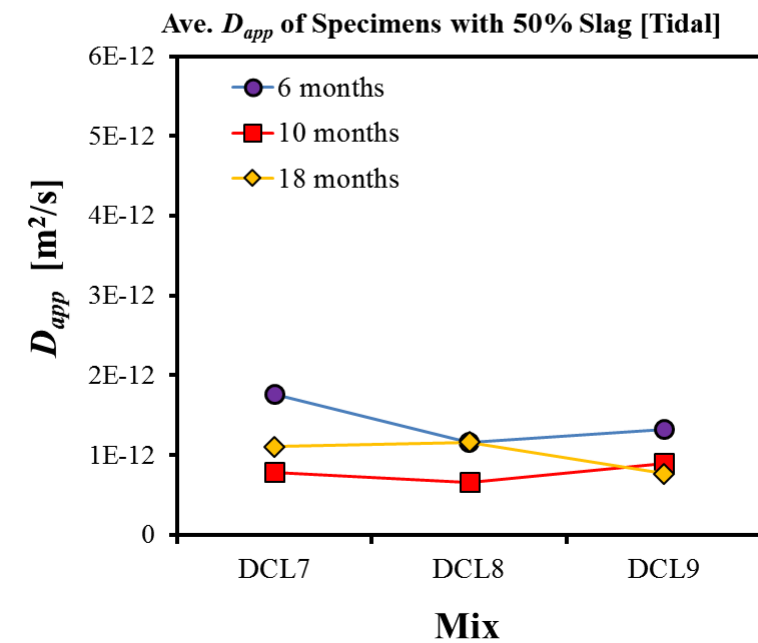
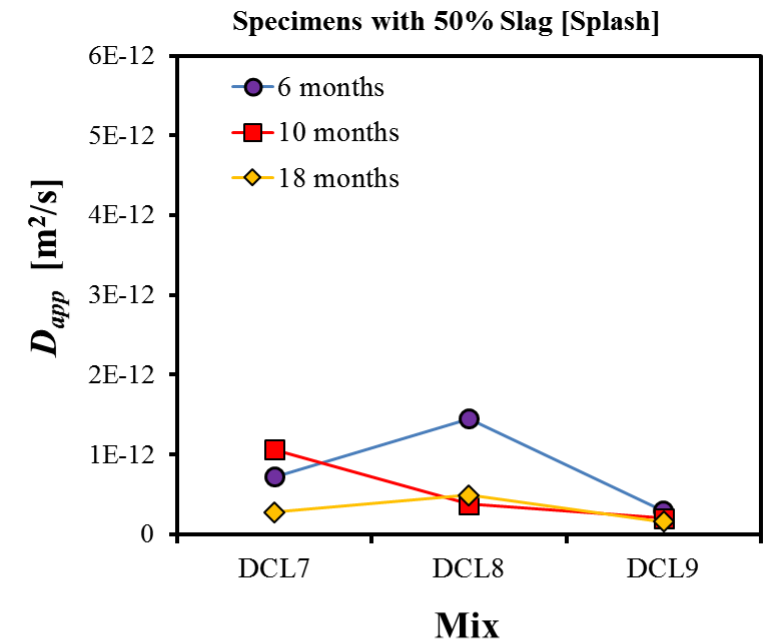
**Appendix K: DCL3, 6, and 9: Apparent Diffusivity Coefficient of Specimens Exposed to 0.1M NaCl Solution**

Figure K.1: Effect of cm on  $D_{app}$  comparing DCL3, 6 and 9 specimen exposed in 0.1 M NaCl



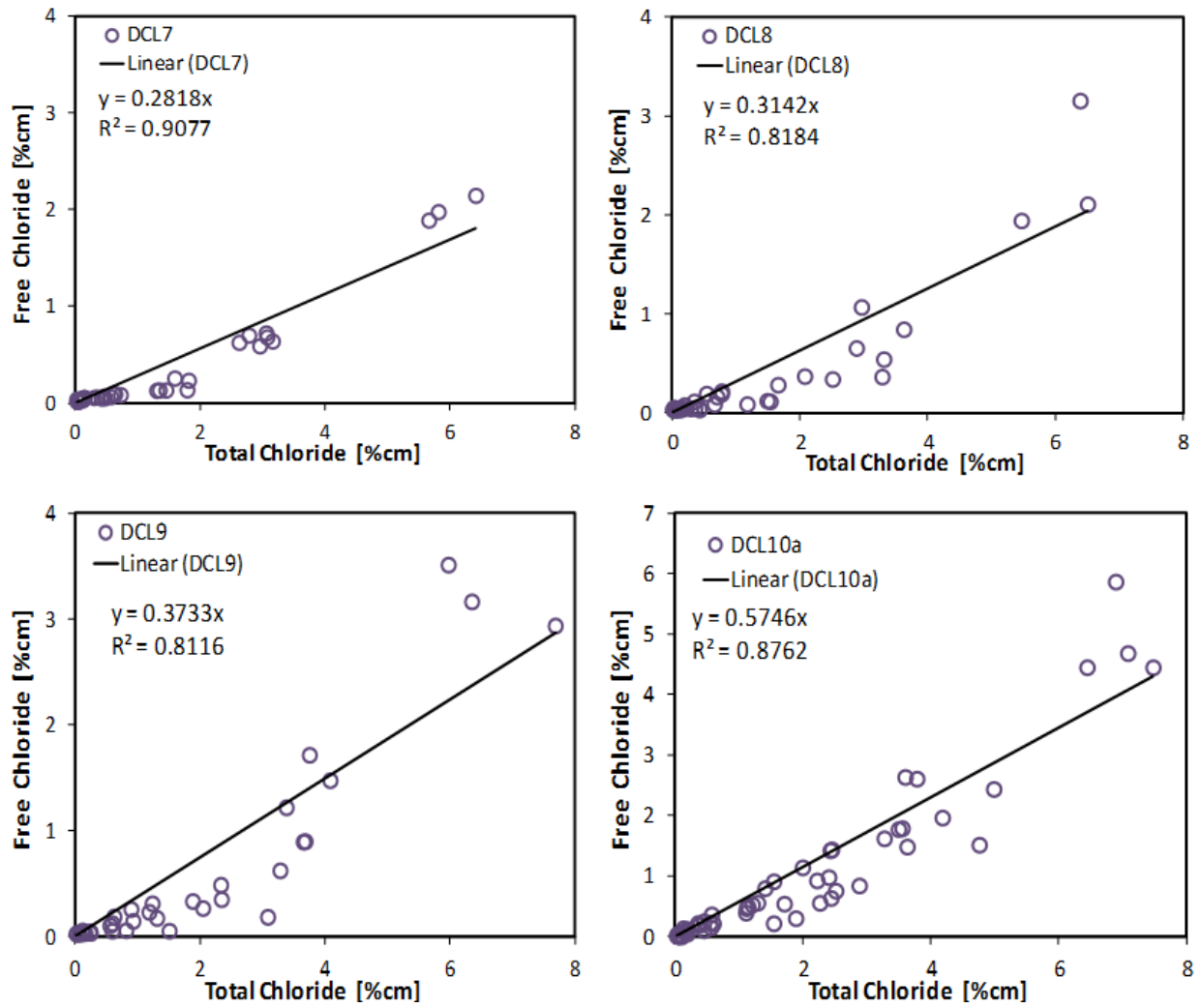
## Appendix L: DCL7, 8, and 9: Apparent Diffusivity Coefficient of Specimens Exposed to Tidal and Splash

Figure L.1: Effect of w/cm on  $D_{app}$  for DCL7, 8 and 9 at elevation A



## Appendix M: DCL7, 8, 9, and 10b: Free vs. Total Chloride Contents

Figure M.1: DCL7, DCL8, DCL9 and DCL10b: Free vs. total chloride contents



## Appendix N: Computed Equivalent Resistivity Values for DCL Mixes (Bulk Diffusion)

Table N.1: Equivalent resistivity vs.  $D_{app}$

Mix	Solution	Curing Regime	Exposure (days)	$D_{app}$ ( $10^{-12}$ m <sup>2</sup> /s)	Equivalent Resistivity (kohm•cm)
DCL1	0.60%	180RT	220	2.41	30.8
	0.60%	180RT	400	1.99	34.3
	3%	NC	365	1.98	21.7
	3%	AC	365	1.75	28.9
	3%	NC=AC	365	1.18	32.6
	3%	721	104	1.56	56.0
	16.5%	NC	365	2.06	21.7
	16.5%	AC	365	2.04	28.9
	16.5%	NC=AC	365	1.24	32.6
	16.5%	721	104	1.55	56.0
DCL2	0.60%	180RT	220	2.07	21.3
	0.60%	180RT	400	1.26	23.1
	3%	NC	365	1.89	16.6
	3%	AC	365	2.66	21.4
	3%	NC<AC	365	2.06	18.4
	3%	NC=AC	365	1.91	21.2
	3%	797	142	1.55	35.0
	16.5%	NC	365	2.25	16.6
	16.5%	AC	365	2.90	21.4
	16.5%	NC<AC	365	3.19	18.4
16.5%	NC=AC	365	1.94	21.2	
16.5%	797	127	1.21	35.0	
DCL3	0.60%	180RT	220	4.43	16.7
	0.60%	180RT	400	2.65	18.2
	3%	NC	365	2.54	13.3
	3%	AC	365	2.60	16.1
	3%	NC<AC	365	2.85	15.0
	3%	NC=AC	365	2.08	17.0
	3%	770	142	1.87	23.5
	16.5%	NC	365	4.73	13.3
	16.5%	AC	365	4.05	16.1
	16.5%	NC<AC	365	3.61	15.0
16.5%	NC=AC	365	3.47	17.0	
16.5%	770	127	2.06	23.5	
DCL4	0.60%	180RT	220	0.88	69.3
	0.60%	180RT	400	0.83	70.4
	3%	NC	365	0.90	64.2
	3%	AC	365	0.88	81.1
	3%	NC=AC	365	0.74	72.6
	3%	716	110	1.01	88.0
	16.5%	NC	365	0.93	64.2
	16.5%	AC	365	0.86	81.1
	16.5%	NC=AC	365	0.93	72.6
	16.5%	716	102	1.48	88.0
DCL5	0.60%	180RT	220	1.35	58.3
	0.60%	180RT	400	0.61	59.5
	3%	NC	365	1.22	52.4
	3%	AC	365	0.87	59.2
	3%	NC=AC	365	1.37	62.1
	3%	716	110	1.56	68.0
	16.5%	NC	365	1.53	52.4
	16.5%	AC	365	1.63	59.2
	16.5%	NC=AC	365	0.87	62.1
	16.5%	716	102	2.91	68.0
DCL6	0.60%	180RT	220	1.93	44.4
	0.60%	180RT	400	1.69	47.0
	3%	NC	365	2.51	35.9
	3%	AC	365	1.33	50.3
	3%	NC=AC	365	1.39	49.8
	3%	763	142	0.84	58.0
	16.5%	NC	365	2.93	35.9
	16.5%	AC	365	2.46	50.3
	16.5%	NC=AC	365	1.14	49.8
	16.5%	763	127	1.96	58.0

Table N.1: Continued

Mix	Solution	Curing Regime	Exposure (days)	$D_{app}$ ( $10^{-12}$ m <sup>2</sup> /s)	Equivalent Resistivity (kohm•cm)	
DCL7	0.60%	180RT	220	2.00	22.1	
	0.60%	180RT	400	0.36	23.9	
	3%	NC	365	1.47	20.8	
	3%	AC	365	1.81	22.2	
	3%	NC=AC	365	1.53	24.0	
	3%	723	111	0.93	29.0	
	16.5%	NC	365	2.60	20.8	
	16.5%	AC	365	2.70	22.2	
	16.5%	NC=AC	365	2.41	24.0	
	16.5%	723	102	1.69	29.0	
DCL8	0.60%	180RT	220	2.98	19.6	
	0.60%	180RT	400	0.95	20.5	
	3%	NC	365	1.96	18.6	
	3%	AC	365	1.11	23.1	
	3%	NC=AC	365	1.64	21.3	
	3%	735	120	1.23	27.5	
	16.5%	NC	365	2.15	18.6	
	16.5%	AC	365	2.40	23.1	
	16.5%	NC=AC	365	1.44	21.3	
	16.5%	735	104	1.42	27.5	
DCL9	0.60%	180RT	220	2.79	17.5	
	0.60%	180RT	400	0.78	17.9	
	3%	NC	365	1.37	16.8	
	3%	AC	365	1.45	20.0	
	3%	NC=AC	365	2.22	18.5	
	3%	756	120	0.73	22.0	
	16.5%	NC	365	2.59	16.8	
	16.5%	AC	365	2.47	20.0	
	16.5%	NC=AC	365	1.45	18.5	
	16.5%	756	104	2.33	22.0	
DCL10	3%	NC	365	3.28	20.2	
	3%	AC	365	2.97	25.5	
	3%	NC<AC	365	2.33	23.0	
	3%	NC=AC	365	1.73	29.5	
	3%	791	143	0.97	34.5	
	16.5%	NC	365	3.88	20.2	
	16.5%	AC	365	4.64	25.5	
	16.5%	NC<AC	365	3.11	23.0	
	16.5%	NC=AC	365	2.36	29.5	
	16.5%	791	138	1.14	34.5	
	DCL10a	0.60%	180RT	220	3.69	23.9
		0.60%	180RT	400	3.16	26.4
		3%	NC	365	3.09	20.1
		3%	AC	365	2.83	22.3
		3%	NC<AC	365	2.75	20.7
		3%	NC=AC	365	1.53	25.5
3%		777	143	1.38	35.0	
16.5%		NC	365	3.87	20.1	
16.5%		AC	365	3.39	22.3	
16.5%		NC<AC	365	2.94	20.7	
16.5%		NC=AC	365	2.43	25.5	
16.5%		777	138	1.46	35.0	
DCL10b		0.60%	180RT	220	3.83	23.2
		0.60%	180RT	400	1.06	26.3
		3%	NC	365	2.74	19.6
		3%	AC	365	2.41	21.9
	3%	NC=AC	365	1.72	24.8	
	3%	742	120		35.0	
	16.5%	NC	365	4.19	19.6	
	16.5%	AC	365	4.55	21.9	
	16.5%	NC=AC	365	2.72	24.8	
	16.5%	742	104	2.27	35.0	
	DCL11	0.60%	180RT	220	4.85	23.0
		0.60%	180RT	400	2.33	26.3
		3%	NC	365	2.25	19.8
		3%	AC	365	2.50	23.6
		3%	NC=AC	365	1.86	24.2
		3%	749	120		36.0
16.5%		NC	365	4.11	19.8	
16.5%		AC	365	3.73	23.6	
16.5%		NC=AC	365	2.65	24.2	
16.5%		749	104	1.72	36.0	

## Appendix O: Historical Weather and Wind Data (Ft. Lauderdale Airport)

Figure O.1: Wind Speed (mean, minimum and maximum)

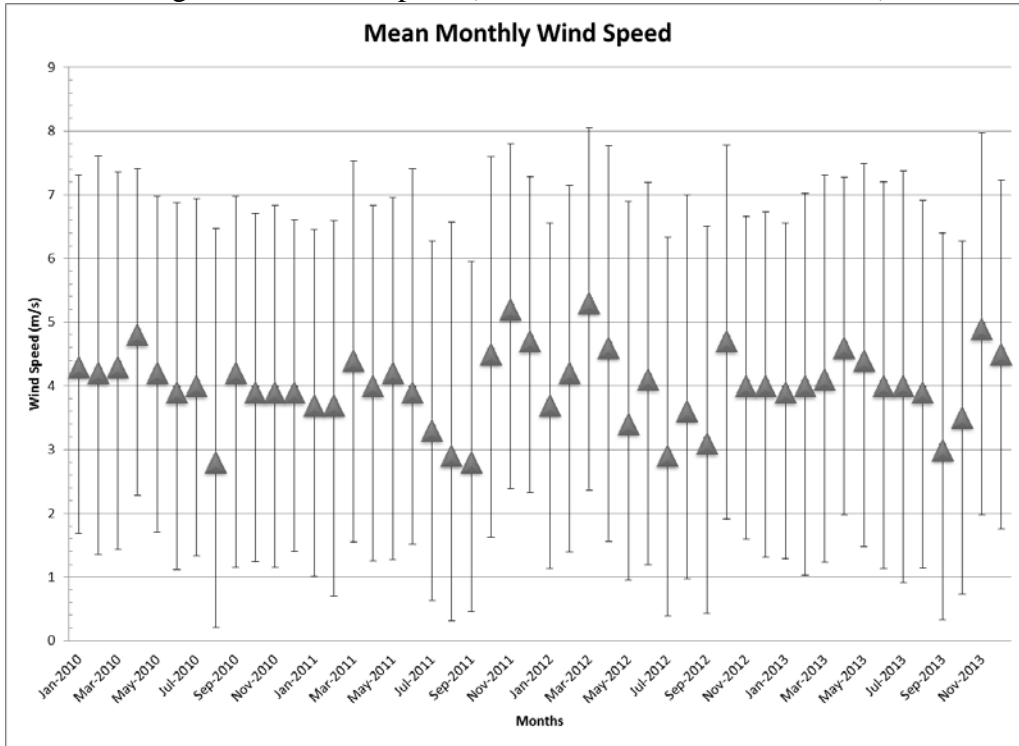


Figure O.2: monthly mean wind direction

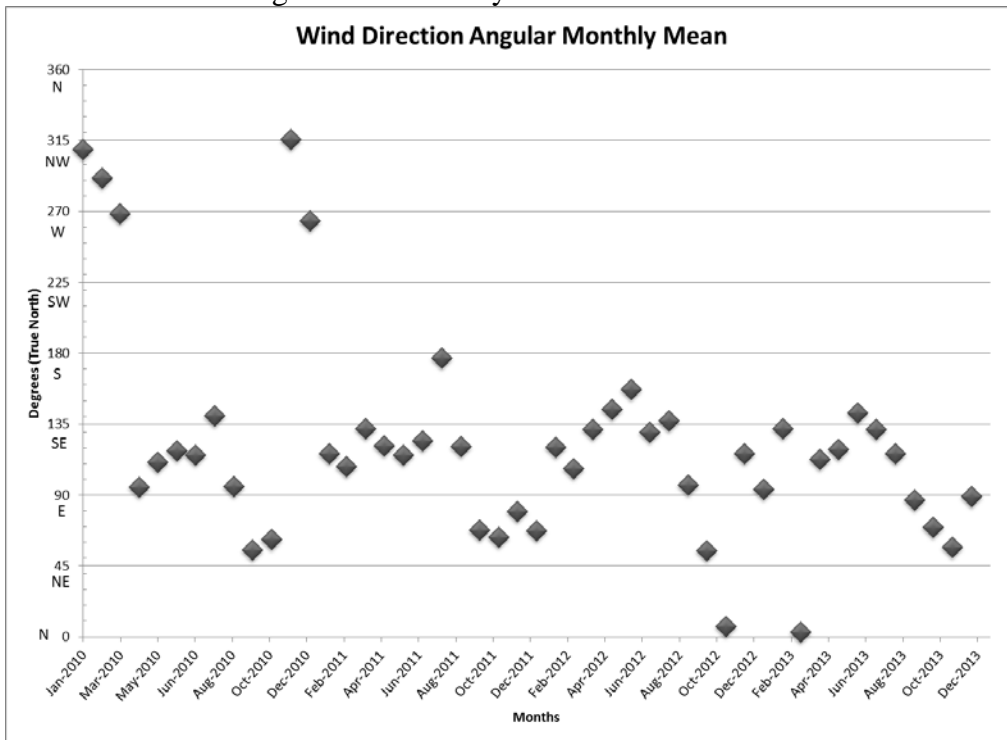


Figure O.3: Monthly mean temperature

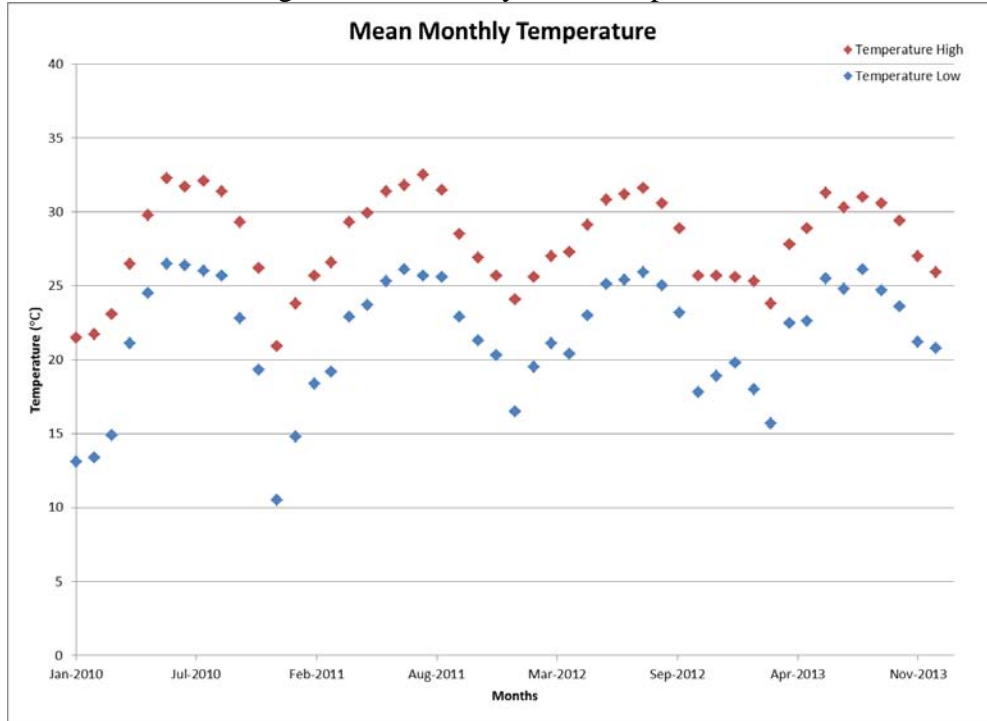


Figure O.4: Mean monthly relative humidity

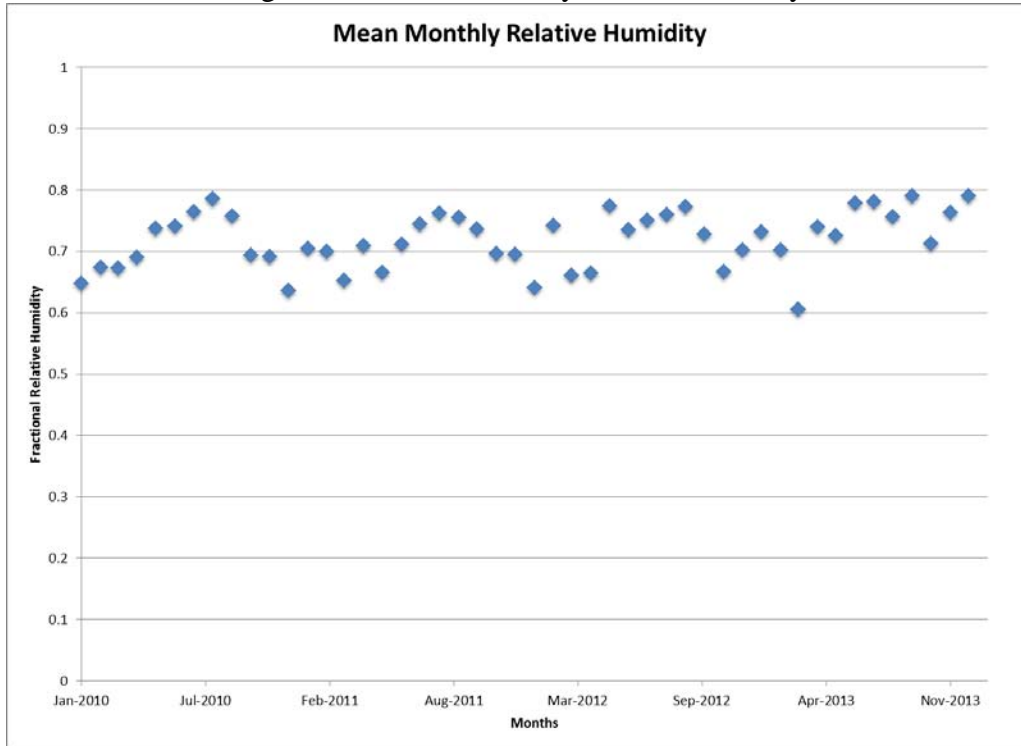
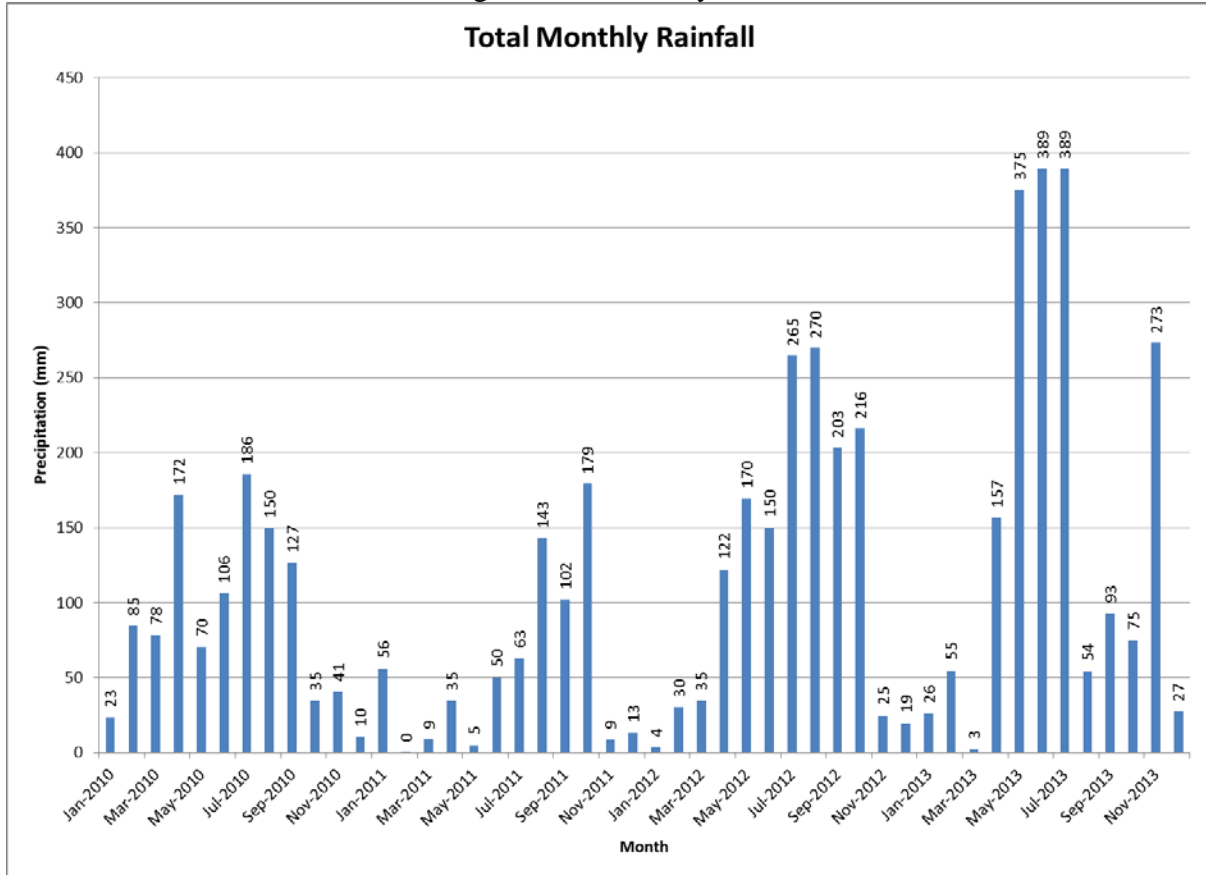


Figure O.5: Monthly rainfall



## Appendix P: Compilation of $D_{app}$ from Previous Projects Sorted by Bridge Number

Table P.1:  $D_{app}$  values from Previous Projects Sorted by Bridge Number

Bridge #	Construction date	Year Visited	Age at Visit	Location	Elevation AHT (m)	Elevation MG (m)	$D_{app}$ ( $m^2/s$ ) $\times 10^{-12}$
10057	1980	1992	12	Pier 54	-0.03		0.348
10057	1980	1992	12	Pier 54	0.51		0.388
10058	1980	1992	12	Pier 54	-0.03		0.634
10058	1980	1992	12	Pier 54	1.22		0.266
10058	1980	1992	12	Pier 37	0.48		0.368
10058	1980	1992	12	Pier 37	2.29		0.204
10092	1983	1992	9	Pier 9	0.13		1.206
10092	1983	1992	9	Pier 9	1.19		0.838
10092	1983	1992	9	Pier 9	2.64		0.756
30148	7/1/1969	6/2/2004	35	Bent 18 Pile 3 EF	0.00		0.255
100300	7/1/1975	11/2/2005	30	Pile 271-3 North Face 10" from corner	0.30		9.109
100300	1975	2009	34			0.69	3.510
100300	1975	2009	34			0.20	1.781
100358	1981	1991	10		1.55		0.164
100358	1981	1991	10		1.93		3.067
100359	1981	1991	10		0.18		2.453
100359	1981	1991	10		1.19		2.044
100585	1996	2009	13			0.41	0.196
100585	1996	2009	13			0.00	0.224
105504	7/1/1926	6/23/2009	83	Pier 9 EF		0.15	0.807
105504	7/1/1926	6/23/2009	83	Pier 6 Cap		2.34	0.068
120084	7/1/1976	3/26/2001	25	Footer	1.22		1.381
120084	7/1/1976	3/26/2001	25	Footer	0.15		1.402
120088	1980	1992	12		0.10		0.368
120088	1980	1992	12		0.13		0.388
120088	1980	1992	12		0.13		1.247
120088	1980	2009	29			0.48	0.188
120088	1980	2009	29			0.48	0.319
120088	1980	2009	29			0.00	0.752
120089	1980/91	2006	15		-0.08		0.050
120089	1980/91	2006	15		-0.15		0.149
120089	1980/91	2006	15		-0.15		0.151
120089	1980/91	2009	18			0.51	0.129
120089	1980/91	2009	18			0.51	0.240
120089	1980/91	2009	18			0.08	0.123
120089	1980/91	2009	29			0.53	3.353
120089	1980/91	2009	29			0.03	3.800
120089	1980/91	2009	29			0.03	2.810

Table P.1 Continued

Bridge #	Construction date	Year Visited	Age at Visit	Location	Elevation AHT (m)	Elevation MG (m)	Dapp (m <sup>2</sup> /s) × 10 <sup>-12</sup>
124115	2007	2009	2			0.51	1.047
124115	2007	2009	2			0.13	0.803
124115	2007	2009	2			0.13	0.963
124116	2007	2009	2			0.46	1.013
124116	2007	2009	2			0.05	1.507
124116	2007	2009	2			0.05	1.360
130103	1980	1991	11		0.76		0.225
130103	1980	1991	11		1.02		0.327
130104	1980	1991	11		0.79		0.920
130104	1980	1991	11		0.74		0.572
130132	1985	1991	6		0.86		0.388
130132	1985	1991	6		1.02		0.348
130132	1985	1991	6		2.34		0.879
130132	1985	1991	6		1.02		0.961
136502	2006/2007	2009	2.5				0.216
136502	2006/2007	2009	2.5				0.235
136502	2006/2007	2009	2.5				0.229
136502	2006/2007	2009	2.5				0.209
136502	2006/2007	2009	2.5				0.088
136502	2006/2007	2009	2.5				0.130
136502	2006/2007	2009	2.5				0.142
136502	2006/2007	2009	2.5				0.313
136502	2006/2007	2009	2.5				0.360
136502	2006/2007	2009	2.5				0.246
136502	2006/2007	2009	2.5				0.287
136502	2006/2007	2009	2.5				0.342
136502	2006/2007	2009	2.5				0.085
136502	2006/2007	2009	2.5				0.163
136502	2006/2007	2009	2.5				0.095
136502	2006/2007	2009	2.5				0.285
136502	2006/2007	2009	2.5				0.388
136502	2006/2007	2009	2.5				0.802
139003	7/1/1966 7/1/1993 redone	6/10/2009	43	Pile 11-3	0.61		0.747
139003	7/1/1966 7/1/1993 redone	6/10/2009	43	Pile 6-3	0.61		3.118
150038	1968/1990	2009	19			0.37	0.392
150038	1968/1990	2009	19			-0.13	0.790
150038	1968/1990	2009	19			-0.13	1.915
150038	1968/1990	2009	19			0.18	1.315
150038	1968/1990	2009	19			-0.13	0.832

Table P.1: Continued

Bridge #	Construction date	Year Visited	Age at Visit	Location	Elevation AHT (m)	Elevation MG (m)	Dapp (m <sup>2</sup> /s) × 10 <sup>-12</sup>
150049	1961/1996	2009	48			0.36	1.009
150050	1962	2009	47			0.18	0.155
150107	1959/1992	2009	50			0.36	1.225
150107	1959/1992	2009	50			-0.13	0.490
150138	1992	1998	6		1.01		0.859
150138	1992	1998	6		1.01		0.409
150138	1992	1998	6		0.67		0.491
150138	1992	1998	6		0.67		0.598
150138	1992	1998	6		0.00		0.266
150138	1992	1998	6		0.30		0.307
150138	1992	1998	6		0.00		0.205
150138	1992	1998	6		0.30		0.123
150138	1992	2009	17		-0.15		0.409
150138	1992	2009	17		-0.15		0.573
150138	1974/1992	2009	17			-0.13	11.500
150138	1974/1992	2009	17			0.41	1.330
150138	1974/1992	2009	17			0.41	0.489
150138	1974/1992	2009	17			-0.08	0.902
150169	1986	1993	7		2.13		0.245
150189	1966	1993	27		1.83		0.184
150189	1985	1996	11		5.49		0.090
150189	1985	1996	11		5.49		0.062
150189	1985	1996	11		5.49		4.700
150189	1985	1996	11		1.83		0.571
150189	1985	1996	11		5.79		0.201
150189	1985	1996	11		1.83		0.086
150189	1985	1996	11		5.79		0.089
150189	1985	1996	11		5.79		0.106
150189	1985	1996	11		18.29		0.226
150189	1985	1996	11		18.29		0.057
150189	1985	1996	11		0.91		1.655
150189	1985	1996	11		18.29		0.064
150189	1985	1996	11		36.58		0.149
150189	1985	1996	11		0.91		0.204
150189	1985	1996	11		0.91		0.204
150189	1985	1996	11		0.91		1.326
150189	1985	1996	11		0.91		0.204
150189	1985	1996	11		0.91		0.204
150189	1985	1996	11		0.91		0.409
150189	1986	1993	7		1.27		0.450
150189	1986	1993	7		2.54		0.838
150189	1986	1993	7		3.25		0.532
150189	1986	1993	7		0.53		0.388
150189	1986	1993	7		0.91		0.307
150189	1986	1993	7		1.02		0.368
150189	1986	1993	7		1.47		0.327

Table P.1: Continued

Bridge #	Construction date	Year Visited	Age at Visit	Location	Elevation AHT (m)	Elevation MG (m)	Dapp (m <sup>2</sup> /s) × 10 <sup>-12</sup>
150189	1986	1993	7		0.00		0.450
150189	1986	1993	7		0.61		0.388
150189	1986	1993	7		1.22		0.245
150189	1986	1993	7		2.44		0.082
150189	1986	1993	7		0.30		0.307
150189	1986	1993	7		0.91		0.225
150189	1986	1993	7		1.52		0.552
150189	1986	1993	7		2.74		0.348
150189	7/1/1986	7/13/1994	8	Pier 15 Nothbound North Face	0.91		0.310
150189	7/1/1986	7/13/1994	8	Pier 30 South Bound North Face North of channel	0.91		0.315
150189	7/1/1986	7/13/1994	8	Pier 30 South Bound North Face North of channel	0.30		0.585
150189	7/1/1986	7/13/1994	8	Pier 1 North North Face	2.08		0.380
150189	7/1/1986	2/2/1997	11	Pier 117-2	1.83		0.079
150189	7/1/1986	2/2/1997	11	Pier 106-1	0.91		0.142
150189	7/1/1986	2/2/1997	11	Pier 116	0.91		0.238
150189	7/1/1986	4/3/1997	11	Pier 155	5.49		0.057
150189	7/1/1986	4/3/1997	11	Pier 151	5.79		0.077
150189	7/1/1986	4/3/1997	11	Pier 126-1	18.29		0.052
150189	1986	2009	23			0.36	0.515
150189	1986	2009	23			0.20	0.258
150189	1986	2009	23			0.28	0.404
150189	1986	2009	23			0.15	1.069
150189	1986	2007	21		0.5		0.110
150200	1962	2000	38		-0.09		1.636
150200	1962	2000	38		0.30		1.636
150200	1962	2000	38		0.30		3.884
150200	1986	2000	14		-0.09		7.360
150200	1986	2000	14		0.30		4.907
150200	1986	2000	14		0.30		3.362
150200	1986	2000	14		0.30		0.818
150200	1986	2000	14		0.61		2.044
150200	1986	2000	14		0.61		4.603
150202	1990	2000	10		0.71		0.069
150202	1990	2000	10		0.71		0.613
150202	1990	2000	10		0.30		1.227
150202	1990	2000	10		0.30		0.818
150202	1990	2000	10		-0.21		0.613
150202	1990	2000	10		-0.21		0.613
150202	1990	2000	10		0.76		0.041
150202	1990	2000	10		0.76		0.204
150202	1990	2000	10		0.30		1.022
150202	1990	2000	10		0.30		1.022
150202	1990	2000	10		-0.09		0.613
150202	1990	2000	10		-0.09		0.613
150202	1990	2000	10		0.61		0.270
150202	1990	2000	10		0.61		0.204

Table P.1: Continued

Bridge #	Construction date	Year Visited	Age at Visit	Location	Elevation AHT (m)	Elevation MG (m)	Dapp (m <sup>2</sup> /s) × 10 <sup>-12</sup>
150210	1991	1999	8		0.51		1.290
150210	1991	1999	8		0.51		0.409
150210	1991	1999	8		0.41		0.879
150210	1991	1999	8		0.41		0.129
150210	1991	1999	8		1.07		0.891
150210	1991	1999	8		1.07		0.818
150210	1991	1999	8		0.06		1.334
150210	1991	1999	8		-0.06		0.818
150210	1991	1999	8		1.07		1.022
150210	1991	1999	8		0.66		1.431
150210	1991	1999	8		-0.15		1.467
150210	1991	1999	8		-0.15		0.409
150210	1991	1999	8		0.97		0.613
150210	1991	1999	8		0.97		0.409
150210	1991	2009	18			0.28	0.178
150210	1991	2009	18			0.28	0.135
150210	1991	2009	18			-0.15	0.257
150210	1991	2009	18			0.53	0.278
150210	1991	2009	18			0.00	0.906
150210	1991	2007	16		0.5		0.730
150211	1991	2000	9		-0.12		0.204
150211	1991	2000	9		0.25		0.409
150211	1991	2000	9		-0.12		0.204
150211	1991	2000	9		0.25		0.204
150211	1991	2000	9		-0.12		0.409
150211	1991	2000	9		0.23		0.613
150214	1992	2009	17			0.30	0.157
150214	1992	2009	17			0.30	0.214
150214	1992	2009	17			0.15	0.221
150221	1996	1998	2		0.30		1.022
150221	1996	1998	2		0.30		0.204
150221	1996	1998	2		-0.06		2.044
150221	1996	1998	2		-0.15		0.613
150243	2001	2009	8			1.12	0.669
150243	2001	2009	8			0.61	1.170
150243	2001	2009	8			0.61	2.825
154259	1993	2000	7		0.30		1.226
154259	1993	2000	7		-0.09		0.422
154259	1993	2000	7		-0.09		0.204
154259	1993	2000	7		0.30		0.068
154259	1993	2000	7		0.30		12.329
154259	1993	2000	7		0.30		0.204
154259	1993	2000	7		-0.15		0.409
154259	1993	2000	7		-0.15		0.409
154259	1993	2000	7		0.12		1.419

Table P.1: Continued

Bridge #	Construction date	Year Visited	Age at Visit	Location	Elevation AHT (m)	Elevation MG (m)	Dapp (m <sup>2</sup> /s) × 10 <sup>-12</sup>
154259	1993	2000	7		0.12		1.227
154259	1993	2000	7		-0.09		2.249
154259	1993	2000	7		0.73		0.613
154259	1993	2000	7		0.57		0.176
154259	1993	2000	7		0.73		2.249
159008	7/1/1966 7/1/1993 redone	6/10/2009	16	Pile 2-2	0.61		0.599
170158	1986	1992	6		0.20		2.453
170158	1986	1992	6		2.41		6.133
170158	1986	1992	6		0.56		0.286
170158	1986	1992	6		2.06		0.041
170158	1986	2000	14		0.02		0.000
170158	1986	2000	14		0.02		0.613
170158	1986	2000	14		0.71		2.044
170158	1986	2000	14		0.10		0.000
170158	1986	2000	14		0.10		0.613
170158	1986	2000	14		0.71		1.022
170158	1986	2000	14		1.37		0.000
170158	1986	2000	14		1.37		0.613
170158	1986	2000	14		0.15		2.249
170158	1986	2000	14		0.15		0.379
340053	1974	2010	36	bent 15, pile cap	1.52		0.909
340053	1974	2010	36	bent 6, pile cap	1.52		0.126
460012	1960	2002	42	H8-2-2	0.03		0.059
460012	1960	2002	42	H8-2-3	-0.04		0.286
460012	1960	2002	42	H8-2-4	-0.04		0.092
460012	1960	2002	42	H8-2-5	0.46		0.032
460012	1960	2002	42	H29-3-2	0.05		0.084
460012	1960	2002	42	H29-3	0.46 C		0.074
460072	1989	2009	20			0.46	0.386
460072	1989	2009	20			0.00	0.347
460072	1989	2009	20			0.00	0.827
460112	2003	2009	6			0.28	0.626
460112	2003	2009	6			0.05	0.516
460112	2003	2009	6			0.18	0.483
480035	1960	2003	43	P4-1-1	0.10		0.240
480035	1960	2003	43		0.1 C		0.044
480035	1960	2003	43		0.23		0.078
480035	1960	2003	43		0.12		0.125
480035	1960	2003	43		0.46		0.061
480035	1960	2003	43	P-185-4-1	0.15		0.096
480035	1960	2003	43	P-185-4-2	0.15		0.055
480035	1960	2003	43	P-213-4-1	0.43		0.086
480035	1960	2003	43	P-213-4-2	0.43 C		0.068
480035	1960	2003	43	P237-1-1	0.09		0.312
480035	1960	2003	43	P252-1-2	0.09		0.343

Table P.1: Continued

Bridge #	Construction date	Year Visited	Age at Visit	Location	Elevation AHT (m)	Elevation MG (m)	Dapp (m <sup>2</sup> /s) × 10 <sup>-12</sup>
480140	1981	1992	11		0.10		0.307
480140	1981	1992	11		1.19		0.204
480140	1981	1992	11		0.53		0.184
480140	1981	2007	26		1.1		0.500
480140	1981	2007	26		0.9		0.140
490003	2003	2004	1	152TPN-2			0.226
490003	2003	2004	1	162WS-1	0.15		0.078
490003	2003	2004	1	162WS-2	0.15		0.052
490003	2003	2004	1	162WS-3	0.30		0.044
490003	2003	2004	1	162WS-4	0.30		0.029
490003	2003	2004	1	163WS-1	0.15		0.502
490003	2003	2004	1	163WS-2	0.15		0.309
490003	2003	2004	1	163WS-3	0.30		0.174
490003	2003	2004	1	163WS-4	0.30		0.240
490003	2003	2004	1	1404-3			0.144
490003	2003	2004	1	1404-4			0.109
490003	2003	2004	1	943-3			0.403
490003*	2003	2009	6			0.38	0.174
490003*	2003	2009	6			0.38	0.288
490003*	2003	2009	6			-0.03	0.302
490003*	2003	2009	6			0.43	0.149
490003*	2003	2009	6			0.18	0.118
490003*	2003	2009	6			0.18	0.140
490003*	2003	2009	6			-0.05	0.562
490003*	2003	2009	6			-0.05	0.361
490031	1988	1992	4		1.04		92.613
490031	1988	1992	4		2.90		19.627
490031	1988	1992	4		0.20		1.268
490031	1988	1992	4		1.96		423.197
490032	1988	2009	21			0.20	0.340
490032	1988	2009	21			0.20	0.690
490032	1988	2009	21			-0.18	0.960
490032	1988	2009	21			0.28	0.344
490032	1988	2009	21			0.28	0.351
570034	1964	2003	39	BR3-2-3	0.62		0.281
570034	1964	2003	39	BR3-2-4	0.62		0.246
570034	1964	2003	39	BR3-2-5	0.15		0.197
570034	1964	2003	39	BR3-2-6	0.15		0.288
570054	1971	2009	38			0.43	1.168
570054	1971	2009	38			0.43	1.659
570054	1971	2009	38			0.10	1.317
570054	1971	2009	38			0.10	2.495
570054	1971	2009	38			0.05	1.250
570054	1971	2009	38			0.05	1.400
570054	1971	2009	38			0.18	1.070
570054	1971	2009	38			0.18	3.700
570054	1971	2009	38			0.38	0.808
570054	1971	2009	38			0.13	0.605

Table P.1: Continued

Bridge #	Construction date	Year Visited	Age at Visit	Location	Elevation AHT (m)	Elevation MG (m)	Dapp (m <sup>2</sup> /s) × 10 <sup>-12</sup>
570082	1979	1992	13		1.09		28.213
570082	1979	1992	13		2.72		0.879
570082	1979	2007	28		0.3		2.000
570082	1979	2007	28		0.2		1.600
700006	1959/90	12/10/2008				0.25	0.199
700006	1959/90	12/10/2008				0.25	0.194
700081	7/1/1971	7/28/2008		Pile 8	0.15		2.338
700174	1978	12/10/2008				0.25	0.943
700174	1985	1991	6		0.79		24.124
700174	7/1/1978	6/1/2011		footer Pier 20		0.53	2.488
700174	7/1/1978	6/1/2011		Crash Wall Pier 14		0.30	4.530
700181	1985	1991	6		0.61		5.520
700181	1985	2011	26	footer Pier 13		0.48	5.630
700181	1985	2011	26	Crashwall Pier 15		0.36	0.929
700181	1985	12/10/2008	23			0.25	3.720
700181	1985	12/10/2008	23			0.25	13.200
700193	1995	12/10/2008	23			0.25	0.782
700193	1995	12/10/2008	23			0.25	1.530
700203	1999	12/10/2008	9			0.25	0.171
700203	1999	12/10/2008	9			0.25	0.320
700203	1999	12/10/2008	9			0.25	0.051
700203	1999	2006	7		-0.10		0.185
700203	1999	2006	7		-0.23		0.132
700203	1999	2006	7		-0.23		0.155
720053	1972	2010	38	Pile 8-4	0.30		0.133
720053	1972	2010	38	Pile 10-2	1.22		0.011
720053	1972	2010	38	at mean high tide	0.00		0.328
720053	1972	2010	38	Pile Crashwall	0.00		0.521
720053	1972	2011	39	Pile 8-2	1.22		0.041
720053	1972	2011	39	Pile 4-8	0.30		0.151
720107	1967	2009	42			0.51	0.386
720107	1967	2009	42			0.51	17.648
720107	1967	2009	42			0.08	0.658
720249	1970/1993	2009	16			0.48	0.048
720249	1970/1993	2009	16			0.08	0.056
720249	1970/1993	2009	16			0.08	0.105
720249	1970/1993	2009	16			0.48	0.286
720249	1970/1993	2009	16			0.48	0.221
720249	1970/1993	2009	16			0.08	0.097
720249	1970/1993	2009	16			0.46	0.912
720249	1970/1993	2009	16			0.05	13.361
720249	1970/1993	2009	16			0.05	2.900
720336	7/1/1967	5/24/2004	37	Bent 9 Pile 6 EF	0.00		1.300

Table P.1: Continued

Bridge #	Construction date	Year Visited	Age at Visit	Location	Elevation AHT (m)	Elevation MG (m)	Dapp (m <sup>2</sup> /s) × 10 <sup>-12</sup>
720343	1970/1995	2009	14			0.46	0.345
720343	1970/1995	2009	14			0.46	0.951
720343	1970/1995	2009	14			0.08	1.428
720343	1970/1995	2009	14			0.08	2.061
720343	1970/1995	2009	14			0.51	0.442
720343	1970/1995	2009	14			0.51	0.094
720343	1970/1995	2009	14			0.08	0.108
720343	1970/1995	2009	14			0.08	0.153
720343	1970/1995	2009	14			0.48	0.246
720343	1970/1995	2009	14			0.48	0.272
720343	1970/1995	2009	14			0.05	0.548
720518	1989	2000	11	0A	0.00		0.409
720518	1989	2000	11	0C	0.00		0.000
720518	1989	2000	11	0D	0.00		1.022
720518	1989	2000	11	1AA	0.30		1.636
720518	1989	2000	11	1C	0.30		0.000
720518	1989	2000	11	1DD	0.30		2.658
720518	1989	2000	11	3A	0.91		0.000
720518	1989	2000	11	3CCC	0.91		0.000
720518	1989	2000	11	3D	0.91		0.000
720518	1989	2000	11	5A	1.52		0.000
720518	1989	2000	11	5C	1.52		0.000
720518	1989	2000	11	5D	1.52		0.204
720570	1991	2009	18			0.46	0.082
720570	1991	2009	18			0.46	0.135
720570	1991	2009	18			0.08	0.180
780089	1976	2009	33			0.51	0.682
780089	1976	2009	33			0.51	2.015
780089	1976	2009	33			0.00	0.874
780090	1975	2009	34			0.46	0.840
780090	1975	2009	34			-0.03	1.201
780090	1975	2009	34			-0.03	2.079
780090	1975	2009	34			0.43	0.971
780090	1975	2009	34			0.10	1.433
780090	1975	2009	34			0.10	1.246
780097	1995	2002	7	1	-0.15		0.409
780097	1995	2002	7	2	-0.15		0.613
780097	1995	2002	7	3	-0.15		0.818
780097	1995	2002	7	4	-0.15		0.613
780097	1995	2002	7	5	0.15		1.022
780097	1995	2002	7	6	0.15		0.818
780097	1995	2002	7	7	0.15		1.022
780097	1995	2002	7	8	0.15		0.818
780099	1995	2009	14			0.76	0.093
780099	1995	2009	14			0.76	0.136
780099	1995	2009	14			0.43	0.312

Table P.1: Continued

Bridge #	Construction date	Year Visited	Age at Visit	Location	Elevation AHT (m)	Elevation MG (m)	Dapp (m <sup>2</sup> /s) × 10 <sup>-12</sup>
780100	1999	2009	10			0.08	1.182
780100	1999	2009	10			0.08	1.793
780100	1999	2009	10			-0.25	1.248
780100	1999	2009	10			0.43	0.372
780100	1999	2009	10			0.43	0.408
780100	1999	2009	10			0.00	0.617
790132	1986	1991	5		0.53		6.338
790132	1983/97	2006	9		-0.15		0.051
790152	1990	2000	10	1	-0.15		8.490
790152	1990	2000	10	2	0.13		34.102
790152	1990	2000	10	3	0.10		2.862
790152	1990	2000	10	4	-0.12		3.271
790152	1990	2000	10	7	0.08		15.511
790152	1990	2000	10	8	0.09		8.178
790152	1990	2000	10	12	0.09		3.775
790152	1990	2000	10	13	0.06		2.249
790152	1990	2000	10	14	0.34		17.384
790152	1990	2000	10	15	0.34		1.227
790152	1990	2000	10	16	0.02		3.902
790152	1990	2000	10	17	0.02		1.636
790152	1990	2000	10	18	0.32		3.511
790152	1990	2000	10	19	0.32		2.249
790152	1990	2000	10	24	-0.09		5.432
790152	1990	2000	10	25	-0.09		1.022
790152	1990	2000	10	26	0.16		7.889
790152	1990	2000	10	27	0.16		1.227
790174	1997	2006	9		-0.20		0.628
790174	1997	2006	9		-0.13		0.329
790174	1997	2009	12			0.36	0.312
790174	1997	2009	12			-0.13	0.406
790174	1997	2009	12			0.36	0.378
790174	1997	2009	12			-0.13	0.503
790175	1997	2009	12			0.28	0.386
790175	1997	2009	12			-0.03	0.255
790187	2001	2006	5		-0.30		0.585
790187	2001	2006	5		-0.10		0.358
790187	2001	2009	8			0.13	0.239
790187	2001	2009	8			-0.10	0.289
790187	2001	2009	8			0.36	0.356
790187	2001	2009	8			0.10	0.186
794004	1959	2009	50			-0.03	0.073
794004	1959	2009	50			0.24	5.100
794004	1959	2009	50			-0.20	17.000
860018	1958	2009	51			0.33	1.000
860018	1958	2009	51			0.33	1.137
860018	1958	2009	51			-0.10	0.576
860018	1958	2009	51			0.25	0.289
860018	1958	2009	51			0.25	0.559
860018	1958	2009	51			-0.05	1.069
860018	1958	2009	51			-0.05	3.039

Table P.1: Continued

Bridge #	Construction date	Year Visited	Age at Visit	Location	Elevation AHT (m)	Elevation MG (m)	Dapp (m <sup>2</sup> /s) × 10 <sup>-12</sup>
860043	1962	2009	47			0.36	1.106
860043	1962	2009	47			0.36	1.449
860043	1962	2009	47			0.00	2.515
860061	1957/1981	2009	28			0.25	1.546
860061	1957/1981	2009	28			0.25	0.646
860061	1957/1981	2009	28			-0.05	0.238
860061	1957/1981	2009	28			0.41	0.727
860061	1957/1981	2009	28			0.41	0.825
860061	1957/1981	2009	28			0.00	0.681
860319	1981	1991	10		0.97		1.411
860319	1981	2007	26		0.6		1.800
860466	1989	1992	3		0.53		3.476
860466	1989	1992	3		2.06		1.676
860466	1989	2009	20			0.36	1.600
860466	1989	2009	20			0.36	2.409
860466	1989	2009	20			-0.08	2.230
860466	1989	2007	18				25.000
860467	1989	1992	3		0.46		0.470
860467	1989	1992	3		1.78		0.552
860467	1989	2009	20			0.30	2.430
860467	1989	2009	20			-0.08	1.530
860467	1989	2007	18		0.7		0.380
870606	1983	1992	9		1.68		0.184
870606	1983	1992	9		0.23		9.200
870606	1983	1992	9		2.16		0.920
870606	1983	2007	24		0.4		5.000
870607	1983	1992	9		0.79		1.754
870607	1983	1992	9		1.02		13.084
870607	1983	1992	9		3.00		1.002
870607	1983	2007	24		1.2		2.900
870660	7/1/1929	6/8/2010	81	West Pier NF	0.91		3.417
870660	7/1/1929	6/8/2010	81	East Pier EF	1.52		1.605
870660	7/1/1929	6/8/2010	81	East Pier EF	1.52		1.537
870772	1995	1998.5	3.5	12	1.75		0.213
870772	1995	1998.5	3.5	13	1.75		0.063
870772	1995	1998.5	3.5	16	0.83		0.818
870772	1995	1998.5	3.5	20	0.80		0.824
870772	1995	1998.5	3.5	21	0.81		0.409
870772	1995	1998.5	3.5	31	0.76		0.961
874663	1985	1993	8		2.21		0.368
874663	1985	1993	8		0.89		0.572
874663	1985	1993	8		1.70		0.245
874664	1985	1993	8		0.64		0.450
874664	1985	1993	8		2.08		0.450
874664	1985	1993	8		1.12		2.453
874664	1985	1993	8		2.31		2.044

Table P.1: Continued

Bridge #	Construction date	Year Visited	Age at Visit	Location	Elevation AHT (m)	Elevation MG (m)	Dapp (m <sup>2</sup> /s) × 10 <sup>-12</sup>
880050	7/1/1967	1/15/2010	43	Pile 3-4	0.30		3.718
880051	7/1/1967	9/29/2009	42	Pile 18-5 EF	0.30		0.452
880051	7/1/1967	1/15/2010	43	Pile 18-5	0.30		0.444
880052	7/1/1967	9/22/2009	42	Pile 4-3 EF	0.30		1.073
890003	1964	2009	45			0.46	0.342
890003	1964	2009	45			0.08	0.456
890003	1964	2009	45			0.08	0.898
890107	1987	1993	6		0.89		4.089
890107	1987	1993	6		2.34		1.574
890107	1987	1993	6		0.51		15.333
890107	1987	1993	6		1.73		0.797
890145 W	2005	2009	4			0.48	0.600
890145 W	2005	2009	4			0.48	1.314
890145 W	2005	2009	4			0.05	0.843
890146 E	2005	2009	4			0.51	0.900
890146 E	2005	2009	4			0.51	0.672
890146 E	2005	2009	4			0.00	0.912
890150	2007	2009	2			0.53	0.116
890150	2007	2009	2			0.53	0.284
890150	2007	2009	2			0.08	0.322
890151	1997	2009	12			0.46	0.108
890151	1997	2009	12			0.08	0.198
890151	1997	2009	12			0.08	0.180
890152	1997	2006	9		-0.18		0.361
890152	1997	2006	9		-0.15		0.540
890152	1997	2006	9		-0.15		0.373
890158	2001	2009	8			0.48	0.112
890158	2001	2009	8			0.05	0.239
890158	2001	2009	8			0.05	0.244
894037	1967	2009	42			0.53	0.098
894037	1967	2009	42			0.53	0.078
900016	1972	2009	37			0.89	1.02
900016	1972	2009	37			0.89	1.62
900016	1972	2009	37			0.30	0.87
900017	1983	1988	5		1.22		6.95
900017	1983	1988	5		1.83		2.86
900017	1983	1988	5		1.37		124.30
900017	1983	1988	5		0.00		9.40
900017	1983	1988	5		0.61		6.75
900017	1983	1988	5		2.44		1.82
900017	1983	1988	5		0.74		15.54
900017	1983	1988	5		1.19		4.70
900017	1983	1988	5		1.88		6.75

Table P.1: Continued

Bridge #	Construction date	Year Visited	Age at Visit	Location	Elevation AHT (m)	Elevation MG (m)	Dapp (m <sup>2</sup> /s) × 10 <sup>-12</sup>
900026	1982	1988	6		1.52		20.04
900026	1982	1988	6		0.00		38.23
900026	1982	1988	6		0.61		31.08
900026	1982	1988	6		1.22		11.04
900026	1982	1988	6		1.83		6.54
900026	1982	1991	9		0.76		25.56
900026	1982	1991	9		1.07		5.72
900045	1972	2009	37			0.25	1.71
900077	1981	1992	11		1.52		8.38
900077	1981	1992	11		1.09		7.97
900077	1981	2007	26		0.06		4.70
900077	1981	2007	26		0.34		6.90
900077	1981	2007	26		0.21		11.00
900077	1981	2007	26		0.01		14.00
900086	7/1/1978	7/29/2003	25	Bent 2 Pile 2 WF	0.30		3.50
900086	7/1/1978	7/29/2003	25	Bent 3 Pile 2 SF	0.30		7.38
900095	1981	2009	28			0.66	3.83
900095	1981	2009	28			0.15	11.74
900095	1981	2009	28			0.15	6.21
900096	1981	2009	28			0.76	17.57
900096	1981	2009	28			0.13	2.16
900096	1981	2009	28			0.13	1.56
900101	1982	2009	27			1.02	1.86
900101	1982	2009	27			0.25	80.00
900101	1982	2009	27			0.89	12.62
900101	1982	2009	27			0.25	3.47
900101	1982	2009	27			0.25	2.36
900103	1981	2009	28			0.38	14.40
900106	1982	2009	27			0.71	4.44
900106	1982	2009	27			0.71	2.72
900106	1982	2009	27			0.18	2.95
900106	1982	2009	27			0.18	2.52
900124	1982	1991	9		0.41		15.54
900124	1982	1991	9		0.69		20.04
900124	1982	2007	25		0.52		10.00
900124	1982	2007	25		0.09		14.00
900125	7/1/1985	7/29/2003	18	Bent 8 Pile 1 SF	0.00		1.12
900126	1982	1991	9		0.61		29.03
900126	1982	1991	9		1.91		20.44
900126	1982	2007	25		0.15		28.00
930349	1982	1993	11		1.24		13.29
930349	1982	1993	11		2.08		6.95
930349	1982	1993	11		0.08		7.16
930349	1982	1993	11		1.37		18.40

Table P.1: Continued

Bridge #	Construction date	Year Visited	Age at Visit	Location	Elevation AHT (m)	Elevation MG (m)	Dapp (m <sup>2</sup> /s) × 10 <sup>-12</sup>
OldStGeorge	1967	2009	42			0.51	0.610
OldStGeorge	1967	2009	42			0.00	0.529
OldStGeorge	1967	2009	42			0.00	0.816
OldStGeorge	1967	2009	39		-1.83		9.18
OldStGeorge	1967	2009	39		-0.30		14.71
OldStGeorge	1967	2009	39		0.91		2.04
OldStGeorge	1967	2009	39		0.18		1.47